
Marine Physical Laboratory

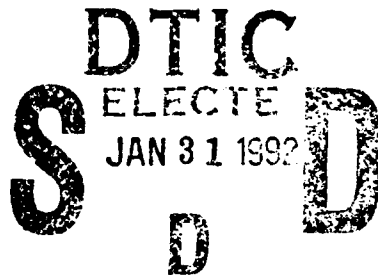
2

AD-A245 317



Localizing Swallow Floats During the July 1989 Experiment

G. C. Chen and W. S. Hodgkiss



MPL Technical Memorandum 421
December 1990

Approved for public release; distribution unlimited.



University of California, San Diego
Scripps Institution of Oceanography

92-02472



REPORT DOCUMENTATION PAGE				Form Approved OMB No. 0704-0188	
1a. REPORT SECURITY CLASSIFICATION UNCLASSIFIED			1b. RESTRICTIVE MARKINGS		
2a. SECURITY CLASSIFICATION AUTHORITY			3. DISTRIBUTION / AVAILABILITY OF REPORT Approved for public release; distribution unlimited.		
2b. DECLASSIFICATION / DOWNGRADING SCHEDULE					
4. PERFORMING ORGANIZATION REPORT NUMBER(S) MPL Technical Memorandum 421 [MPL-U-28/90]			5. MONITORING ORGANIZATION REPORT NUMBER(S)		
6a. NAME OF PERFORMING ORGANIZATION University of California, San Diego		6b. OFFICE SYMBOL (If applicable) MPL	7a. NAME OF MONITORING ORGANIZATION Naval Research Laboratory		
6c. ADDRESS (City, State, and ZIP Code) Marine Physical Laboratory Scripps Institution of Oceanography San Diego, California 92152			7b. ADDRESS (City, State, and ZIP Code) 4555 Overlook Avenue, S.W. Washington, D.C. 20375-5000		
8a. NAME OF FUNDING / SPONSORING ORGANIZATION Naval Research Laboratory		8b. OFFICE SYMBOL (If applicable) ONR	9. PROCUREMENT INSTRUMENT IDENTIFICATION NUMBER N00014-88-K-2040		
8c. ADDRESS (City, State, and ZIP Code) 4555 Overlook Avenue, S.W. Washington, D.C. 20375-5000			10. SOURCE OF FUNDING NUMBERS		
			PROGRAM ELEMENT NO.	PROJECT NO.	TASK NO.
11. TITLE (Include Security Classification) LOCALIZING SWALLOW FLOATS DURING THE JULY 1989 EXPERIMENT					
12. PERSONAL AUTHOR(S) G. C. Chen and W. S. Hodgkiss					
13a. TYPE OF REPORT tech memo		13b. TIME COVERED FROM _____ TO _____		14. DATE OF REPORT (Year, Month, Day) December 1990	
15. PAGE COUNT					
16. SUPPLEMENTARY NOTATION					
17. COSATI CODES			18. SUBJECT TERMS (Continue on reverse if necessary and identify by block number) Swallow floats, Kalman filter, least squares filter, VLF acoustic data		
FIELD	GROUP	SUB-GROUP			
19. ABSTRACT (Continue on reverse if necessary and identify by block number) Results from localizing Swallow floats using range data collected during the 8-9 July 1989 experiment are presented herein. As part of the Downslope Conversion experiment, the Swallow float deployment was conducted near 34° 50' N, 122° 20' W, about 150 km west, northwest of Pt. Arguello, California. Three Swallow floats were deployed to the ocean bottom and 9 freely drifting floats were ballasted to depths starting at 600 m and spaced every 400 m, to 3800 m. Two localization methods, least squares filter and Kalman filter, were applied to the experiment data so that their results can be compared. Due to the high process noise experienced by the freely drifting floats during the experiment and the quasi vertical line array deployment geometry, the two filters performs comparably. The rms position error is estimated to be less than 3.3 m for the Kalman filter and less than 4.6 m for the least squares filter. Both filters appear to be capable of estimating float positions to within the desired accuracy of one-tenth of a wavelength at the highest frequency of interest 20 Hz (7.5 m) in order to effectively beam-form the VLF acoustic data.					
20. DISTRIBUTION / AVAILABILITY OF ABSTRACT <input type="checkbox"/> UNCLASSIFIED/UNLIMITED <input checked="" type="checkbox"/> SAME AS RPT. <input type="checkbox"/> DTIC USERS			21. ABSTRACT SECURITY CLASSIFICATION UNCLASSIFIED		
22a. NAME OF RESPONSIBLE INDIVIDUAL W.S. Hodgkiss			22b. TELEPHONE (Include Area Code) (619) 534-1798		22c. OFFICE SYMBOL MPL

Localizing Swallow floats during the July 1989 Experiment

G. C. Chen and W. S. Hodgkiss

Marine Physical Laboratory
Scripps Institution of Oceanography
San Diego, CA 92152

ABSTRACT

Results from localizing Swallow floats using range data collected during the 8-9 July 1989 experiment are presented herein. As part of the Downslope Conversion experiment, the Swallow float deployment was conducted near $34^{\circ} 50' N$, $122^{\circ} 20' W$, about 150 km west, northwest of Pt. Arguello, California. Three Swallow floats were deployed to the ocean bottom and 9 freely drifting floats were ballasted to depths starting at 600 m and spaced every 400 m, to 3800 m.

Two localization methods, least squares filter and Kalman filter, were applied to the experiment data so that their results can be compared. Due to the high process noise experienced by the freely drifting floats during the experiment and the quasi vertical line array deployment geometry, the two filters performs comparably. The rms position error is estimated to be less than 3.3 m for the Kalman filter and less than 4.6 m for the least squares filter. Both filters appear to be capable of estimating float positions to within the desired accuracy of one-tenth of a wavelength at the highest frequency of interest 20 Hz (7.5 m) in order to effectively beam-form the VLF acoustic data.

Accession For	
NTIS	<input checked="" type="checkbox"/>
CRA&I	<input type="checkbox"/>
DTIC TAB	<input type="checkbox"/>
Unannounced	<input type="checkbox"/>
Justification	
By	
Distribution /	
Availability Codes	
Dist	Avail and/or Special
A-1	

1. Introduction

This report presents the results from localizing Swallow floats using range data collected during the July 1989 experiment which took place between 8 and 9 July near $34^{\circ} 50' \text{ N}$, $122^{\circ} 20' \text{ W}$, about 150 km west, northwest of Pt. Arguello, California. In this experiment, 12 Swallow floats were deployed; 9 were freely drifting in the water column in a quasi vertical line array geometry with a vertical float separation of about 400 m, starting at about 600 m depth to about 3800 m; and 3 were tethered to the ocean bottom so that stable absolute position fixes could be obtained for the freely drifting midwater floats. Detailed information about the experiment is contained in the experiment trip report [1].

The theoretical basis and simulation results for the two localization methods, least squares filter and Kalman filter, can be found in [2,3]. A comprehensive procedure for estimating float positions using data from the April 1987 experiment was documented in [4]. The emphasis here is on the use of the filters and interpretation of the results using data from the July 1989 experiment.

This report is organized as follows. Following this introduction section, Section 2 reviews the two filters from the performance criteria point of view. The desire here is to provide the necessary background for discussion in the subsequent sections. Section 3 describes the inputs to the filters while Sections 4 and 5 discuss approaches to filter tuning and the outputs from the filters respectively. Lastly, summary of the localization results is given in Section 6.

2. Localization Methods

The function of the localization filter is to algorithmically compute float positions from noisy range measurements in a statistical sense depending on the optimality criterion chosen. In this section, two such filters developed at the Marine Physical Laboratory (MPL) are reviewed from the performance criteria point of view.

2.1. Generalized Least Squares Filter

The generalized (or weighted) least squares filter [5,6] involves using the current set of range measurements, Z_n , which are related to the set of float positions X_n by the expression:

$$Z_n = h(X_n) + V_n \quad (\text{measurement model}) \quad (2.1)$$

where h is the nonlinear function which gives the ideal (noiseless) connection between the range measurements and the float positions, and V_n is the set of range measurement errors. These errors are also known as the residuals with zero means and second-order statistics described by:

$$E \begin{bmatrix} V_n & V_n^T \end{bmatrix} = R_n \delta_{nm} \quad (\text{measurement statistics}) \quad (2.2)$$

i.e. the errors are mutually uncorrelated.

The least squares method is concerned with determining the most probable set of float positions which is defined as the set of float positions that minimizes the weighted sum of the squares of the residuals:

$$\underset{X_n}{\text{minimize}} \begin{bmatrix} Z_n - h(X_n) \end{bmatrix}^T W_n \begin{bmatrix} Z_n - h(X_n) \end{bmatrix}$$

where W_n is the weighting matrix chosen as the inverse of the range covariance matrix R_n , and the weighted least squares filter's position estimate is:

$$\hat{X}_n = \left[H^T R_n H \right]^{-1} H^T R_n Z_n \quad (2.3)$$

where:

$$H = \frac{\partial h(X_n)}{\partial X} = \frac{\partial h}{\partial X} \Big|_{x_n} \quad (2.4)$$

Thus, the least squares filter estimates current float positions using only current set of measurements and an estimate of the measurement error statistics.

2.2. Kalman Filter

The Kalman filter [3,6,7,8,9] attempts to better estimate float positions by taking advantage of the knowledge of float dynamics and incorporating a fading memory of past data into the estimator structure. In addition to the measurement model (2.1) and statistics (2.2), Kalman filter also uses the system model (float dynamics), the system statistics, and the initial conditions. The system model is given by:

$$X_n = \Phi X_{n-1} + \Gamma \ddot{X}_{n-1} \quad (\text{system model}) \quad (2.5)$$

where Φ is the state transition matrix which relates X_{n-1} to X_n , Γ the matrix which relates the accelerations to the float positions, and \ddot{X}_{n-1} the set of accelerations with zero means and second-order statistics described by:

$$E \left[\ddot{X}_n \ddot{X}_n^T \right] = Q_n \delta_{nm} \quad (\text{system statistics}) \quad (2.6)$$

The initial conditions are:

$$\hat{X}_0 = E(X_0) \quad (2.7)$$

$$P_0 = E \left[(X_0 - \hat{X}_0)(X_0 - \hat{X}_0)^T \right] \quad (2.8)$$

where \hat{X}_0 is the estimate of the initial float positions, and P_0 the estimate of the error variance in the initial float positions.

The operation of the Kalman filter can be viewed as a predictor-corrector process [10]. First, suppose we have available to us the previous float position estimates X_{n-1} and associated position covariance matrix P_{n-1} :

$$P_{n-1} = E \left[(X_{n-1} - \hat{X}_{n-1}) (X_{n-1} - \hat{X}_{n-1})^T \right] \quad (2.9)$$

and we would like to obtain the best estimate of the current float positions based on the previous estimate. We are in the "prediction phase" of the process. The system model (2.5) is used to predict the float positions and the associated position covariance matrix:

$$\hat{X}_n(-) = \Phi \hat{X}_{n-1} \quad (2.10)$$

$$P_n(-) = \Phi P_{n-1} \Phi^T + \Gamma \ddot{X}_n \Gamma^T \quad (2.11)$$

The "minus" is introduced here (following the notation in reference [6]) as a reminder that this is our best estimate prior to incorporating the measurement. We now seek to use the measurement Z_n to improve the estimate $\hat{X}_n(-)$. We choose a linear blending of the noisy measurement and the $\hat{X}_n(-)$ in accordance with the equation:

$$\hat{X}_n = \hat{X}_n(-) + K_n \left[Z_n - h(\hat{X}_n(-)) \right] \quad (2.12)$$

The optimal choice of K_n , the Kalman gain, is to minimize a scalar sum of the diagonal elements of the position covariance matrix P_n :

$$\underset{K_n}{\text{minimize}} \left\{ \text{trace} \left[P_n \right] \right\}$$

where:

$$P_n = E \left[(X_n - \hat{X}_n) (X_n - \hat{X}_n)^T \right] \quad (2.13)$$

K_n is obtained as:

$$K_n = P_n(-) H_n^T \left[H_n P_n(-) H_n^T + R_n \right]^{-1} \quad (2.14)$$

or in a simpler form:

$$K_n = P_n H_n^T R_n^{-1} \quad (2.15)$$

where:

$$H_n = \left. \frac{\partial h(X_n)}{\partial X} \right|_{X_n = \hat{X}_n(-)} \quad (2.16)$$

We then use the current set of range measurements Z_n to determine the innovations. The innovation is defined as:

$$Z_n - h\left[\hat{X}_n(-)\right]$$

which is the difference between the actual range measurement and the predicted range measurement (2.10). Now we enter the "correction phase" of the process. That is, we correct or update the predicted positions based on the new information in the range measurements - the innovation. The innovation is weighted by the Kalman gain K_n to correct the predicted positions $\hat{X}_n(-)$ as described in (2.12). The associated position covariance matrix (2.11) is corrected as well:

$$P_n = \left[I - K_n H_n \right] P_n(-) \quad (2.17)$$

The predictor-corrector process then repeats until all measurements are consumed.

A useful interpretation [6] of the Kalman gain (2.15) is that the gain is "proportional" to the uncertainty in the position estimates, and "inversely proportional" to the range measurement noise. In other words, if the range measurement errors are large and the predicted position errors are small, the innovation is due chiefly to the noise and only small change in the predicted positions should be made. On the other hand, small measurement noise and large uncertainty in the position estimates suggest that the innovation

contains considerable information about errors in the position estimates. Therefore, the difference between the actual and the predicted range measurement will be used as a basis for strong corrections to the position estimates.

In short, the Kalman filter estimates float positions by weighting a current set of measurements against previous position estimates propagated forward in time using an equation of motion. Thus, the Kalman filter uses current measurements as well as past measurements in a fading memory fashion, estimates of the measurement error statistics and acceleration error (process noise) statistics, and the float dynamics. It has been shown [3] that the Kalman filter outperforms the least squares filter in the presence of high measurement noise and when the process noise is low because of its ability to track float motion and effectively smooth noisy measurements.

3. Inputs to localization filter

This section presents the inputs to both filters using data from the July 1989 experiment. Based on discussion in the previous section, input data falls under four categories: measurement data, measurement statistics, initial estimates and process noise.

3.1. Measurement Data

Range measurements used by the filters are derived quantities computed from 8 kHz pulse travel time measurements between floats (or from float to surface) using an estimate of the sound speed. Thus, measurement data includes travel time estimates and sound speed estimates.

3.1.1. Travel Time Estimates

Measurement of pulse travel times has received a great deal of attention during the process of the Swallow float system development in the past few years. References [1,11,12] have addressed this subject in detail. In brief, each float is equipped with an acoustic transducer which transmits and receives 8 kHz pulses. Pulses are transmitted by the floats in a preprogrammed sequence. A different float transmits every 45 seconds; 12 floats were deployed in this experiment and each float transmits every 9 minutes. A given float receives pulses transmitted by other floats as well as its own arrivals (surface echoes, bottom bounces, or mixtures of both). Since only direct path pulses between floats and surface echo pulses from one float to itself are of interest, an edge detector program [11,3,4] was used to detect and extract such pulses which correspond to the first arrivals in a narrow range time window.

Surface echo travel time measurements are obtained by subtracting outgoing pulse transmit times from pulse arrival times, whereas interfloat travel time measurements are obtained by subtracting pulse transmit time according to the transmitting float from pulse arrival times at the receiving float. Since two time bases are involved,

interfloat travel time measurements contain a bias due to variation in the float clock rates. It has been shown [12] that the bias can be reduced significantly by averaging reciprocal path interfloat travel time measurements. Because interfloat measurements were not made simultaneously, travel time measurements must be interpolated by a factor of 12 before reciprocal path measurements can be averaged.

Figures 3.1 through 3.12 show the leading edge of each float's detection of its own transmitted and surface echo 8 kHz pulses. The vertical axes in the figures have been scaled from travel time to depth, using half of 1500 m/s for sound speed. The line of dots at approximately 0 depth corresponds to the detection of the outgoing 8 kHz pings and the second line of dots corresponds to the detection of the incoming pulses i.e. surface echo pulses. Note that the lines of dots terminate prematurely for floats 4 and 5 in Figures 3.5 and 3.6, respectively. Float 4 stopped recording data 4 hours too early and float 5's automatic ballast release time was set incorrectly [1]. Figures 3.13 through 3.78 (except Figures 3.13, 3.14, and 3.24) show the direct path pulse detections between floats. Figures 3.13, 3.14 and 3.24 show the surface reflected pulse detections between the bottomed floats, 9, 10 and 11. The direct path pulses between the bottomed floats were not detected because the sound speed gradient bends nearly all of the sound energy upward over the 6.3 km distance which separates the floats. Direct path travel times can be calculated from surface reflection travel times using equation (3.1) [4]:

$$\left[\tau_{ij}^A \right]_{\text{direct path}}^2 = \frac{c_{avg}^2}{c_{ij}^2} \left\{ \left[\tau_{ij}^A \right]_{\text{surface reflection}}^2 - \tau_{ii} \tau_{jj} \right\} \quad (3.1)$$

where τ_{ij}^A is the interfloat travel time, τ_{ii} and τ_{jj} the individual float surface echo travel times, c_{avg} the harmonic mean sound speed for a vertical path from the surface to the bottom, and c_{ij} the sound speed at the depth of floats i and j.

Figures 3.79 through 3.87 contain the surface echo travel time measurements for the freely drifting floats. Figures 3.88, 3.89 and 3.90 show the surface echo travel

time measurements for the bottomed floats, 9, 10 and 11. As pointed out in [4], the bottomed floats' surface measurements like these are expected to be approximately constant because the floats themselves are approximately stationary; they are tethered to the ocean bottom by 3.05-meter lines. Noise in the surface echo pulse arrival time is thought to be caused by scattering of the pulse at the rough, moving sea surface and destructive interference among multiple arrivals at the receiver. Since filter performance can be improved by substituting a constant for the actual measurements, the most probable value i.e. the mode of the travel time measurements (5.402 seconds for float 9, 5.422 seconds for float 10, and 5.404 seconds for float 11) will be used as the travel time estimates.

Figures 3.91a, 3.92a, and 3.93a show the averaged surface bounce path travel times between the bottomed floats. Like the bottom float surface echo travel times, the interfloat travel time should be approximately constant because the floats are approximately stationary. Figures 3.91b, 3.92b, and 3.93b show the direct path travel time estimates between the bottomed floats, calculated using equation (3.1) and the actual surface echo travel times, whereas Figures 3.91c, 3.92c, and 3.93c show the direct path travel time estimates, calculated using equation (3.1) and the constant value (mode) estimates of the surface echo travel times. Because the underlying direct path travel time must be approximately constant, the modes of Figures 3.91c, 3.92c, and 3.93c will be used as the direct path travel time estimates (4.025 seconds for path between floats 9 and 10, 4.157 seconds for path between floats 9 and 11, and 4.132 seconds for path between floats 10 and 11).

Figures 3.94 through 3.127 contain the remaining interfloat travel time estimates calculated by averaging interpolated reciprocal path measurements.

3.1.2. Sound Speed Estimates

The sound speed profile for the upper 1000 meters was obtained from 5 expendable bathythermograph (XBT) measurements [13] made from the R/V New

Horizon near the deployment site at various times during the Swallow float experiment and historical salinity data for area 24, 3rd quarter of the year, in the upper 1000 meters archived by the National Oceanographic Data Center [13]. The sound speed profile for the lower 3100 meters was obtained from a conductivity-temperature-depth CTD station [14] carried out on July 11, 1989 near the center of the float-triangle where all the freely drifting floats were put into the water. Using the equation given by Mackenzie [15], the composite sound speed profile was calculated and plotted in Figure 3.128. Harmonic mean sound speeds for each interfloat and float to surface path were also calculated and are given in Appendix 1.

3.2. Measurement Statistics

The measurement error variance estimates are used to weight the measurements so that greater weight is given to measurement with a smaller error variance. Since travel time measurement error and sound speed estimate error are assumed to be uncorrelated, the measurement error variance for float pair ij can be expressed as [4]:

$$\sigma_{r_{ij}}^2 = (\hat{\tau}_{ij}^s)^2 \sigma_{c_{ij}}^2 + (\hat{c}_{ij})^2 \sigma_{\tau_{ij}}^2 \quad (3.2)$$

where $\hat{\tau}_{ij}^s$ is the estimated travel time between float i and j , $\sigma_{c_{ij}}^2$ the sound speed error variance in \hat{c}_{ij} , \hat{c}_{ij} the estimated harmonic sound speed between float i and j , and $\sigma_{\tau_{ij}}^2$ the travel time error variance between float i and j .

3.2.1. Travel Time Variances

It has been shown [12] that the variance of a bottomed float's surface echo travel time measurements can be used as an estimate of the variance of the measurement error, because the true surface echo times are approximately constant. Subtracting the means from the surface echo travel time estimates produces estimates of the travel time estimate errors. The variances of the error time series are given in Table 3.1.

Table 3.1. Estimated Variance of Bottomed Float Travel Time, July 1989 Experiment		
Float Numbers		Variance, msec ²
9	9	115
10	10	110
11	11	97
9	10	78
9	11	64
10	11	142

In the previous section, the bottomed float surface echo travel time measurements were ruled as too noisy to be used directly in estimating the float positions, and the mode of the travel time measurements was taken as the travel time estimate. The variance of the error in the constant estimate (mode) is expected to be much smaller than the variance of the error in the measurement. Based upon the predicted maximum vertical movement of a tethered bottom float and wave height in the sea surface during the deployment (about 3 meters), the error in the mode is taken to be mean zero and have variance 6 msec². By the same token, the interfloat travel time variance is taken to be 4 msec² [4] based upon the predicted maximum horizontal movement of a bottom float. Table 3.2 summarizes the estimated error variances of the bottomed float travel time estimates.

The surface echo travel time estimate error for the freely drifting floats cannot be estimated directly. Because these floats were deployed shallower than the bottom floats, their variances are expected to be lower than the values in Table 3.1 but higher than those in Table 3.2. An arbitrary, yet logical, choice of error variances for the freely drifting float surface echo travel time estimates are listed in Table 3.3.

Table 3.2. Estimated Variance of Bottomed Float Travel Time Based on Predicted Float Movement, July 1989 Experiment

Float Numbers		Variance, msec ²
9	9	6
10	10	6
11	11	6
9	10	4
9	11	4
10	11	4

Table 3.3 Estimated Variance of Freely Drifting Float Travel Time, July 1989 Experiment

Float Numbers		Variance, msec ²
0	0	6
1	1	10
2	2	20
3	3	30
4	4	40
5	5	50
6	6	60
7	7	70
8	8	80

Travel time error variance for float pairs in which one of the floats is not stationary can be estimated from the difference between reciprocal path travel time measurements [12]. The difference in clock rates causes the travel time difference to be a linear function of time. The difference also appears to contain second order time dependence due to difference in clock accelerations. Subtracting a second order fit from the travel time difference produces an estimate of the error in the travel time estimates. Figures 3.129 through 3.191 contain interfloat travel time differences along with second

order curves fitted to the differences and the corresponding error estimate time series. The variances of the error time series are summarized in Appendix 2.

3.2.2. Sound Speed Variances

It has been shown [2,4] that the variance of the sound speed estimate at a particular depth is just under $0.4 \text{ (meter/sec)}^2$ in the North Pacific Ocean. The variance of the harmonic mean sound speed for a given path would be expected to be less than that in the sound speed at a particular depth due to averaging effect. The error in the harmonic mean sound speed is estimated to be $0.1 \text{ (meter/sec)}^2$ for the 1989 experiment.

3.3. Initial Estimates

The MPL implementation of the filters requires an initial estimate of the float positions. Additionally, the Kalman filter requires an initial estimate of the float velocities and the initial position and velocity variance estimates. Before estimating the initial positions, we must first define a coordinate system. The coordinate system for the float localization is established in which the origin lies at the surface directly above float 9. The Z axis is vertical, positive downwards and extends through float 9, and the X axis is oriented such that float 10 lies in the XZ plane. The positions of floats 9, 10 and 11 are taken to be the ship's position when the floats were launched into the water. Figure 3.192 shows a plane view of the coordinate system. The locations of the freely drifting floats will be estimated relative to these axes.

3.3.1. Initial Position Estimates

The time for the initial float position chosen for float localization is record 1003, 00:00 July 9 1989, at which 7 of the 9 freely drifting floats had reached equilibrium depth. The MPL implementation of the least squares filter requires a rough initial position estimate to bootstrap the filter. The rough initial positions are taken to be the ship's

position relative to the coordinate system when the floats were launched into the water using depths taken from Figures 3.1 through 3.12. Table 3.6 lists the rough initial position estimate.

Table 3.6. Rough Initial Position Estimate Record 1003, 00:00 July 9 1989			
Float	X	Y	Z
9	0	0	4050
10	6150	0	4050
11	3075	5500	4050
0	3075	2750	570
1	3075	2750	990
2	3075	2750	1380
3	3075	2750	1670
4	3075	2750	2080
5	3075	2750	2490
6	3075	2750	2840
7	3075	2750	3350
8	3075	2750	3650

Using the rough initial position estimates in Table 3.6, the travel time estimates for record 1003, the travel time variance estimates given in Tables 3.2 and 3.3 and Appendix 2, and the sound speeds and sound speed variances given in Appendix 1, the least squares filter produced the position estimate given in Table 3.7. It has a root mean squared (rms) residual of 2.67 meters. Since an initial position estimate is determined to be satisfactory when the least squares filter converges to a position estimate which results in an rms residual of less than 7.5 meters [4], the position estimate at record 1003 is taken as a good initial position estimate and will be used by the Kalman filter.

Table 3.7. Initial Position Estimate Produced by the Least Squares Filter for Record 1003, 00:00, July 9 1989

Float	X	Y	Z
9	0	0	4039
10	6131	0	4051
11	3103	5518	4041
0	3779	-1456	574
1	4887	82	999
2	3885	162	1380
3	4425	969	1674
4	4110	1398	2081
5	4092	1482	2489
6	3870	1754	2841
7	2875	2085	3353
8	2824	1871	3650

3.3.2. Initial Velocity Estimates

Using the good initial position estimates, the least squares filter was again run for the first 13 records (9 minute period) from records 1003 to 1015. The position estimates produced by the filter were used to calculate the position change rates $\frac{X_{n+1}-X_n}{45}$ meters/second. Twelve such successive position change rates were then averaged to produce the initial velocity estimates. Table 3.8 lists the velocity estimates for record 1003, 00:00, 9 July 1989.

3.3.3. Initial Position and Velocity Variance Estimates

The estimate of the variances in the initial positions and velocities is also needed by the Kalman filter. The estimate suggested by [4] will be used and is listed in Table 3.9.

Table 3.8. Initial Velocity Estimate (in meters/second),
Record 1003, 00:00, July 1989 Experiment

Float	X	Y	Z
9	0	0	0
10	0	0	0
11	0	0	0
0	0.061	-0.040	-0.004
1	0.025	-0.058	0.005
2	-0.015	-0.040	0.001
3	0.028	-0.027	0.006
4	0.003	0.001	0.013
5	-0.003	0.001	0.015
6	0.002	0.017	0.027
7	-0.010	0.021	0.005
8	-0.036	-0.003	0.025

Table 3.9. Estimate of Initial Position and Velocity Variance
Used by the Kalman Filter, July 1989 Experiment

Float	Position, meters ²			Velocity, (m/sec) ²		
	X	Y	Z	X	Y	Z
9	0	0	0.01	0	0	0
10	0.01	0	0.01	0	0	0
11	0.01	0.01	0.01	0	0	0
0	0.01	0.01	0.01	0.0001	0.0001	0.00001
1	0.01	0.01	0.01	0.0001	0.0001	0.00001
2	0.01	0.01	0.01	0.0001	0.0001	0.00001
3	0.01	0.01	0.01	0.0001	0.0001	0.00001
4	0.01	0.01	0.01	0.0001	0.0001	0.00001
5	0.01	0.01	0.01	0.0001	0.0001	0.00001
6	0.01	0.01	0.01	0.0001	0.0001	0.00001
7	0.01	0.01	0.01	0.0001	0.0001	0.00001
8	0.01	0.01	0.01	0.0001	0.0001	0.00001

3.4. Process Noise

The last piece of information required by the Kalman filter is the float acceleration variance, also known as the process noise, described in equation (2.6). The process

noise is a parameter used by the Kalman filter to determine how much weight to give to its own track of the float relative to the measurements. When the model (i.e. filter) process noise matches the true process noise experienced by the float during the experiment, the Kalman filter is performing optimally and will have more estimates falling inside the predefined confidence interval [16]. However, there is no easy way of estimating the true process noise. One approach suggested by [4] is to run the filter several times, each time with a different process noise value and the one which minimizes the innovation power will be selected as the candidate. We will use this matched processing technique with values ranging from 10^{-12} to 5×10^{-8} (meter/second²)² in search of the true process noise.

4. Filter tuning

4.1. Least Squares Filter

Using the good initial positions given in Table 3.7, the sound speeds and sound speed variances given in Appendix 1, the travel time estimates for records 1003 to 2120, and the travel time variances given in Tables 3.2 and 3.3 and Appendix 2, the least squares filter produced position estimates with an average rms of 2.7 meters. The residual is low and indicates that the position estimate is acceptable. However, a close inspection of the residual sequences $[Z_n - h(X_n)]$ reveals that:

$$E \left[z_{\text{direct path between 9 \& 10}} - h(x_{\text{direct path between 9 \& 10}}^n) \right] = 1.3 \text{ meters} \quad (4.1)$$

$$E \left[z_{\text{direct path between 9 \& 11}} - h(x_{\text{direct path between 9 \& 11}}^n) \right] = 3.0 \text{ meters} \quad (4.2)$$

$$E \left[z_{\text{direct path between 10 \& 11}} - h(x_{\text{direct path between 10 \& 11}}^n) \right] = 1.2 \text{ meters} \quad (4.3)$$

$$E \left[z_{\text{float 9 surface echo}} - h(x_{\text{float 9 surface echo}}^n) \right] = 1.5 \text{ meters} \quad (4.4)$$

$$E \left[z_{\text{float 10 surface echo}} - h(x_{\text{float 10 surface echo}}^n) \right] = 4.9 \text{ meters} \quad (4.5)$$

$$E \left[z_{\text{float 11 surface echo}} - h(x_{\text{float 11 surface echo}}^n) \right] = 0.6 \text{ meters} \quad (4.6)$$

By definition, residuals in the measurement model are to be mean zero:

$$E \left[V_n \right] = E \left[Z_n - h(X_n) \right] = 0 \quad (4.7)$$

The bias contained in the residual sequences (4.1) - (4.6) is an indication that the mode values selected as the travel time estimates may not be the optimal choice for the July 1989 data set. In order to improve the filter performance, trends in the residual sequences must be removed. An iterative procedure was developed to achieve this and is described as follows:

1. Compute $\Delta\tau_{ij} = \frac{E[z_{ij} - h(x_{ij}^n)]}{c_{ij}}$ where $i = 9, 10, 11$ and $j = 9, 10, 11$.
2. Update $\tau_{ij} = \tau_{ij} - \Delta\tau_{ij}$.
3. Rerun the least squares filter.
4. If all $\left| E[z_{ij} - h(x_{ij}^n)] \right| < 1$ meter then stop; otherwise go to step 1.

The procedure was applied to the July 1989 data set. After 10 iterations, all 6 expected residuals converged to within 1 meter, and the least squares filter produced the position estimate with an average rms of 2.3 meters. The residual is lower than 2.7 meters and indicates that the position estimate for records 1003 to 2120 is closer to the true float positions. The constant value estimates used in the 10th run listed in Table 4.1 will replace the mode values as the new travel time estimates and will be used by the Kalman filter.

Table 4.1. Bottomed Float Surface Echo and Direct Path Between Bottomed Floats Travel Time Estimate, July 1989 Experiment	
Float Path	Travel Time Estimate (seconds)
9-10	4.028 (was 4.025)
9-11	4.152 (was 4.157)
10-11	4.130 (was 4.132)
9-9	5.401 (was 5.402)
10-10	5.409 (was 5.422)
11-11	5.405 (was 5.404)

4.2. Kalman Filter

The measurements, sound speed and variance estimates, and the initial estimates were applied to the Kalman filter. Using process noise values ranging from 10^{-12} to 5×10^{-8} (meters/second²)², the Kalman filter was run 24 times. Table 4.2 lists the mean inno-

vation power resulting from each run.

Table 4.2. Mean Innovation Power Produced by the Kalman Filter, July 1989 Experiment	
Process Noise (meters/second ²) ²	Mean Innovation Magnitude (meters)
1×10 ⁻¹²	7.0671
2×10 ⁻¹²	6.0969
3×10 ⁻¹²	5.6302
5×10 ⁻¹²	5.1290
7×10 ⁻¹²	4.8450
1×10 ⁻¹¹	4.5793
2×10 ⁻¹¹	4.1538
3×10 ⁻¹¹	3.9536
5×10 ⁻¹¹	3.7460
7×10 ⁻¹¹	3.6335
1×10 ⁻¹⁰	3.5331
2×10 ⁻¹⁰	3.3866
3×10 ⁻¹⁰	3.3269
5×10 ⁻¹⁰	3.2753
7×10 ⁻¹⁰	3.2546
1×10 ⁻⁹	3.2435
2×10 ⁻⁹	3.2539
3×10 ⁻⁹	3.2808
5×10 ⁻⁹	3.3401
7×10 ⁻⁹	3.3974
1×10 ⁻⁸	3.4770
2×10 ⁻⁸	3.6933
3×10 ⁻⁸	3.9648
5×10 ⁻⁸	6.8216

It has been shown using simulations [4] that the process noise which minimizes the power in the innovations sequence produces a position estimate with the smallest true rms error. The minimum is seen to occur at 10⁻⁹ which is the same found for the 1987 experiment [4]. Thus, process noise for the July 1989 experiment is estimated to be 10⁻⁹ (m/s²)².

5. Discussion of Localization Results

In this section, the outputs from the localization filters are discussed. Of interest are:

- RMS position error estimate
- RMS residual/innovation
- Float position estimate
- Distance difference between filters
- Float depth variation
- Float speed estimate

The curves shown in Figure 5.1 are the mean innovation power $|I|$, the Kalman filter's estimate of the rms position error, and the least squares filter's estimate of the rms position error. The vertical axis is rms error or mean innovation magnitude in meters. The horizontal axis is the estimate of process noise given to the Kalman filter as a parameter. Simulations [2] have shown that the true rms error in the Kalman filter's position estimate was always bracketed by the mean magnitude of the innovation and the filter's estimate of the rms error. Therefore, the rms error in the Kalman filter estimate is thought to be less than 3.3 meters. The least squares filter's estimate of rms float position error is 2.3 meters. Simulation results have indicated that the true rms error in the least squares filter's position estimate is no more than about twice the estimated error. Accordingly, the rms error in the least squares filter estimate is thought to be less than 4.6 meters.

The rms residual for the least squares estimates and the rms innovation for the Kalman filter estimates are shown as a function of measurement (Swallow float record) number in Figure 5.2. Both rms residual and innovation contain large spikes around records 1600 and 1700. These spikes are due to missing surface echo travel time meas-

urements in floats 6 and 8's data and the values determined by the adaptive linear predictor must still contain large errors.

Figures 5.3a and 5.3b show the filters' float horizontal position estimates between records 1003 and 2120. Both position estimates indicate that the freely drifting floats dispersed away from the center of the float triangle with floats 0 and 1 moving to the northwest, floats 2 and 3 to the west, float 4 to the southwest, and floats 5, 6, 7 and 8 to the southeast. The drifting pattern was probably due to the complex water movement (including eddies, wind-driven surface currents and the California Current) near the experiment site. The filters' float depth estimates are also plotted in Fig 5.4a and 5.4b.

The distance between the two filters' estimates is plotted for each float as a function of measurement number in Figure 5.5. The curves are, in descending order, from floats 0 through 11. The distance between the two position estimates is relatively small for all floats with an rms difference less than 3 meters for most of the experiment.

Figures 5.6 through 5.8 show the enlarged version of the Kalman filter's float depth estimates as a function of measurement number. The floats oscillate irregularly about slowly varying means with periods on the order of 30 to 90 minutes which corresponds roughly to internal wave periods. The slowly increasing depth trend, except for float 0, is probably caused by gradual compression of the float as it gets colder.

The float speed estimates derived from the Kalman filter's X, Y, and Z velocity component estimates are plotted in Figures 5.9 through 5.11. The float speeds appear to be rather unsteady (i.e., high process noise) throughout the experiment. The large scale speed oscillation with periods on the order of 4 to 12 hours, depending on float equilibrium depth, is thought to be caused by the tidal currents. Average float speeds for the freely drifting floats are listed in Table 5.1.

Table 5.1. Average Float Speed, July 1989 Experiment

Float Number	Average Speed (meters/hour)
0	350
1	170
2	220
3	180
4	80
5	40
6	110
7	90
8	120

6. Summary

In this report, two localization methods, generalized least squares filter and Kalman filter, were reviewed from the performance criteria point of view. The inputs to both filters using data from the July 1989 experiment were described in detail. The procedures for tuning the filters were described and the results from both filters were discussed and compared. The rms position error is estimated to be less than 3.3 m for the Kalman filter and less than 4.6 m for the least squares filter. Due to the high process noise experienced by the floats during the experiment and the quasi vertical line array deployment geometry [3], the two filters perform comparably. The two position estimates have an rms difference of less than 3 meters for most of the experiment. Both methods appear to be capable of estimating float positions to within the desired accuracy of one-tenth of a wavelength at the highest frequency of interest 20 Hz (7.5 m) in order to effectively beamform the VLF acoustic data.

Acknowledgements

We would like to thank Gerald D'Spain for discussions related to this report. This work was supported by the Office of Naval Research under contract #N00014-88-K-2040.

References

- [1] G. C. Chen, G. L. D'Spain, W. S. Hodgkiss, and G. L. Edmonds, "Freely drifting Swallow float array: July, 1989 trip report" MPL TM-420, Marine Physical Laboratory, Scripps Institution of Oceanography, San Diego, CA, 1990.
- [2] R. L. Culver, "Localizing and beamforming freely-drifting VLF acoustic sensors" SIO Ref. 88-16, Marine Physical Laboratory, Scripps Institution of Oceanography, San Diego, CA, 1988. Also, Ph.D. dissertation, University of California, San Diego, 1988.
- [3] R. L. Culver and W. S. Hodgkiss, "Comparison of Kalman and least squares filters for locating Autonomous very low frequency acoustic sensors," *IEEE J. Oceanic Eng.*, vol. 13, pp. 282-290, 1988.
- [4] R. L. Culver and W. S. Hodgkiss, "Localizing Swallow floats during the April 1987 Experiment" Marine Physical Laboratory, Scripps Institution of Oceanography, San Diego, CA (in press).
- [5] H. W. Sorenson, *Parameter Estimation*. New York: Marcel Dekker, 1980.
- [6] A. Gelb (Ed.), *Applied Optimal Estimation*, Mass.: MIT Press, 1974.
- [7] R. G. Brown, *Introduction to Random Signal Analysis and Kalman Filtering*, New York: John Wiley & Sons, 1983.
- [8] H. W. Sorenson, *Kalman Filtering: Theory and Application*. New York: IEEE Press, 1985.
- [9] W. S. Hodgkiss, "Kalman filter, phase locked loops, and optimal (MAP) demodulation," Naval Undersea Center (NUC), San Diego, CA, NUC TN-1772, 1977.
- [10] J. V. Candy, *Signal Processing: The Modern Approach*, New York: McGraw-Hill, 1988.
- [11] W. S. Hodgkiss and V. C. Anderson, "Acoustic positioning for an array of freely drifting sensors," *IEEE J. Oceanic Eng.*, vol. OE-8, pp. 116-119, 1983.
- [12] R. L. Culver, G. L. D'Spain, W. S. Hodgkiss, and G. L. Edmonds, "Estimating 8 kHz pulse travel times and travel time errors from Swallow float localization system measurements" Marine Physical Laboratory, Scripps Institution of Oceanography, San Diego, CA (in press).
- [13] J. Churgin and S. J. Halminski, Temperature, Salinity, Oxygen, and Phosphate in Waters off the United States, Eastern North Pacific, National Oceanographic Data Center, 3, (1974).
- [14] R. M. Olivera, "Downslope Conversion Experiment: Environmental Data Report", MPL TM-414 Marine Physical Laboratory, Scripps Institution of Oceanography, San Diego, CA, 1990.
- [15] K. V. Mackenzie, "Nine-term equation for sound speed in the oceans" *J. Acoust. Soc. Am.*, 70 (3), 1981.
- [16] Y. Bar-Shalom and T. E. Fortman, *Tracking and Data Association*, Florida: Academic Press, 1988.

Appendix 1 - Harmonic Mean Sound Speed Estimates

Harmonic Mean Sound Speed Estimates		
Floats	Sound Speed, m/msec	Error Variance, (m/msec) ²
9 & 10	1.5237	0.1 × 10 ⁻⁶
9 & 11	1.5237	0.1 × 10 ⁻⁶
9 & 0	1.4975	0.1 × 10 ⁻⁶
9 & 1	1.4999	0.1 × 10 ⁻⁶
9 & 2	1.5024	0.1 × 10 ⁻⁶
9 & 3	1.5043	0.1 × 10 ⁻⁶
9 & 4	1.5075	0.1 × 10 ⁻⁶
9 & 5	1.5108	0.1 × 10 ⁻⁶
9 & 6	1.5143	0.1 × 10 ⁻⁶
9 & 7	1.5178	0.1 × 10 ⁻⁶
9 & 8	1.5213	0.1 × 10 ⁻⁶
10 & 11	1.5237	0.1 × 10 ⁻⁶
10 & 0	1.4975	0.1 × 10 ⁻⁶
10 & 1	1.4999	0.1 × 10 ⁻⁶
10 & 2	1.5024	0.1 × 10 ⁻⁶
10 & 3	1.5043	0.1 × 10 ⁻⁶
10 & 4	1.5075	0.1 × 10 ⁻⁶
10 & 5	1.5108	0.1 × 10 ⁻⁶
10 & 6	1.5143	0.1 × 10 ⁻⁶
10 & 7	1.5178	0.1 × 10 ⁻⁶
10 & 8	1.5213	0.1 × 10 ⁻⁶
11 & 0	1.4975	0.1 × 10 ⁻⁶
11 & 1	1.4999	0.1 × 10 ⁻⁶
11 & 2	1.5024	0.1 × 10 ⁻⁶
11 & 3	1.5043	0.1 × 10 ⁻⁶
11 & 4	1.5075	0.1 × 10 ⁻⁶
11 & 5	1.5108	0.1 × 10 ⁻⁶
11 & 6	1.5143	0.1 × 10 ⁻⁶
11 & 7	1.5178	0.1 × 10 ⁻⁶
11 & 8	1.5213	0.1 × 10 ⁻⁶
0 & 1	1.4809	0.1 × 10 ⁻⁶
0 & 2	1.4820	0.1 × 10 ⁻⁶
0 & 3	1.4830	0.1 × 10 ⁻⁶
0 & 4	1.4849	0.1 × 10 ⁻⁶
0 & 5	1.4872	0.1 × 10 ⁻⁶
0 & 6	1.4897	0.1 × 10 ⁻⁶
0 & 7	1.4926	0.1 × 10 ⁻⁶
0 & 8	1.4955	0.1 × 10 ⁻⁶

Harmonic Mean Sound Speed Estimates		
Floats	Sound Speed, m/msec	Error Variance, (m/msec) ²
1 & 2	1.4832	0.1×10^{-6}
1 & 3	1.4844	0.1×10^{-6}
1 & 4	1.4865	0.1×10^{-6}
1 & 5	1.4890	0.1×10^{-6}
1 & 6	1.4917	0.1×10^{-6}
1 & 7	1.4948	0.1×10^{-6}
1 & 8	1.4978	0.1×10^{-6}
2 & 3	1.4860	0.1×10^{-6}
2 & 4	1.4883	0.1×10^{-6}
2 & 5	1.4909	0.1×10^{-6}
2 & 6	1.4939	0.1×10^{-6}
2 & 7	1.4970	0.1×10^{-6}
2 & 8	1.5002	0.1×10^{-6}
3 & 4	1.4898	0.1×10^{-6}
3 & 5	1.4926	0.1×10^{-6}
3 & 6	1.4957	0.1×10^{-6}
3 & 7	1.4989	0.1×10^{-6}
3 & 8	1.5022	0.1×10^{-6}
4 & 5	1.4954	0.1×10^{-6}
4 & 6	1.4986	0.1×10^{-6}
4 & 7	1.5020	0.1×10^{-6}
4 & 8	1.5053	0.1×10^{-6}
5 & 6	1.5018	0.1×10^{-6}
5 & 7	1.5052	0.1×10^{-6}
5 & 8	1.5086	0.1×10^{-6}
6 & 7	1.5086	0.1×10^{-6}
6 & 8	1.5120	0.1×10^{-6}
7 & 8	1.5155	0.1×10^{-6}
9 & 9	0.7478	0.1×10^{-6}
10 & 10	0.7478	0.1×10^{-6}
11 & 11	0.7478	0.1×10^{-6}
0 & 0	0.7423	0.1×10^{-6}
1 & 1	0.7415	0.1×10^{-6}
2 & 2	0.7415	0.1×10^{-6}
3 & 3	0.7418	0.1×10^{-6}
4 & 4	0.7424	0.1×10^{-6}
5 & 5	0.7433	0.1×10^{-6}
6 & 6	0.7443	0.1×10^{-6}
7 & 7	0.7456	0.1×10^{-6}
8 & 8	0.7469	0.1×10^{-6}

Appendix 2 - Reciprocal Path Travel Time Variances

Variances of Reciprocal Path Travel Time Measurement Differences Minus a Second Order Fit, July 1989 Experiment	
Floats	Variance, msec ²
9 & 0	2.5637
9 & 1	0.8505
9 & 2	1.0208
9 & 3	1.9094
9 & 4	0.6386
9 & 5	0.1996
9 & 6	0.3951
9 & 7	0.8572
9 & 8	0.6349
10 & 0	0.9729
10 & 1	0.8914
10 & 2	0.7811
10 & 3	0.9248
10 & 4	0.5736
10 & 5	0.2852
10 & 6	1.7845
10 & 7	0.7622
10 & 8	0.8752
11 & 0	1.5452
11 & 1	1.4314
11 & 2	0.8876
11 & 3	1.6525
11 & 4	0.5814
11 & 5	0.2615
11 & 6	1.1790
11 & 7	0.8512
11 & 8	0.3782
0 & 1	1.2800
0 & 2	1.8693
0 & 3	2.1737
0 & 4	3.8525
0 & 5	1.0472
0 & 6	2.5033
0 & 7	1.9553
0 & 8	2.0692

Variances of Reciprocal Path Travel Time Measurement Differences Minus a Second Order Fit, July 1989 Experiment	
Floats	Variance, msec ²
1 & 2	1.4894
1 & 3	2.7448
1 & 4	2.1325
1 & 5	0.4147
1 & 6	2.4348
1 & 7	1.5548
1 & 8	1.0353
2 & 3	0.9688
2 & 4	0.8213
2 & 5	1.5815
2 & 6	1.4629
2 & 7	1.3690
2 & 8	1.5648
3 & 4	0.3759
3 & 5	0.7077
3 & 6	2.2006
3 & 7	0.8939
3 & 8	2.3961
4 & 5	0.4745
4 & 6	0.3362
4 & 7	1.1722
4 & 8	2.3950
5 & 6	0.4461
5 & 7	0.5171
5 & 8	0.2398
6 & 7	0.9575
6 & 8	0.7759
7 & 8	0.8713

Pulse Leading Edges. Float 0 listening to itself, July 1989

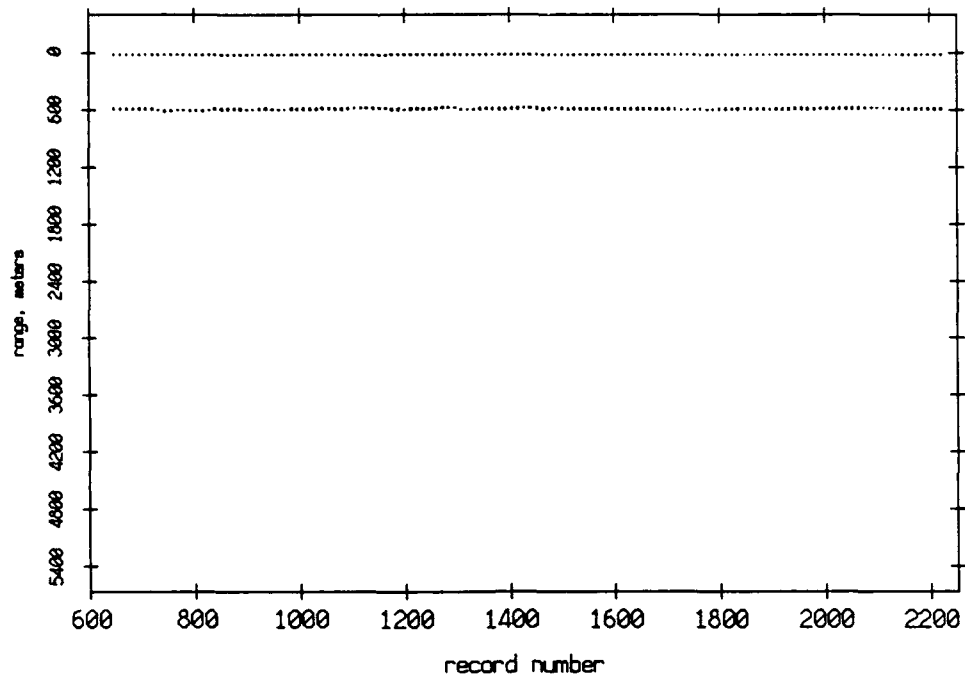


Figure 3.1

Pulse Leading Edges. Float 1 listening to itself, July 1989

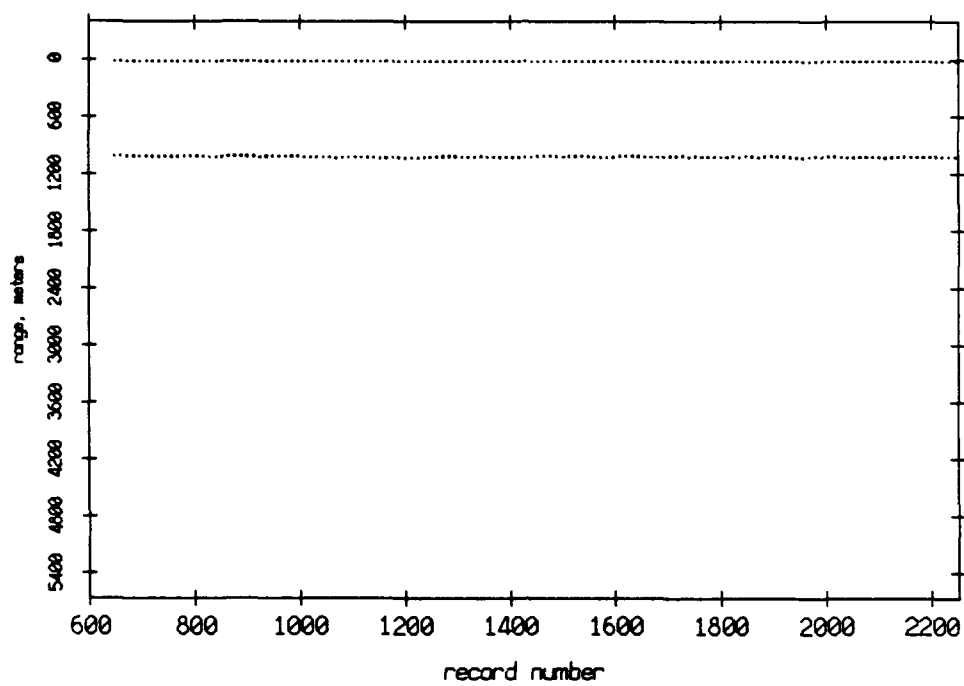


Figure 3.2

Pulse Leading Edges. Float 2 listening to itself, July 1989

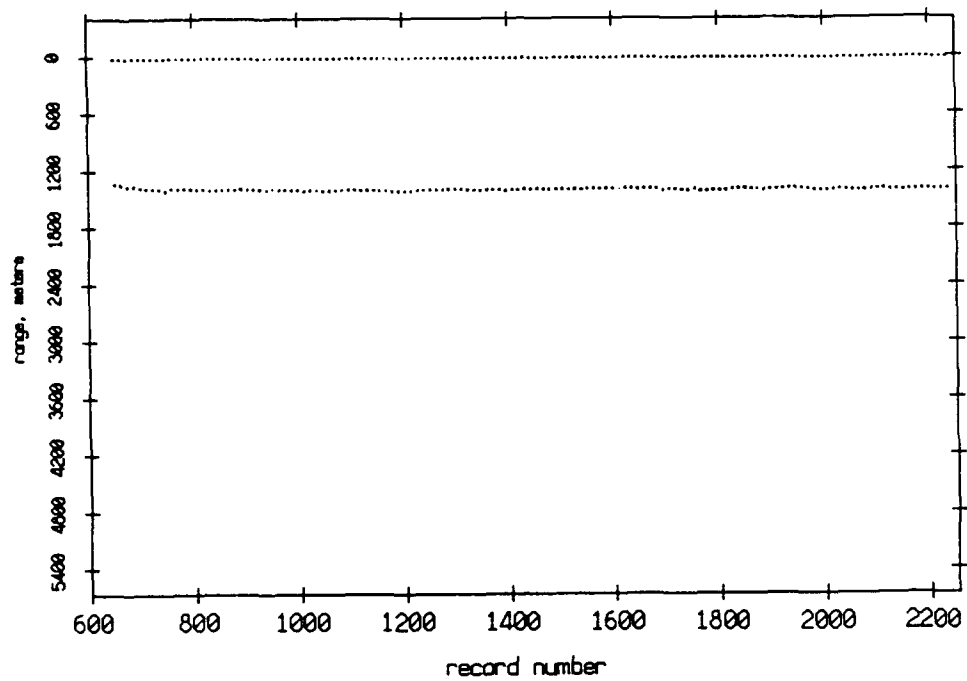


Figure 3.3

Pulse Leading Edges. Float 3 listening to itself, July 1989

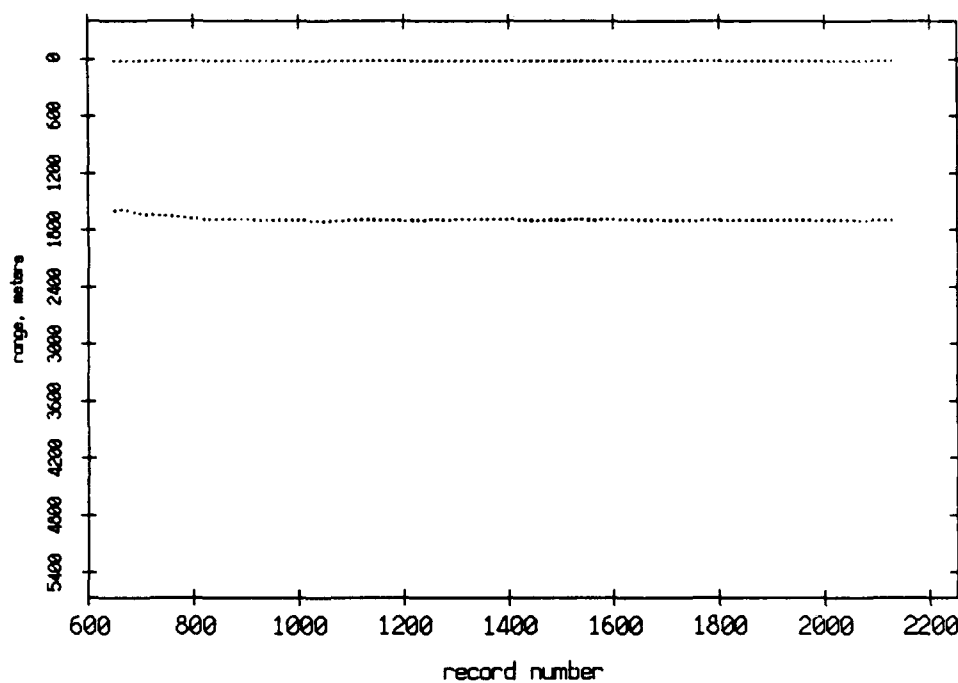


Figure 3.4

Pulse Leading Edges. Float 4 listening to itself, July 1989

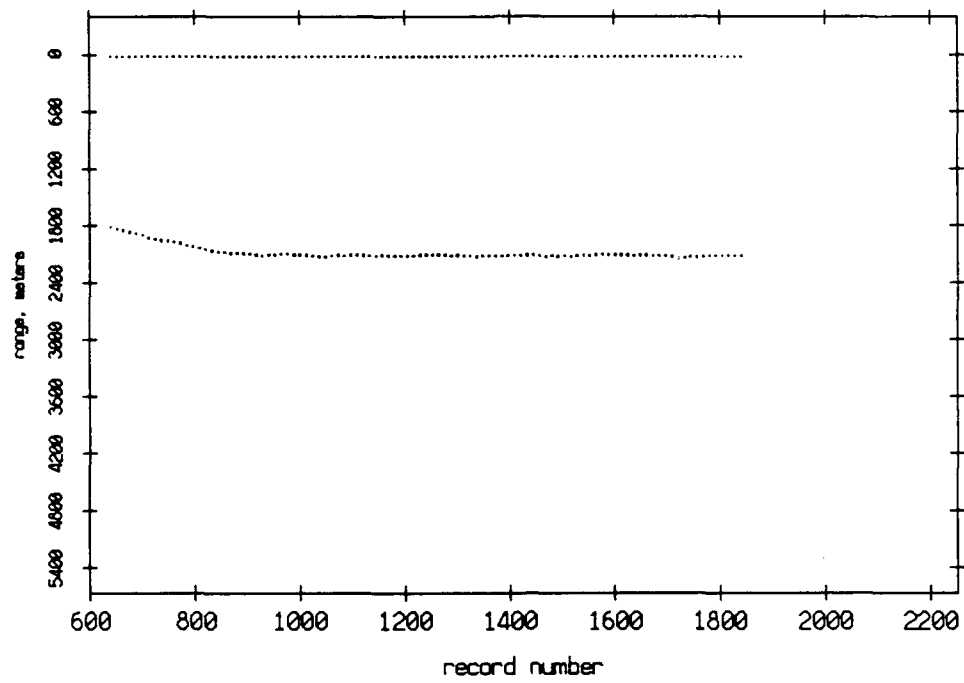


Figure 3.5

Pulse Leading Edges. Float 5 listening to itself, July 1989

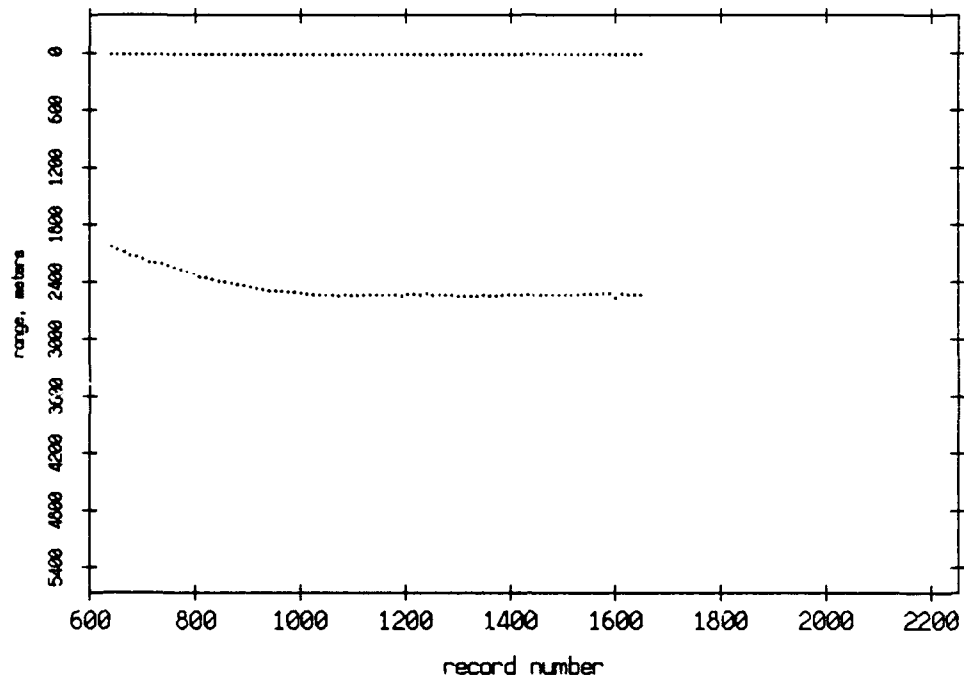


Figure 3.6

Pulse Leading Edges. Float 6 listening to itself, July 1989

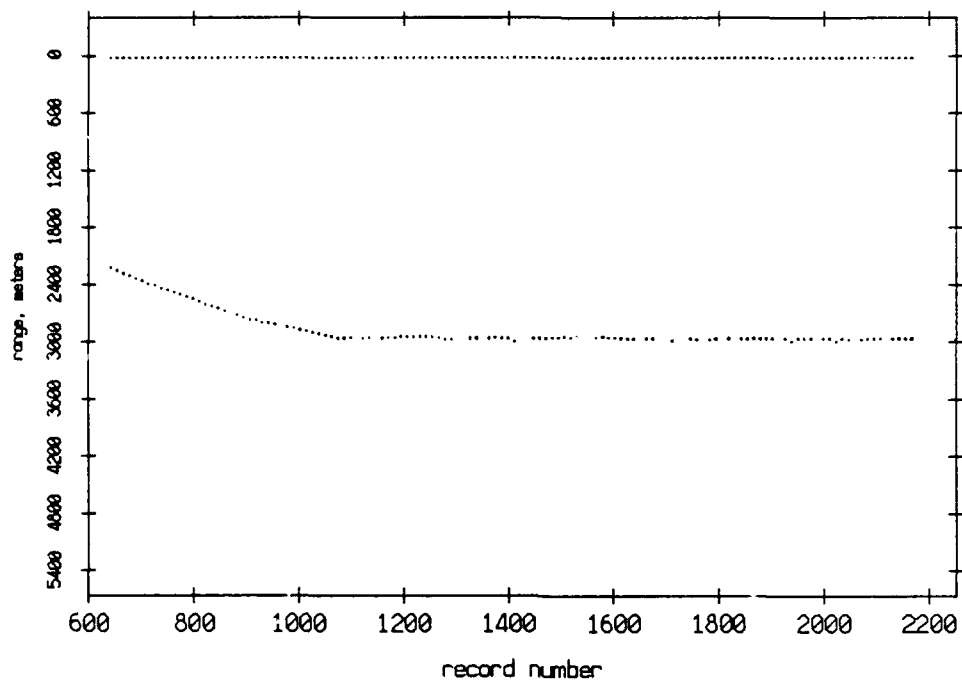


Figure 3.7

Pulse Leading Edges. Float 7 listening to itself, July 1989

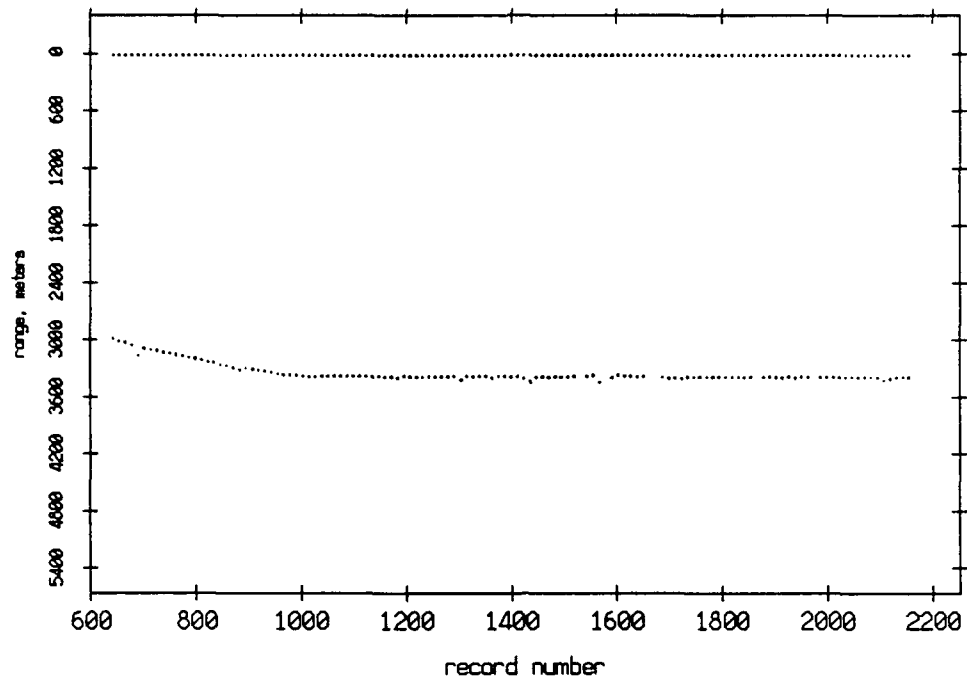


Figure 3.8

Pulse Leading Edges. Float 8 listening to itself, July 1989

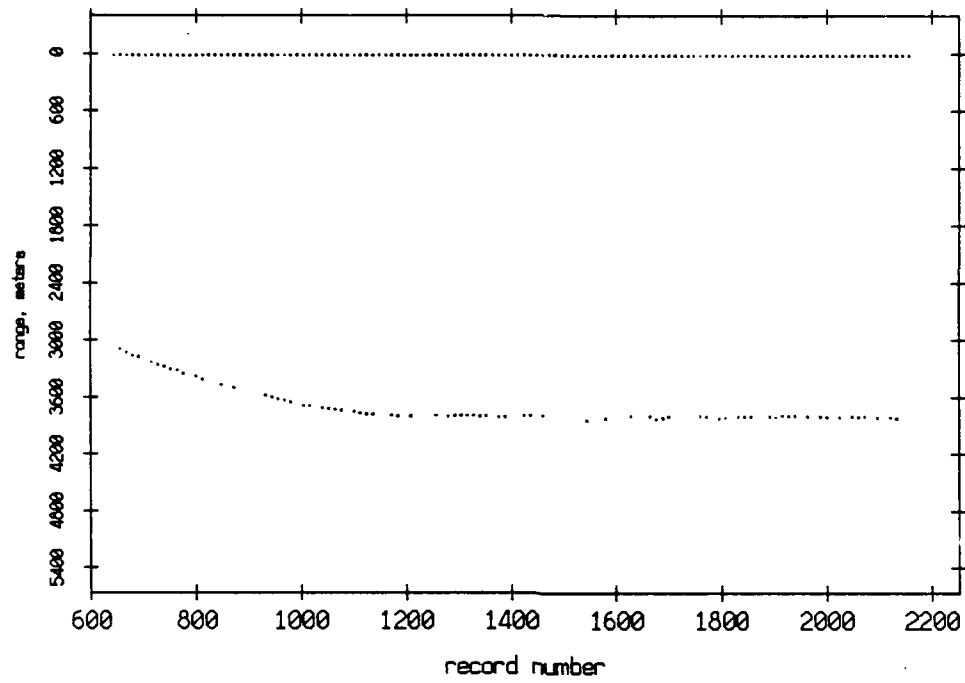


Figure 3.9

Pulse Leading Edges. Float 9 listening to itself, July 1989

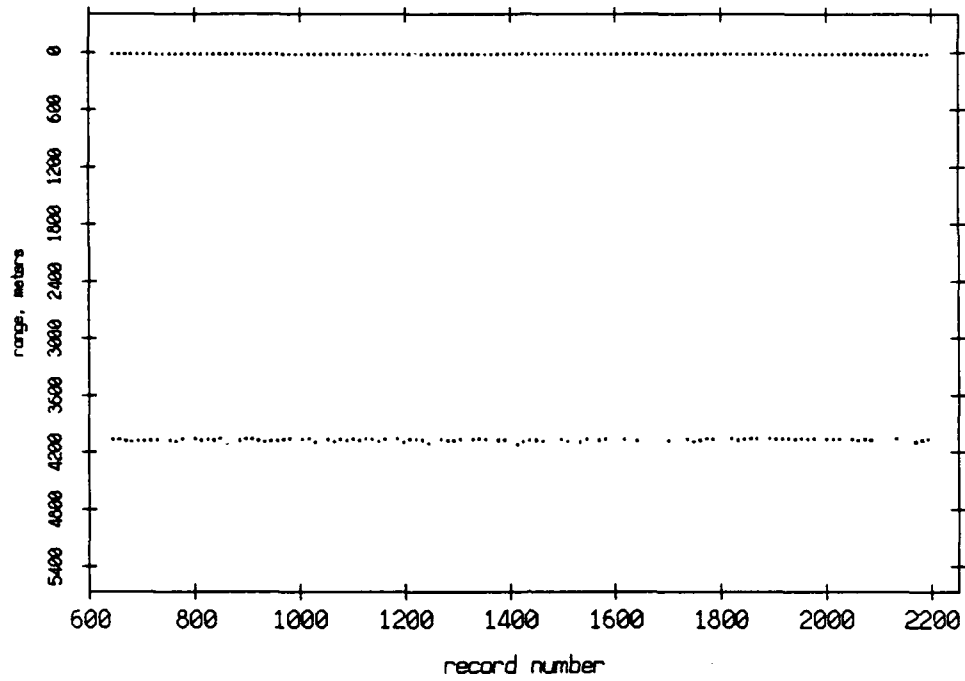


Figure 3.10

Pulse Leading Edges. Float 10 listening to itself, July 1989

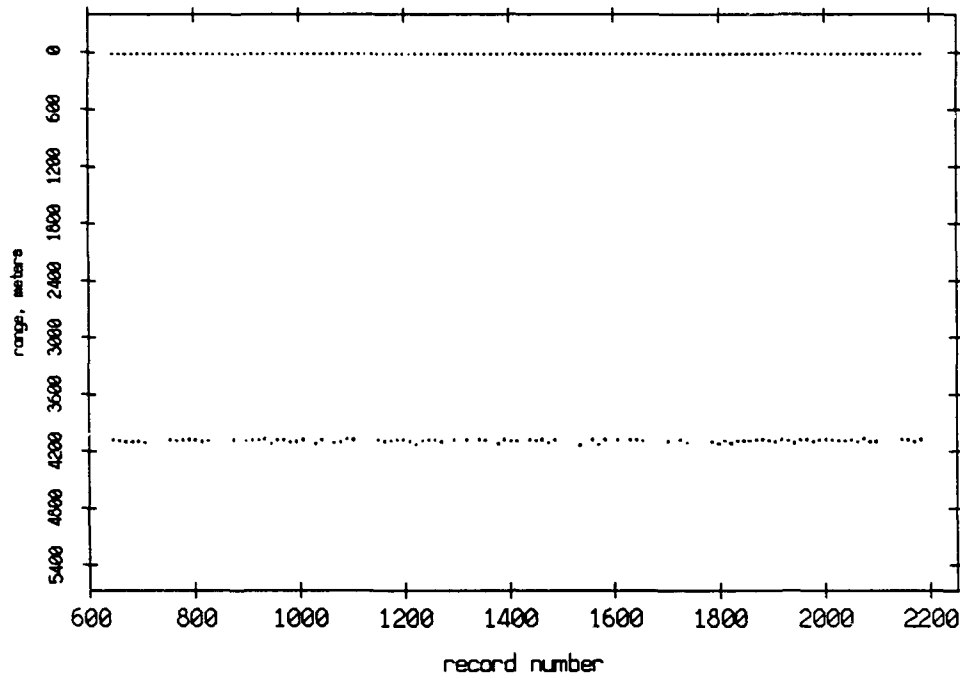


Figure 3.11

Pulse Leading Edges. Float 11 listening to itself, July 1989

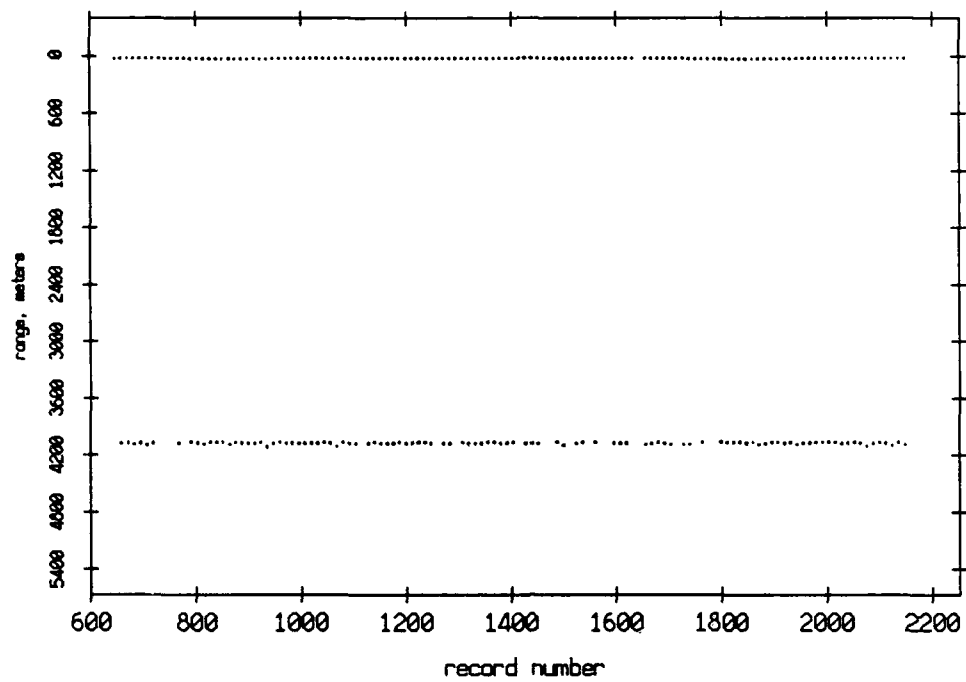
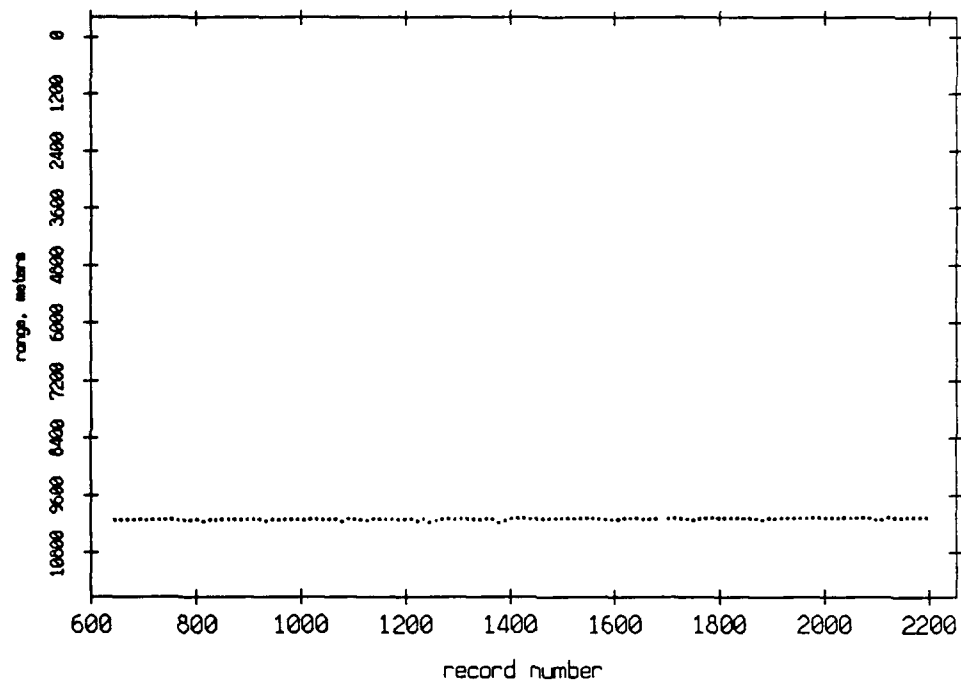


Figure 3.12

Pulse Leading Edges. Float 9 listening to Float 10, July 1989



Pulse Leading Edges. Float 10 listening to Float 9, July 1989

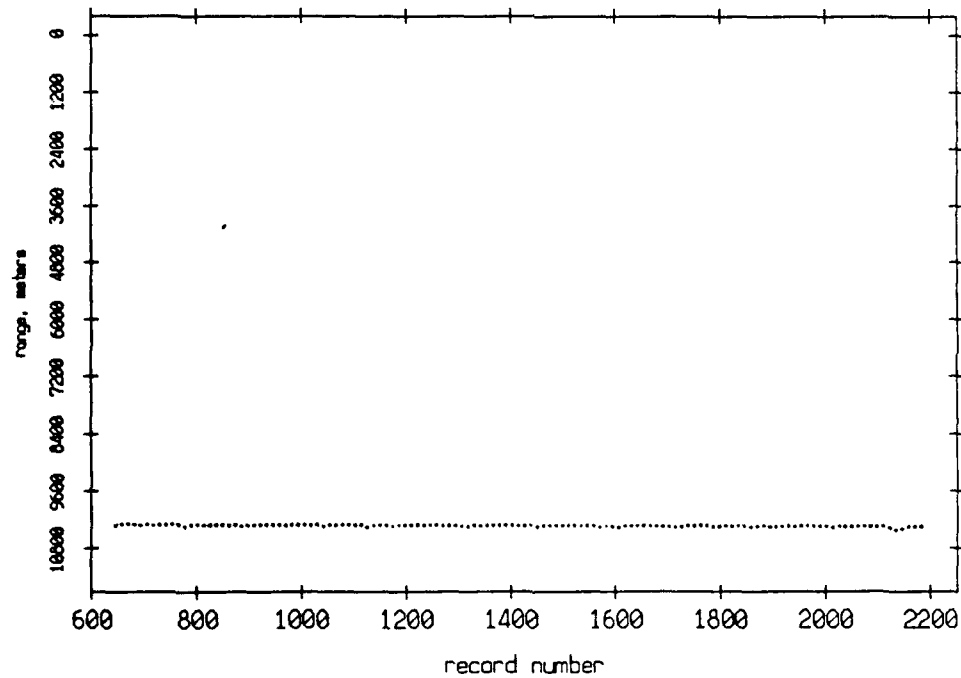
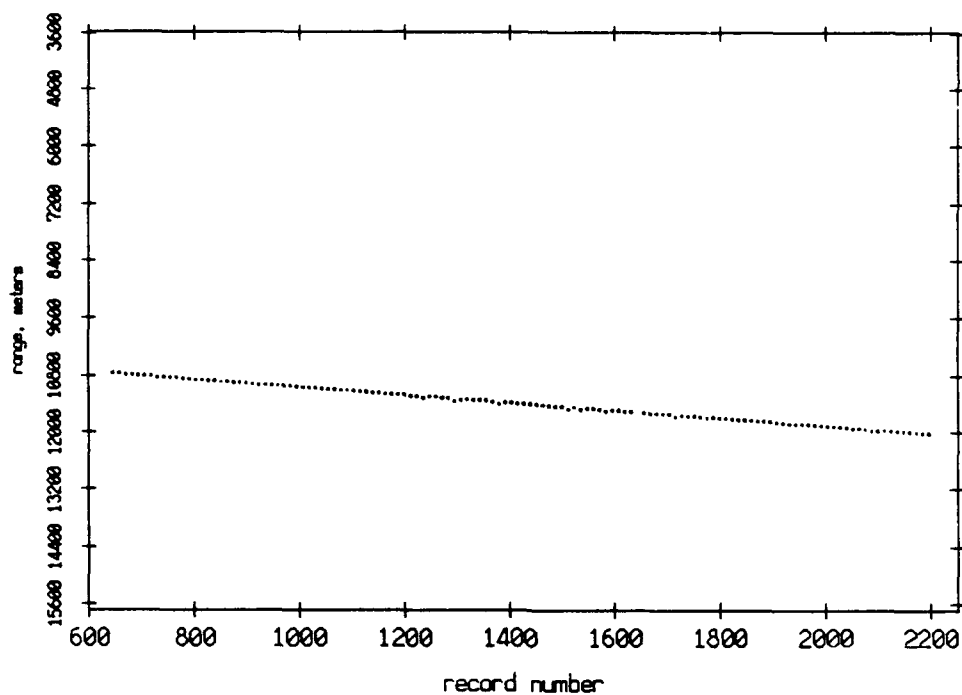


Figure 3.13

Pulse Leading Edges. Float 9 listening to Float 11, July 1989



Pulse Leading Edges. Float 11 listening to Float 9, July 1989

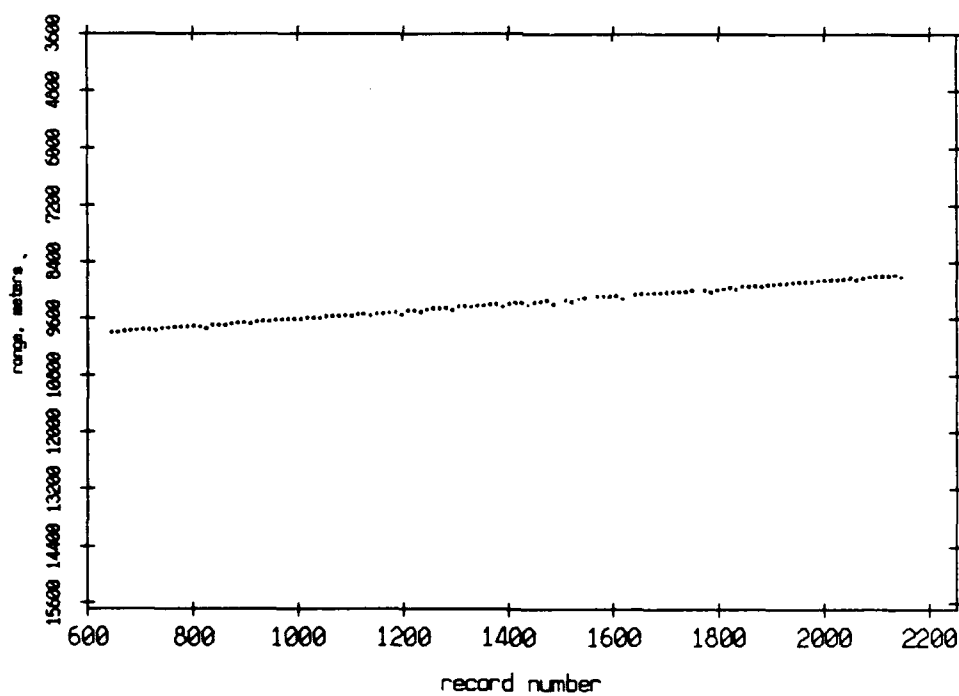
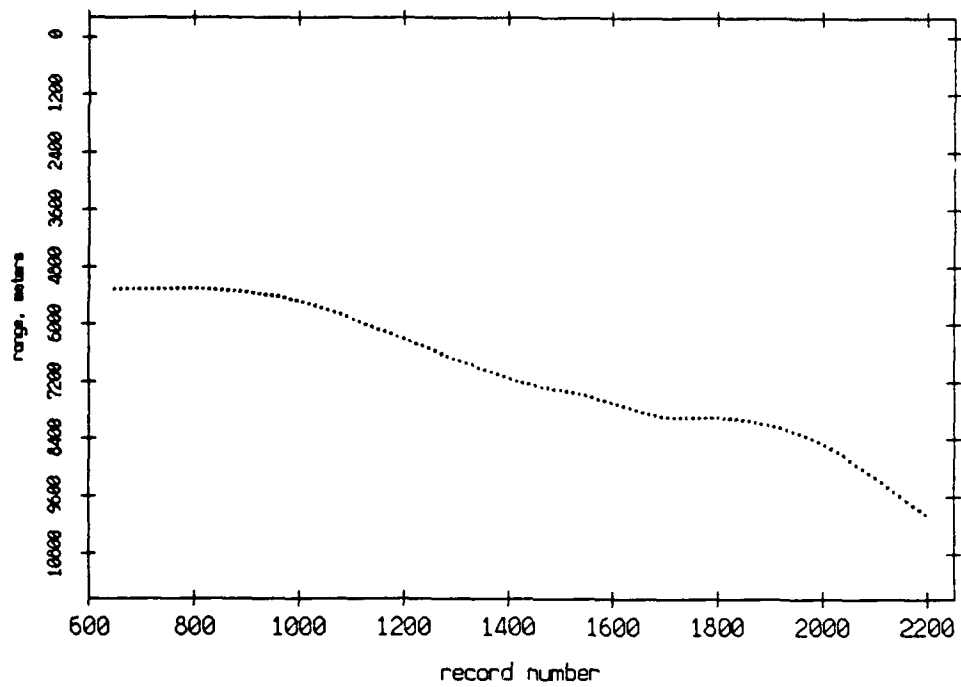


Figure 3.14

Pulse Leading Edges. Float 9 listening to Float 0, July 1989



Pulse Leading Edges. Float 0 listening to Float 9, July 1989

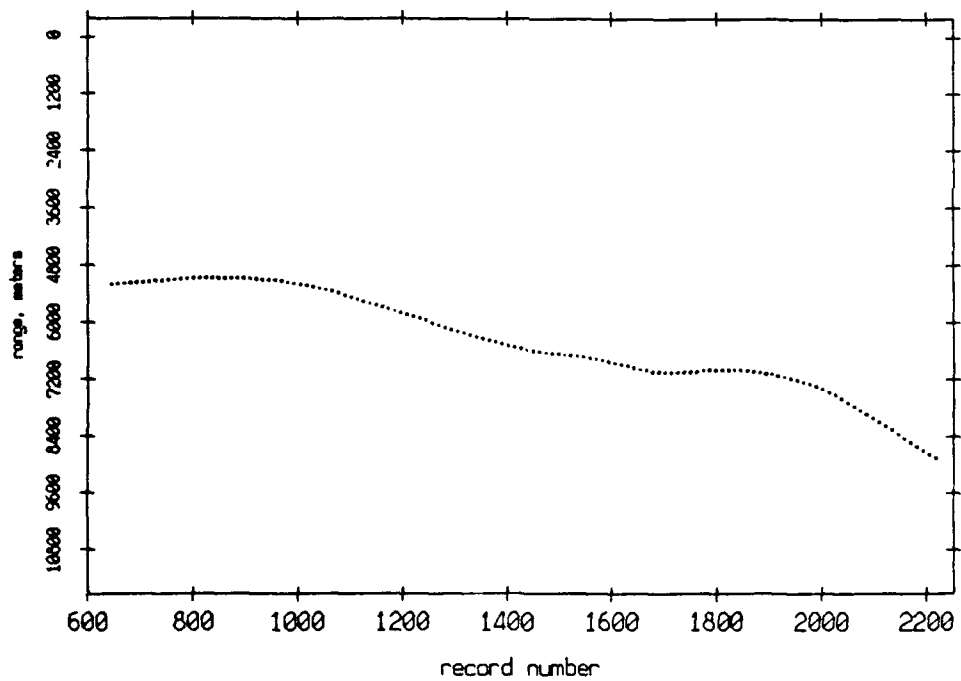
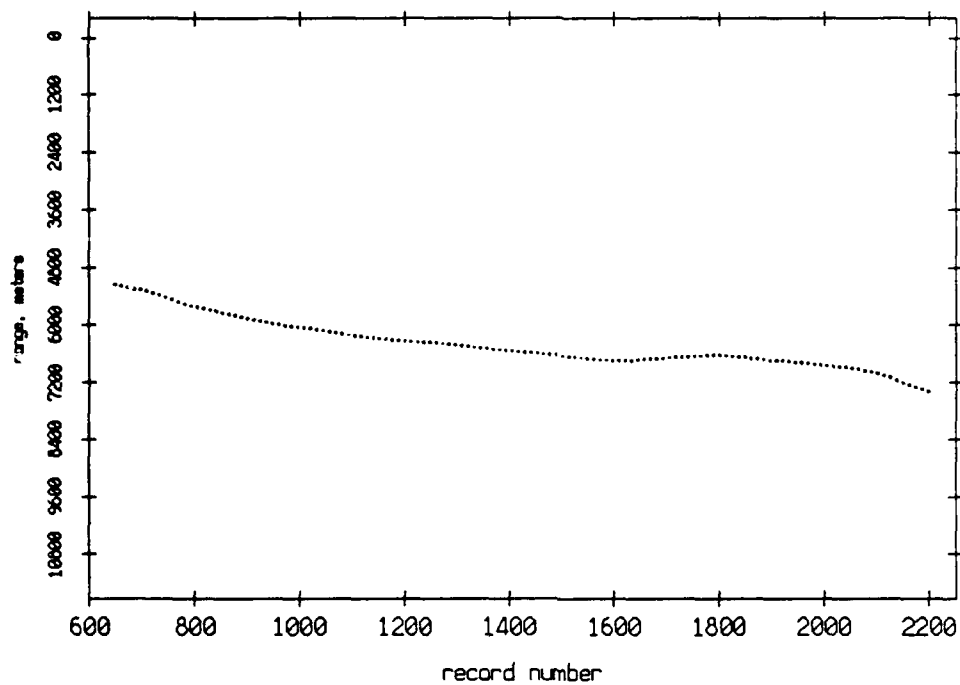


Figure 3.15

Pulse Leading Edges. Float 9 listening to Float 1, July 1989



Pulse Leading Edges. Float 1 listening to Float 9, July 1989

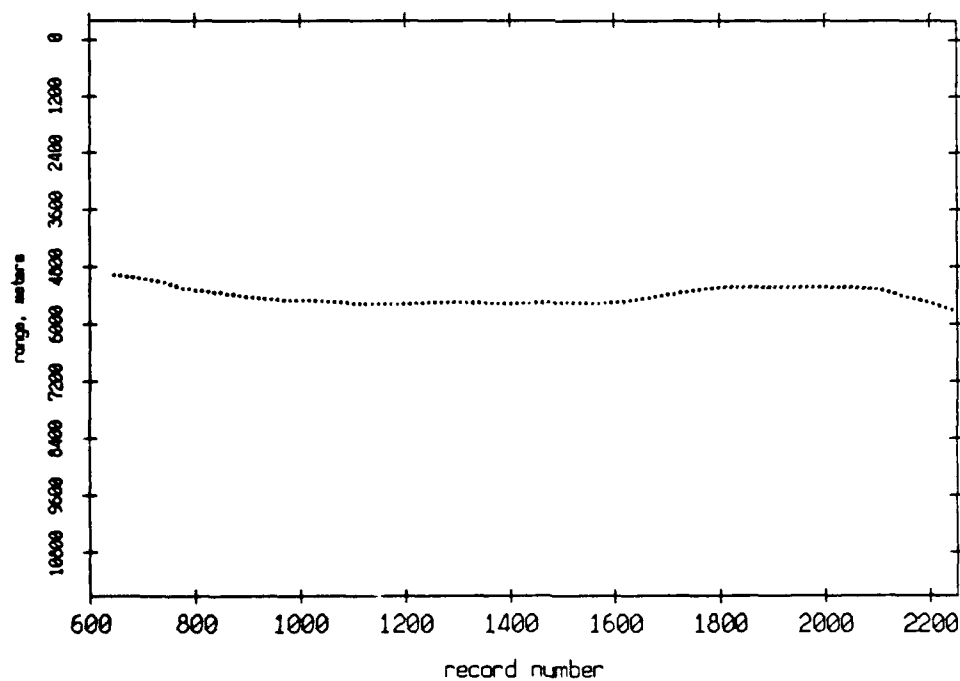
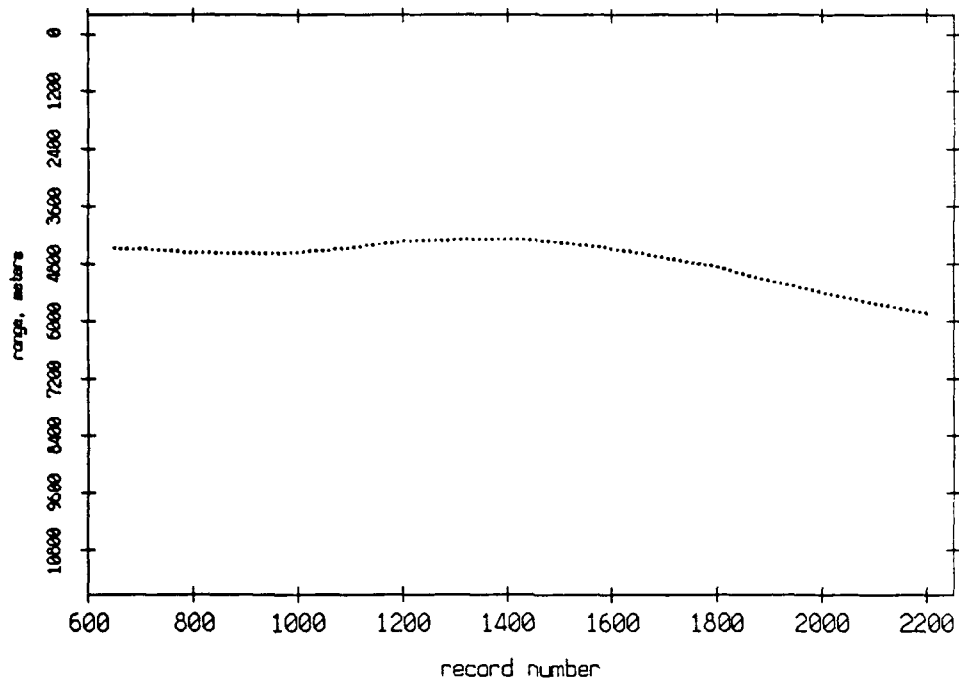


Figure 3.16

Pulse Leading Edges. Float 9 listening to Float 2, July 1989



Pulse Leading Edges. Float 2 listening to Float 9, July 1989

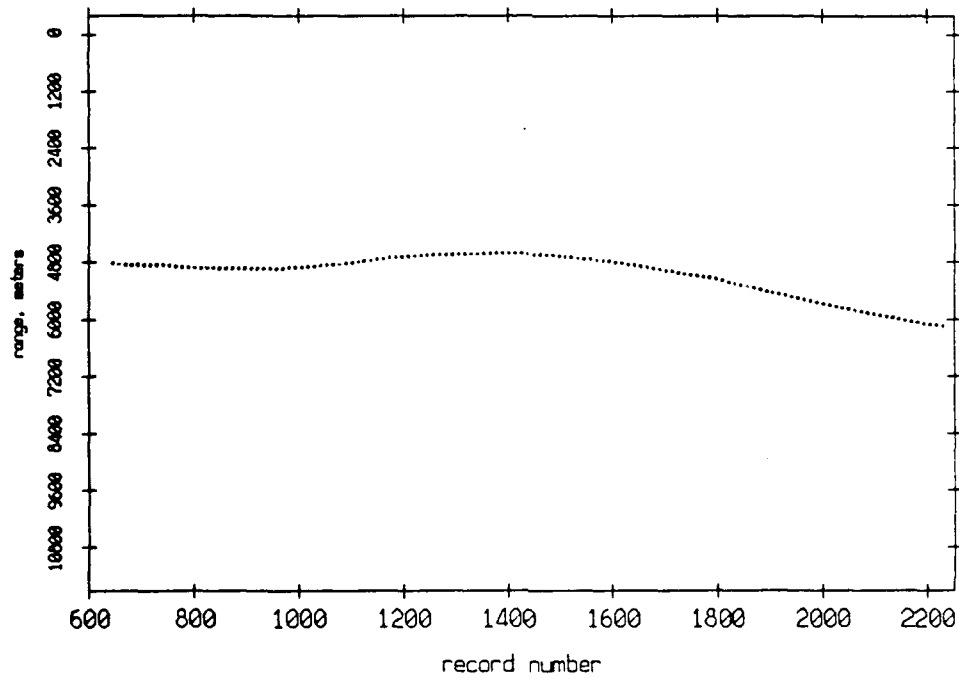
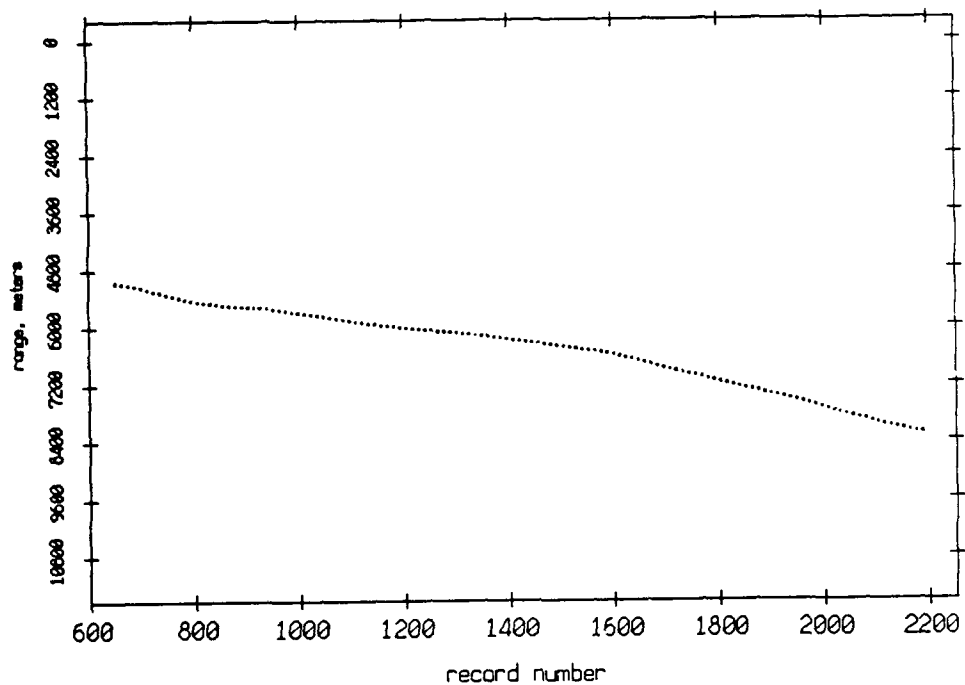


Figure 3.17

Pulse Leading Edges. Float 9 listening to Float 3, July 1989



Pulse Leading Edges. Float 3 listening to Float 9, July 1989

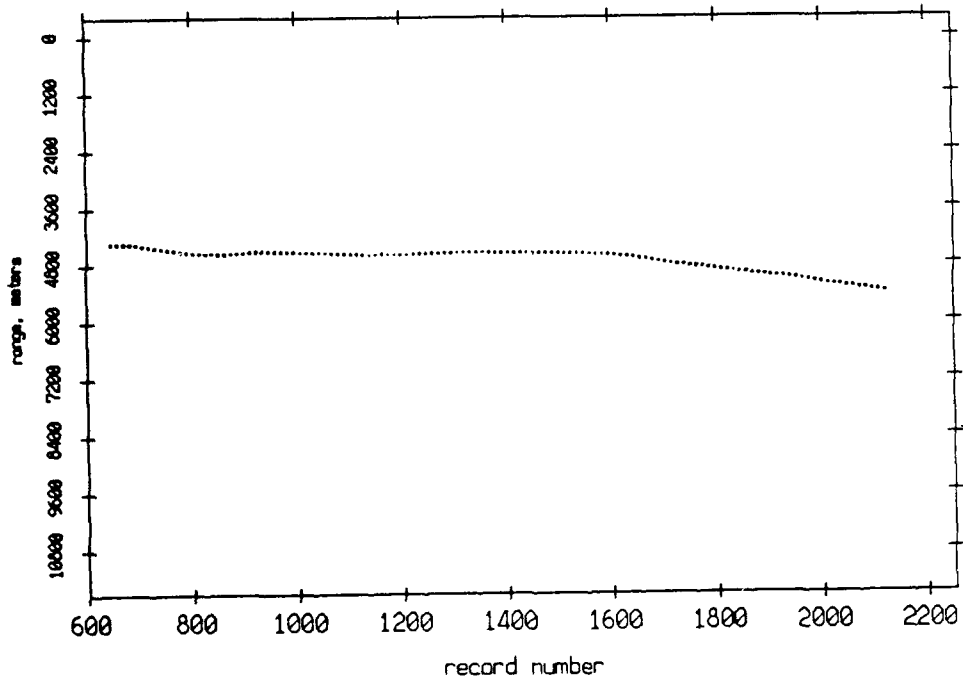
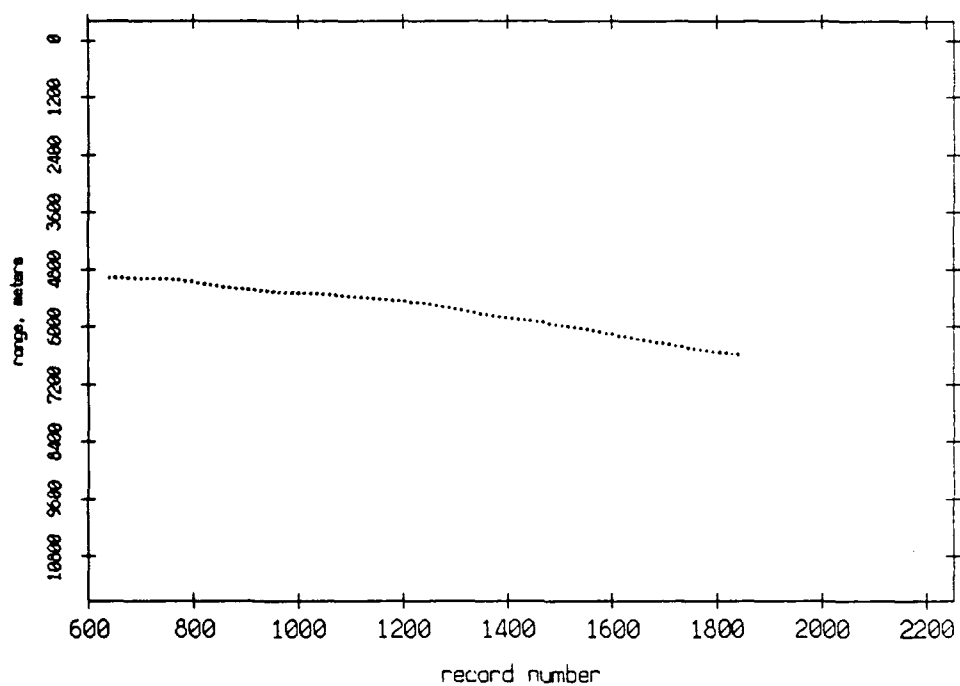


Figure 3.18

Pulse Leading Edges. Float 9 listening to Float 4, July 1989



Pulse Leading Edges. Float 4 listening to Float 9, July 1989

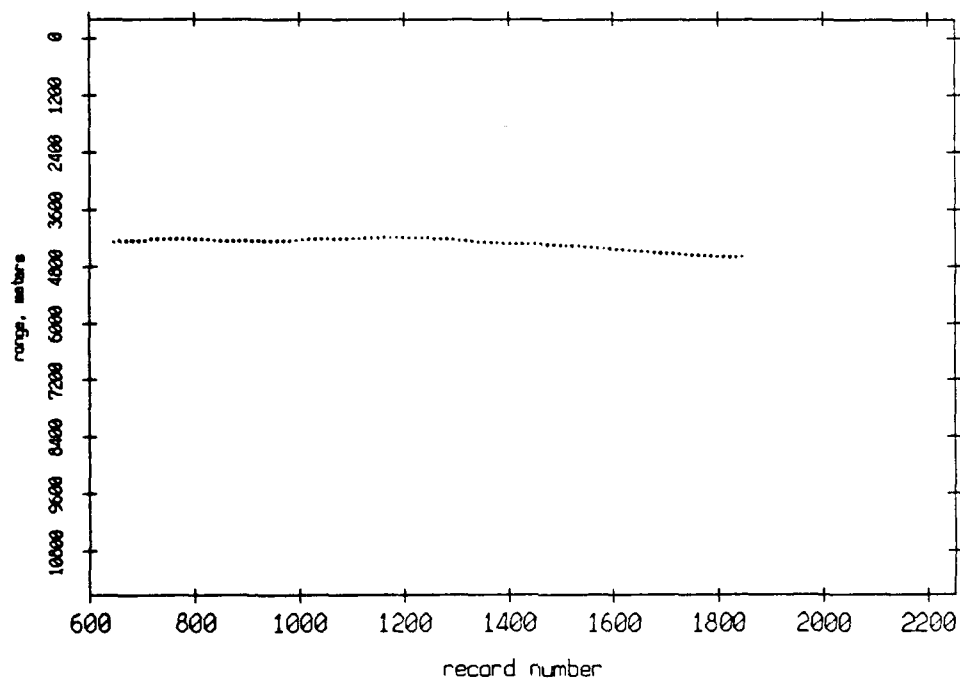
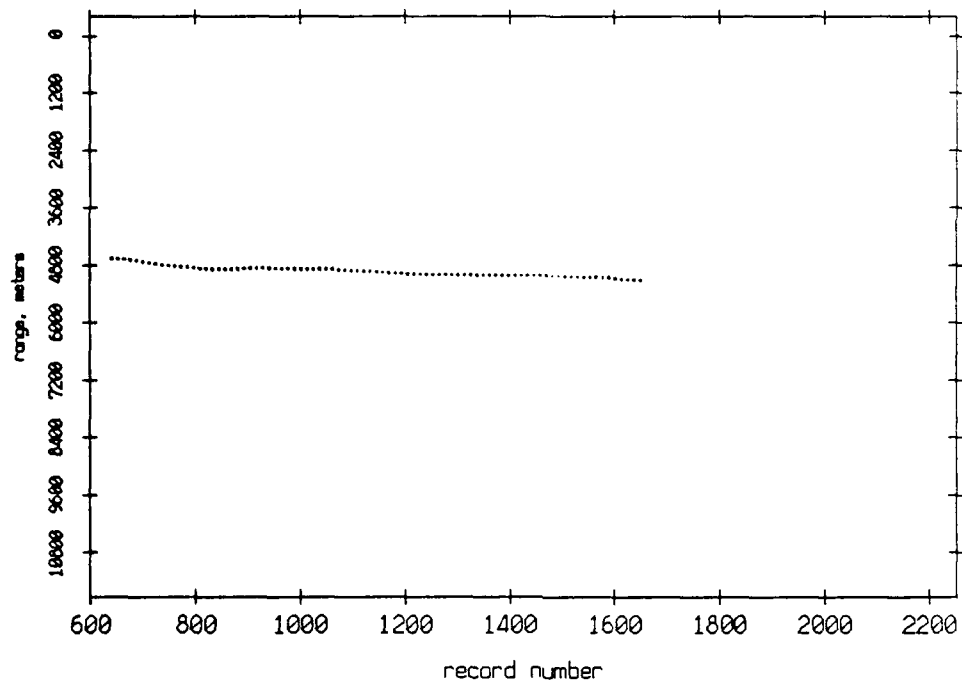


Figure 3.19

Pulse Leading Edges. Float 9 listening to Float 5, July 1989



Pulse Leading Edges. Float 5 listening to Float 9, July 1989

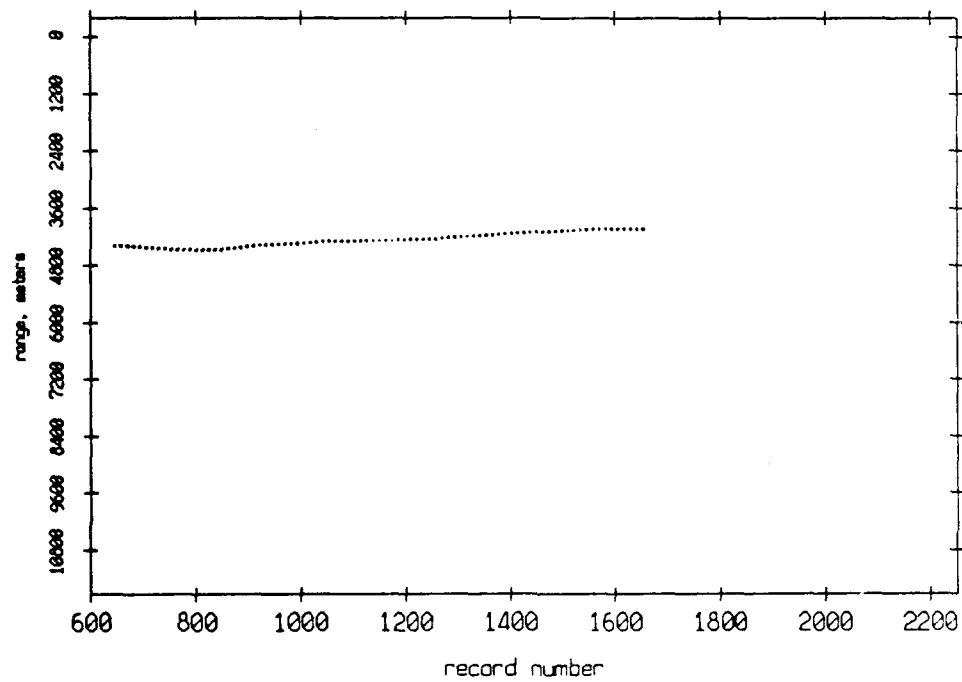
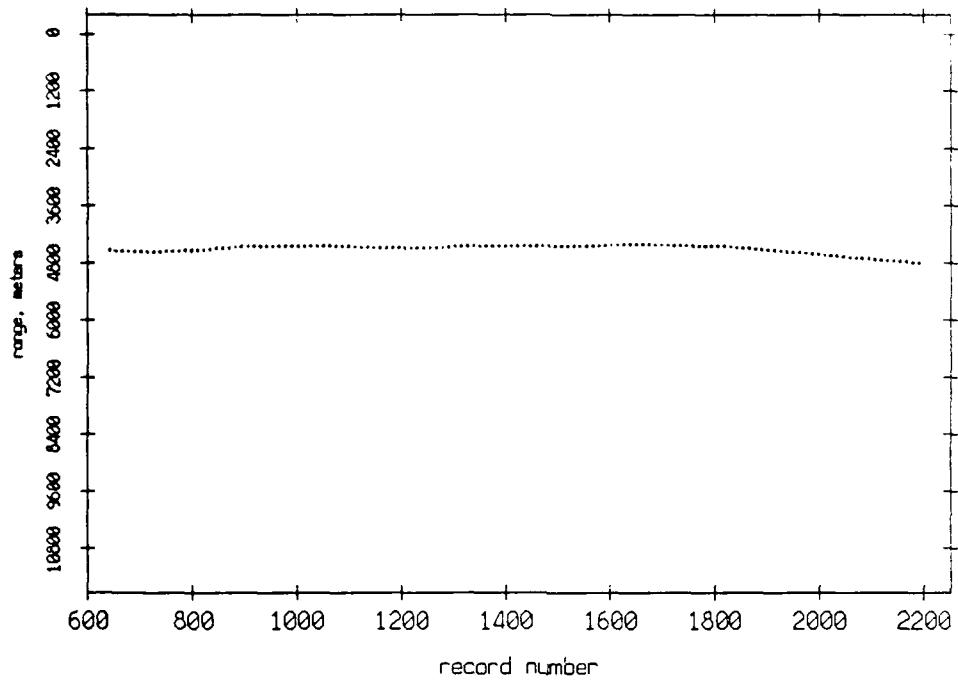


Figure 3.20

Pulse Leading Edges. Float 9 listening to Float 6, July 1989



Pulse Leading Edges. Float 6 listening to Float 9, July 1989

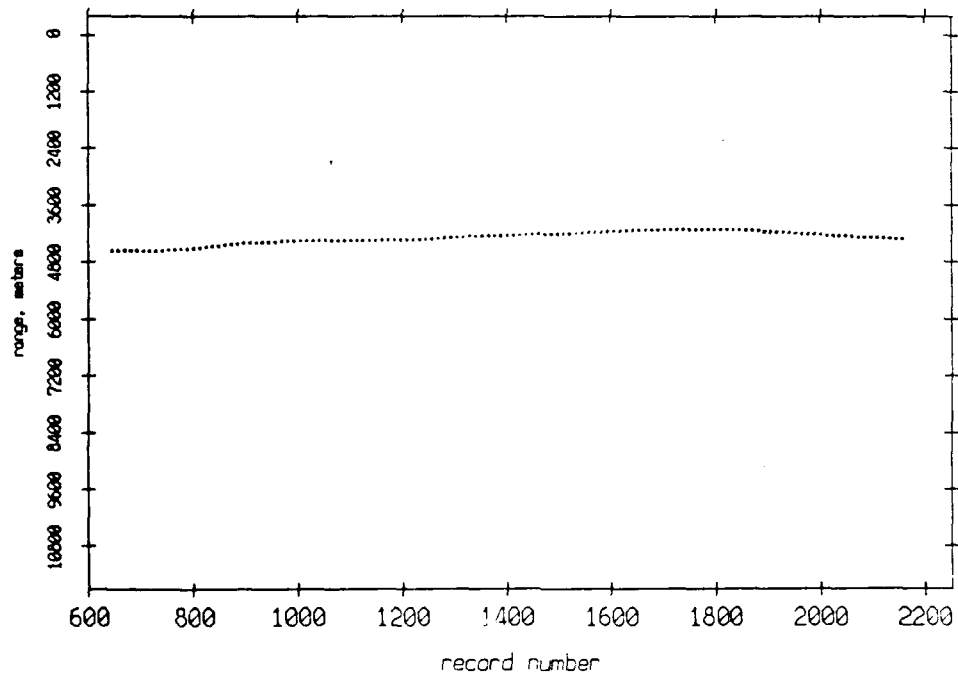
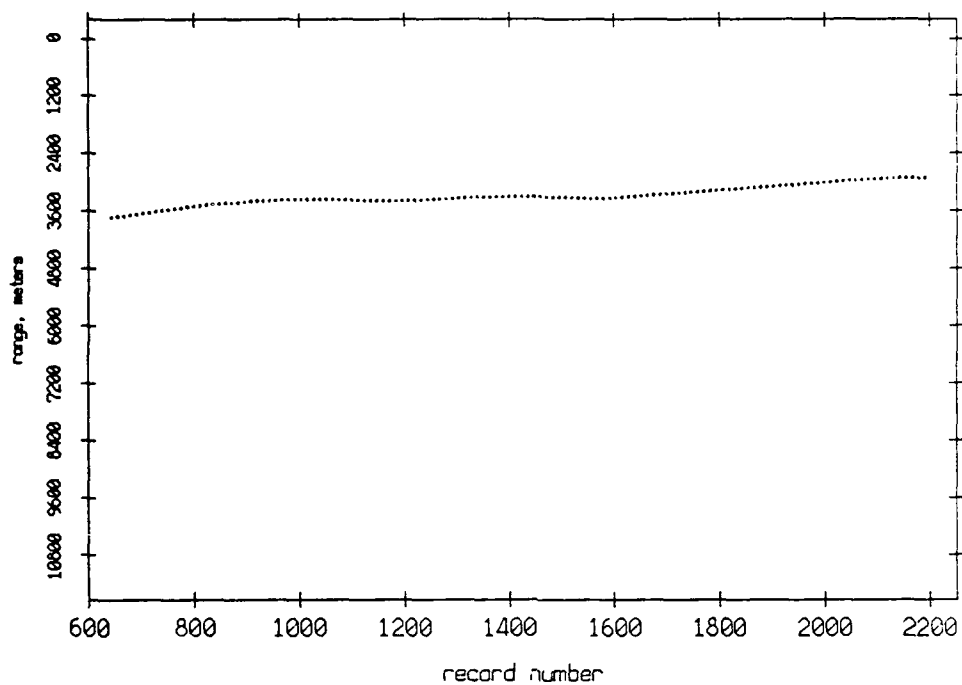


Figure 3.21

Pulse Leading Edges. Float 4 listening to Float 7, July 1989



Pulse Leading Edges. Float 7 listening to Float 9, July 1989

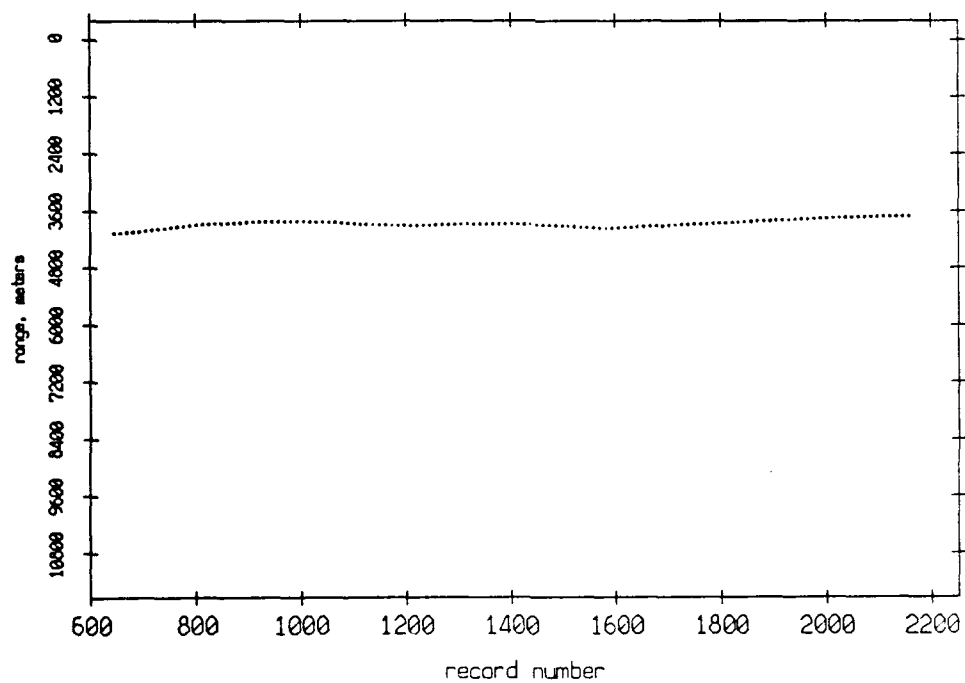
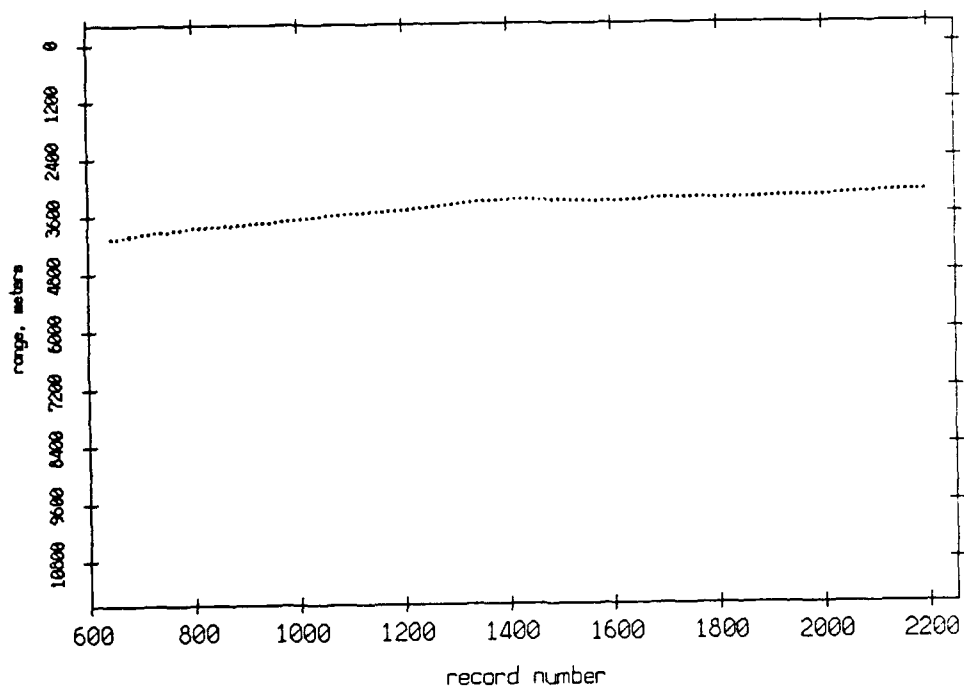


Figure 3.22

Pulse Leading Edges. Float 9 listening to Float 8, July 1989



Pulse Leading Edges. Float 8 listening to Float 9, July 1989

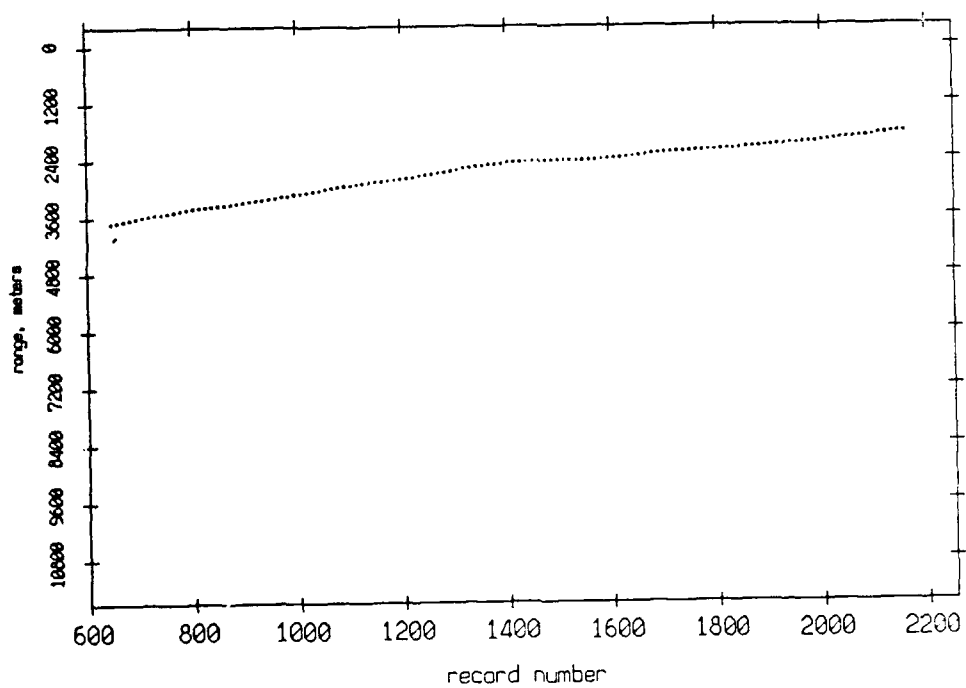
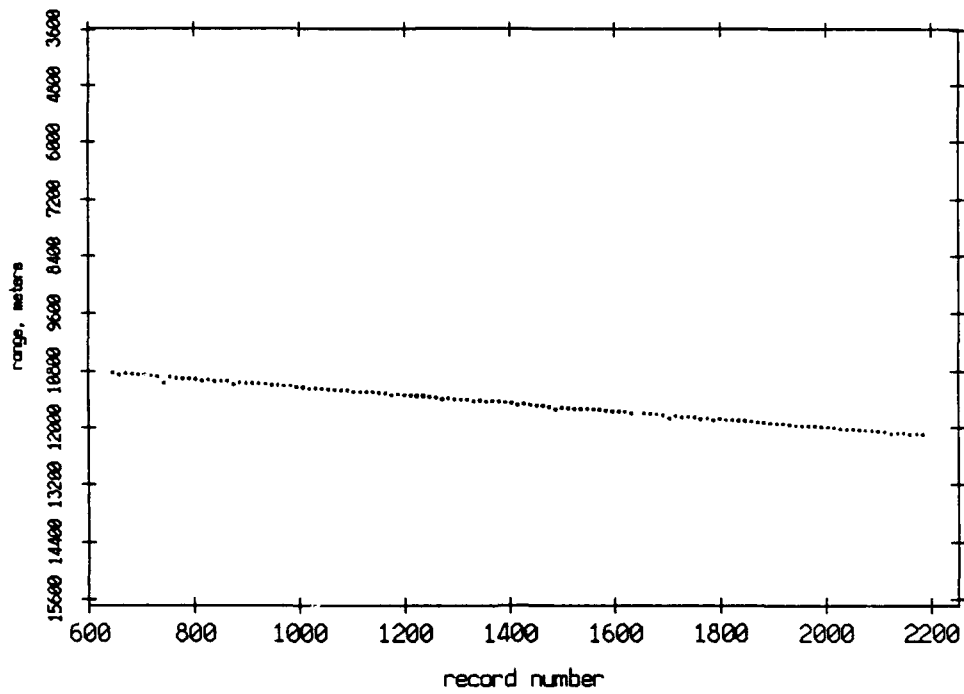


Figure 3.23

Pulse Leading Edges. Float 10 listening to Float 11, July 1989



Pulse Leading Edges. Float 11 listening to Float 10, July 1989

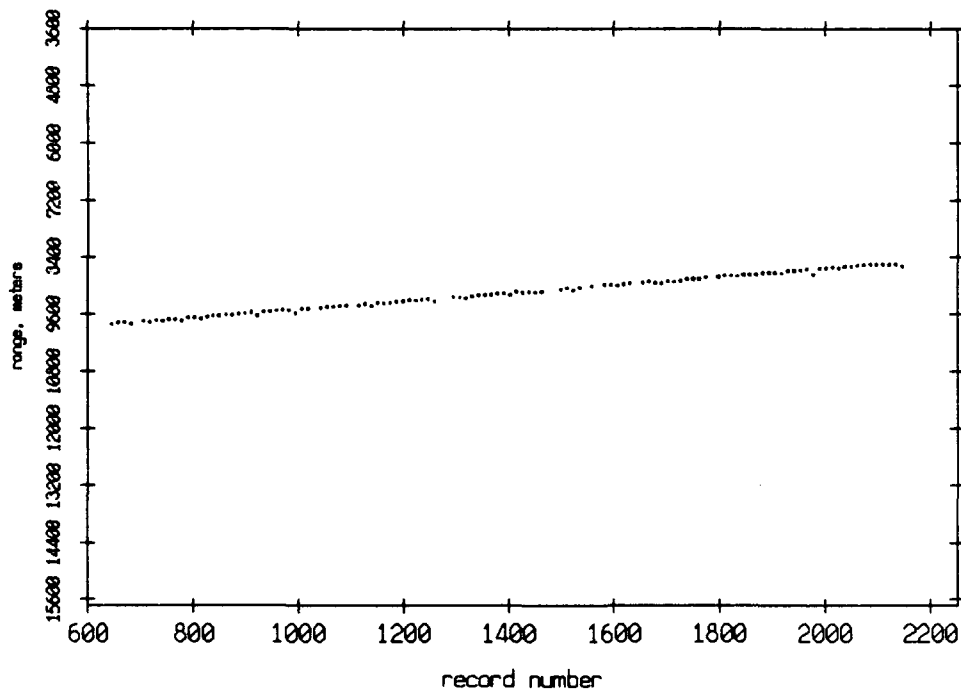
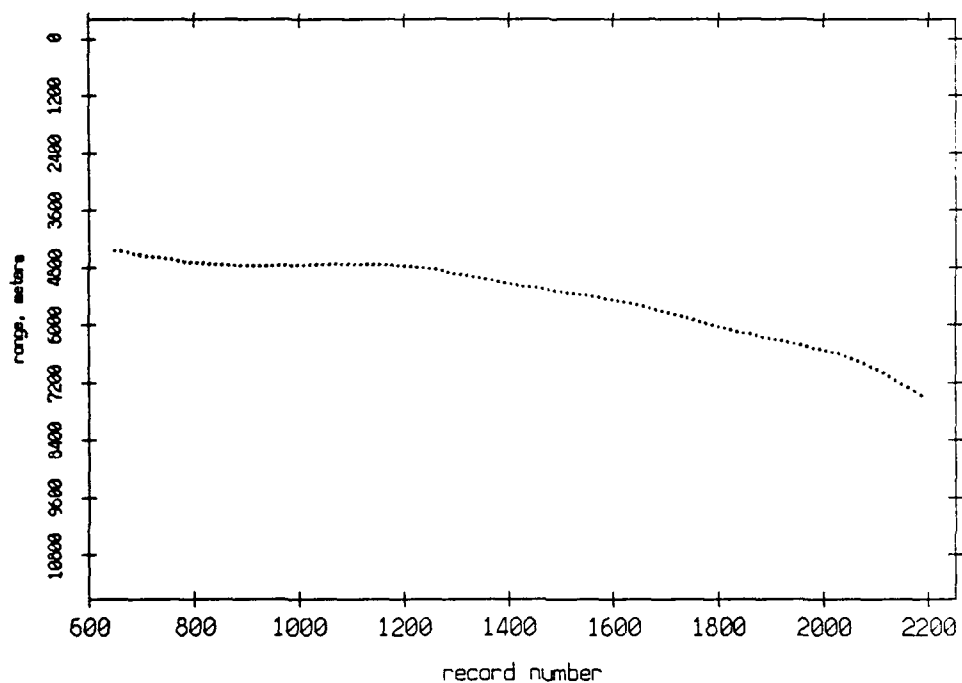


Figure 3.24

Pulse Leading Edges. Float 10 listening to Float 0, July 1989



Pulse Leading Edges. Float 0 listening to Float 10, July 1989

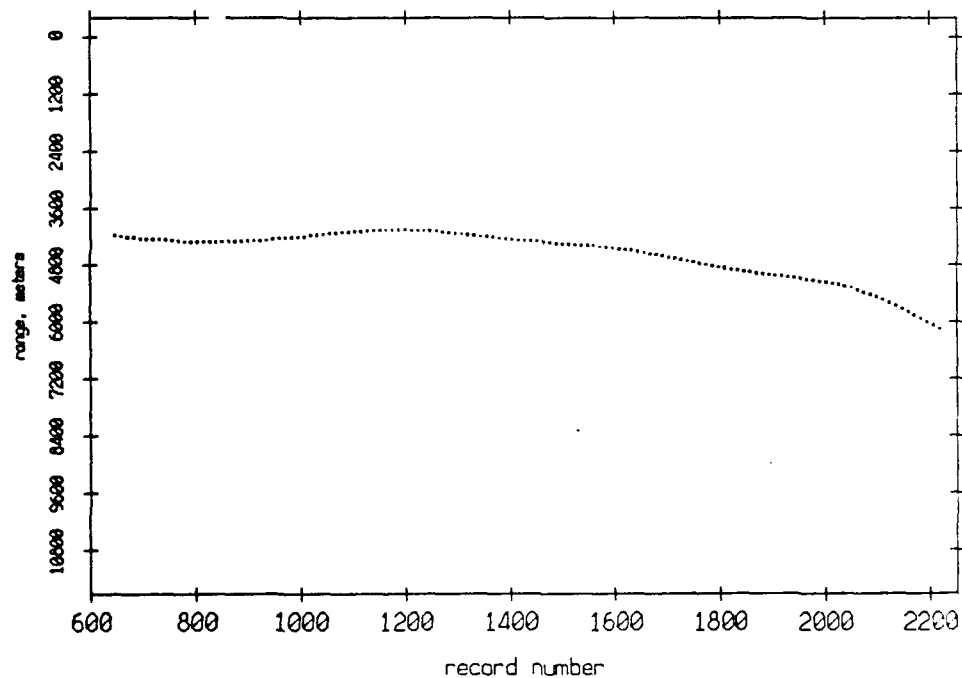
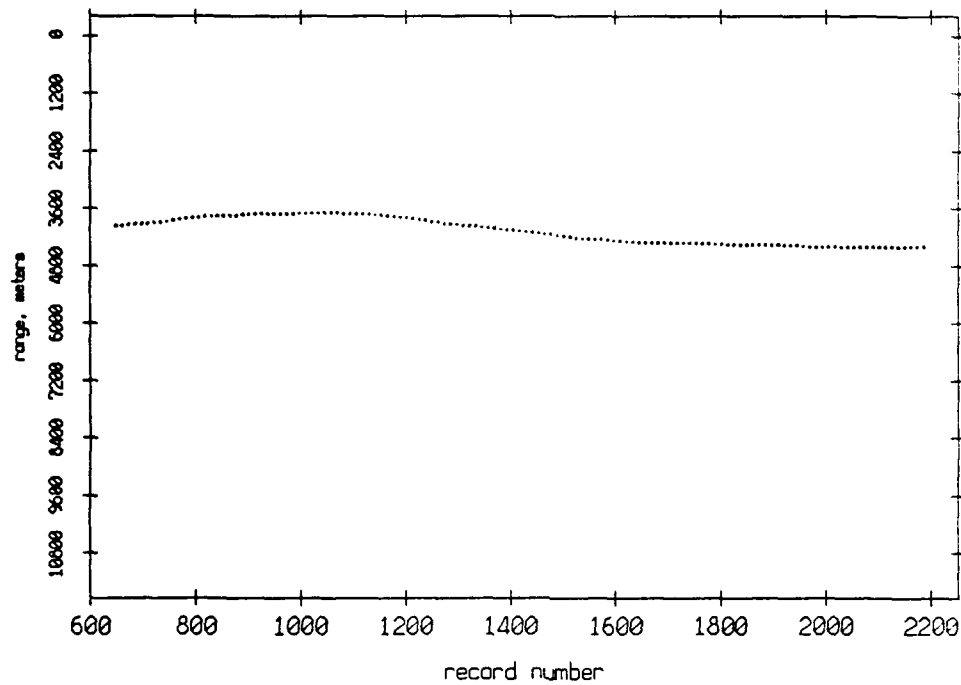


Figure 3.25

Pulse Leading Edges. Float 10 listening to Float 1, July 1989



Pulse Leading Edges. Float 1 listening to Float 10, July 1989

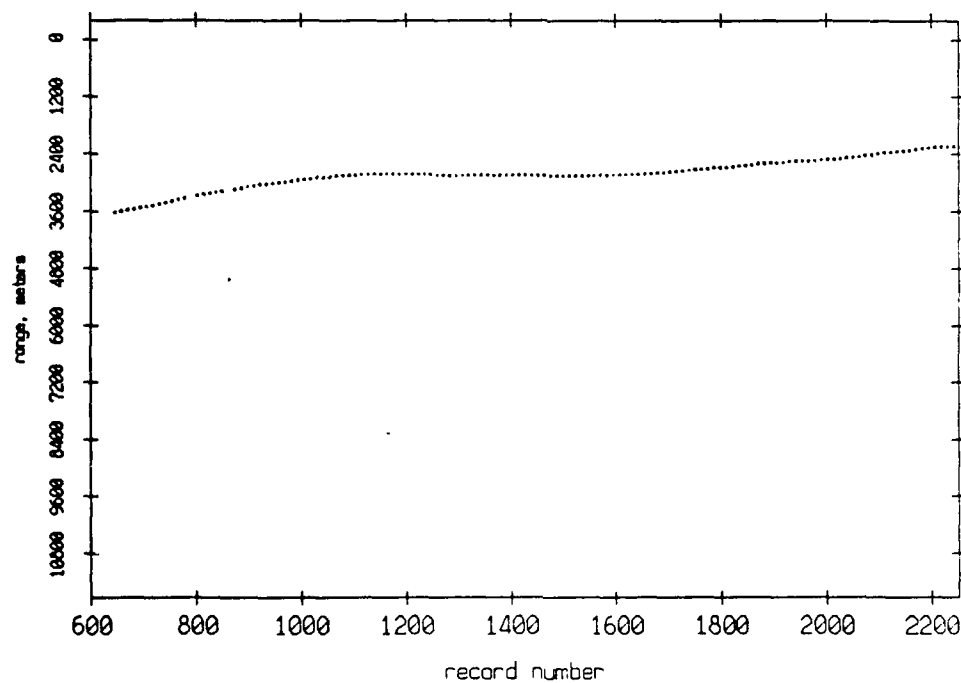
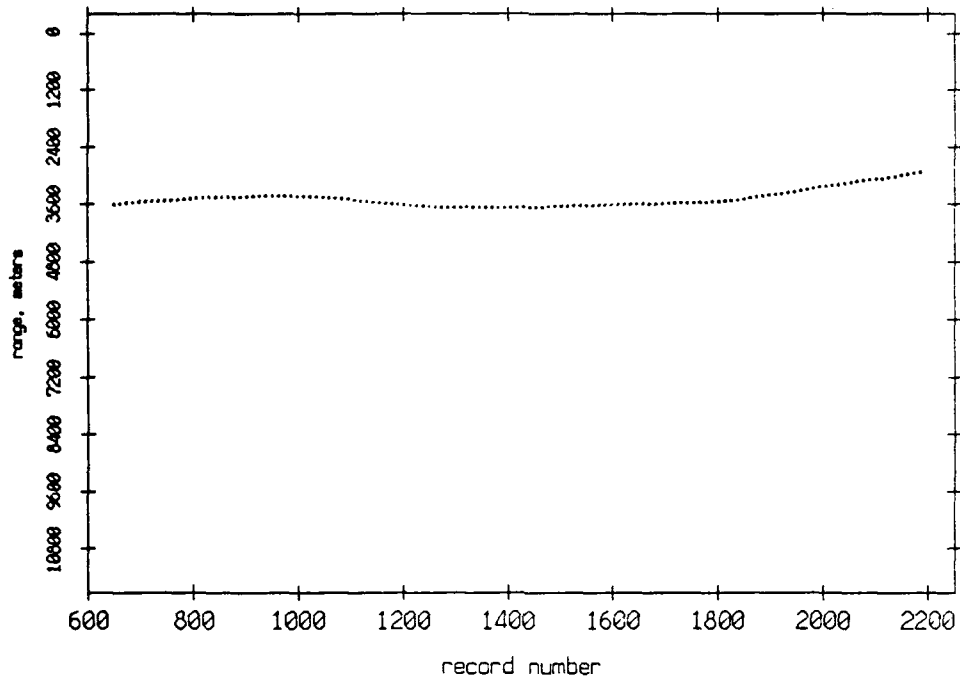


Figure 3.26

Pulse Leading Edges. Float 10 listening to Float 2, July 1989



Pulse Leading Edges. Float 2 listening to Float 10, July 1989

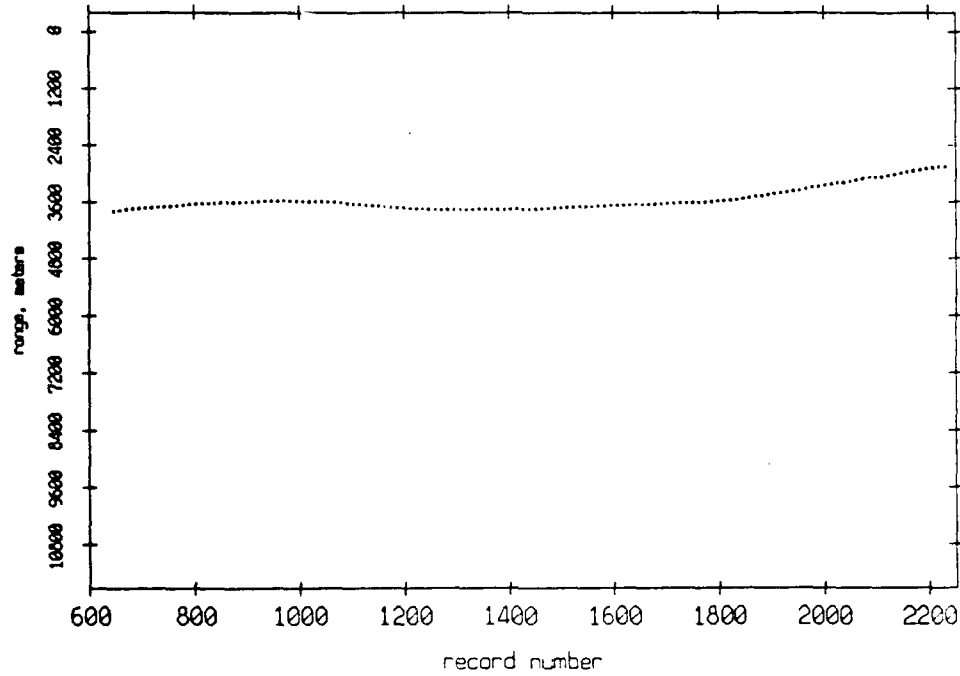
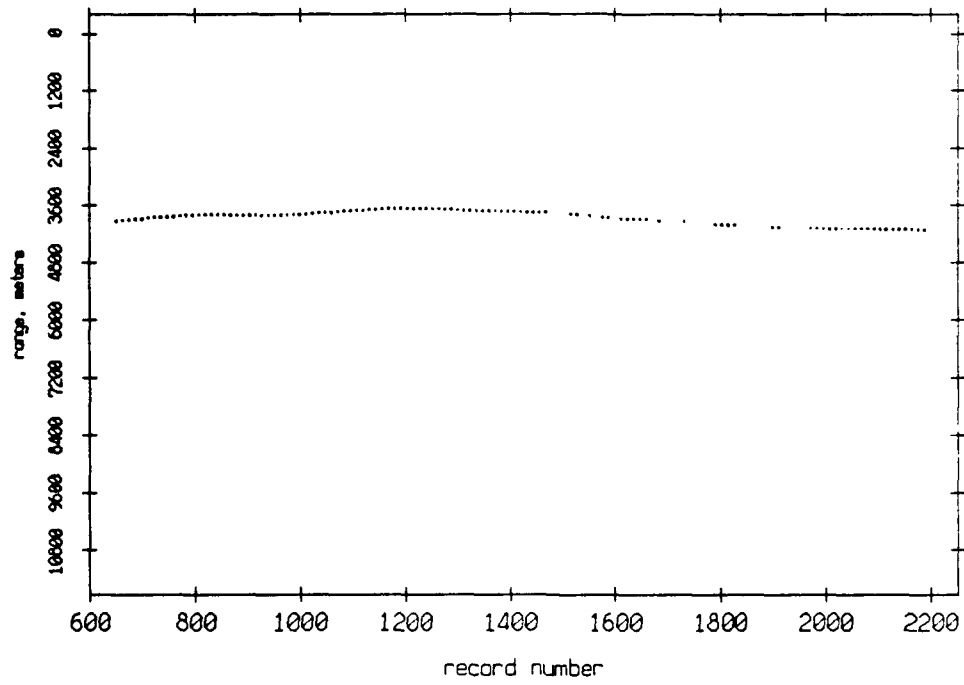


Figure 3.27

Pulse Leading Edges. Float 10 listening to Float 3, July 1989



Pulse Leading Edges. Float 3 listening to Float 10, July 1989

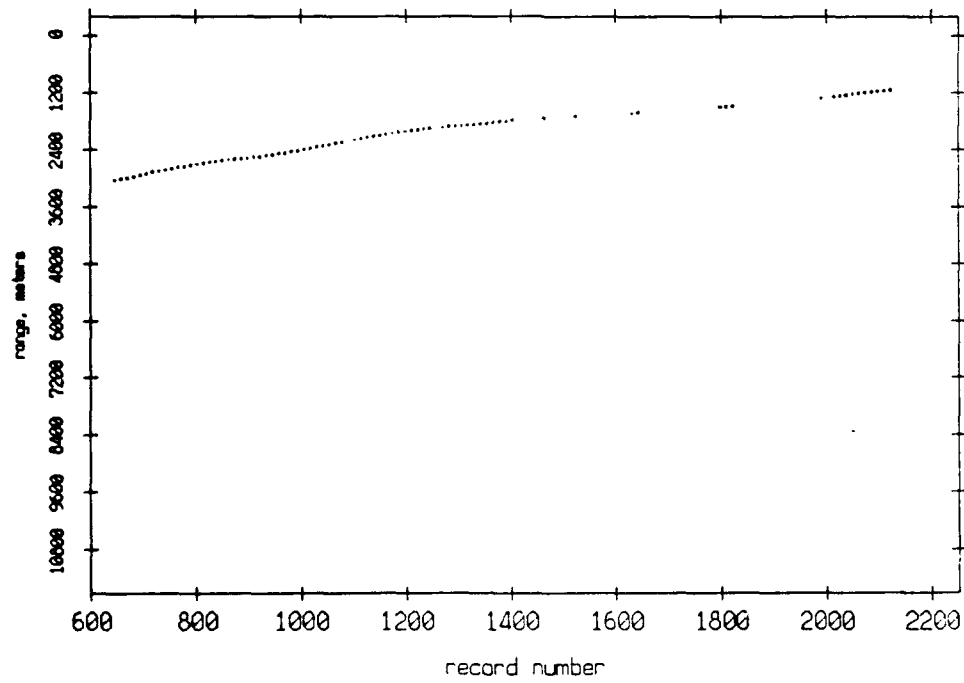
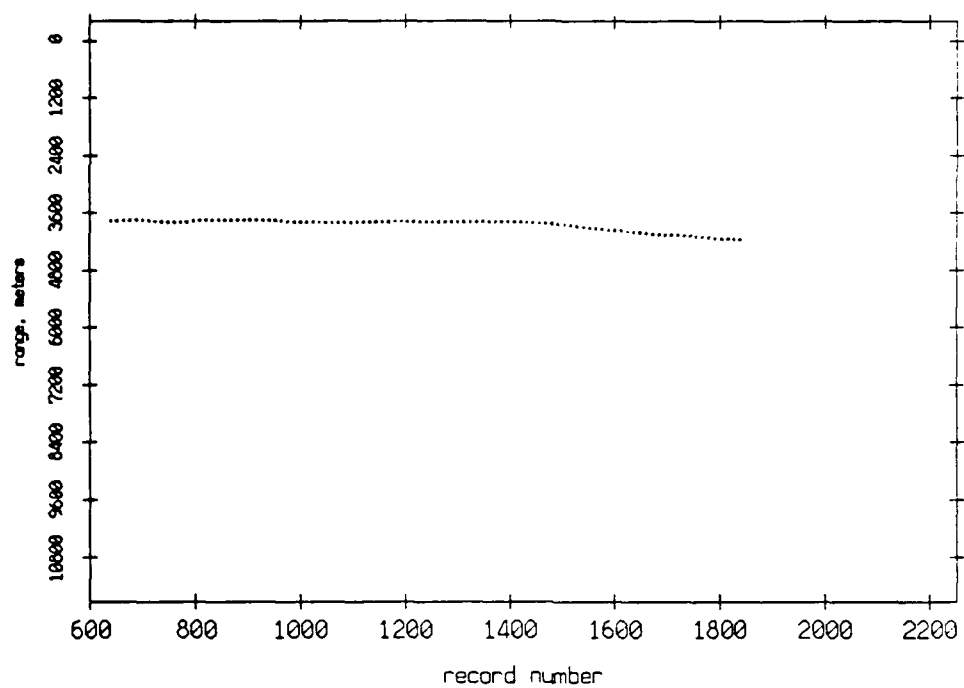


Figure 3.28

Pulse Leading Edges. Float 10 listening to Float 4, July 1989



Pulse Leading Edges. Float 4 listening to Float 10, July 1989

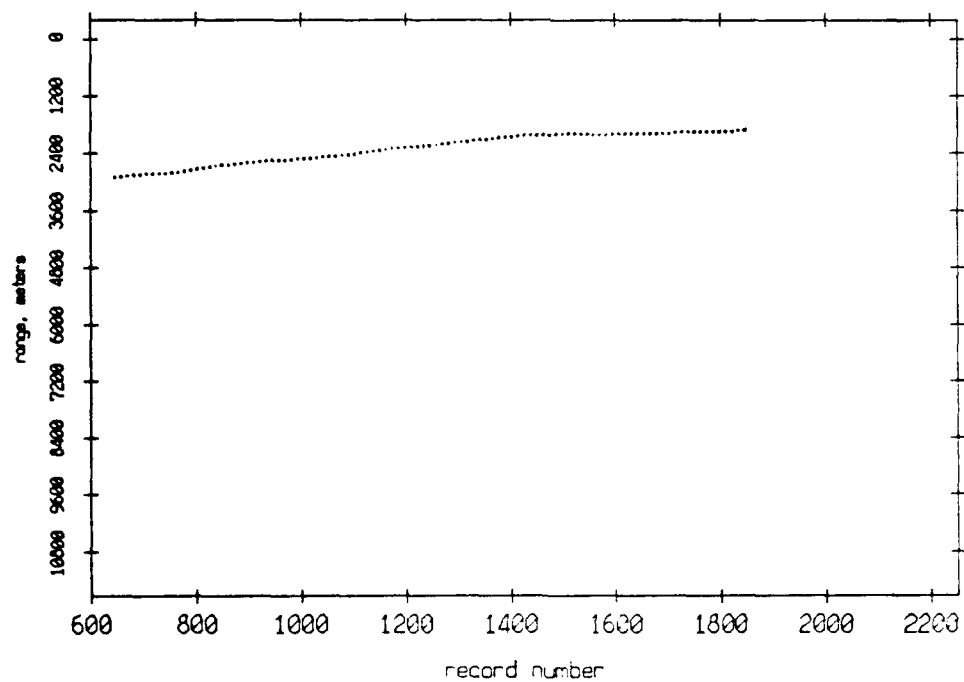
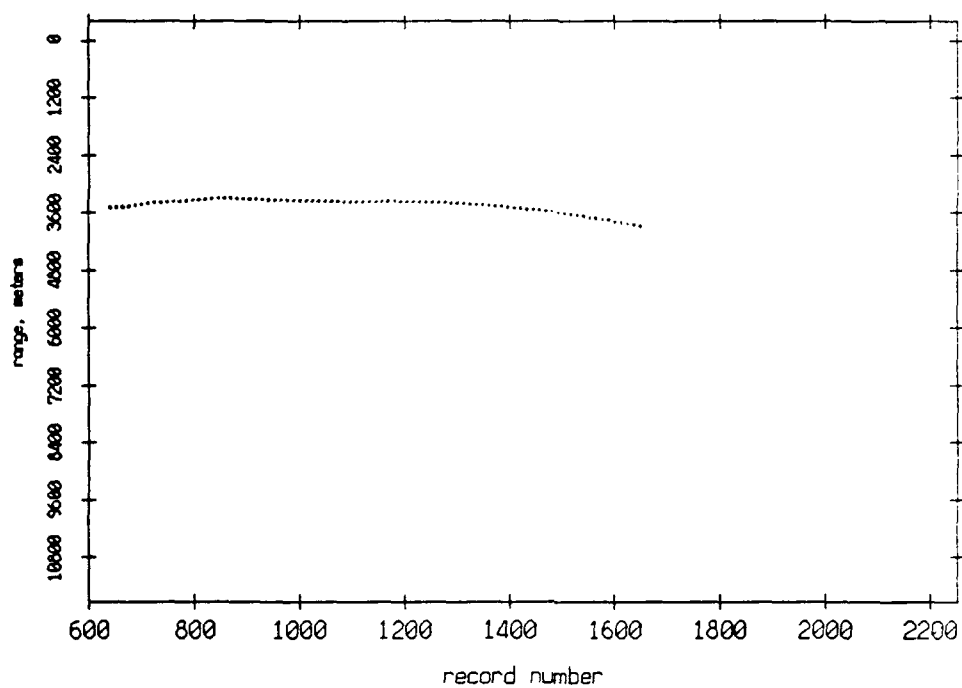


Figure 3.29

Pulse Leading Edges. Float 10 listening to Float 5, July 1989



Pulse Leading Edges. Float 5 listening to Float 10, July 1989

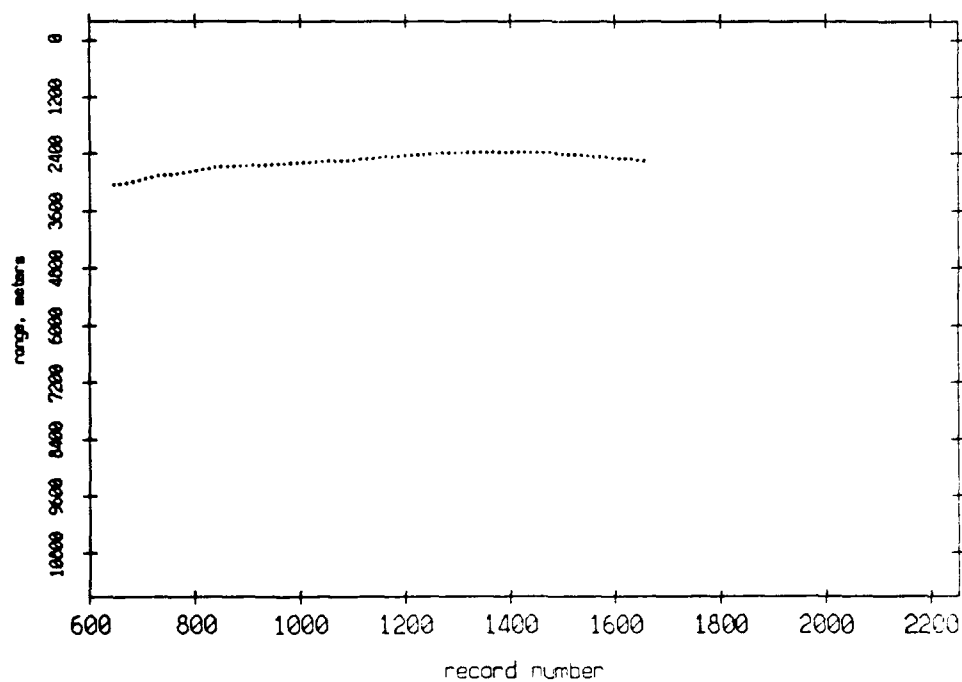
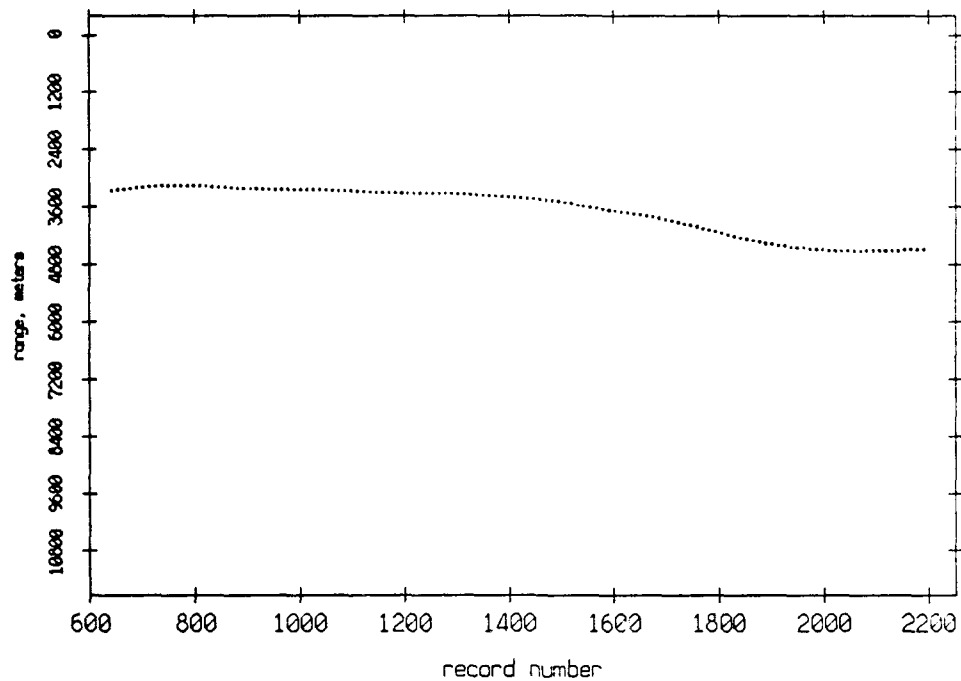


Figure 3.30

Pulse Leading Edges. Float 10 listening to Float 6, July 1989



Pulse Leading Edges. Float 6 listening to Float 10, July 1989

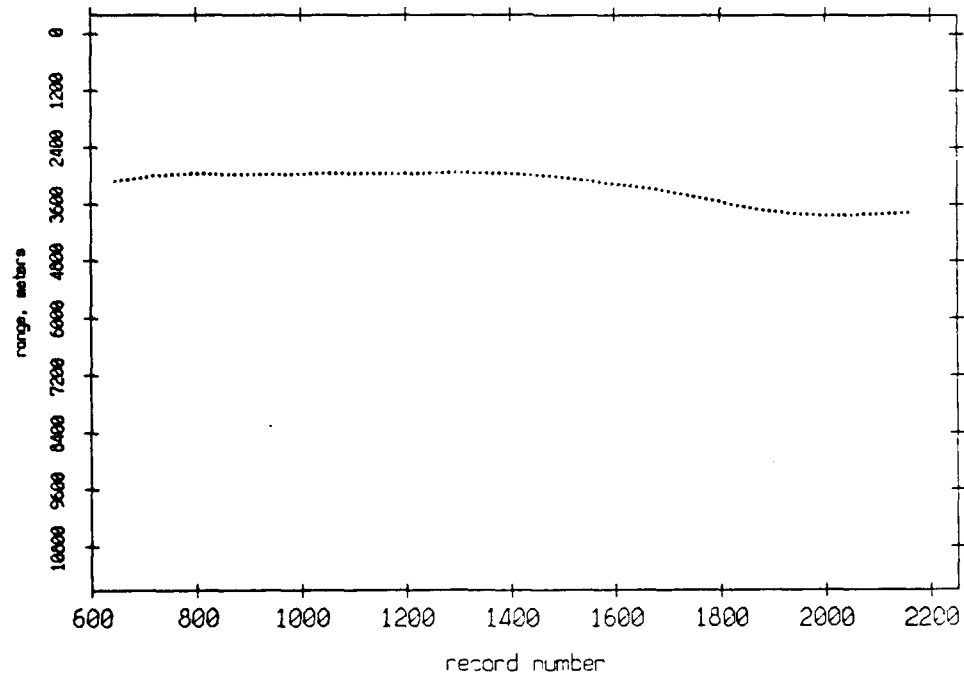
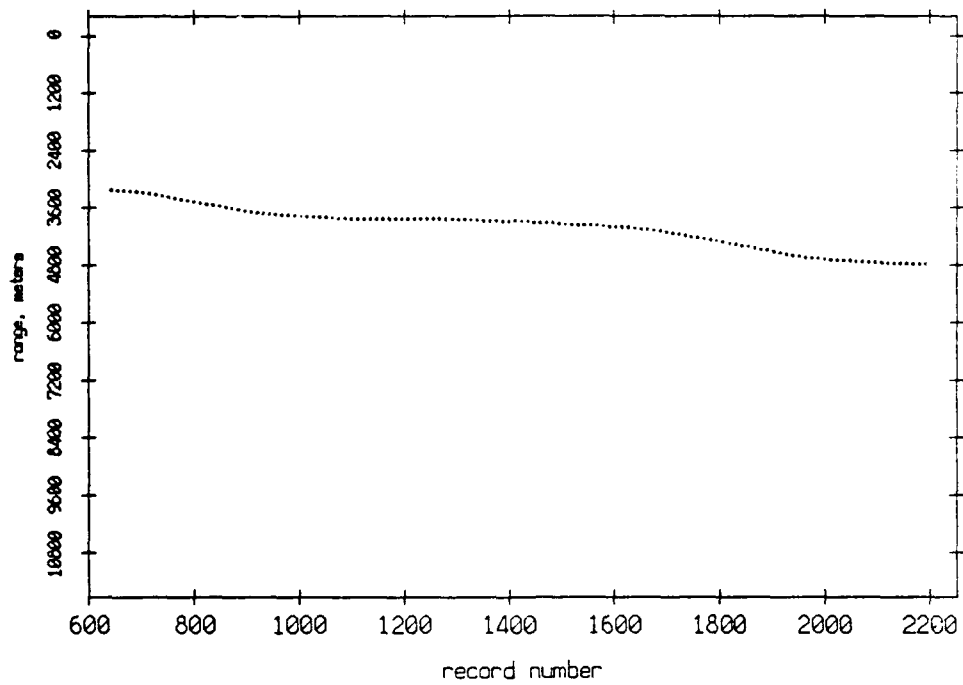


Figure 3.31

Pulse Leading Edges. Float 10 listening to Float 7, July 1989



Pulse Leading Edges. Float 7 listening to Float 10, July 1989

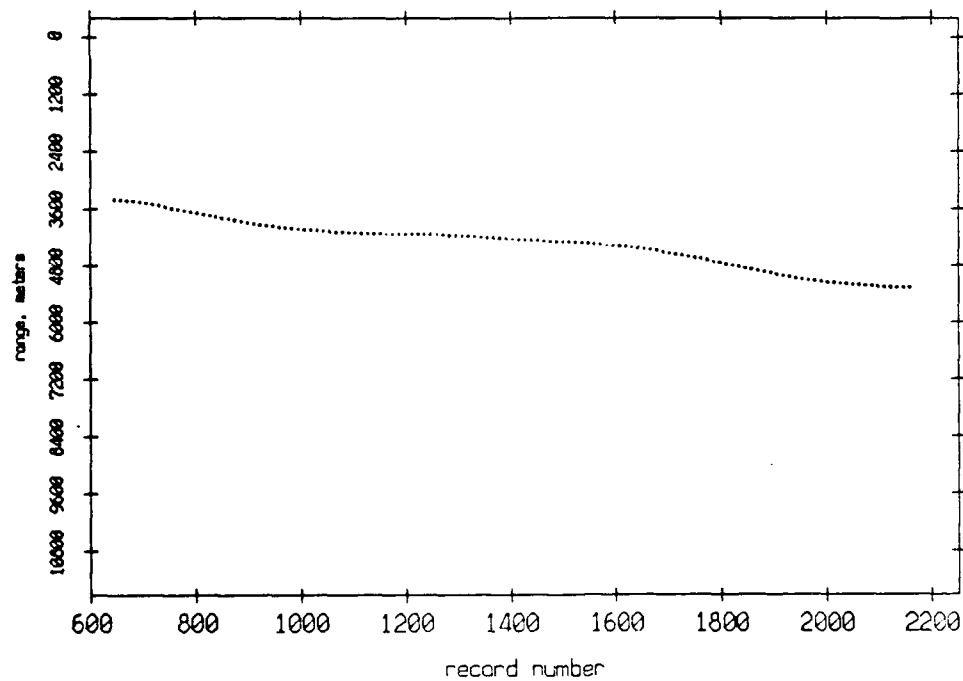
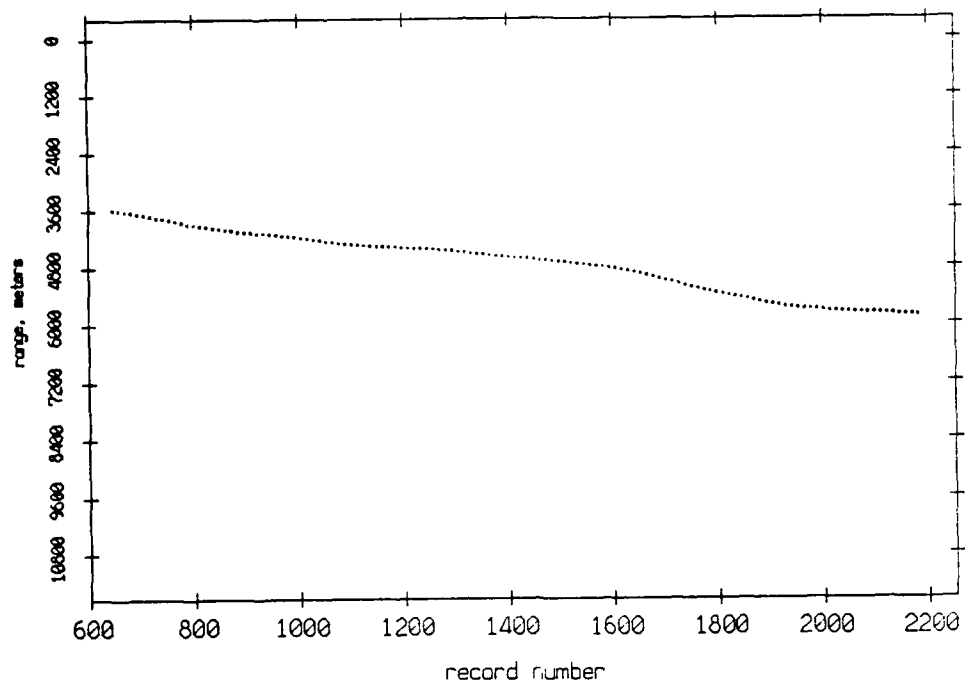


Figure 3.32

Pulse Leading Edges. Float 10 listening to Float 8, July 1989



Pulse Leading Edges. Float 8 listening to Float 10, July 1989

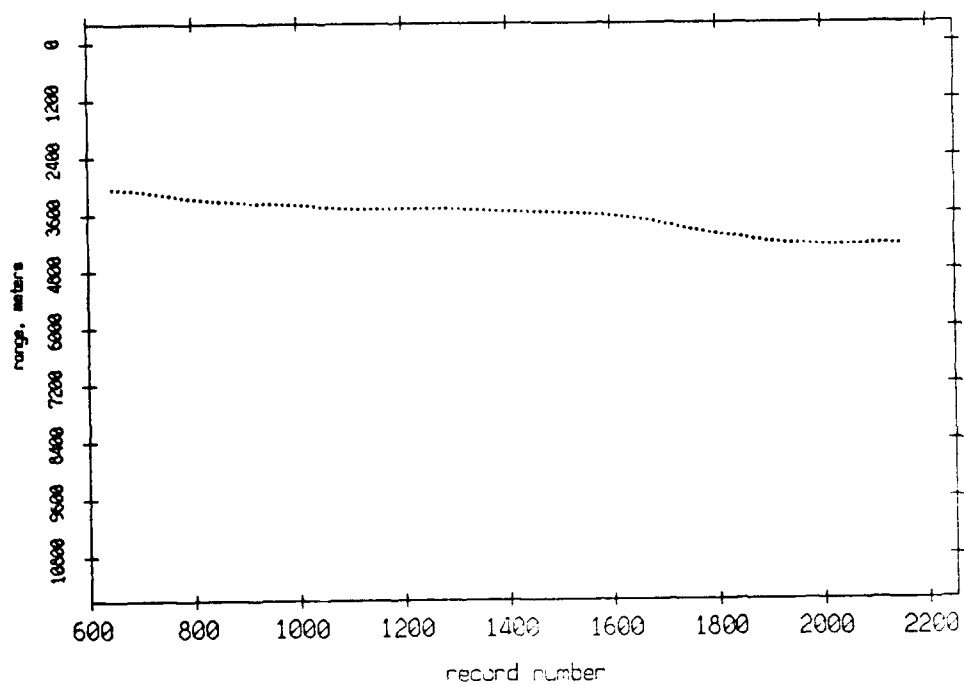
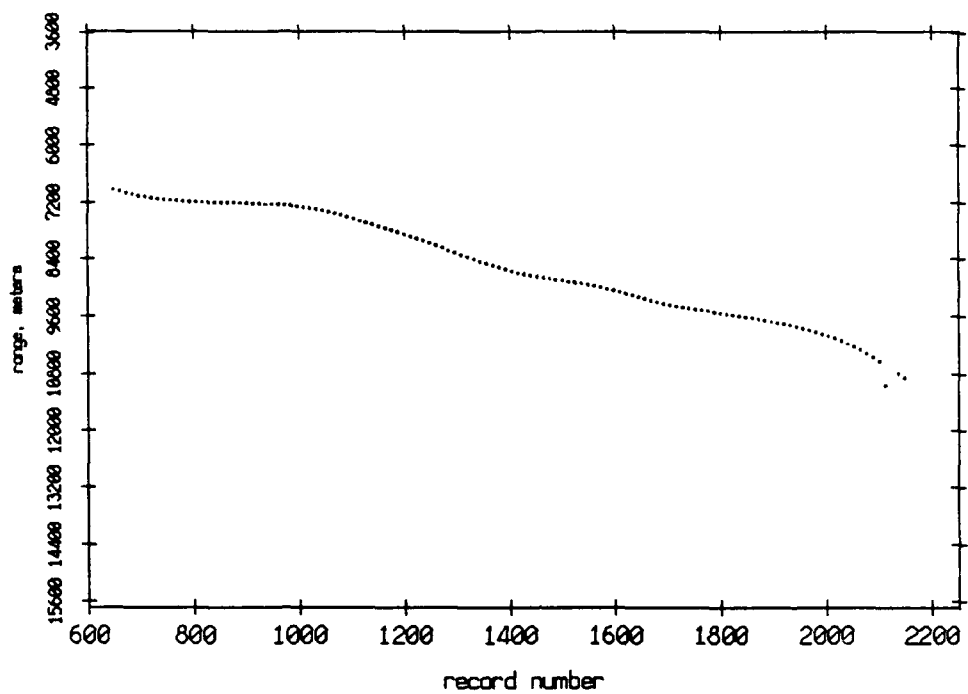


Figure 3.33

Pulse Leading Edges. Float 11 listening to Float 0, July 1989



Pulse Leading Edges. Float 0 listening to Float 11, July 1989

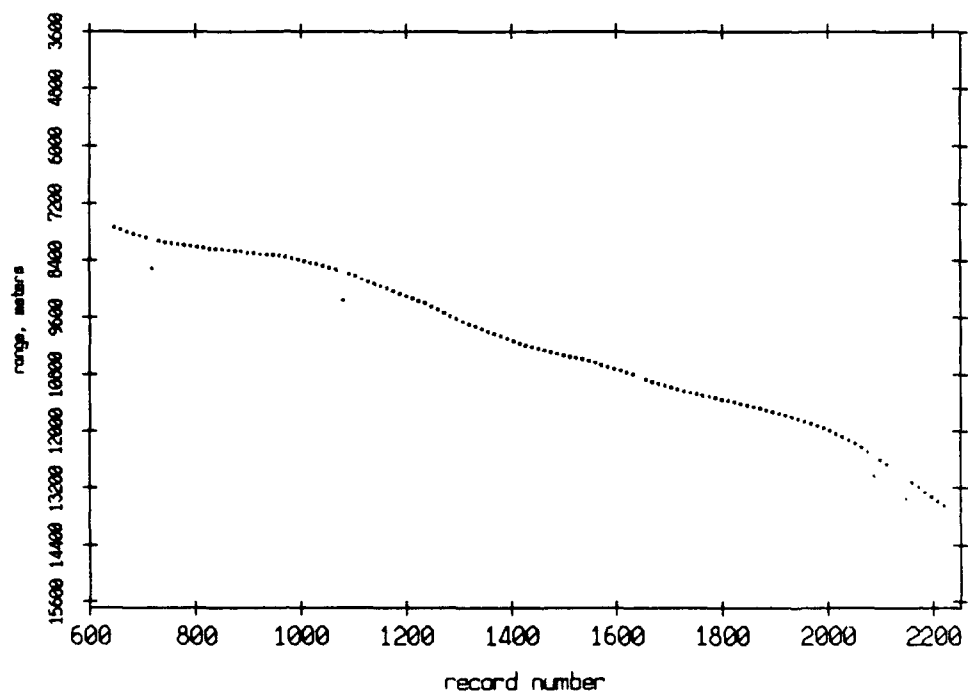
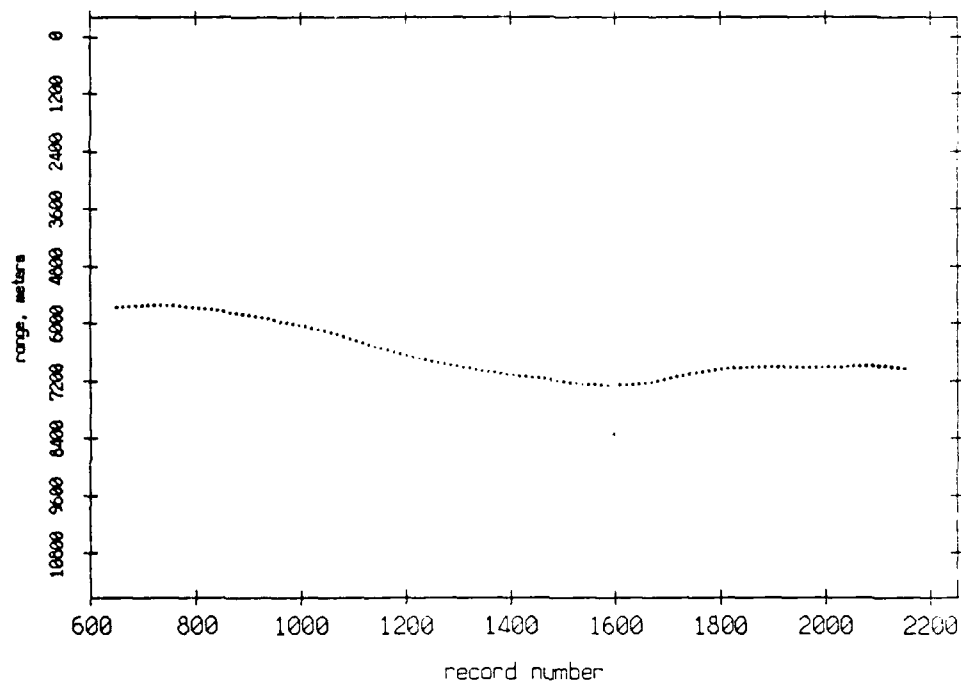


Figure 3.34

Pulse Leading Edges. Float 11 listening to Float 1, July 1989



Pulse Leading Edges. Float 1 listening to Float 11, July 1989

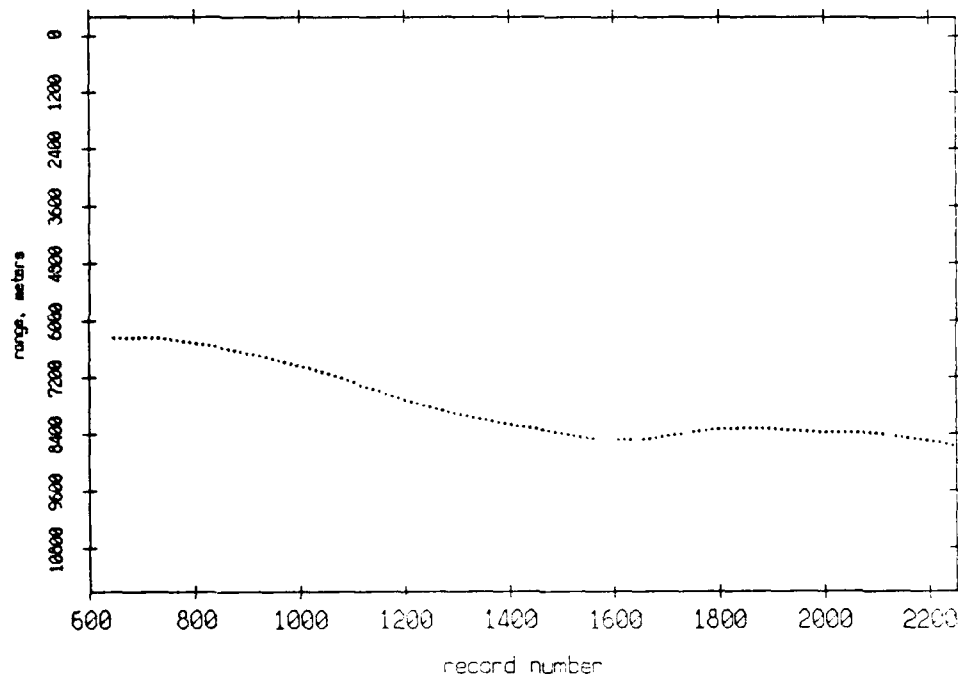
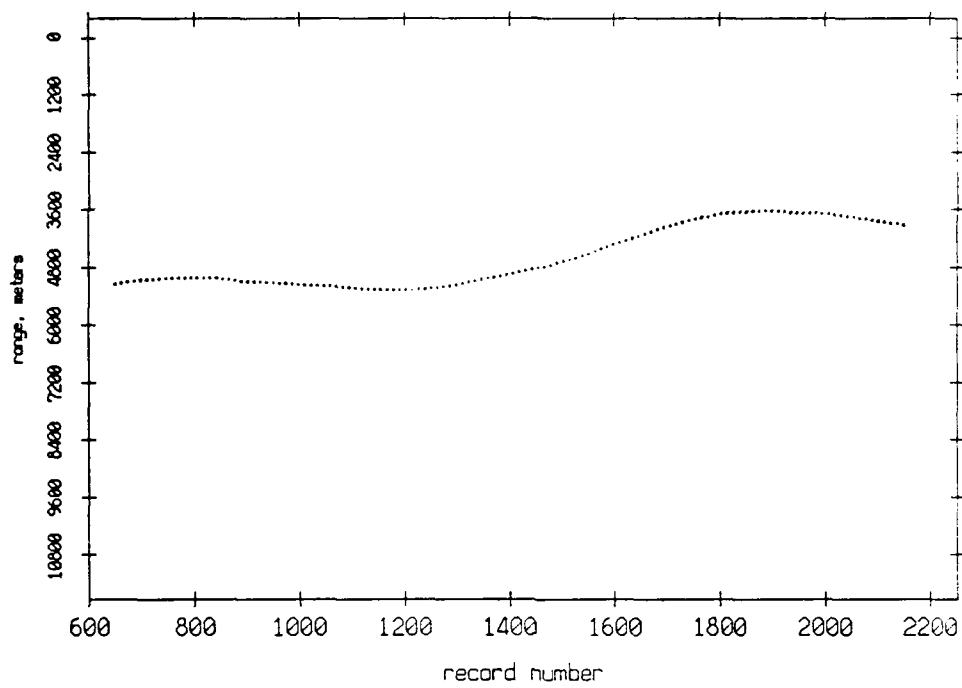


Figure 3.35

Pulse Leading Edges. Float 11 listening to Float 2, July 1989



Pulse Leading Edges. Float 2 listening to Float 11, July 1989

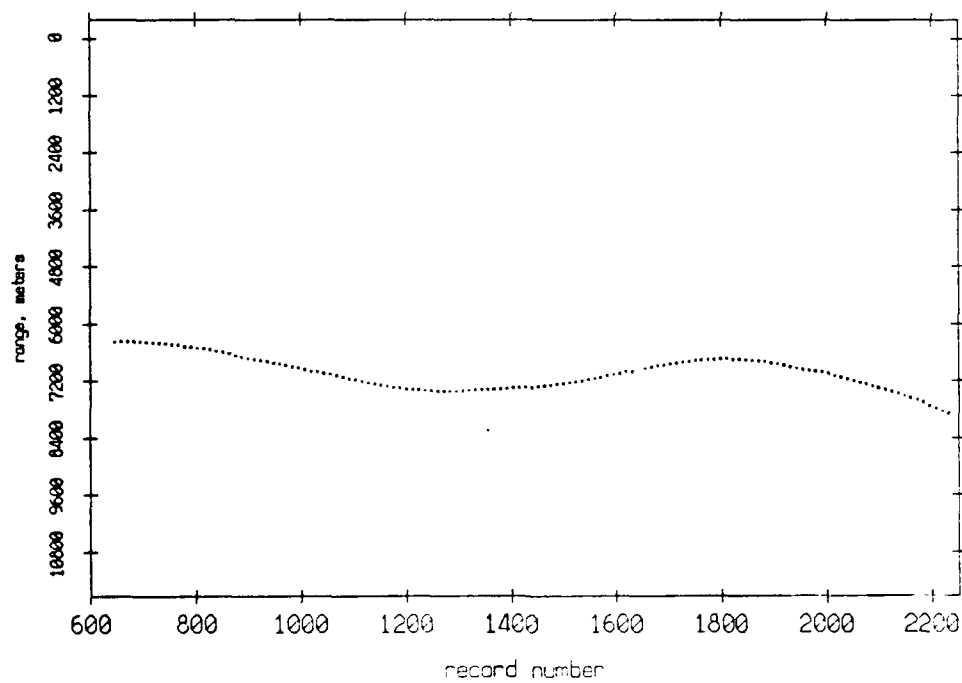
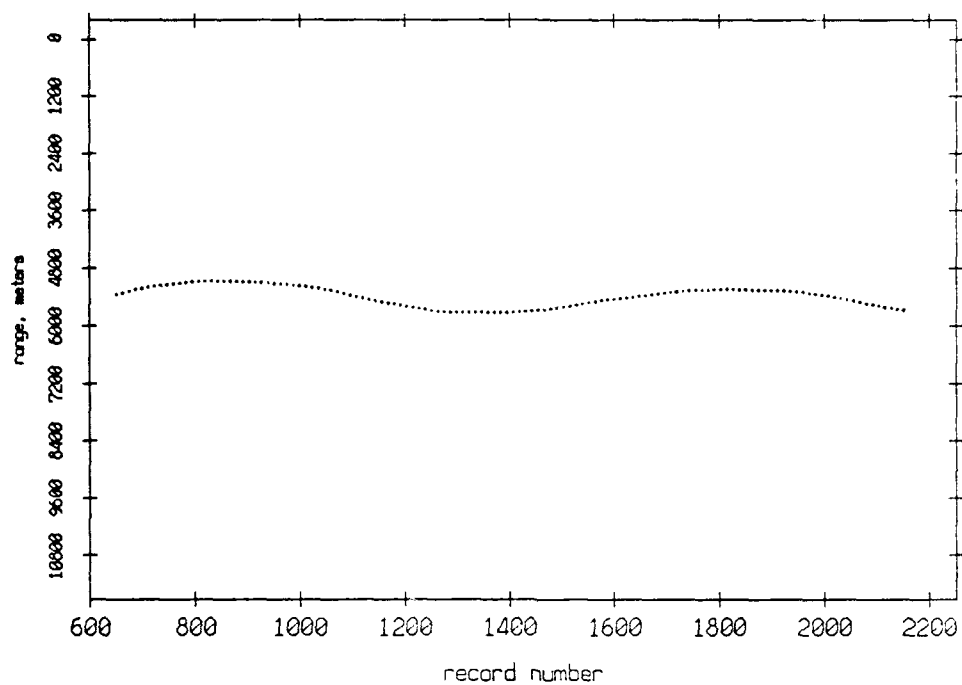


Figure 3.36

Pulse Leading Edges. Float 11 listening to Float 3, July 1989



Pulse Leading Edges. Float 3 listening to Float 11, July 1989

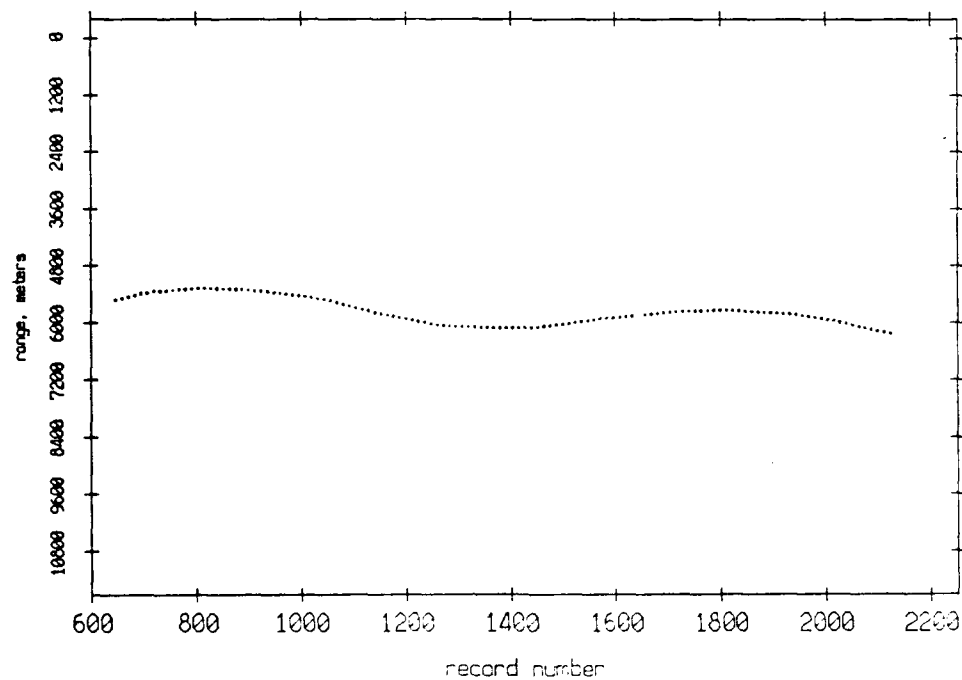
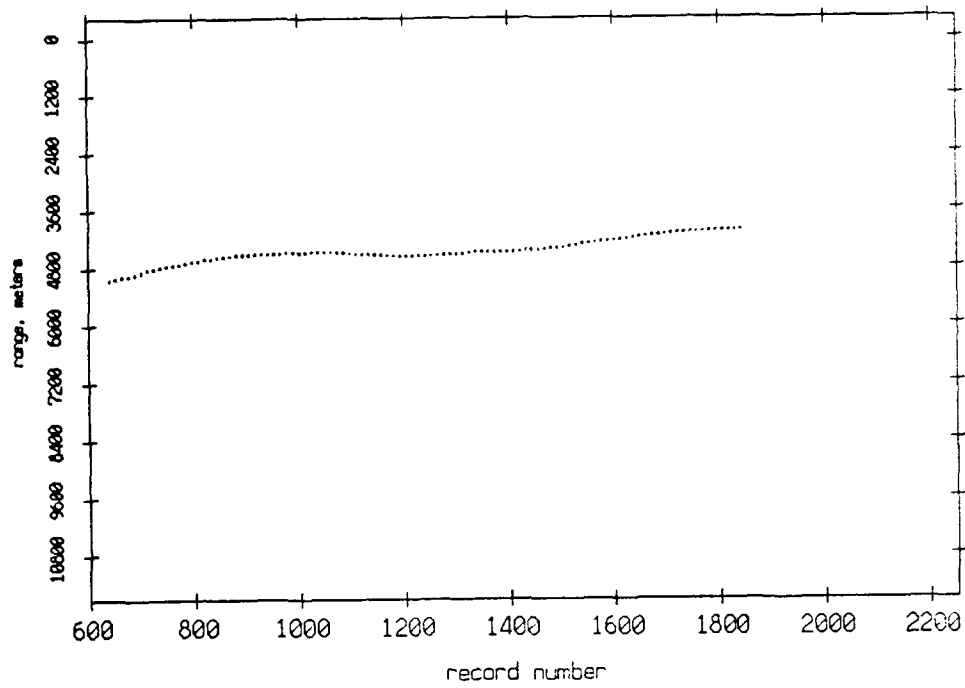


Figure 3.37

Pulse Leading Edges. Float 11 listening to Float 4, July 1989



Pulse Leading Edges. Float 4 listening to Float 11, July 1989

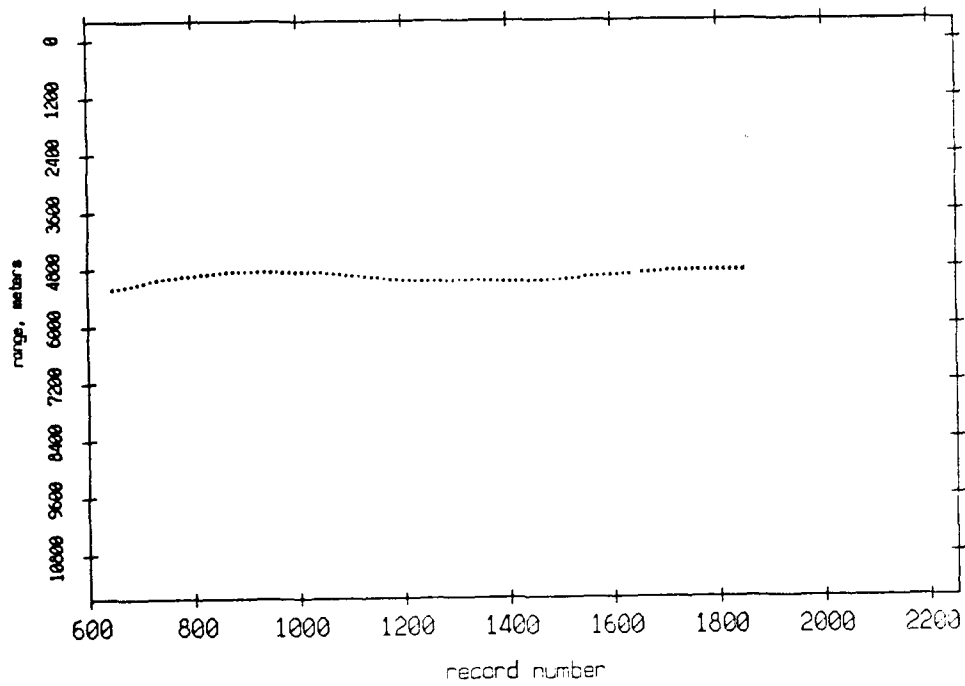
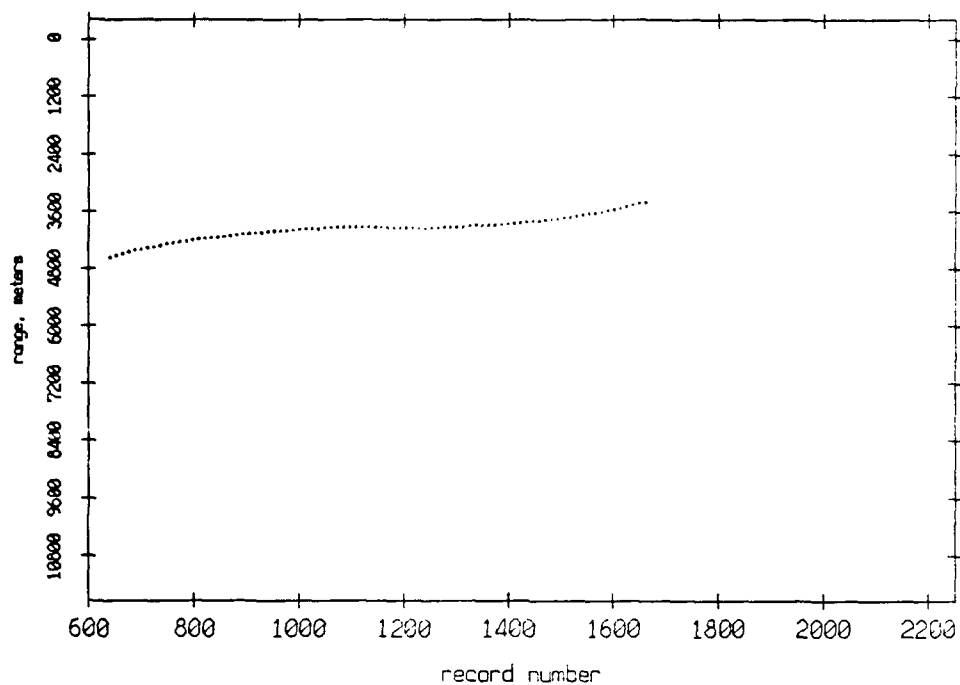


Figure 3.38

Pulse Leading Edges. Float 11 listening to Float 5, July 1989



Pulse Leading Edges. Float 5 listening to Float 11, July 1989

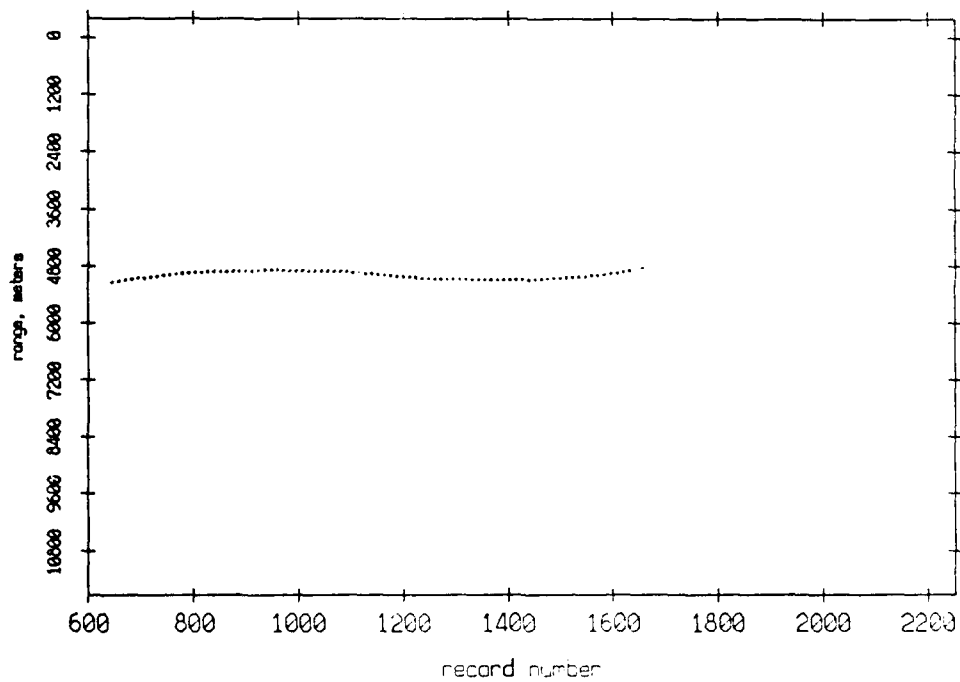
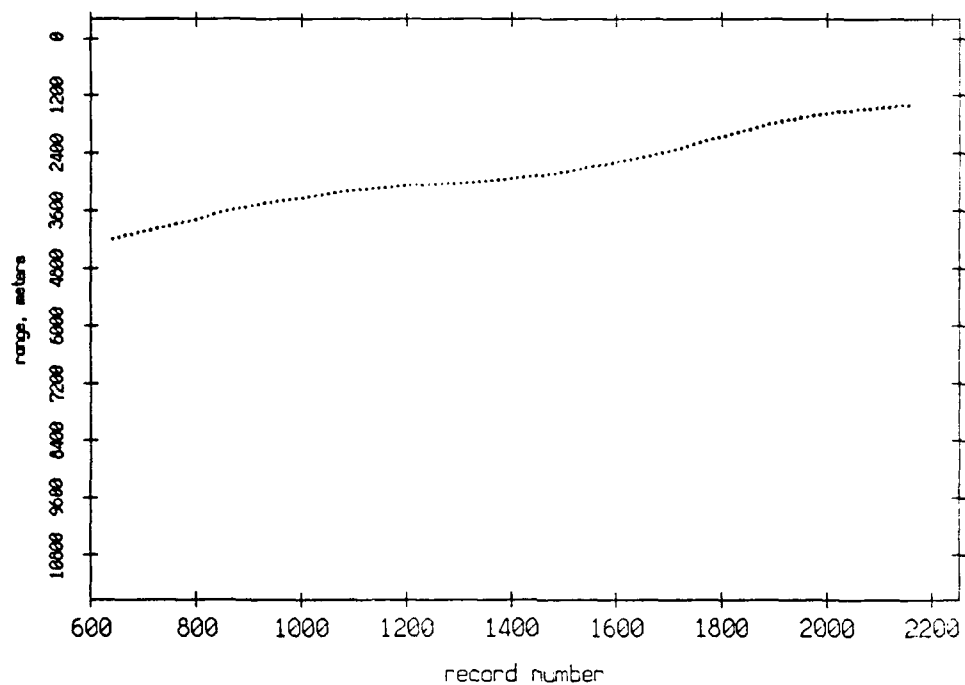


Figure 3.39

Pulse Leading Edges. Float 11 listening to Float 6, July 1989



Pulse Leading Edges. Float 6 listening to Float 11, July 1989

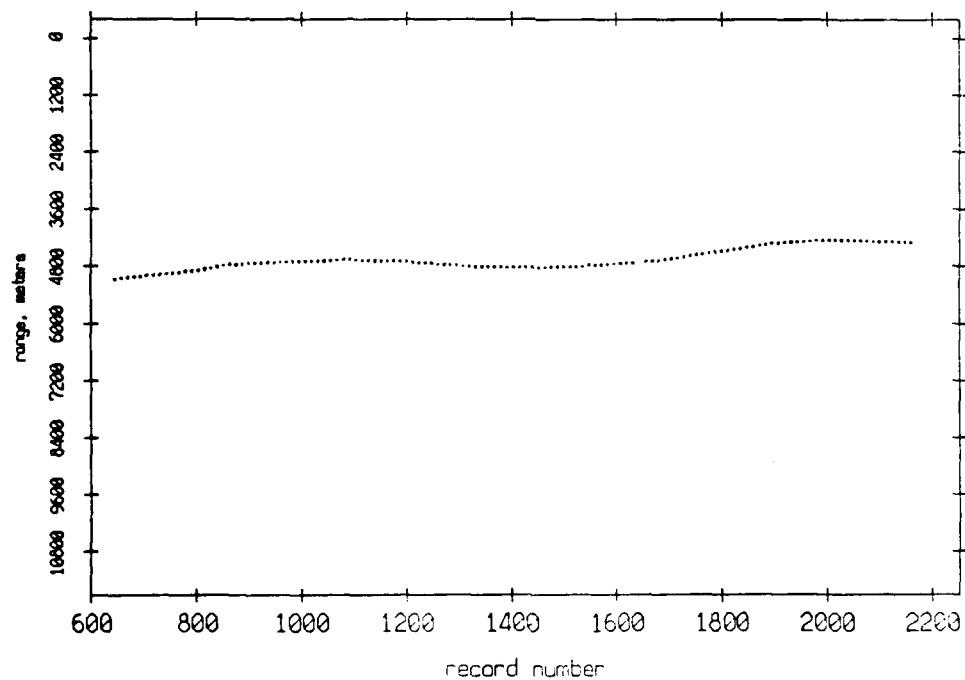
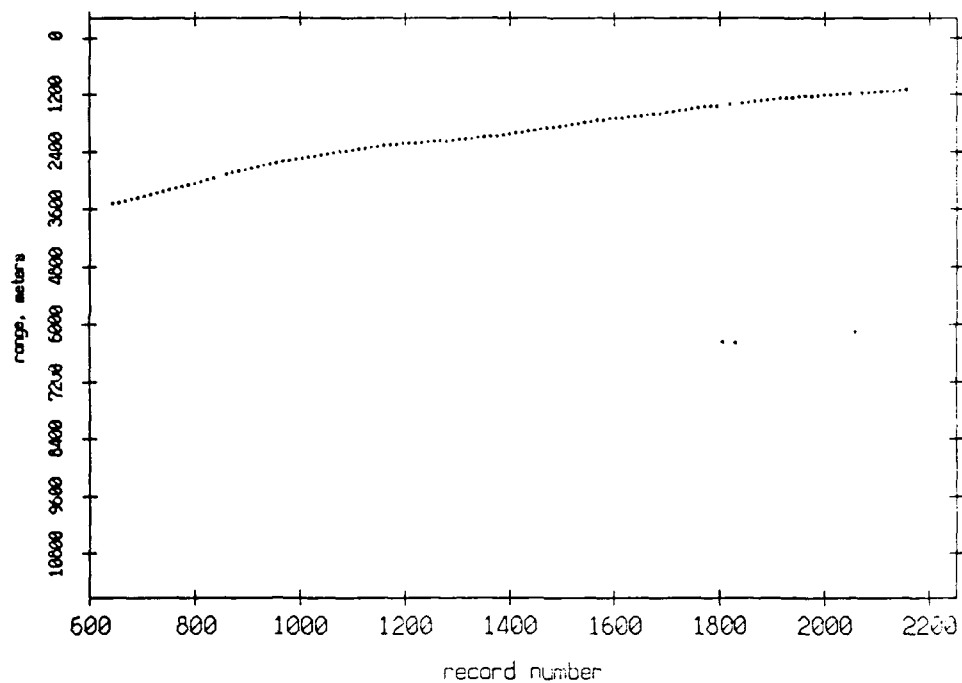


Figure 3.40

Pulse Leading Edges. Float 11 listening to Float 7, July 1989



Pulse Leading Edges. Float 7 listening to Float 11, July 1989

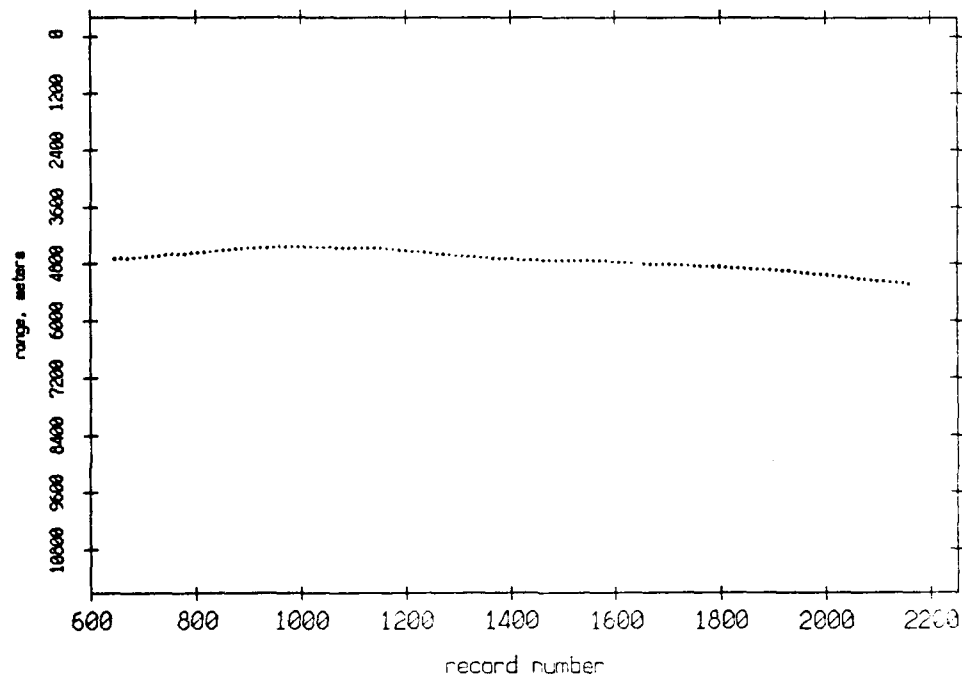
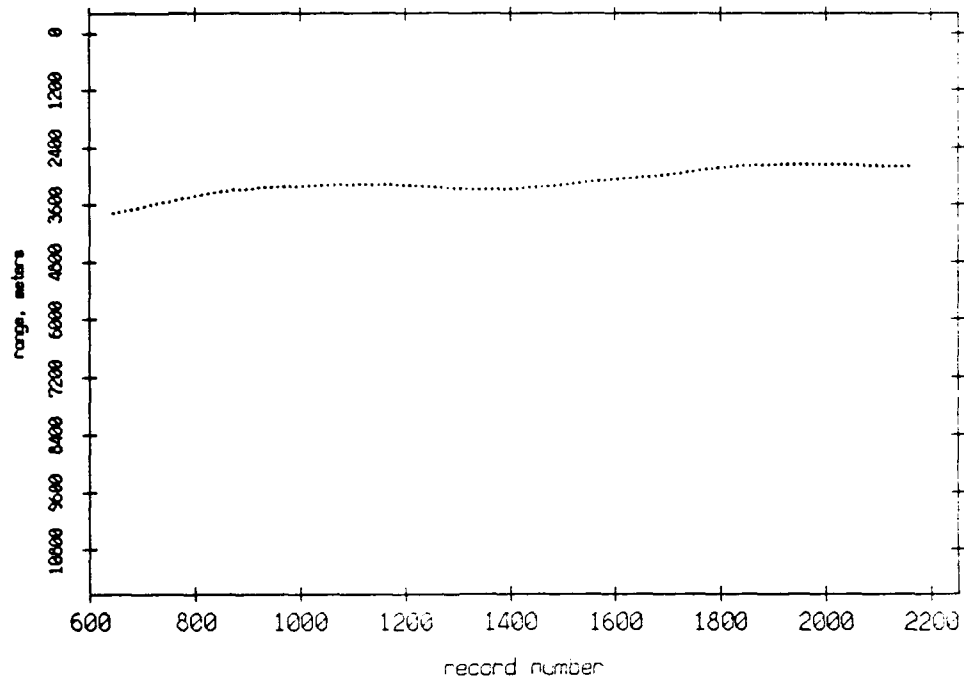


Figure 3.41

Pulse Leading Edges. Float 11 listening to Float 8, July 1989



Pulse Leading Edges. Float 8 listening to Float 11, July 1989

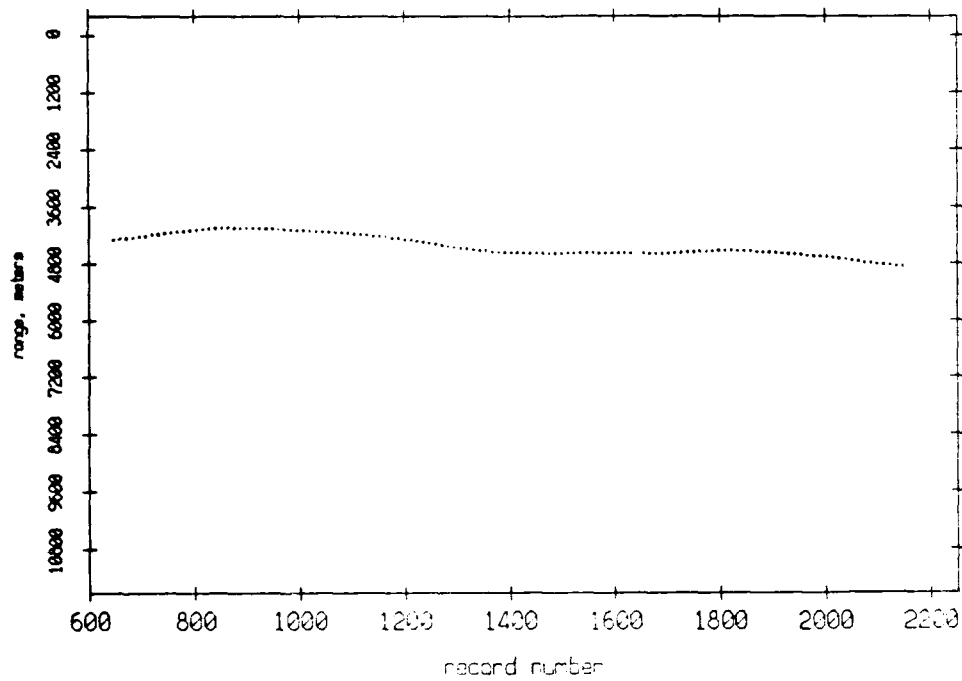
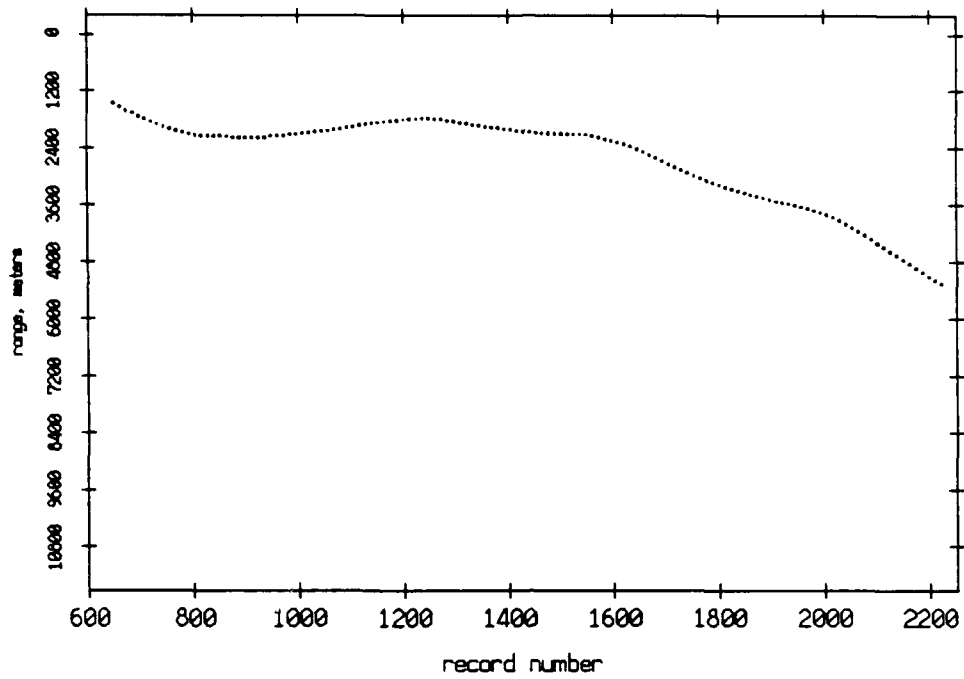


Figure 3.42

Pulse Leading Edges. Float 0 listening to Float 1, July 1989



Pulse Leading Edges. Float 1 listening to Float 0, July 1989

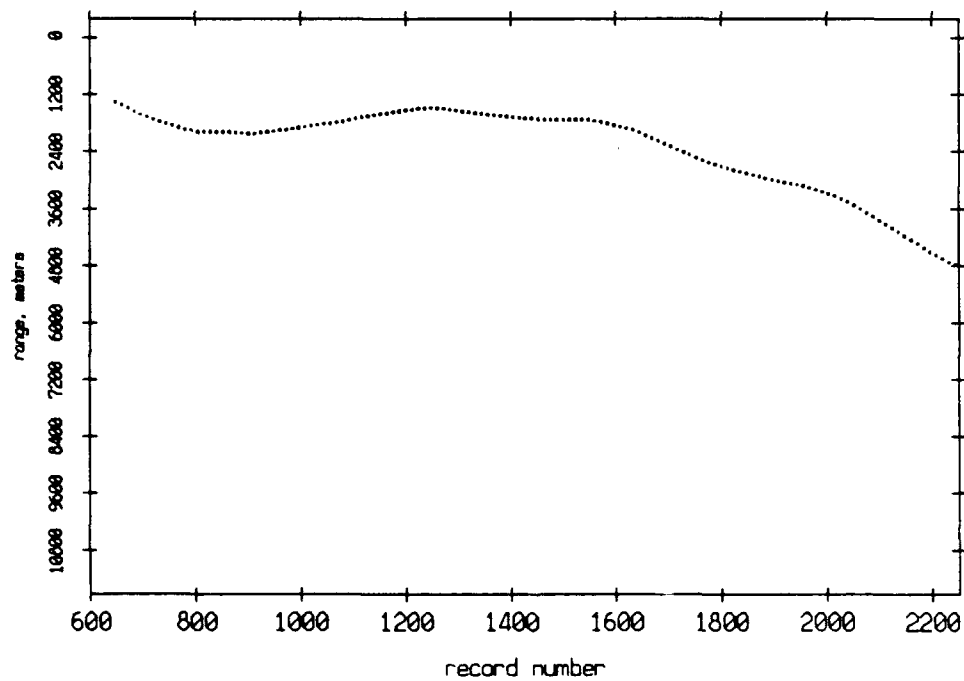
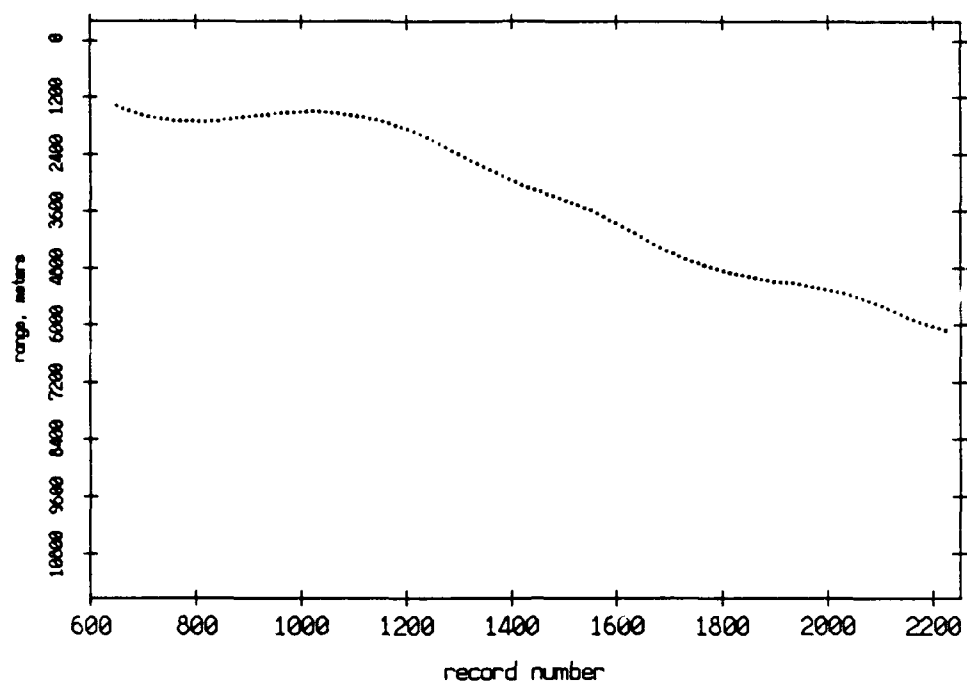


Figure 3.43

Pulse Leading Edges. Float 0 listening to Float 2, July 1989



Pulse Leading Edges. Float 2 listening to Float 0, July 1989

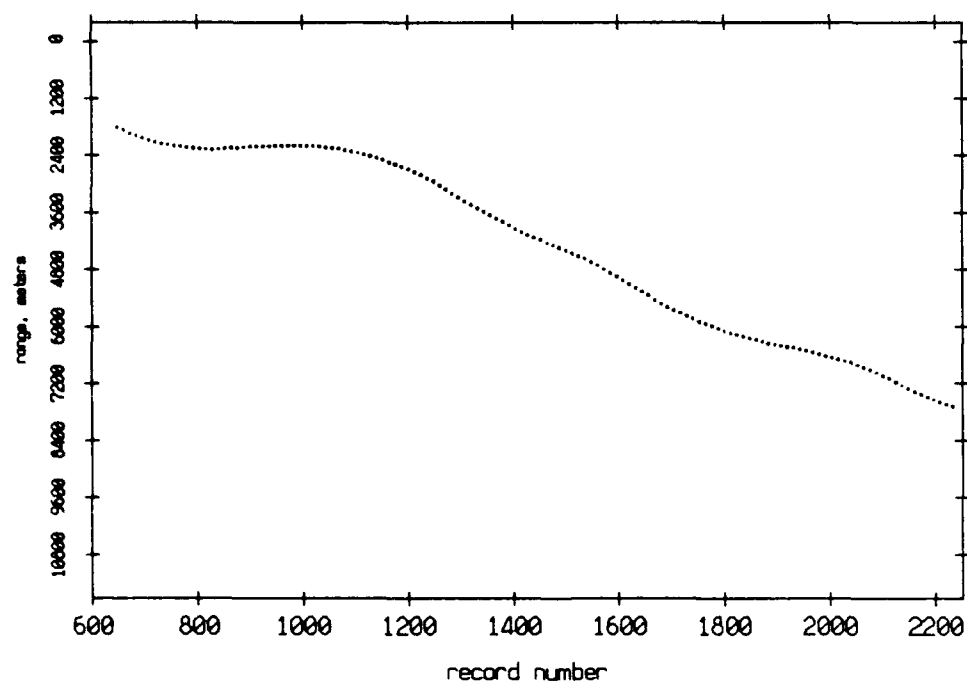
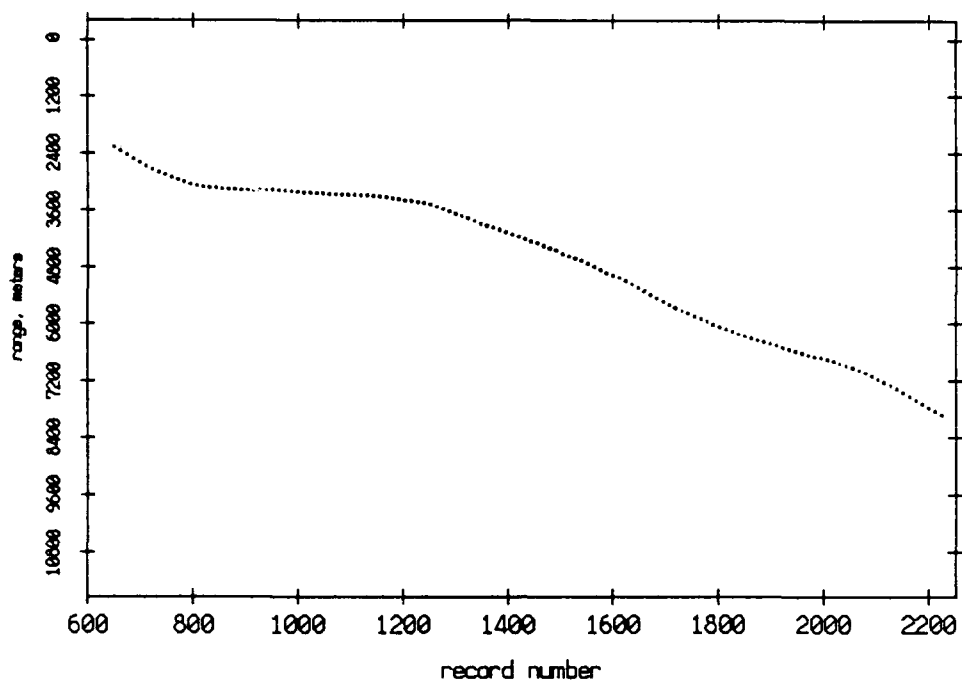


Figure 3.44

Pulse Leading Edges. Float 0 listening to Float 3, July 1989



Pulse Leading Edges. Float 3 listening to Float 0, July 1989

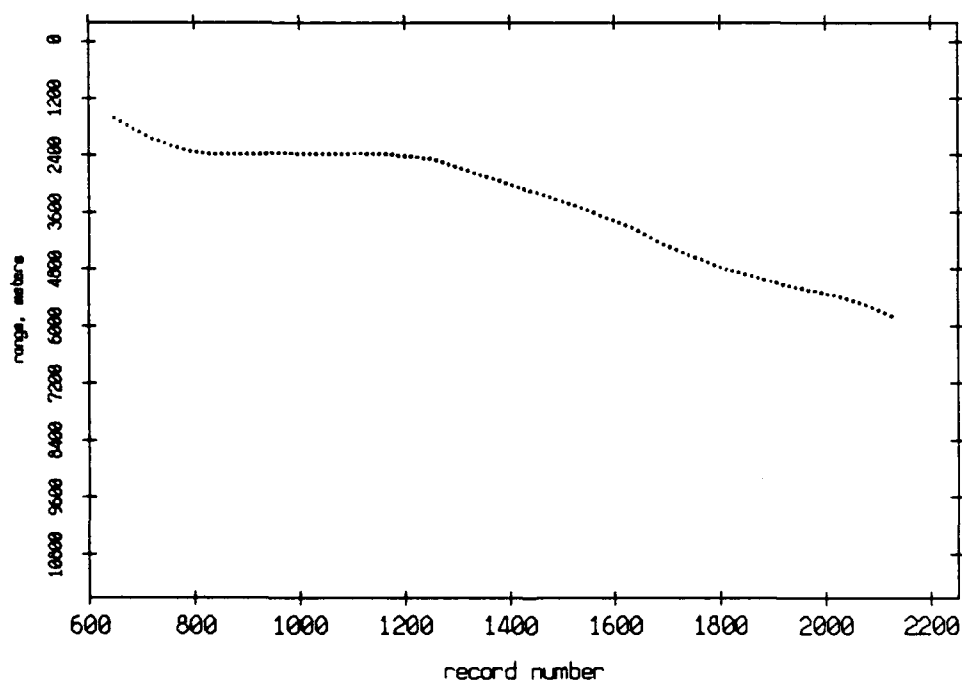
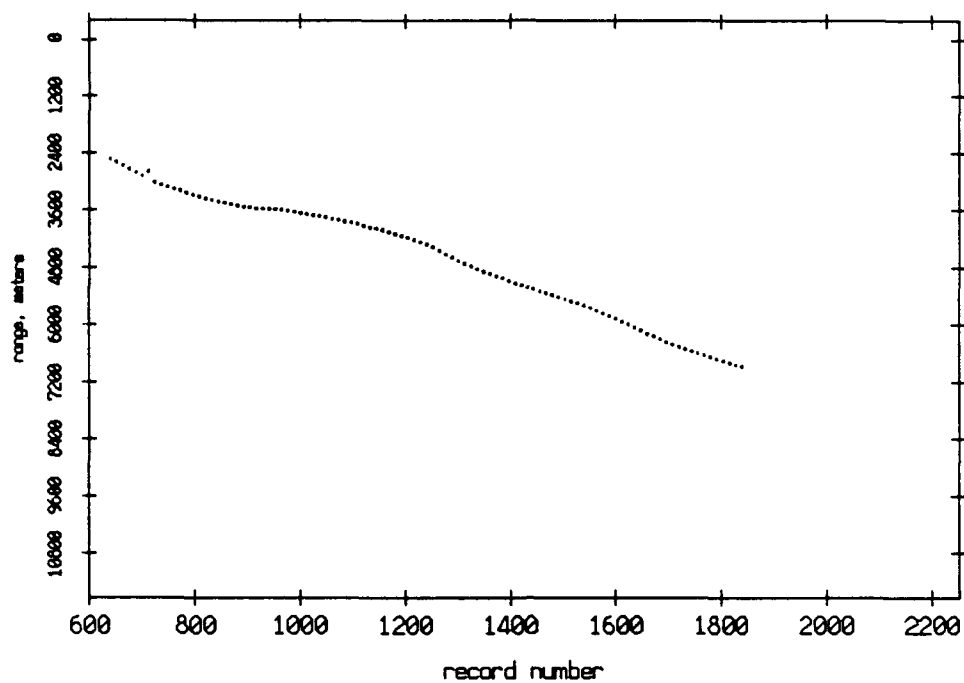


Figure 3.45

Pulse Leading Edges. Float 0 listening to Float 4, July 1989



Pulse Leading Edges. Float 4 listening to Float 0, July 1989

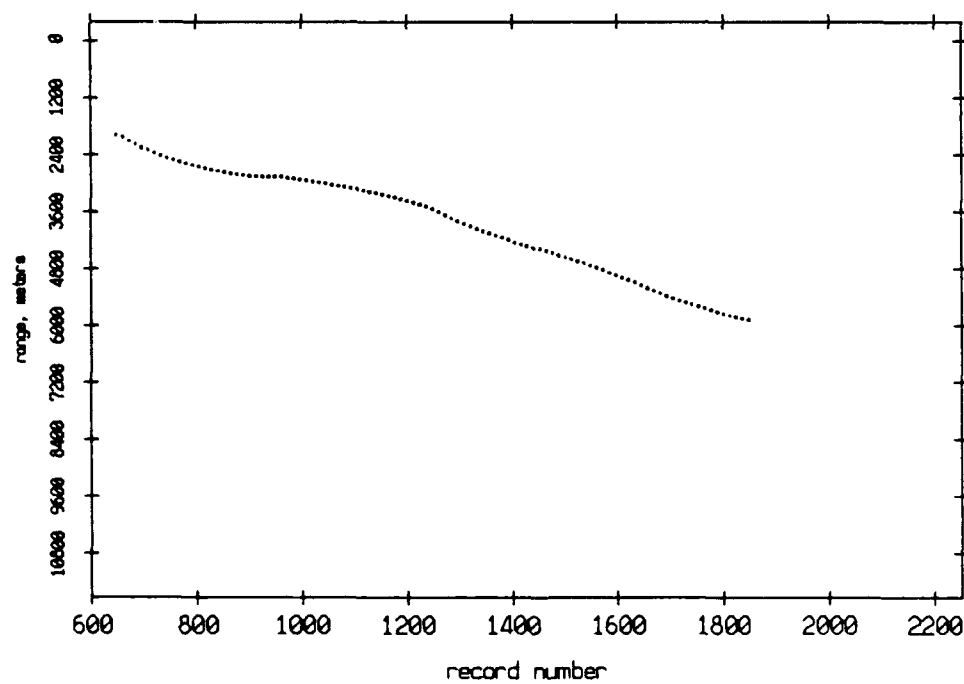
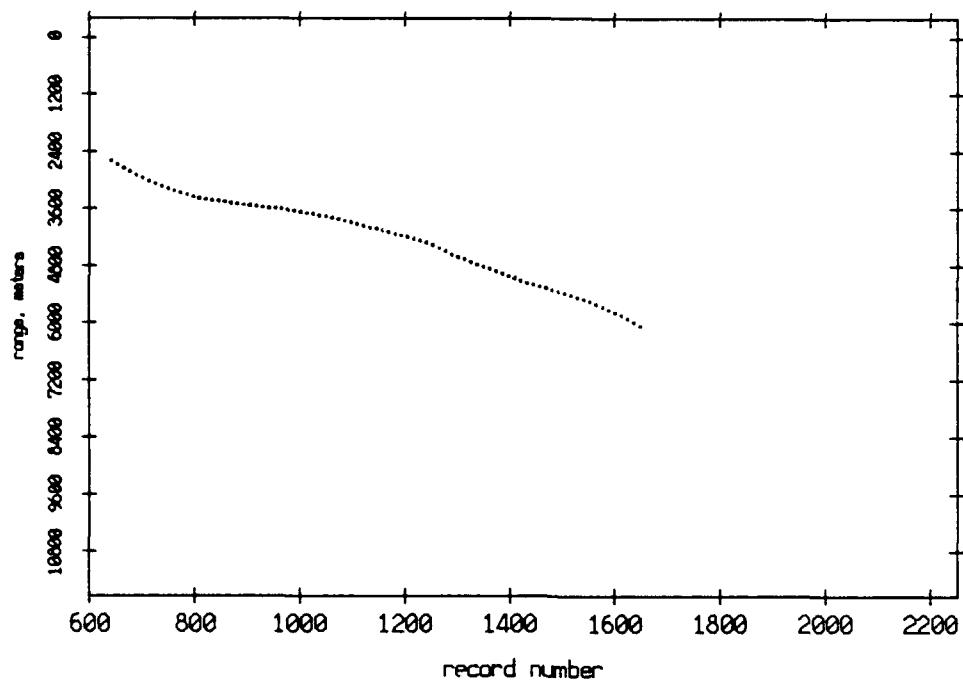


Figure 3.46

Pulse Leading Edges. Float 0 listening to Float 5, July 1989



Pulse Leading Edges. Float 5 listening to Float 0, July 1989

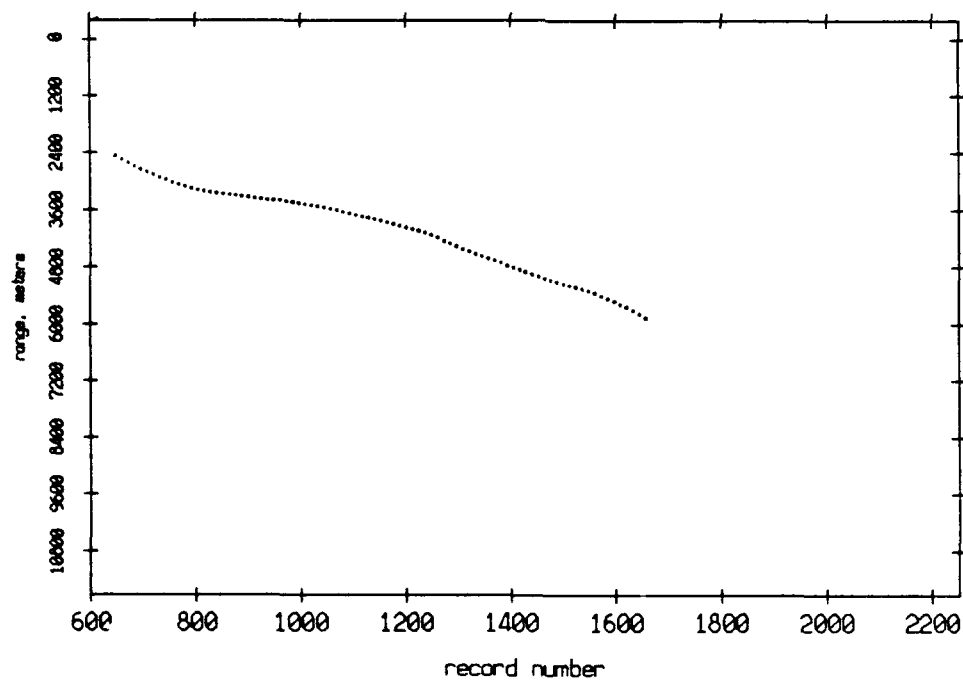
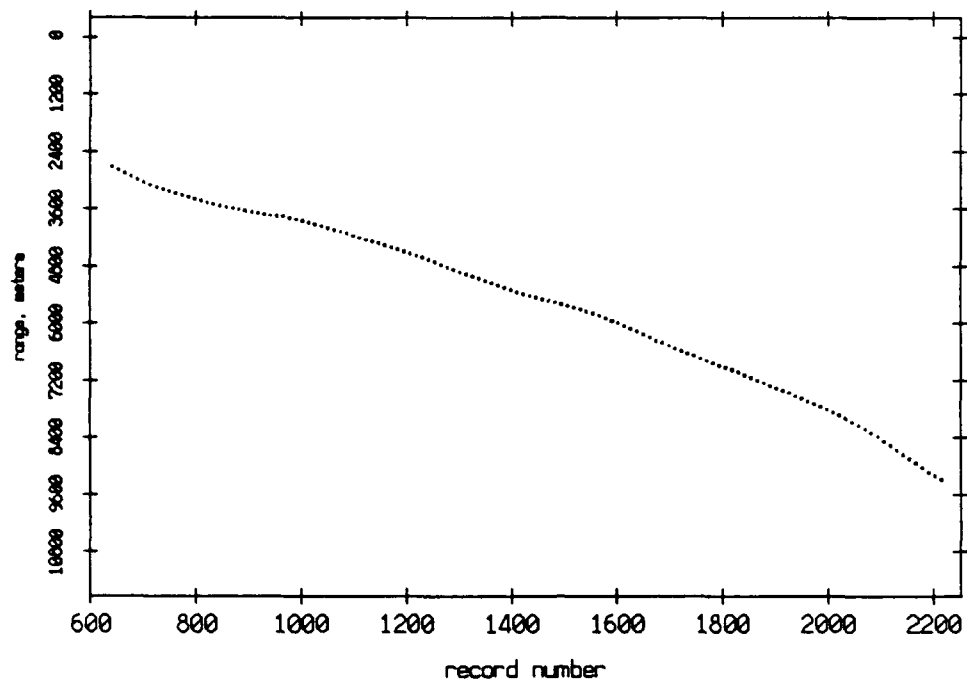


Figure 3.47

Pulse Leading Edges. Float 0 listening to Float 6, July 1989



Pulse Leading Edges. Float 6 listening to Float 0, July 1989

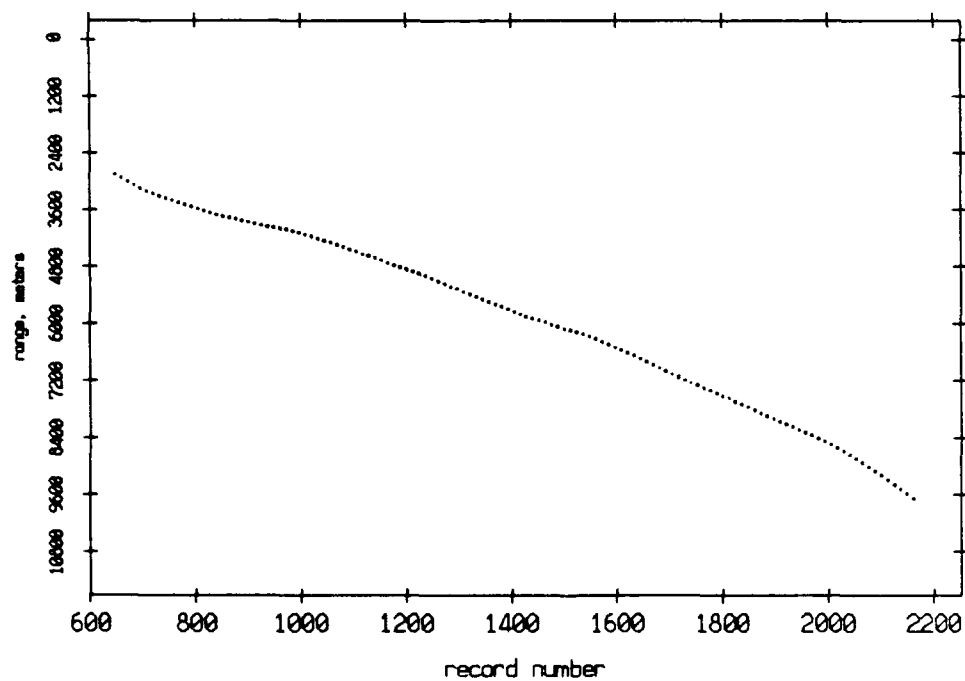
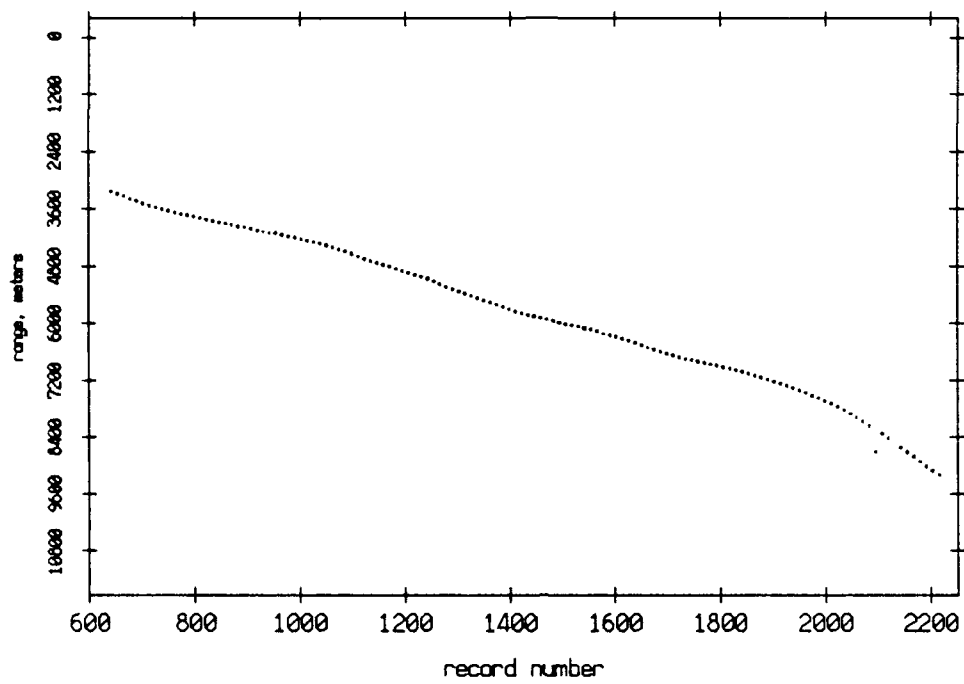


Figure 3.48

Pulse Leading Edges. Float 0 listening to Float 7, July 1989



Pulse Leading Edges. Float 7 listening to Float 0, July 1989

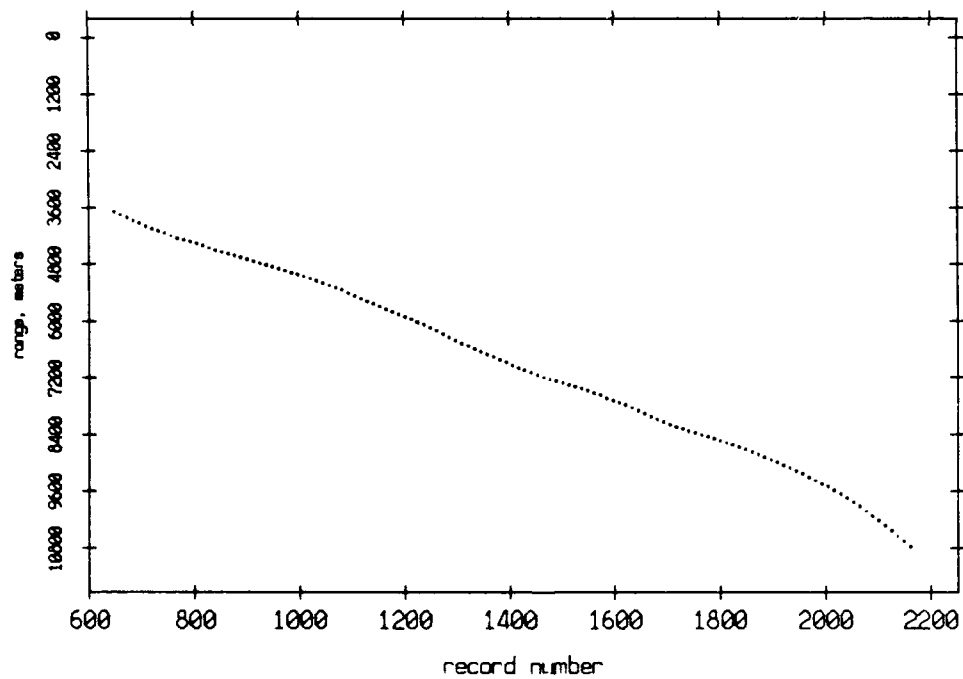
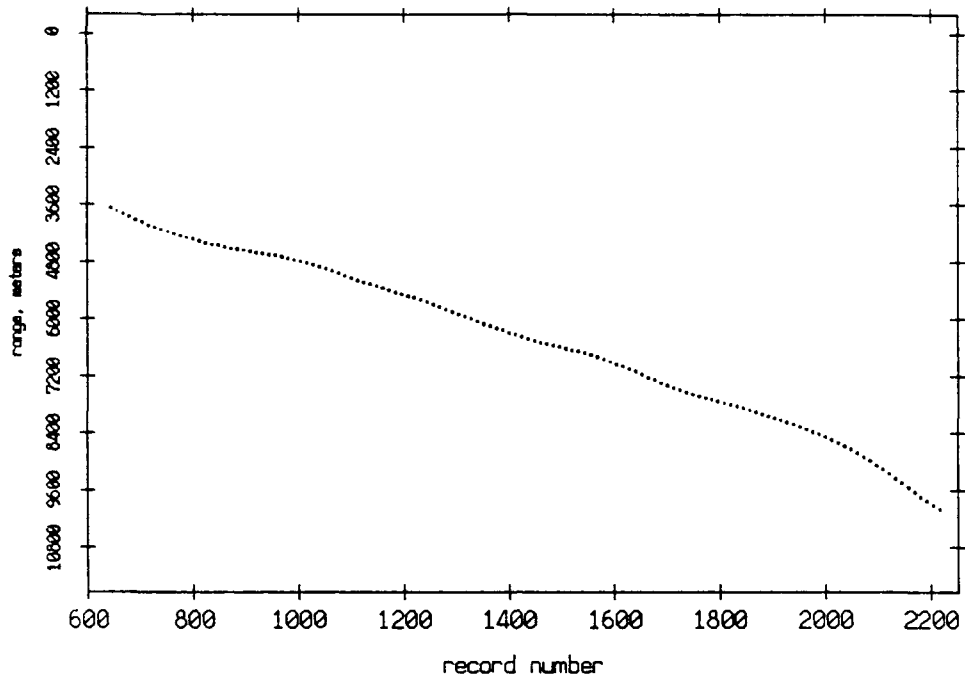


Figure 3.49

Pulse Leading Edges. Float 0 listening to Float 8, July 1989



Pulse Leading Edges. Float 8 listening to Float 0, July 1989

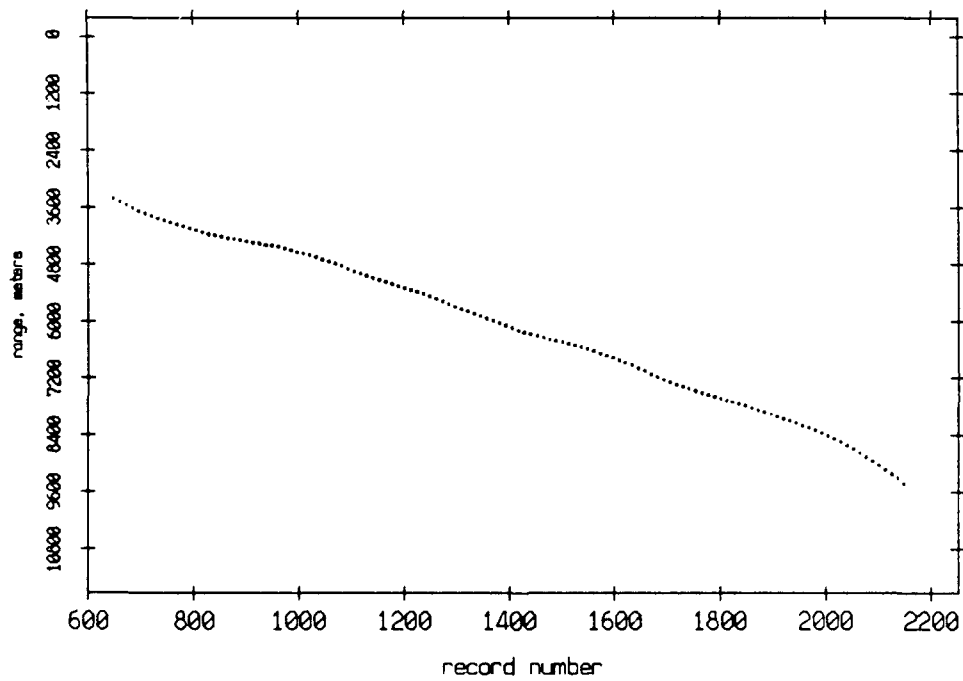
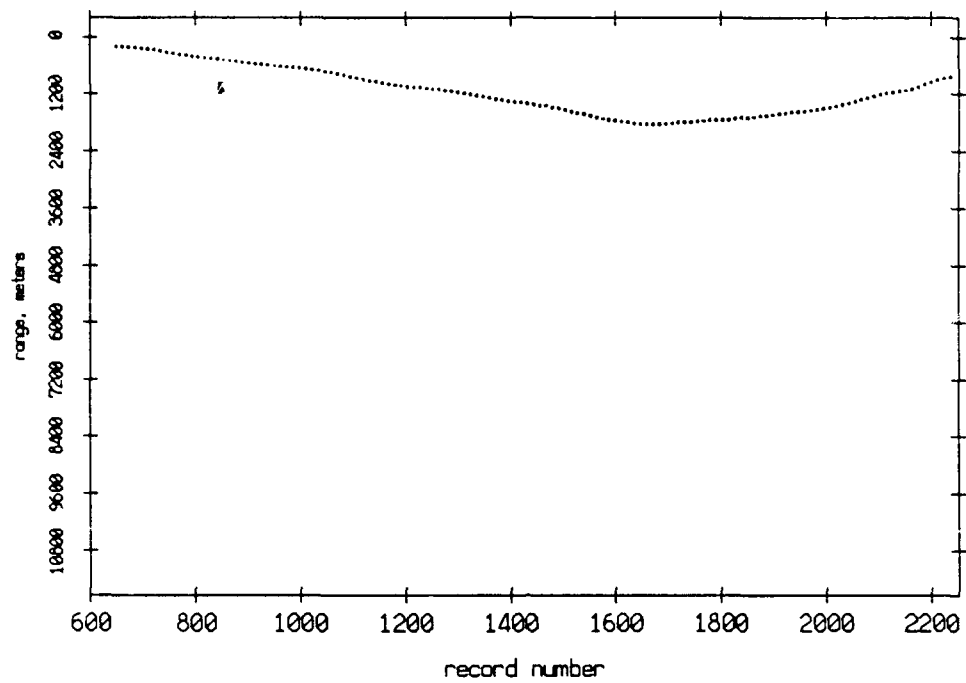


Figure 3.50

Pulse Leading Edges. Float 1 listening to Float 2, July 1989



Pulse Leading Edges. Float 2 listening to Float 1, July 1989

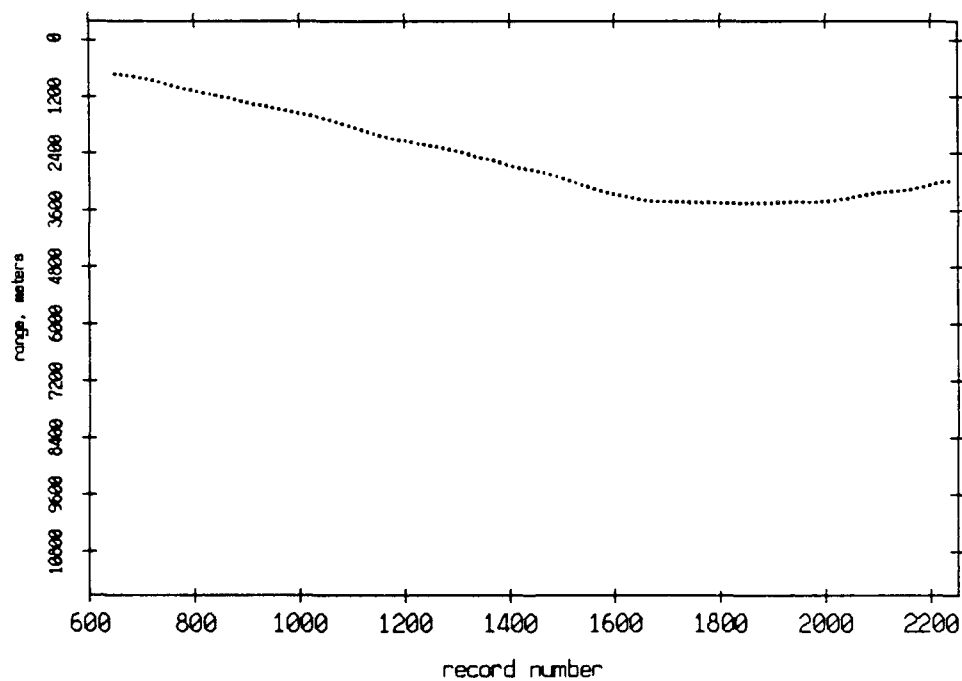
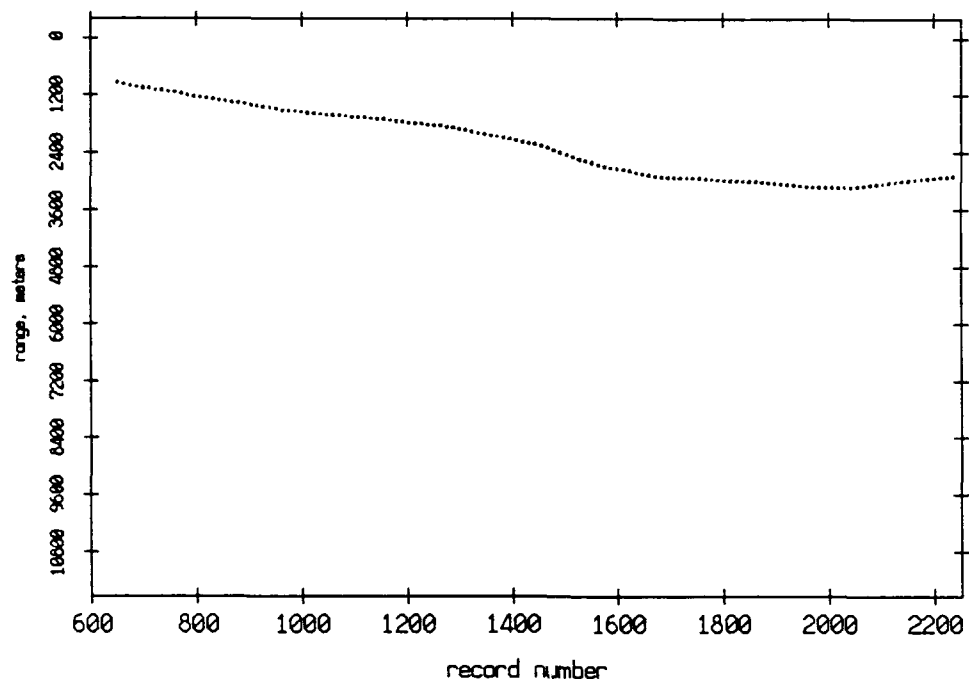


Figure 3.51

Pulse Leading Edges. Float 1 listening to Float 3, July 1989



Pulse Leading Edges. Float 3 listening to Float 1, July 1989

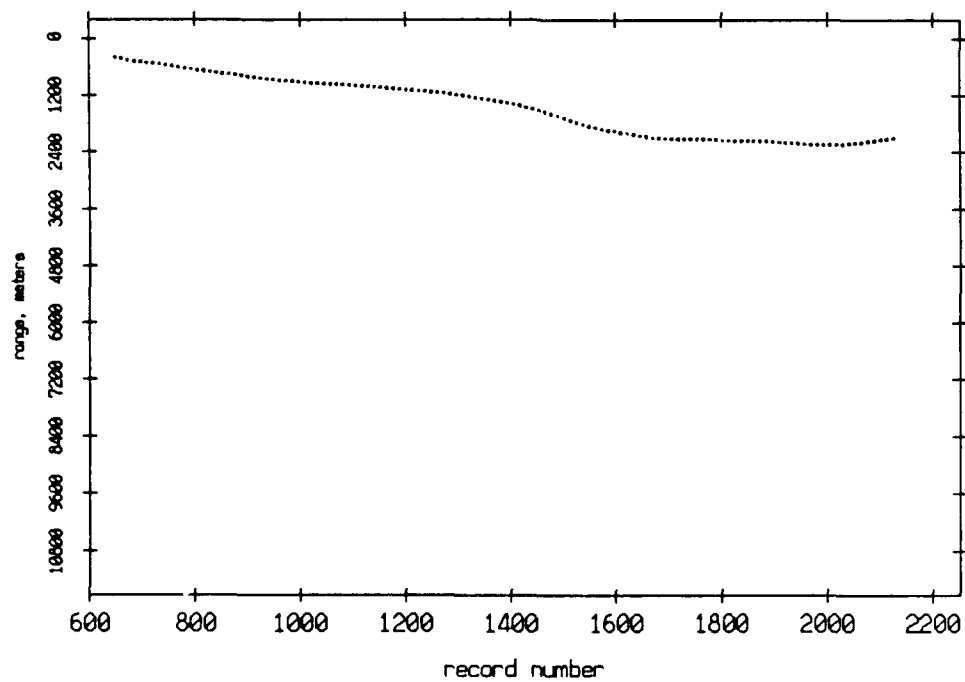
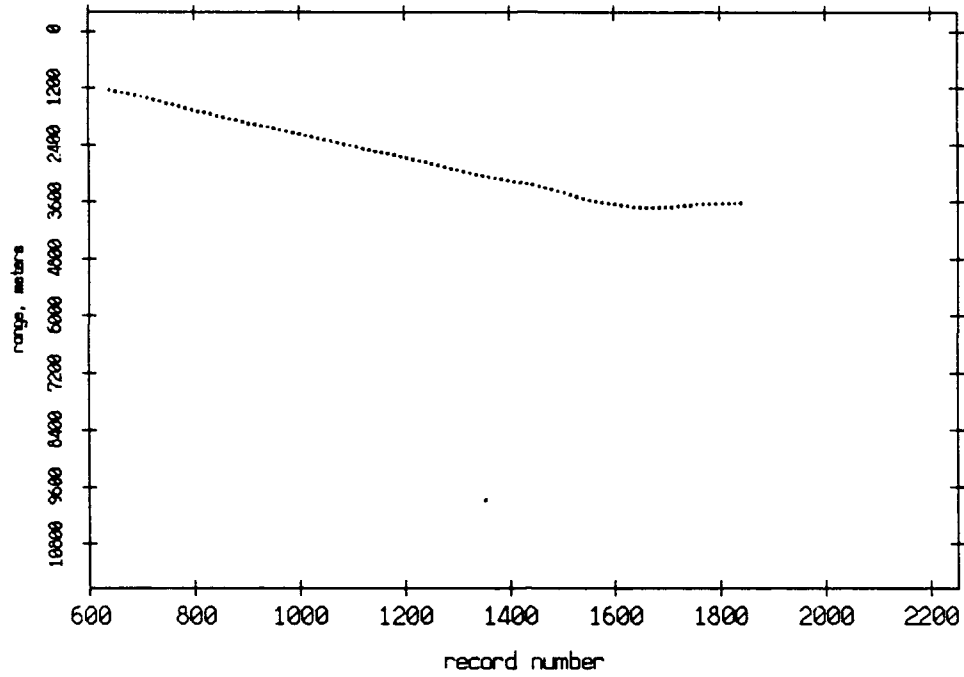


Figure 3.52

Pulse Leading Edges. Float 1 listening to Float 4, July 1989



Pulse Leading Edges. Float 4 listening to Float 1, July 1989

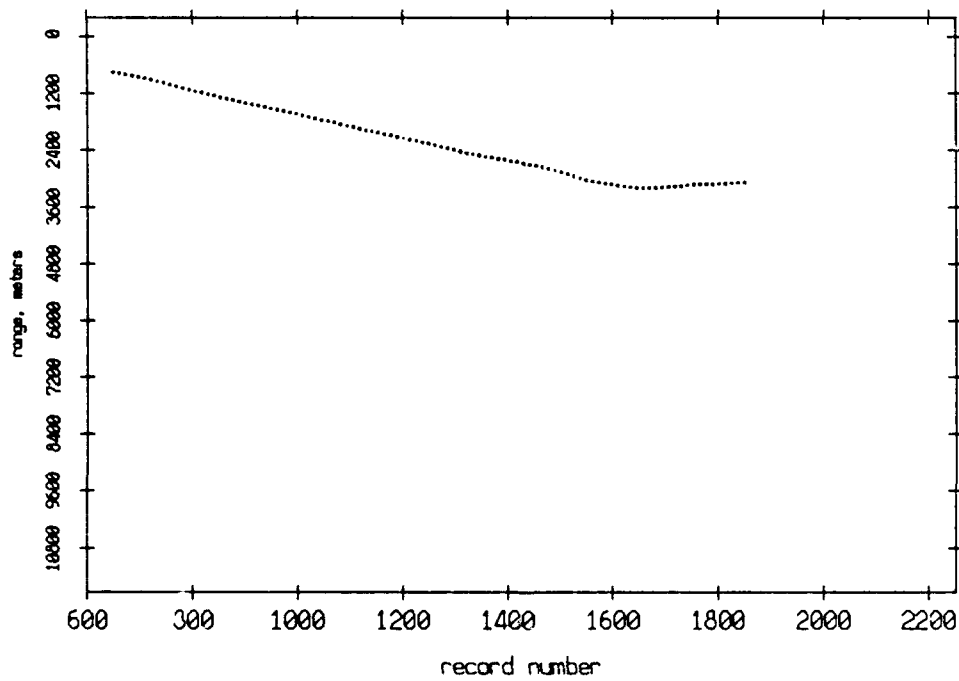
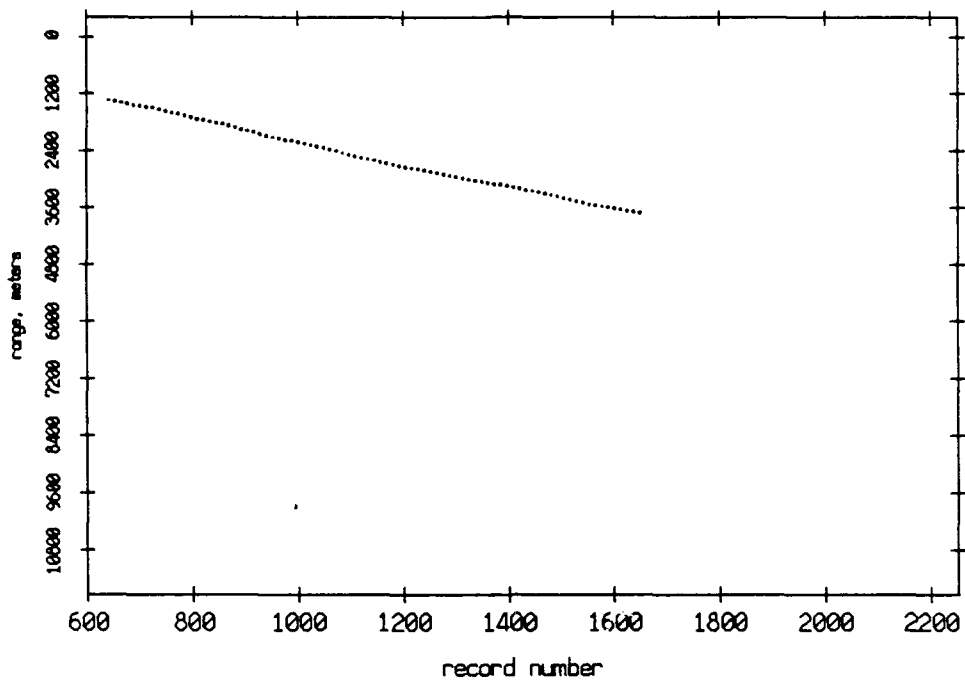


Figure 3.53

Pulse Leading Edges. Float 1 listening to Float 5, July 1989



Pulse Leading Edges. Float 5 listening to Float 1, July 1989

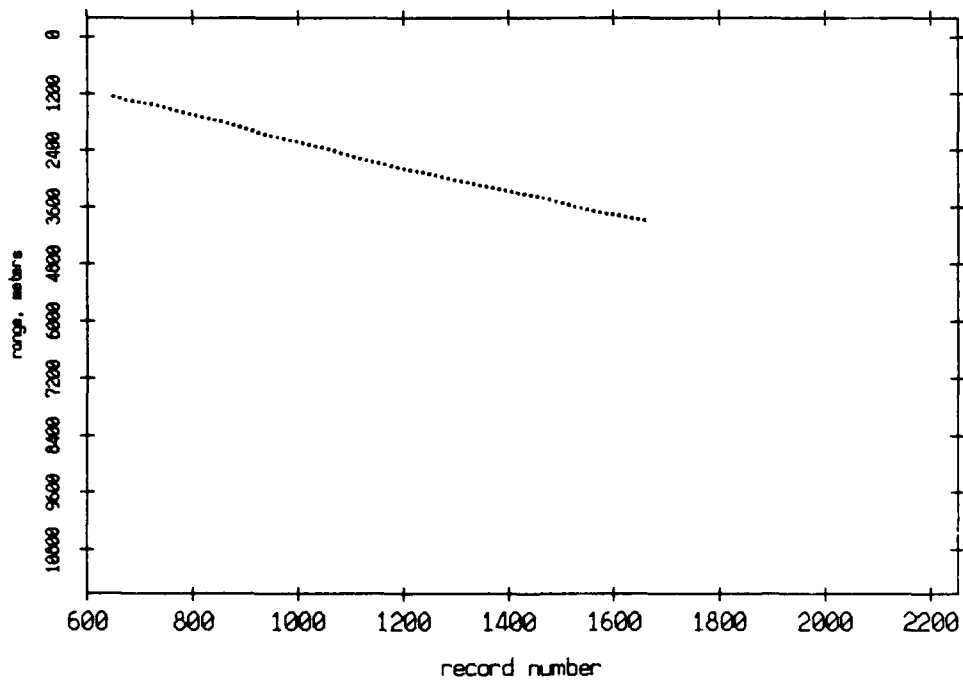
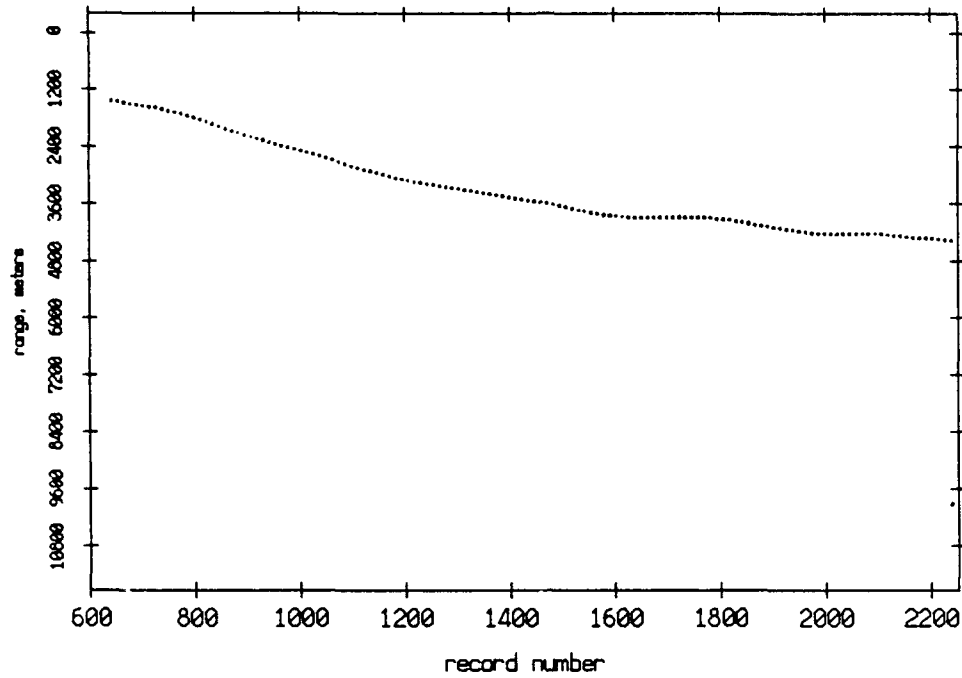


Figure 3.54

Pulse Leading Edges. Float 1 listening to Float 6, July 1989



Pulse Leading Edges. Float 6 listening to Float 1, July 1989

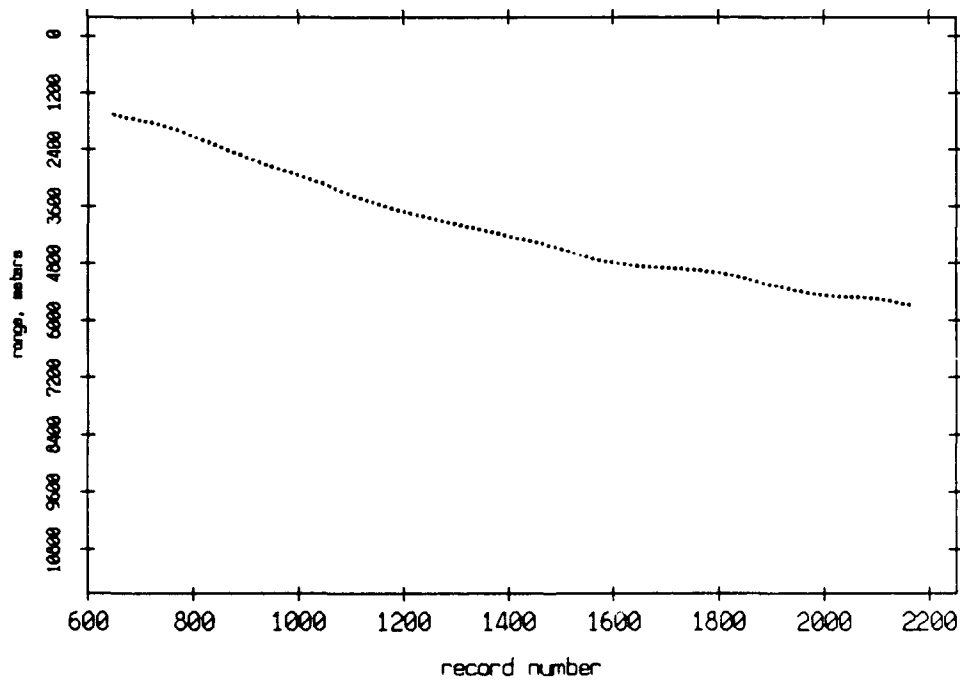
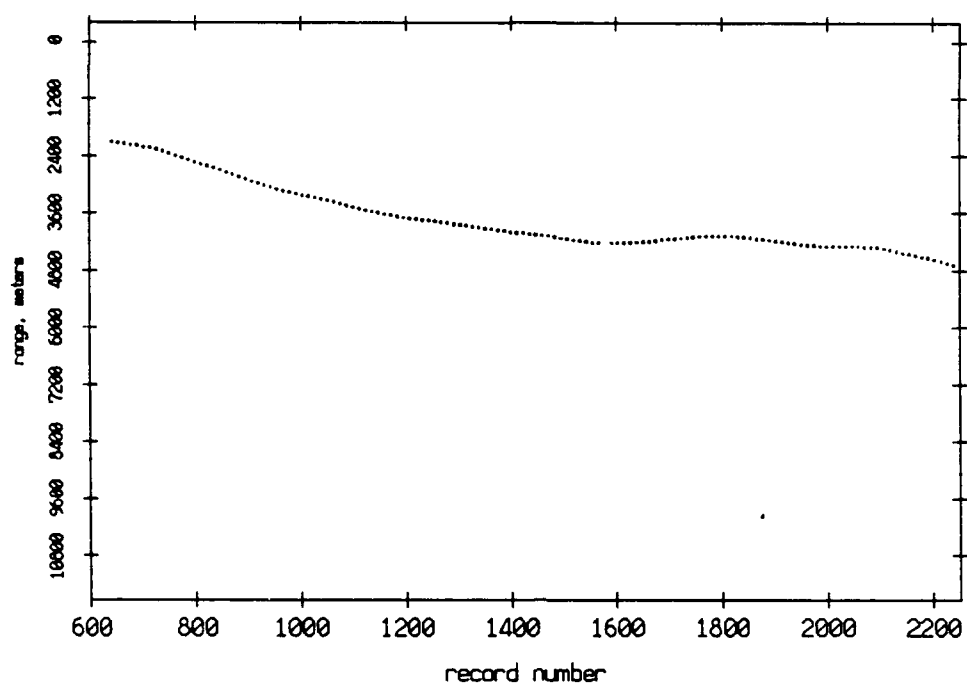


Figure 3.55

Pulse Leading Edges. Float 1 listening to Float 7, July 1989



Pulse Leading Edges. Float 7 listening to Float 1, July 1989

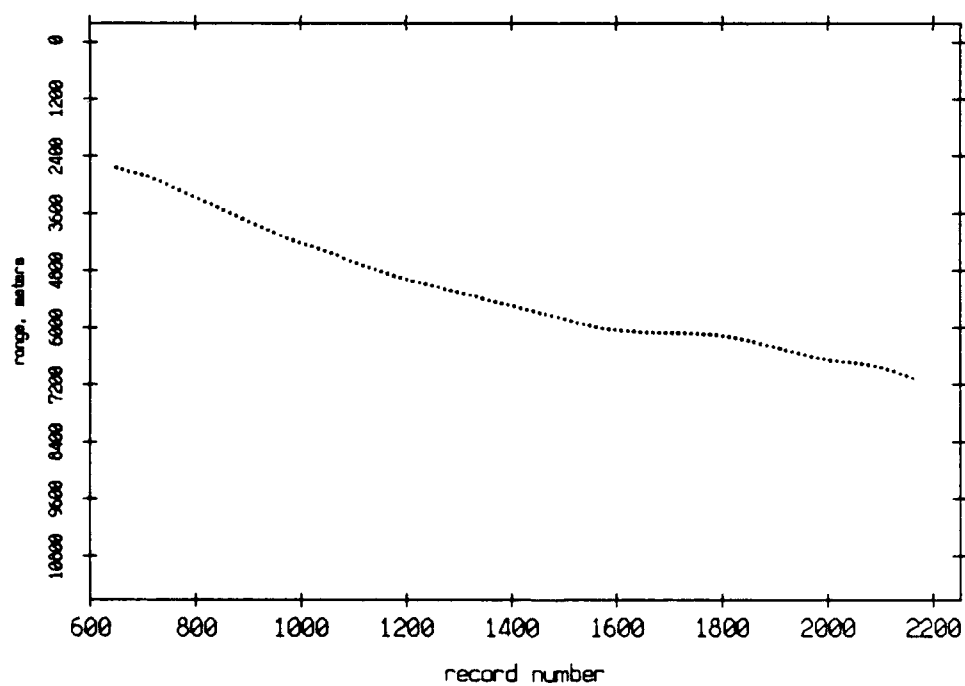
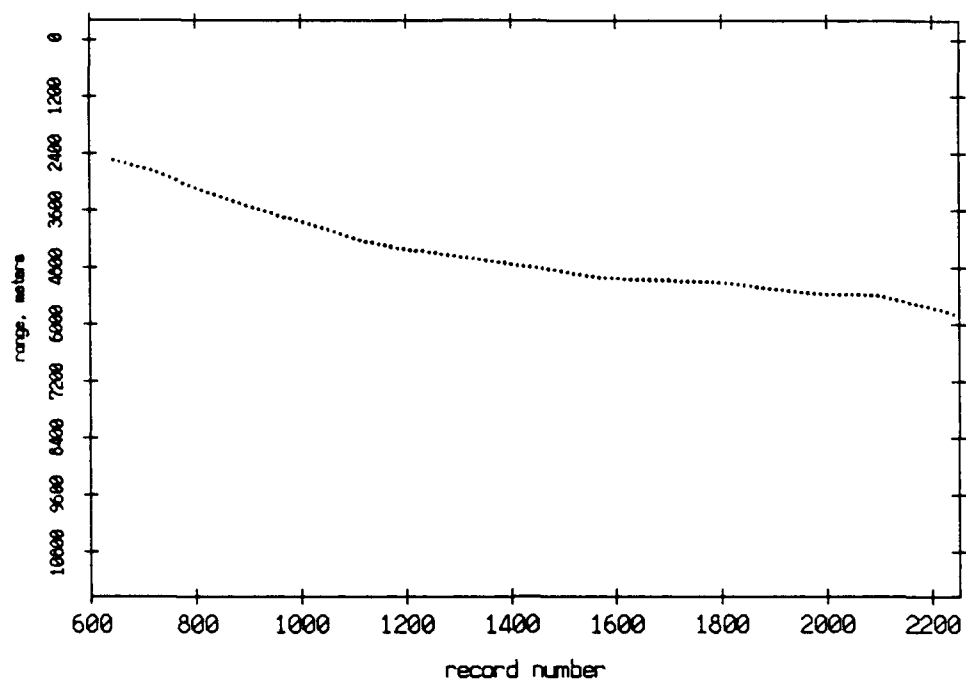


Figure 3.56

Pulse Leading Edges. Float 1 listening to Float 8, July 1989



Pulse Leading Edges. Float 8 listening to Float 1, July 1989

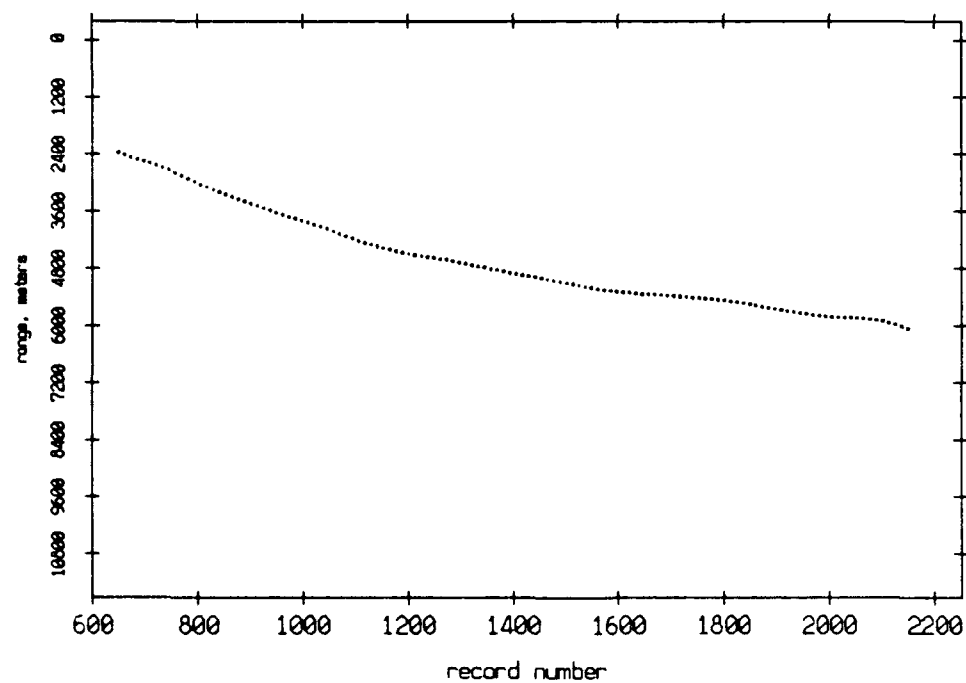
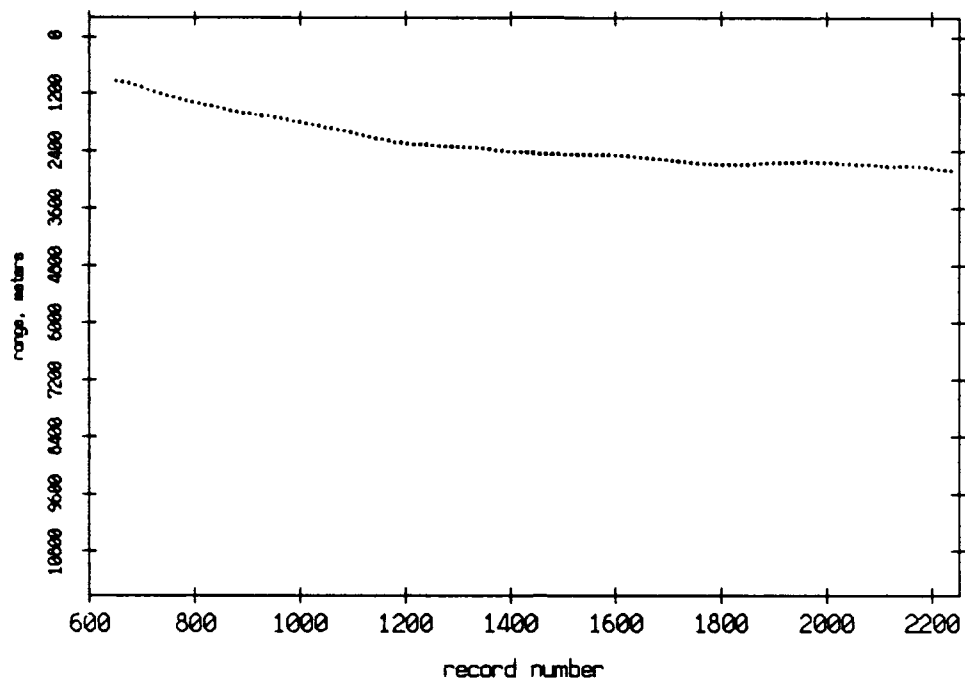


Figure 3.57

Pulse Leading Edges. Float 2 listening to Float 3, July 1989



Pulse Leading Edges. Float 3 listening to Float 2, July 1989

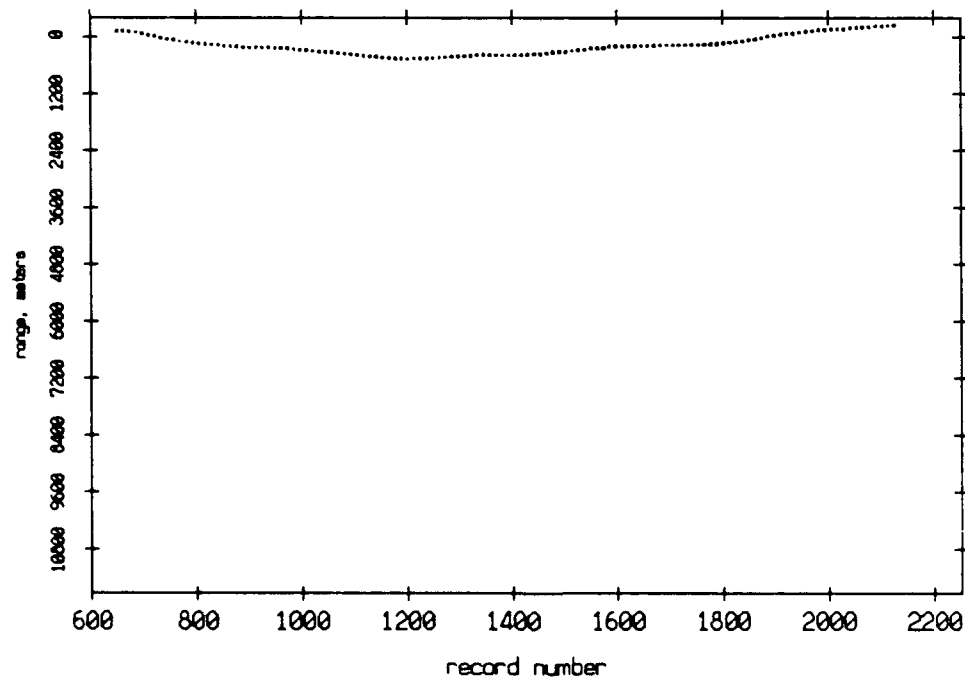
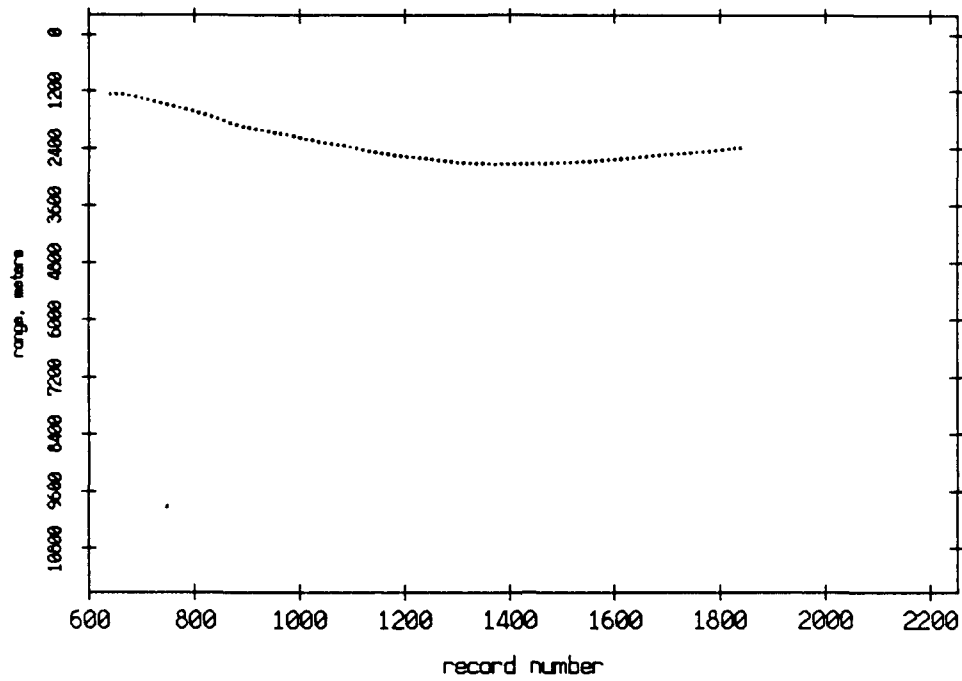


Figure 3.58

Pulse Leading Edges. Float 2 listening to Float 4, July 1989



Pulse Leading Edges. Float 4 listening to Float 2, July 1989

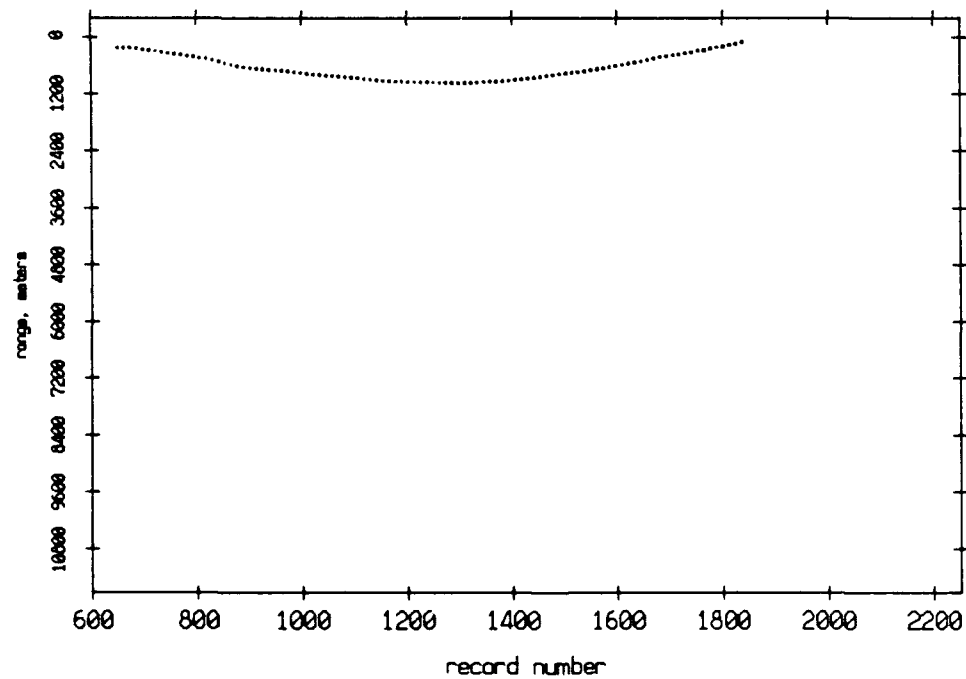
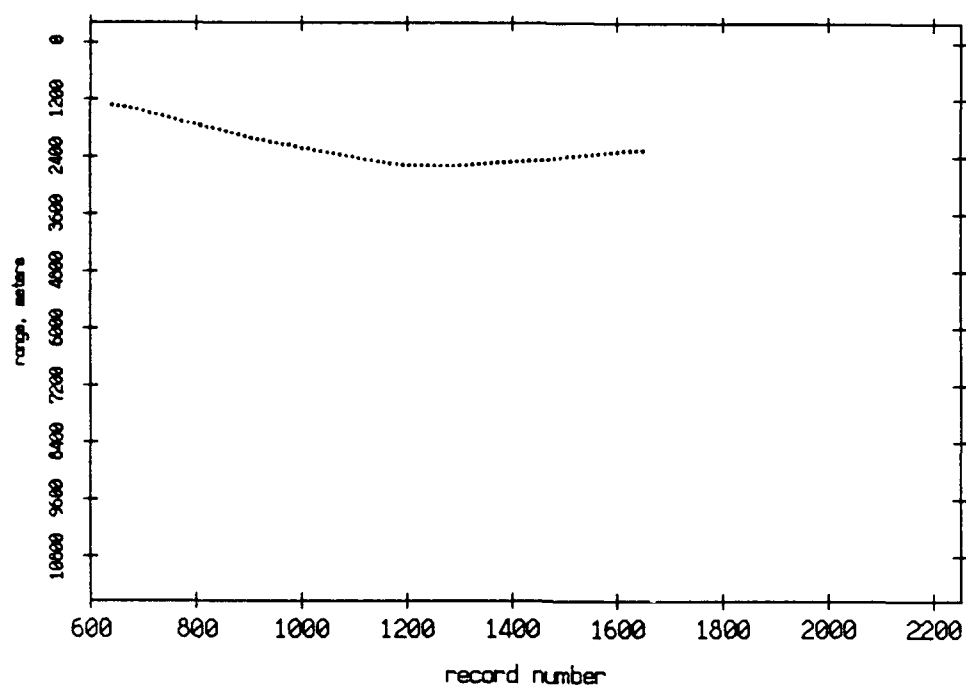


Figure 3.59

Pulse Leading Edges. Float 2 listening to Float 5, July 1989



Pulse Leading Edges. Float 5 listening to Float 2, July 1989

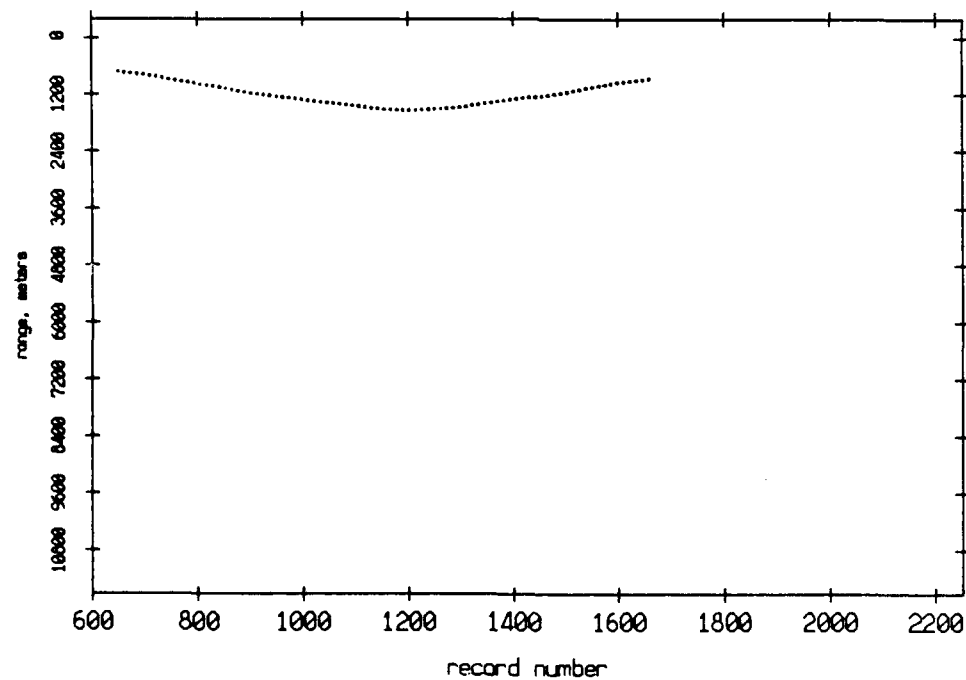
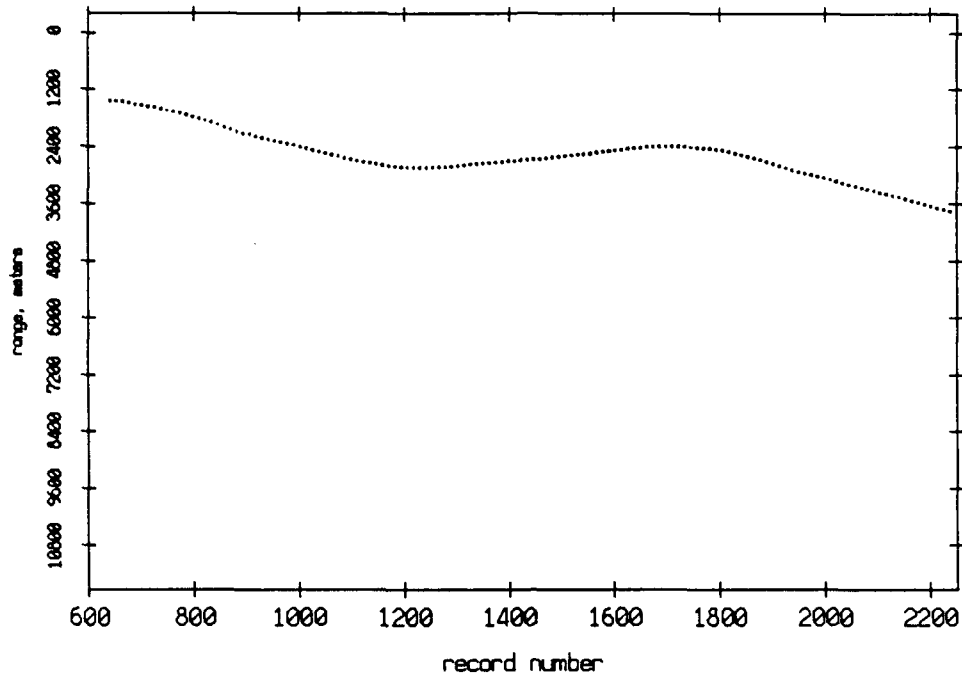


Figure 3.60

Pulse Leading Edges. Float 2 listening to Float 6, July 1989



Pulse Leading Edges. Float 6 listening to Float 2, July 1989

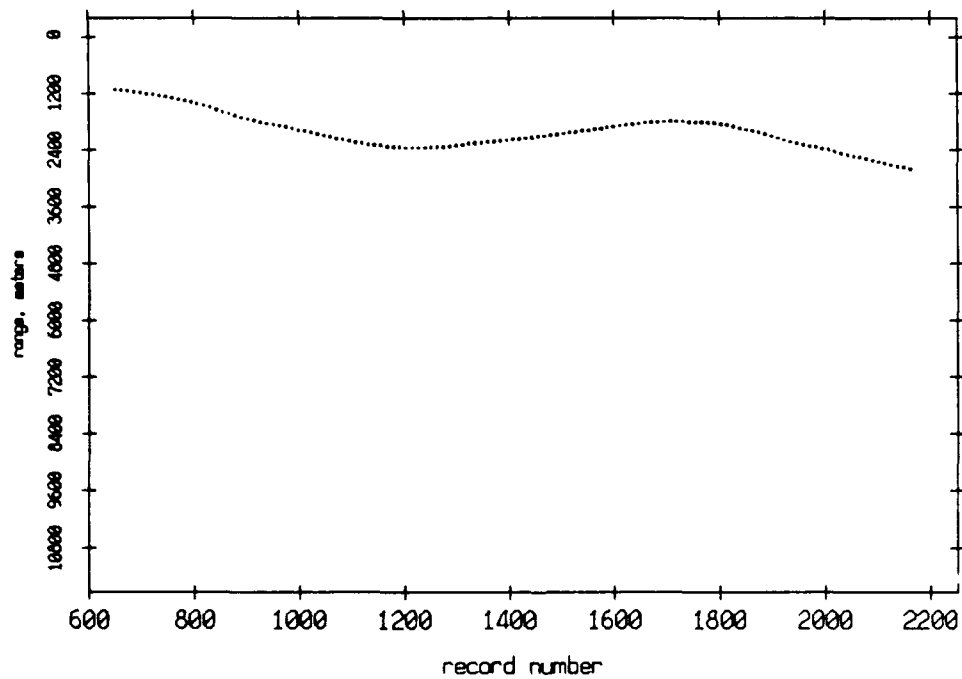
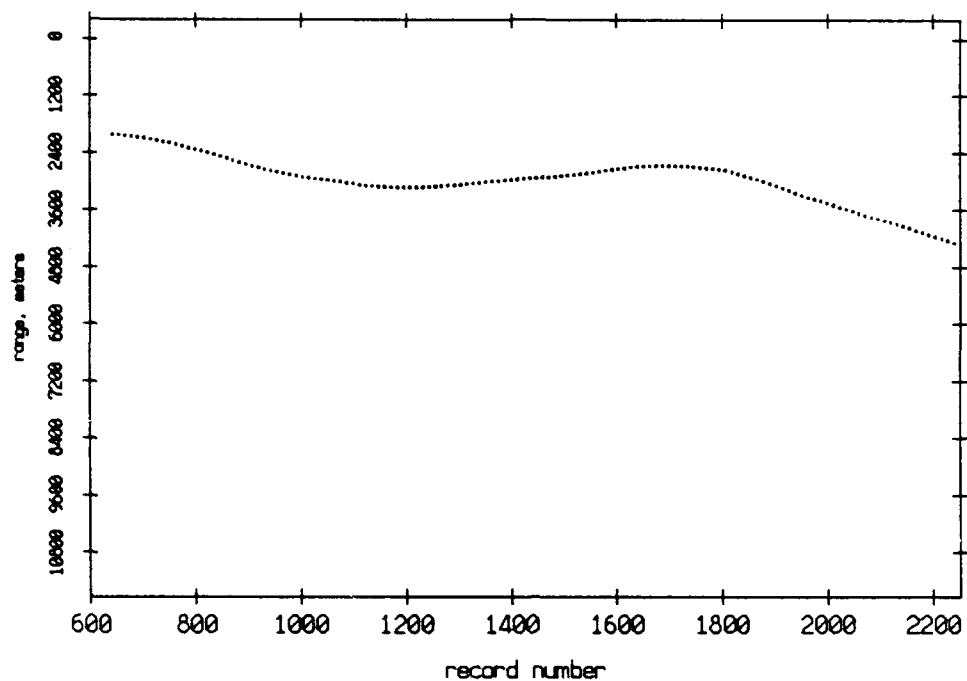


Figure 3.61

Pulse Leading Edges. Float 2 listening to Float 7, July 1989



Pulse Leading Edges. Float 7 listening to Float 2, July 1989

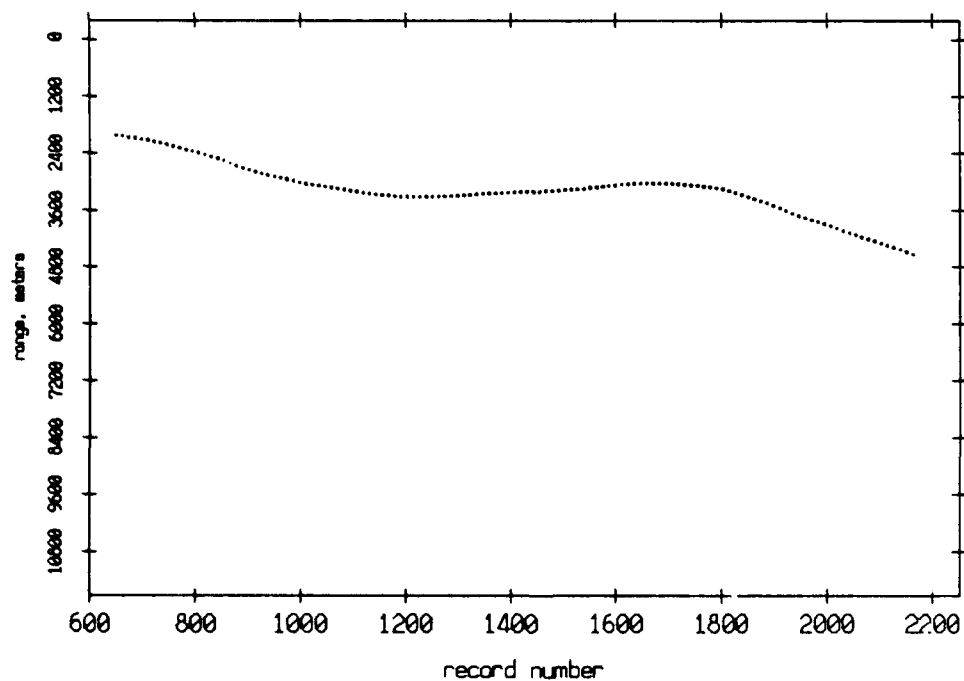
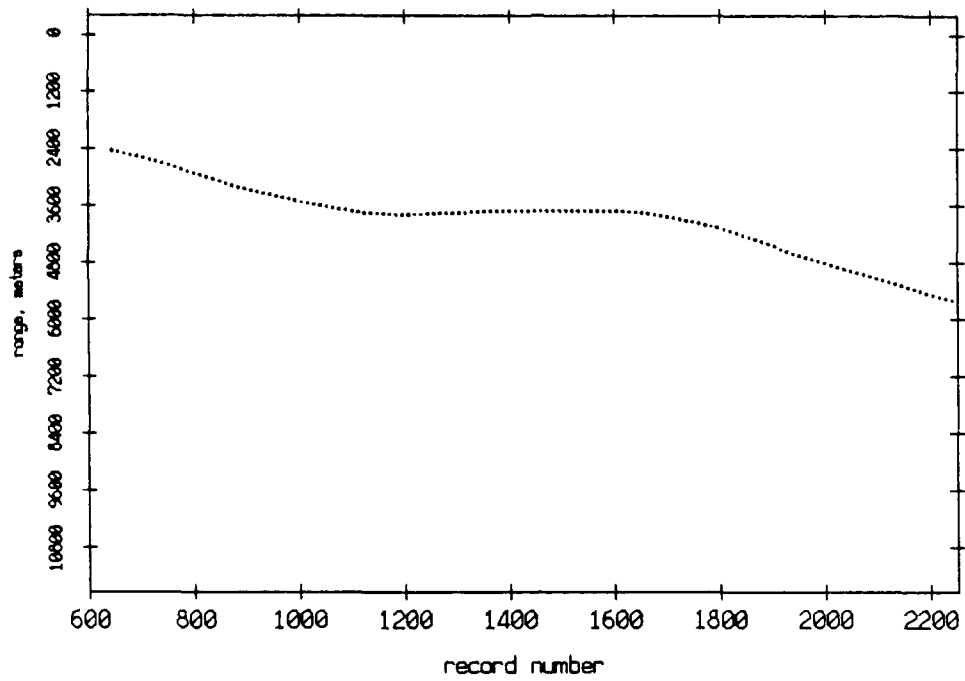


Figure 3.62

Pulse Leading Edges. Float 2 listening to Float 8, July 1989



Pulse Leading Edges. Float 8 listening to Float 2, July 1989

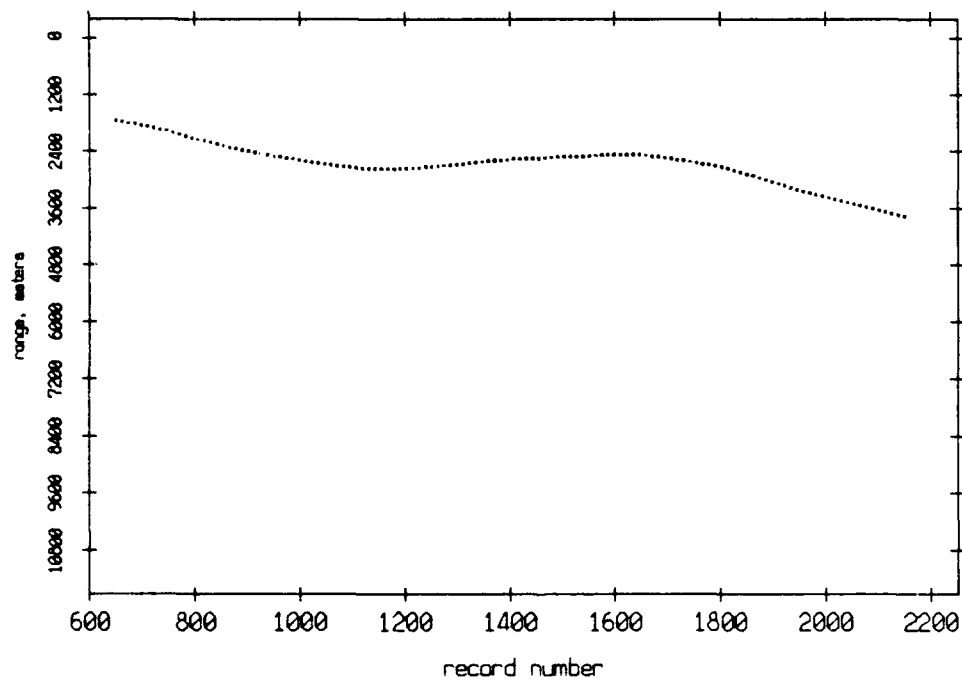
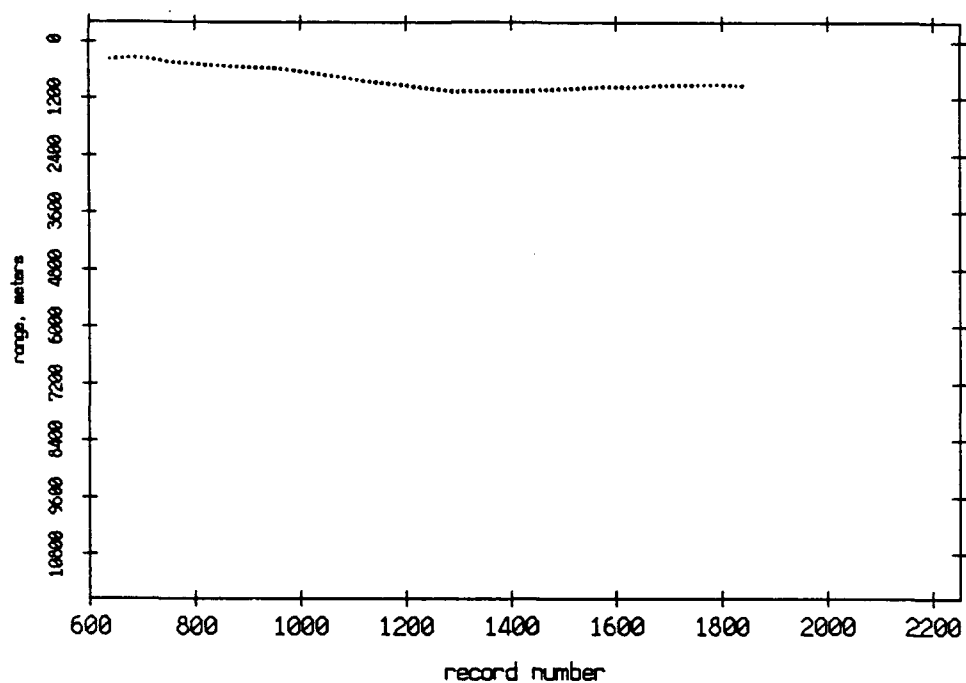


Figure 3.63

Pulse Leading Edges. Float 3 listening to Float 4, July 1989



Pulse Leading Edges. Float 4 listening to Float 3, July 1989

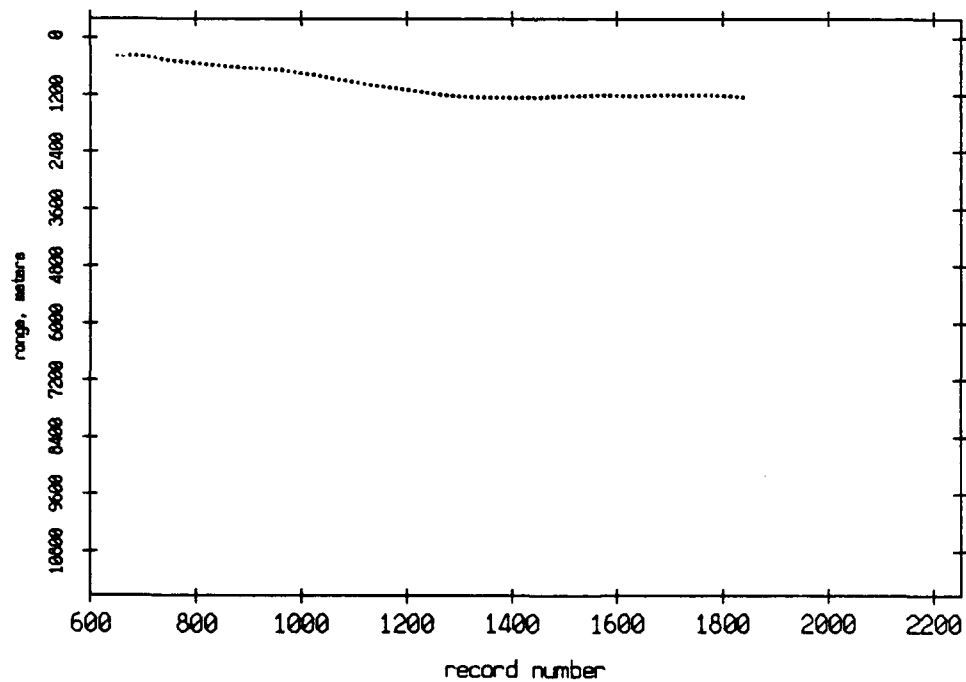
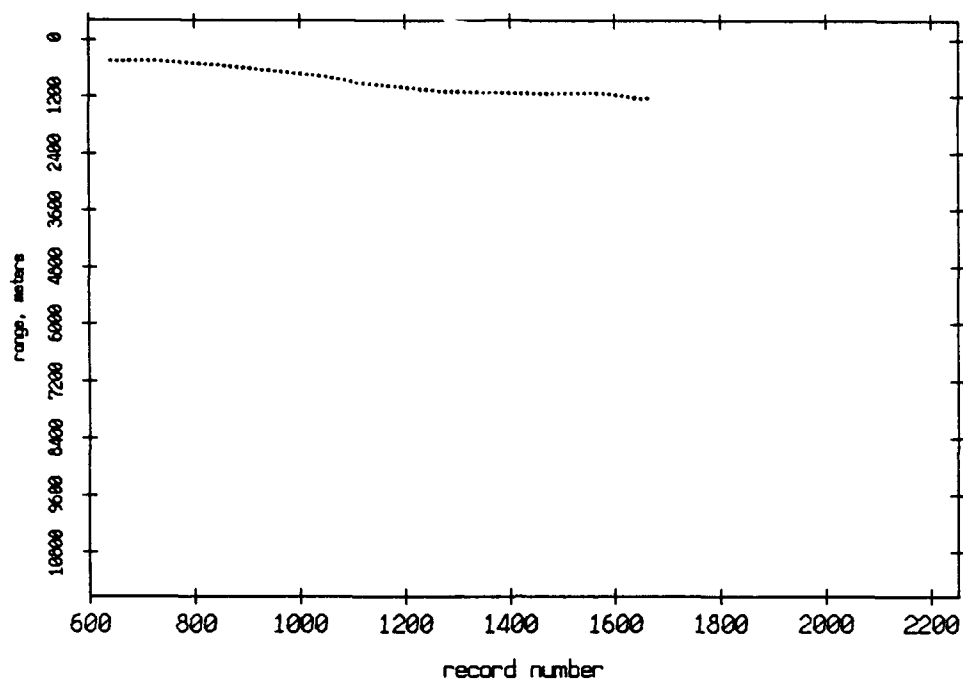


Figure 3.64

Pulse Leading Edges. Float 3 listening to Float 5, July 1989



Pulse Leading Edges. Float 5 listening to Float 3, July 1989

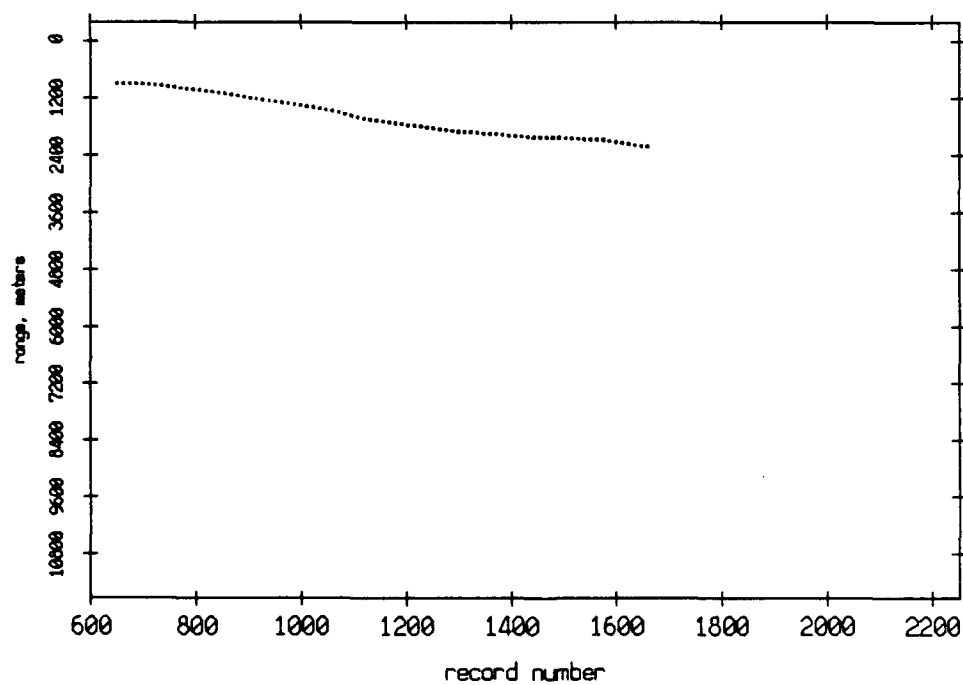
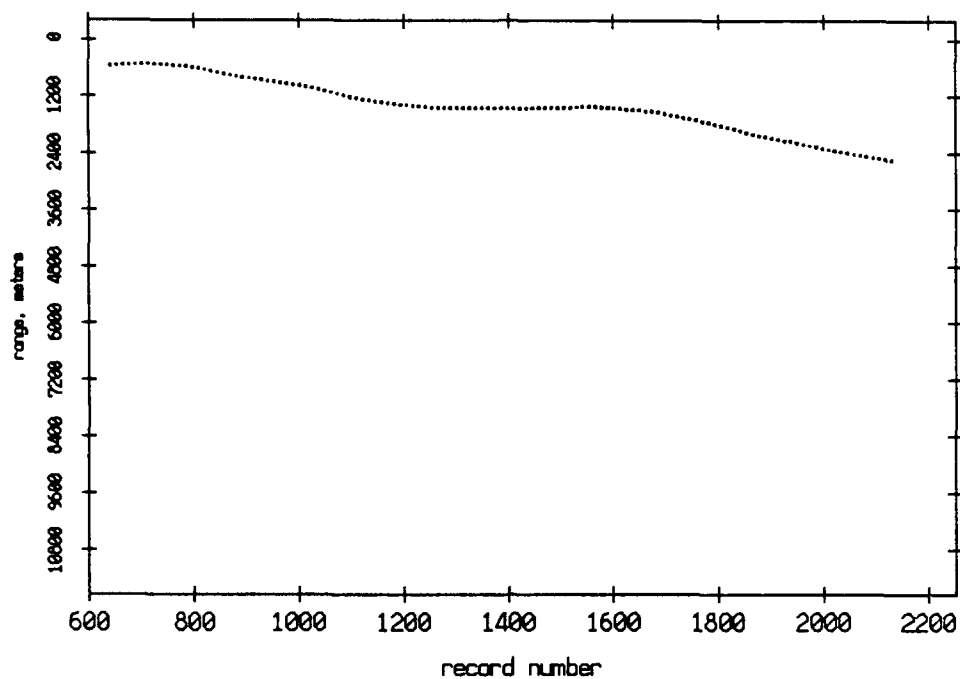


Figure 3.65

Pulse Leading Edges. Float 3 listening to Float 6, July 1989



Pulse Leading Edges. Float 6 listening to Float 3, July 1989

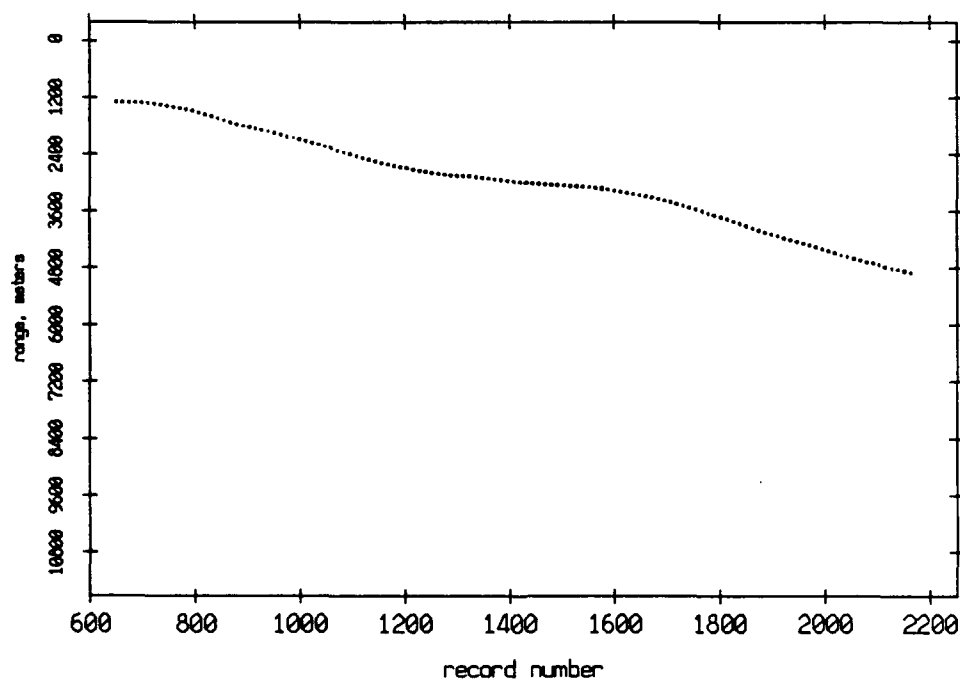
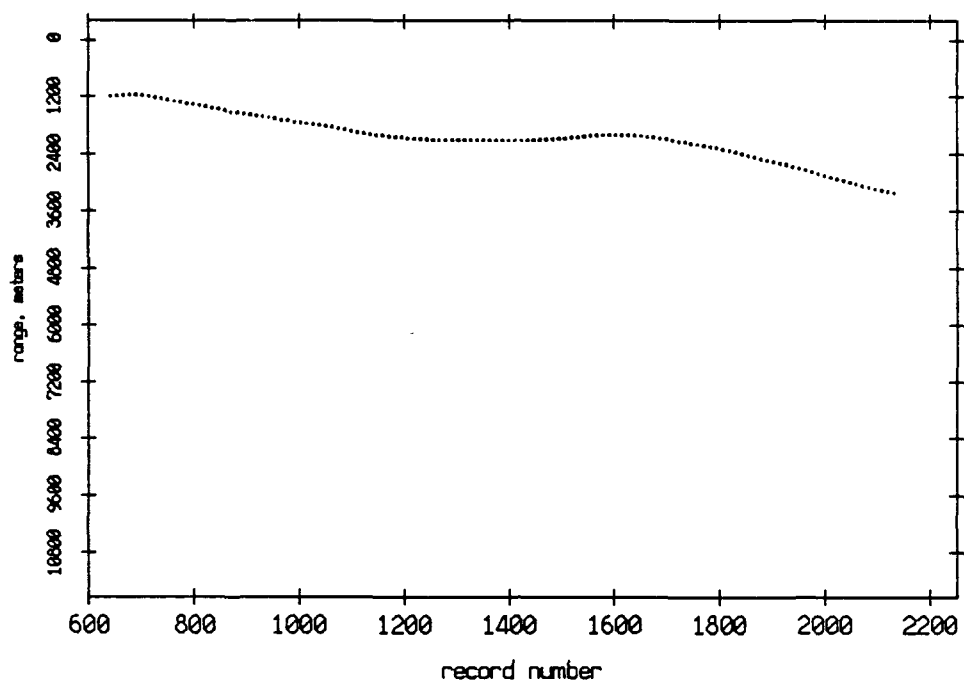


Figure 3.66

Pulse Leading Edges. Float 3 listening to Float 7, July 1989



Pulse Leading Edges. Float 7 listening to Float 3, July 1989

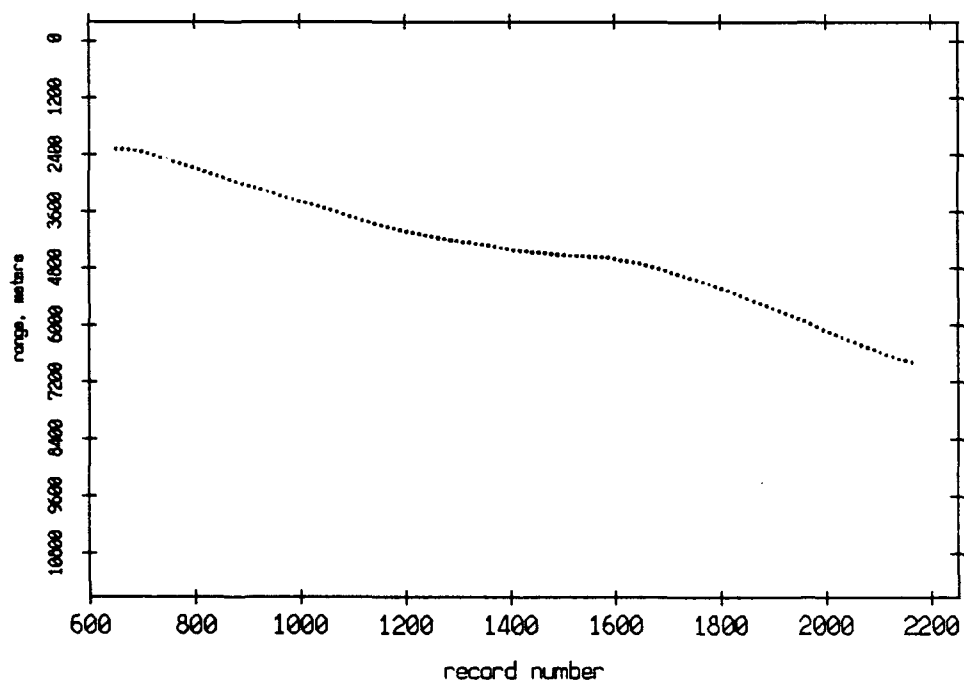
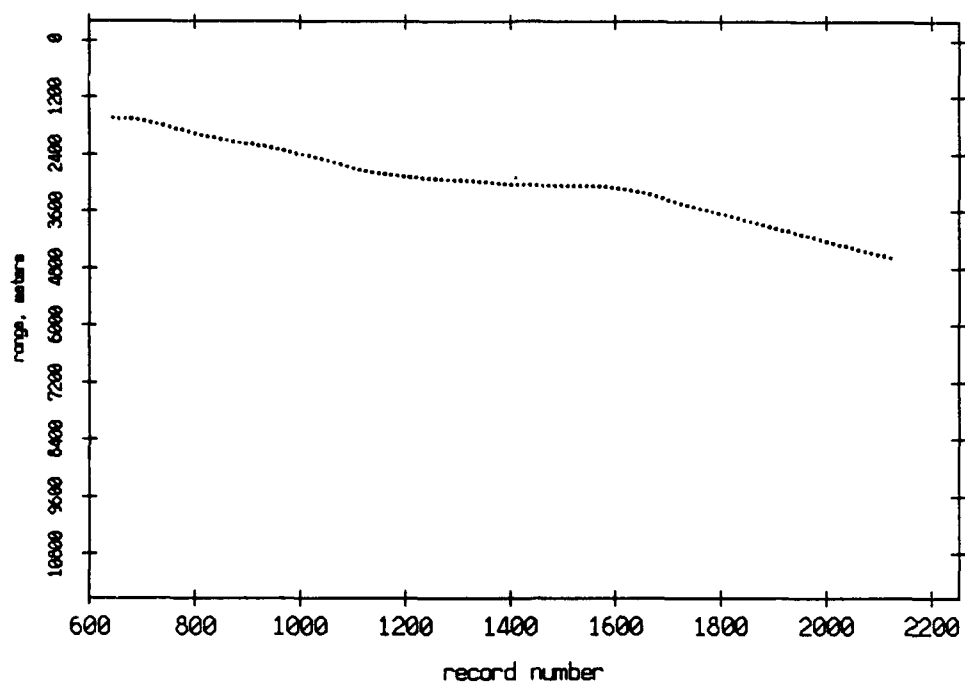


Figure 3.67

Pulse Leading Edges. Float 3 listening to Float 8, July 1989



Pulse Leading Edges. Float 8 listening to Float 3, July 1989

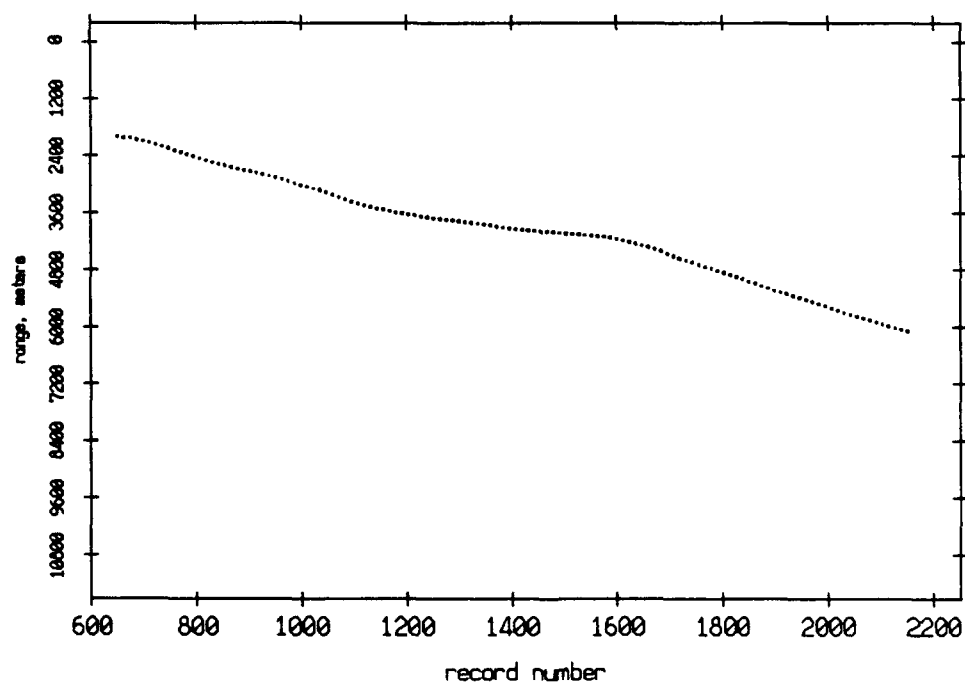
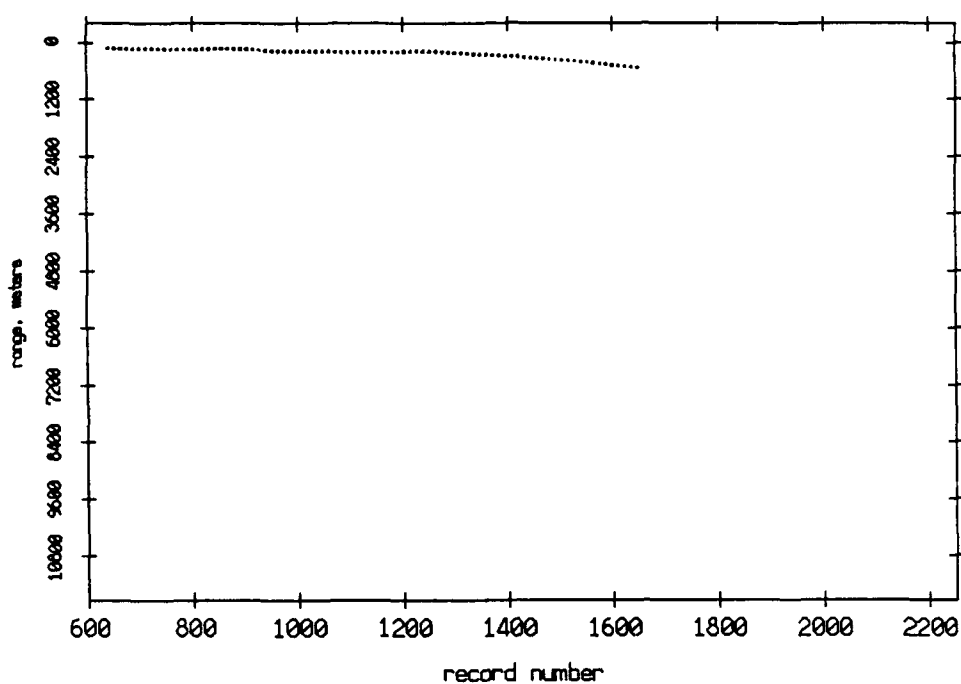


Figure 3.68

Pulse Leading Edges. Float 4 listening to Float 5, July 1989



Pulse Leading Edges. Float 5 listening to Float 4, July 1989

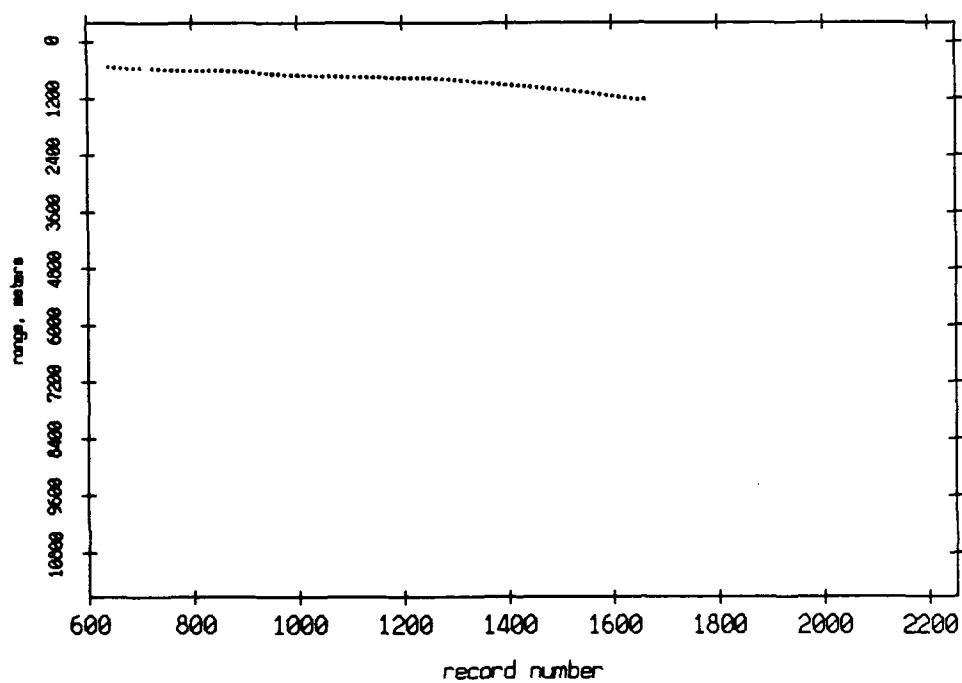
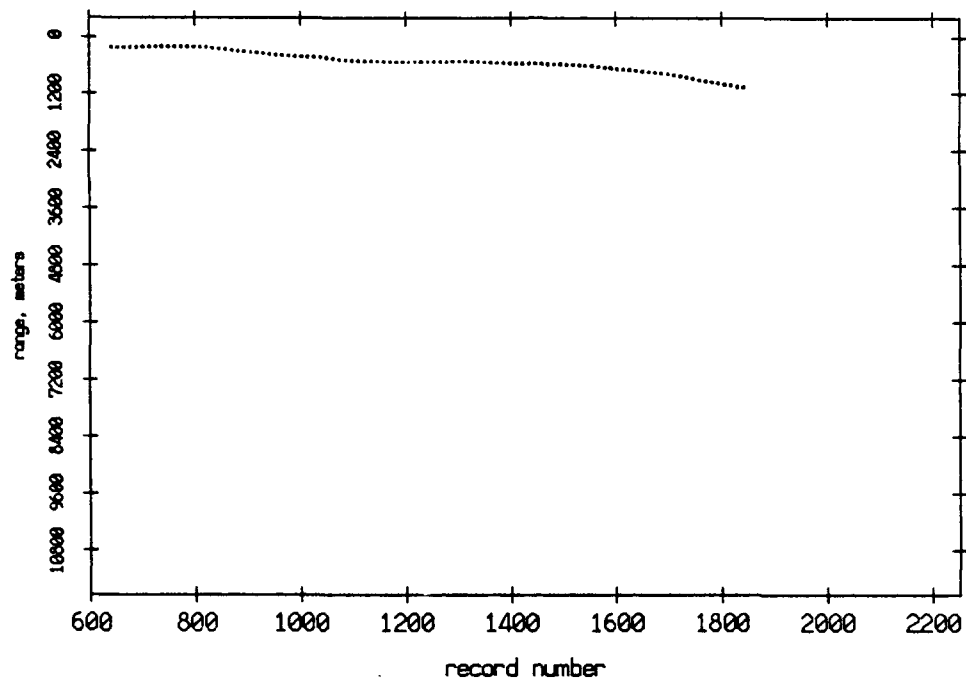


Figure 3.69

Pulse Leading Edges. Float 4 listening to Float 6, July 1989



Pulse Leading Edges. Float 6 listening to Float 4, July 1989

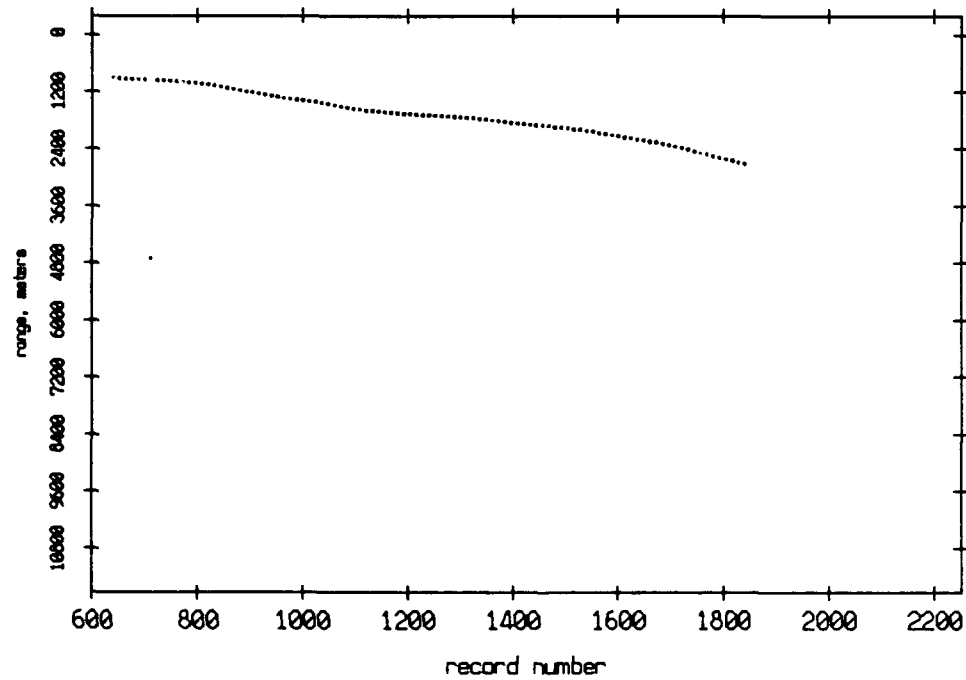
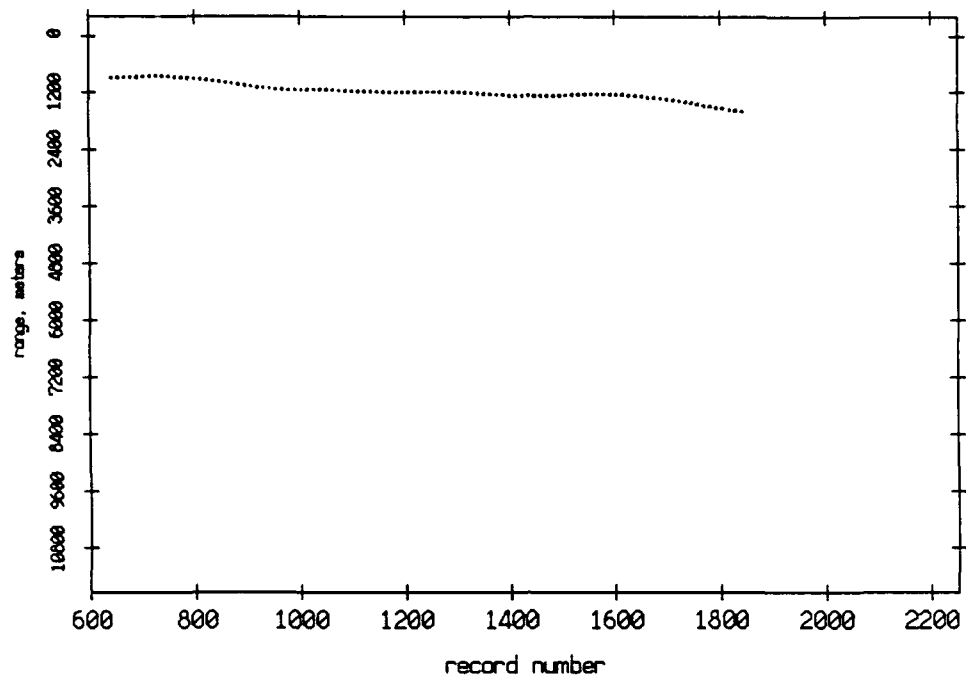


Figure 3.70

Pulse Leading Edges. Float 4 listening to Float 7, July 1989



Pulse Leading Edges. Float 7 listening to Float 4, July 1989

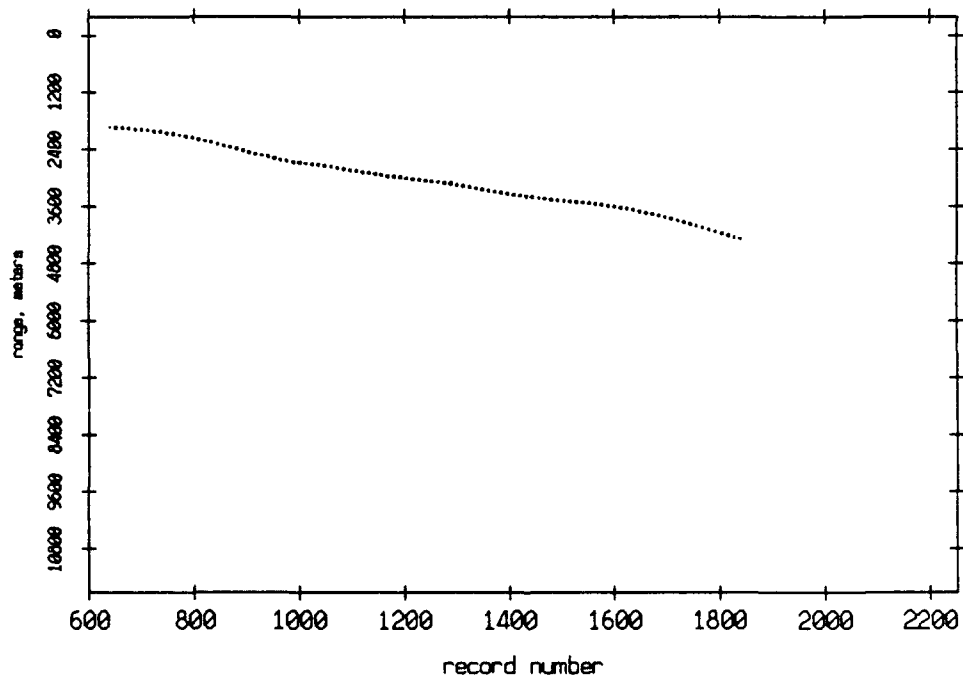
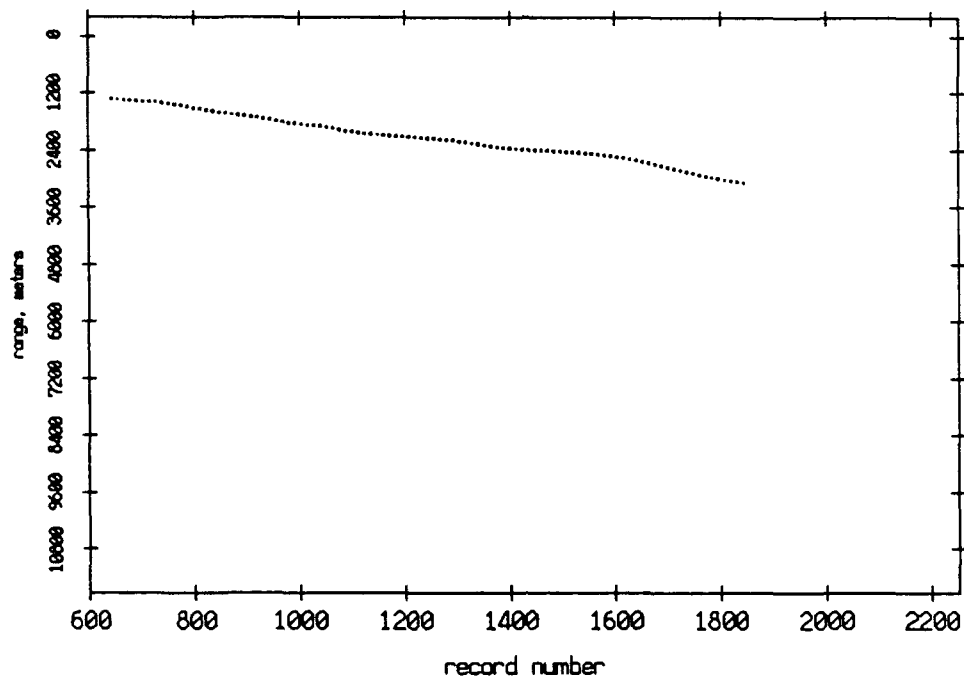


Figure 3.71

Pulse Leading Edges. Float 4 listening to Float 8, July 1989



Pulse Leading Edges. Float 8 listening to Float 4, July 1989

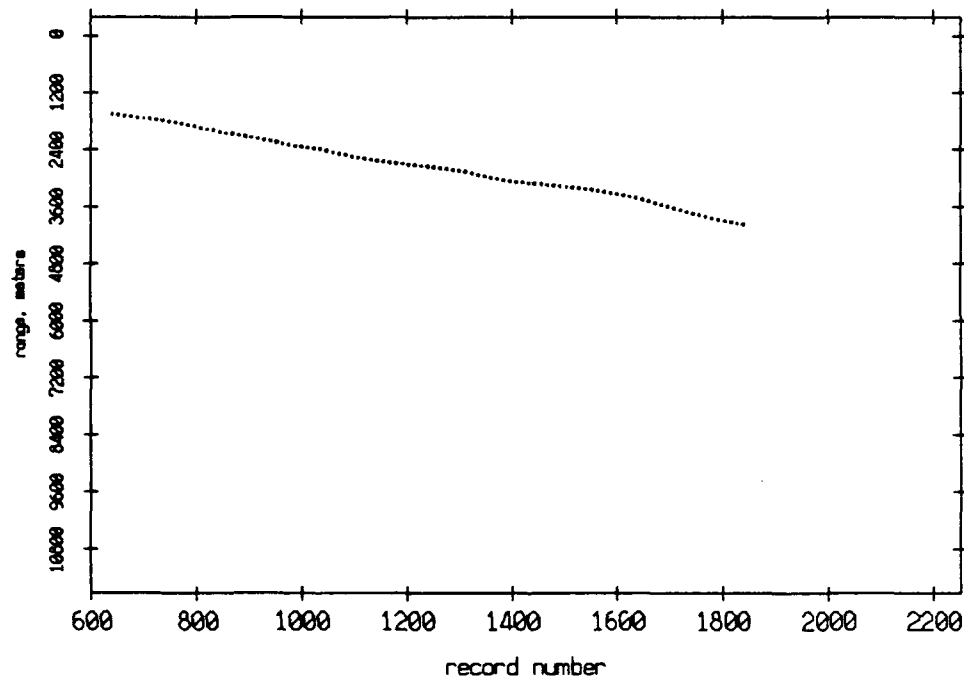
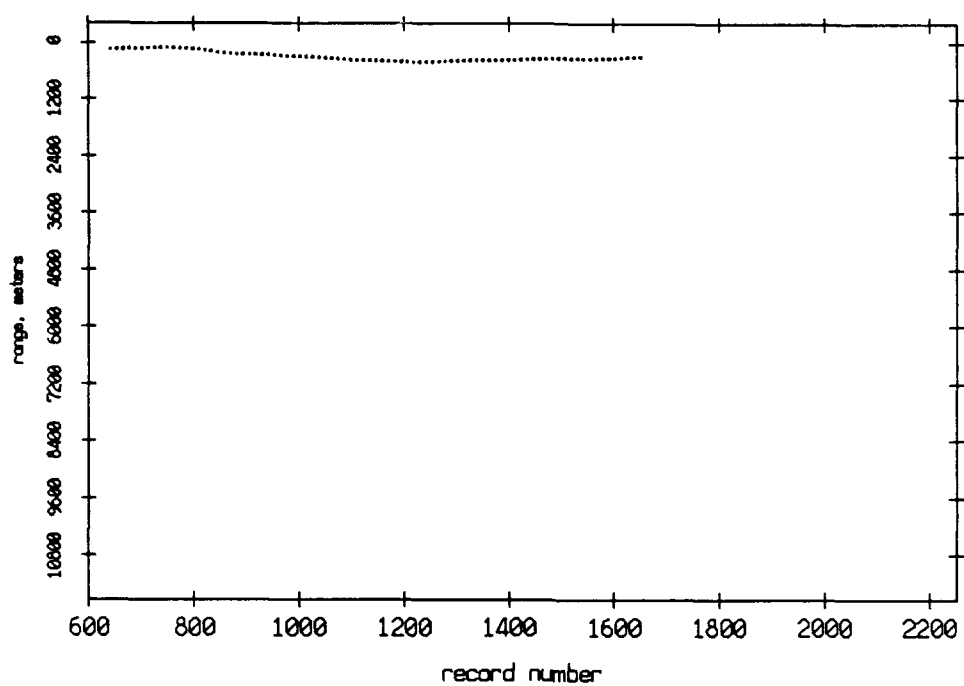


Figure 3.72

Pulse Leading Edges. Float 5 listening to Float 6, July 1989



Pulse Leading Edges. Float 6 listening to Float 5, July 1989

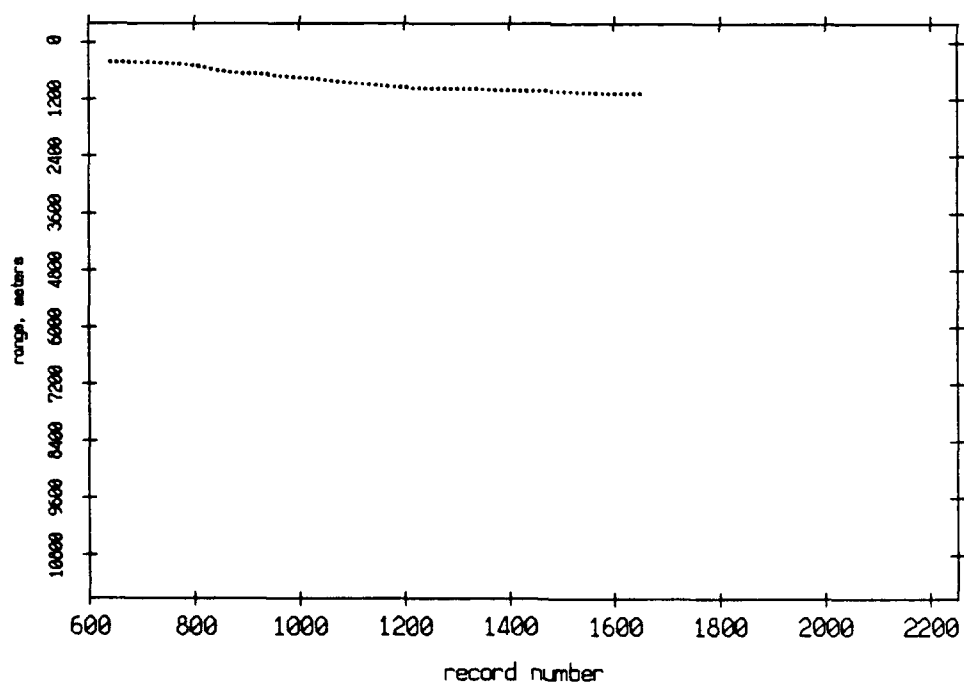
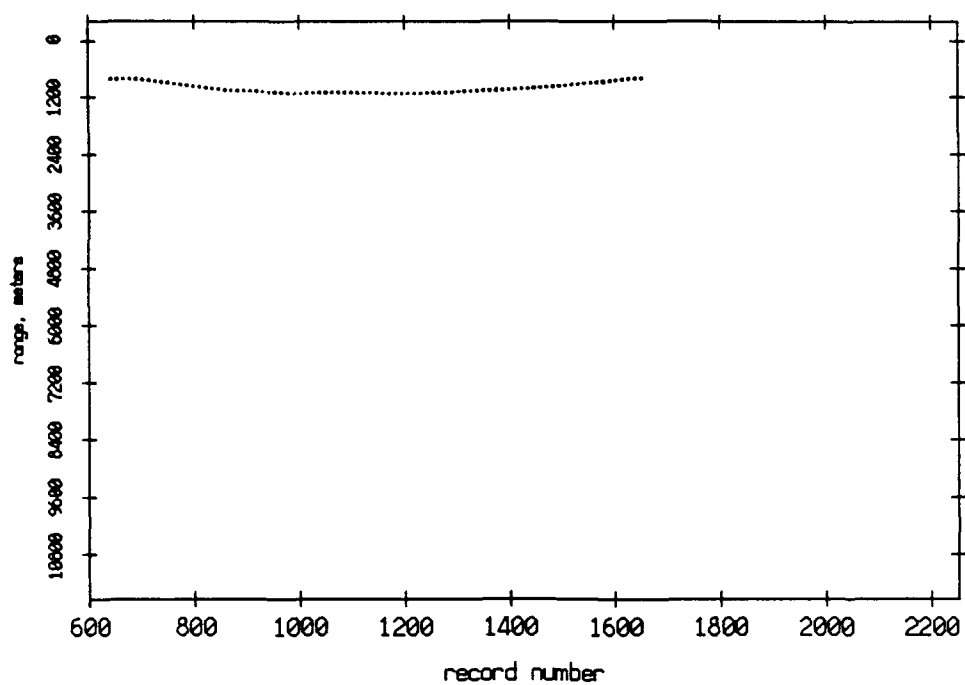


Figure 3.73

Pulse Leading Edges. Float 5 listening to Float 7, July 1989



Pulse Leading Edges. Float 7 listening to Float 5, July 1989

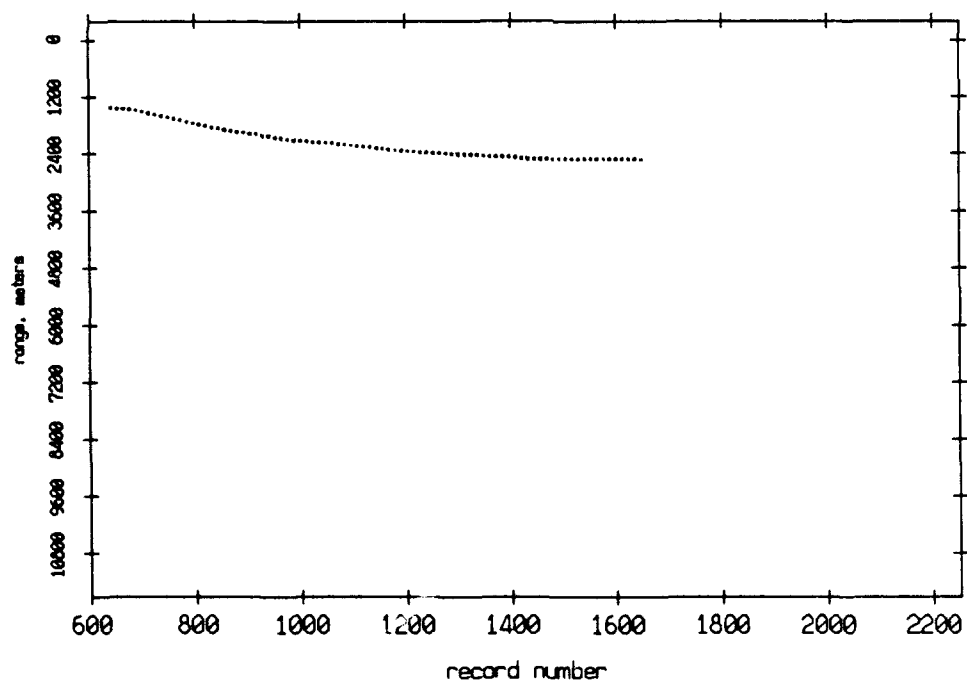
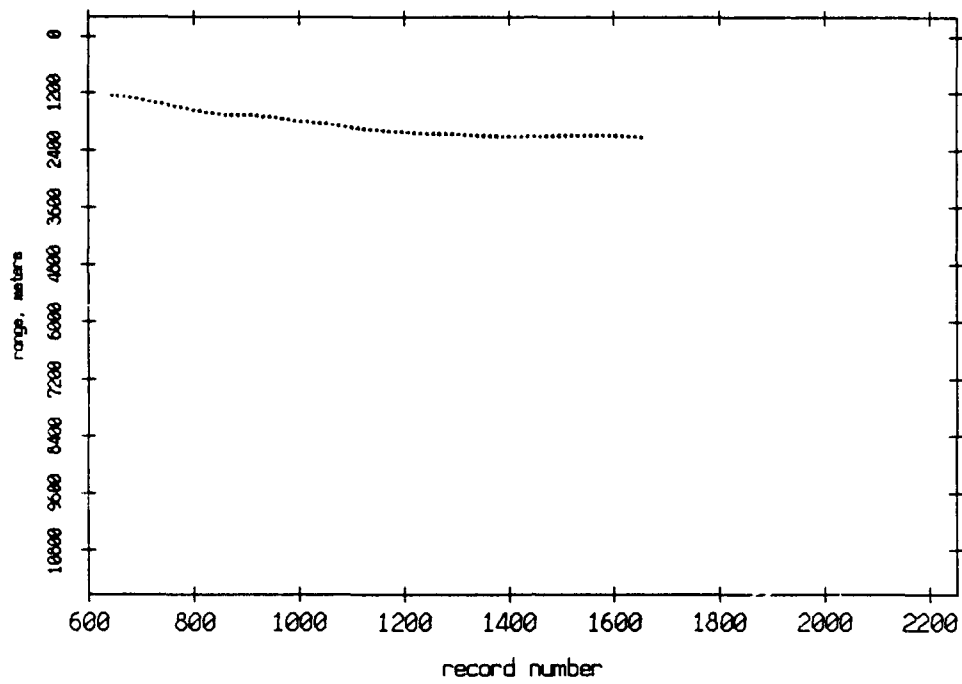


Figure 3.74

Pulse Leading Edges. Float 5 listening to Float 8, July 1989



Pulse Leading Edges. Float 8 listening to Float 5, July 1989

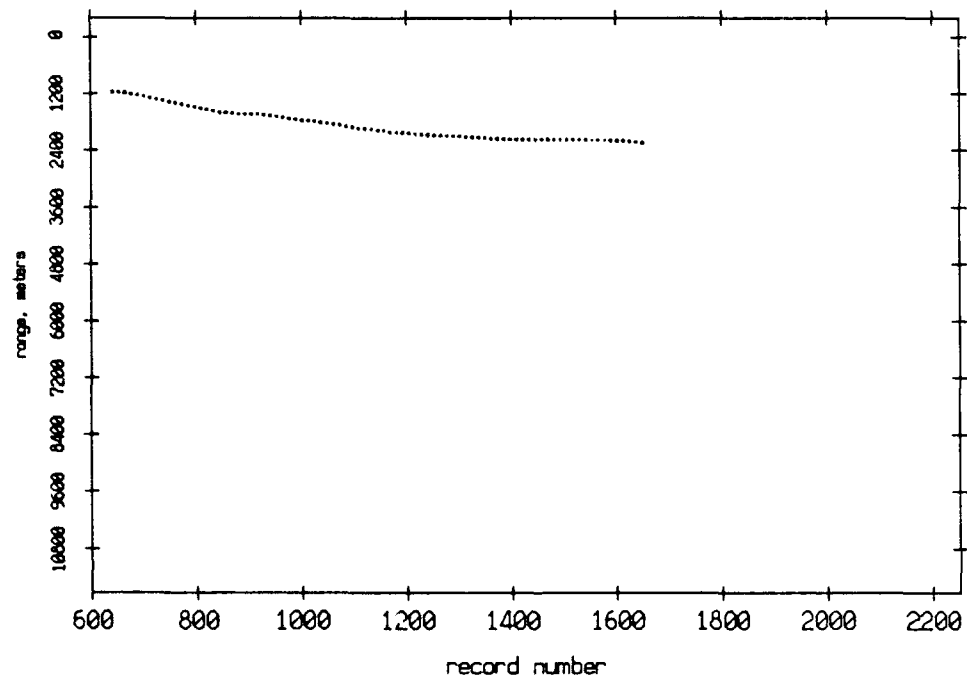
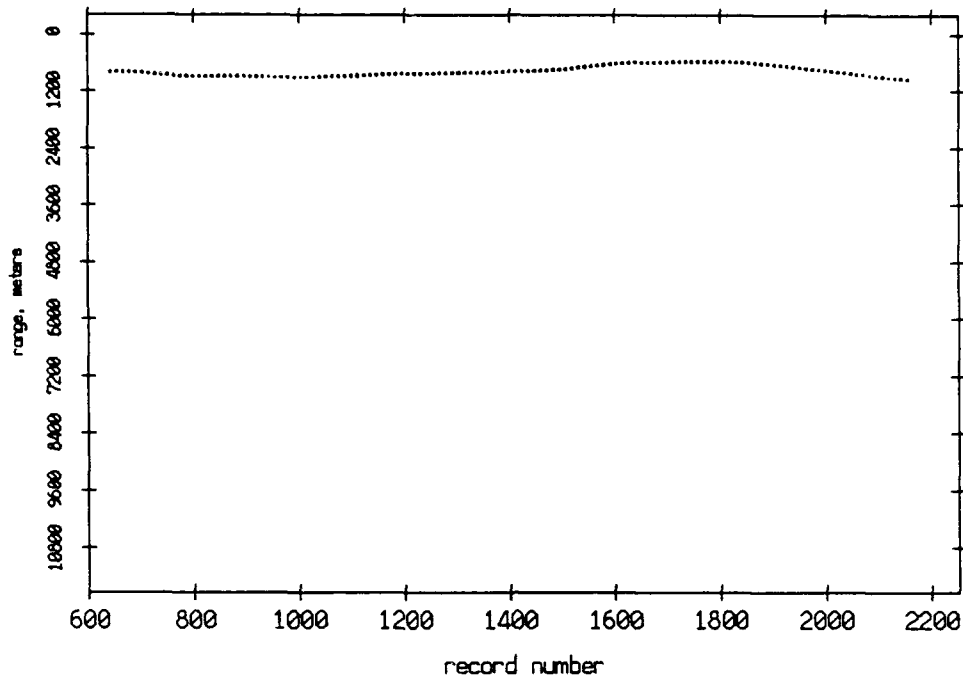


Figure 3.75

Pulse Leading Edges. Float 6 listening to Float 7, July 1989



Pulse Leading Edges. Float 7 listening to Float 6, July 1989

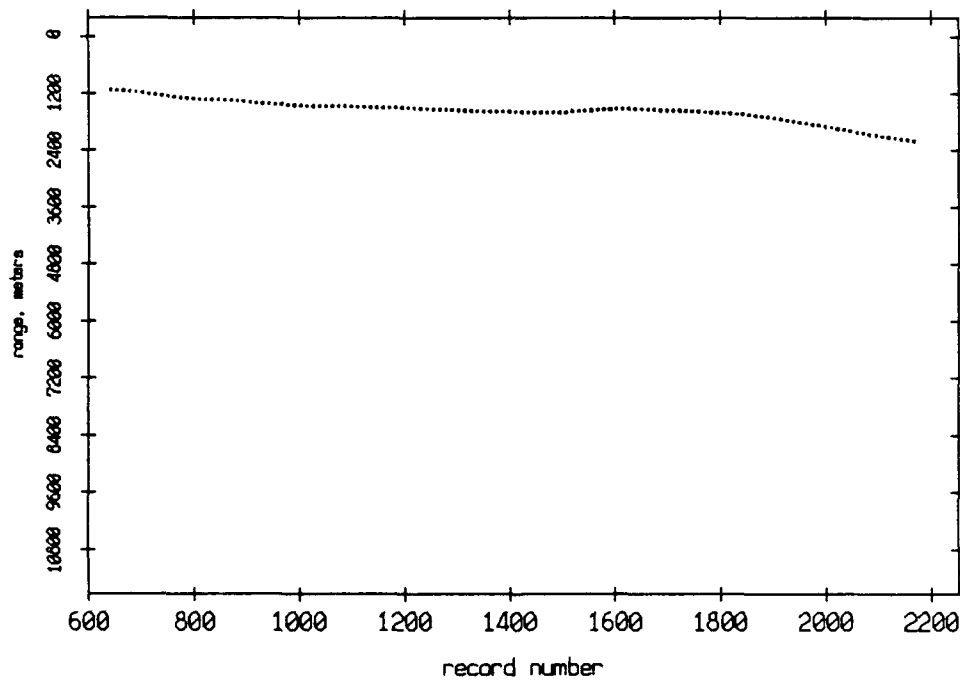
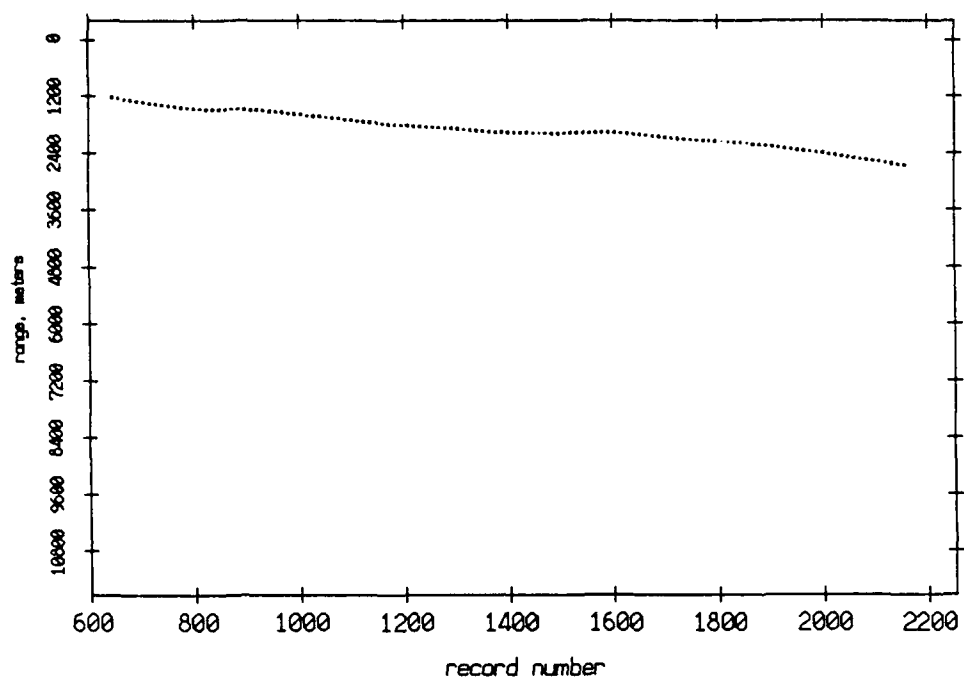


Figure 3.76

Pulse Leading Edges. Float 6 listening to Float 8, July 1989



Pulse Leading Edges. Float 8 listening to Float 6, July 1989

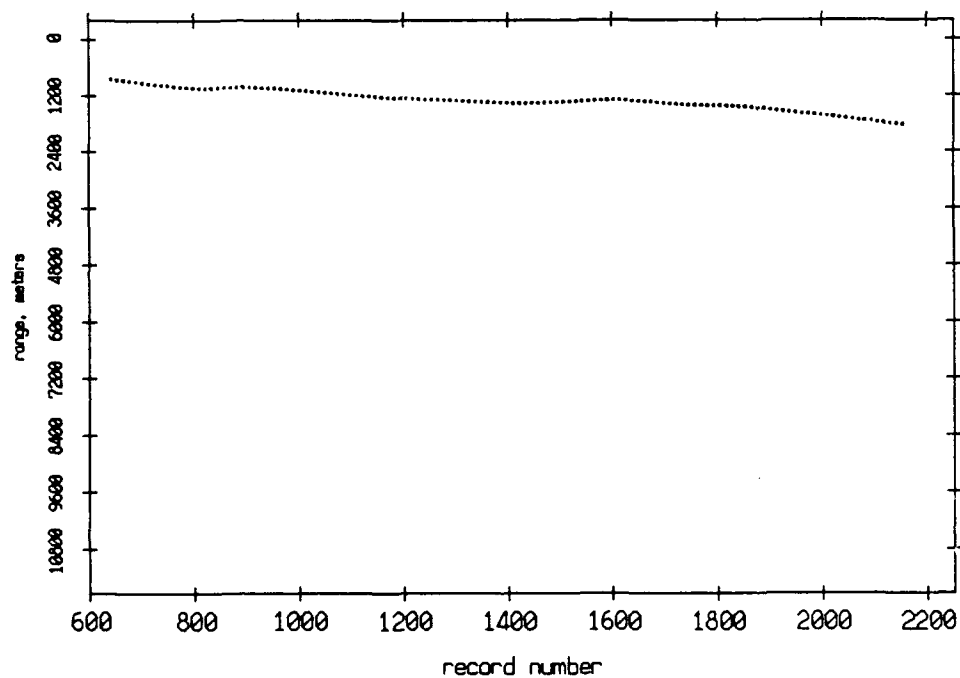
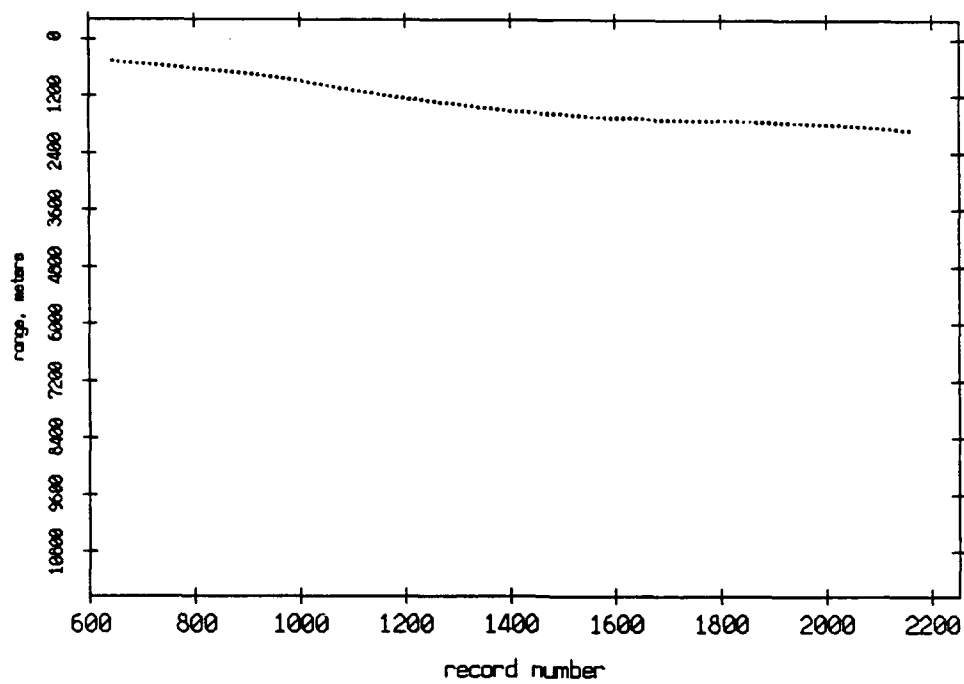


Figure 3.77

Pulse Leading Edges. Float 7 listening to Float 8, July 1989



Pulse Leading Edges. Float 8 listening to Float 7, July 1989

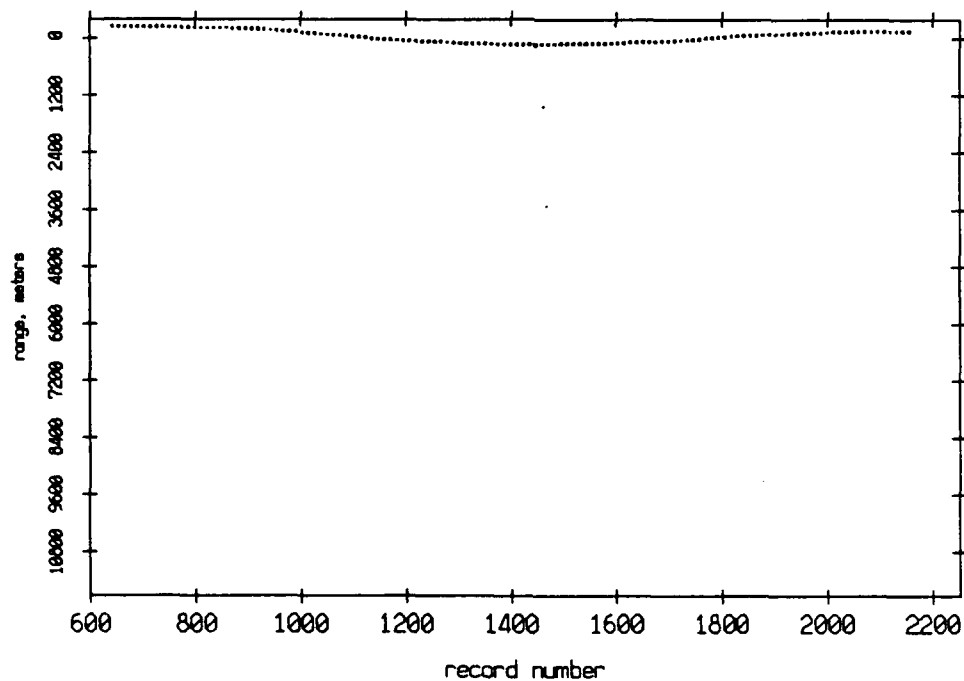


Figure 3.78

Surface echo travel time estimate, float 0, July 1989

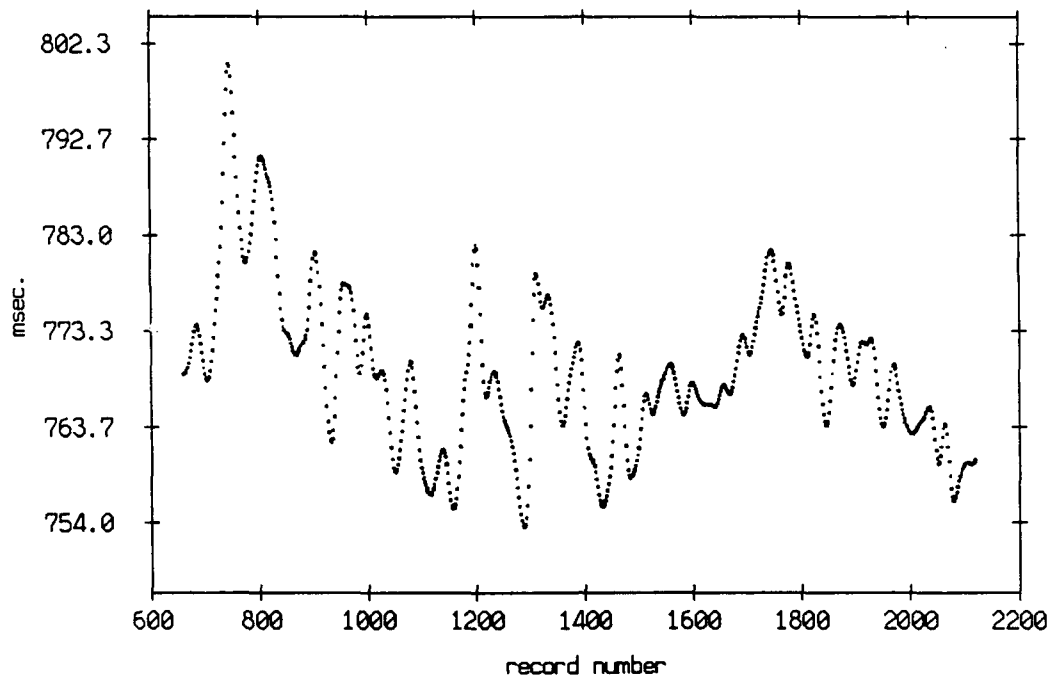


Figure 3.79

Surface echo travel time estimate, float 1, July 1989

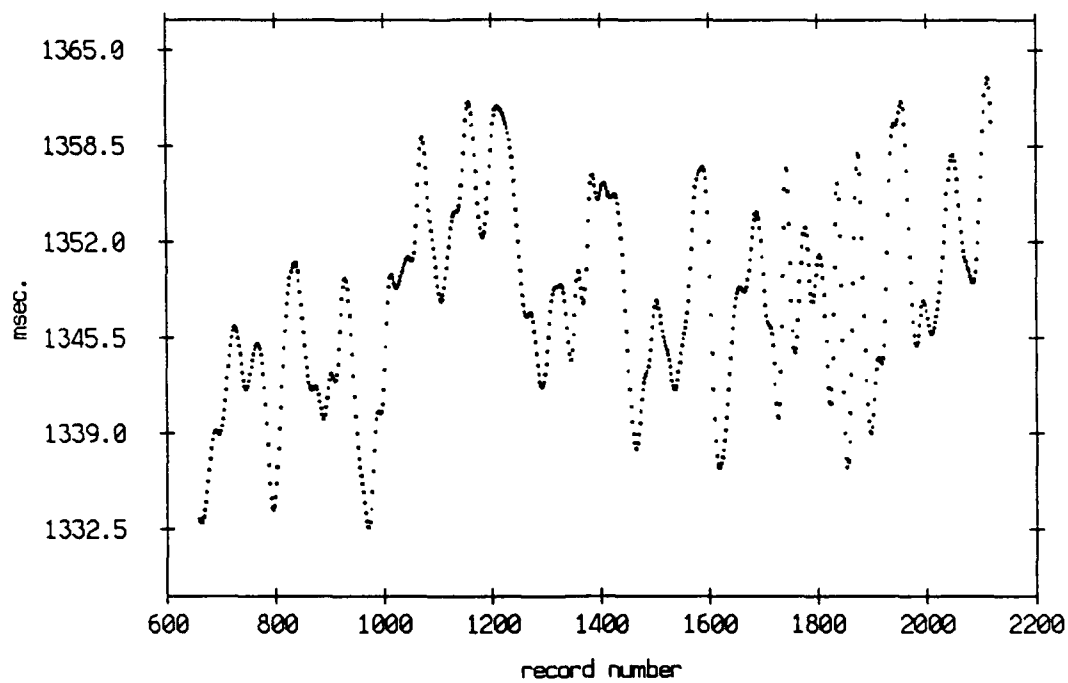


Figure 3.80

Surface echo travel time estimate, float 2, July 1989

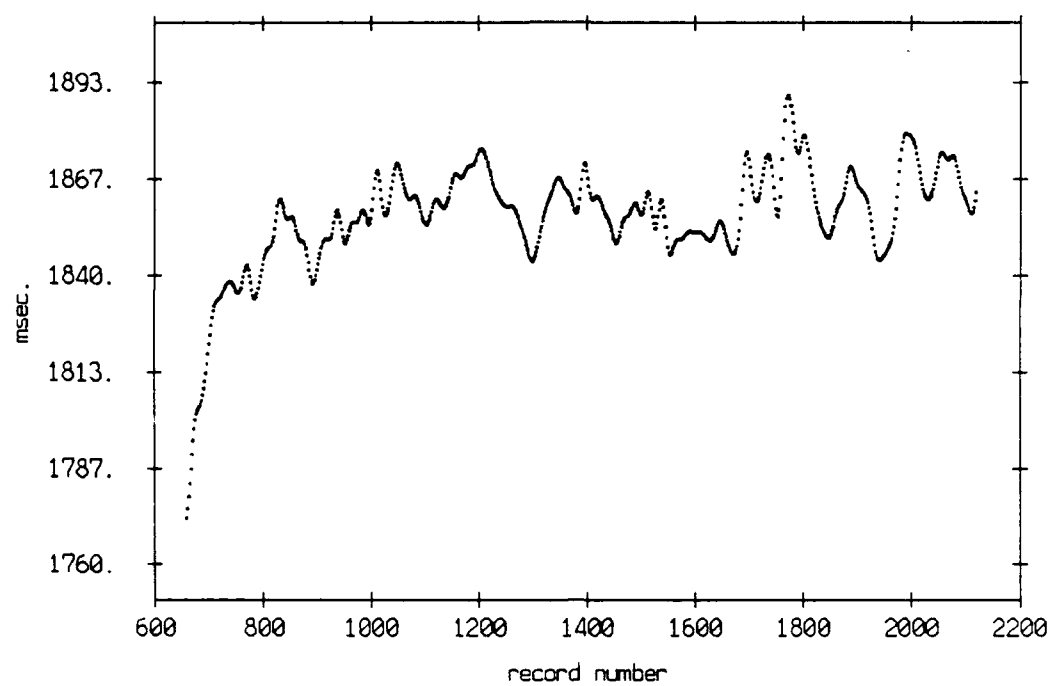


Figure 3.81

Surface echo travel time estimate, float 3, July 1989

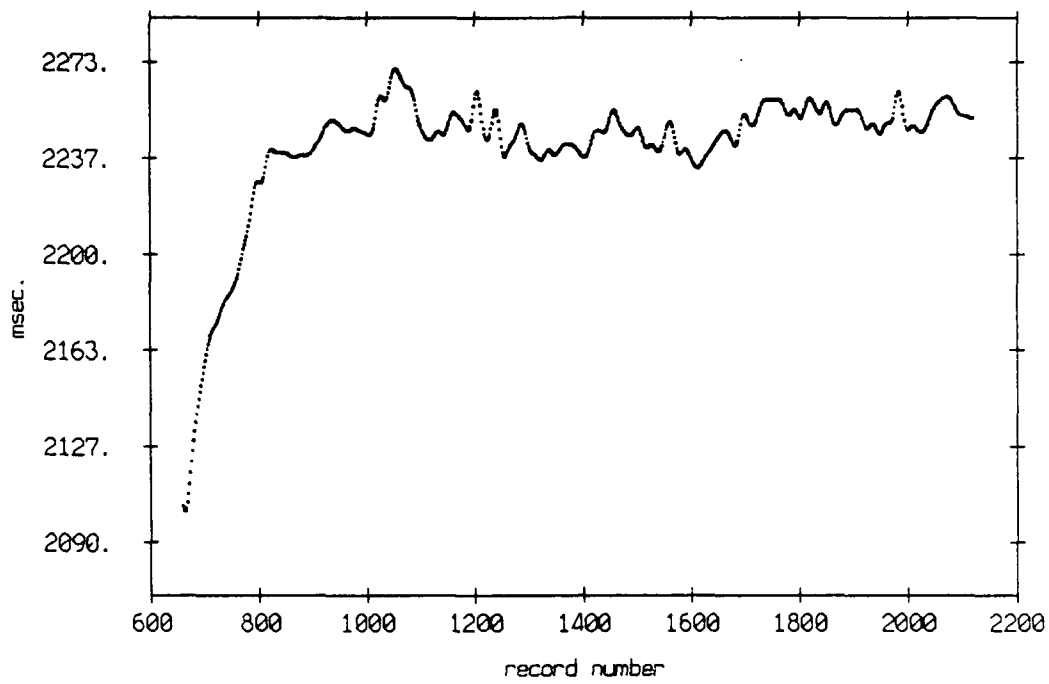


Figure 3.82

Surface echo travel time estimate, float 4, July 1989

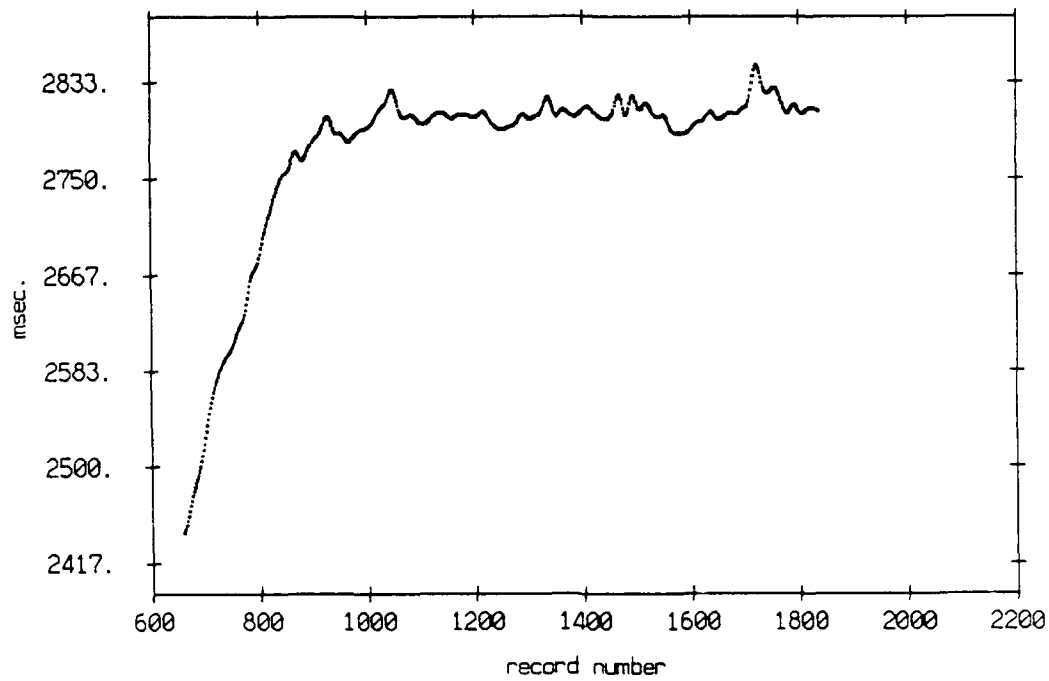


Figure 3.83

Surface echo travel time estimate, float 5, July 1989

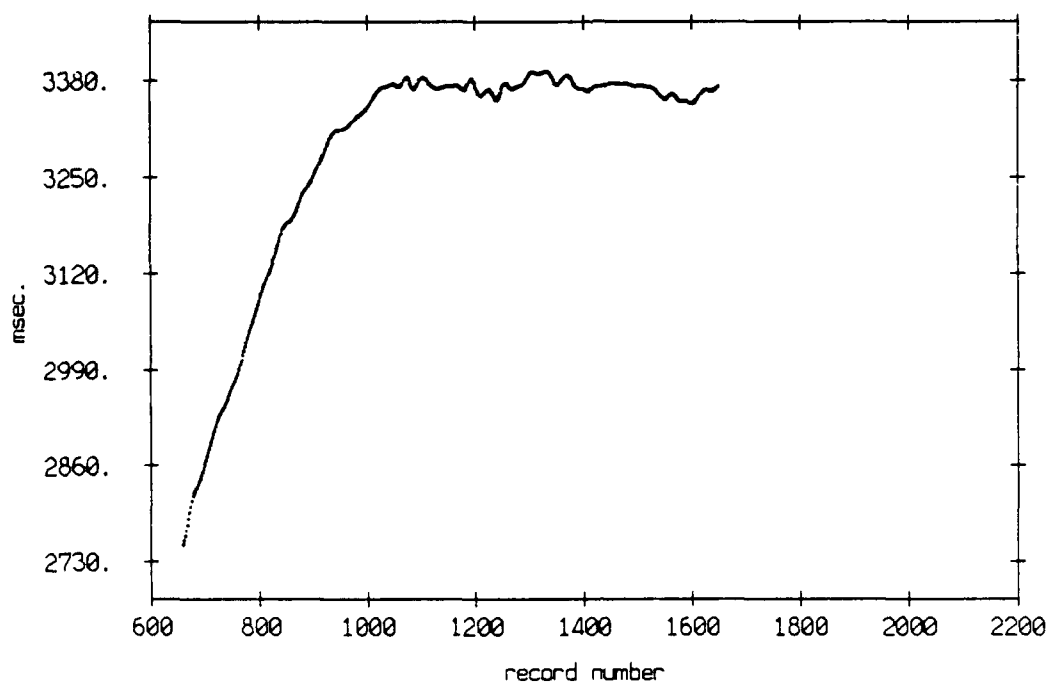


Figure 3.84

Surface echo travel time estimate, float 6, July 1989

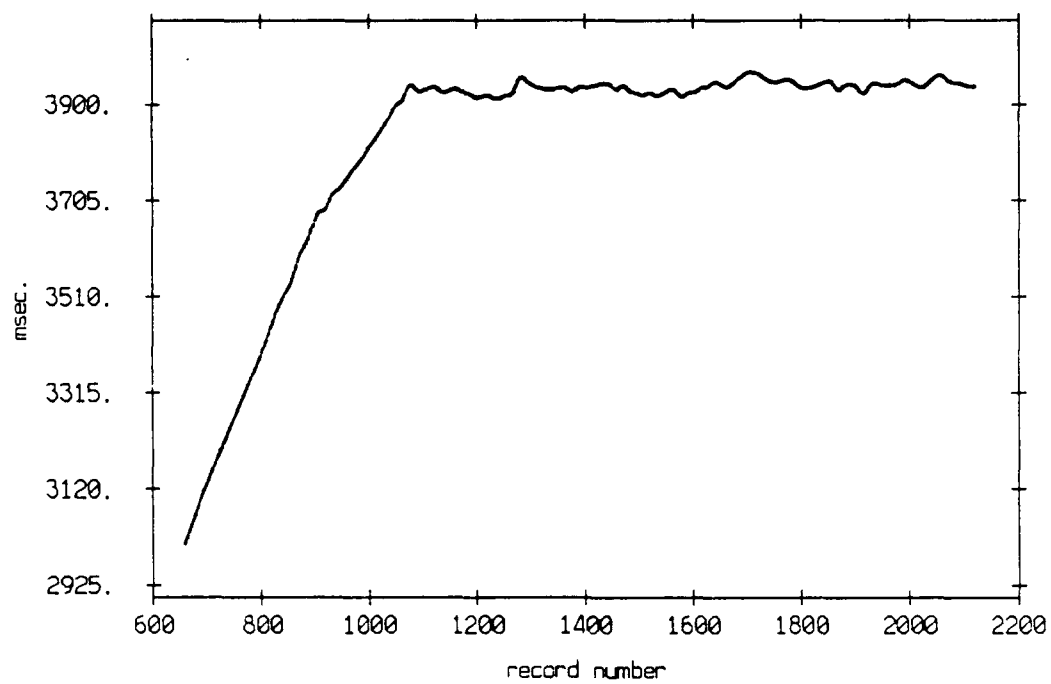


Figure 3.85

Surface echo travel time estimate, float 7, July 1989

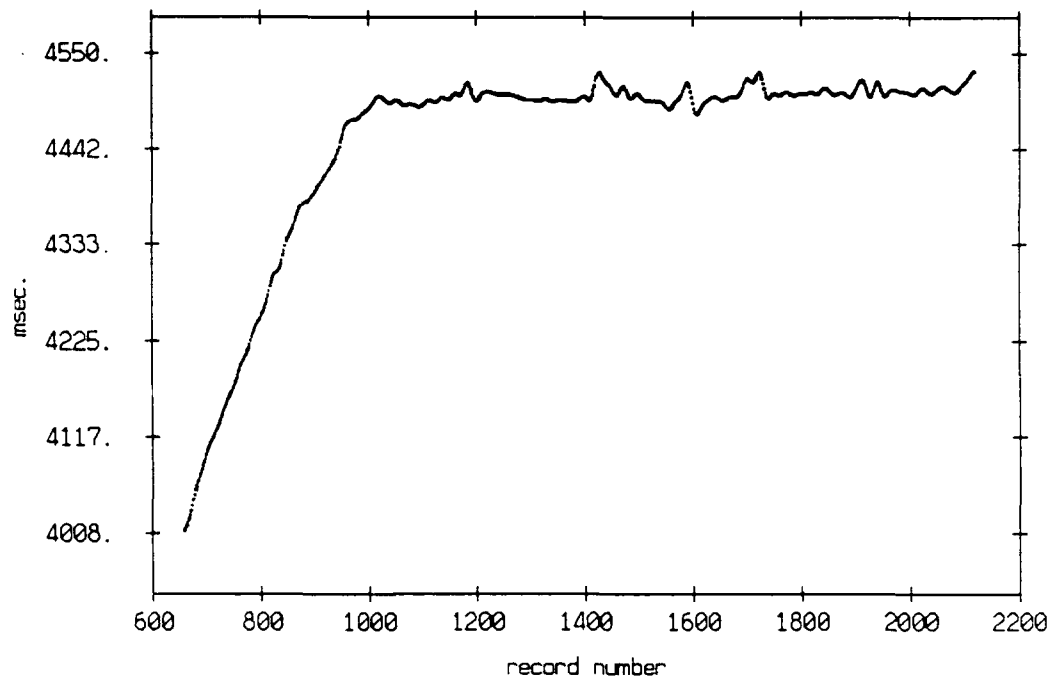


Figure 3.86

Surface echo travel time estimate, float 8, July 1989

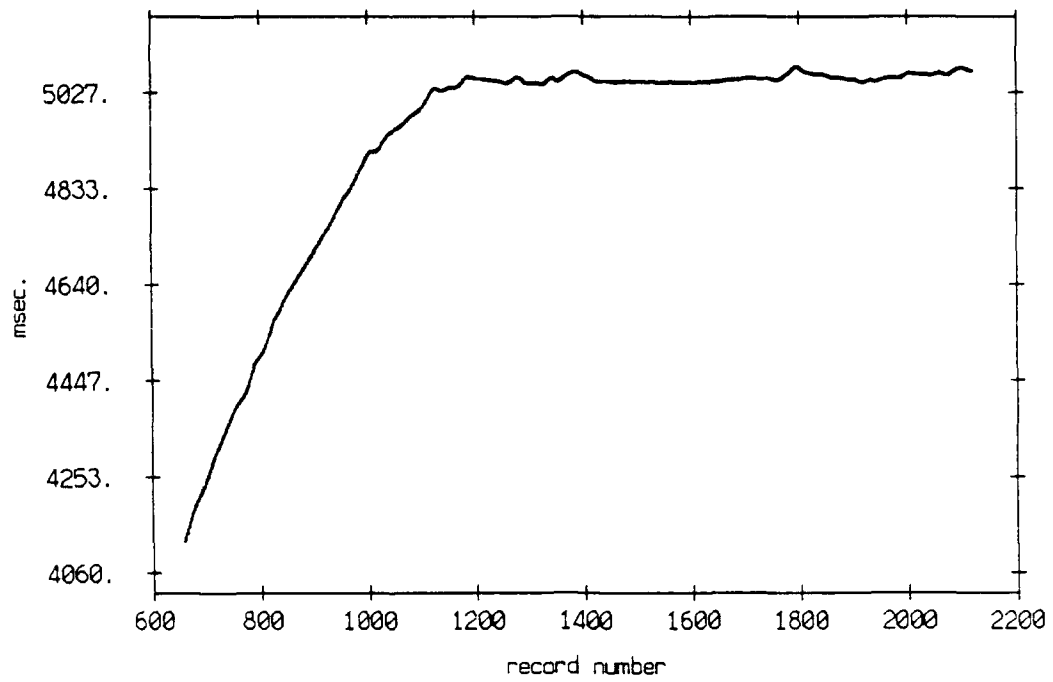
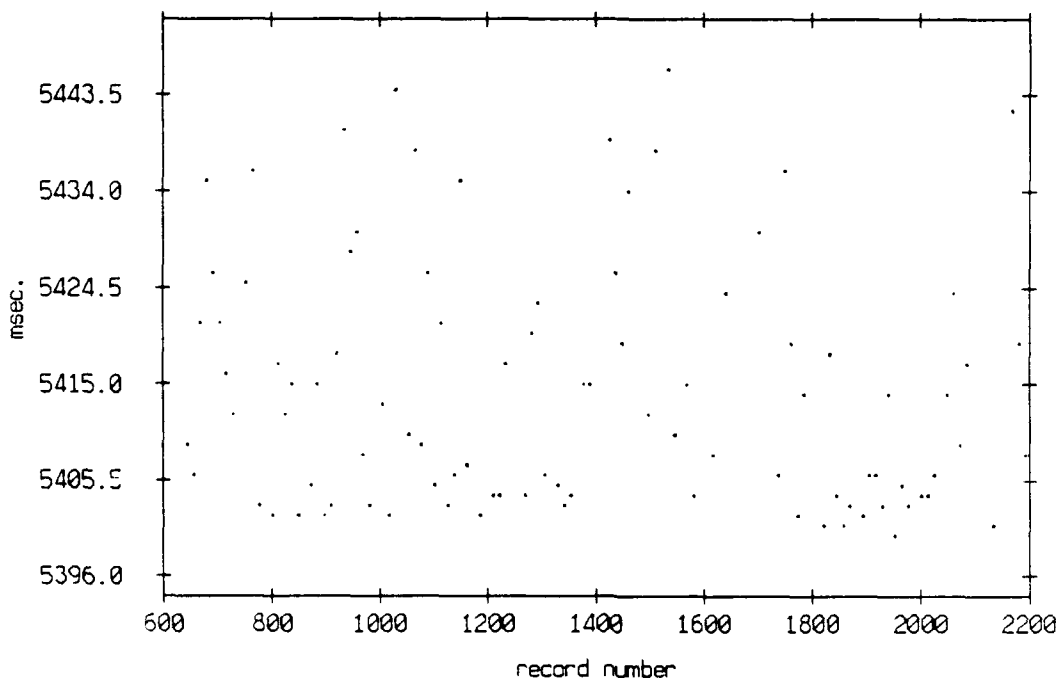


Figure 3.87

Surface echo travel time estimate, float 9, July 1989



Float 9 histogram of surface echo travel time minus the mean 5414.3, July 1989 experiment

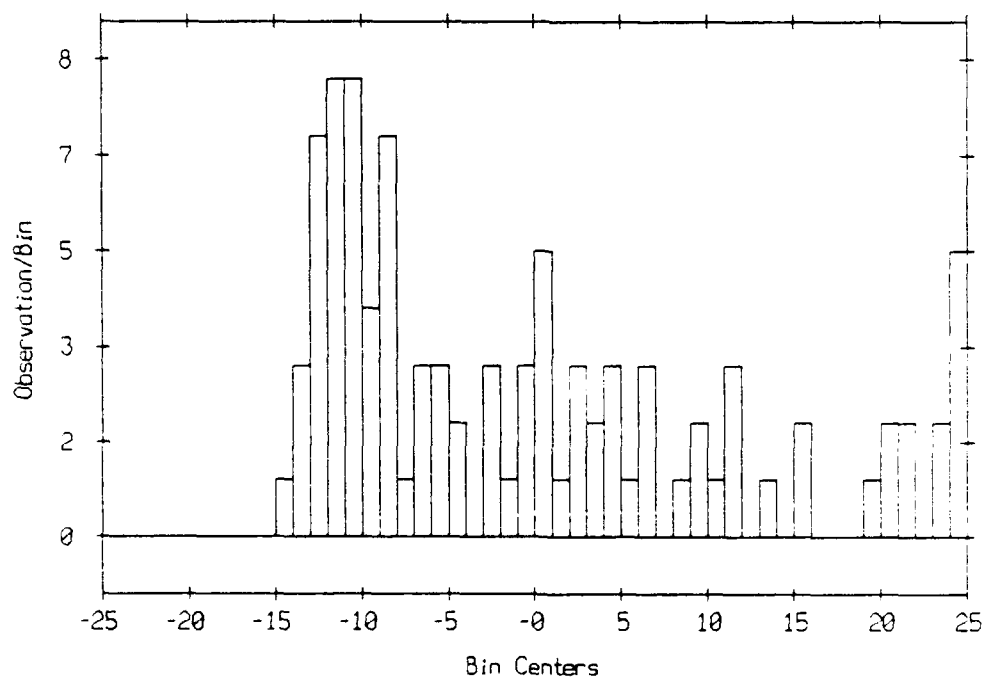
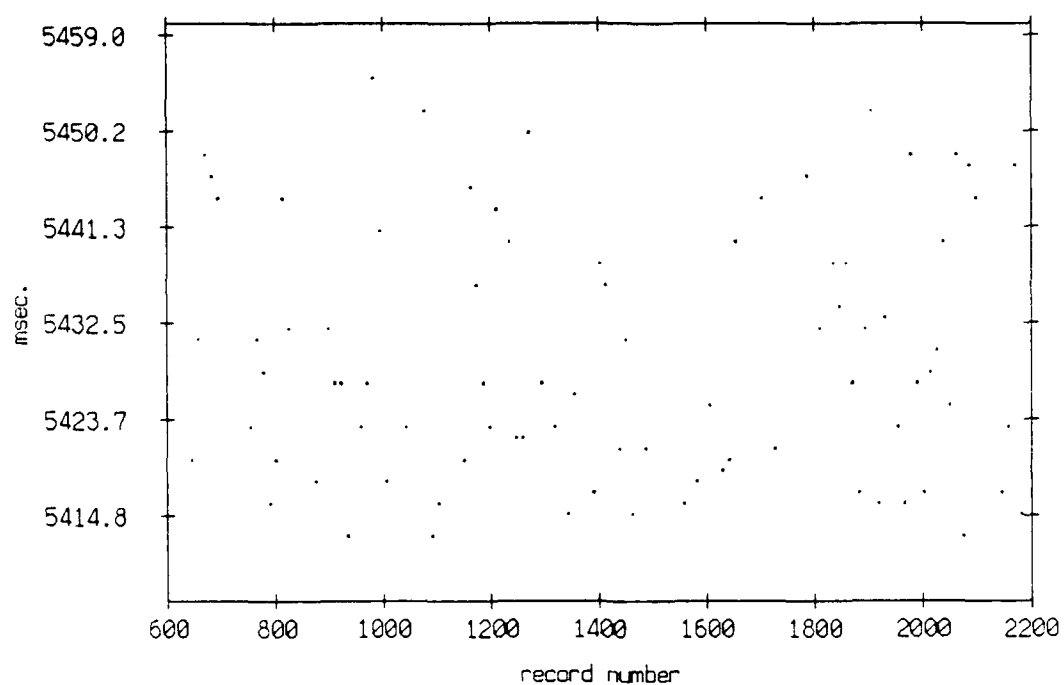


Figure 3.88

Surface echo travel time estimate, float 10, July 1989



Float 10 histogram of surface echo travel time minus the mean 5429.4, July 1989 experiment

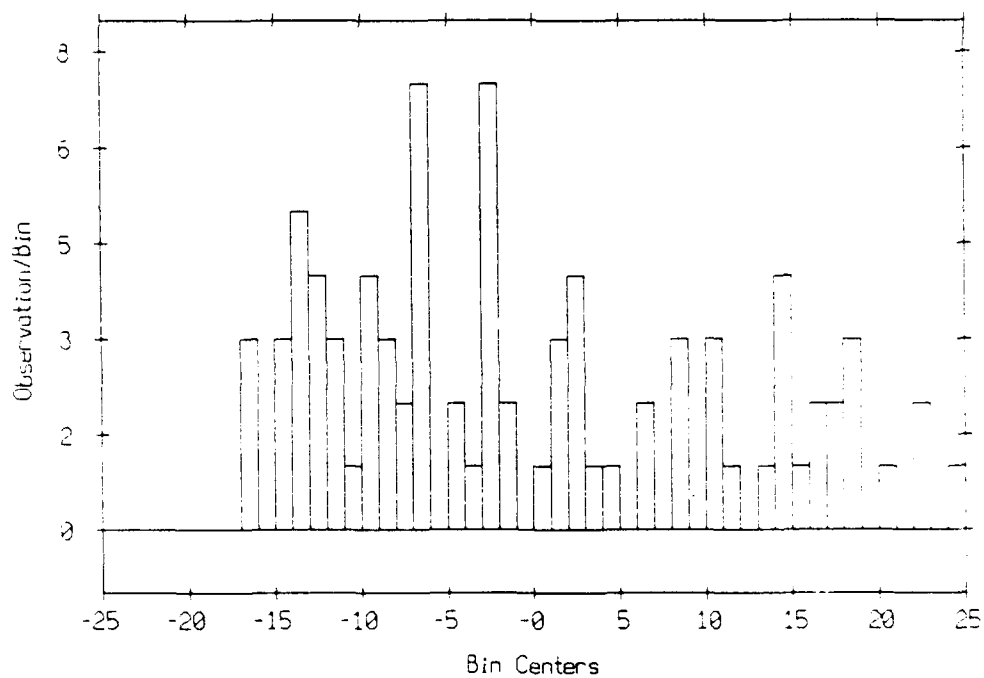


Figure 3.89

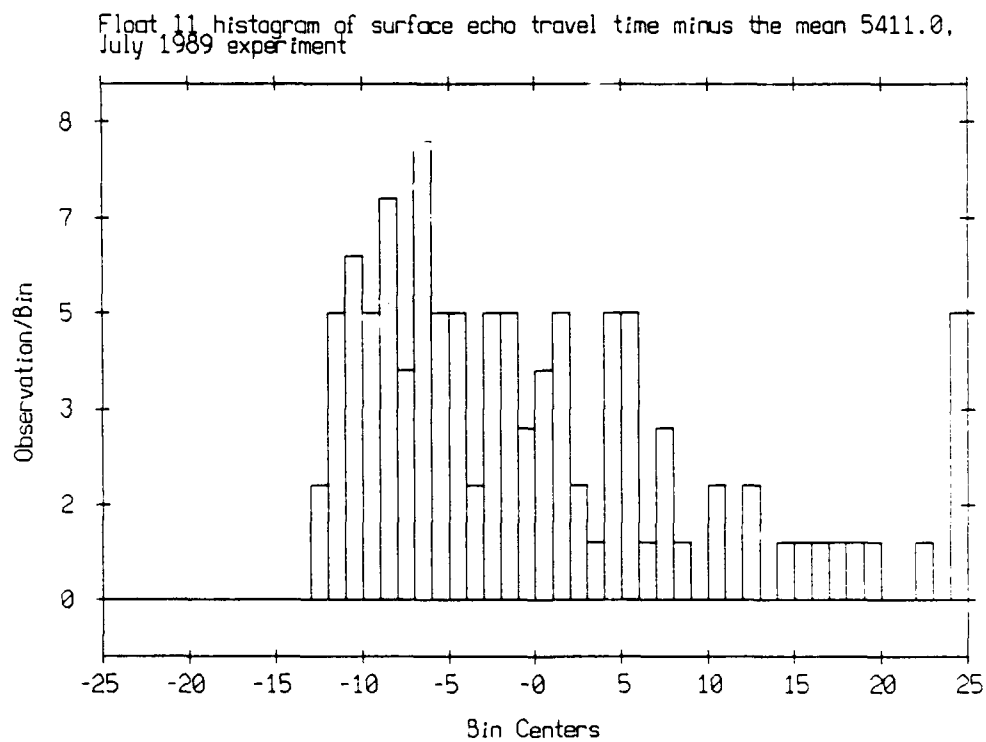
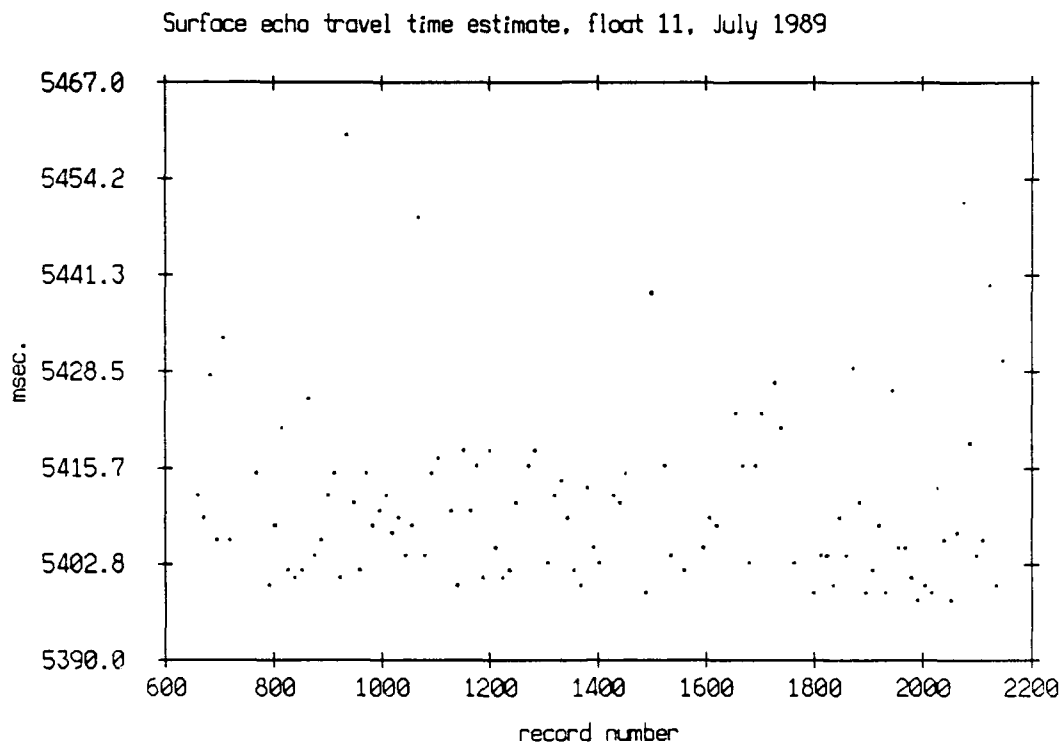


Figure 3.90

Travel time estimate, floats 9 and 10, July 1989
Surface Bounce

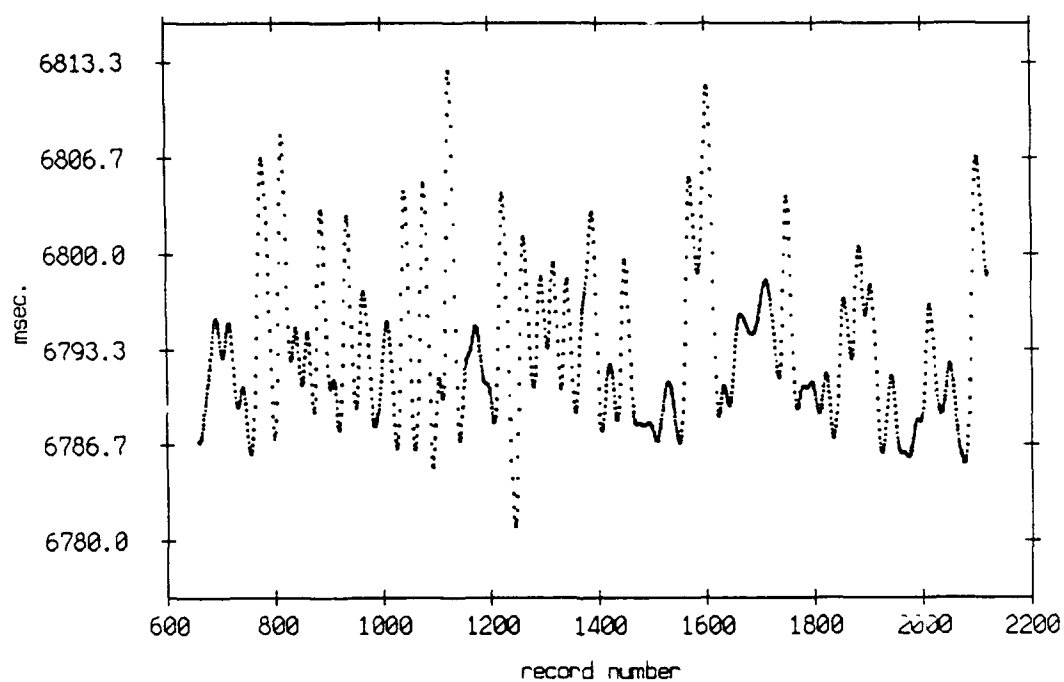


Figure 3.91a

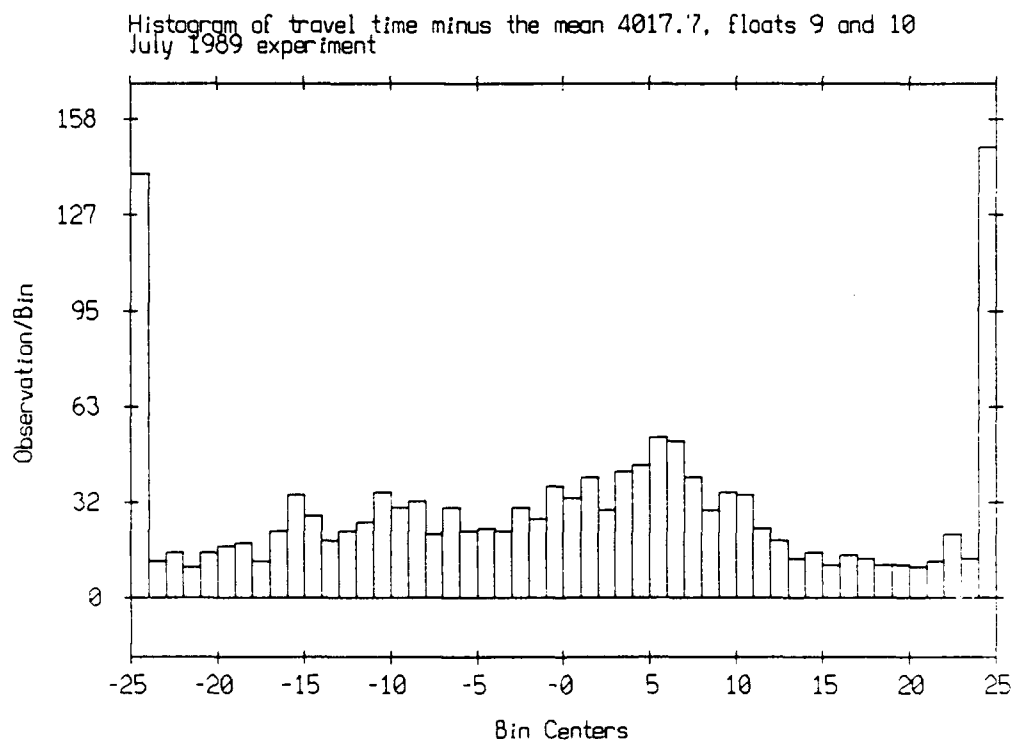
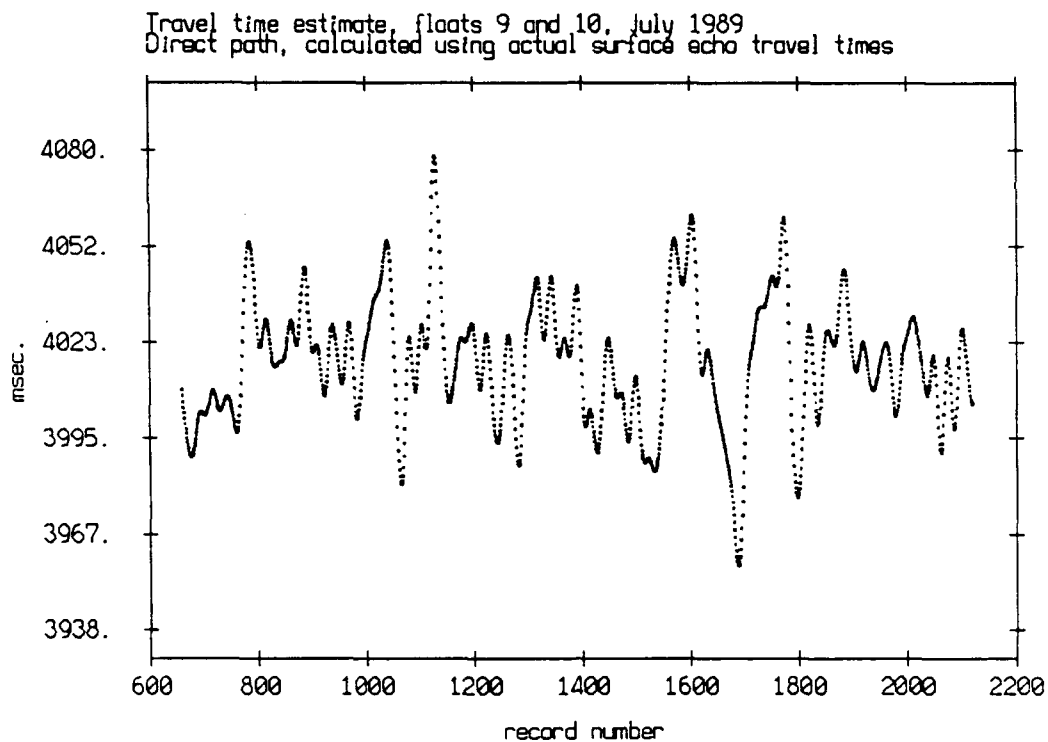


Figure 3.91b

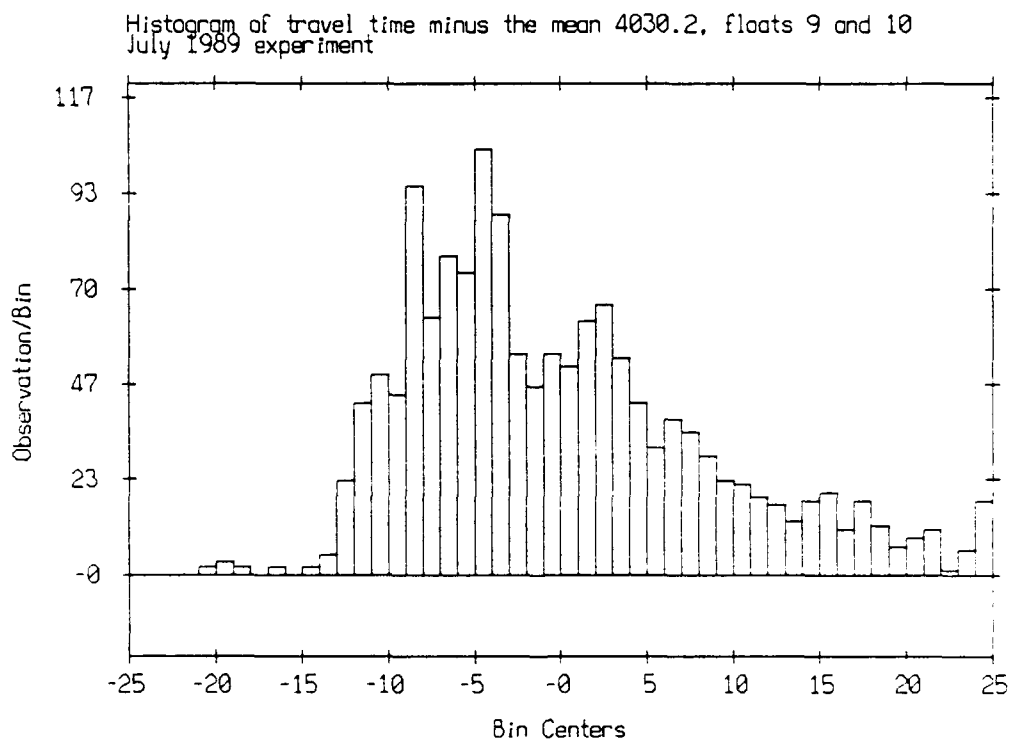
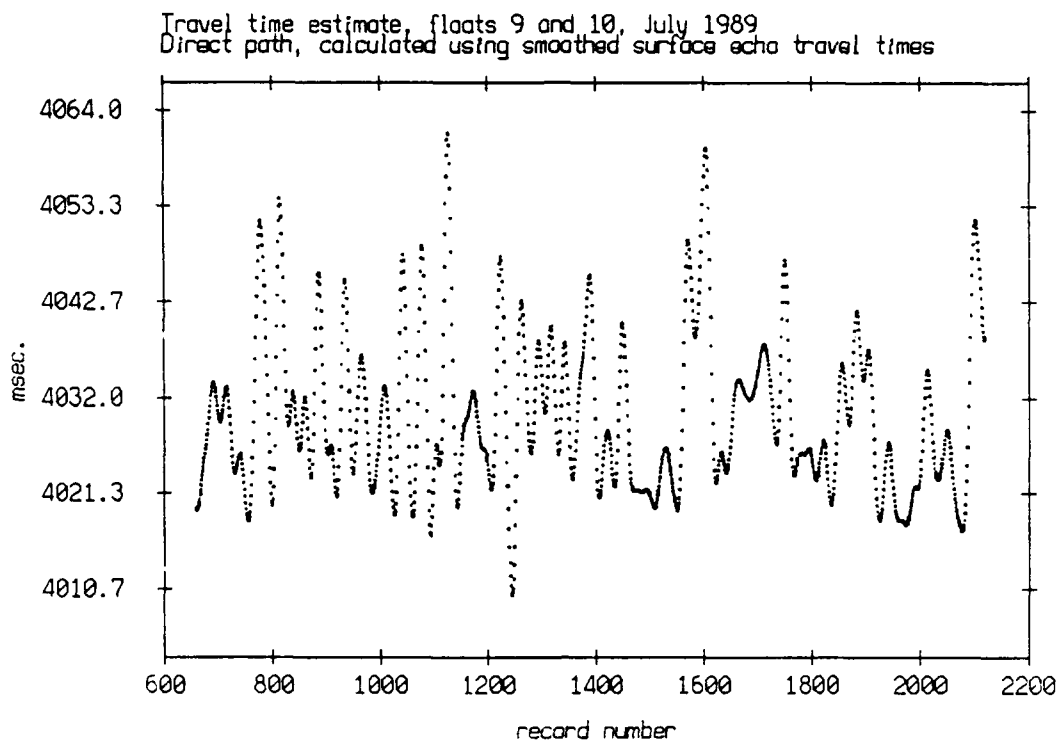


Figure 3.91c

Travel time estimate, floats 9 and 11, July 1989
Surface Bounce

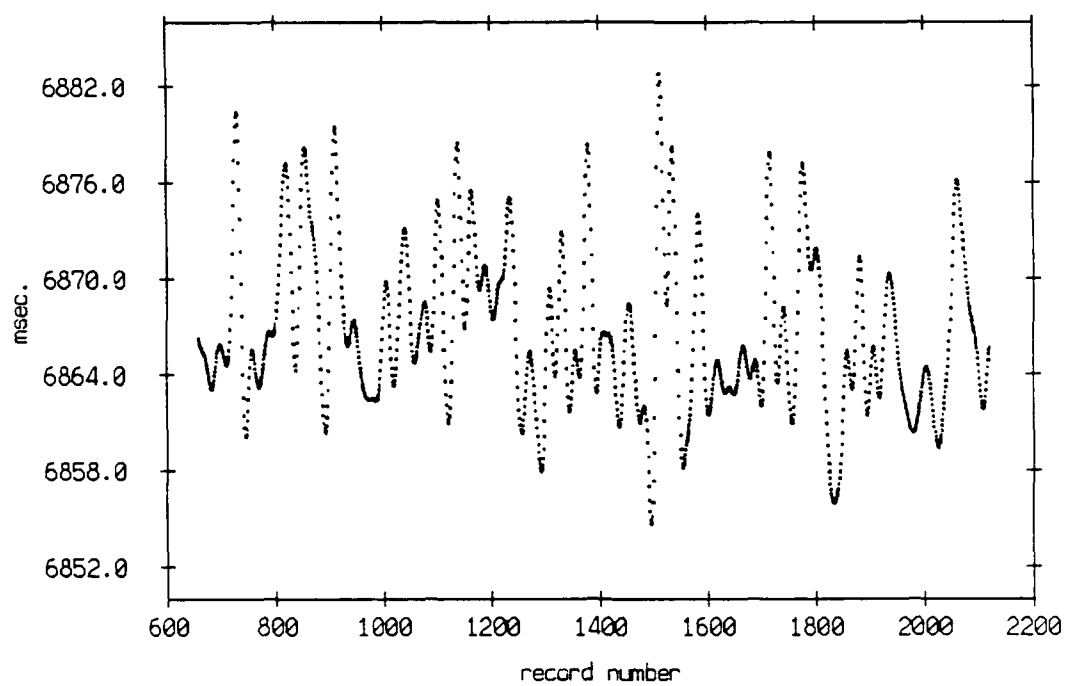


Figure 3.92a

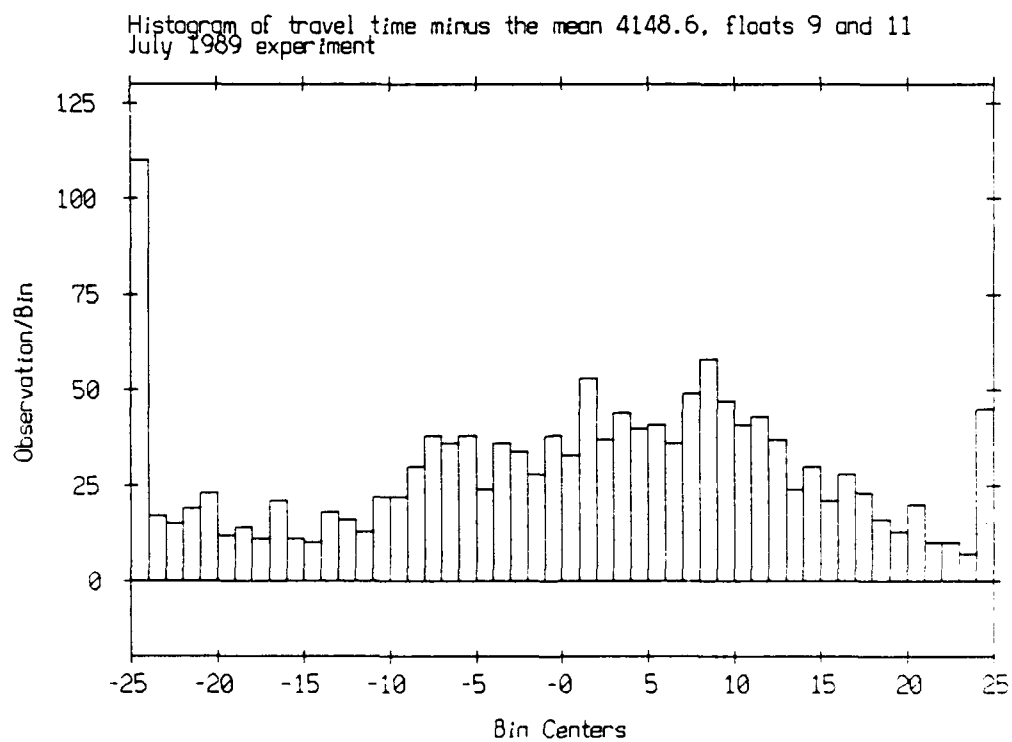
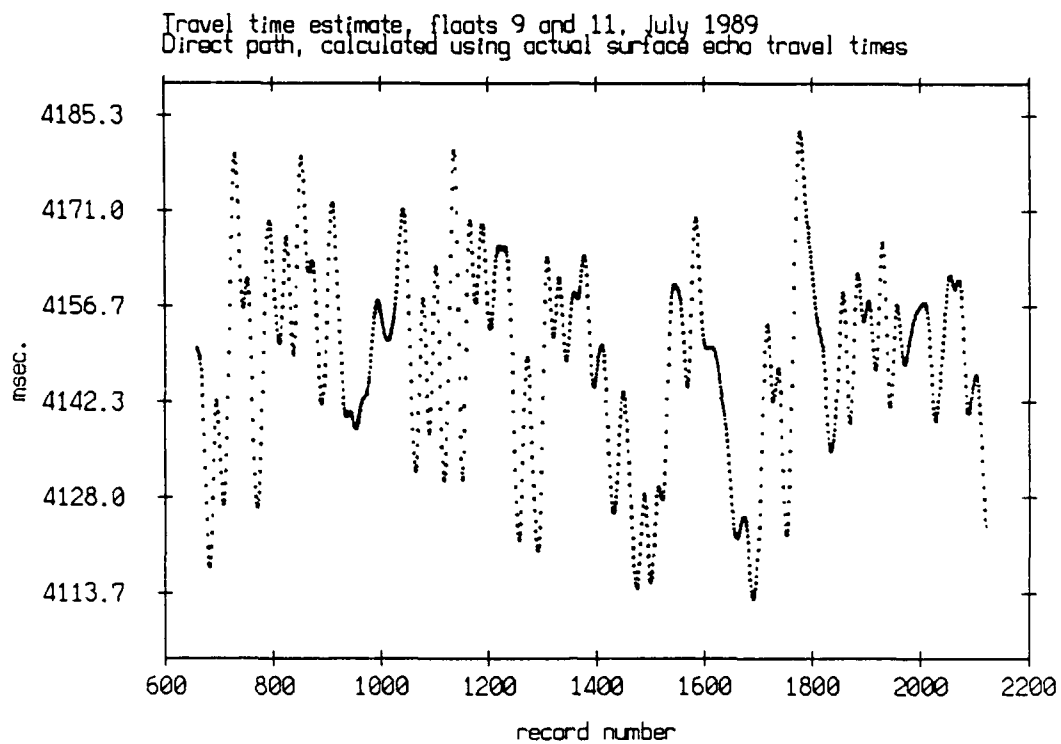
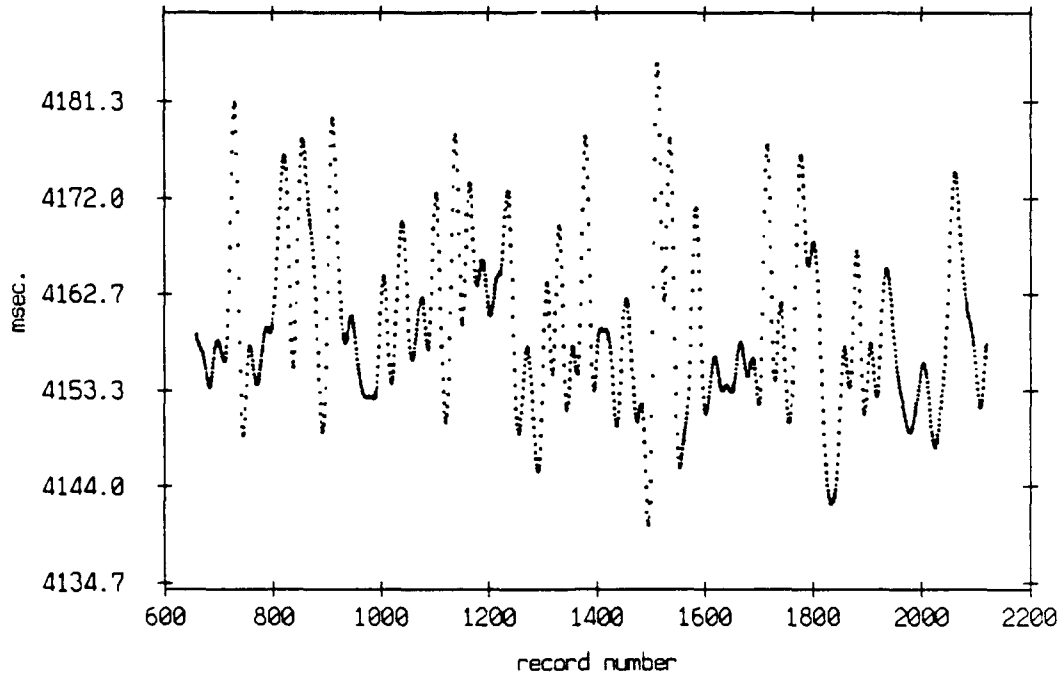


Figure 3.92b

Travel time estimate, floats 9 and 11, July 1989
 Direct path, calculated using smoothed surface echo travel times



Histogram of travel time minus the mean 4159.4, floats 9 and 11
 July 1989 experiment

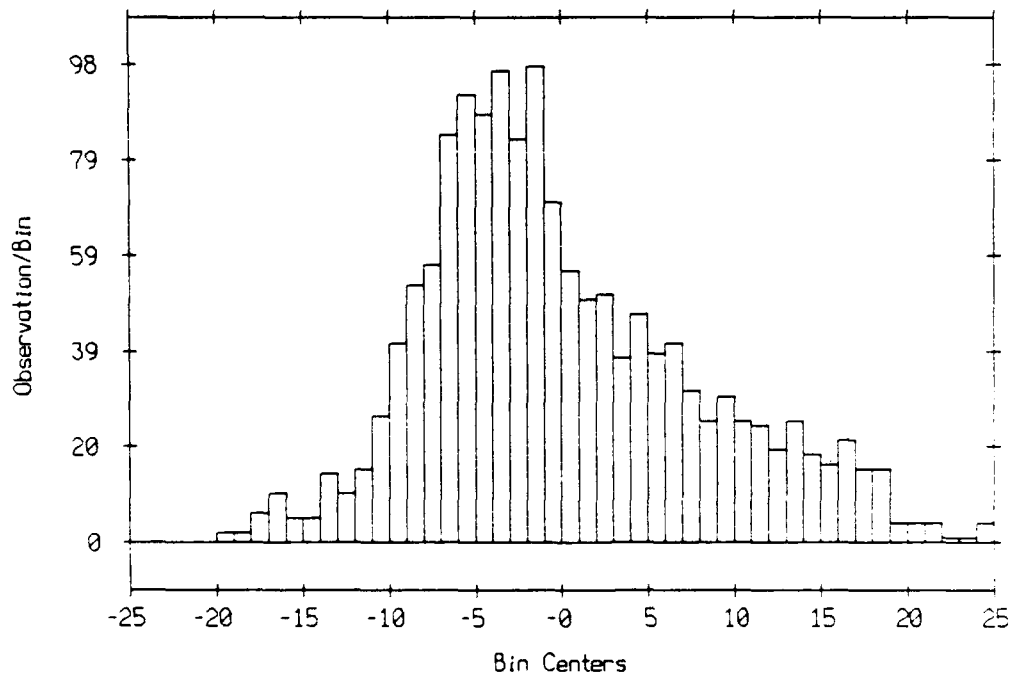


Figure 3.92c

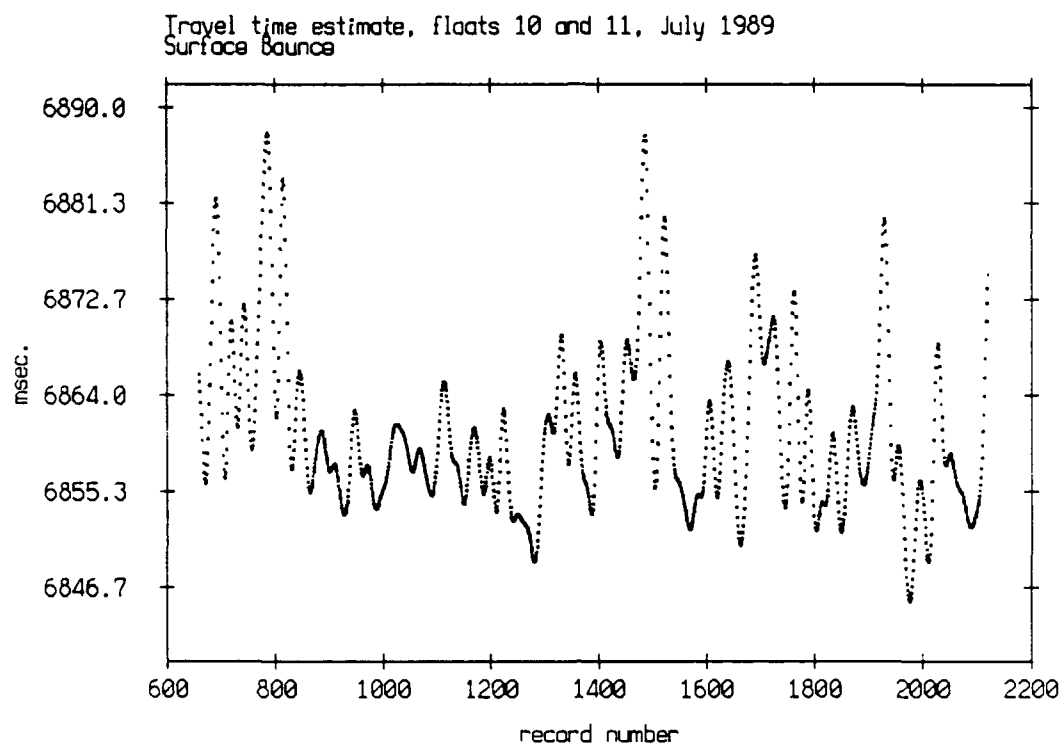


Figure 3.93a

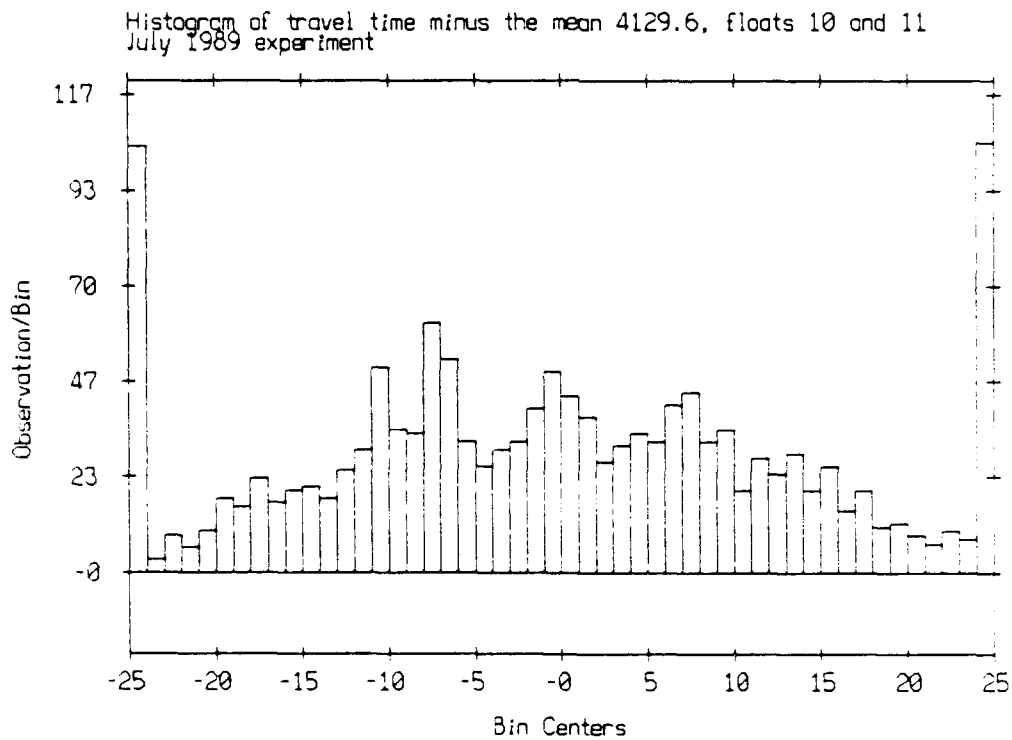
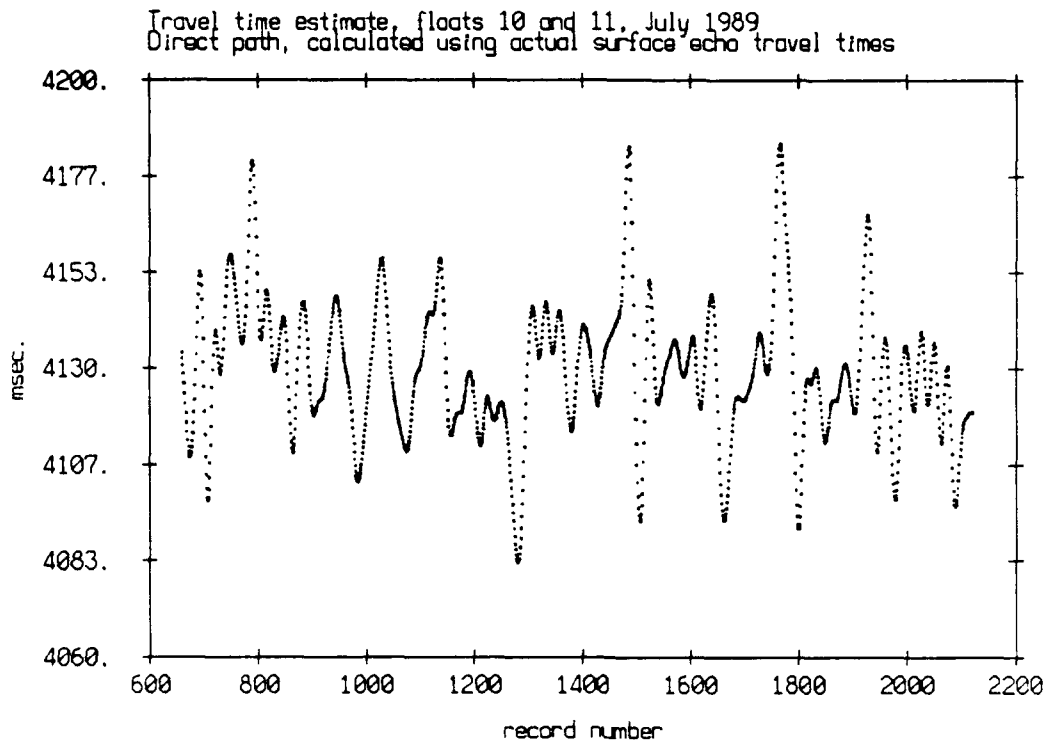


Figure 3.93b

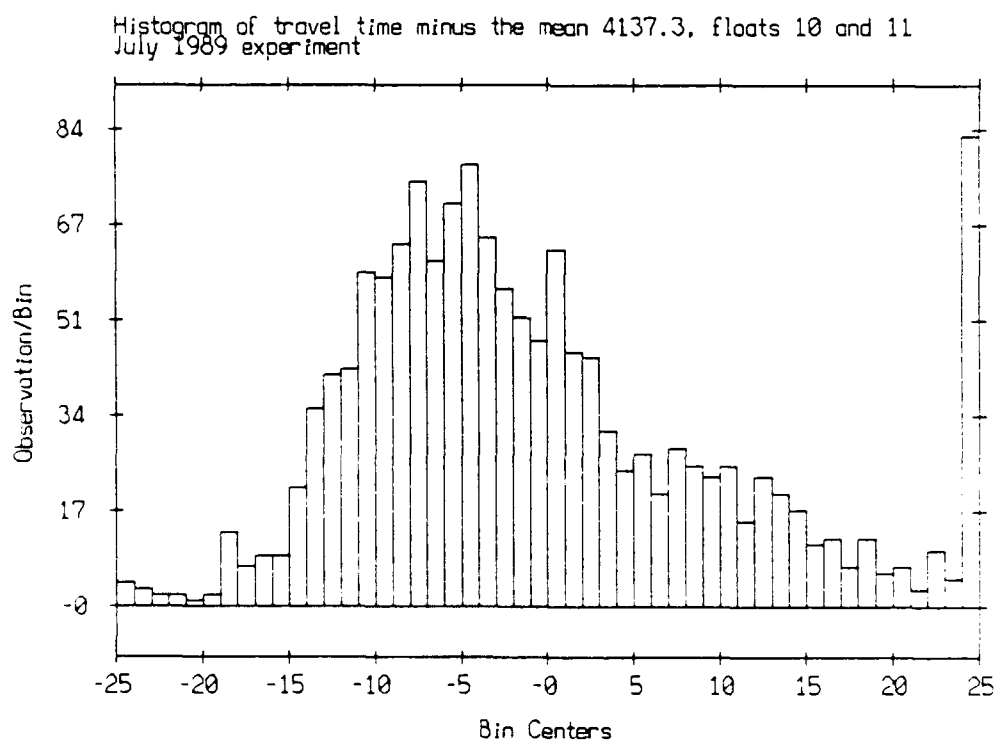
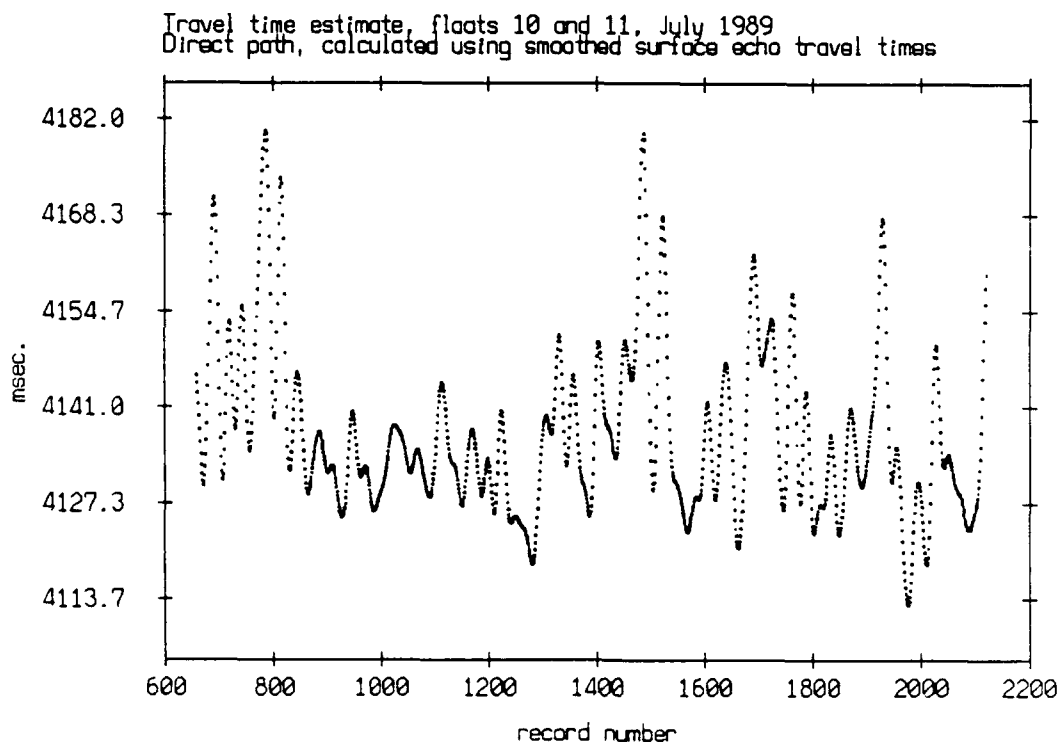
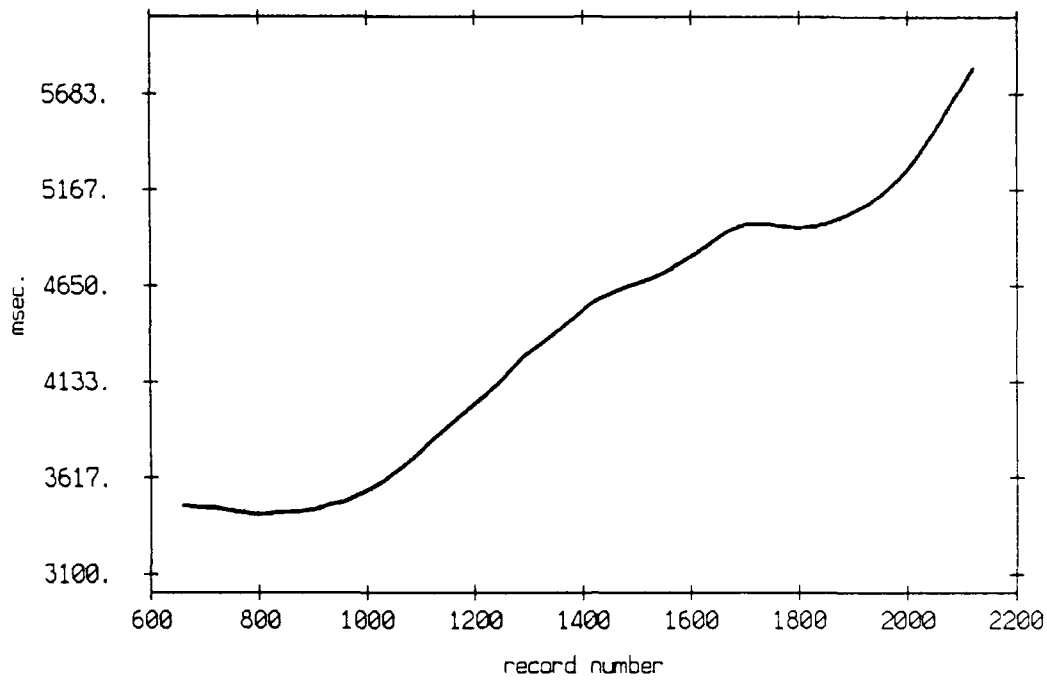


Figure 3.93c

Travel time estimate, floats 9 and 0, July 1989



Travel time estimate, floats 9 and 1, July 1989

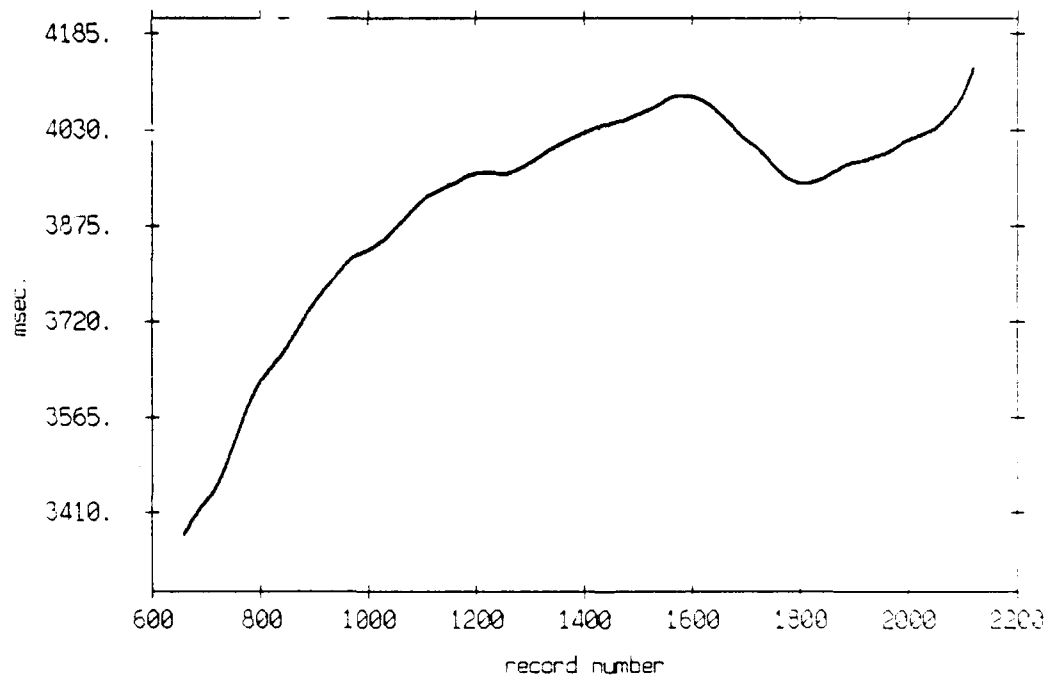
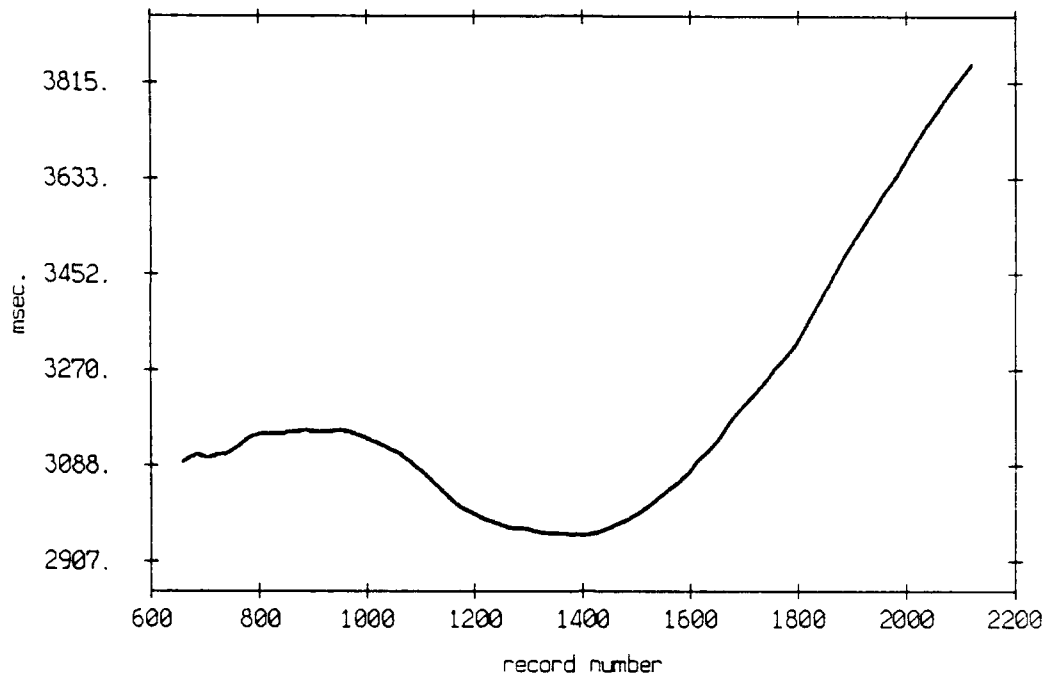


Figure 3.94

Travel time estimate, floats 9 and 2, July 1989



Travel time estimate, floats 9 and 3, July 1989

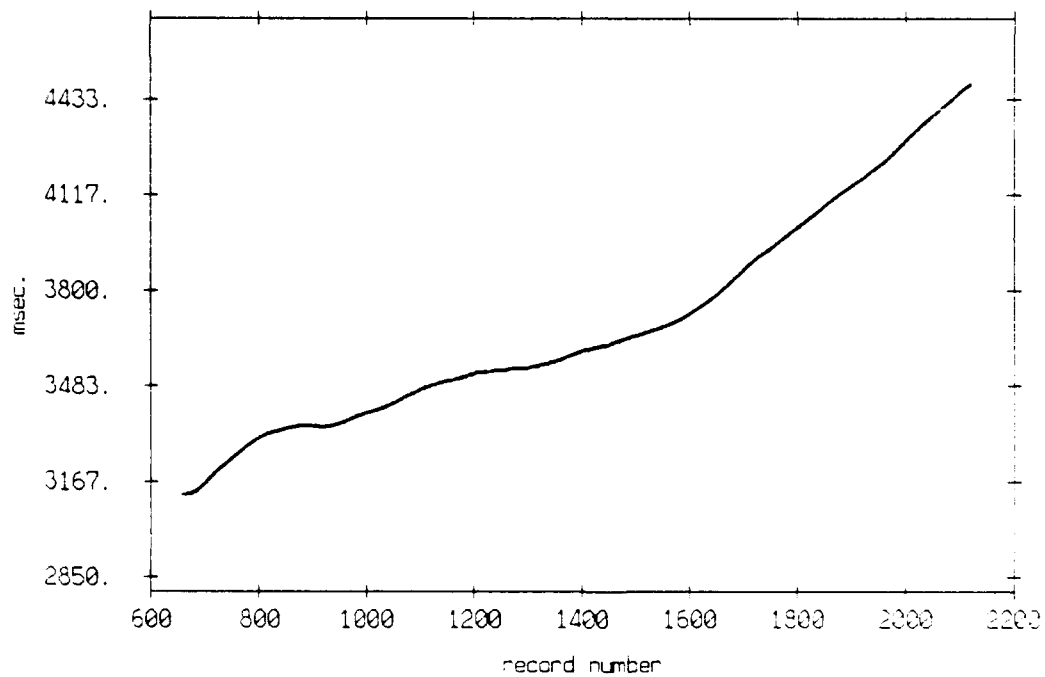


Figure 3.95

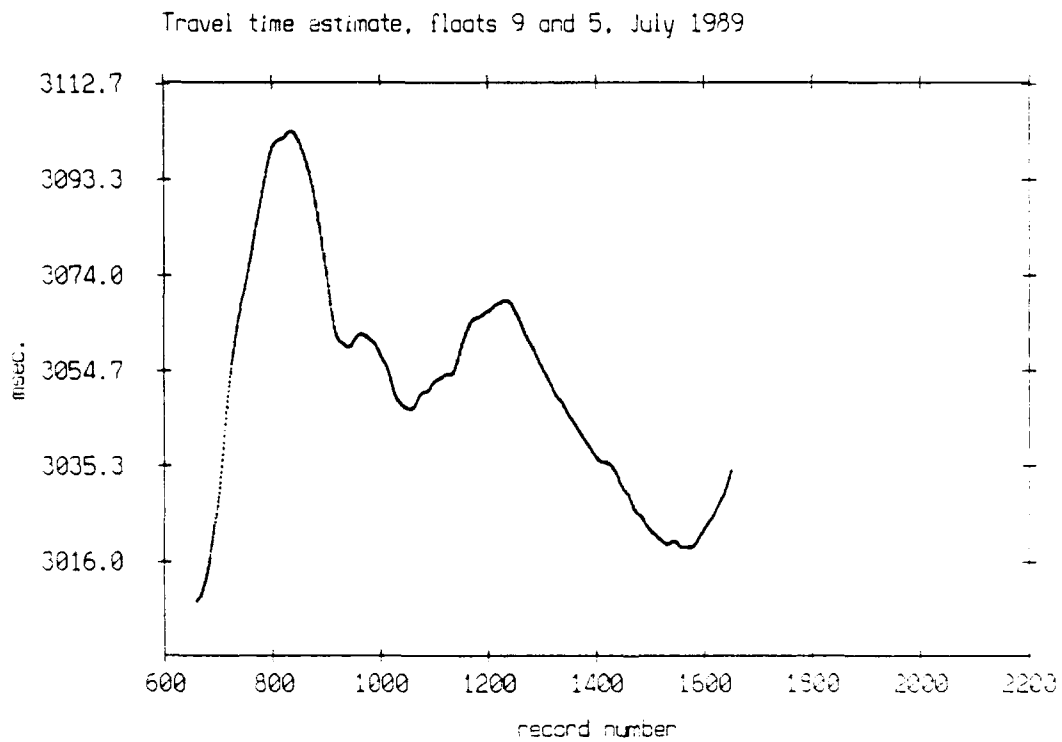
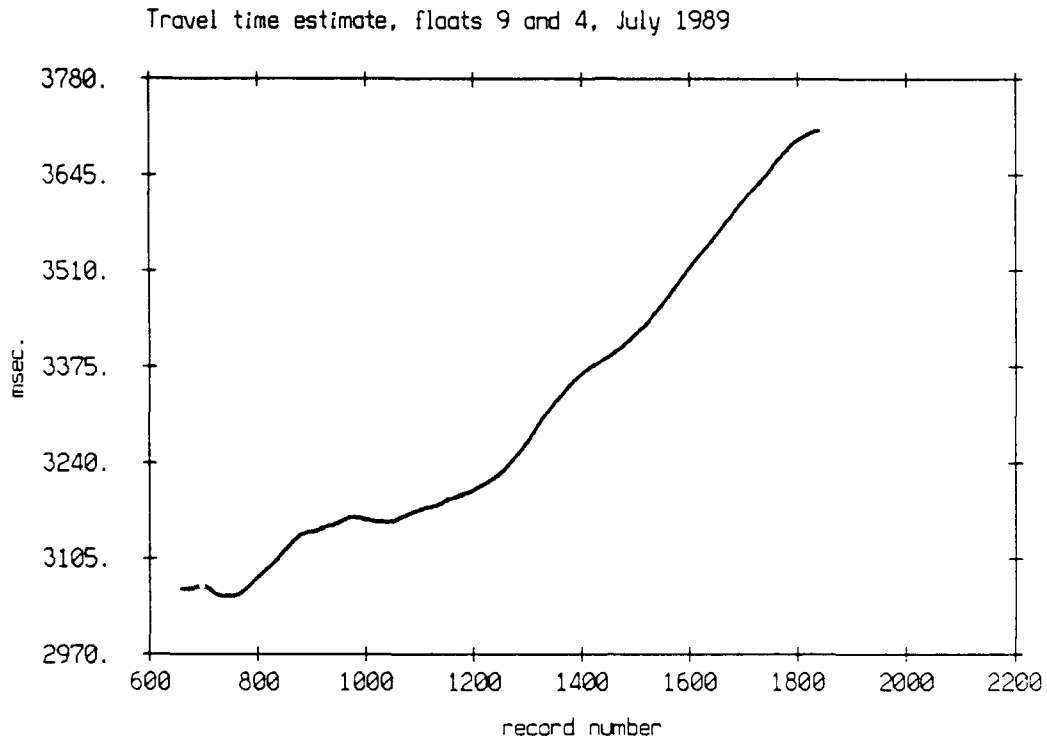
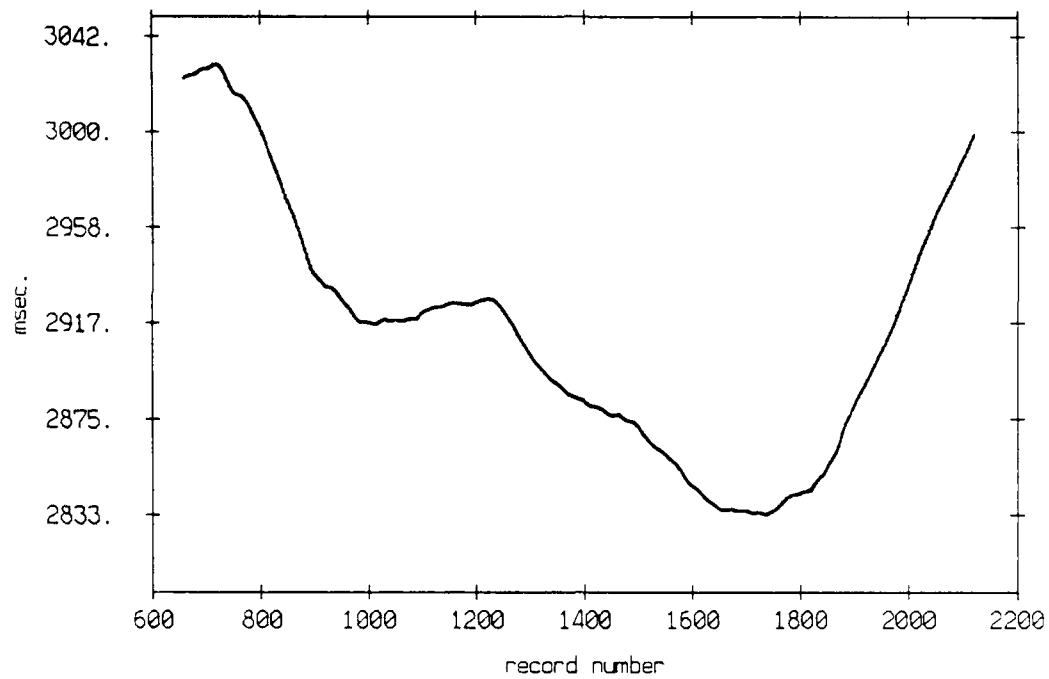


Figure 3.96

Travel time estimate, floats 9 and 6, July 1989



Travel time estimate, floats 9 and 7, July 1989

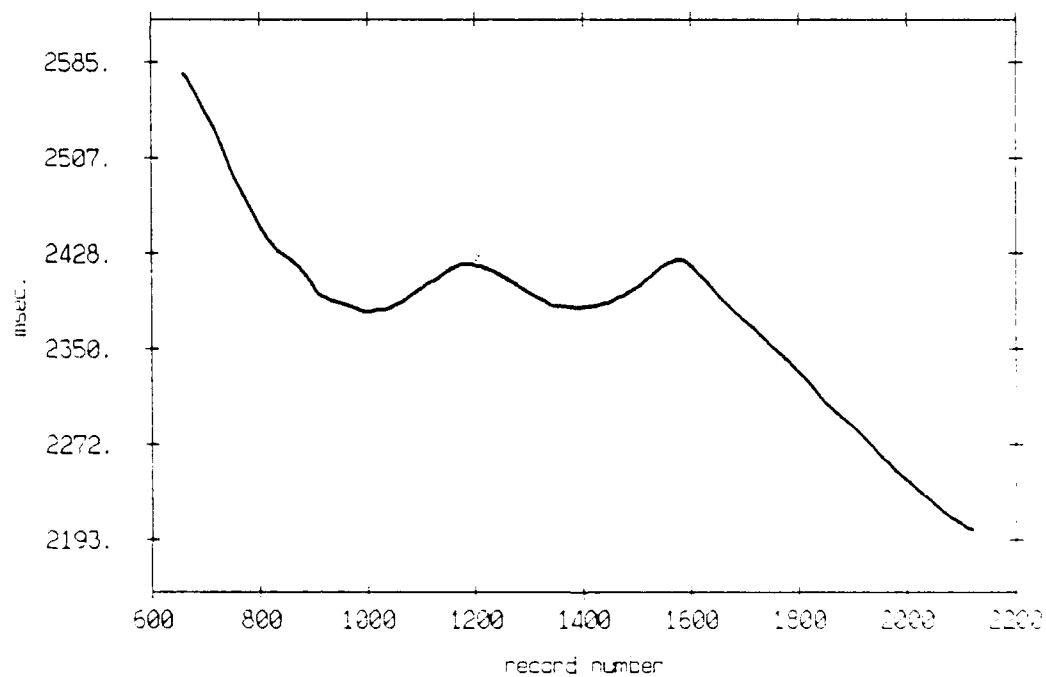


Figure 3.97

Travel time estimate, floats 9 and 8, July 1989

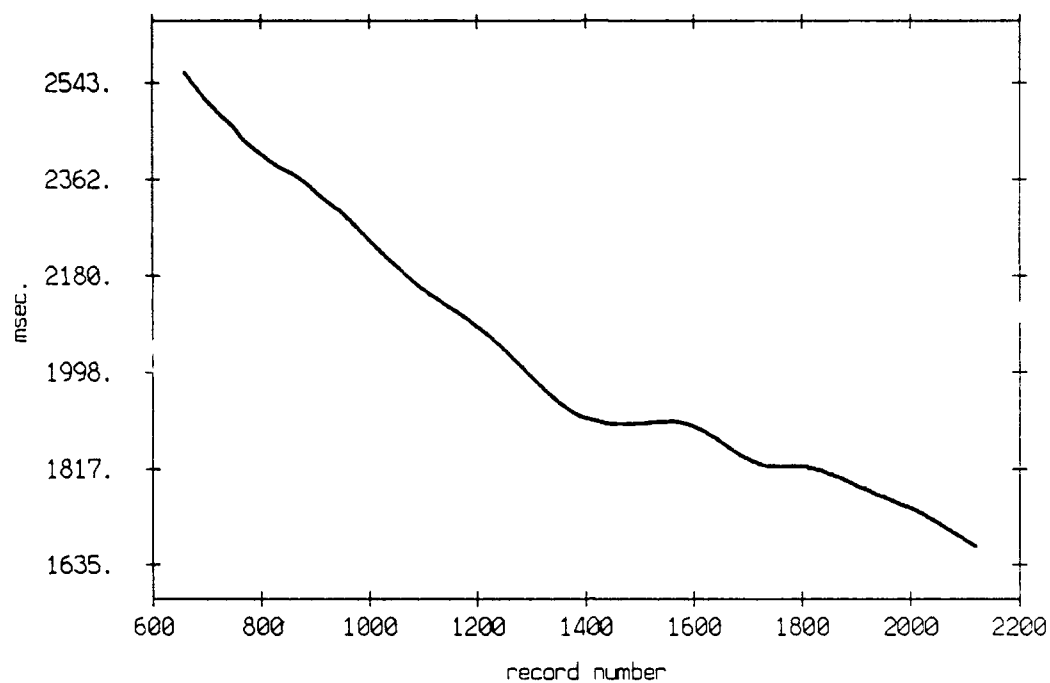
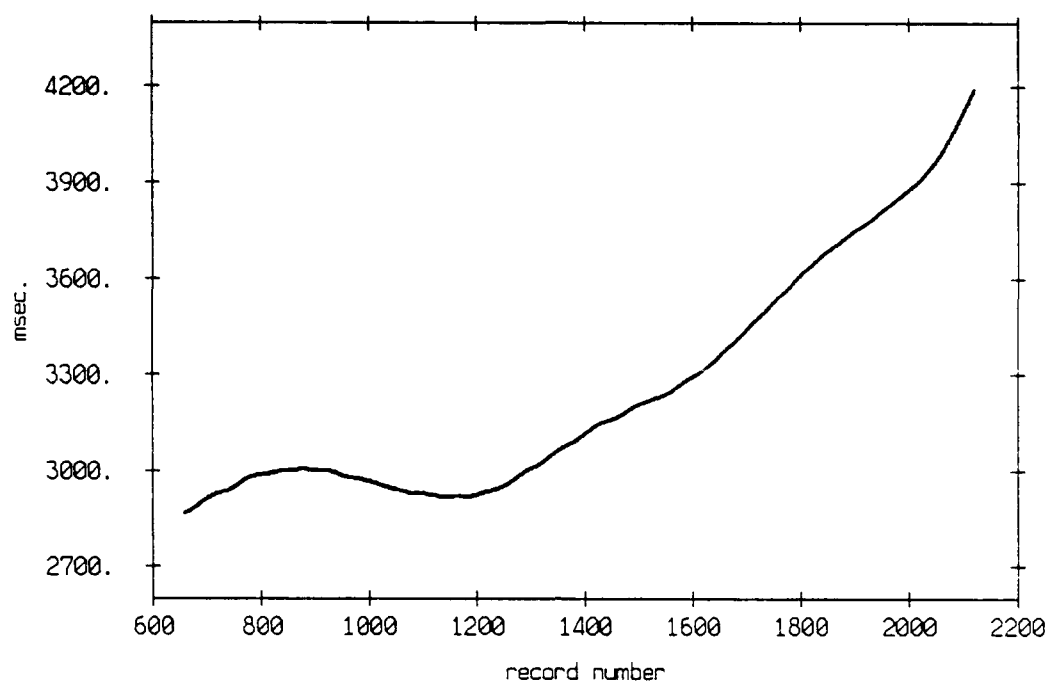


Figure 3.98

Travel time estimate, floats 10 and 0, July 1989



Travel time estimate, floats 10 and 1, July 1989

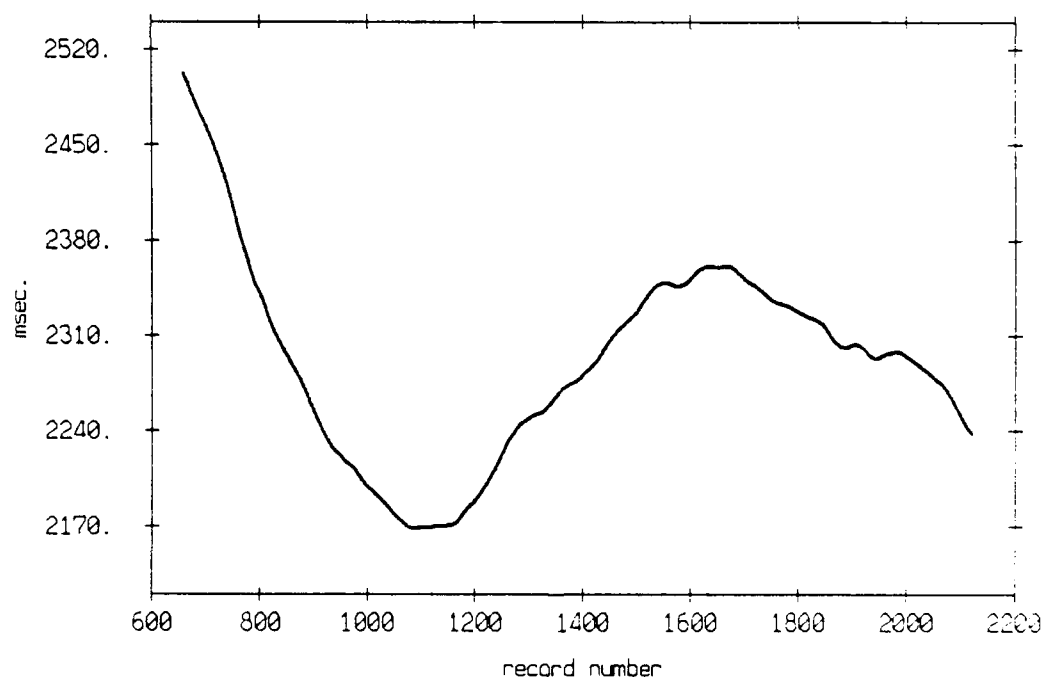
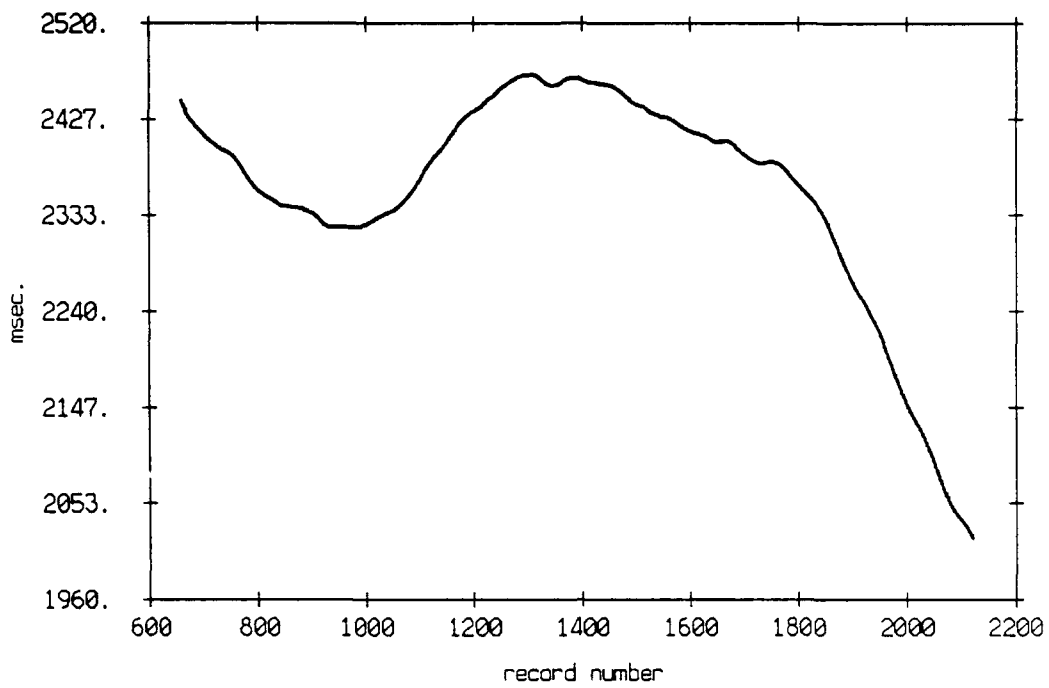


Figure 3.99

Travel time estimate, floats 10 and 2, July 1989



Travel time estimate, floats 10 and 3, July 1989

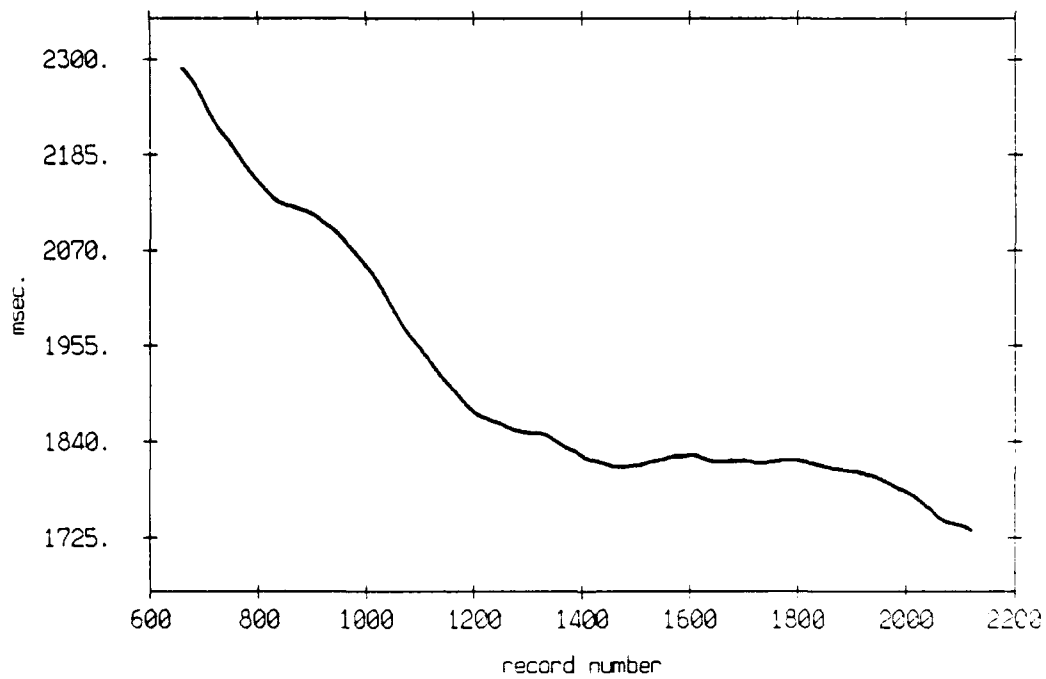
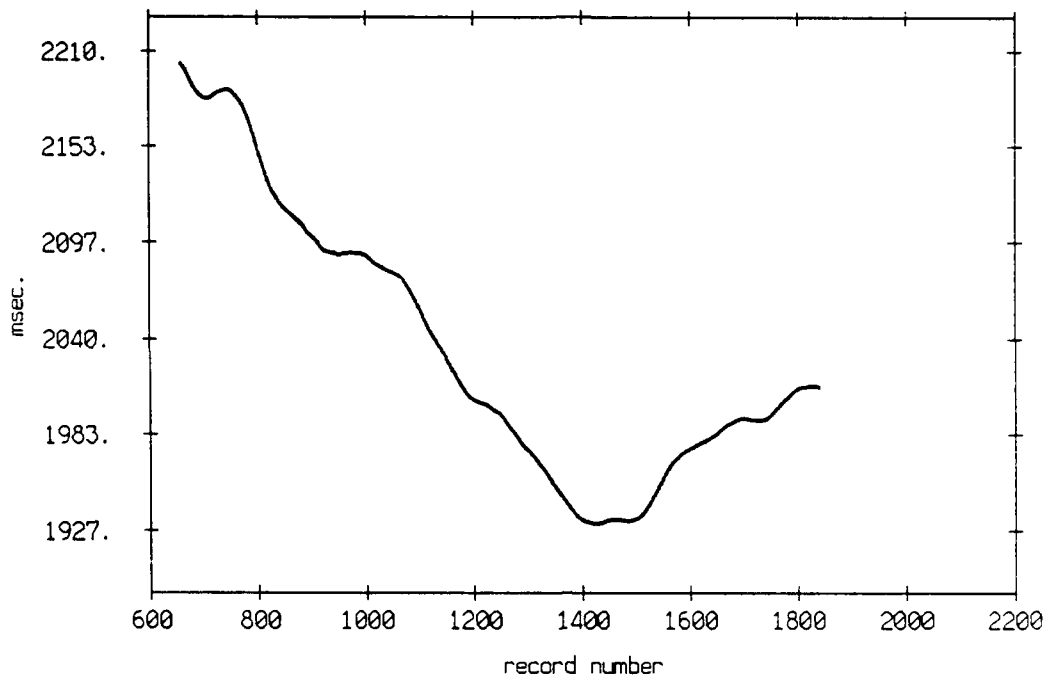


Figure 3.100

Travel time estimate, floats 10 and 4, July 1989



Travel time estimate, floats 10 and 5, July 1989

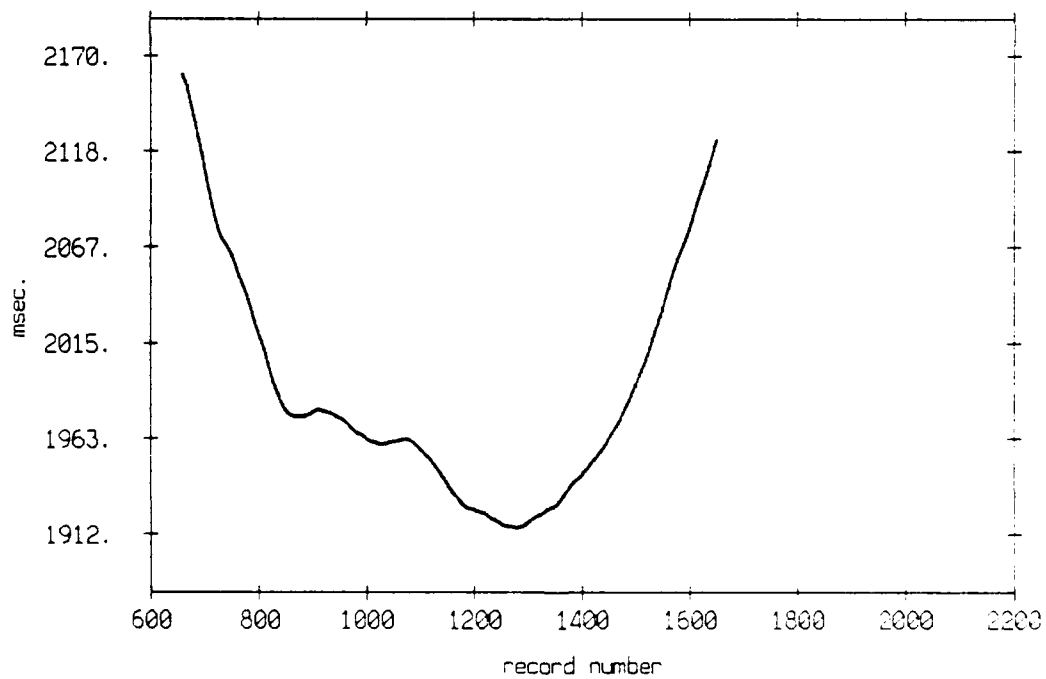
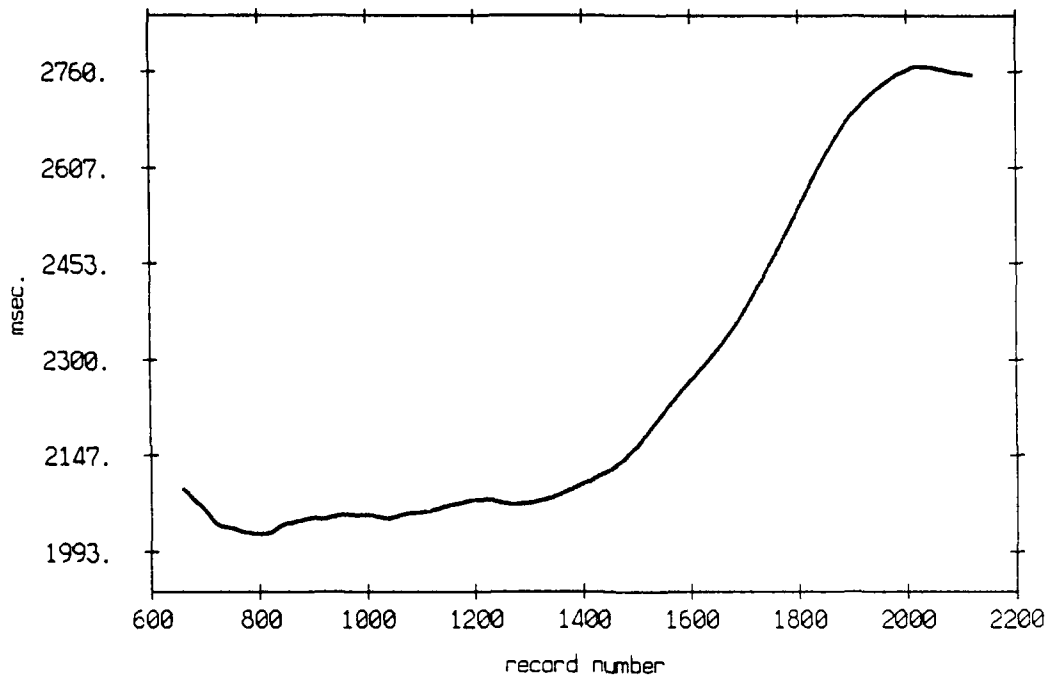


Figure 3.101

Travel time estimate, floats 10 and 6, July 1989



Travel time estimate, floats 10 and 7, July 1989

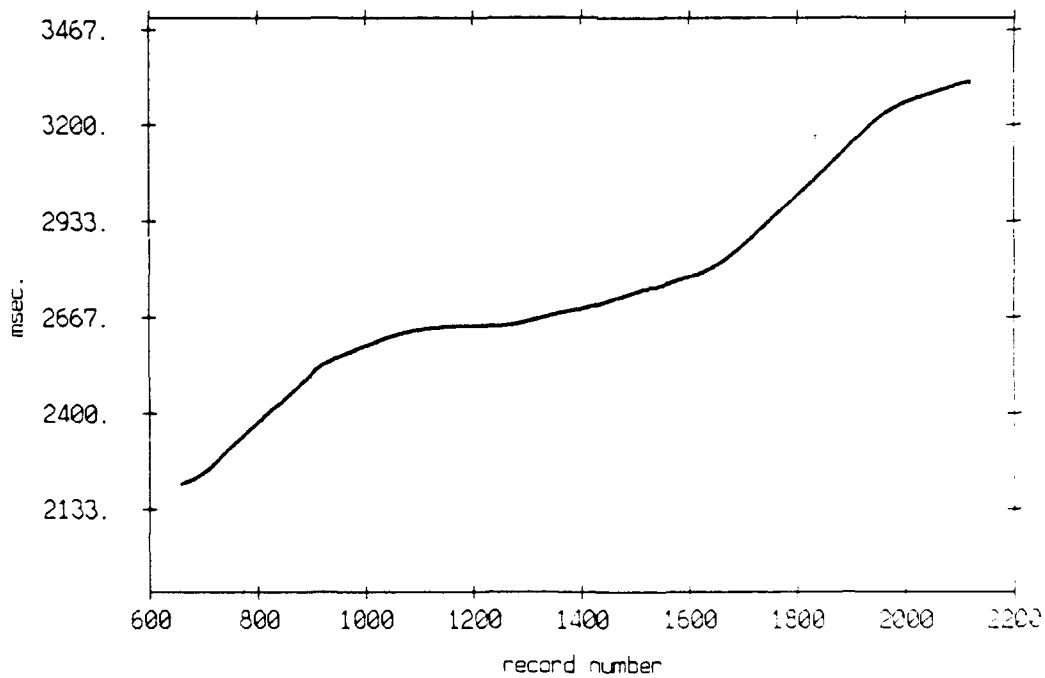


Figure 3.102

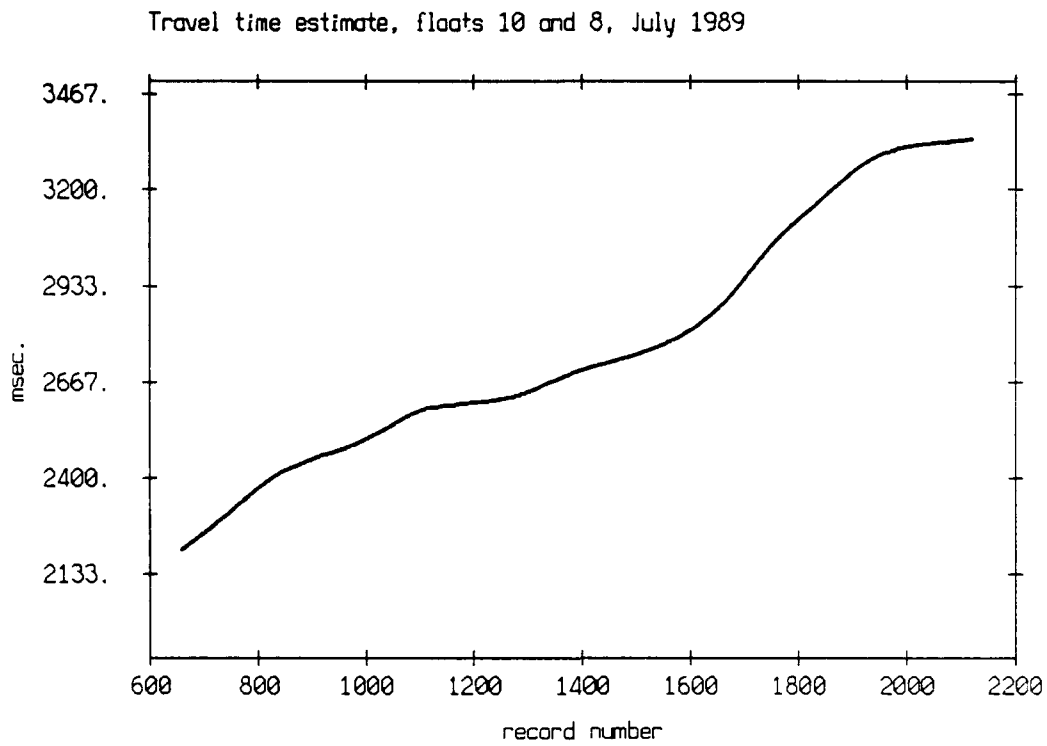
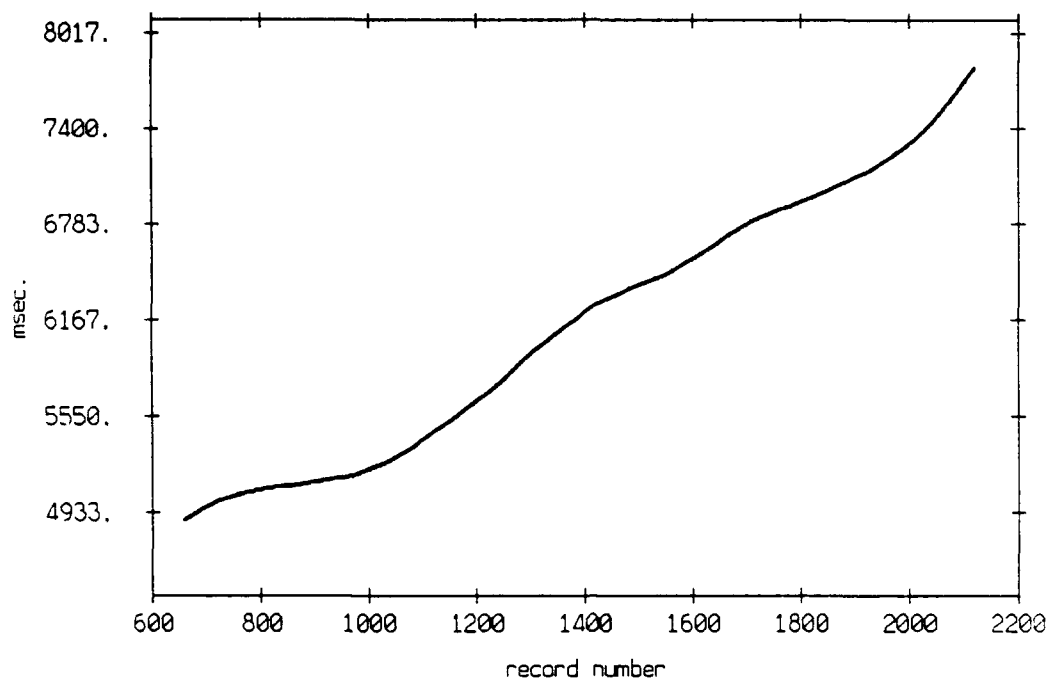


Figure 3.103

Travel time estimate, floats 11 and 0, July 1989



Travel time estimate, floats 11 and 1, July 1989

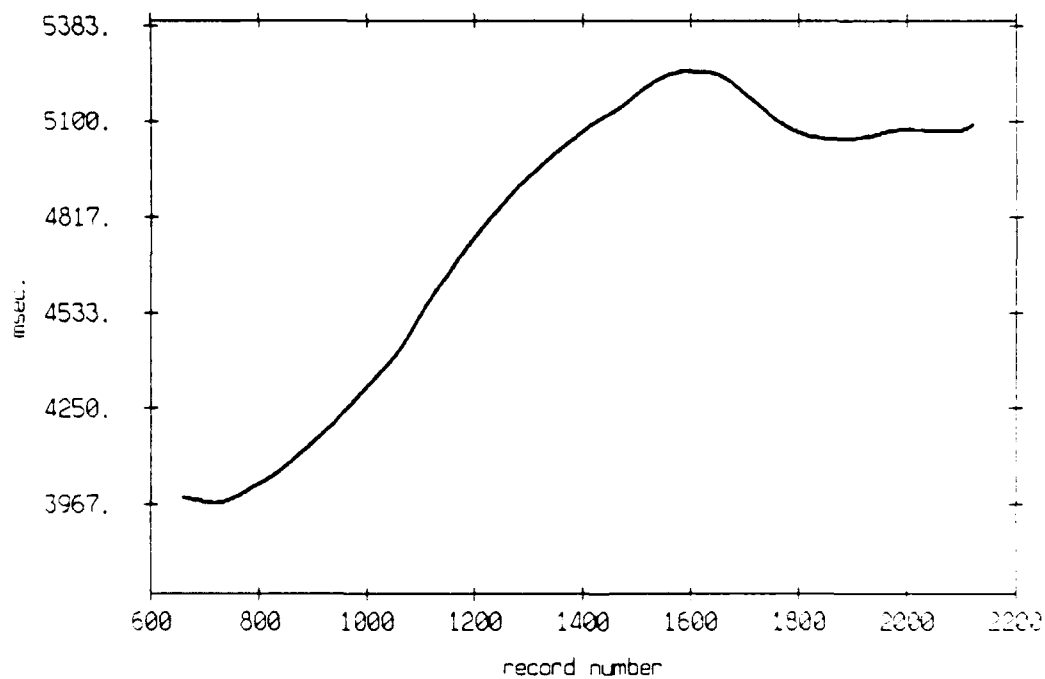
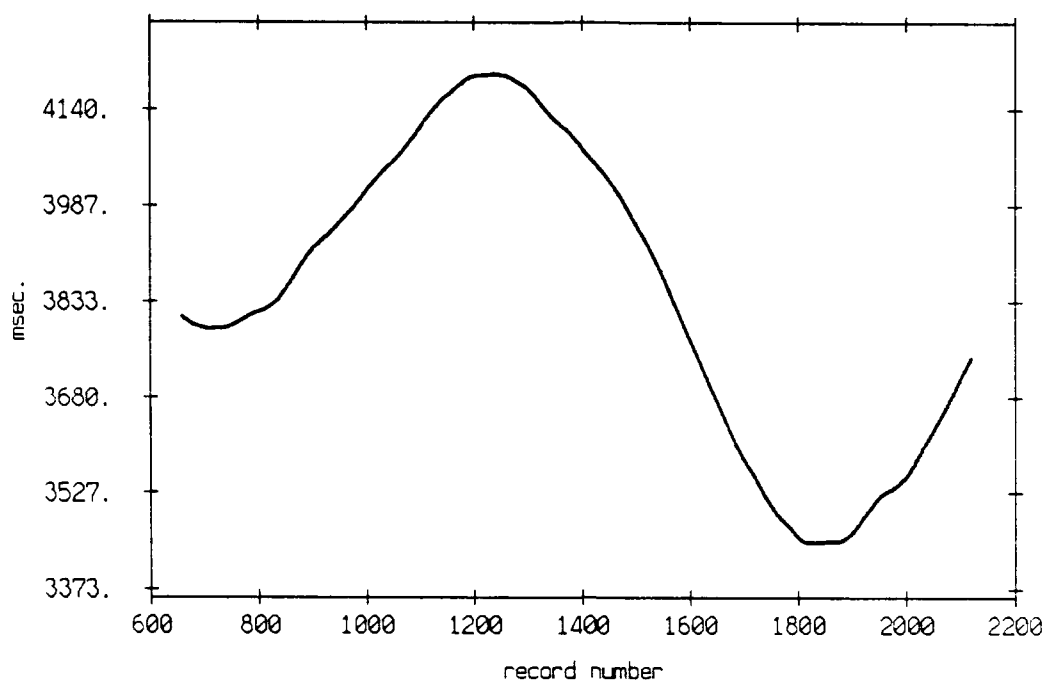


Figure 3.104

Travel time estimate, floats 11 and 2, July 1989



Travel time estimate, floats 11 and 3, July 1989

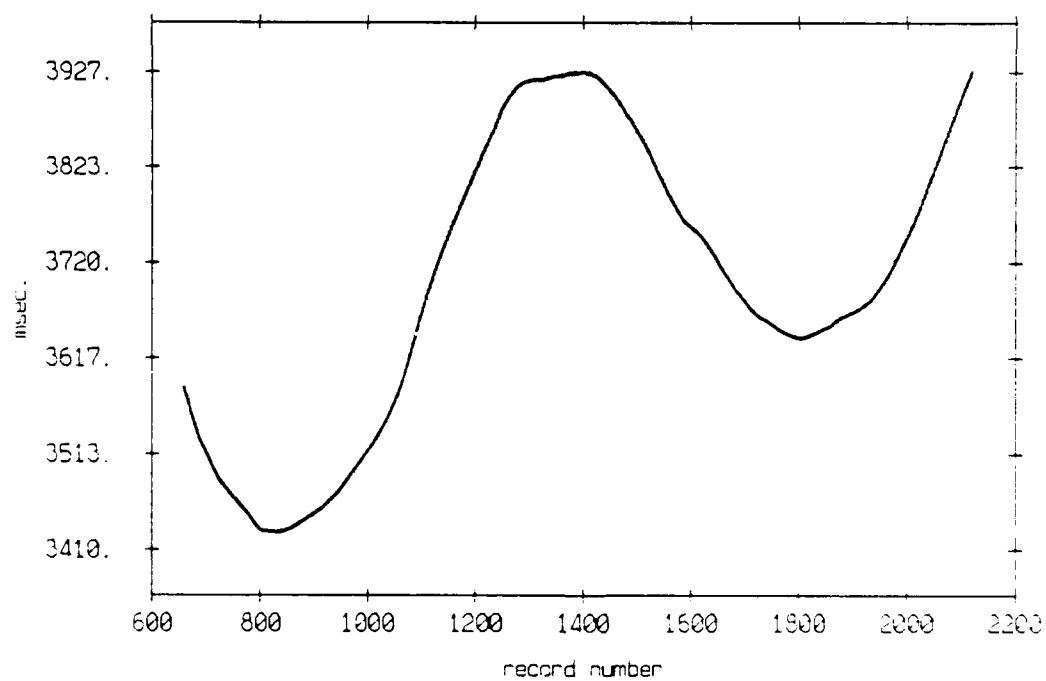
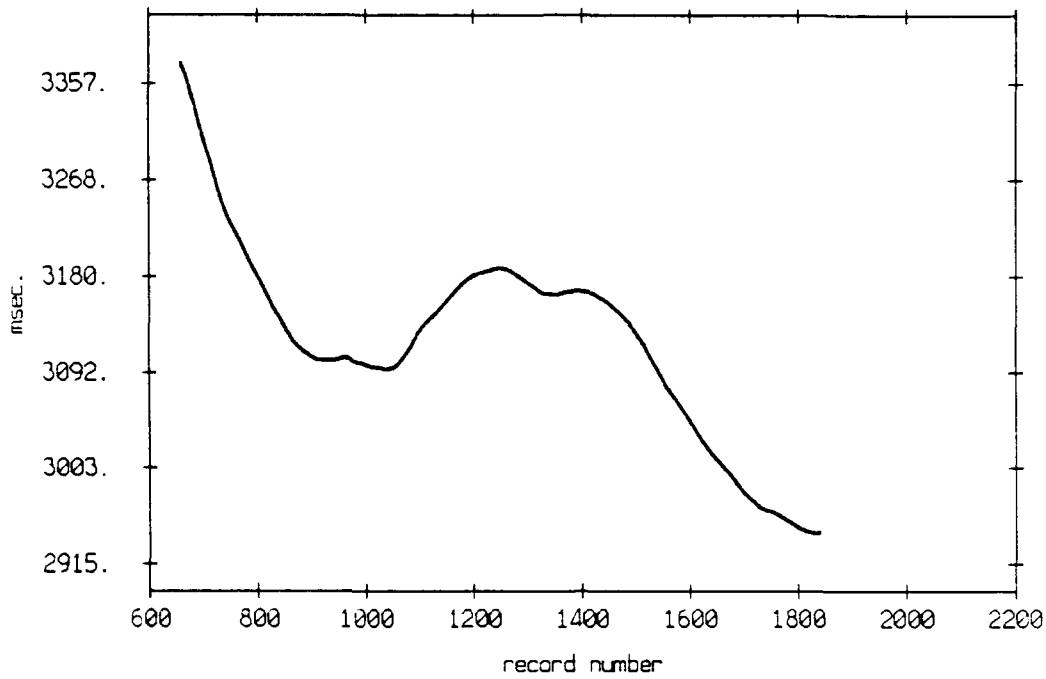


Figure 3.105

Travel time estimate, floats 11 and 4, July 1989



Travel time estimate, floats 11 and 5, July 1989

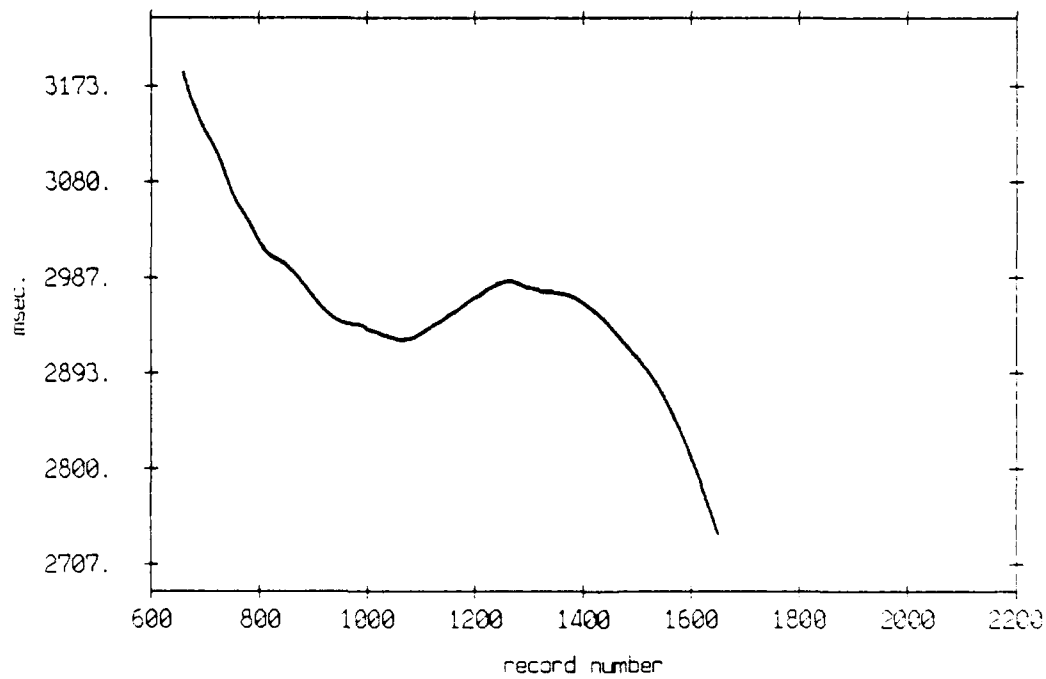


Figure 3.106

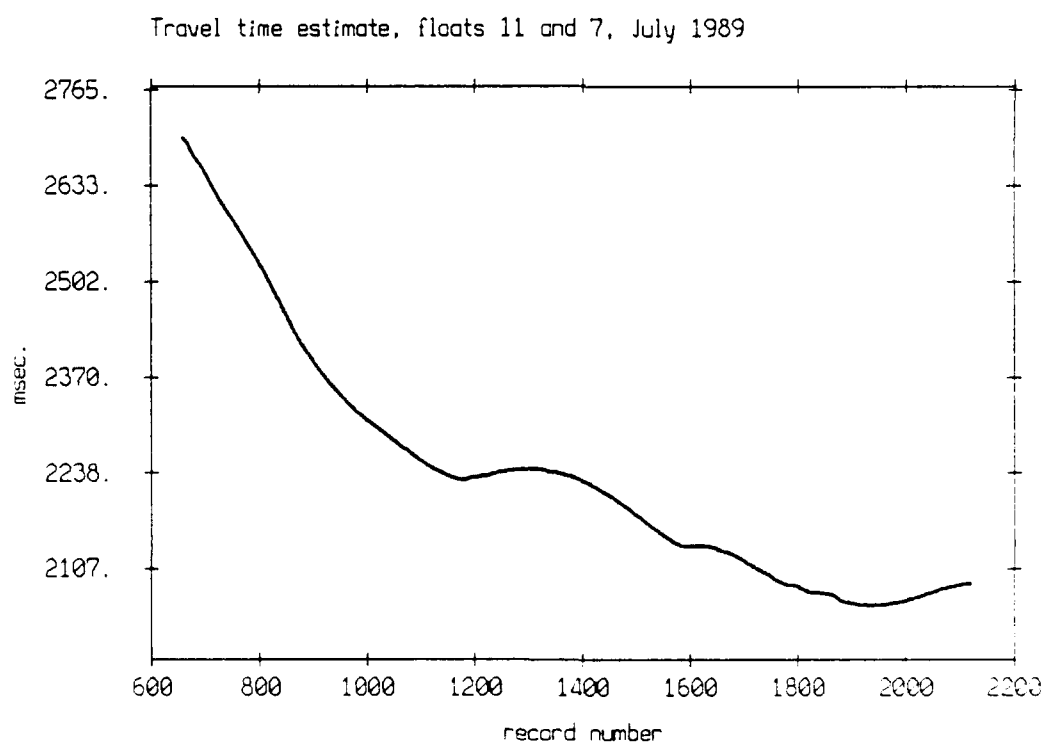
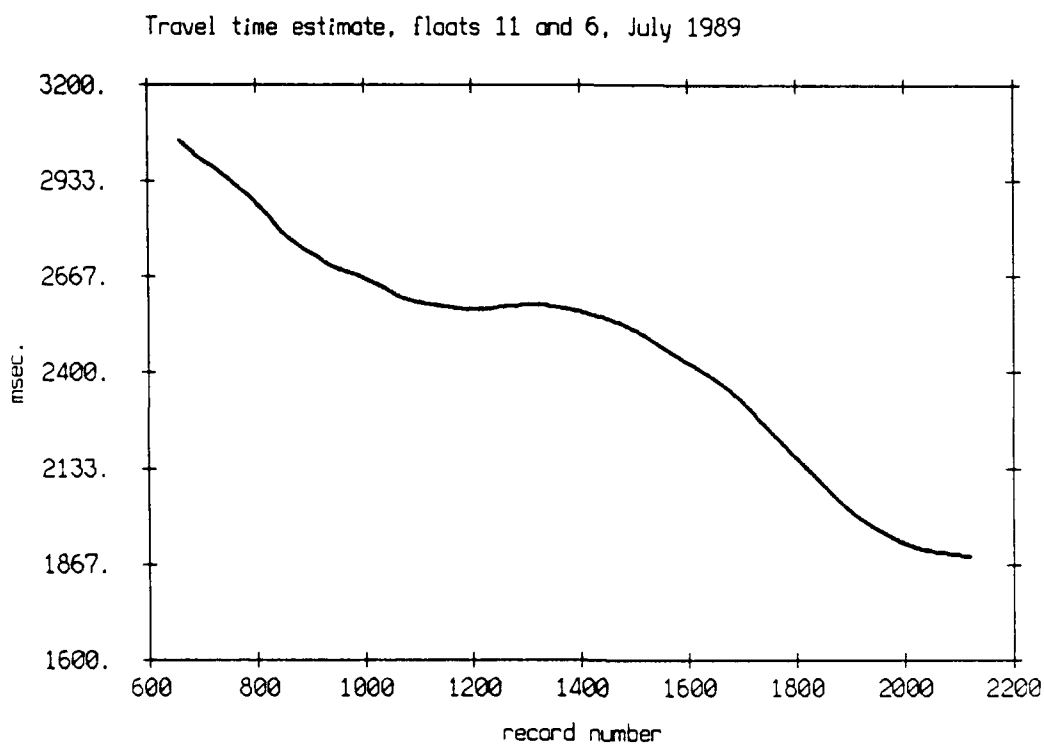
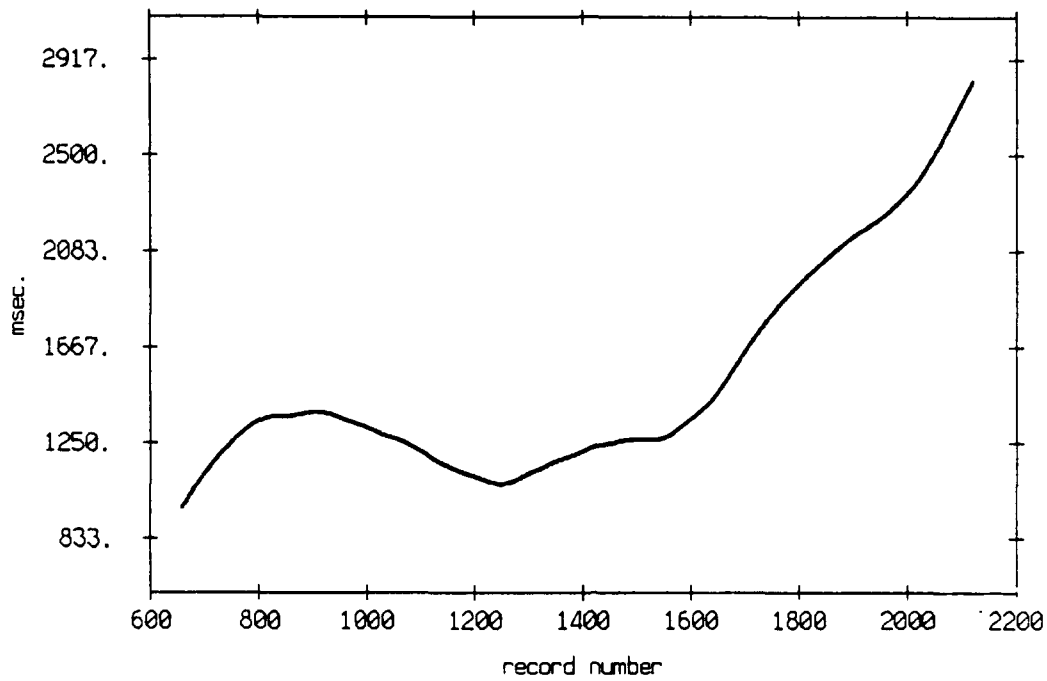


Figure 3.107

Travel time estimate, floats 0 and 1, July 1989



Travel time estimate, floats 0 and 2, July 1989

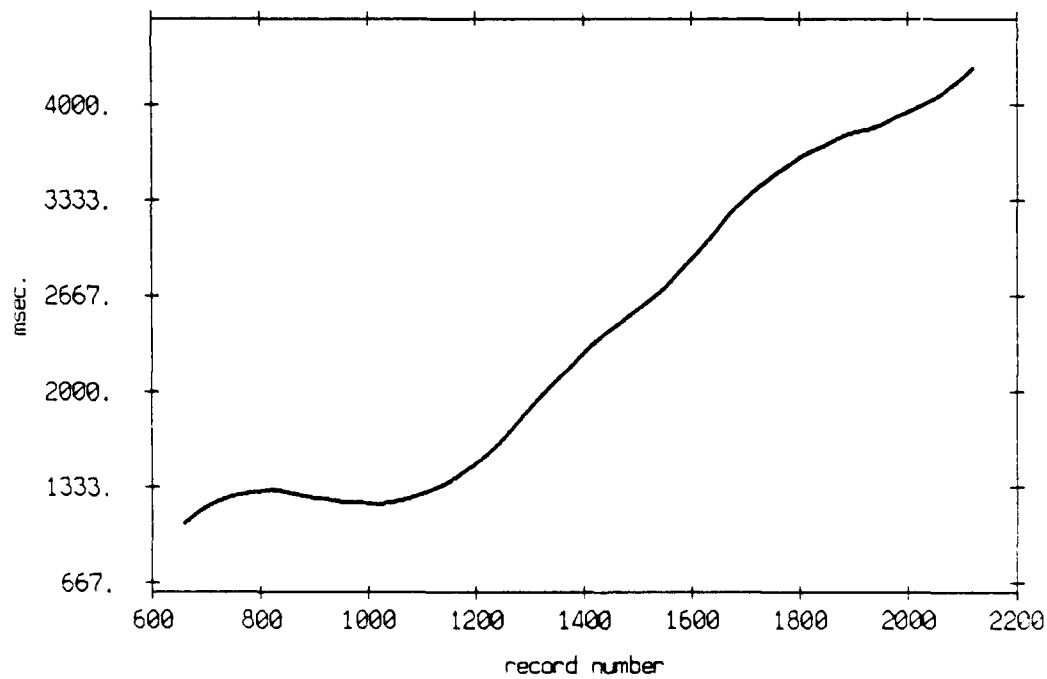
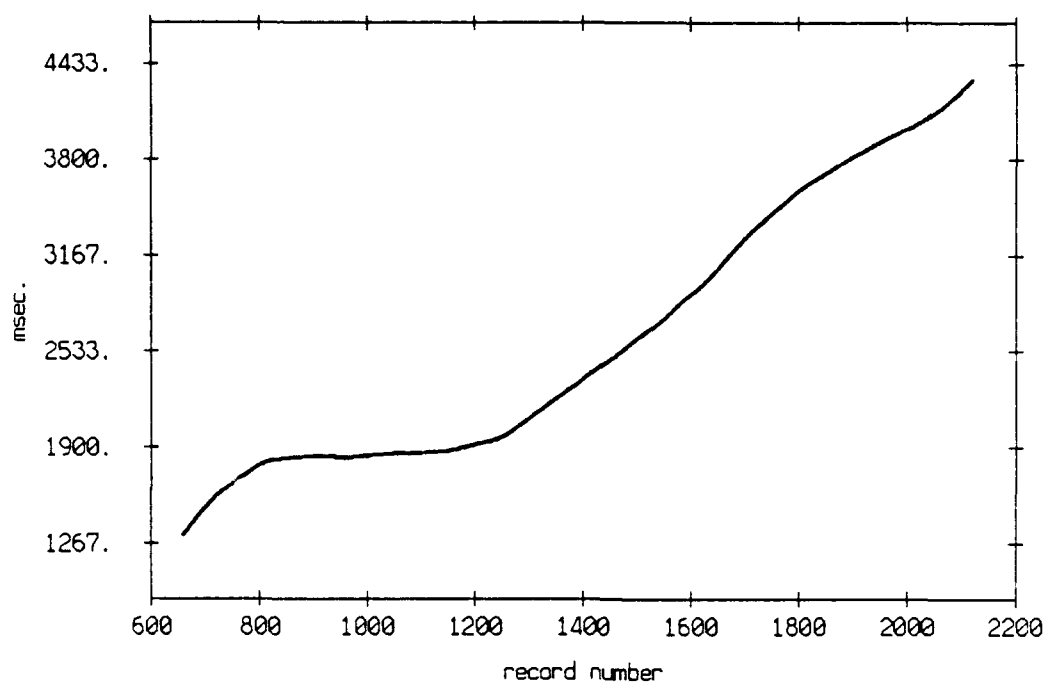


Figure 3.108

Travel time estimate, floats 0 and 3, July 1989



Travel time estimate, floats 0 and 4, July 1989

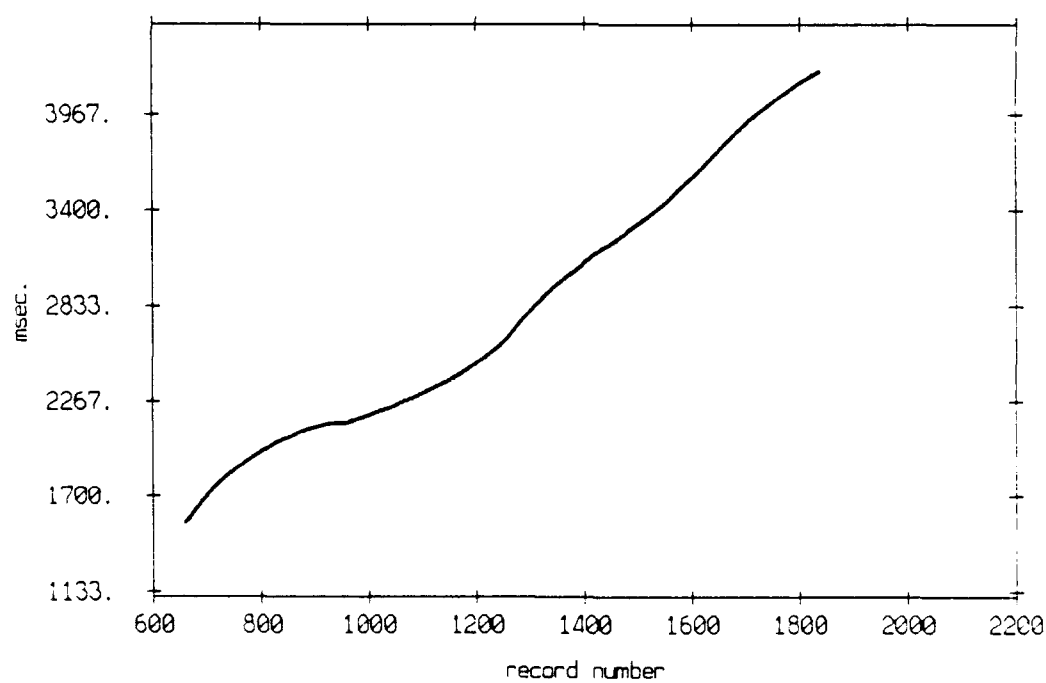


Figure 3.109

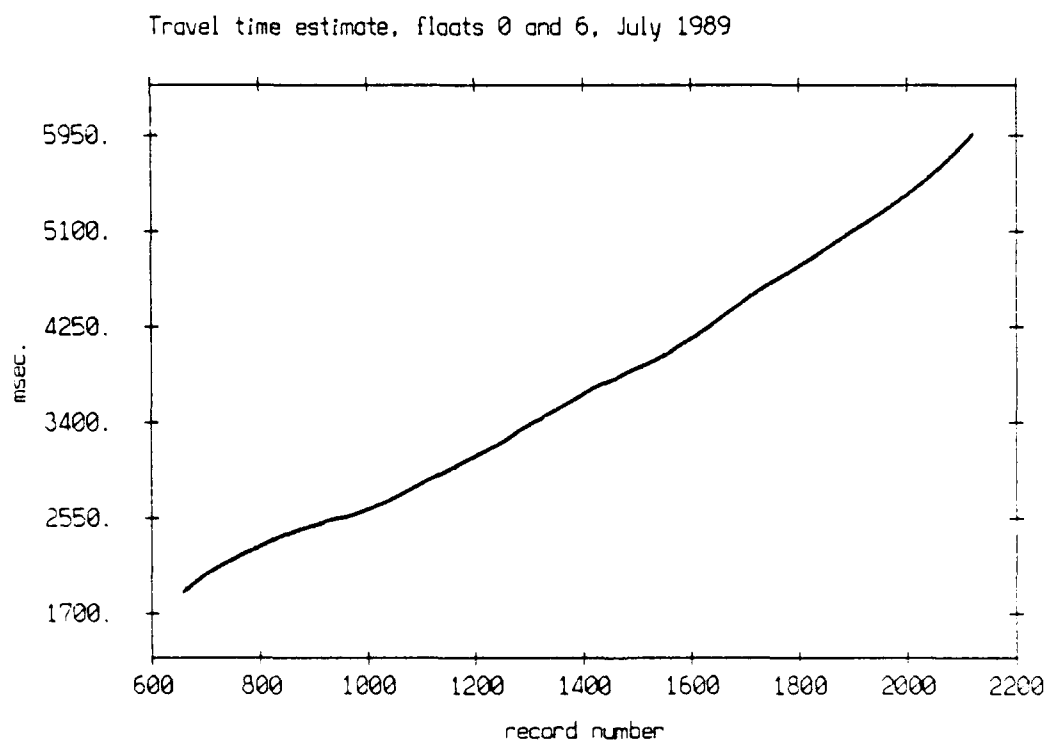
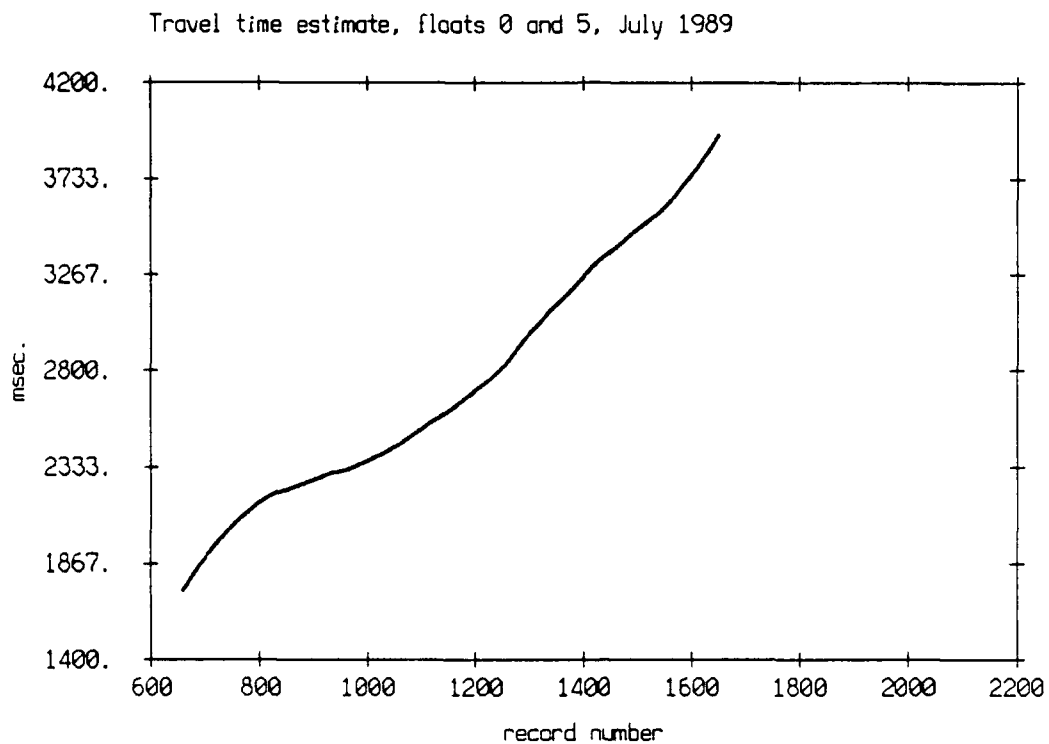
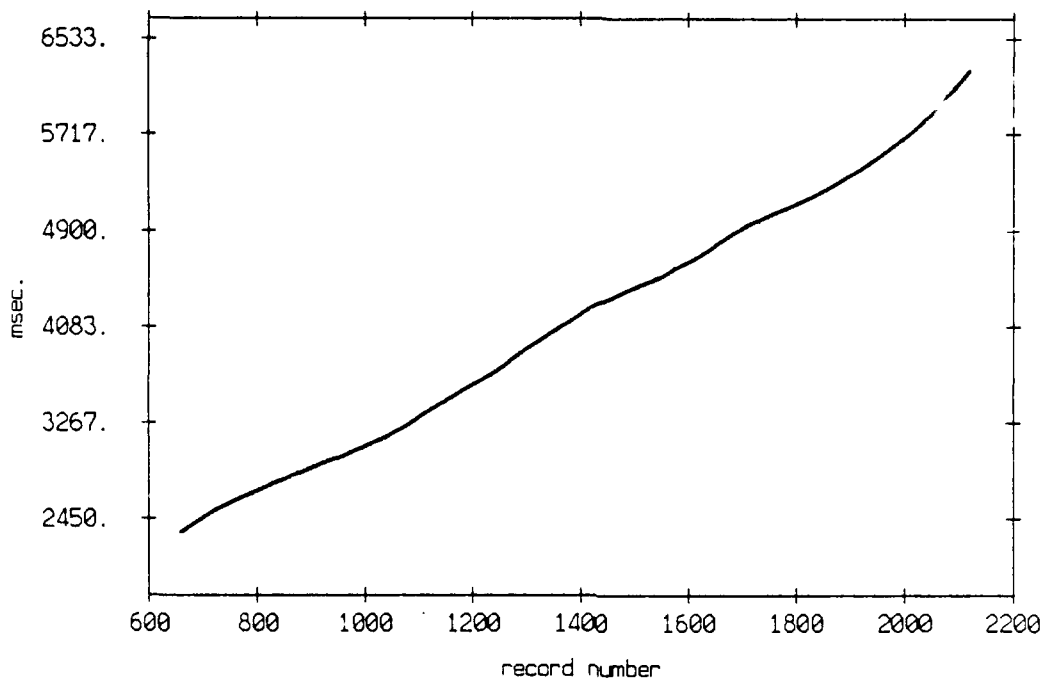


Figure 3.110

Travel time estimate, floats 0 and 7, July 1989



Travel time estimate, floats 0 and 8, July 1989

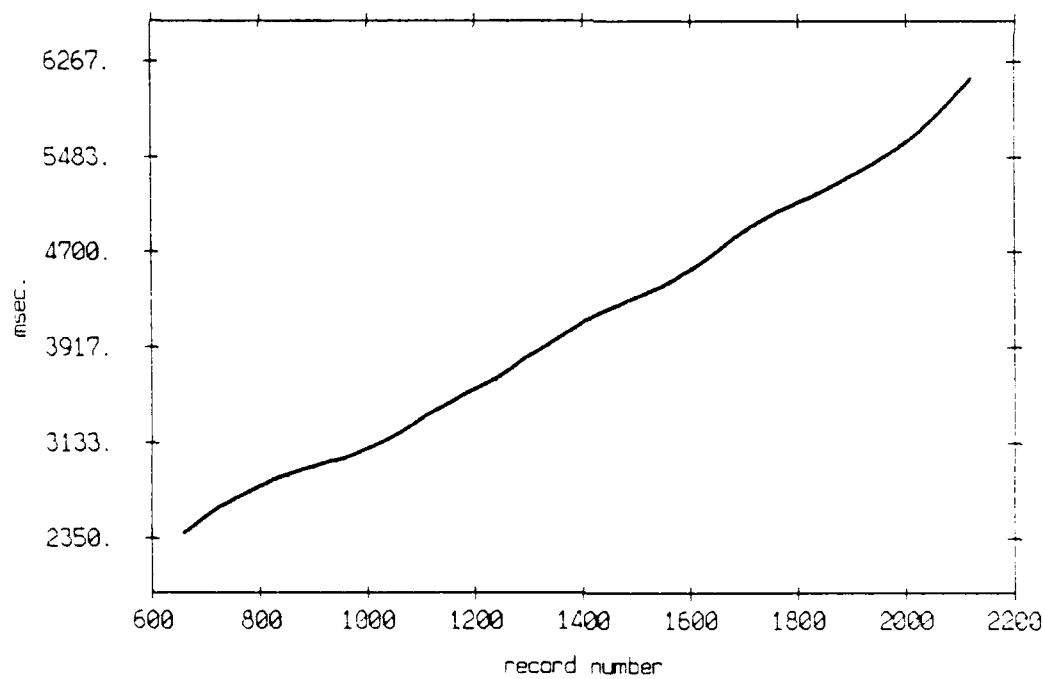
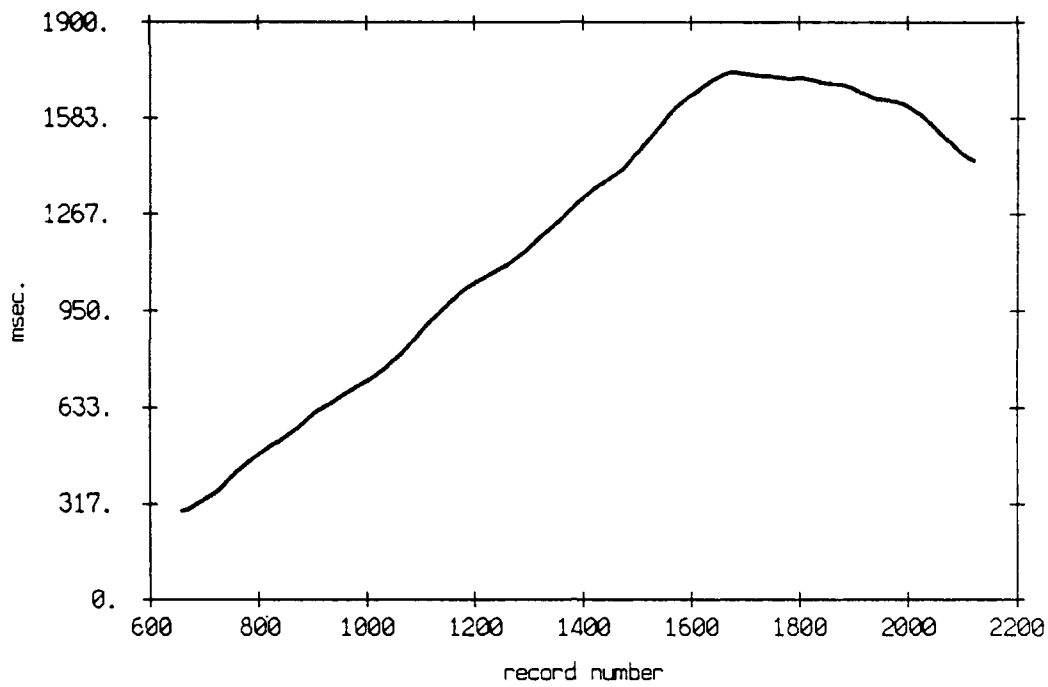


Figure 3.111

Travel time estimate, floats 1 and 2, July 1989



Travel time estimate, floats 1 and 3, July 1989

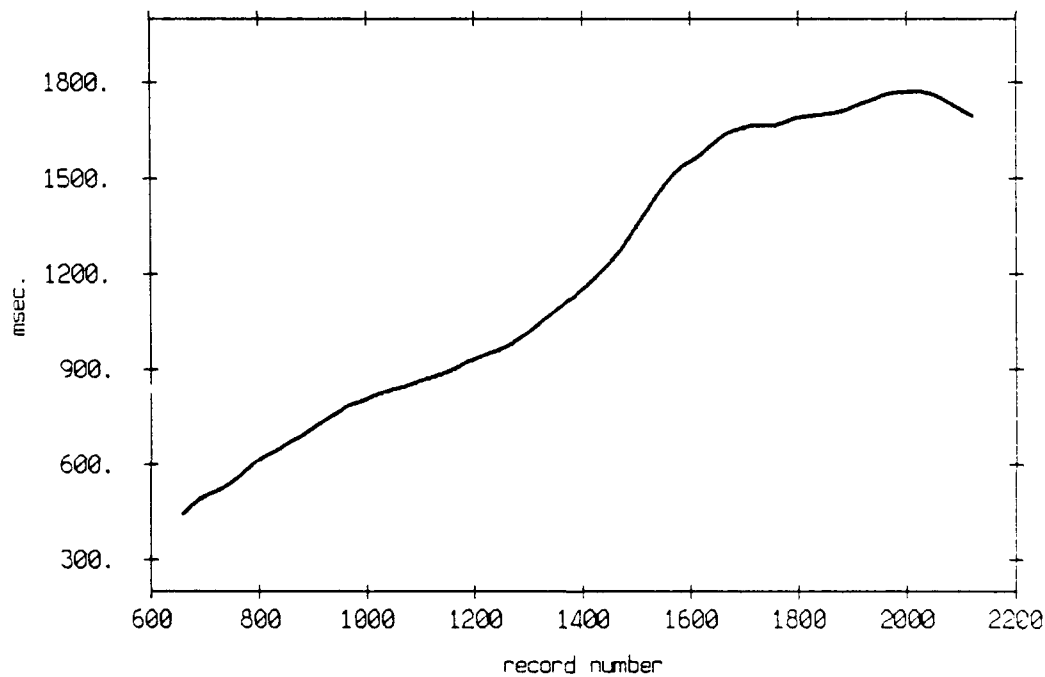
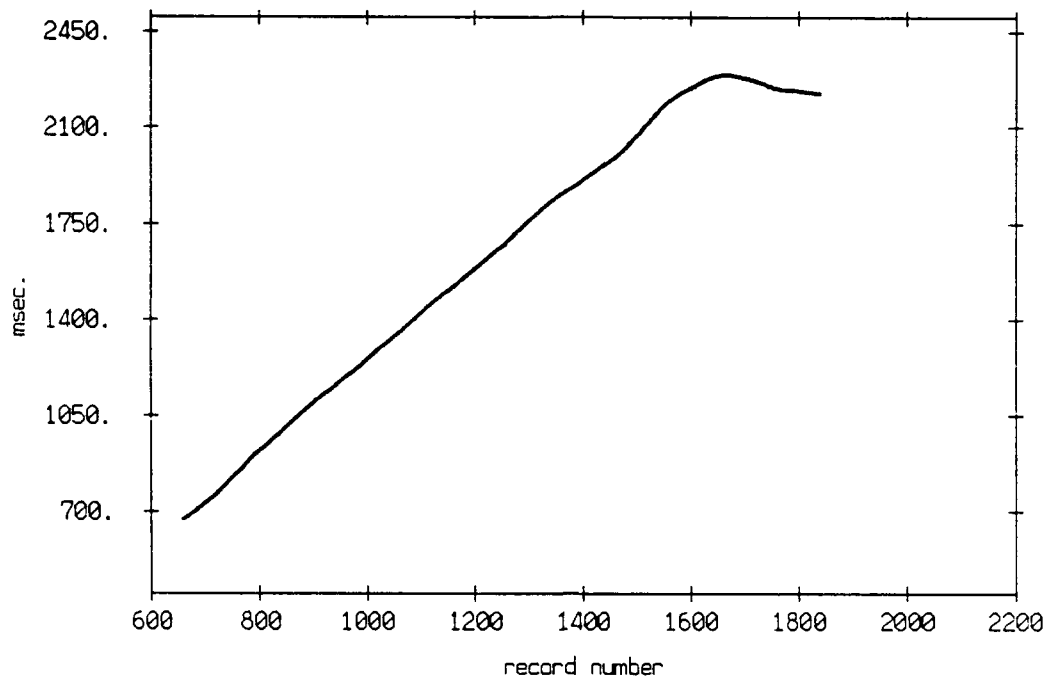


Figure 3.112

Travel time estimate, floats 1 and 4, July 1989



Travel time estimate, floats 1 and 5, July 1989

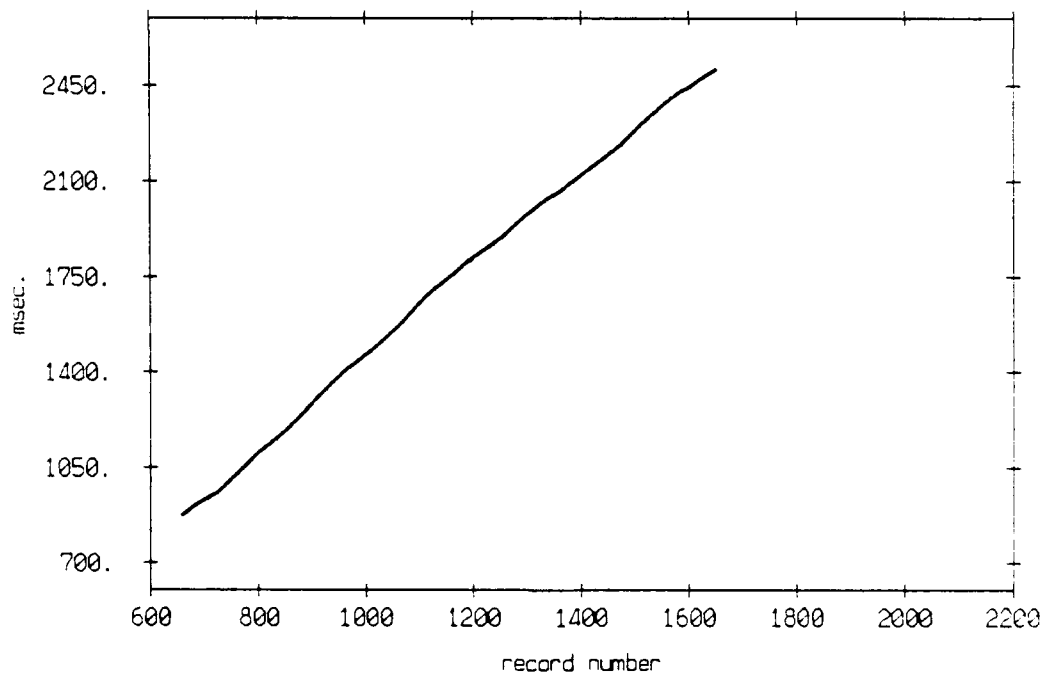
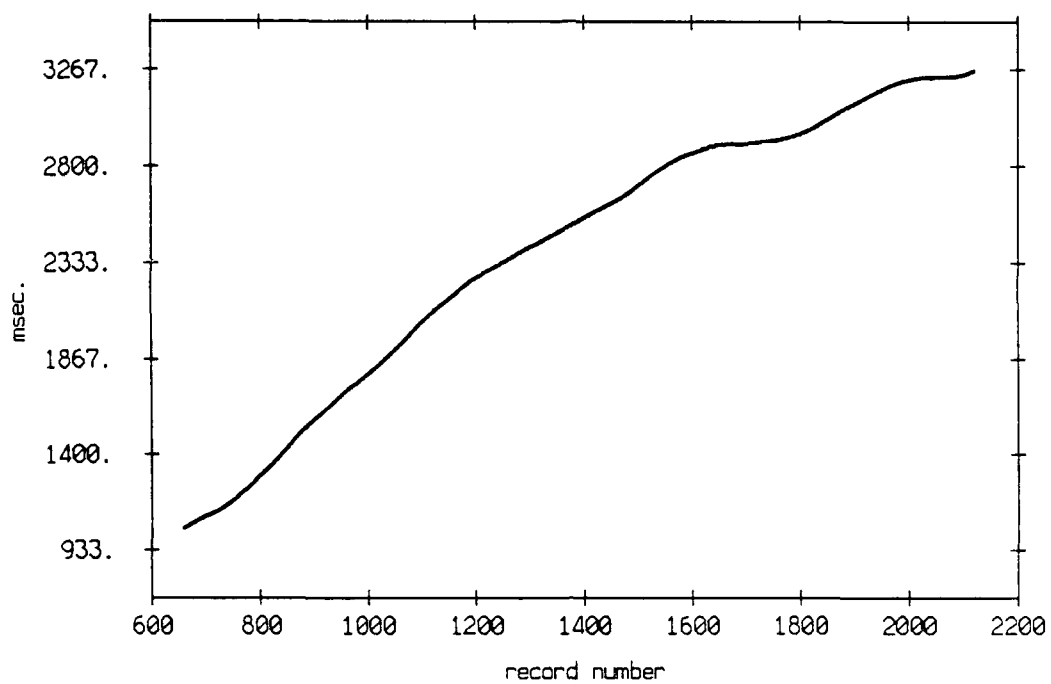


Figure 3.113

Travel time estimate, floats 1 and 6, July 1989



Travel time estimate, floats 1 and 7, July 1989

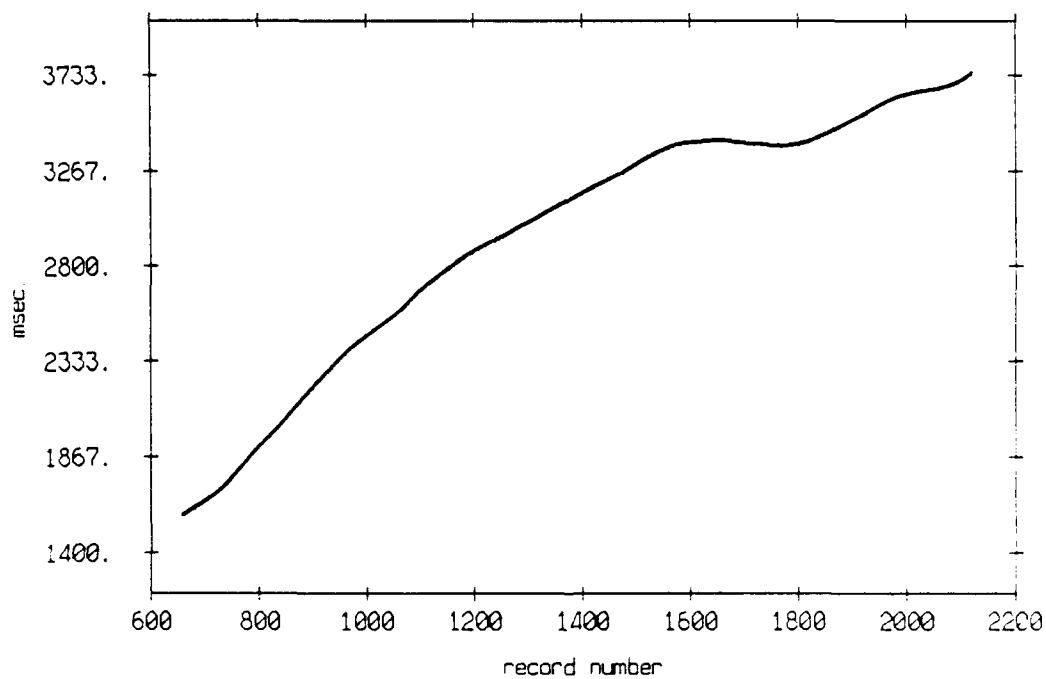


Figure 3.114

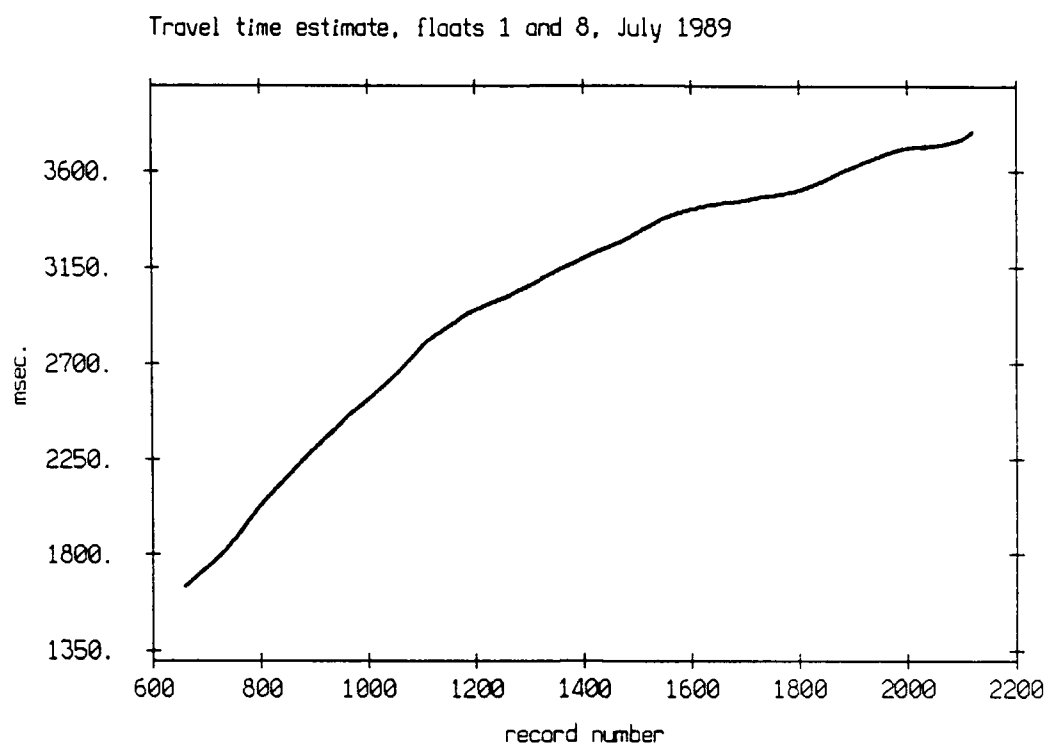
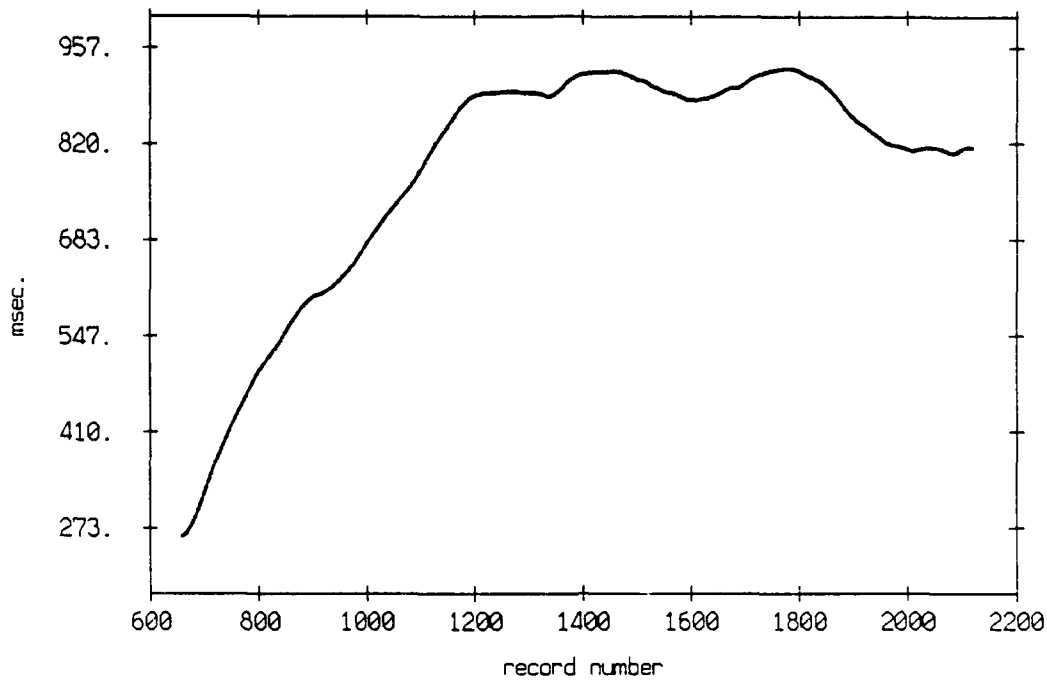


Figure 3.115

Travel time estimate, floats 2 and 3, July 1989



Travel time estimate, floats 2 and 4, July 1989

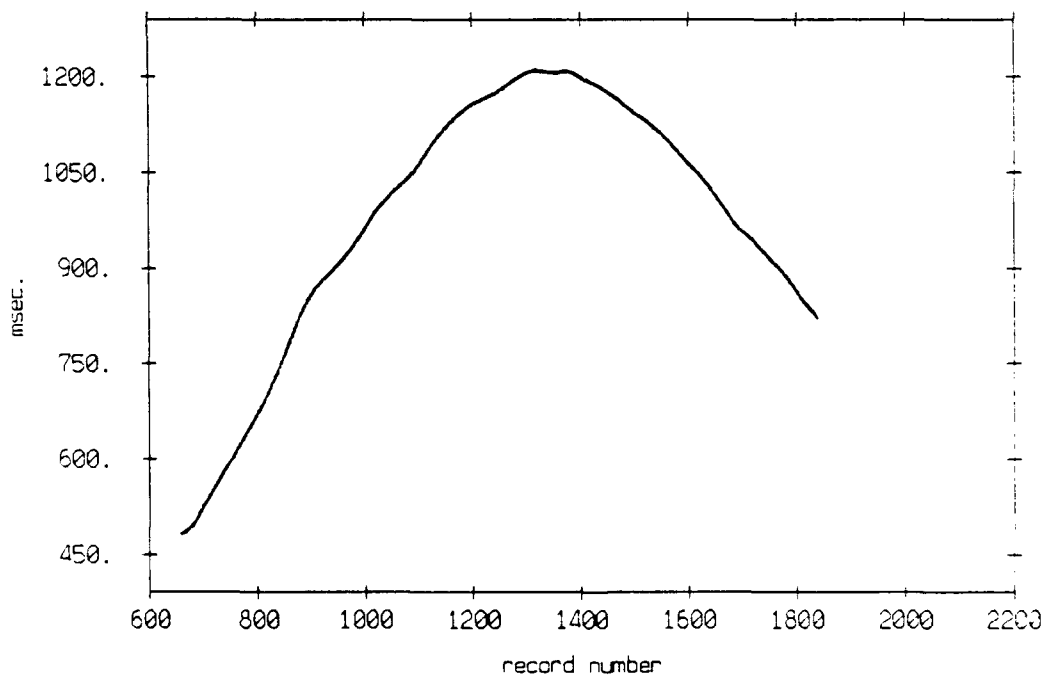
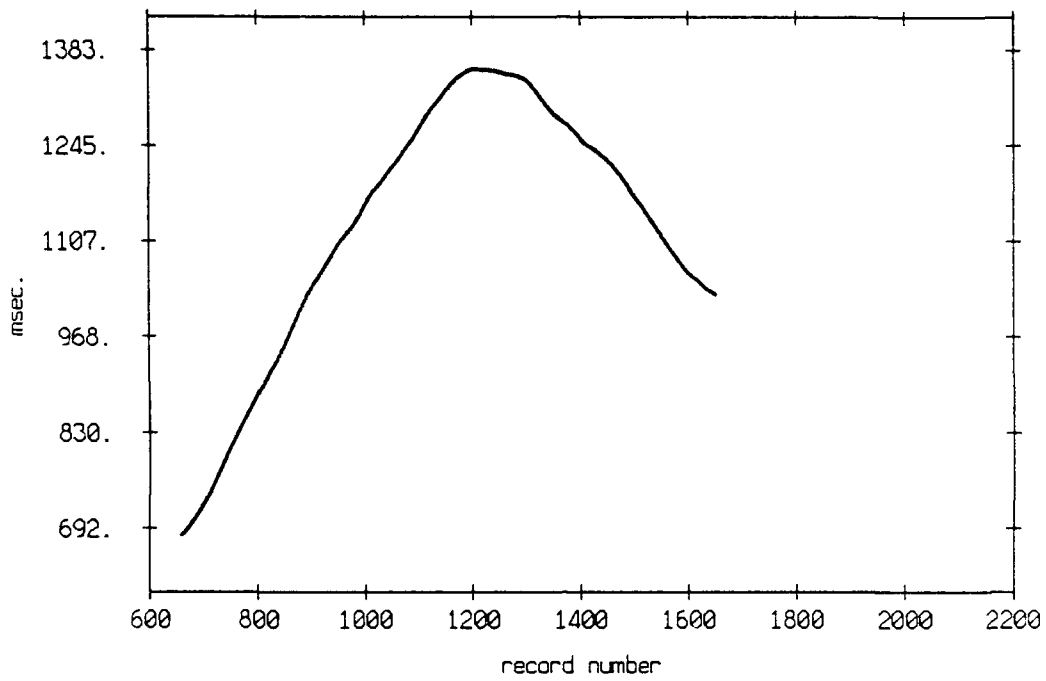


Figure 3.116

Travel time estimate, floats 2 and 5, July 1989



Travel time estimate, floats 2 and 6, July 1989

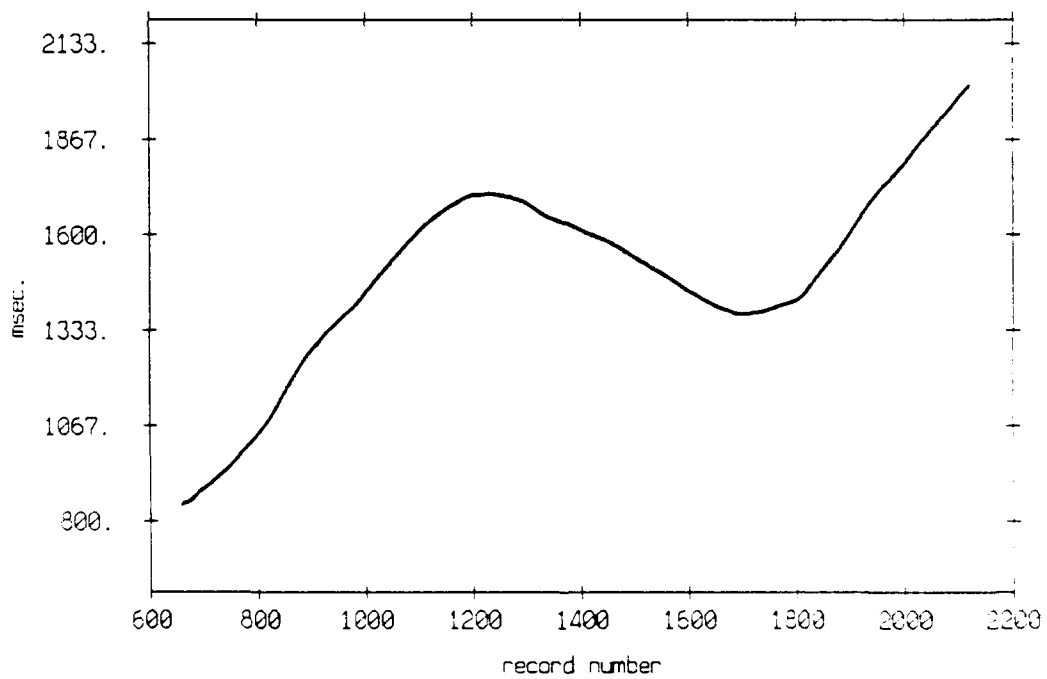
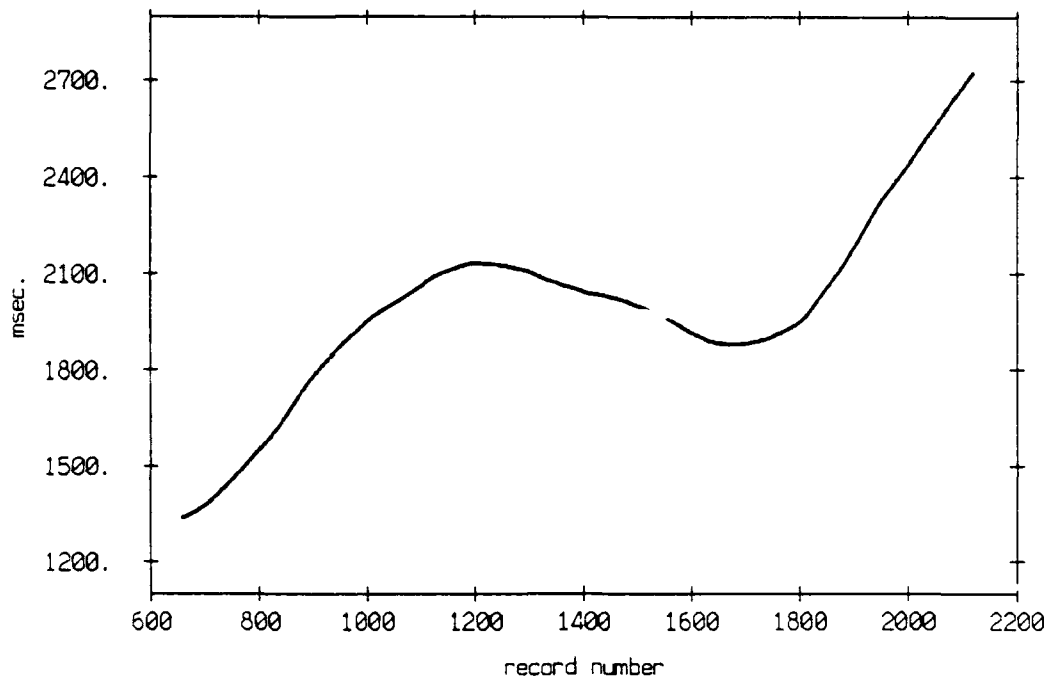


Figure 3.117

Travel time estimate, floats 2 and 7, July 1989



Travel time estimate, floats 2 and 8, July 1989

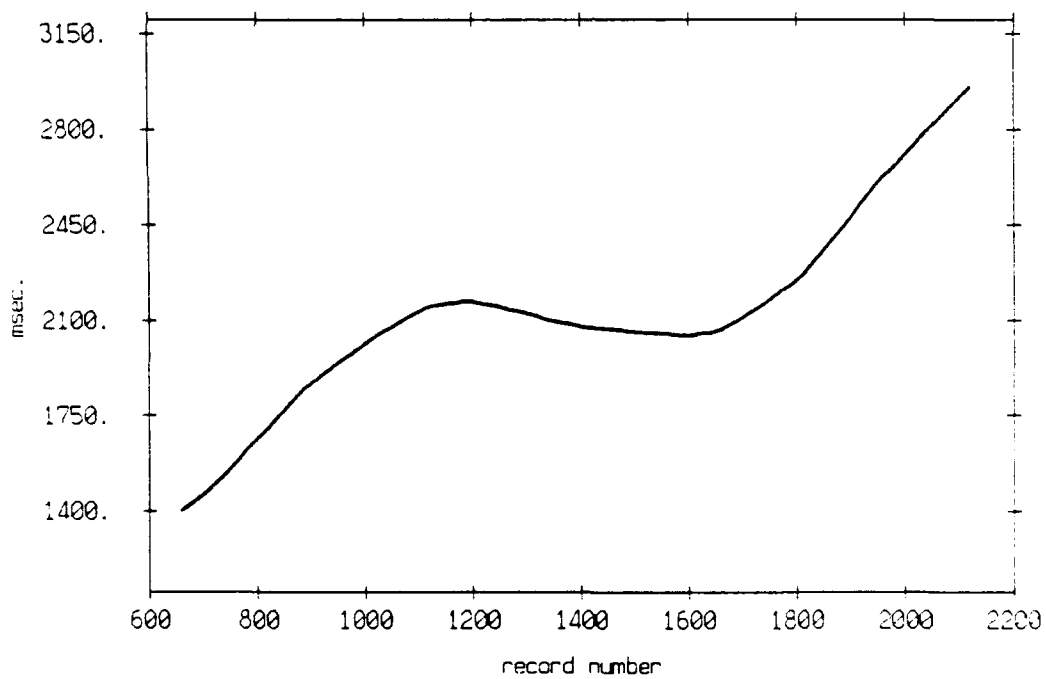
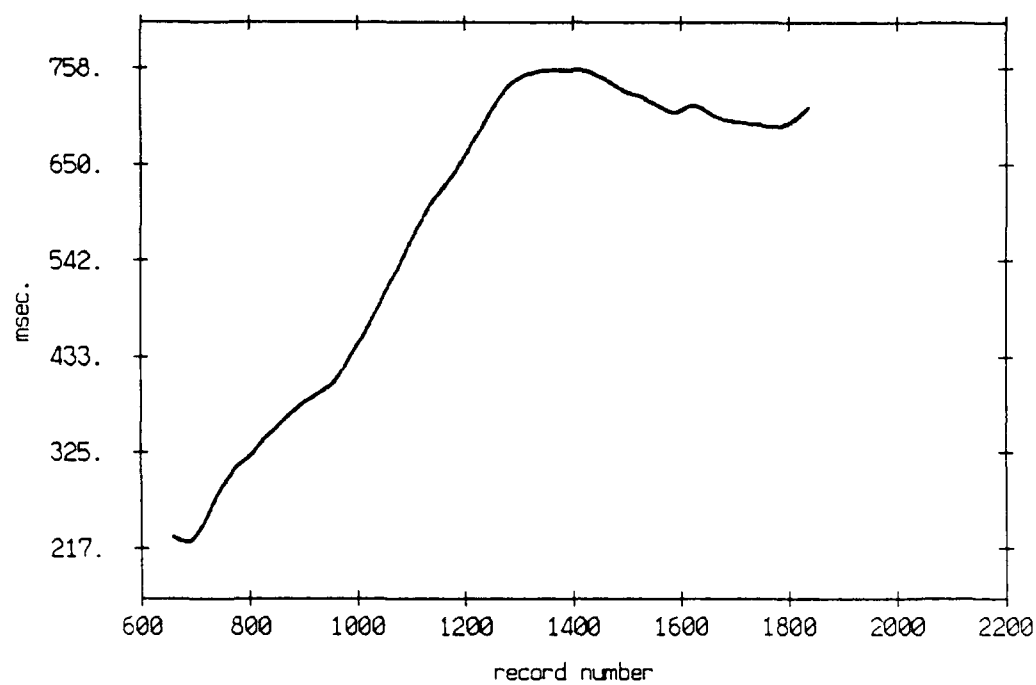


Figure 3.118

Travel time estimate, floats 3 and 4, July 1989



Travel time estimate, floats 3 and 5, July 1989

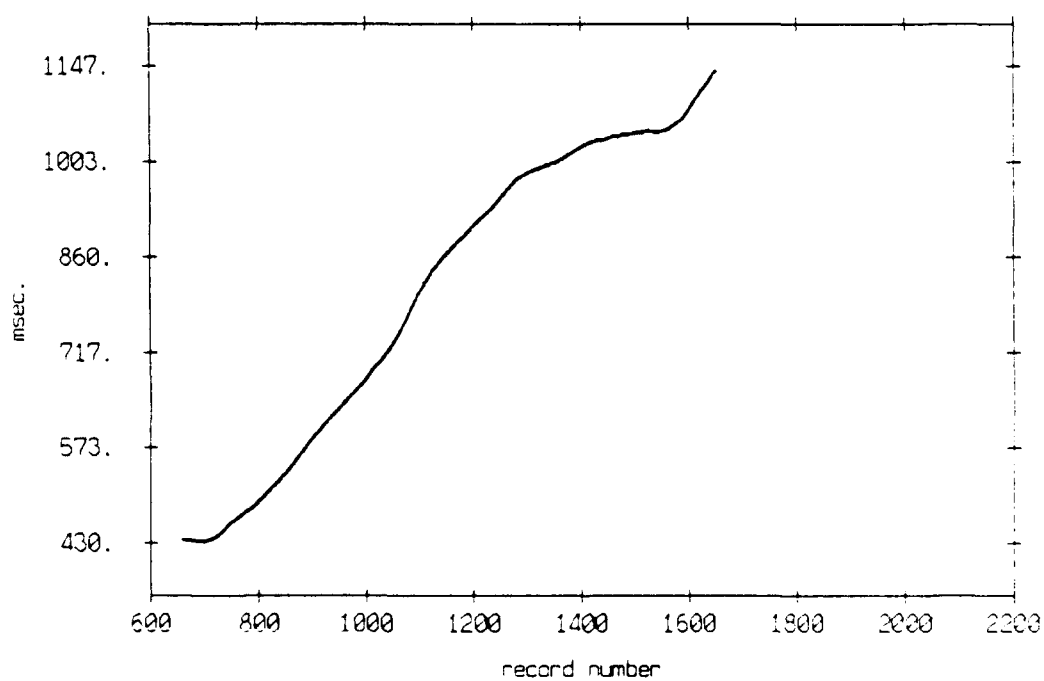
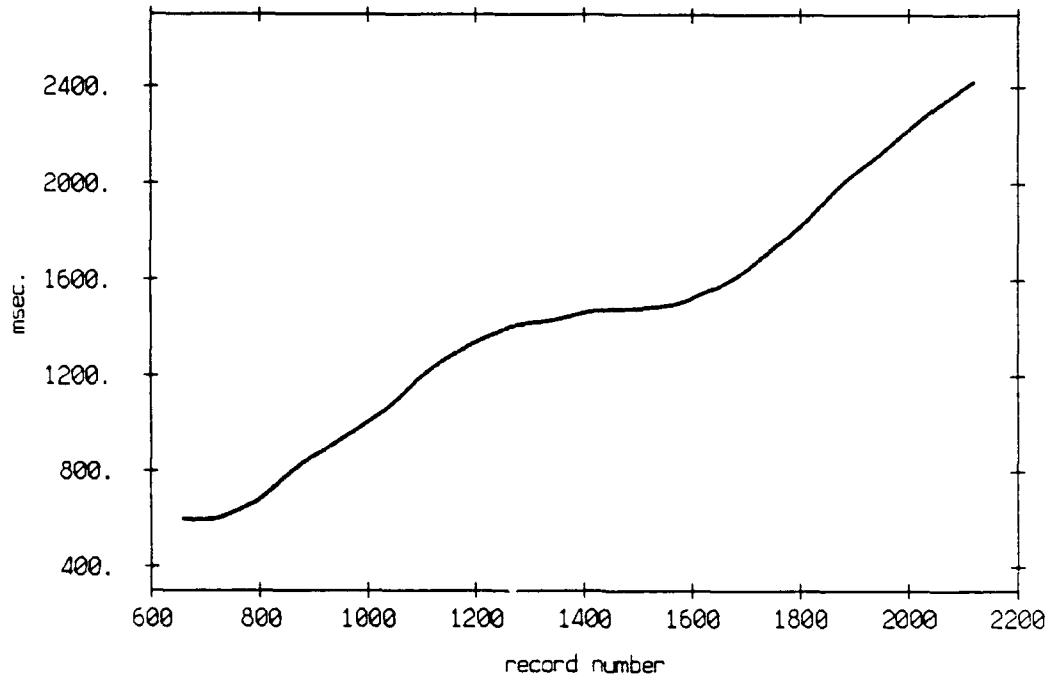


Figure 3.119

Travel time estimate, floats 3 and 6, July 1989



Travel time estimate, floats 3 and 7, July 1989

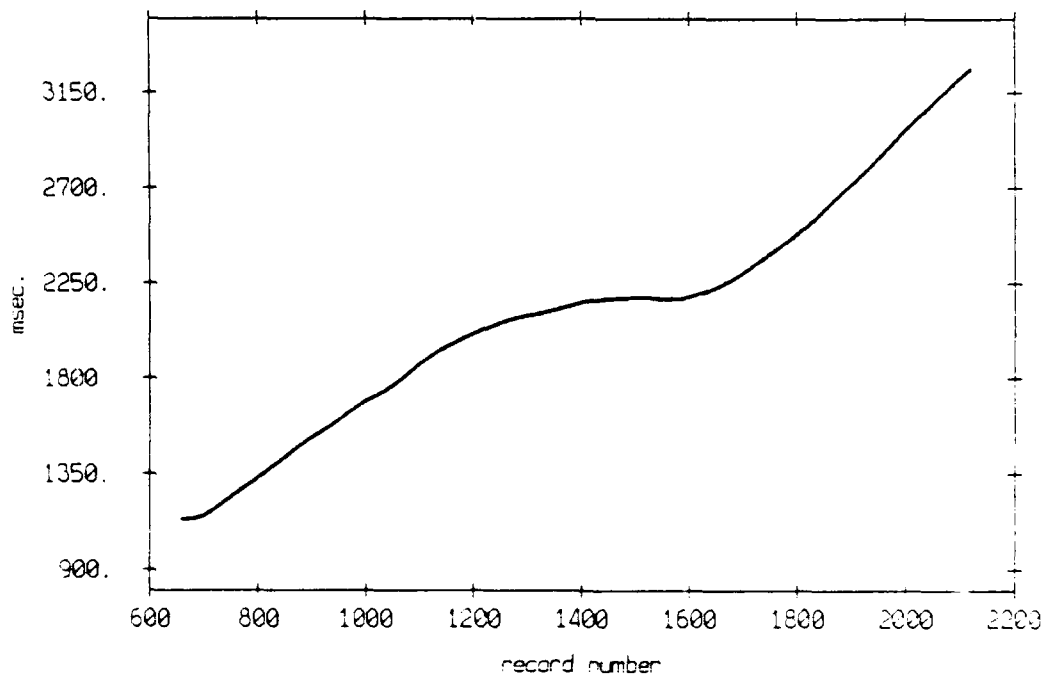


Figure 3.120

Travel time estimate, floats 3 and 8, July 1989

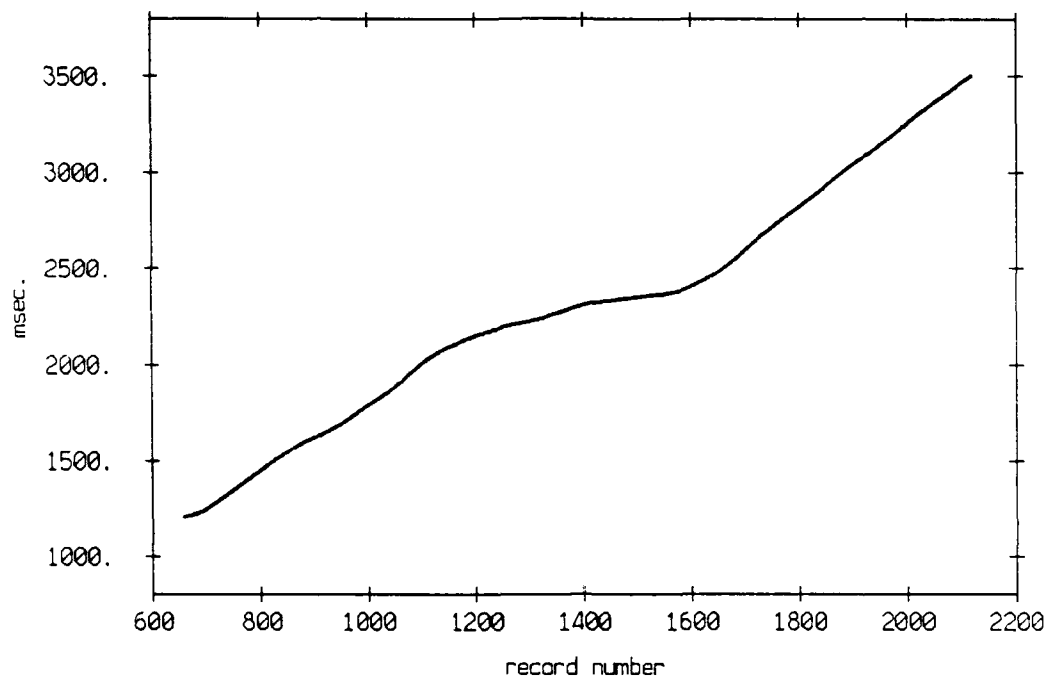
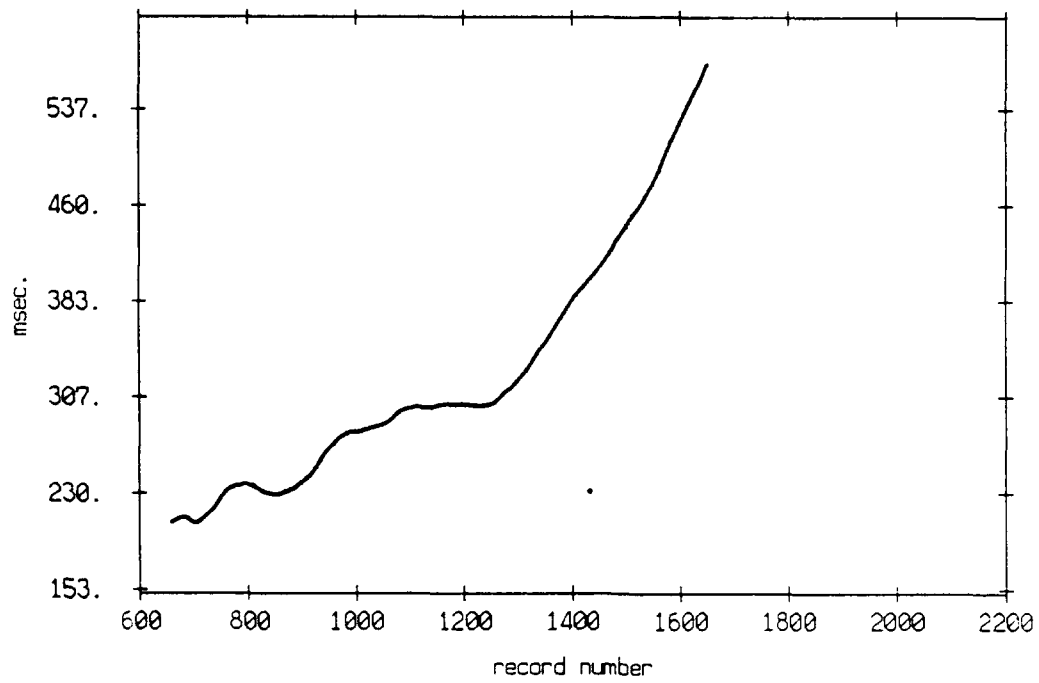


Figure 3.121

Travel time estimate, floats 4 and 5, July 1989



Travel time estimate, floats 4 and 6, July 1989

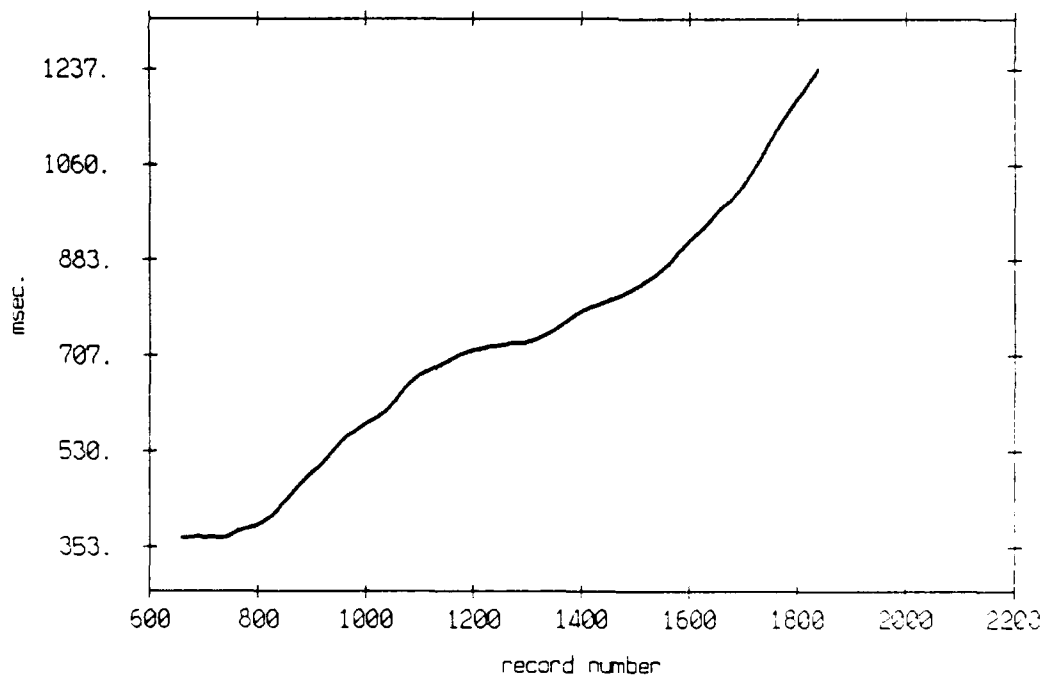


Figure 3.122

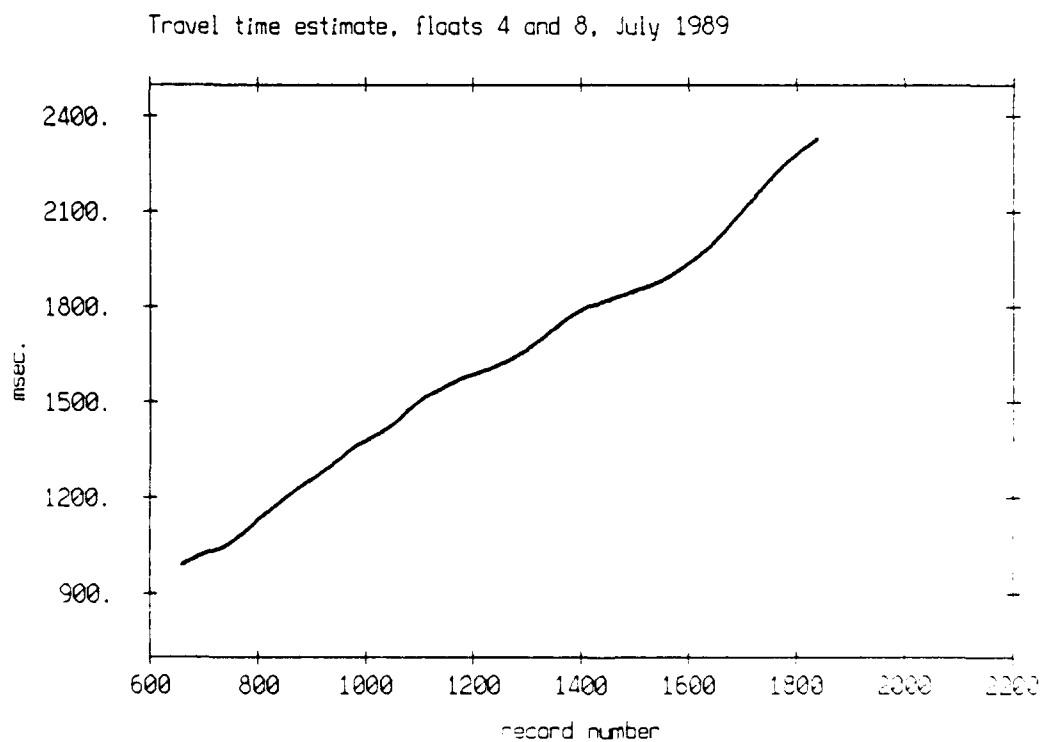
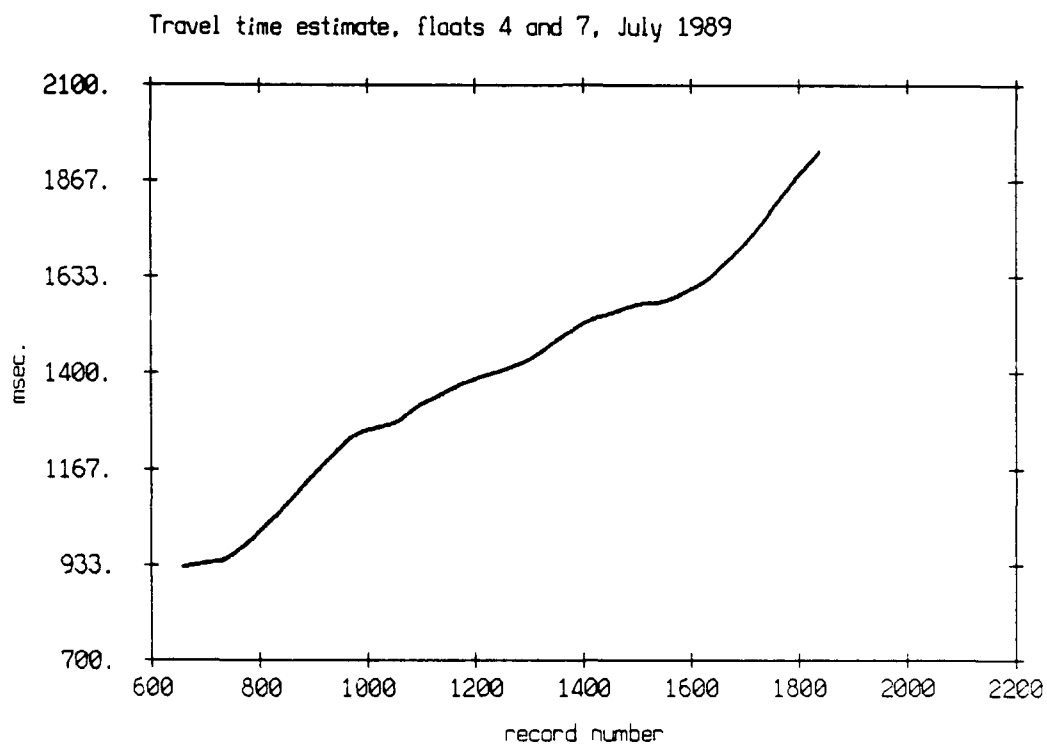
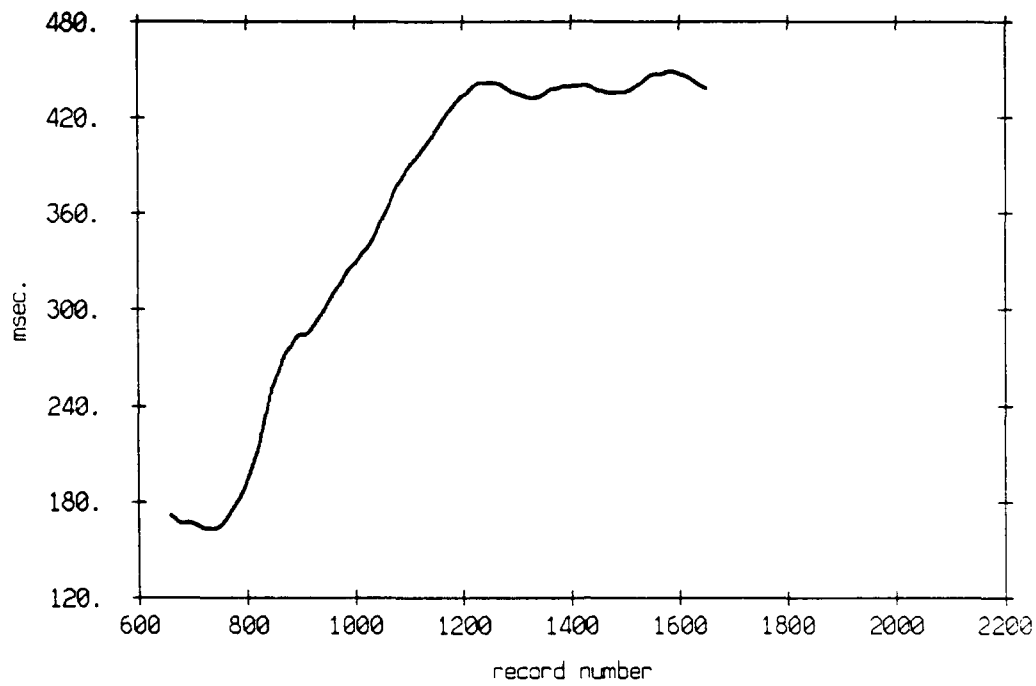


Figure 3.123

Travel time estimate, floats 5 and 6, July 1989



Travel time estimate, floats 5 and 7, July 1989

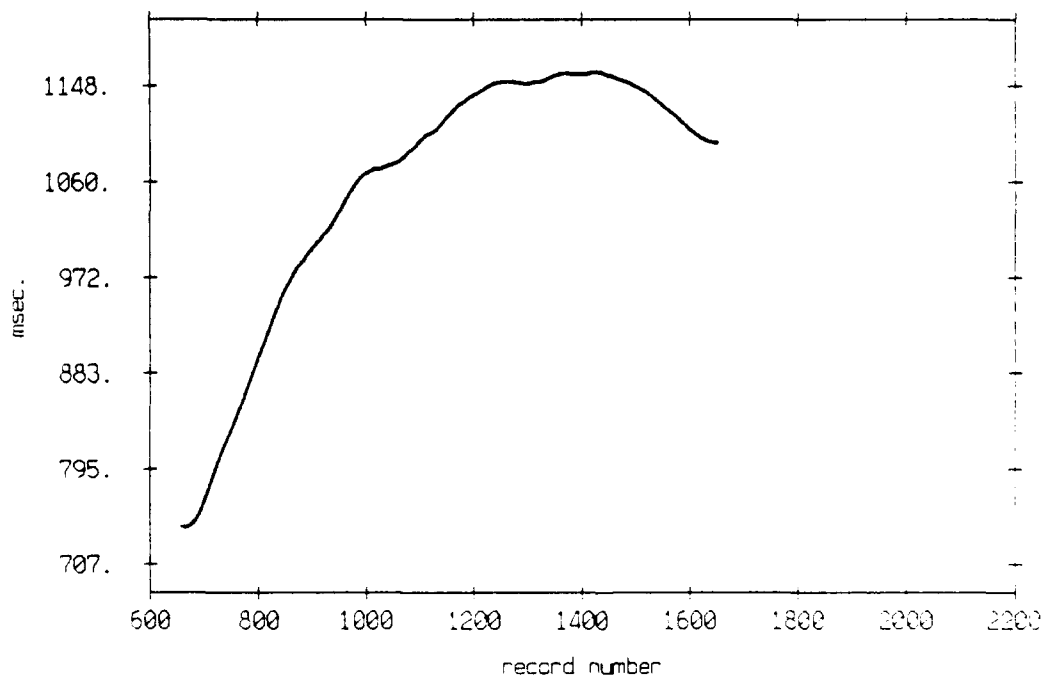


Figure 3.124

Travel time estimate, floats 5 and 8, July 1989

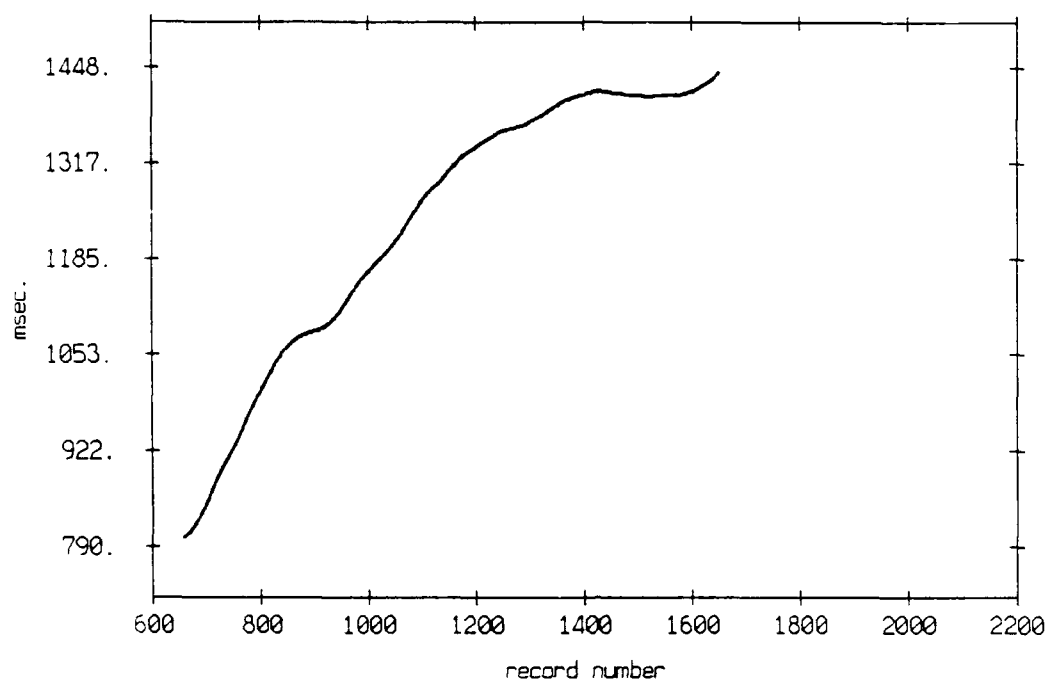
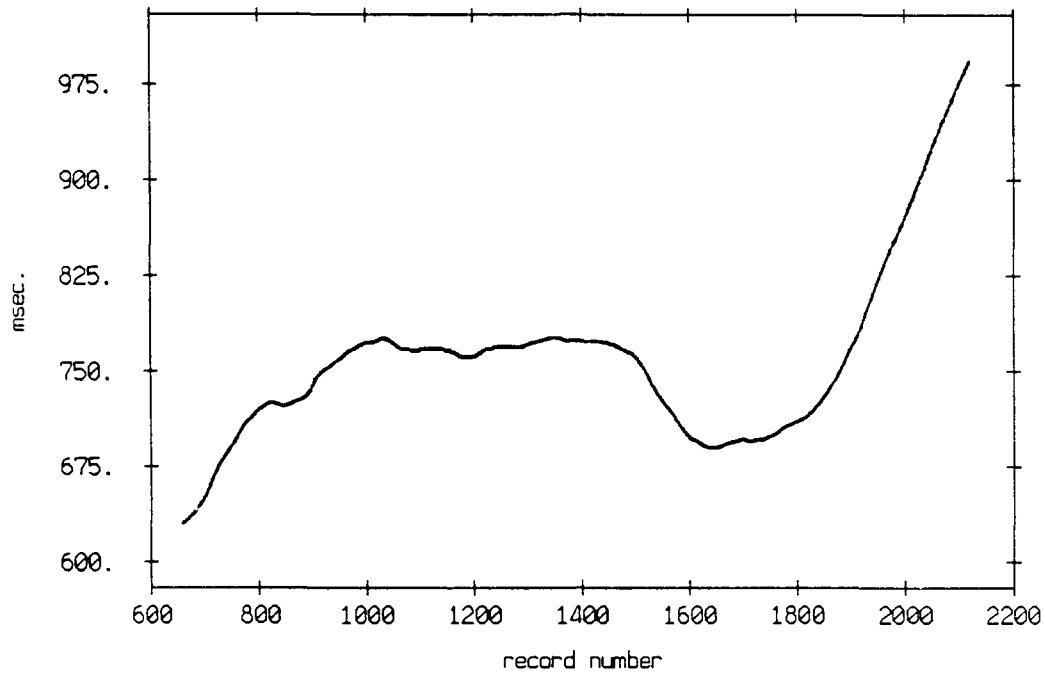


Figure 3.125

Travel time estimate, floats 6 and 7, July 1989



Travel time estimate, floats 6 and 8, July 1989

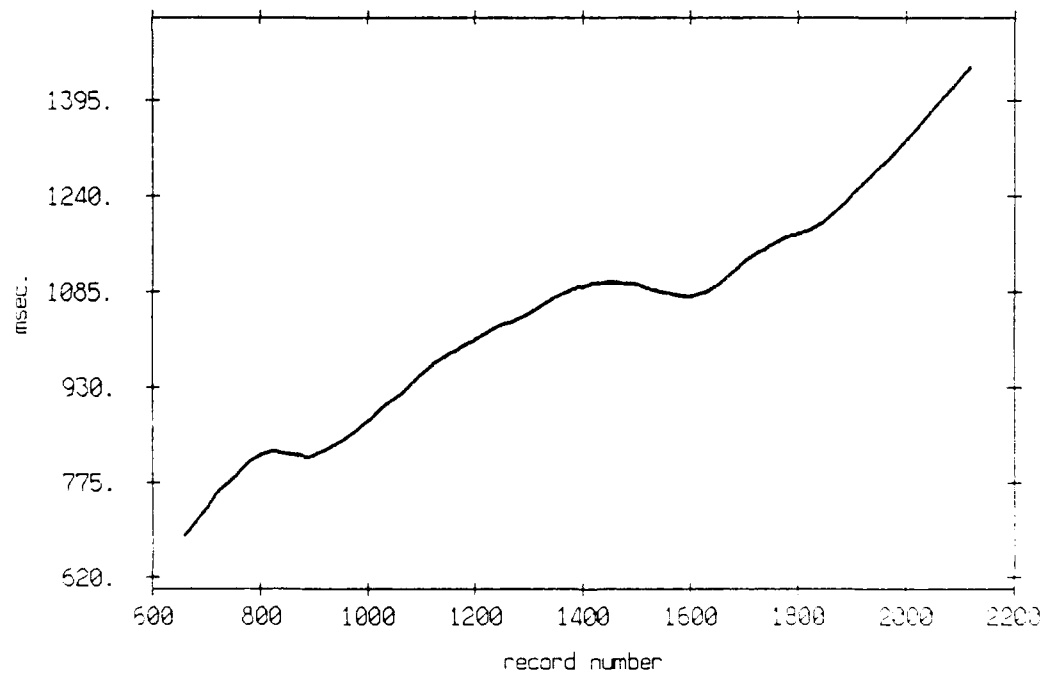


Figure 3.126

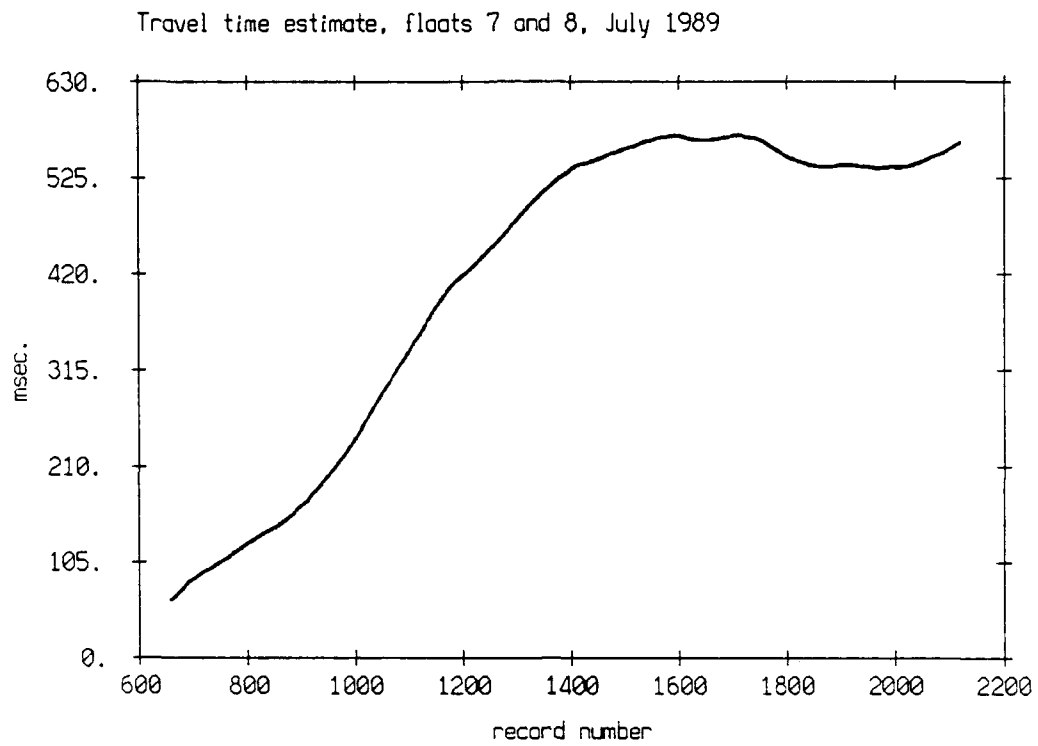


Figure 3.127

Sound Speed Profiles, July 1989 Experiment

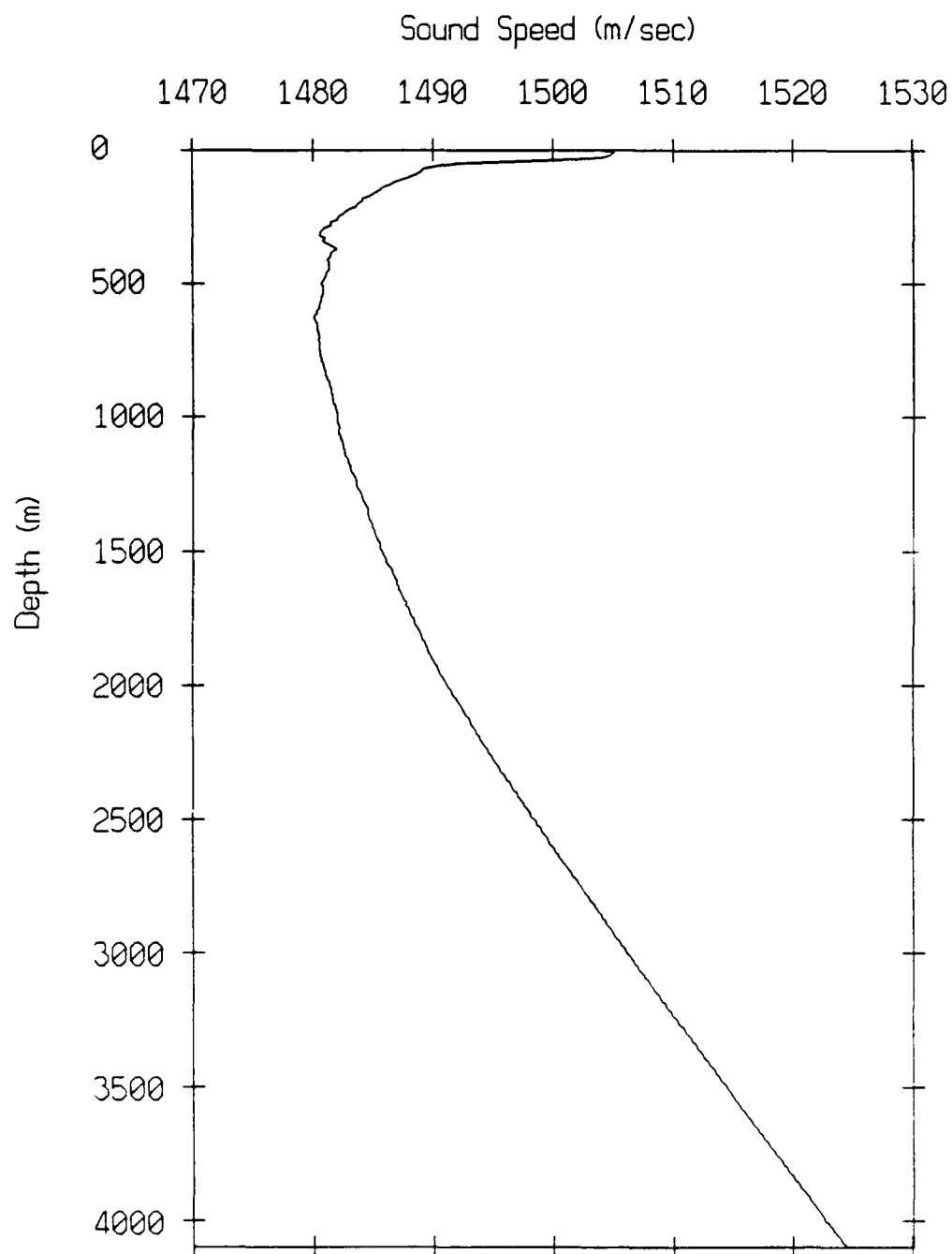
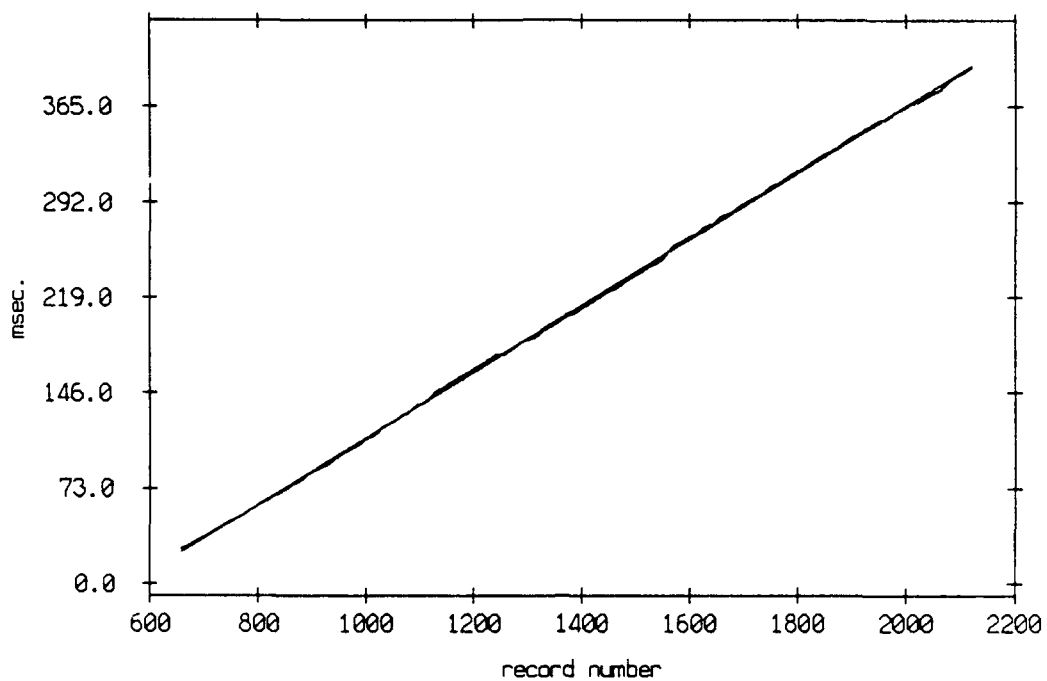


Figure 3.128

Travel time difference, floats 9 and 0, July 1989, and a second order fit, coefficients are: -0.00399 25.55177 and -143.75967



Travel time difference minus second order fit, floats 9 and 0

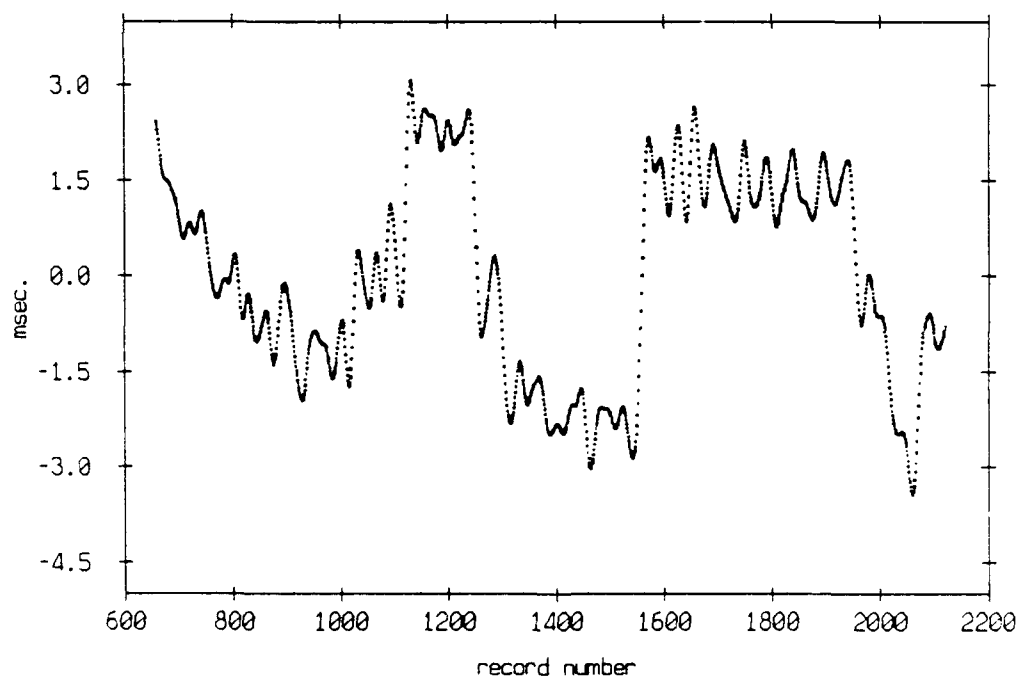


Figure 3.129

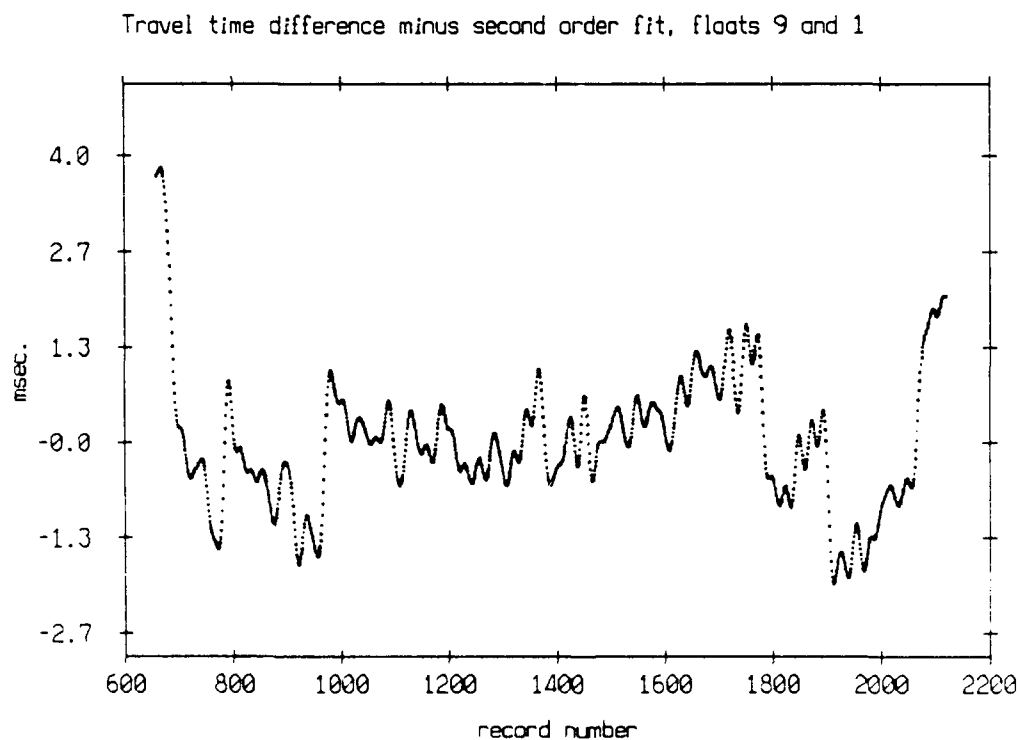
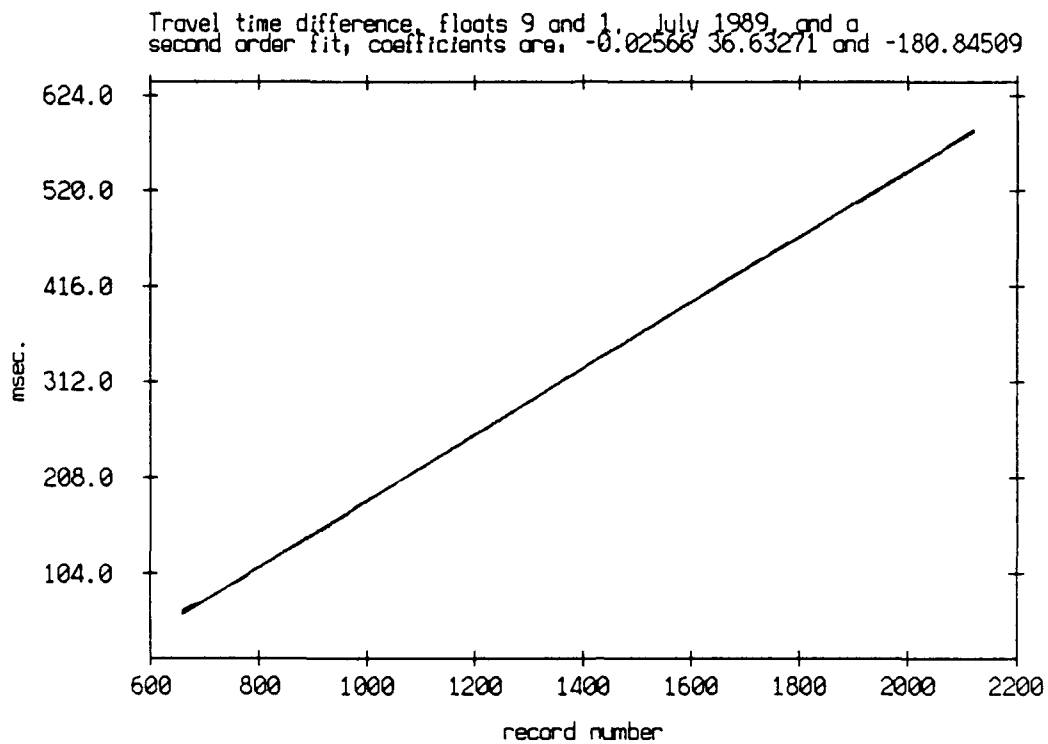


Figure 3.130

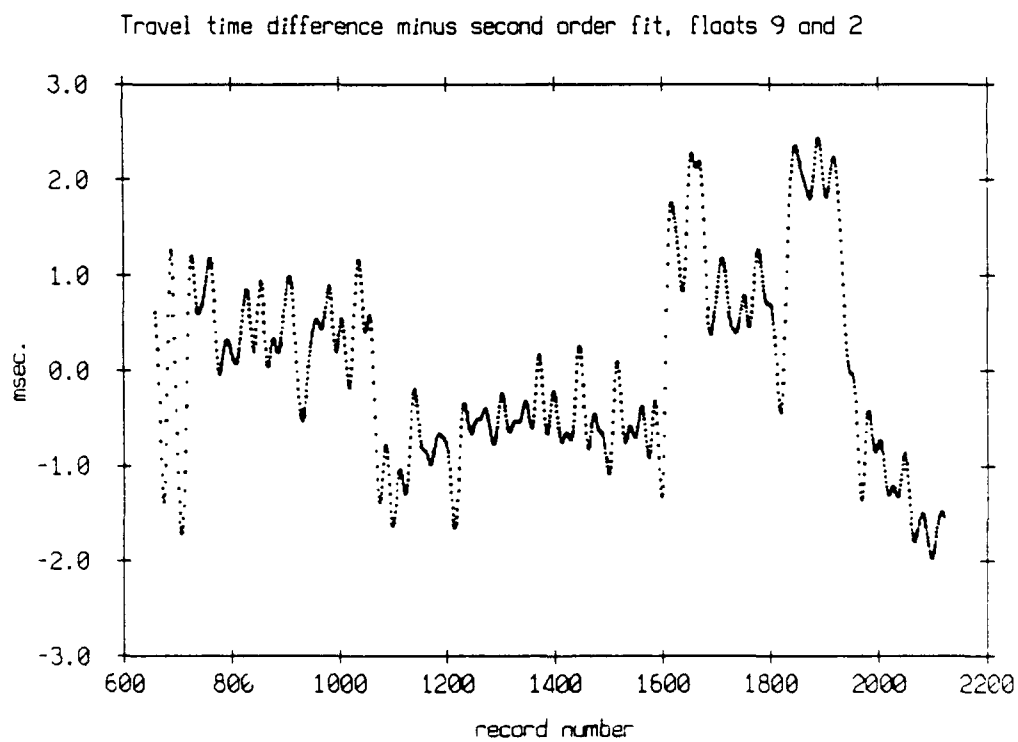
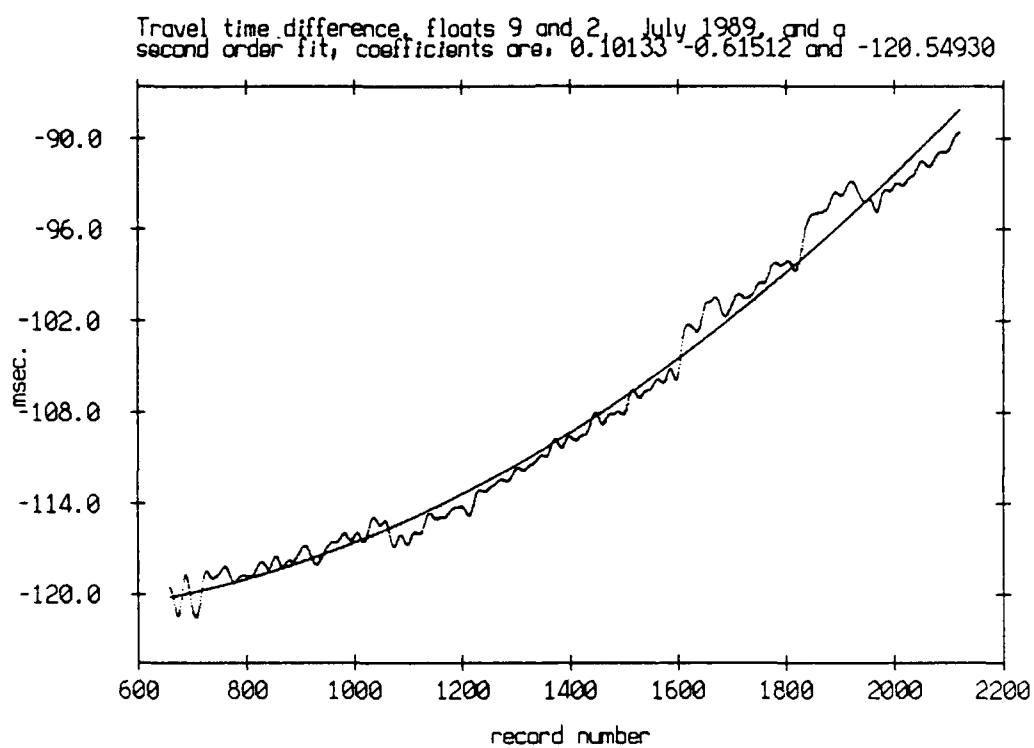
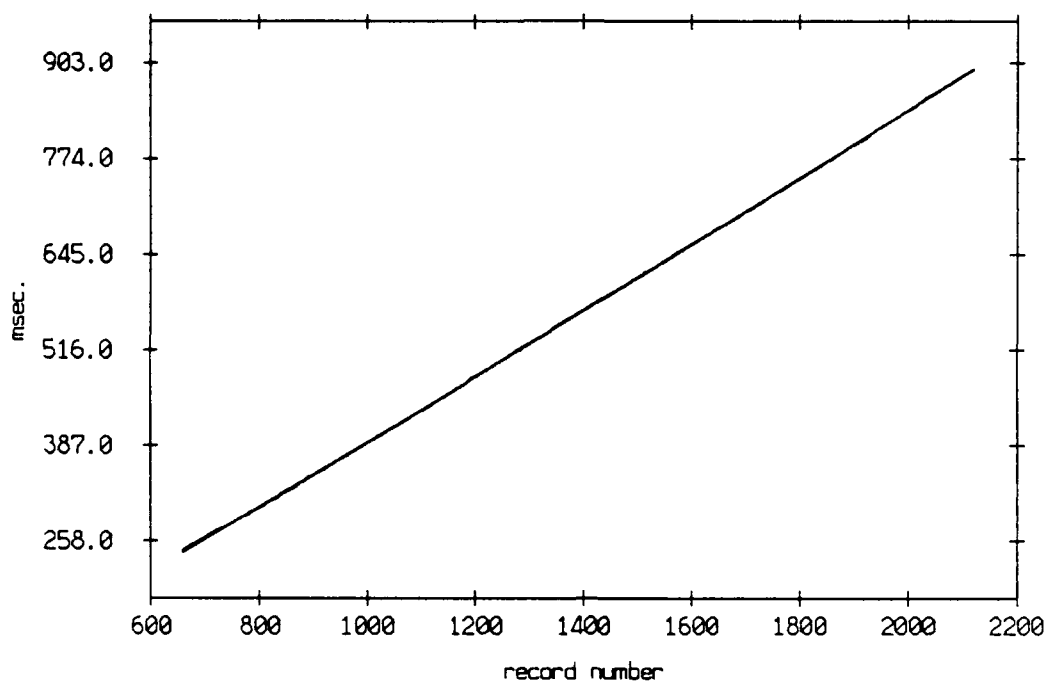


Figure 3.131

Travel time difference, floats 9 and 3, July 1989, and a second order fit, coefficients are: 0.07953 42.33369 and -39.60468



Travel time difference minus second order fit, floats 9 and 3

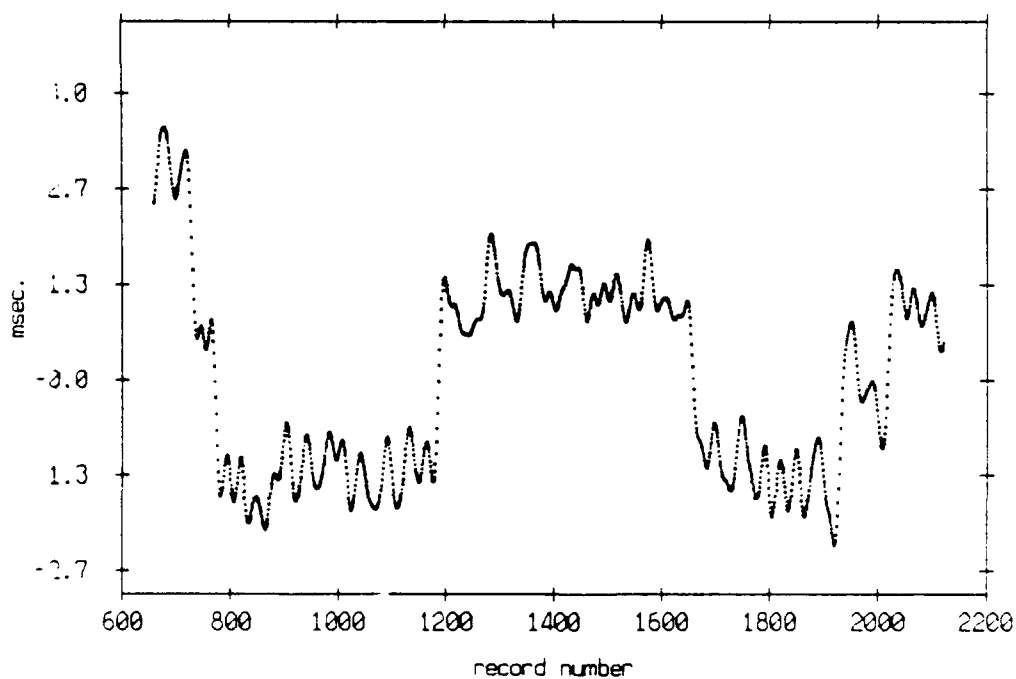
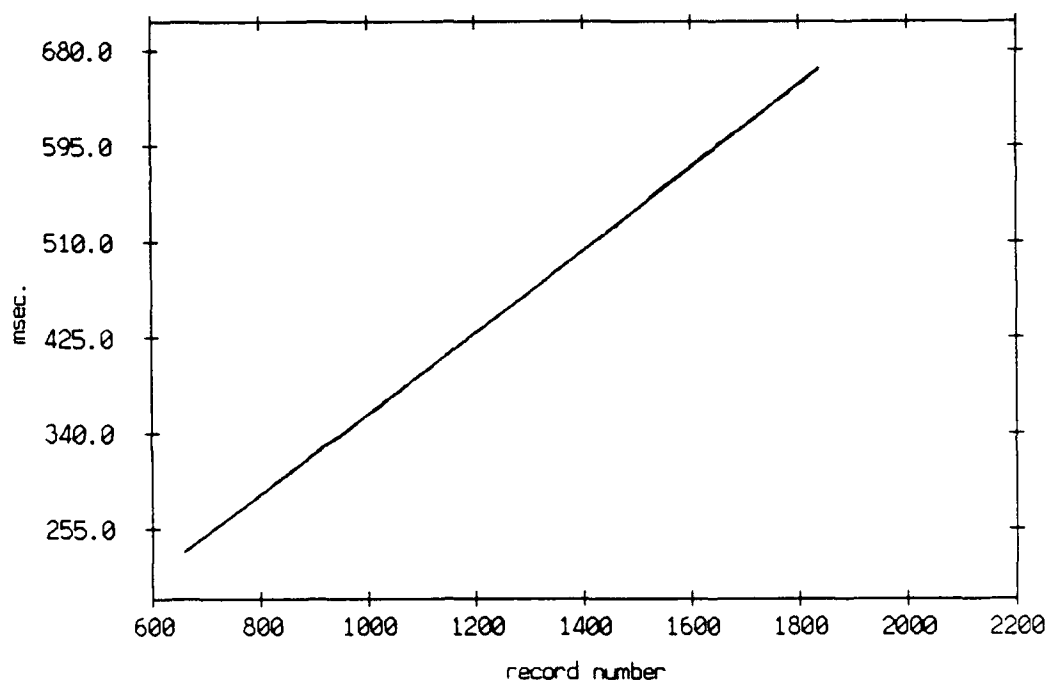


Figure 3.132

Travel time difference, floats 9 and 4, July 1989, and a
second order fit, coefficients are: 0.07021 34.60133 and 4.20795



Travel time difference minus second order fit, floats 9 and 4

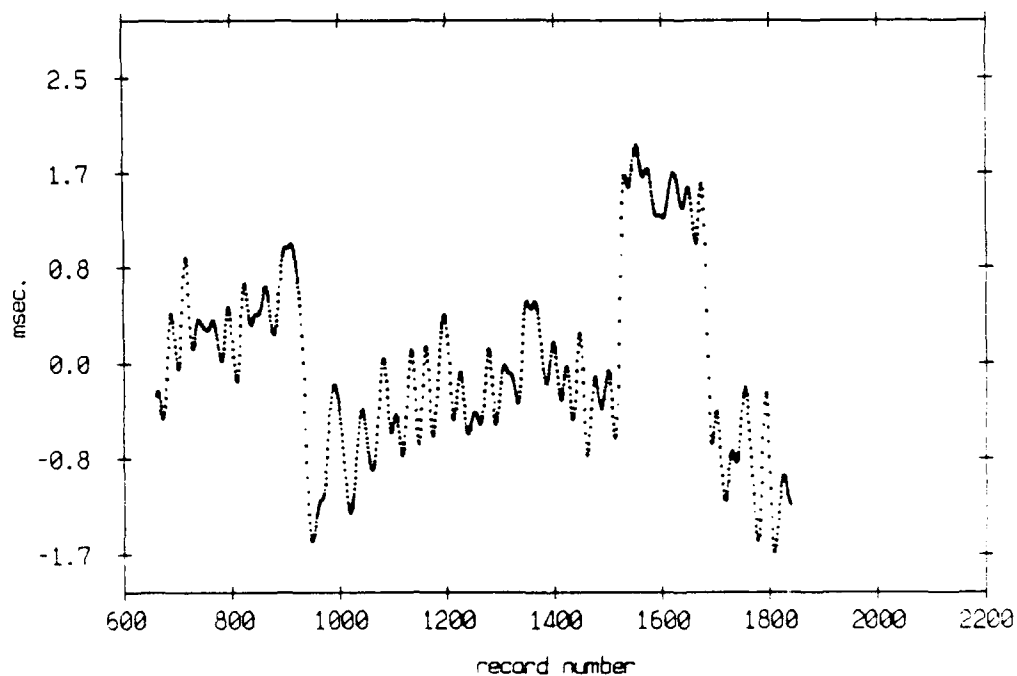


Figure 3.133

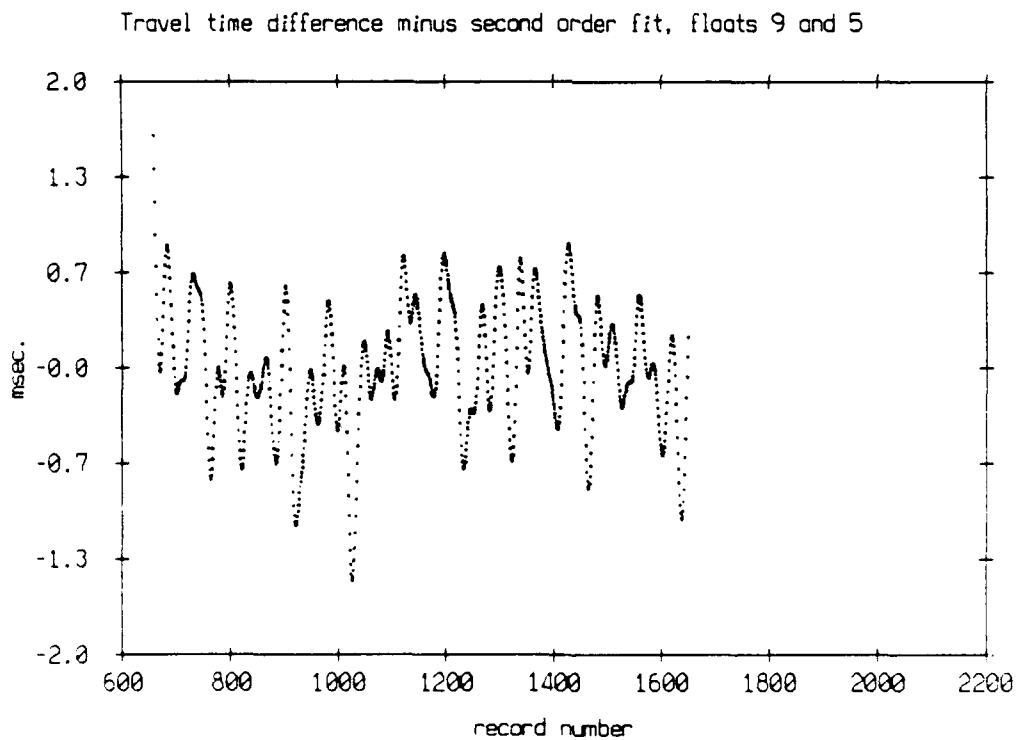
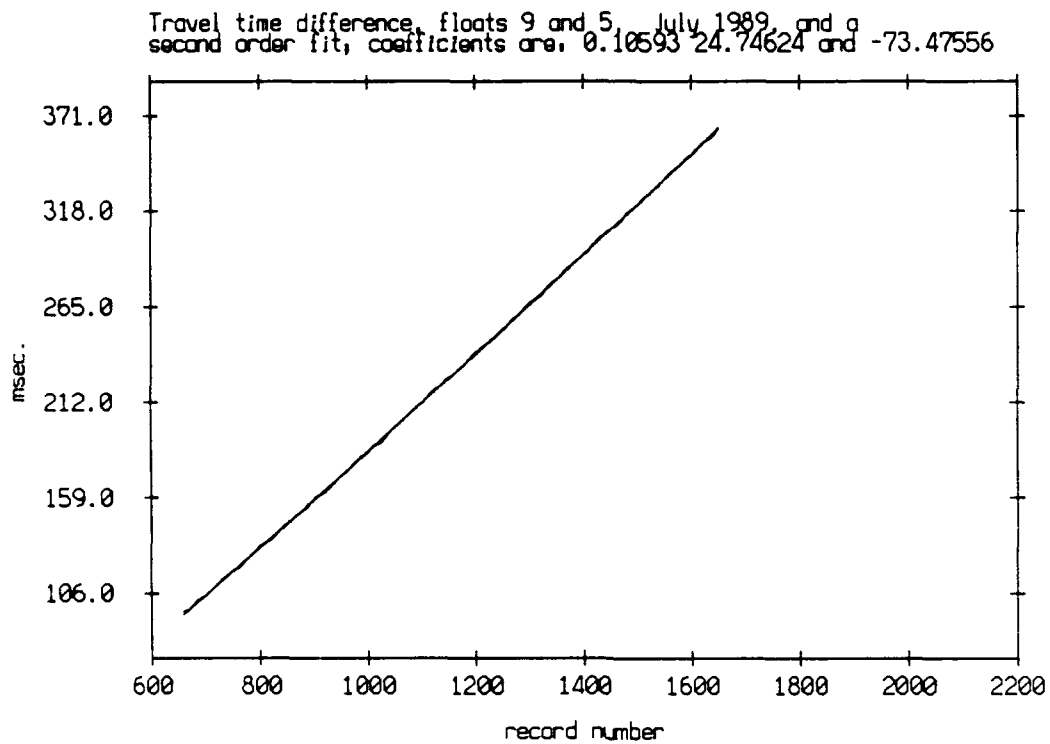


Figure 3.134

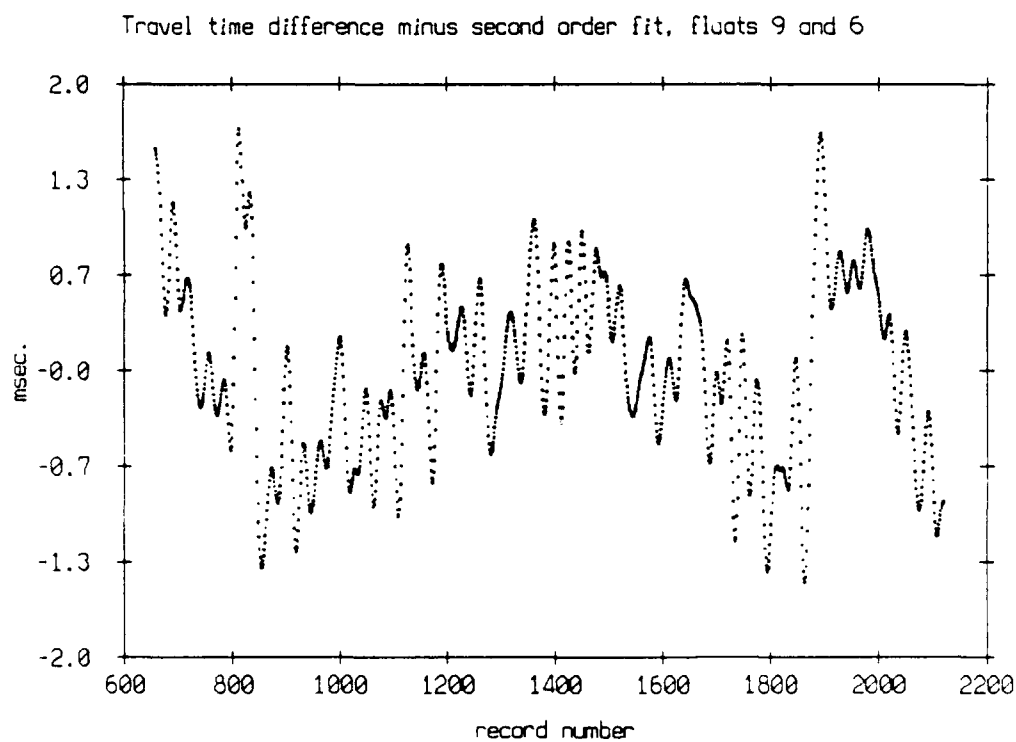
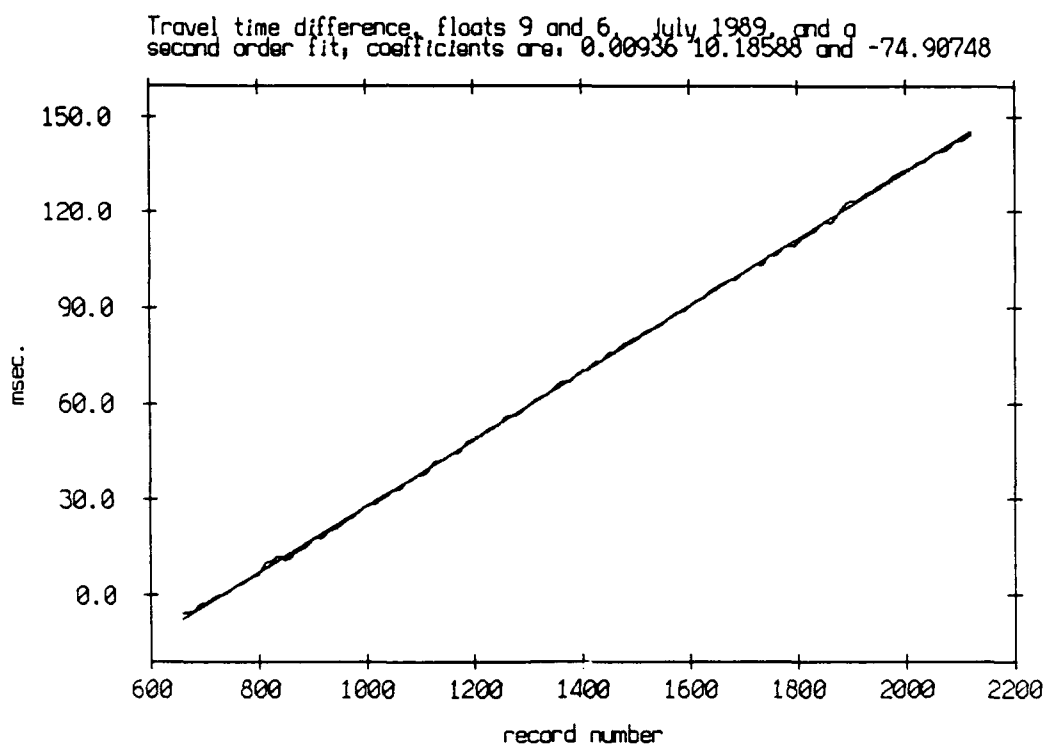


Figure 3.135

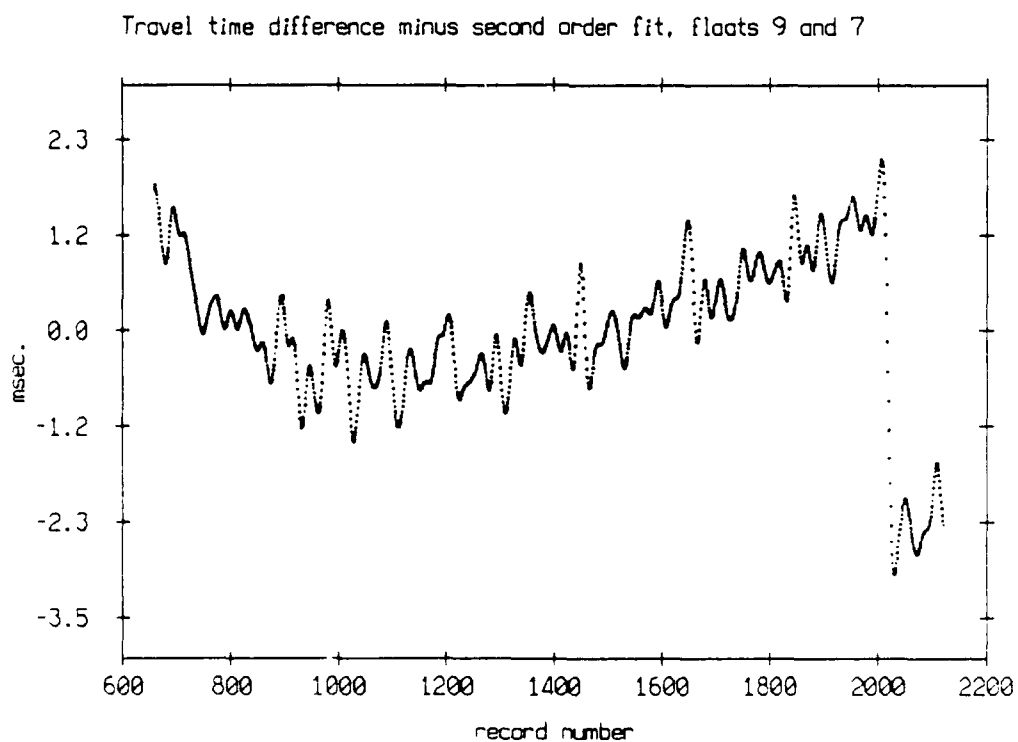
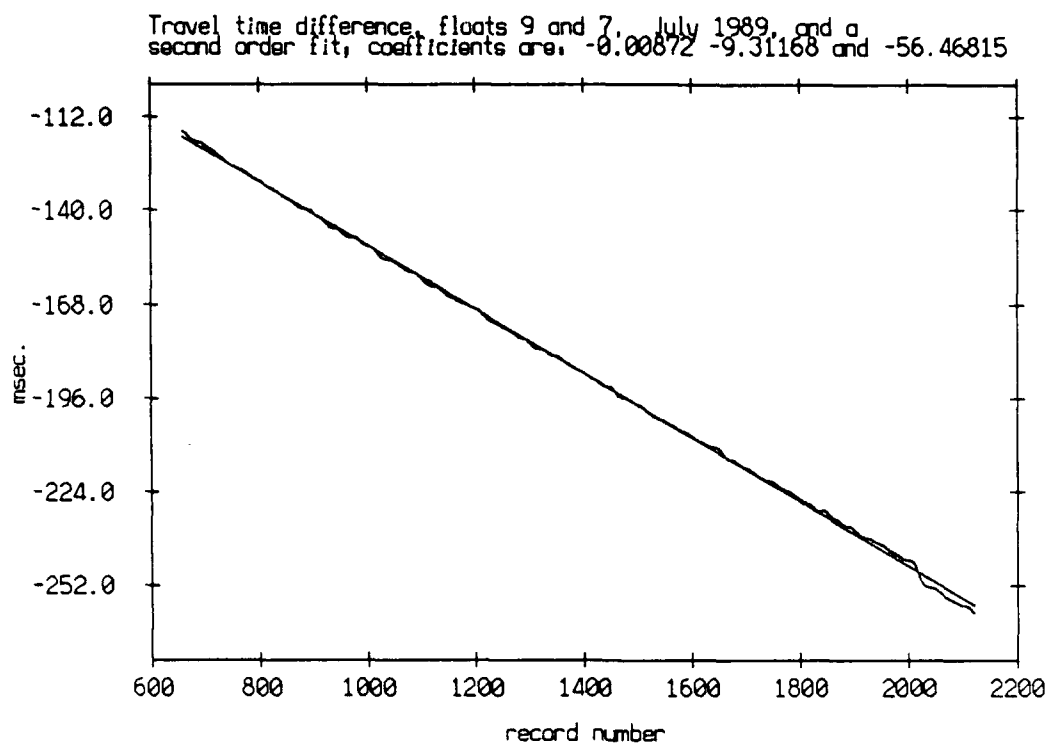


Figure 3.136

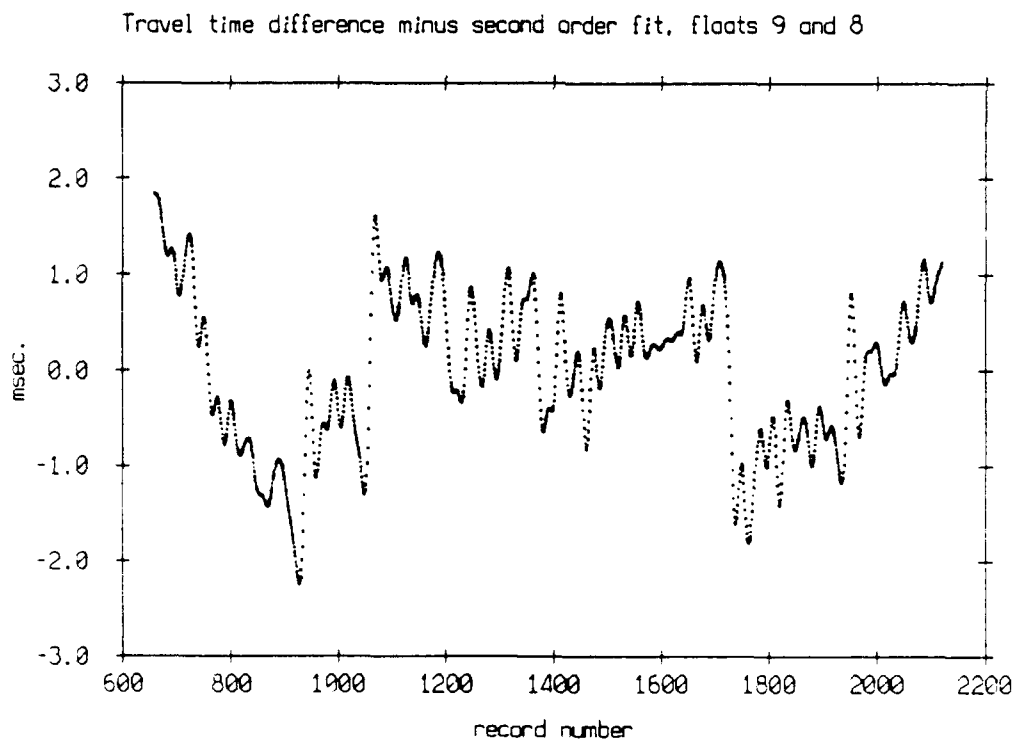
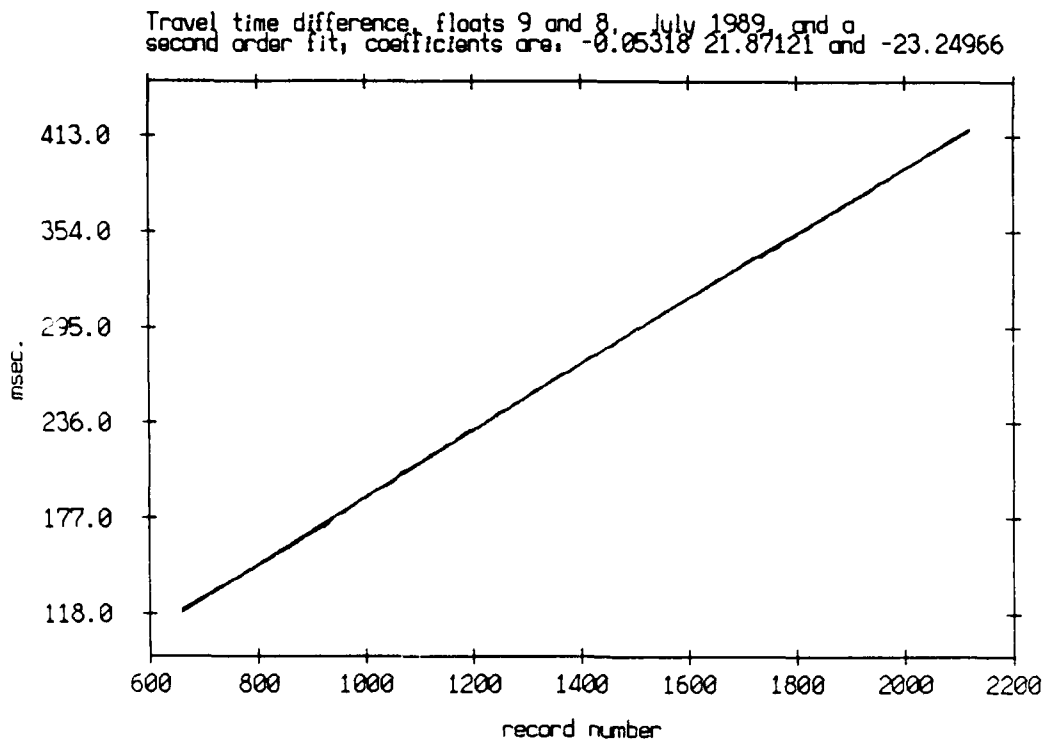


Figure 3.137

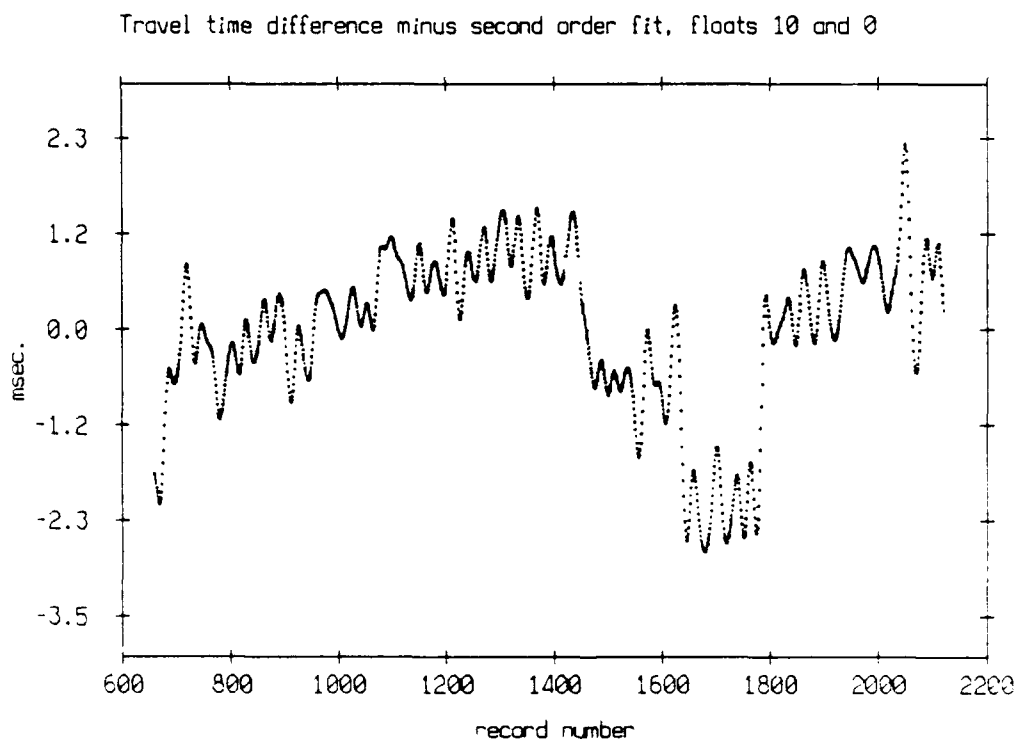
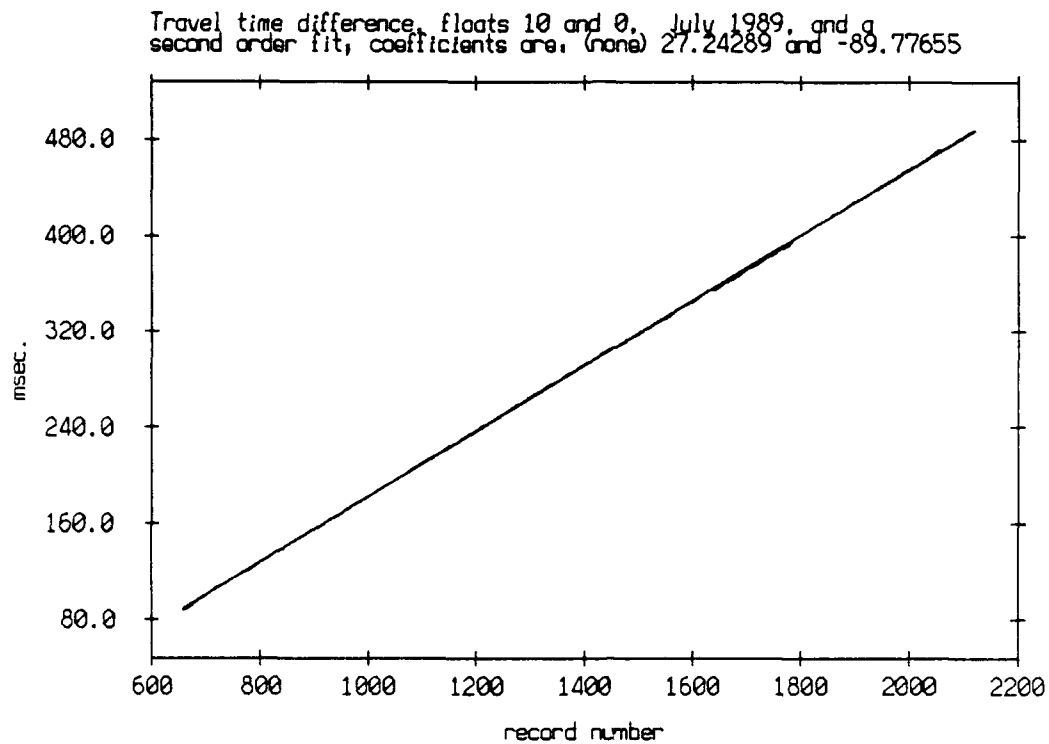


Figure 3.138

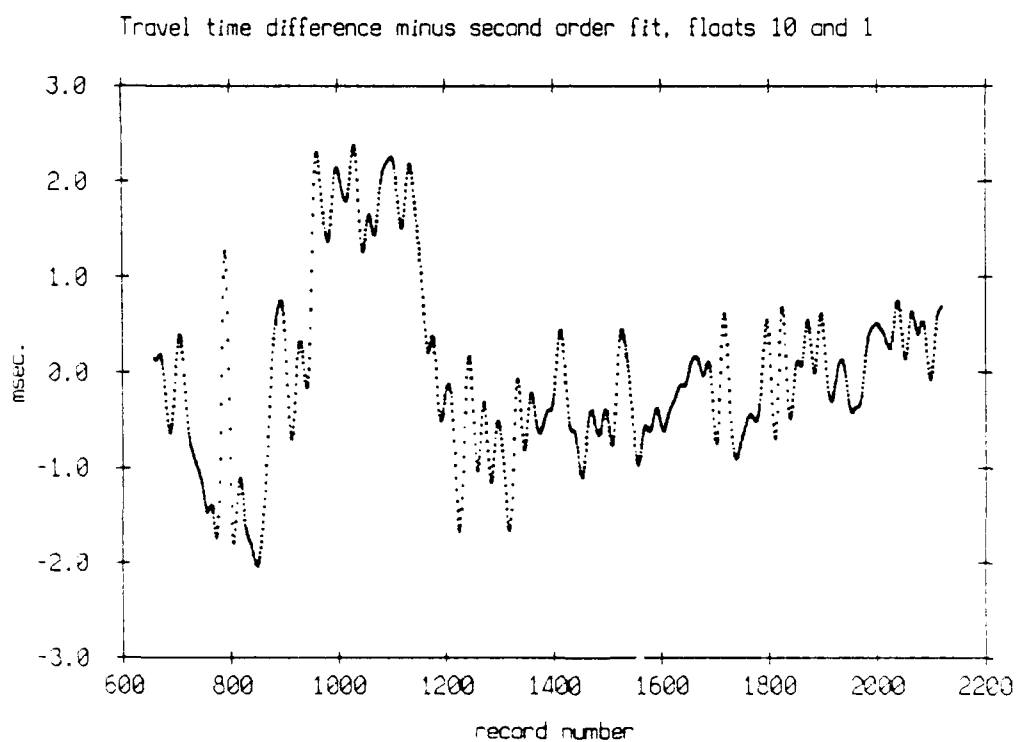
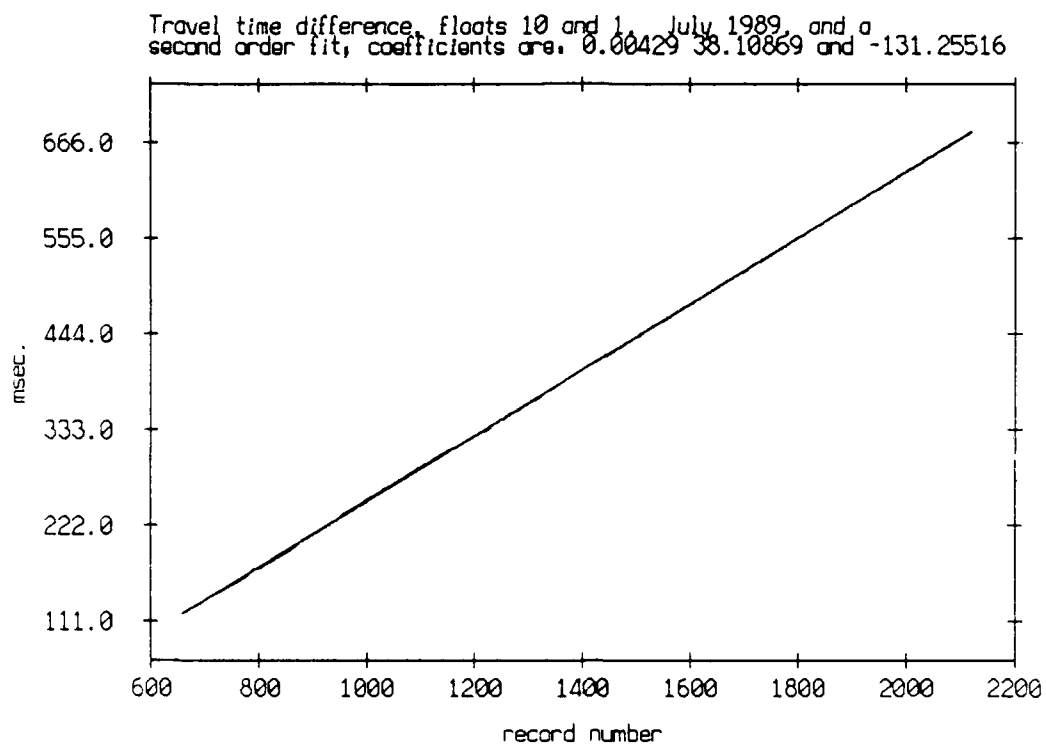
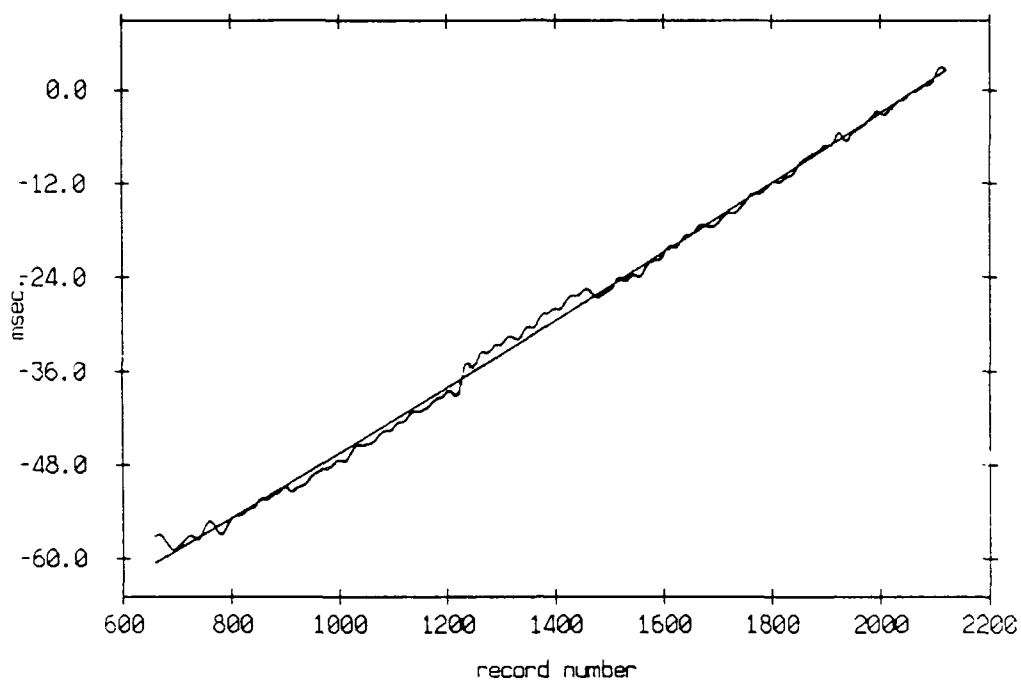


Figure 3.139

Travel time difference, floats 10 and 2, July 1989, and a second order fit, coefficients are: 0.01703 3.83972 and -86.58073



Travel time difference minus second order fit, floats 10 and 2

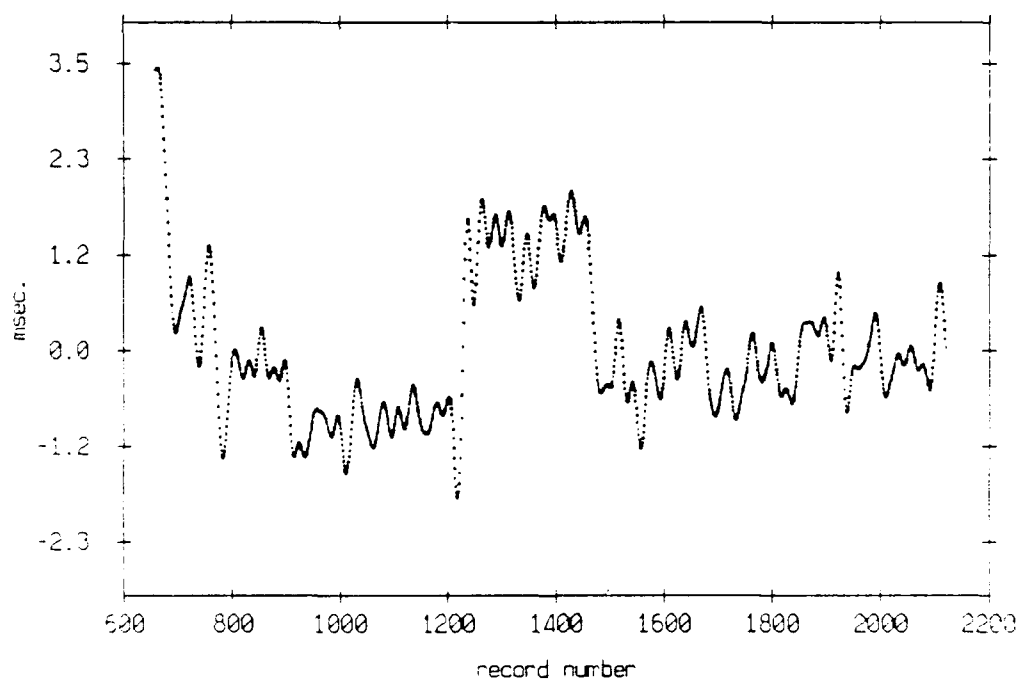
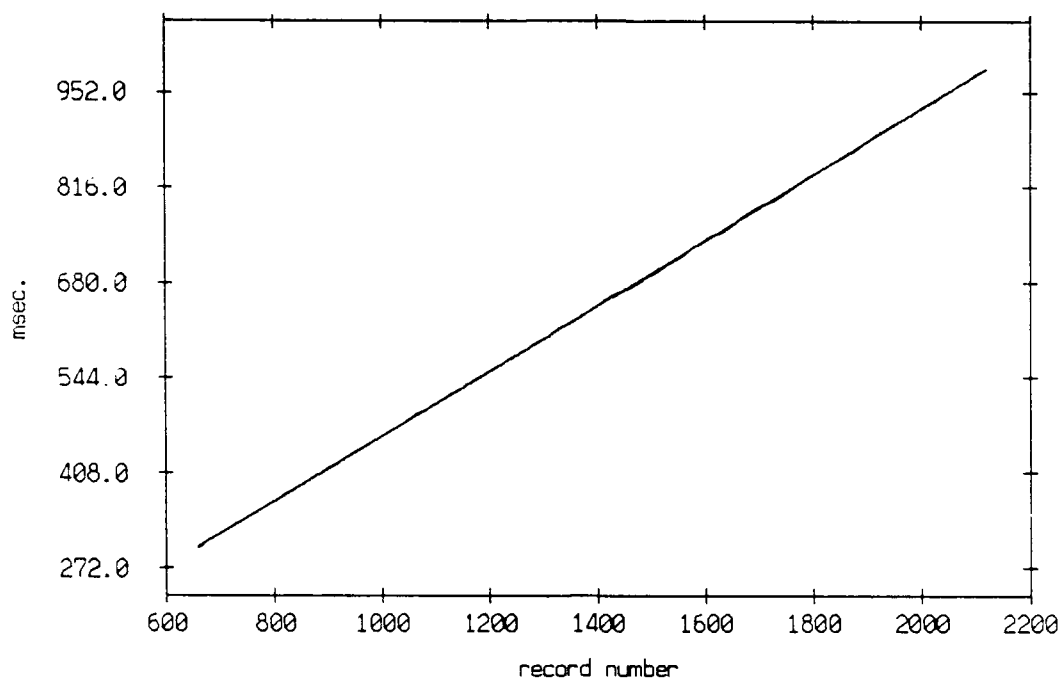


Figure 3.140

Travel time difference, floats 10 and 3, July 1989, and a
second order fit, coefficients are, 0.04859 45.28195 and 3.27728



Travel time difference minus second order fit, floats 10 and 3

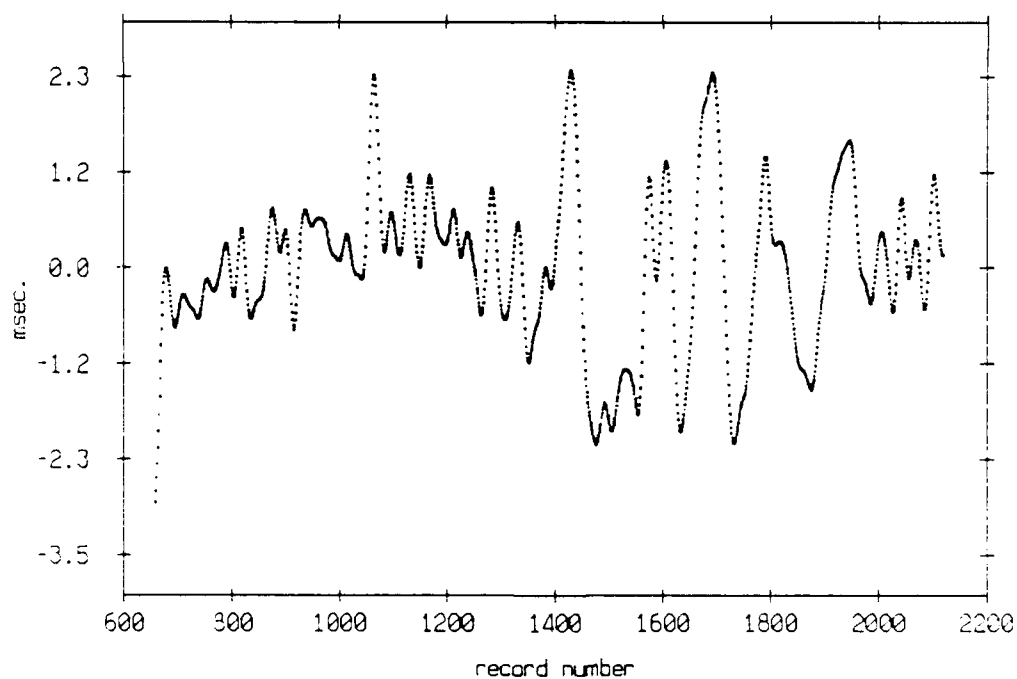


Figure 3.141

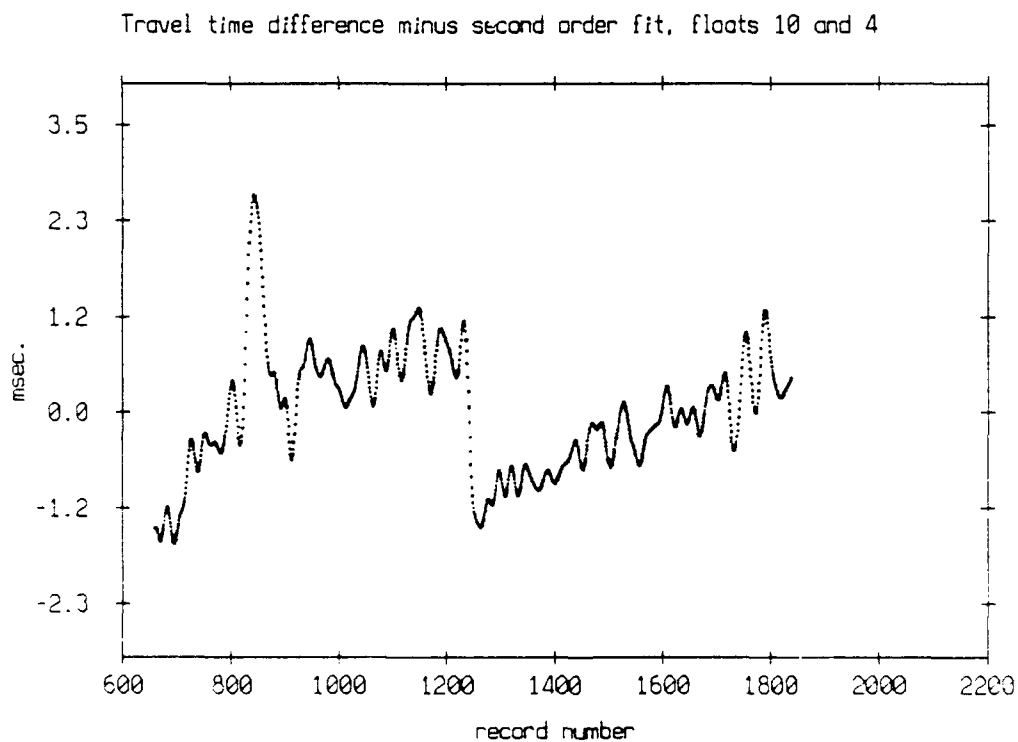
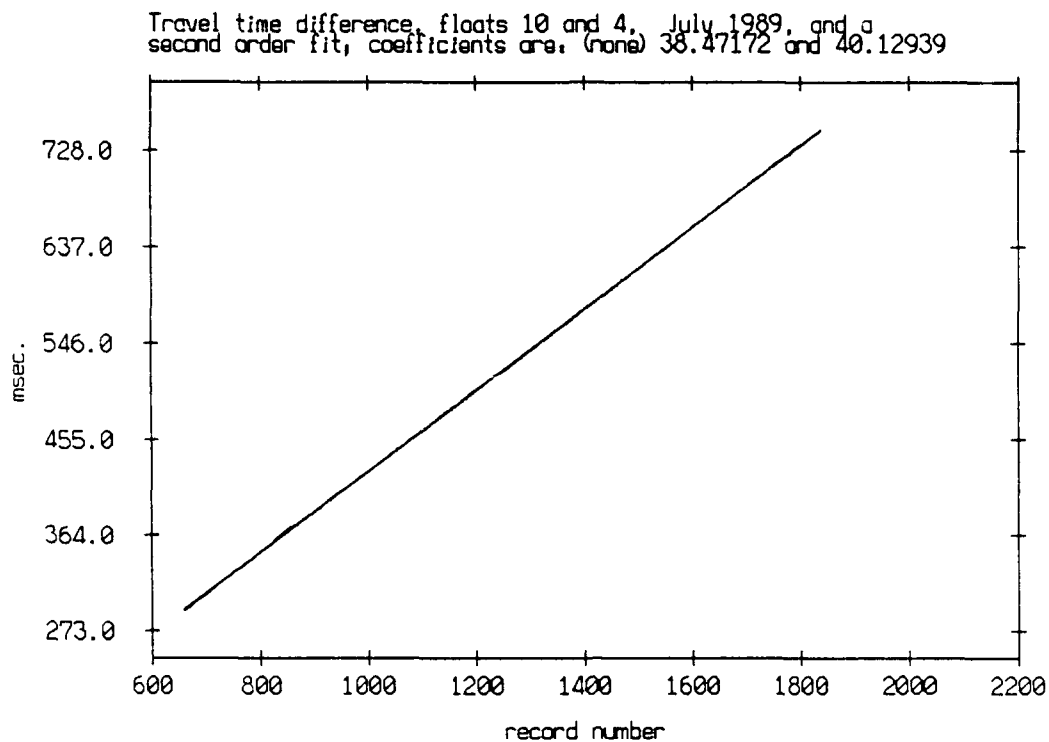


Figure 3.142

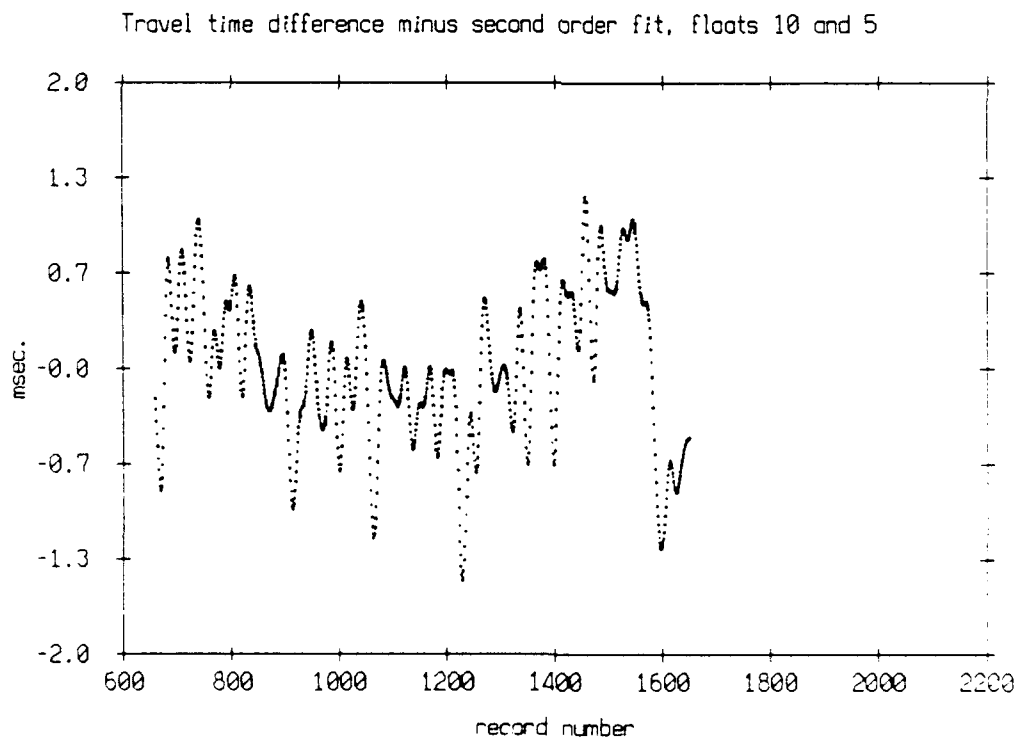
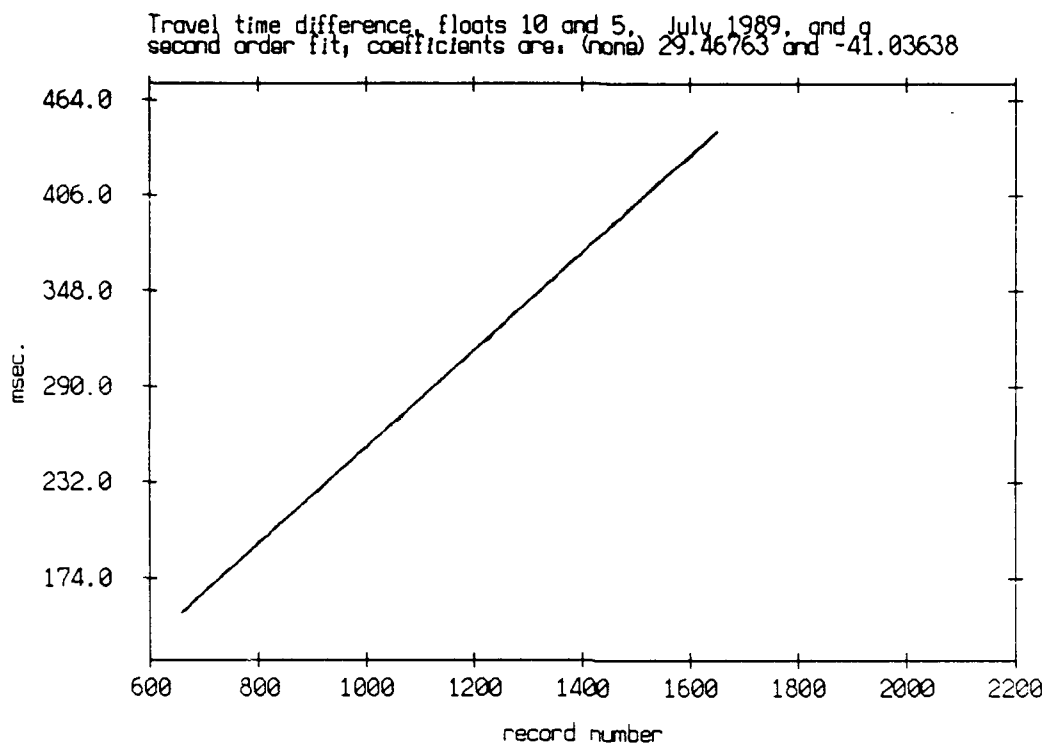


Figure 3.143

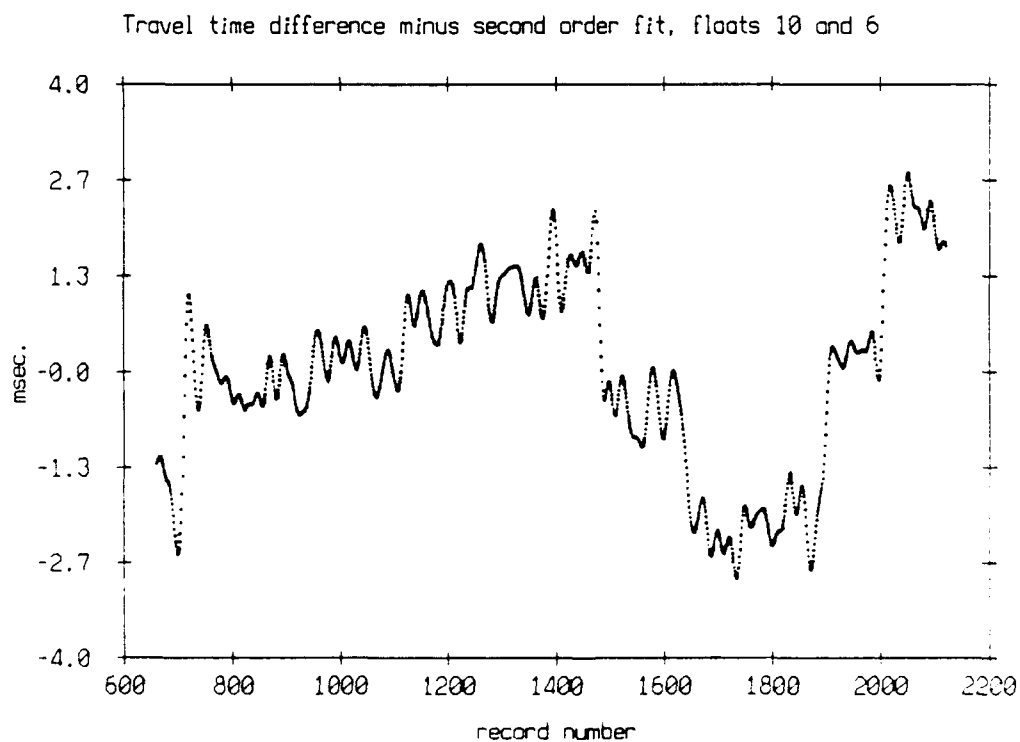
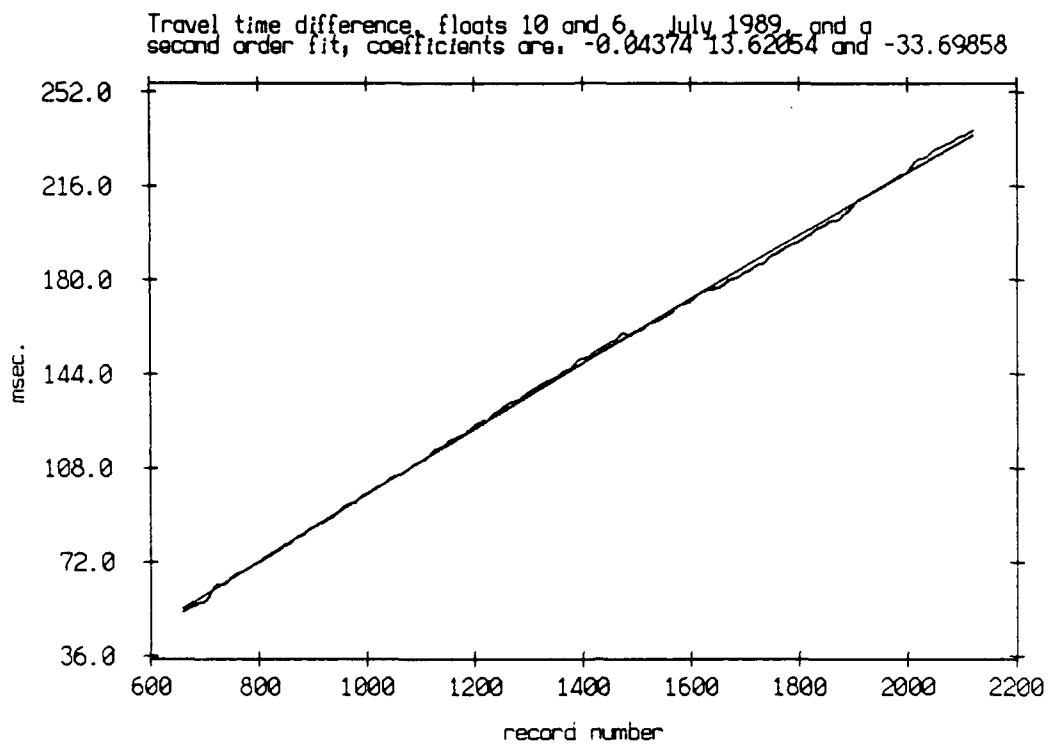


Figure 3.144

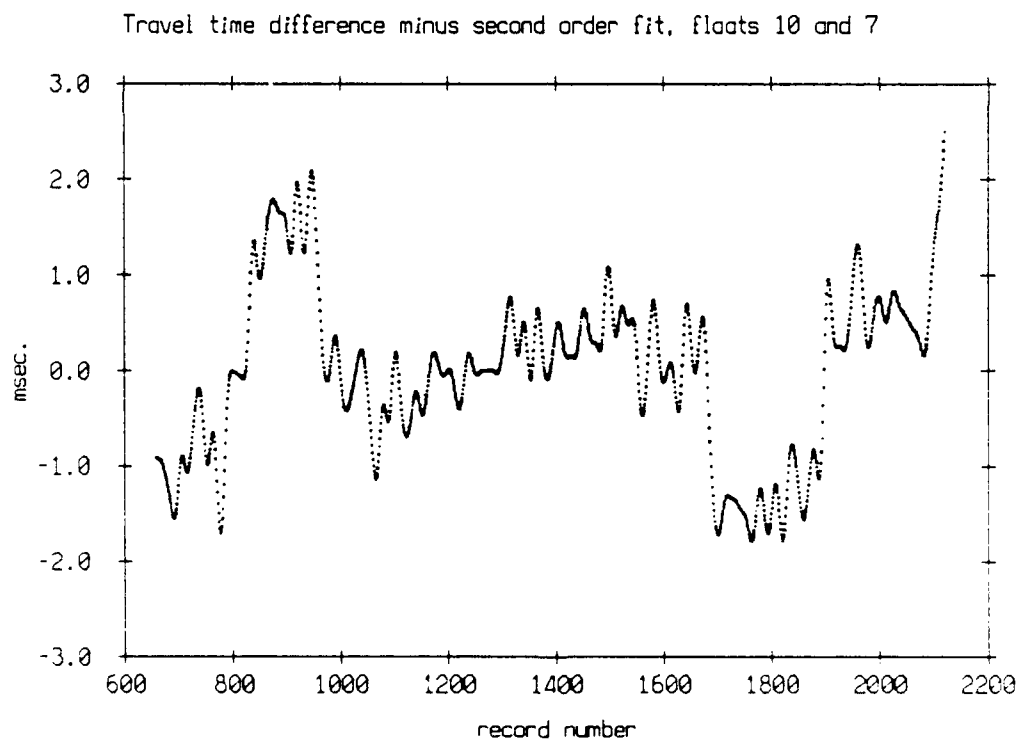
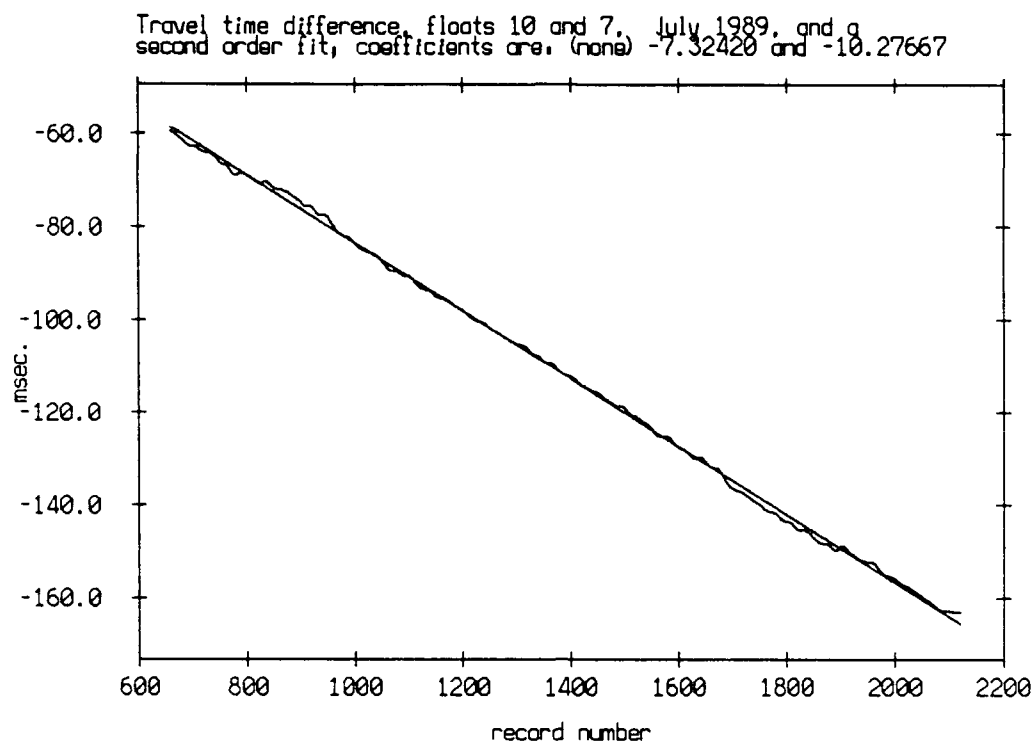


Figure 3.145

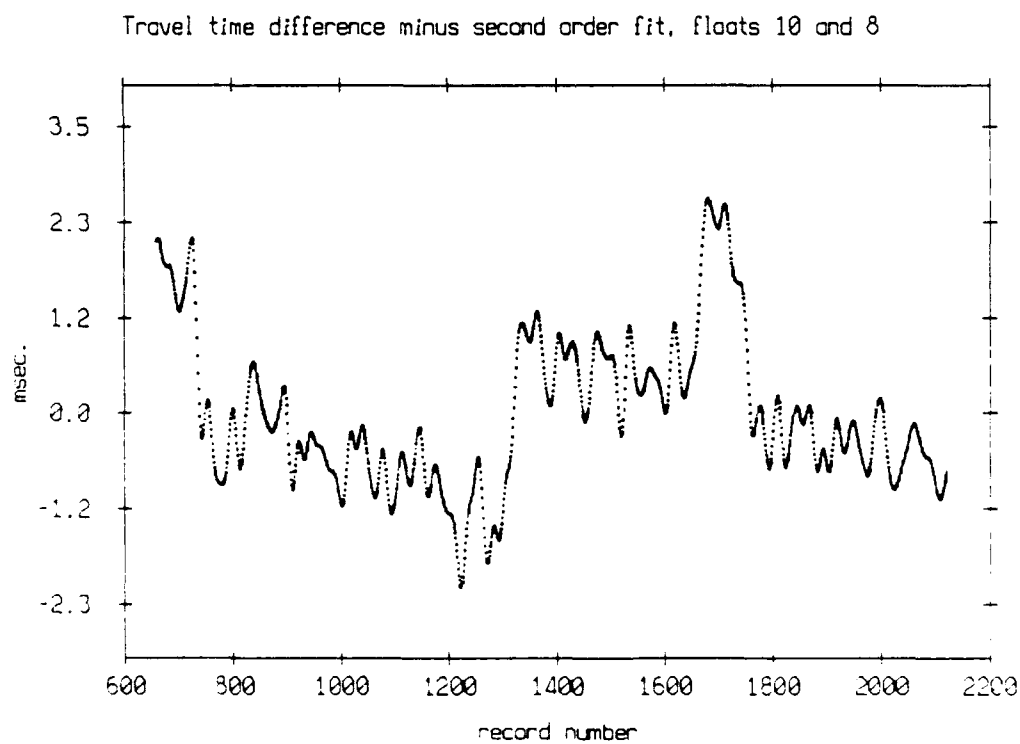
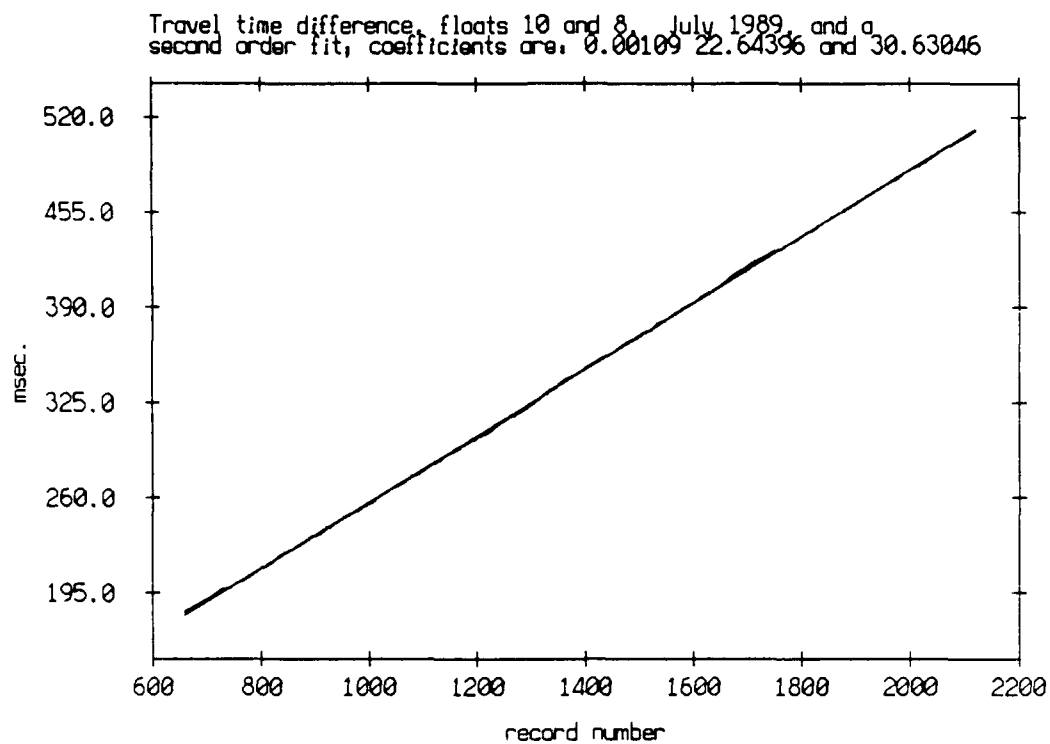


Figure 3.146

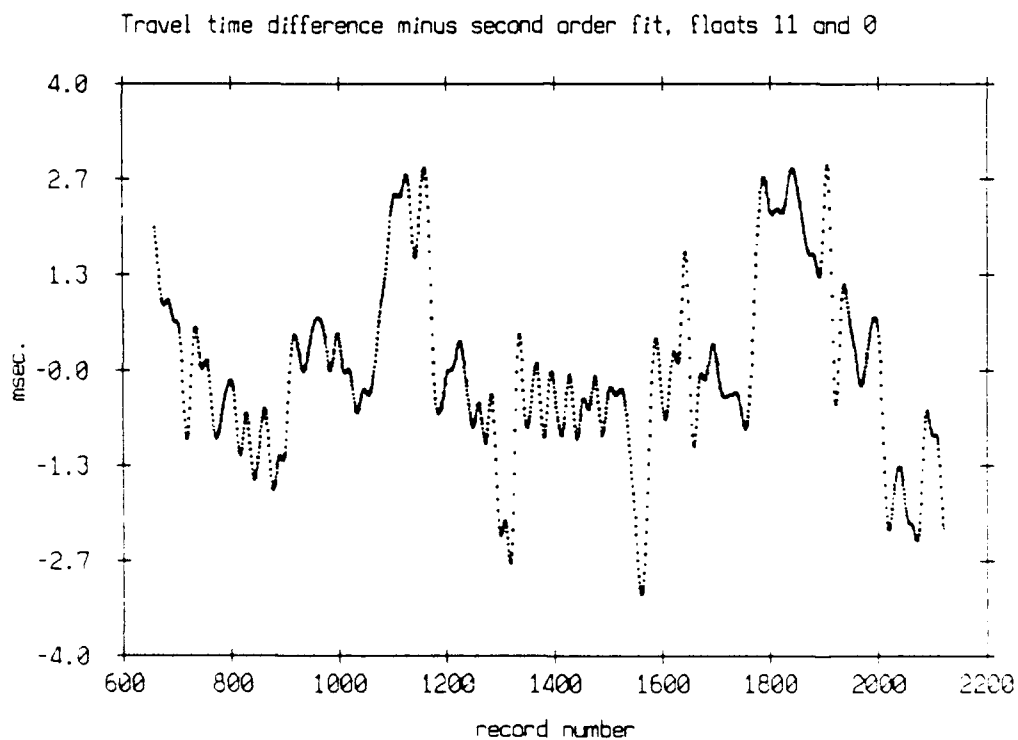
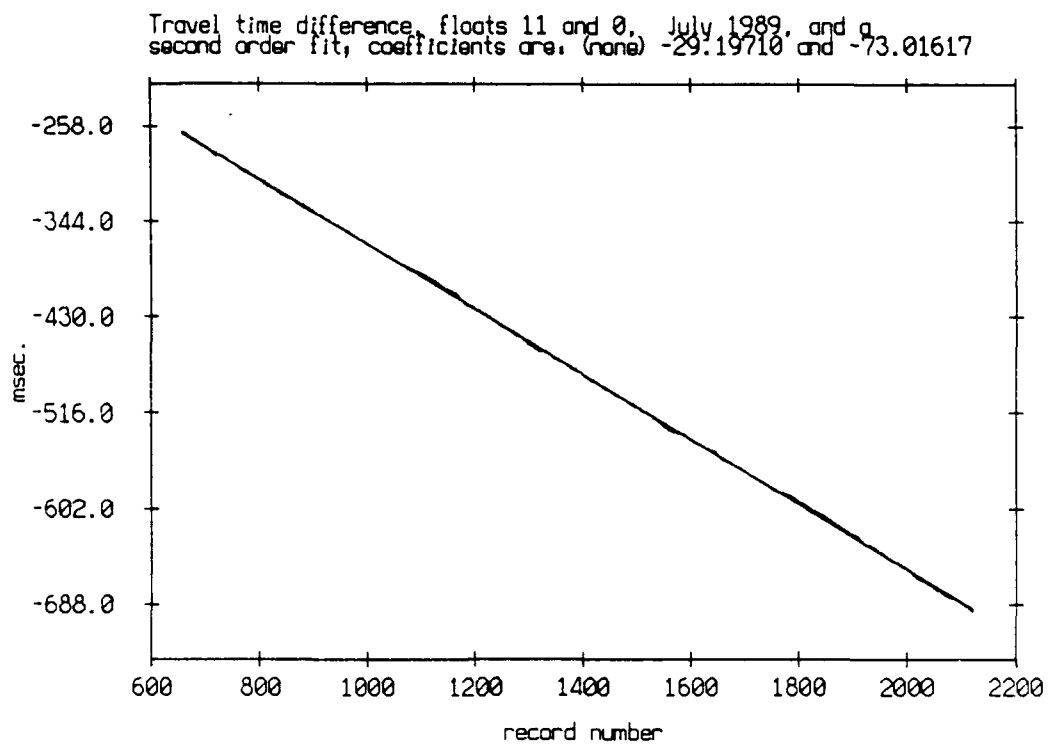


Figure 3.147

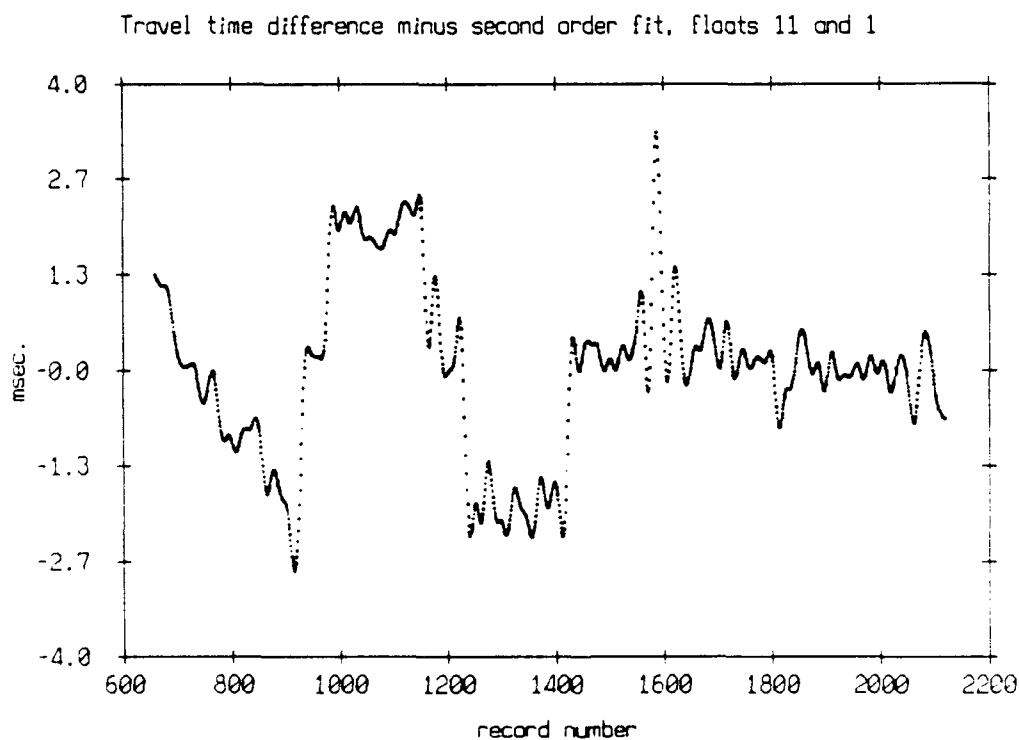
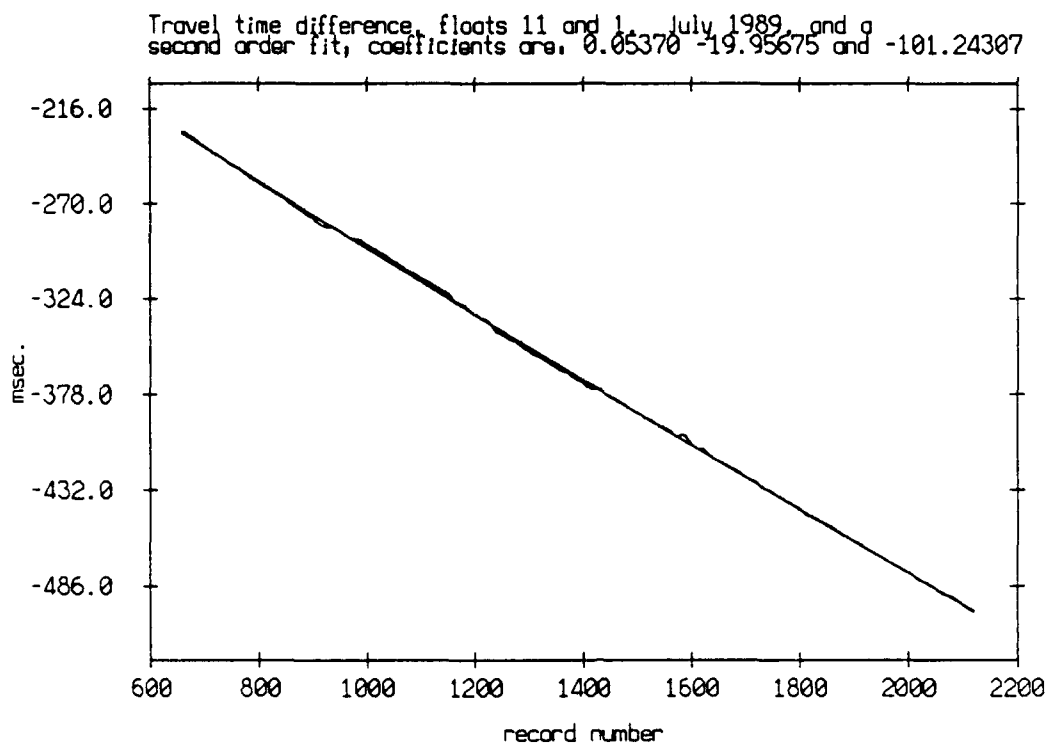


Figure 3.148

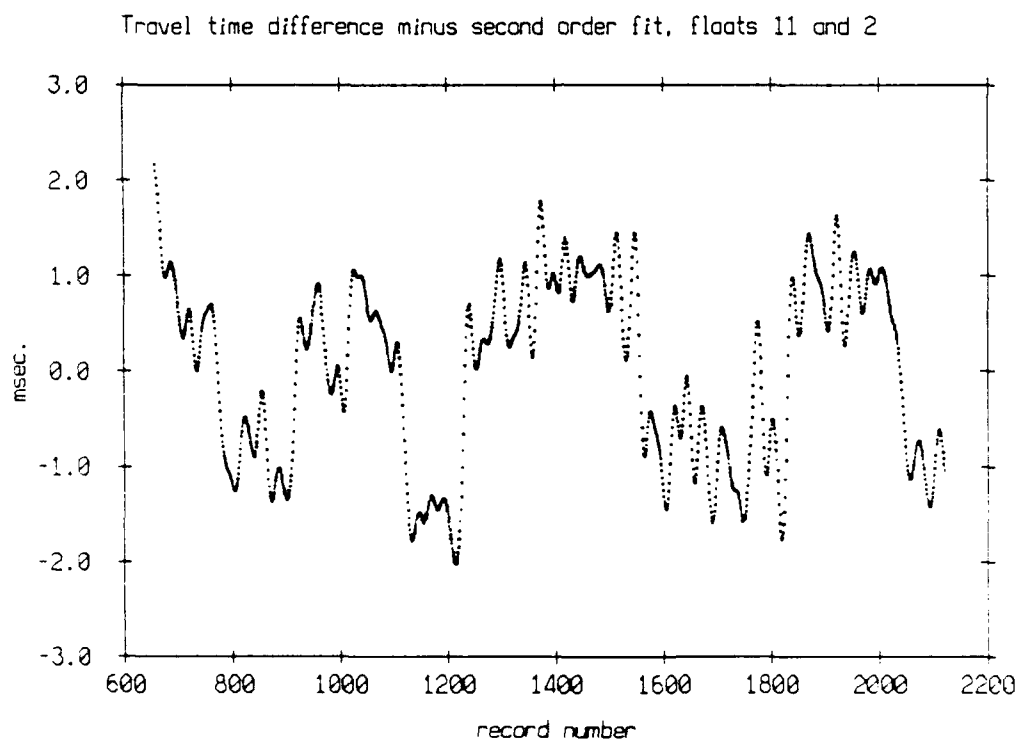
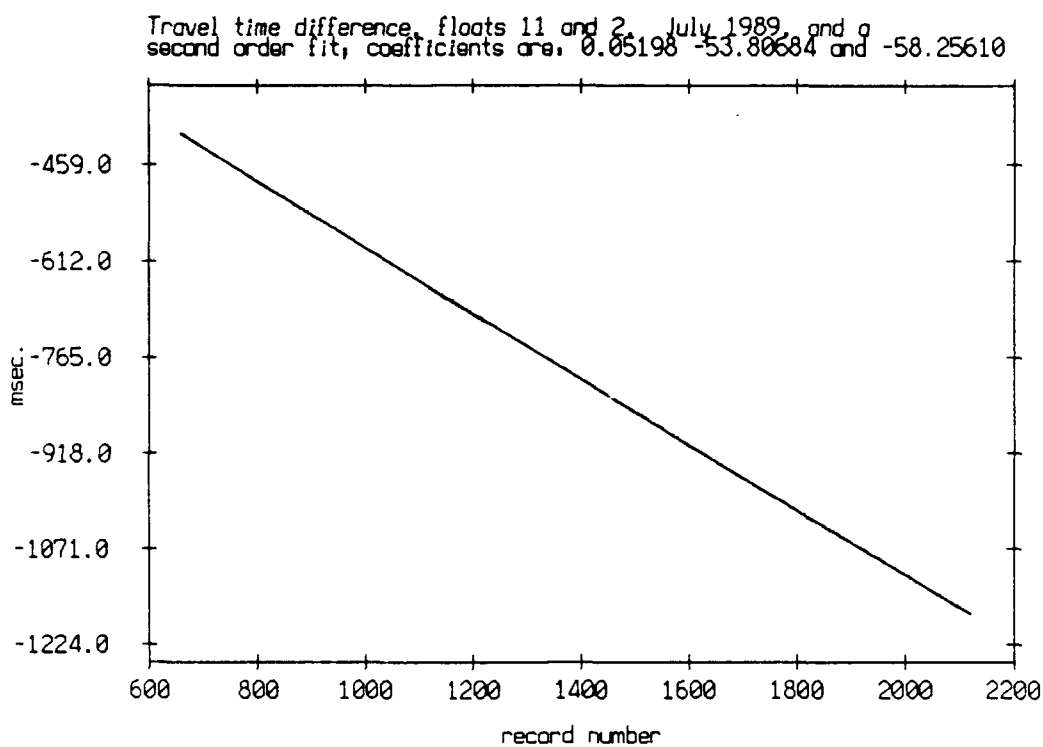


Figure 3.149

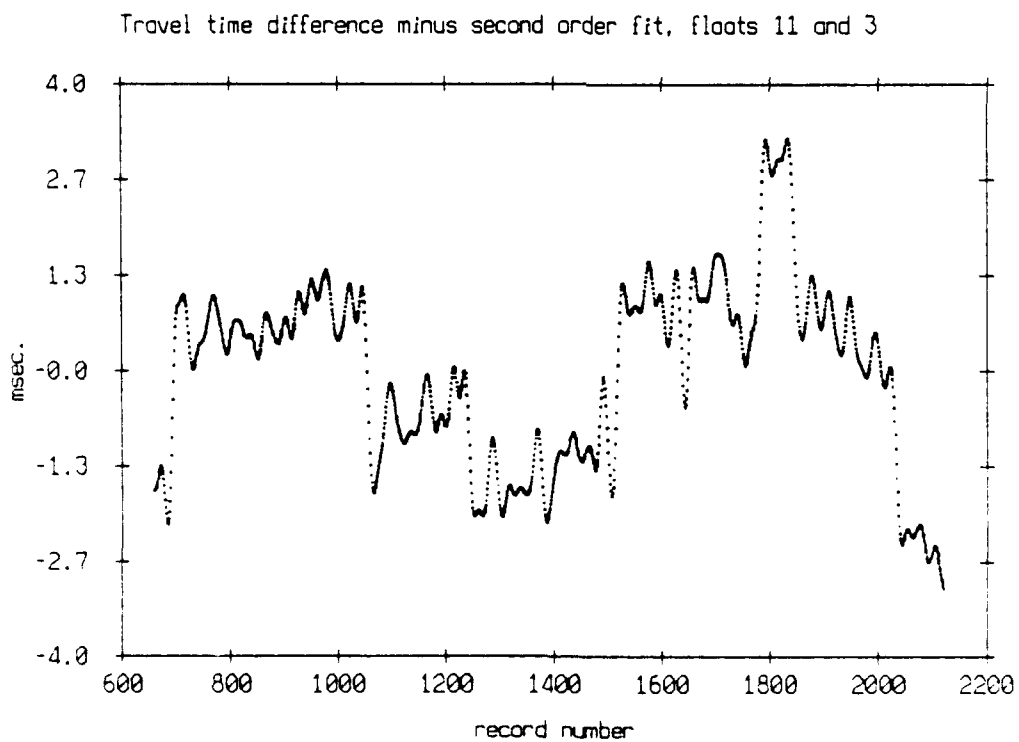
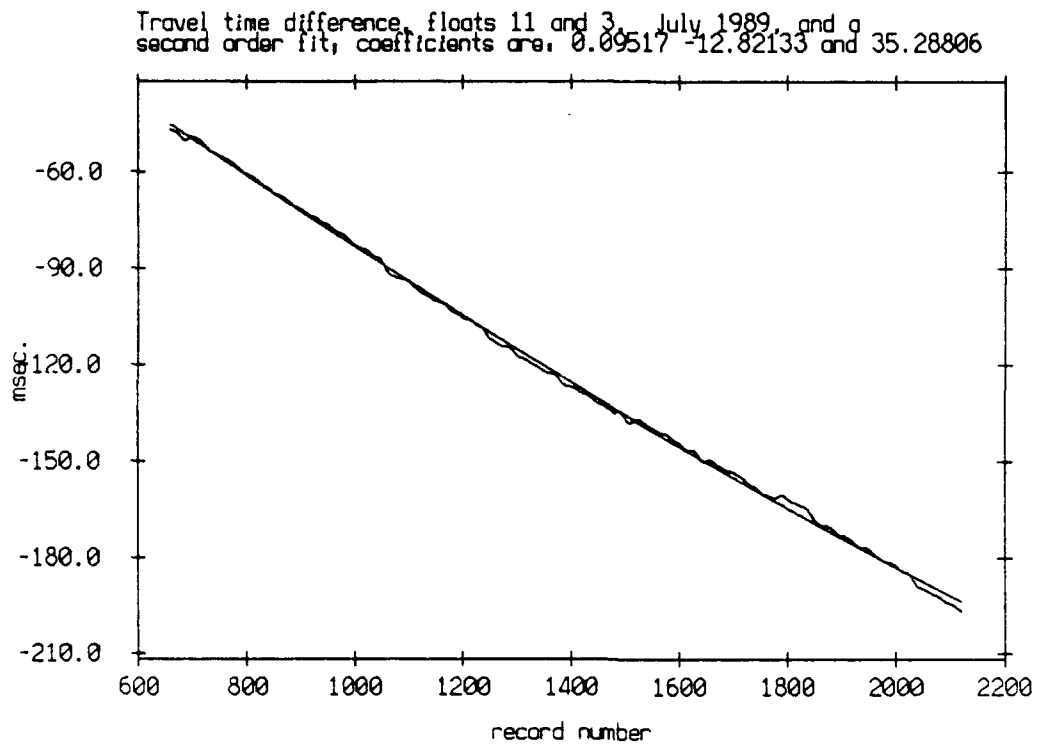


Figure 3.150

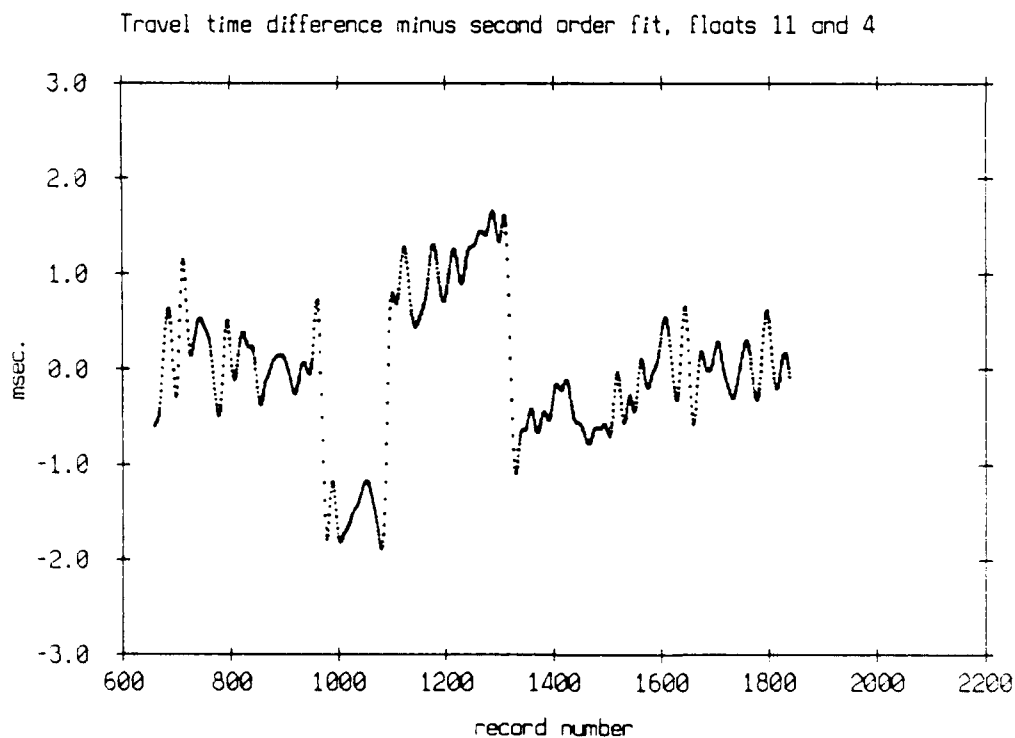
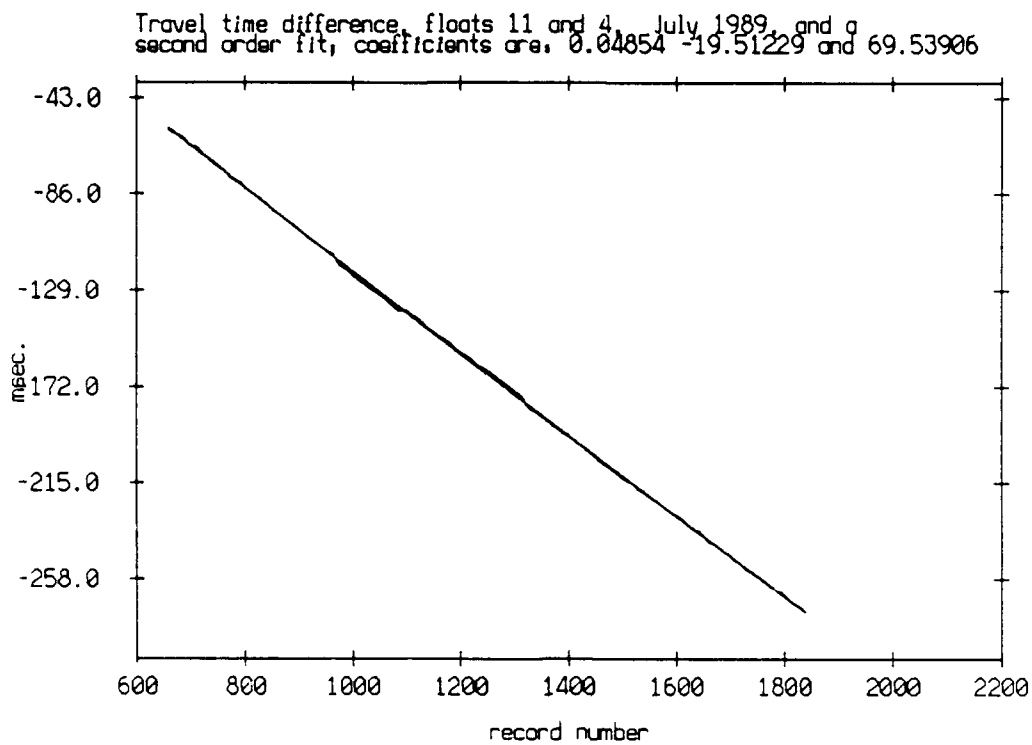


Figure 3.151

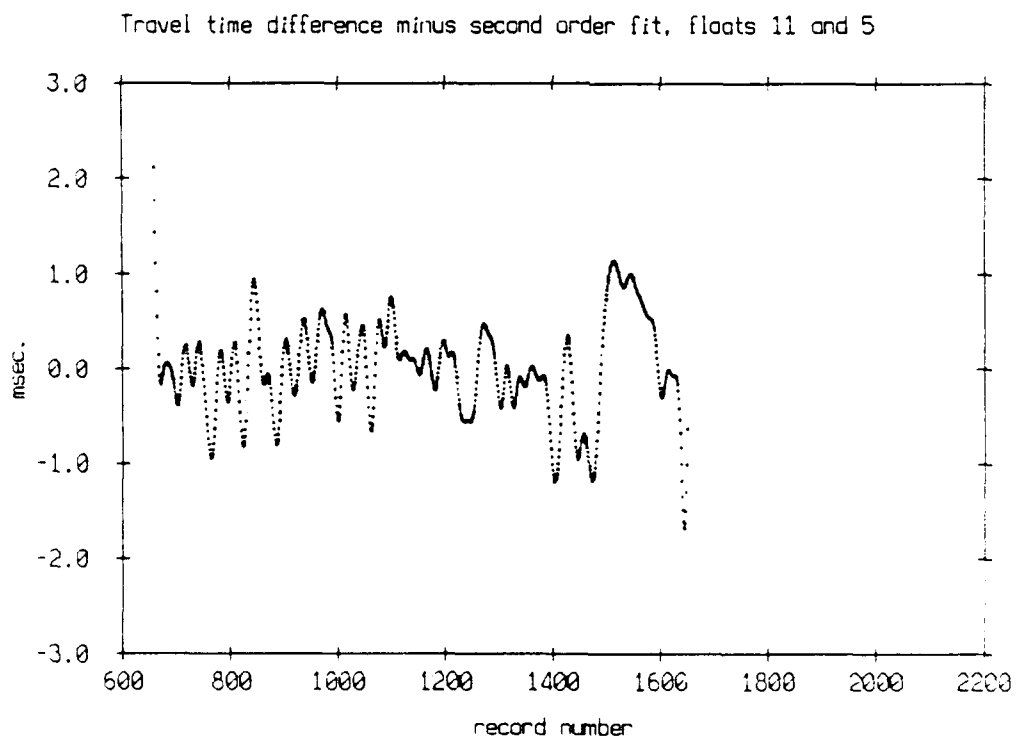
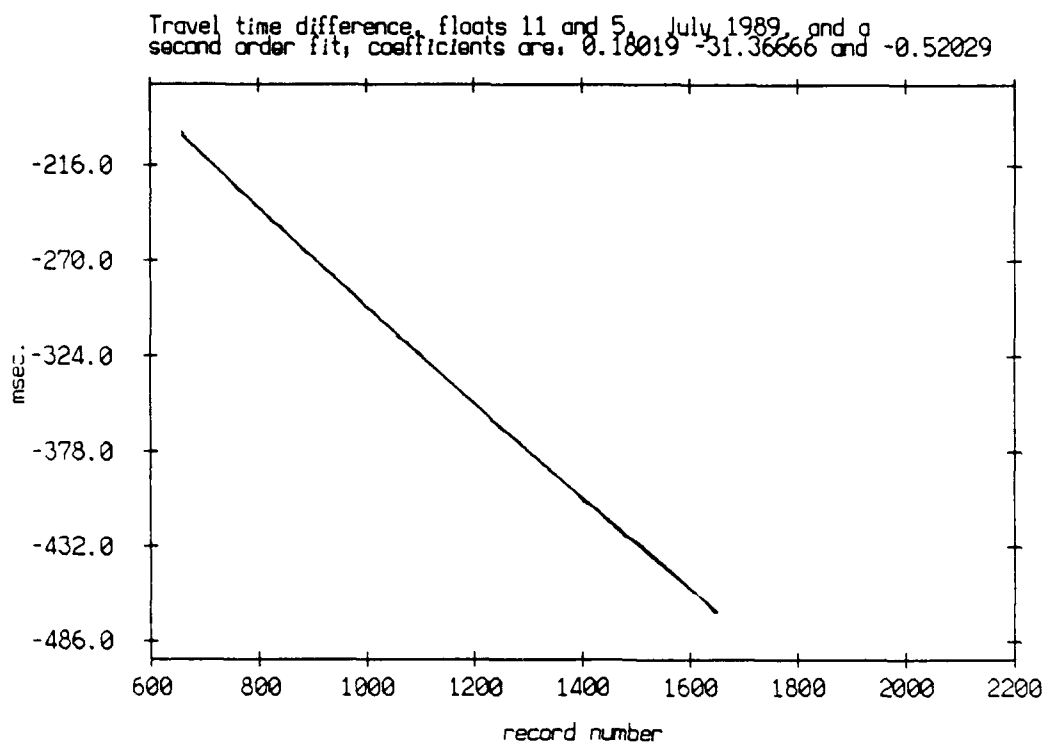


Figure 3.152

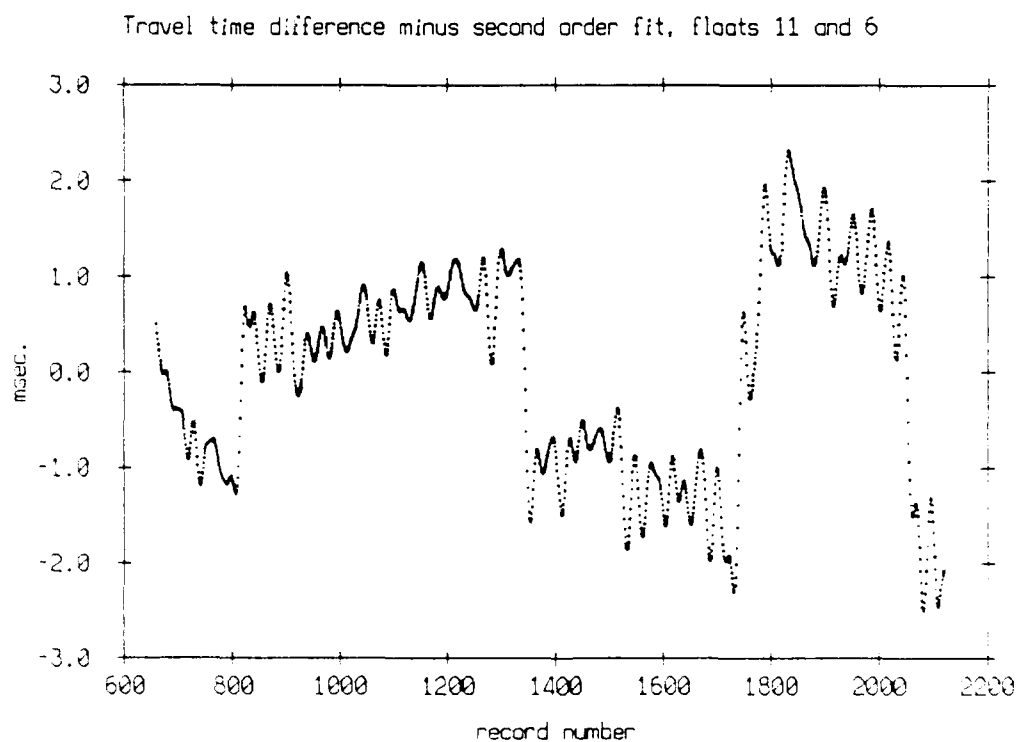
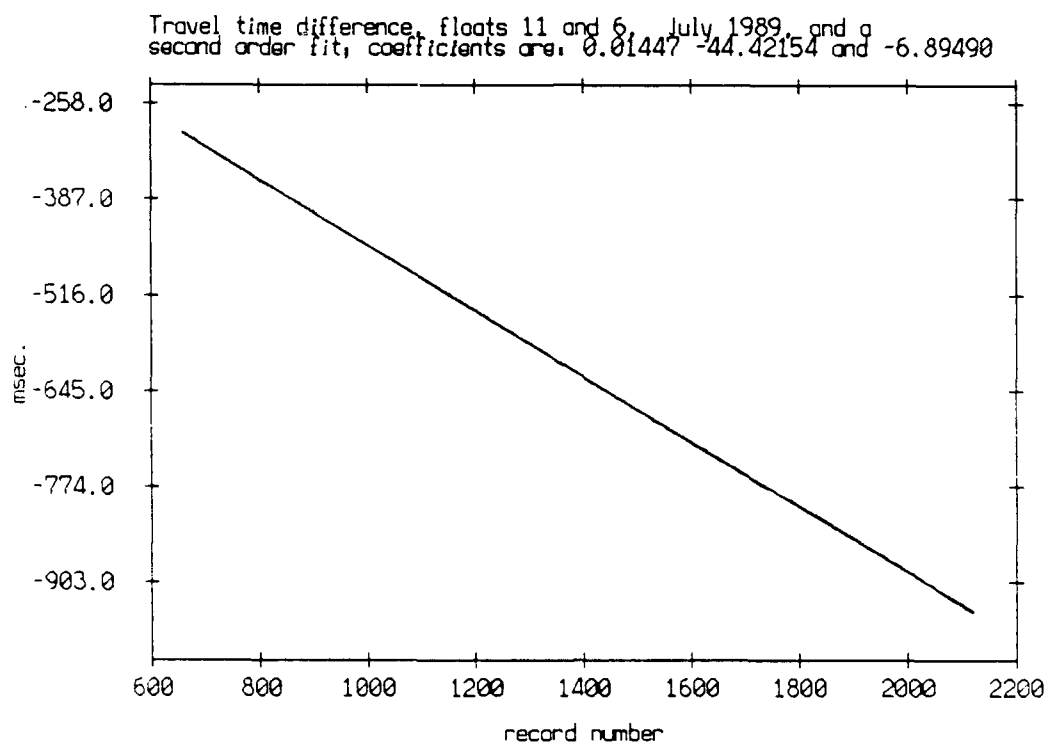


Figure 3.153

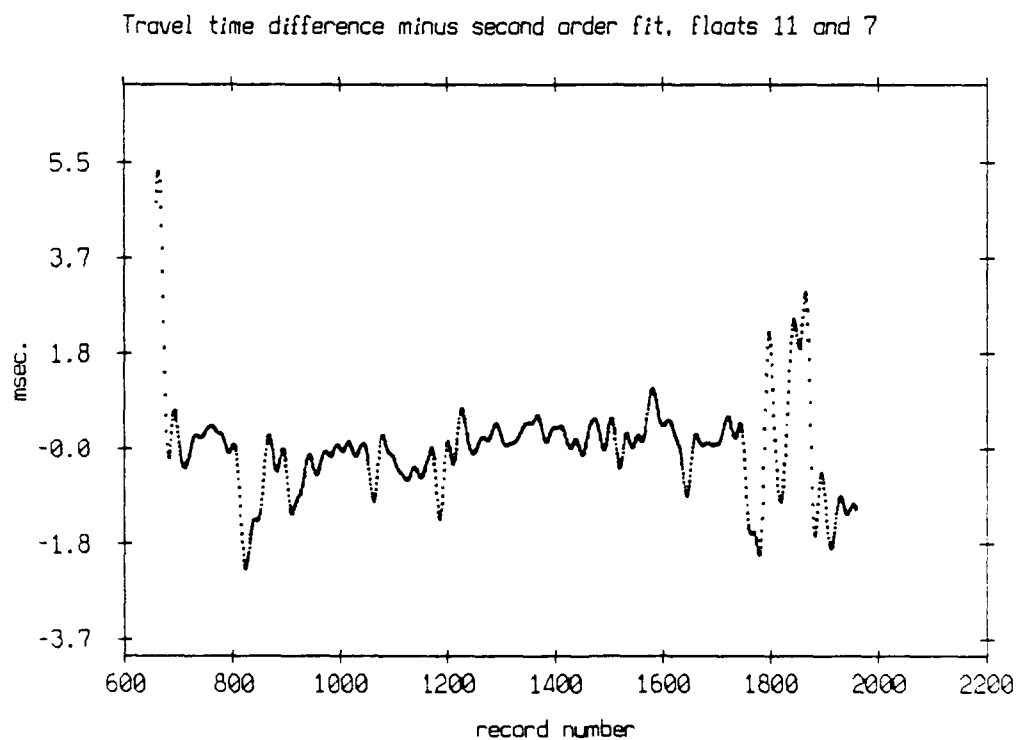
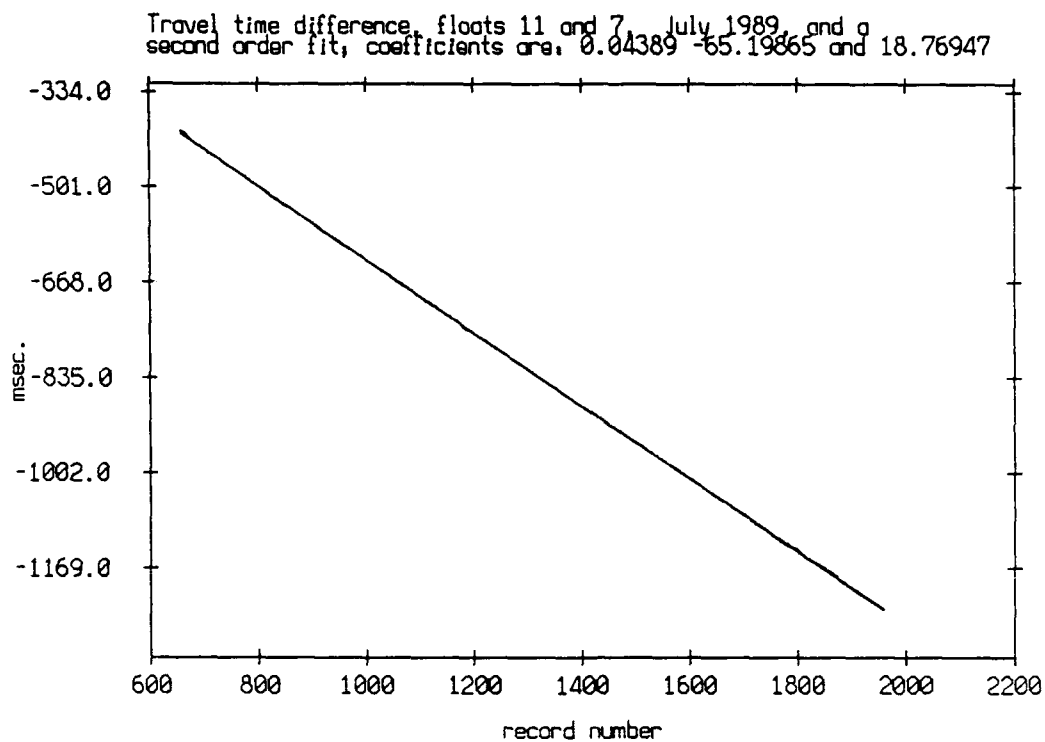
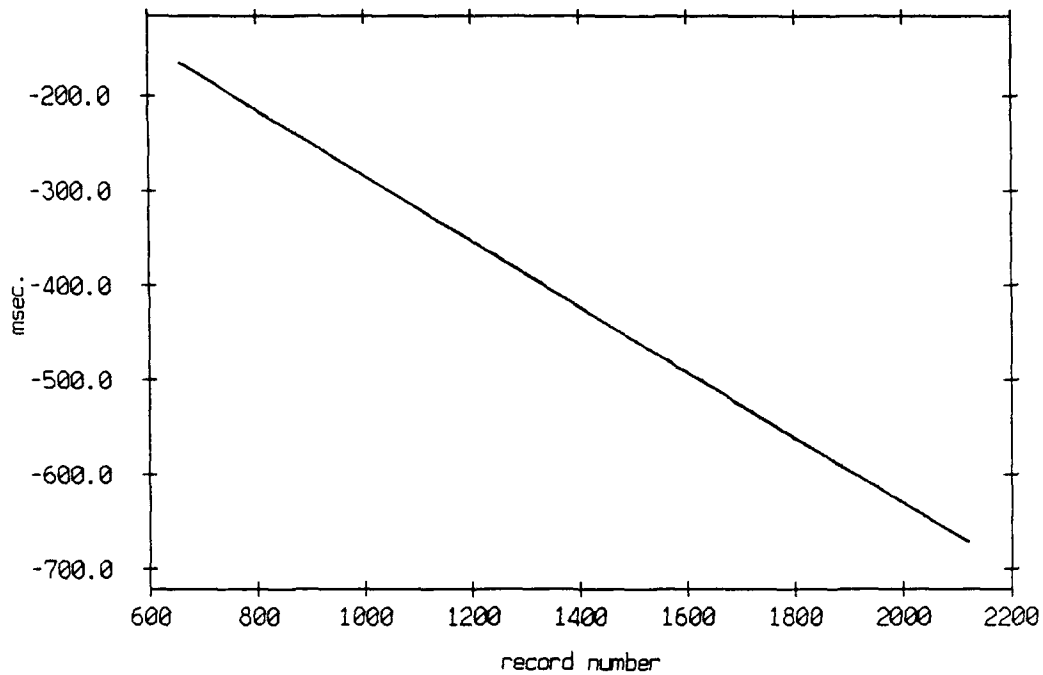


Figure 3.154

Travel time difference, floats 11 and 8, July 1989, and a
second order fit, coefficients are: 0.01572 -35.06775 and 64.42834



Travel time difference minus second order fit, floats 11 and 8

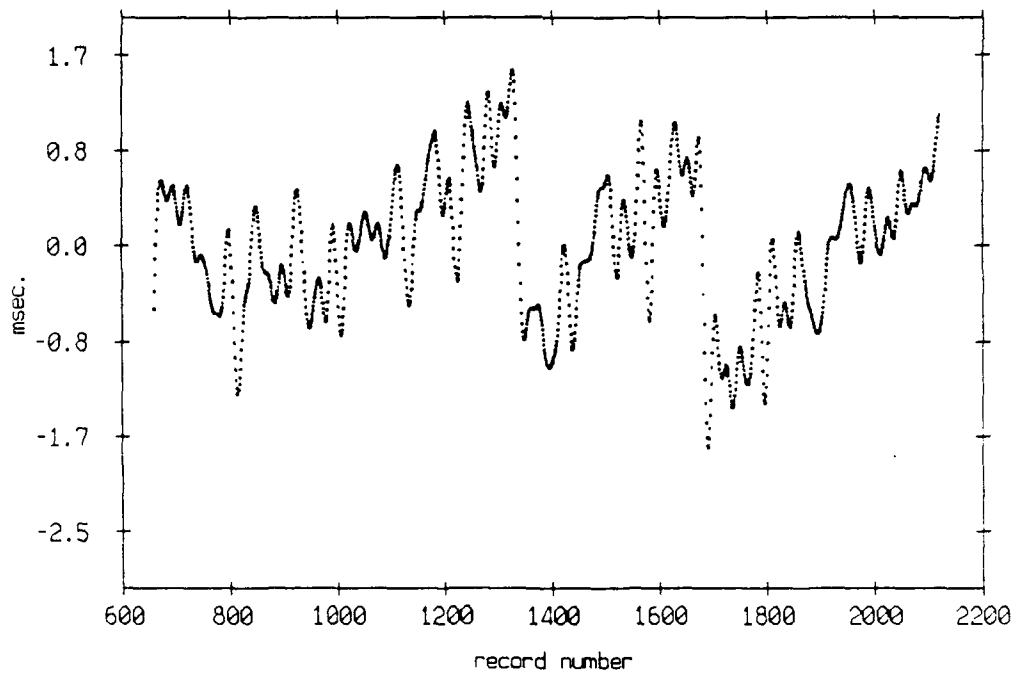


Figure 3.155

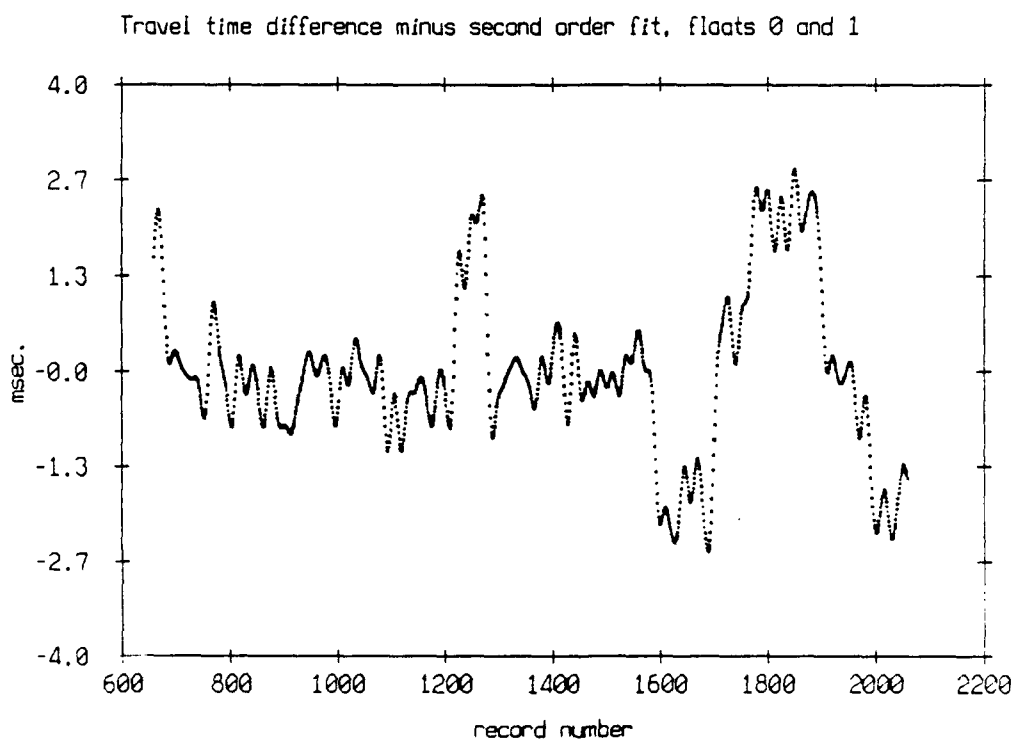
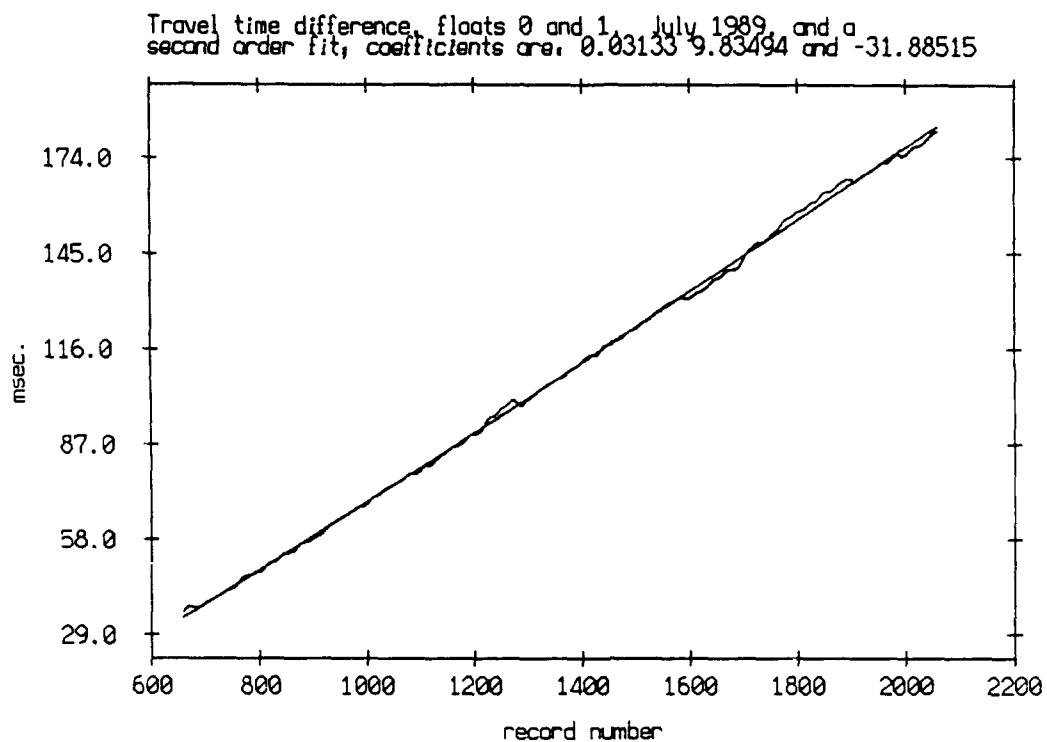


Figure 3.156

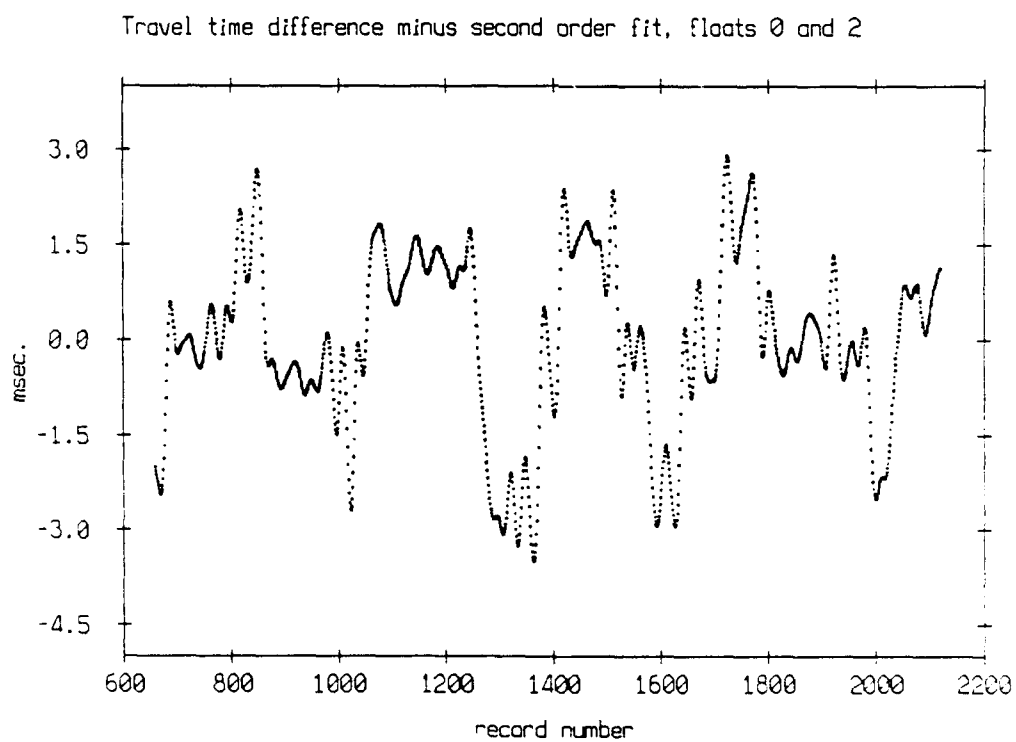
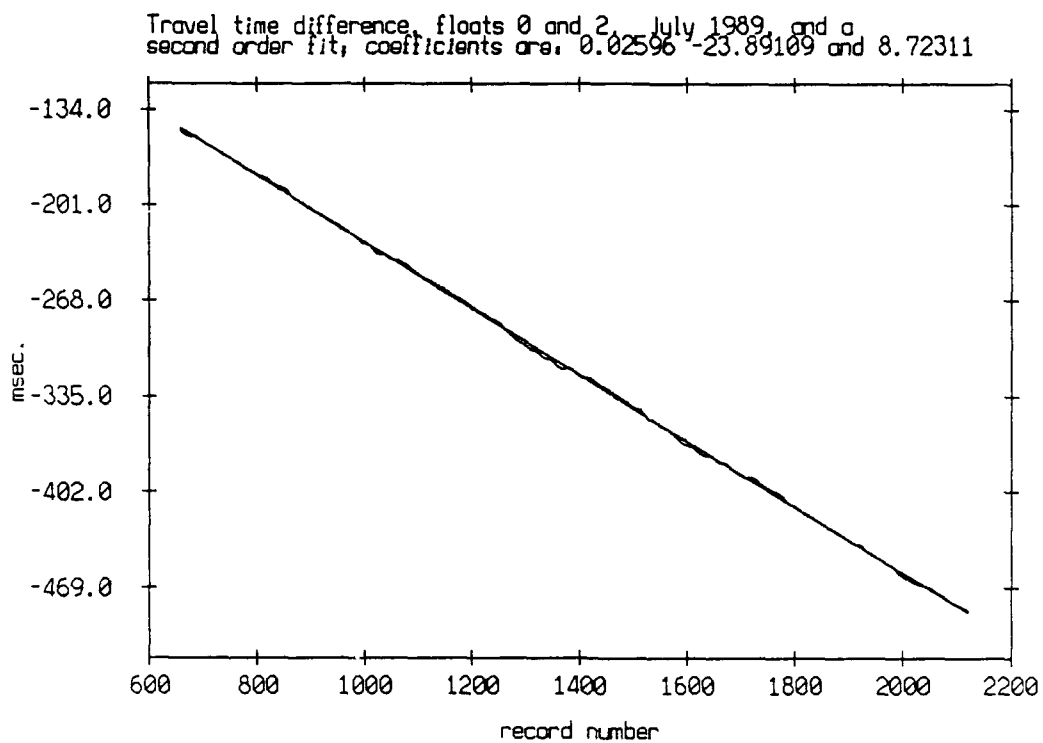
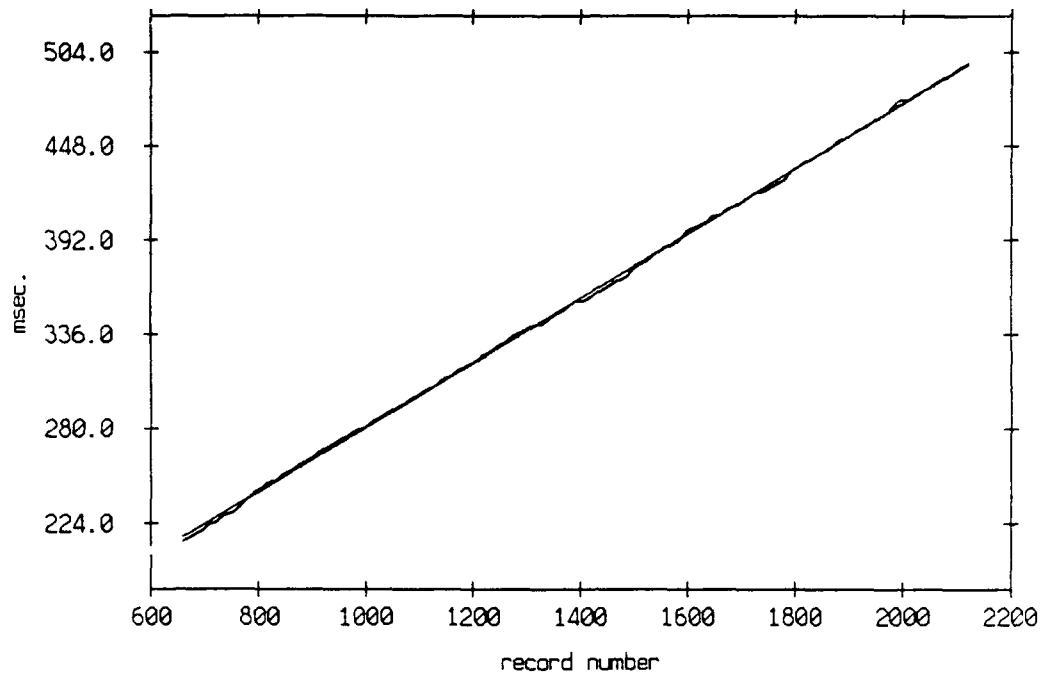


Figure 3.157

Travel time difference, floats 0 and 3, July 1989, and a second order fit, coefficients are: 0.01238 18.85915 and 91.22421



Travel time difference minus second order fit, floats 0 and 3

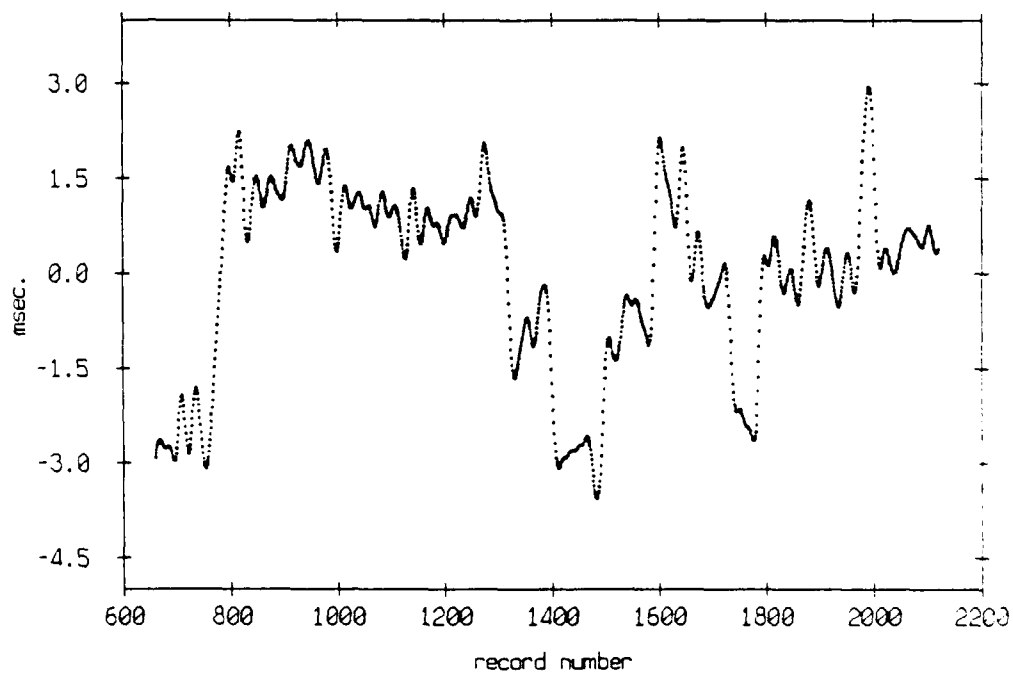


Figure 3.158

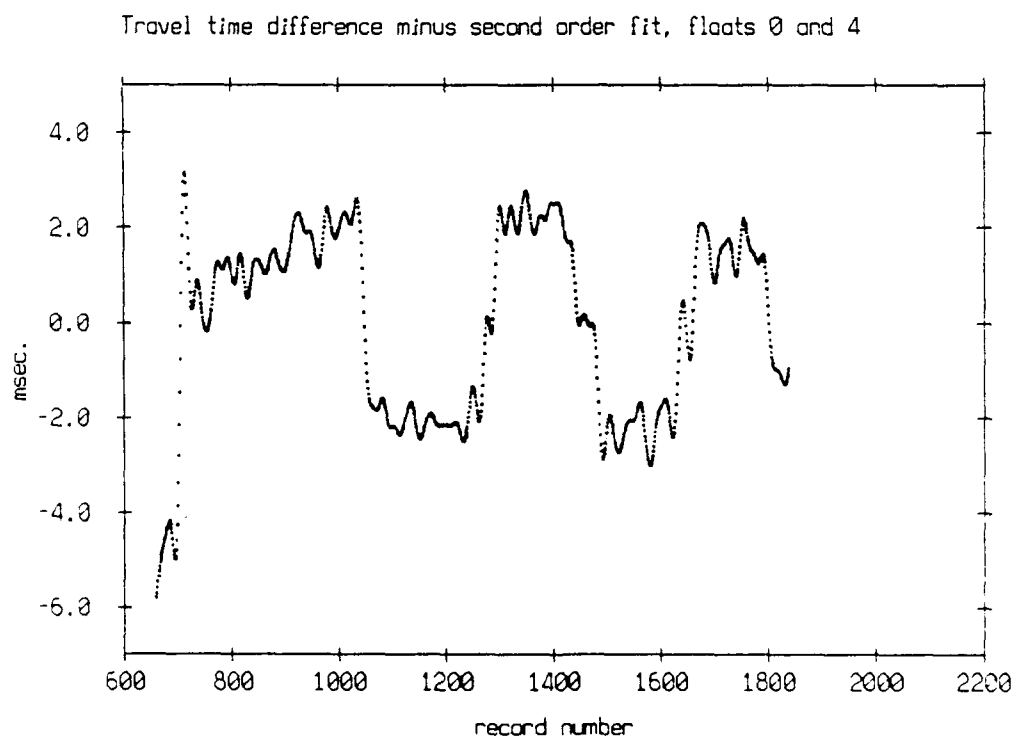
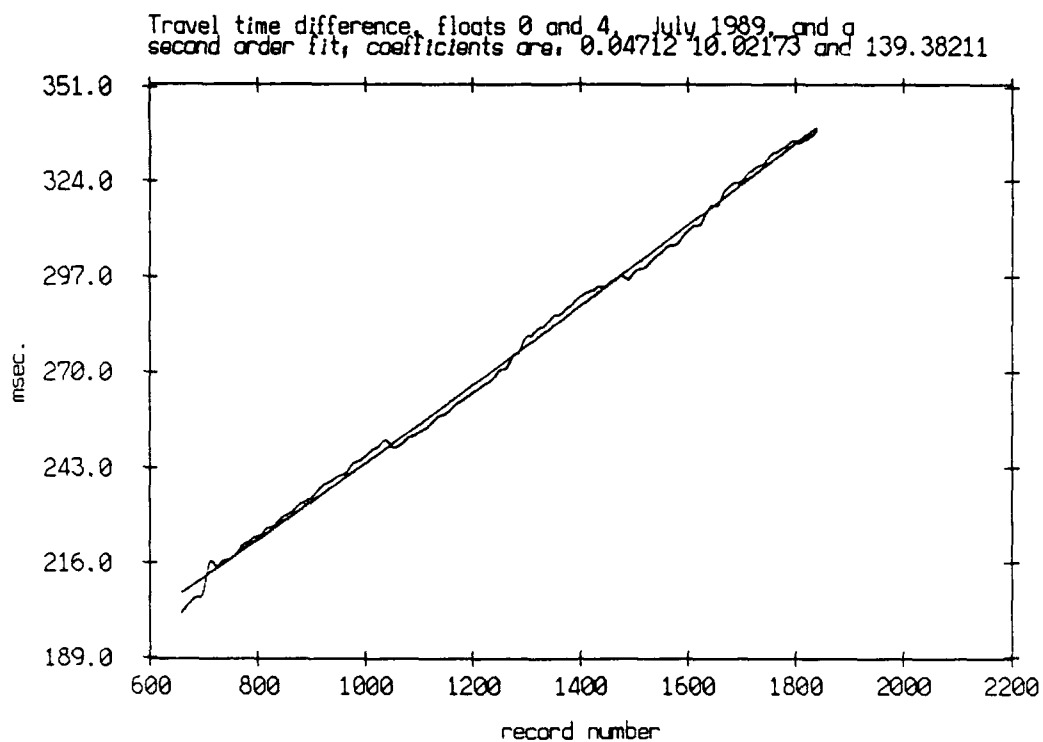


Figure 3.159

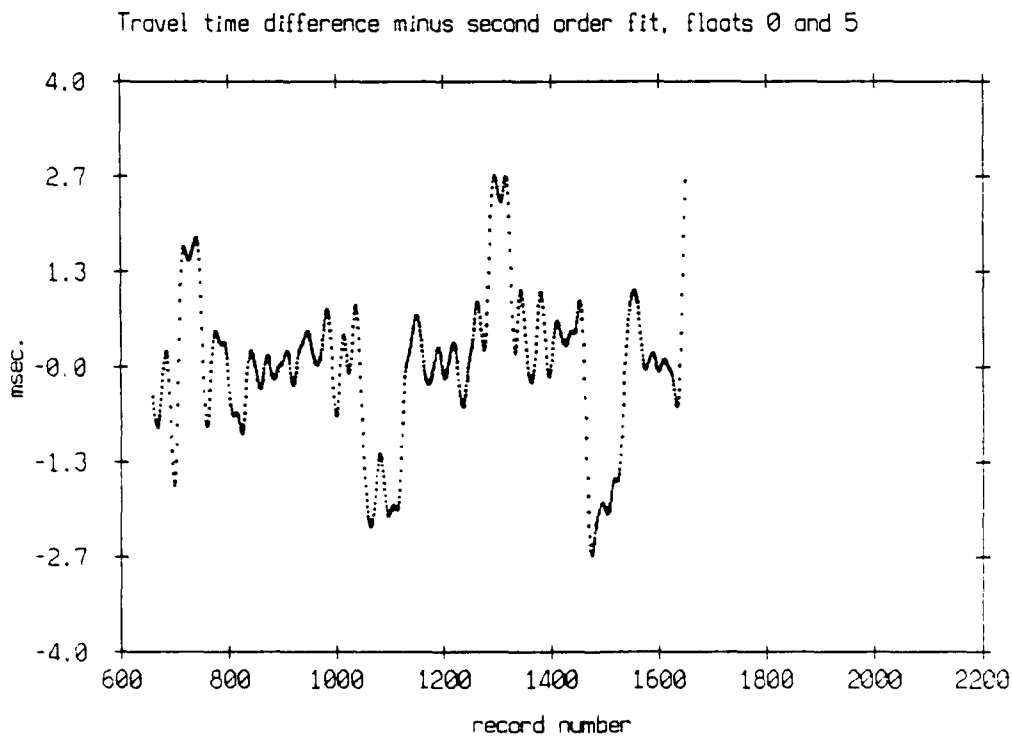
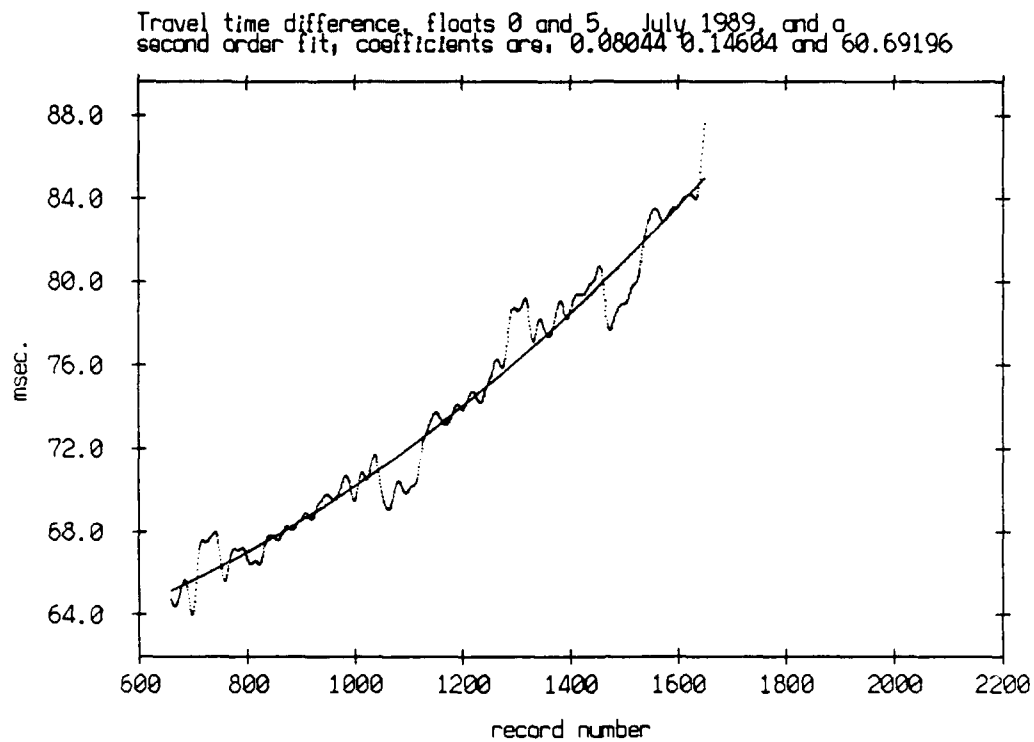
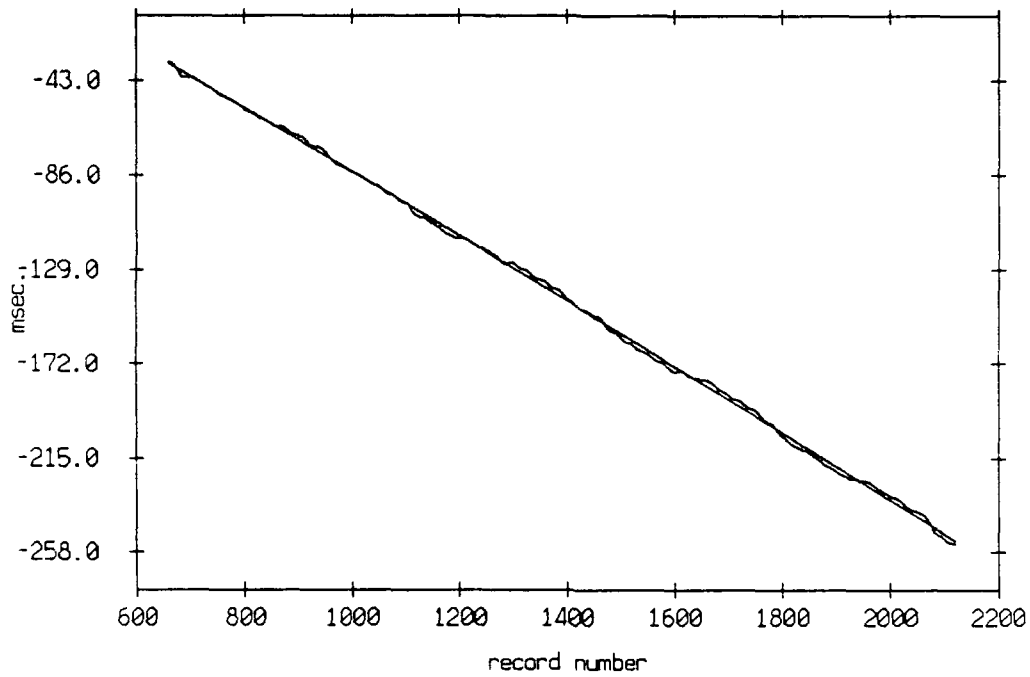


Figure 3.160

Travel time difference, floats 0 and 6, July 1989, and a second order fit, coefficients are, -0.04036 -13.76737 and 57.26703



Travel time difference minus second order fit, floats 0 and 6

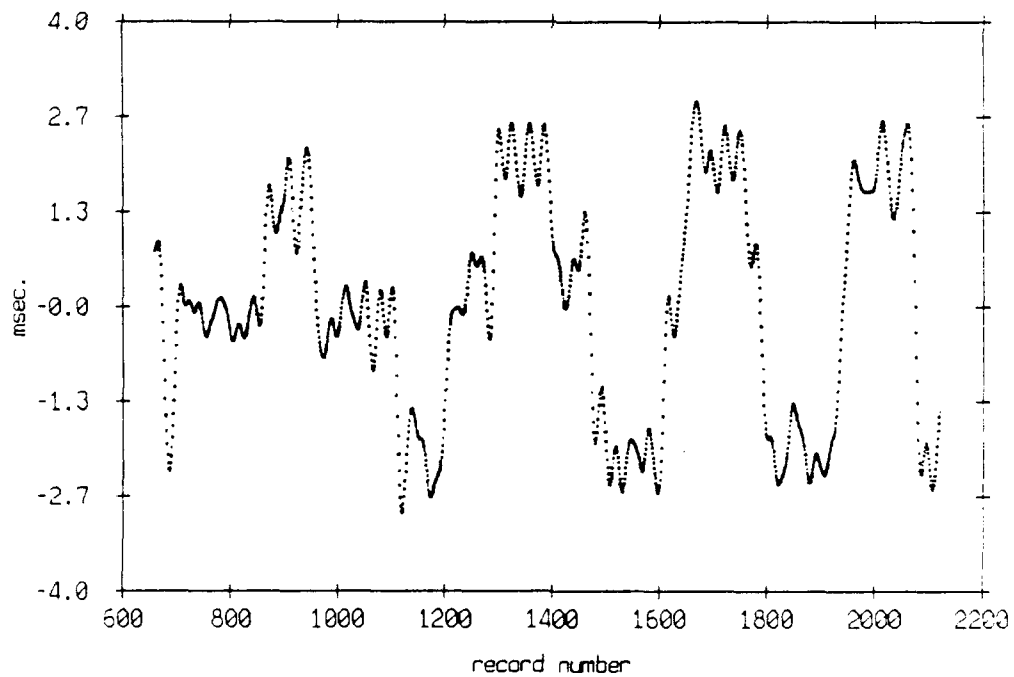


Figure 3.161

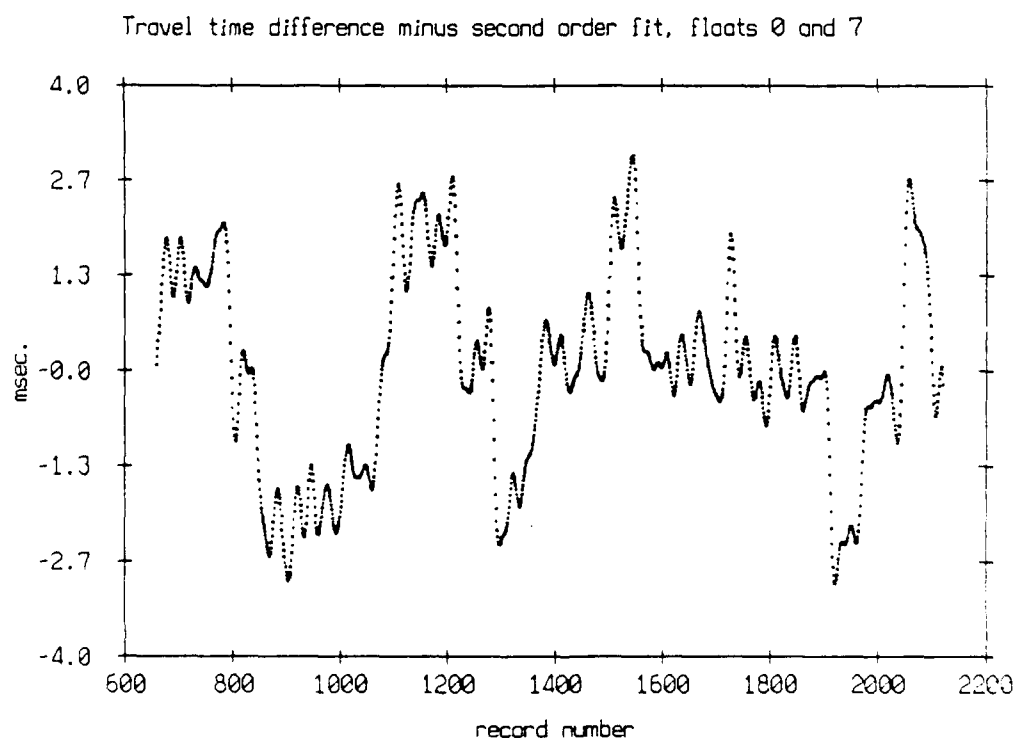
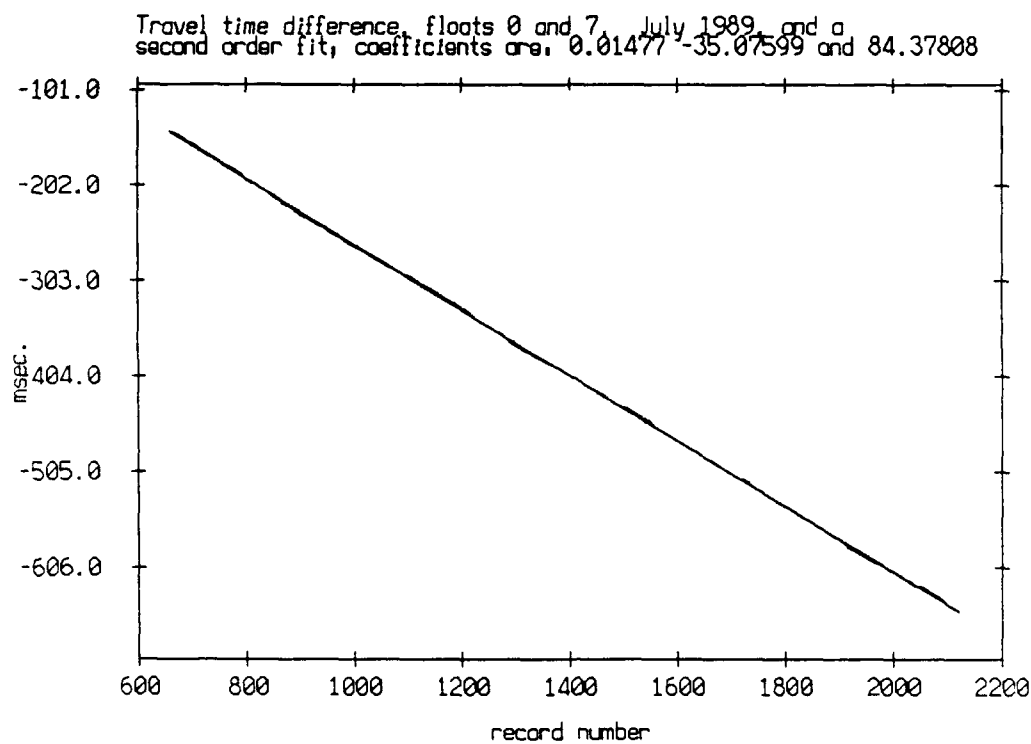
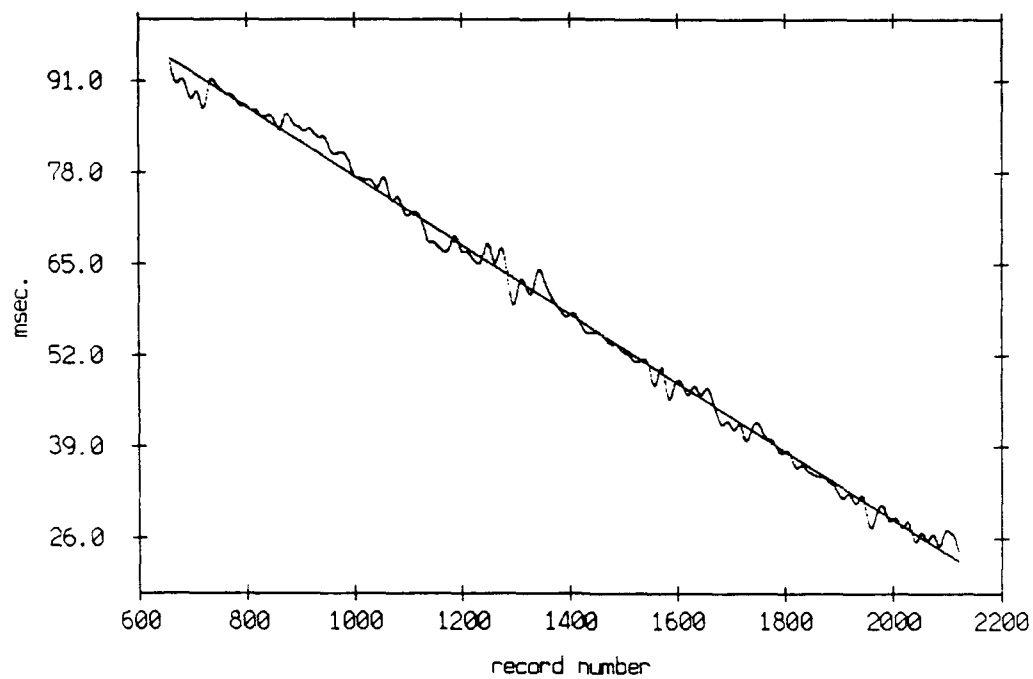


Figure 3.162

Travel time difference, floats 0 and 8, July 1989, and a
second order fit, coefficients are, 0.00207 -4.94819 and 126.70593



Travel time difference minus second order fit, floats 0 and 8

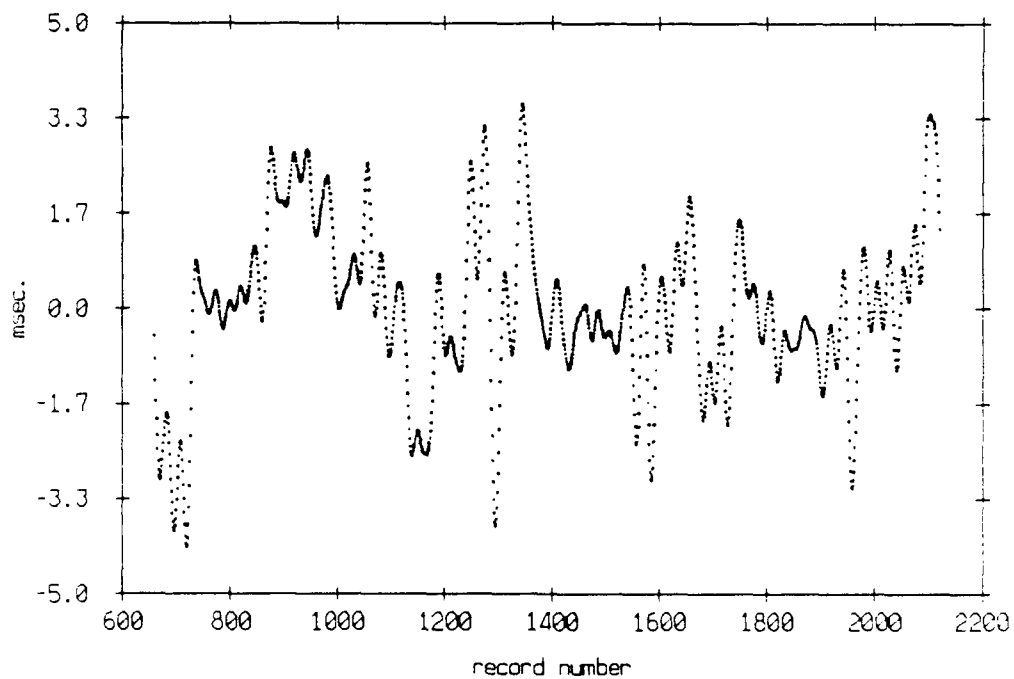


Figure 3.163

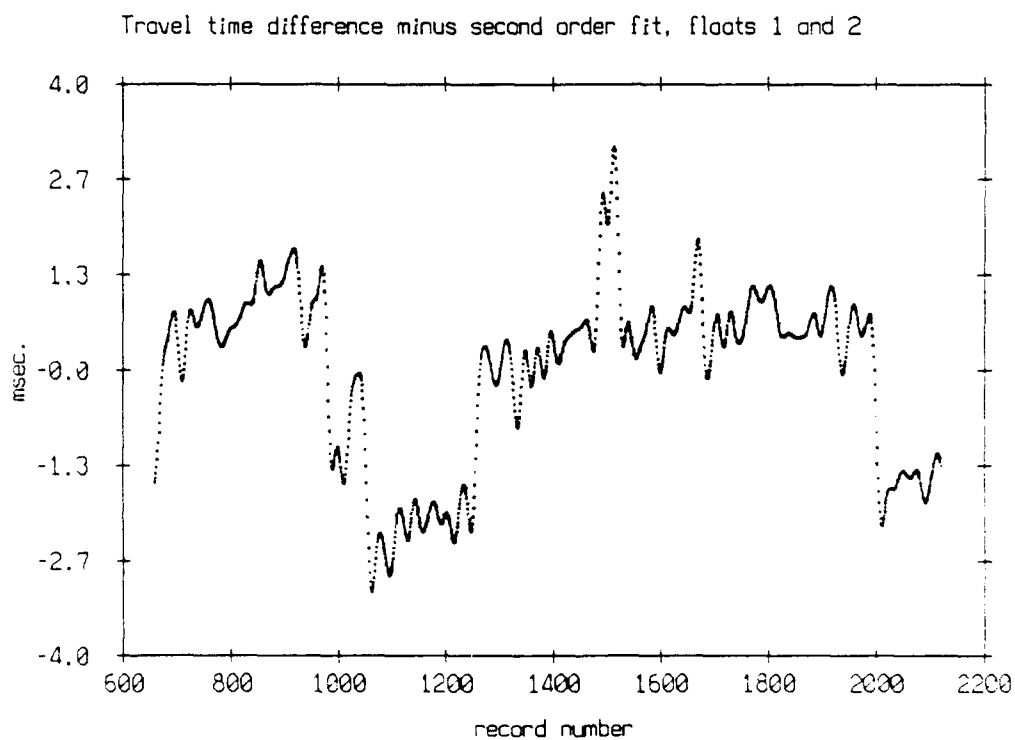
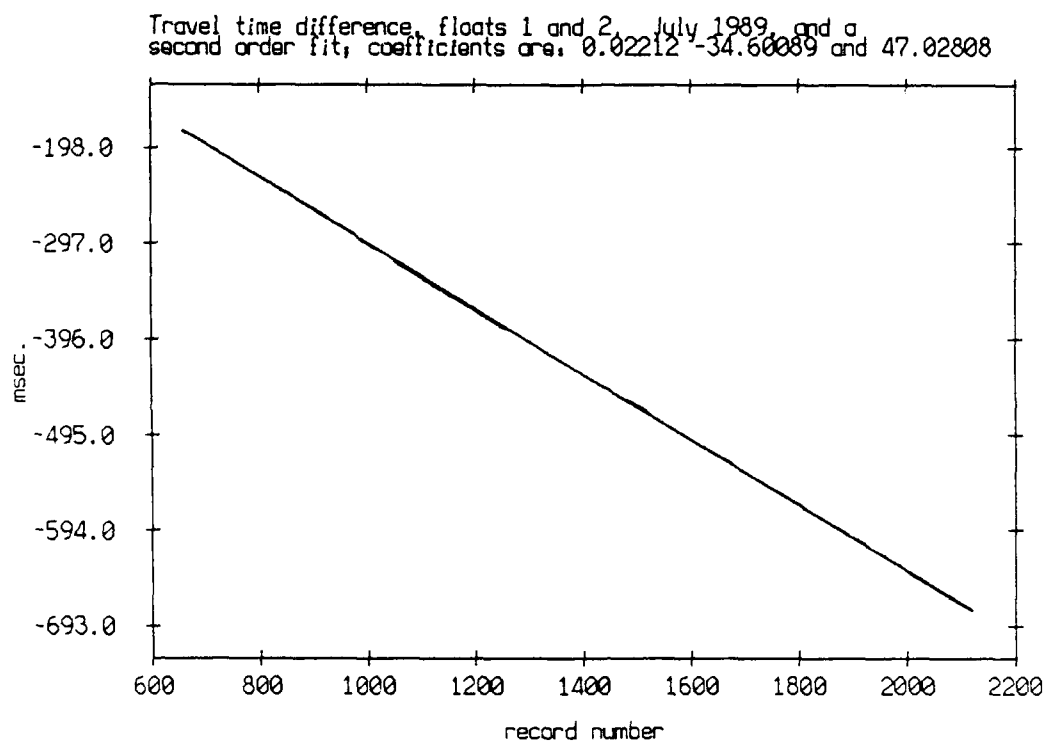


Figure 3.164

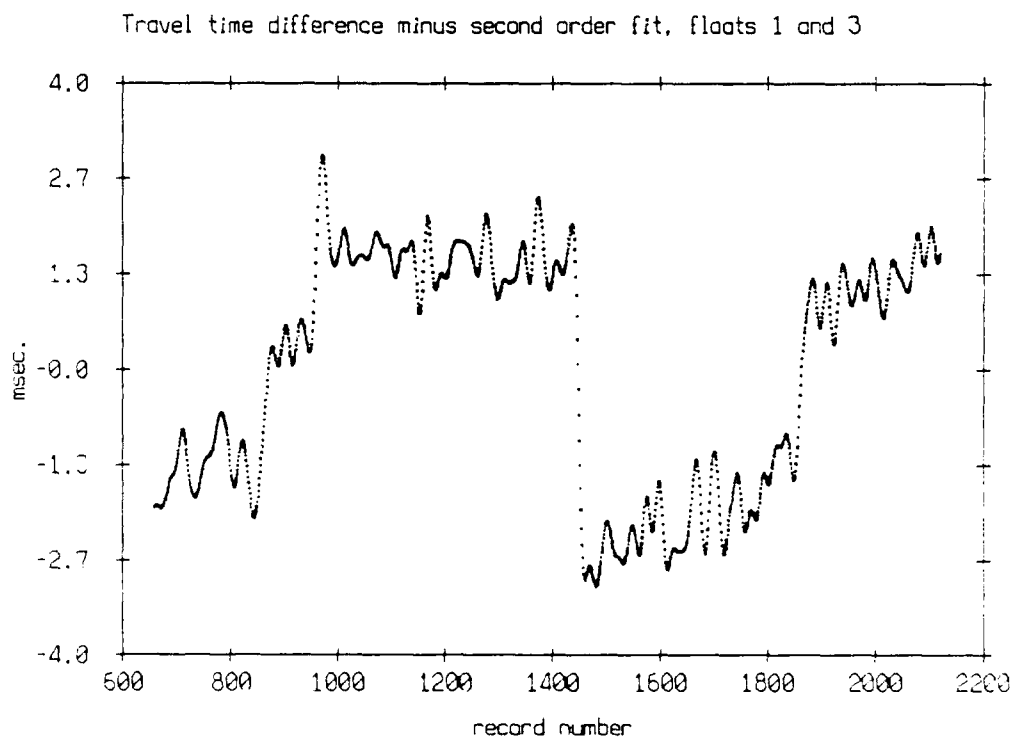
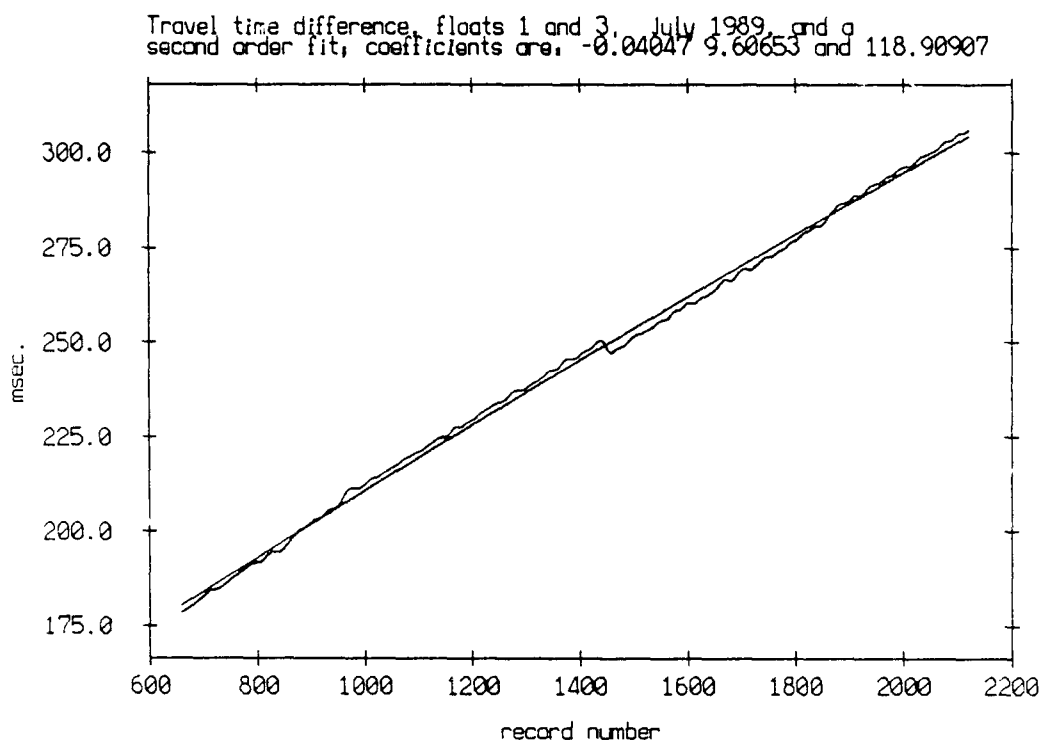
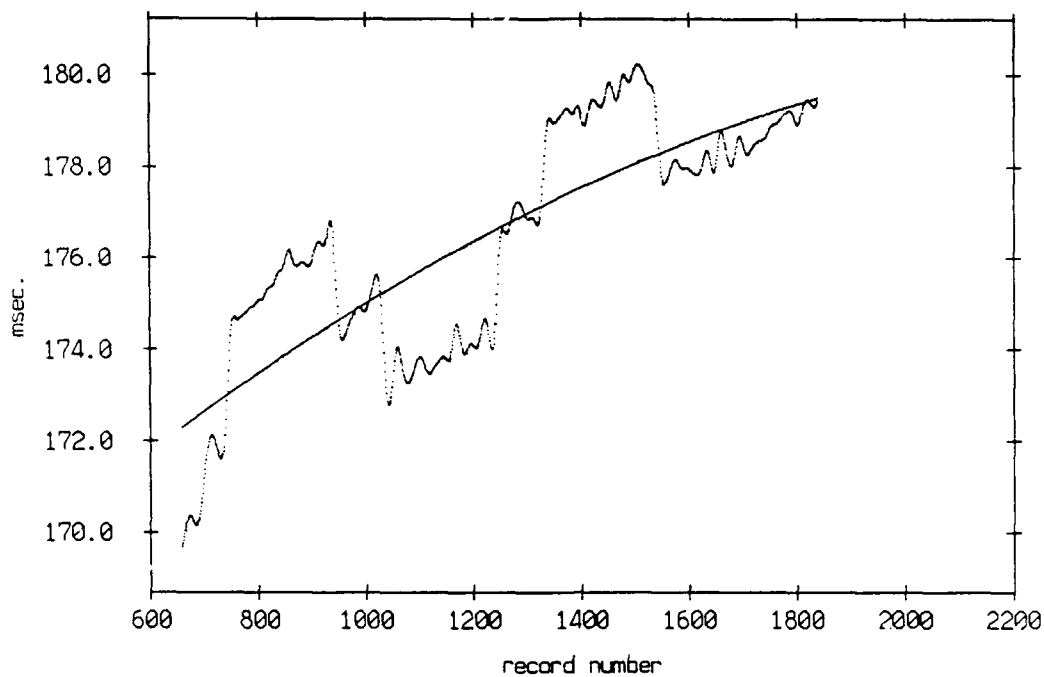


Figure 3.165

Travel time difference, floats 1 and 4, July 1989, and a second order fit, coefficients are: -0.02242 1.17007 and 165.56229



Travel time difference minus second order fit, floats 1 and 4

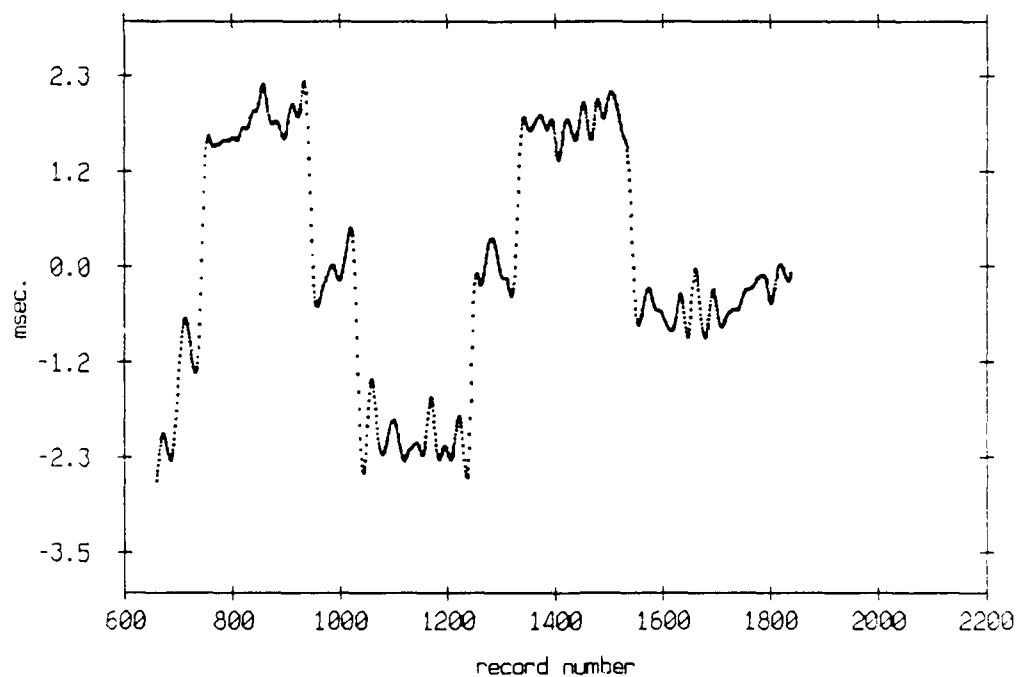


Figure 3.166

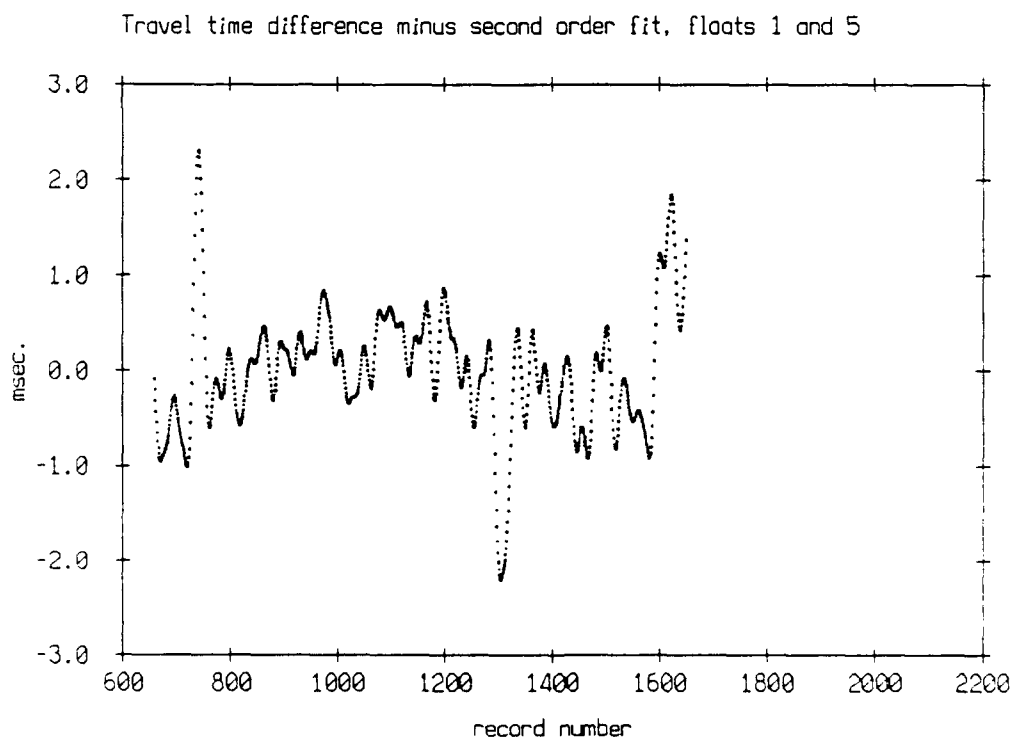
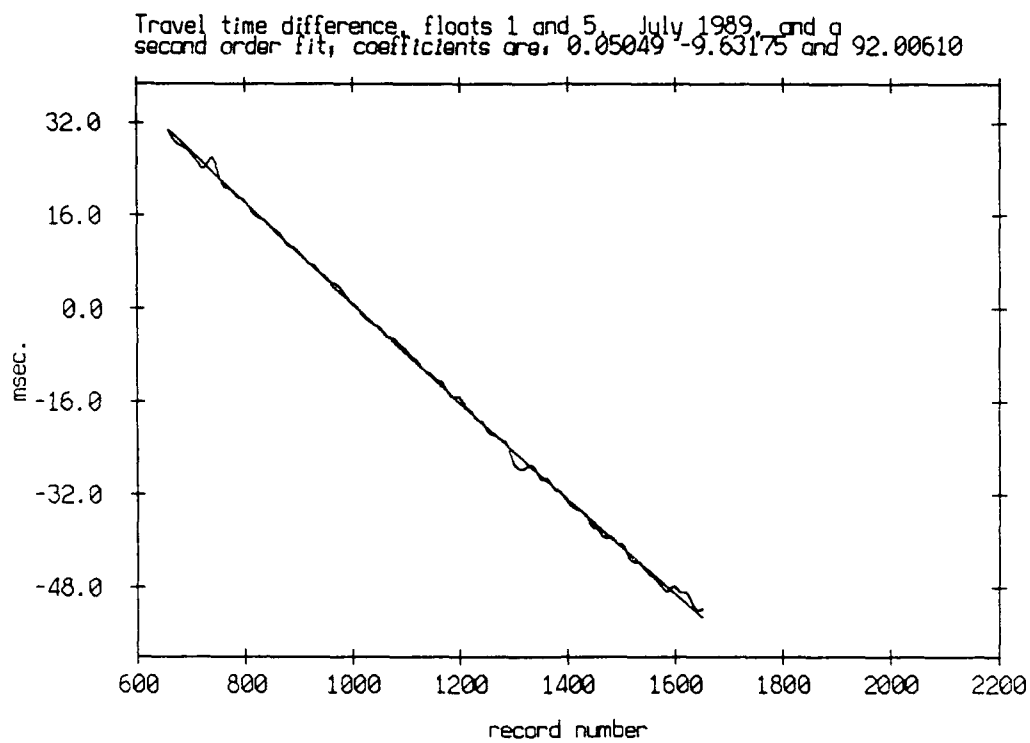


Figure 3.167

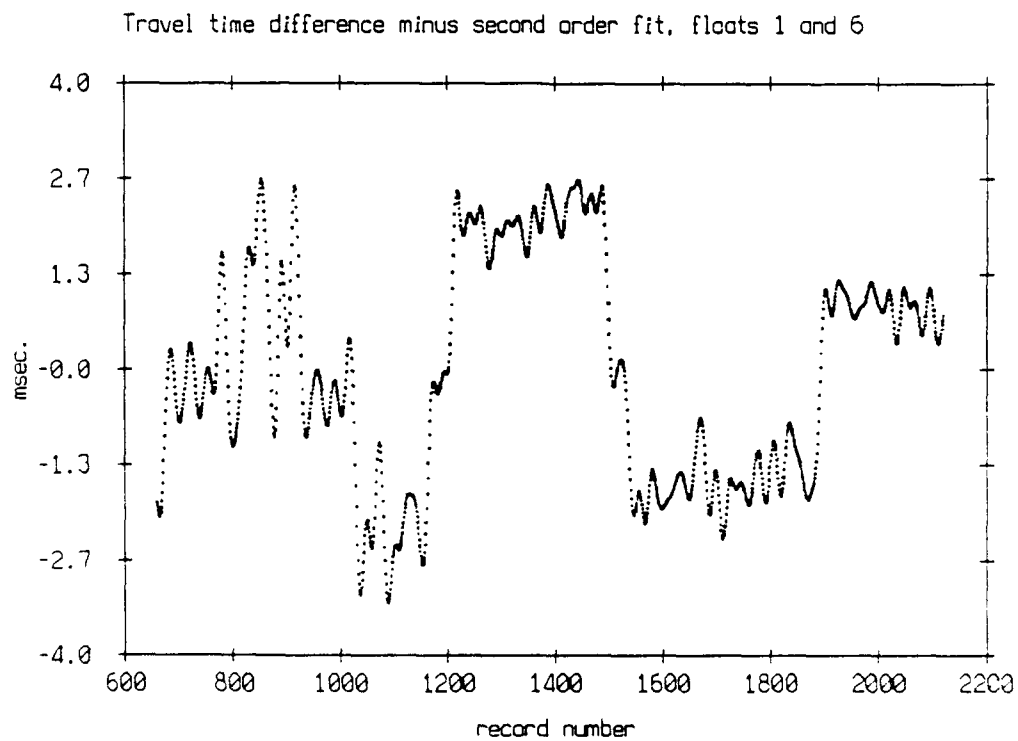
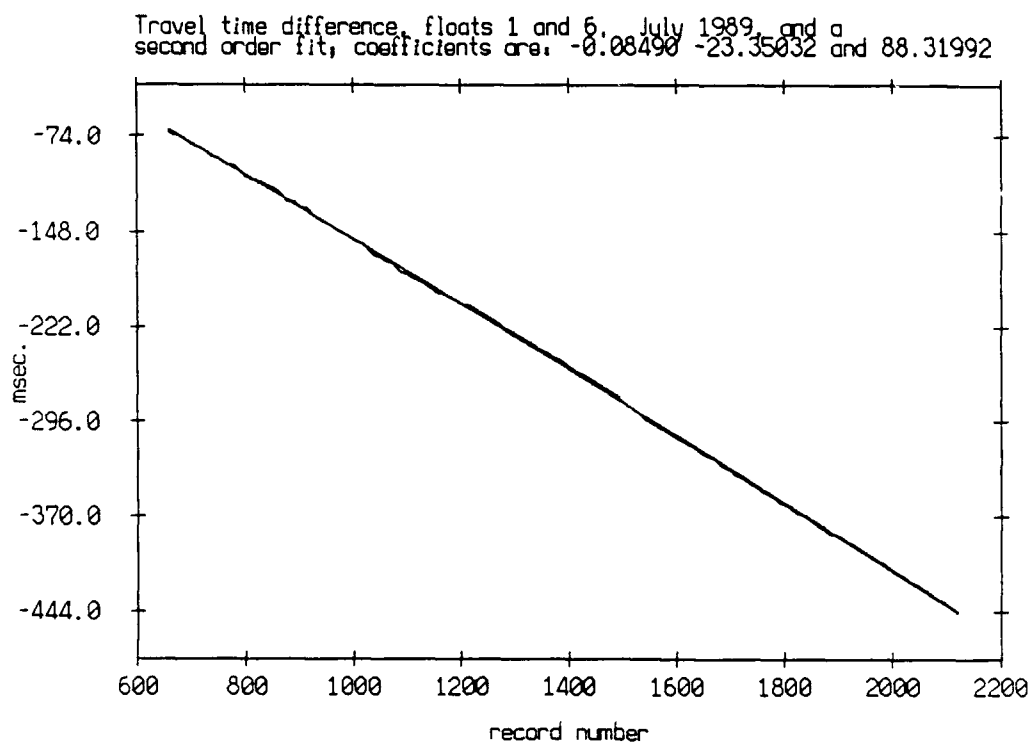
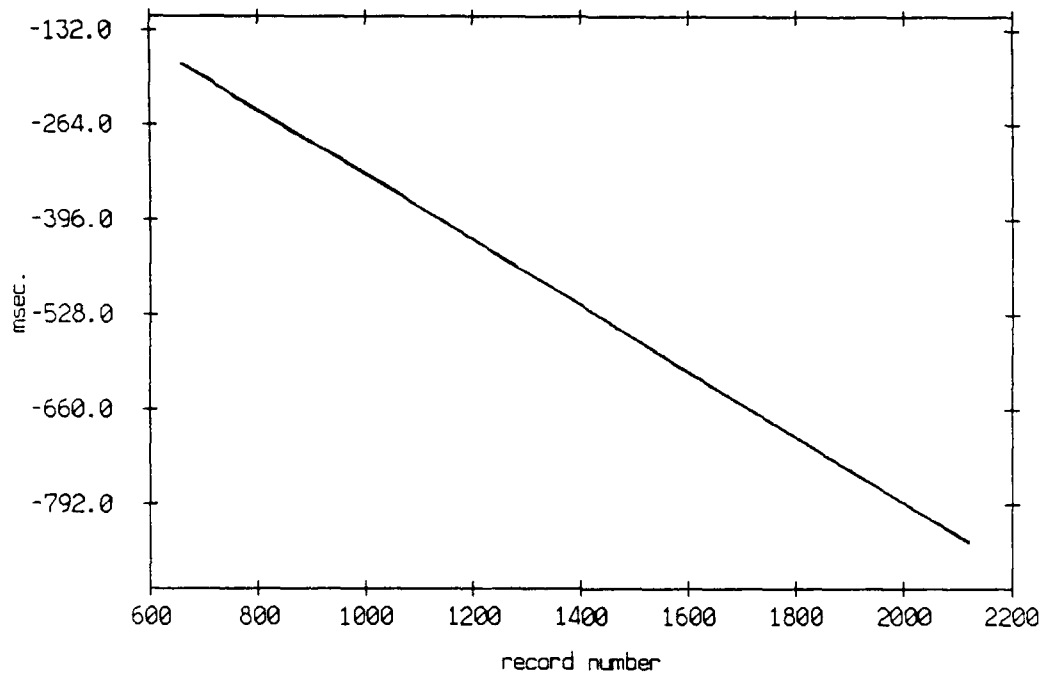


Figure 3.168

Travel time difference, floats 1 and 7, July 1989, and a second order fit, coefficients are, -0.03788 -44.52425 and 114.87286



Travel time difference minus second order fit, floats 1 and 7

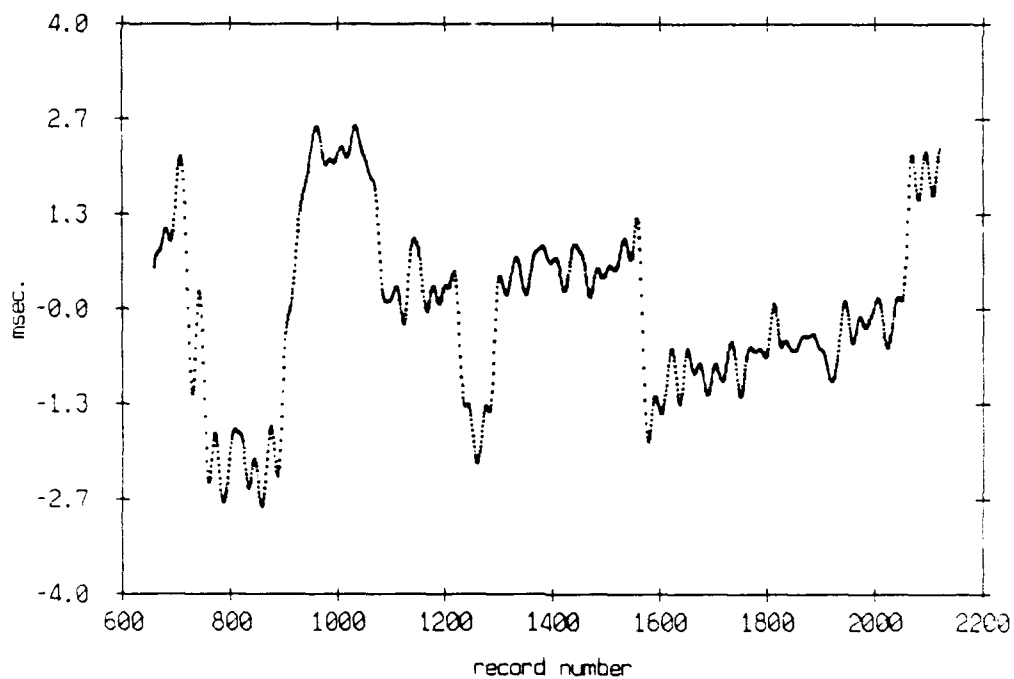
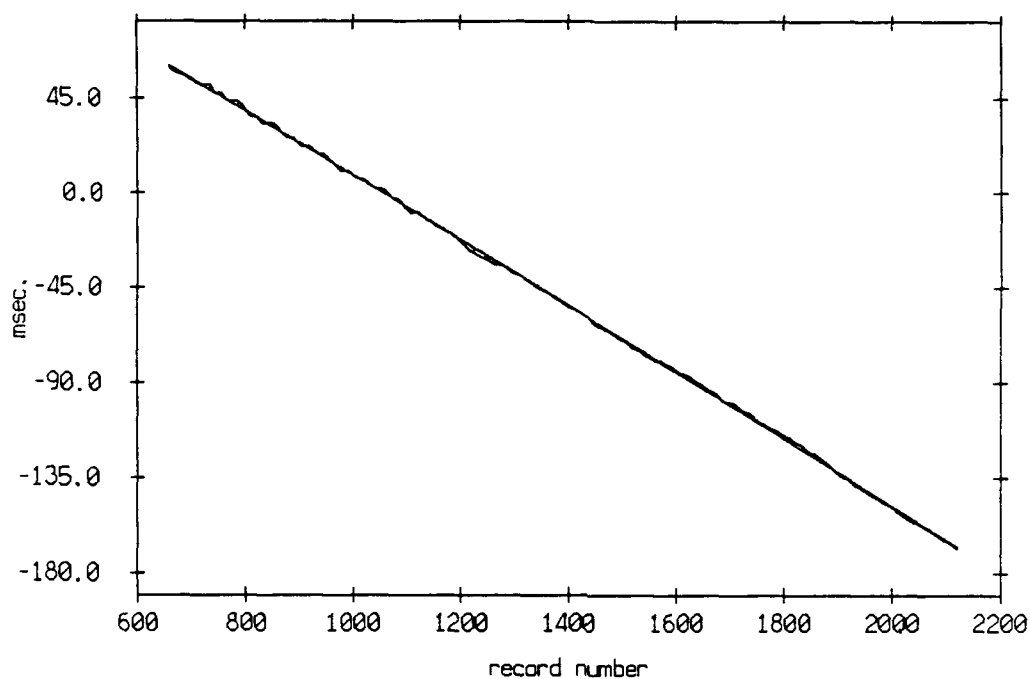


Figure 3.169

Travel time difference, floats 1 and 8, July 1989, and a
second order fit, coefficients are: -0.03449 -14.65317 and 158.19537



Travel time difference minus second order fit, floats 1 and 8

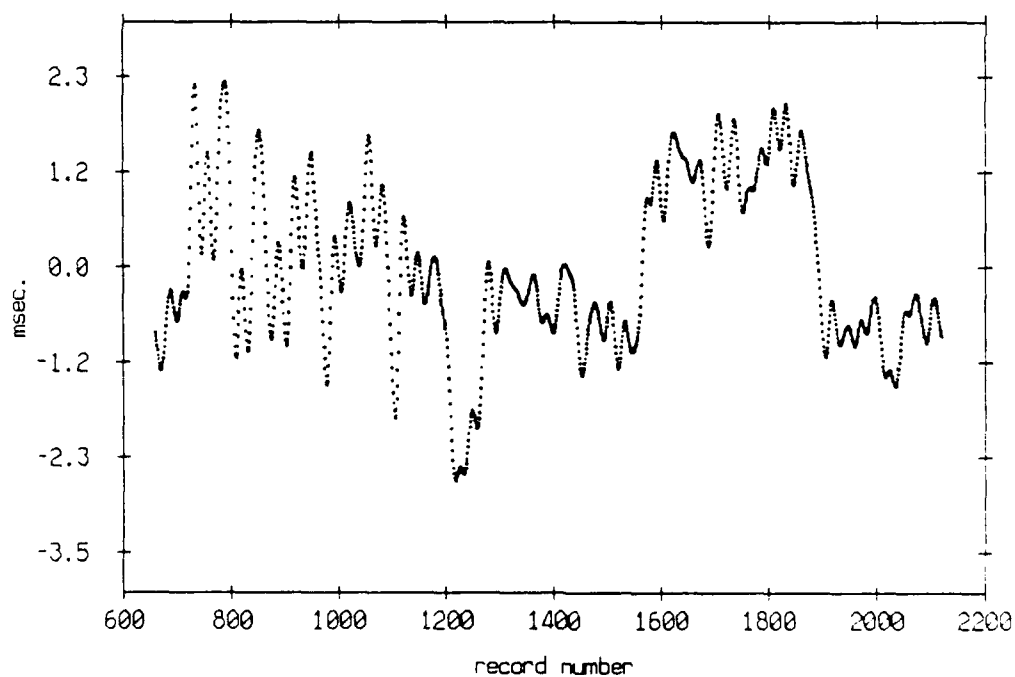
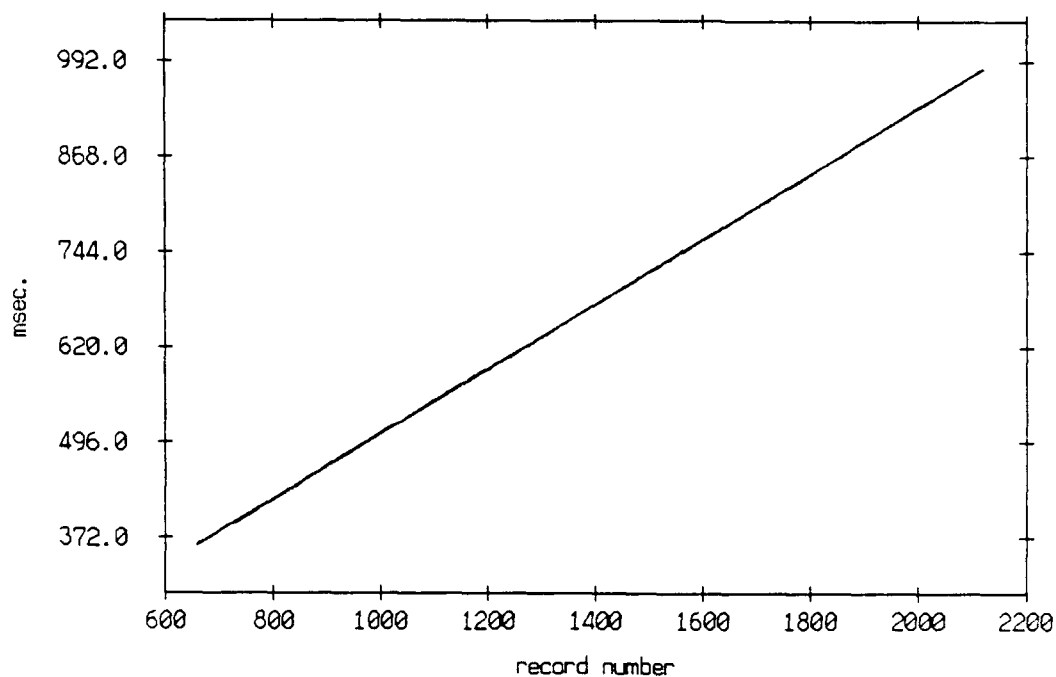


Figure 3.170

Travel time difference, floats 2 and 3, July 1989, and a second order fit, coefficients are, 0.01816 41.85386 and 86.79614



Travel time difference minus second order fit, floats 2 and 3

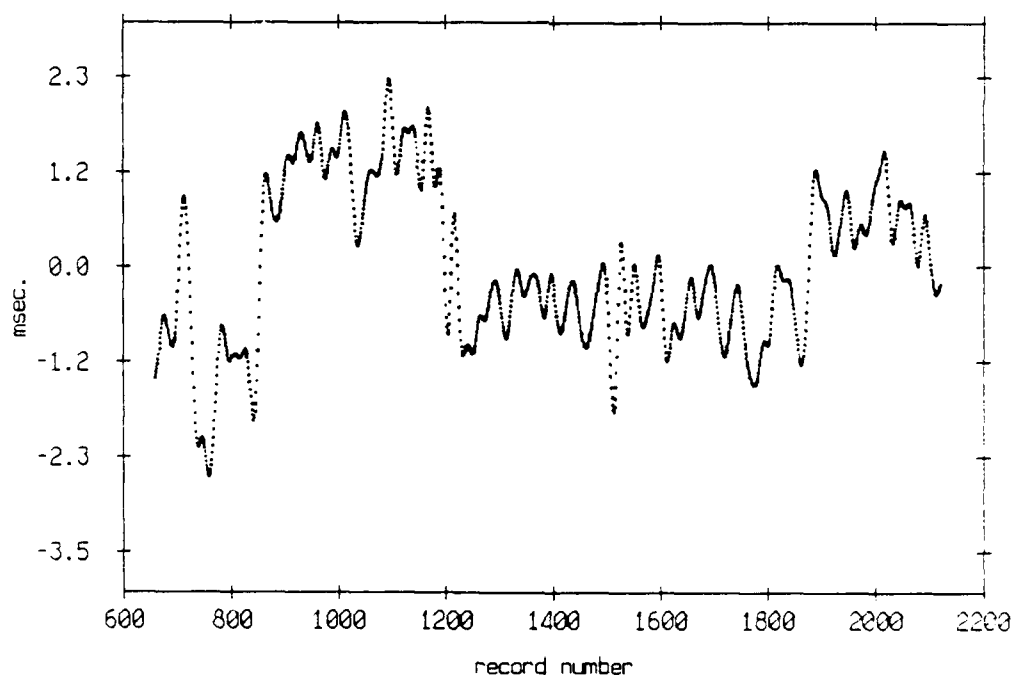
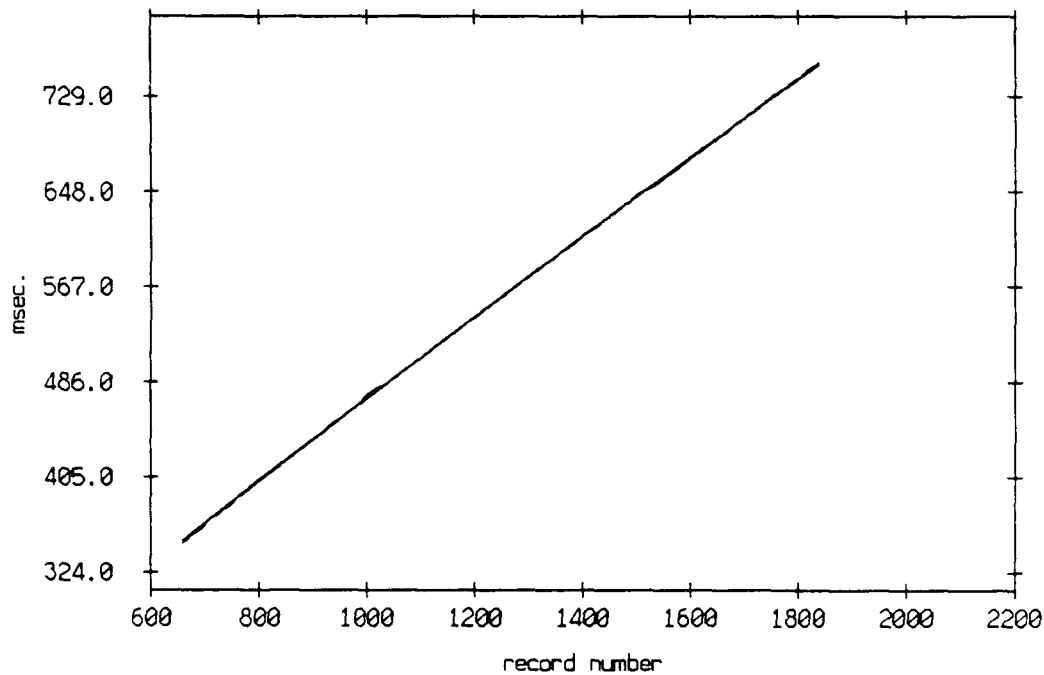


Figure 3.171

Travel time difference, floats 2 and 4, July 1989, and a second order fit, coefficients are, -0.12803 37.56519 and 109.27396



Travel time difference minus second order fit, floats 2 and 4

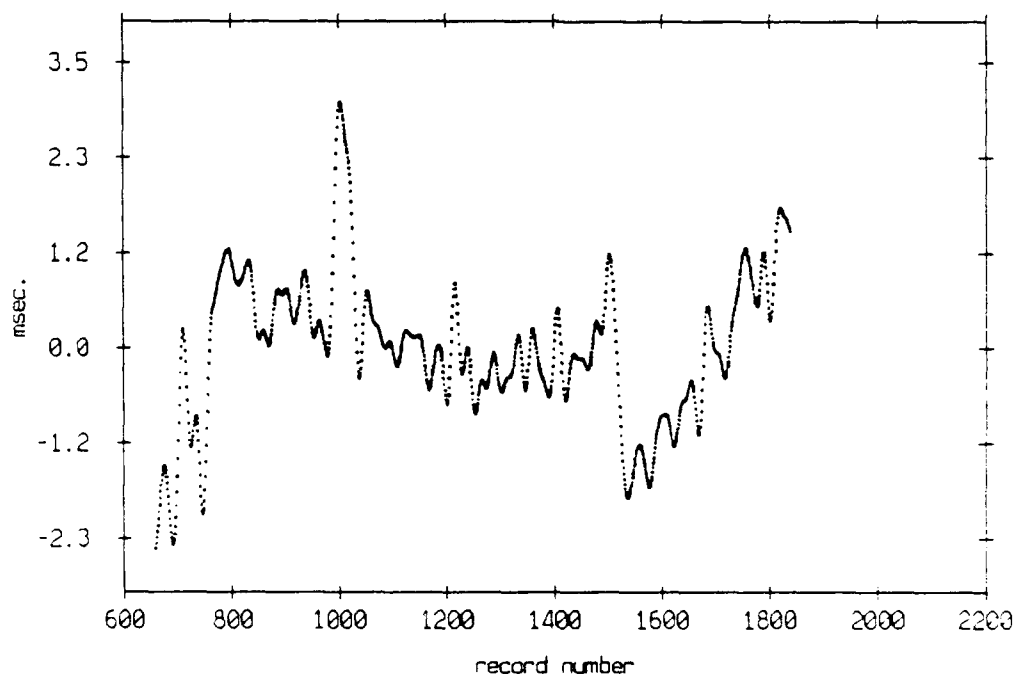
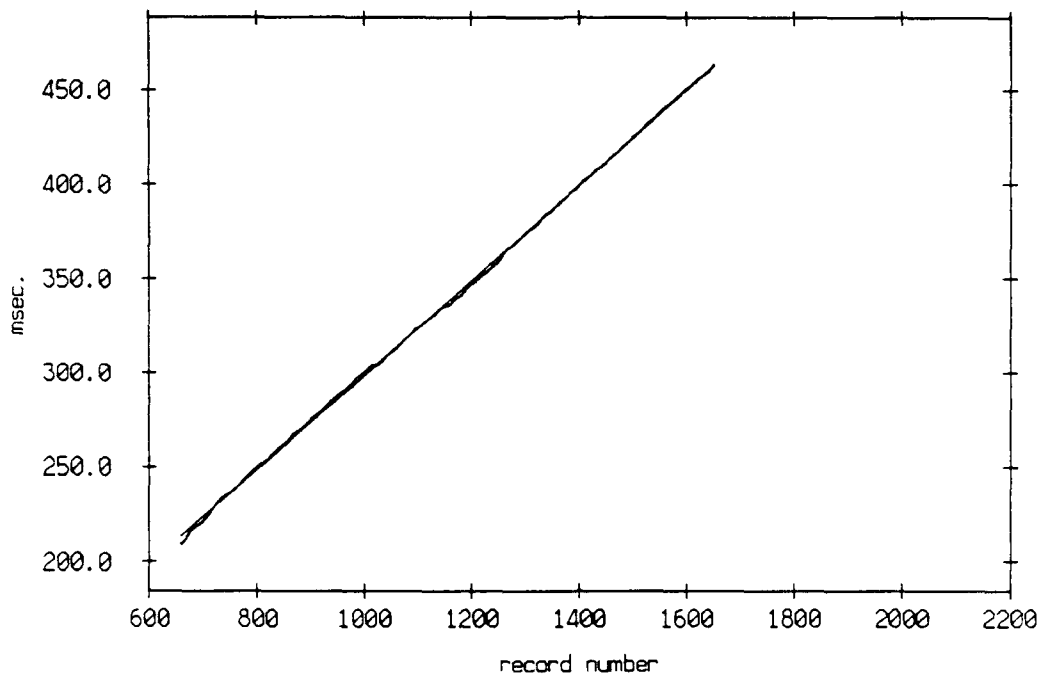


Figure 3.172

Travel time difference, floats 2 and 5, July 1989, and a
second order fit, coefficients are: 0.02849 24.51210 and 50.82257



Travel time difference minus second order fit, floats 2 and 5

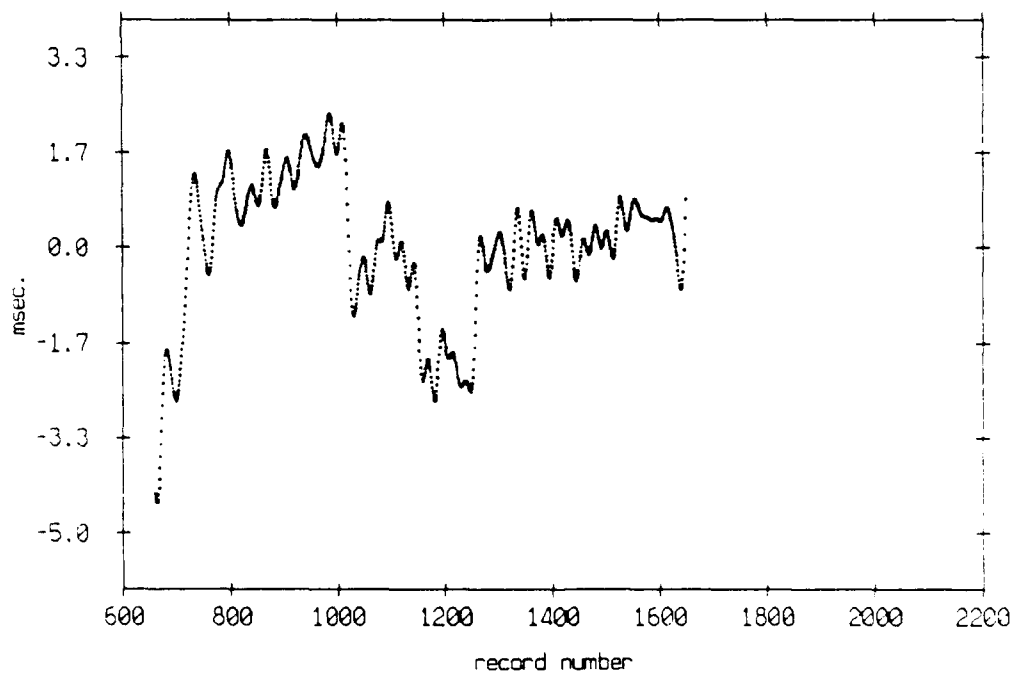


Figure 3.173

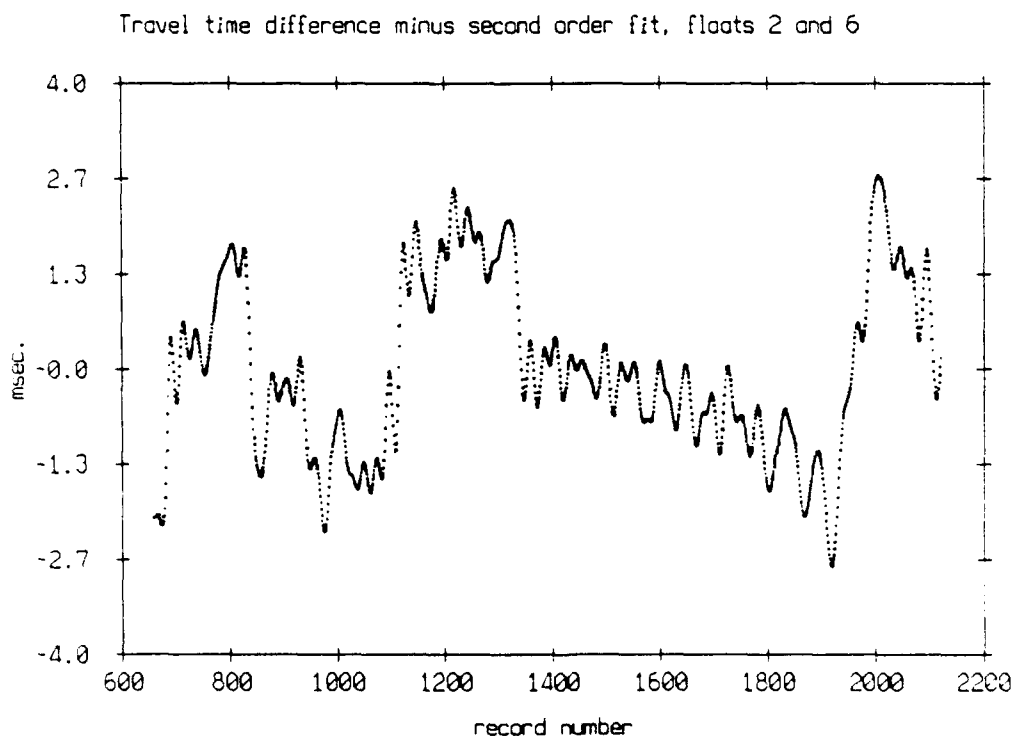
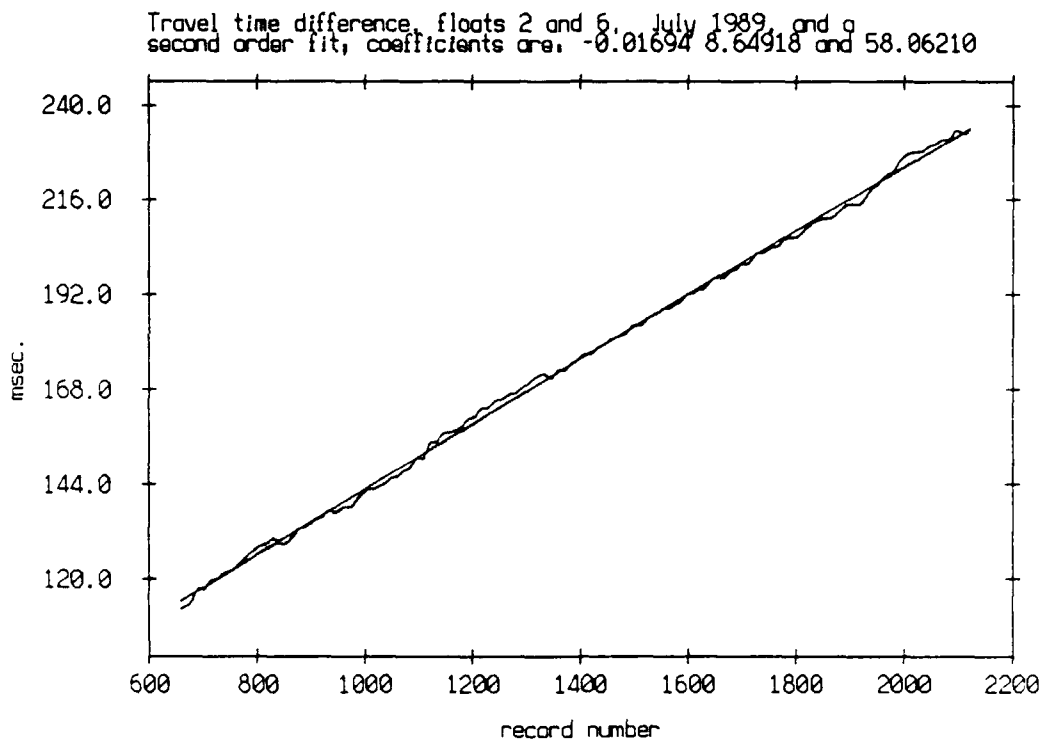
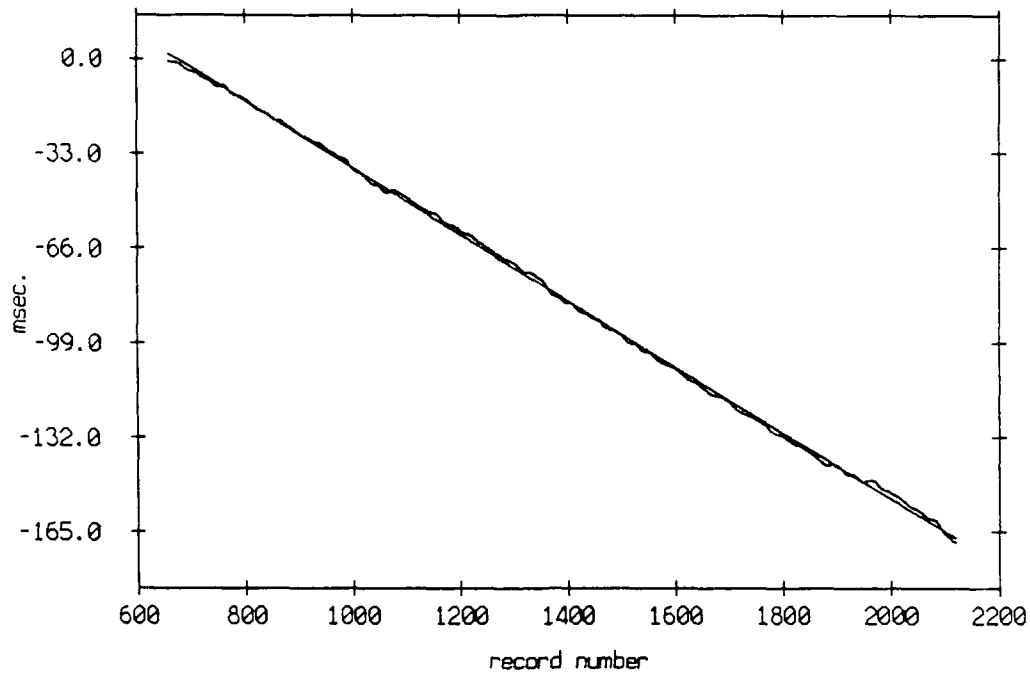


Figure 3.174

Travel time difference, floats 2 and 7, July 1989, and a
second order fit, coefficients are: 0.00913 -11.82151 and 79.21877



Travel time difference minus second order fit, floats 2 and 7

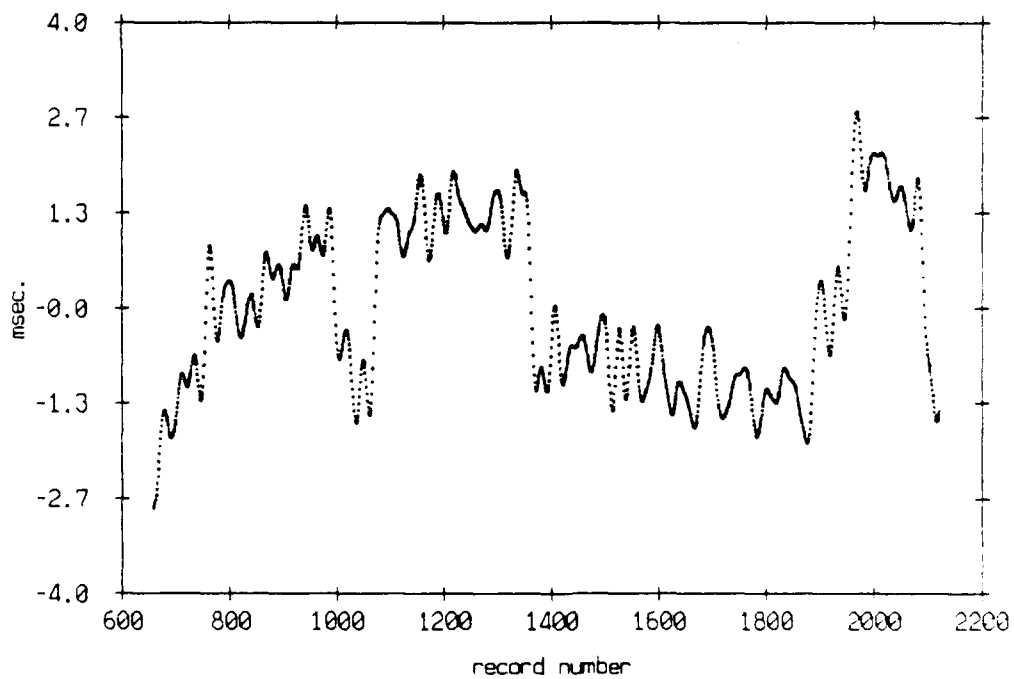


Figure 3.175

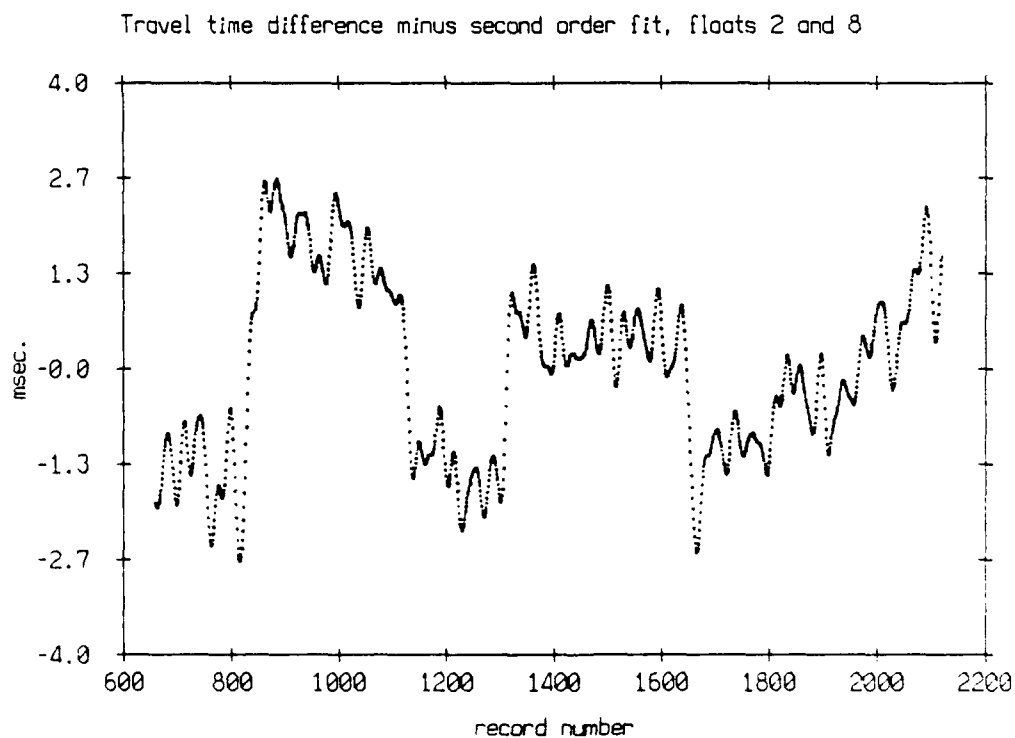
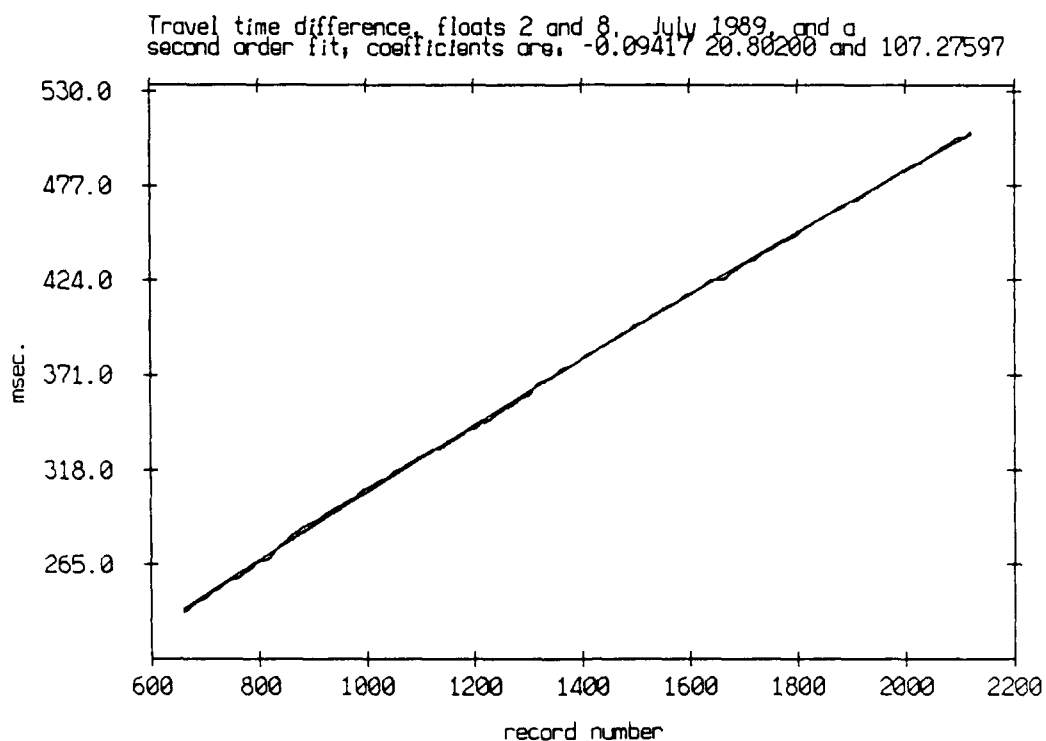
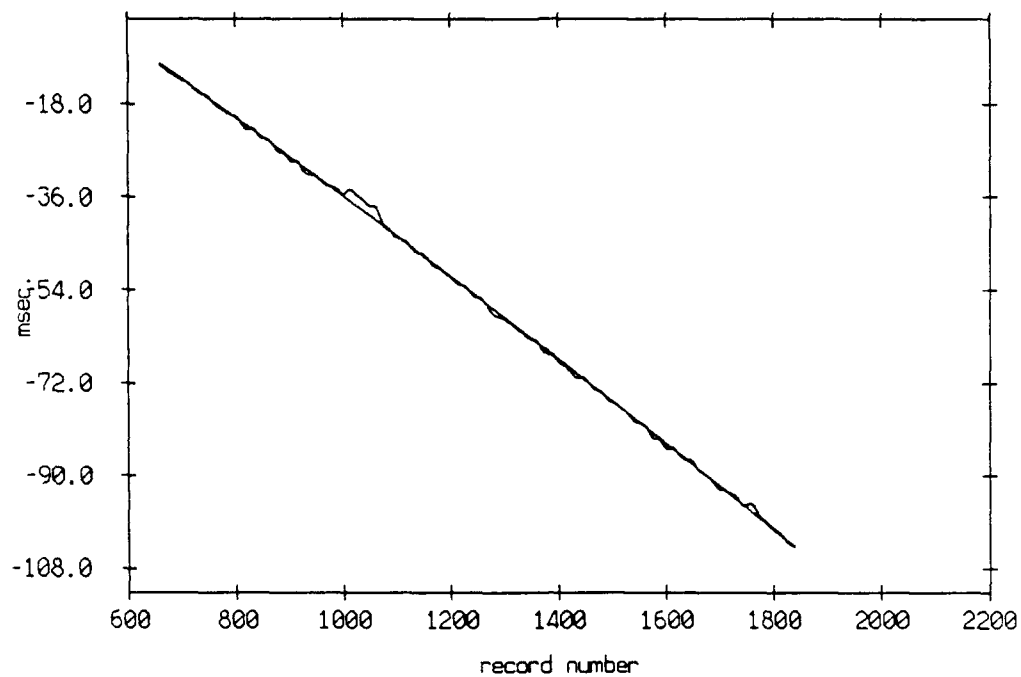


Figure 3.176

Travel time difference, floats 3 and 4, July 1989, and a second order fit, coefficients are, -0.04826 -6.73761 and 36.29120



Travel time difference minus second order fit, floats 3 and 4

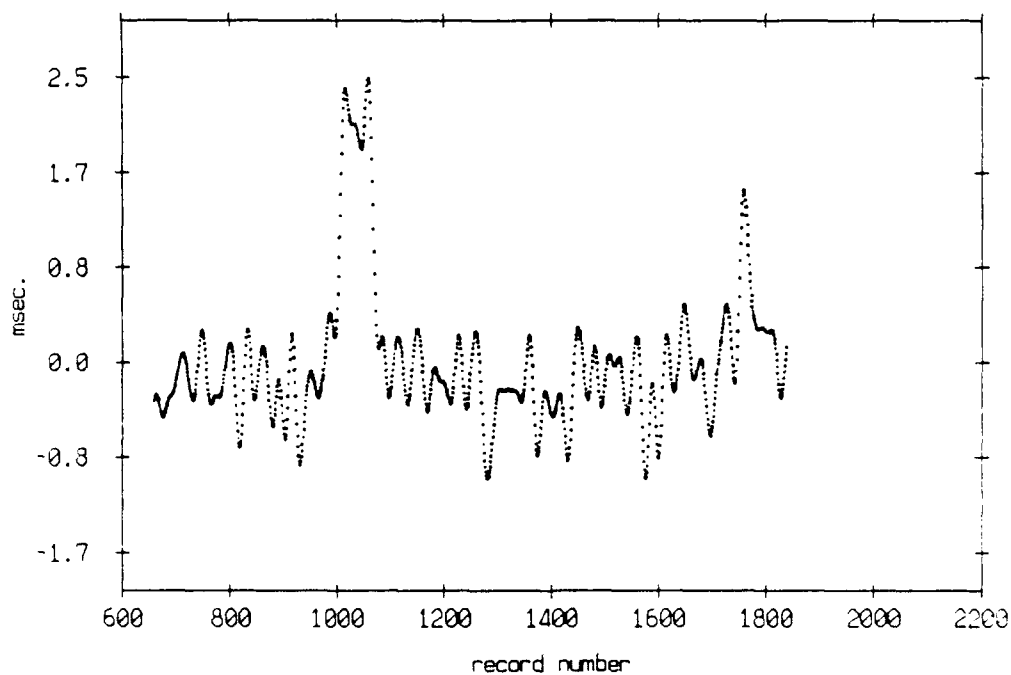


Figure 3.177

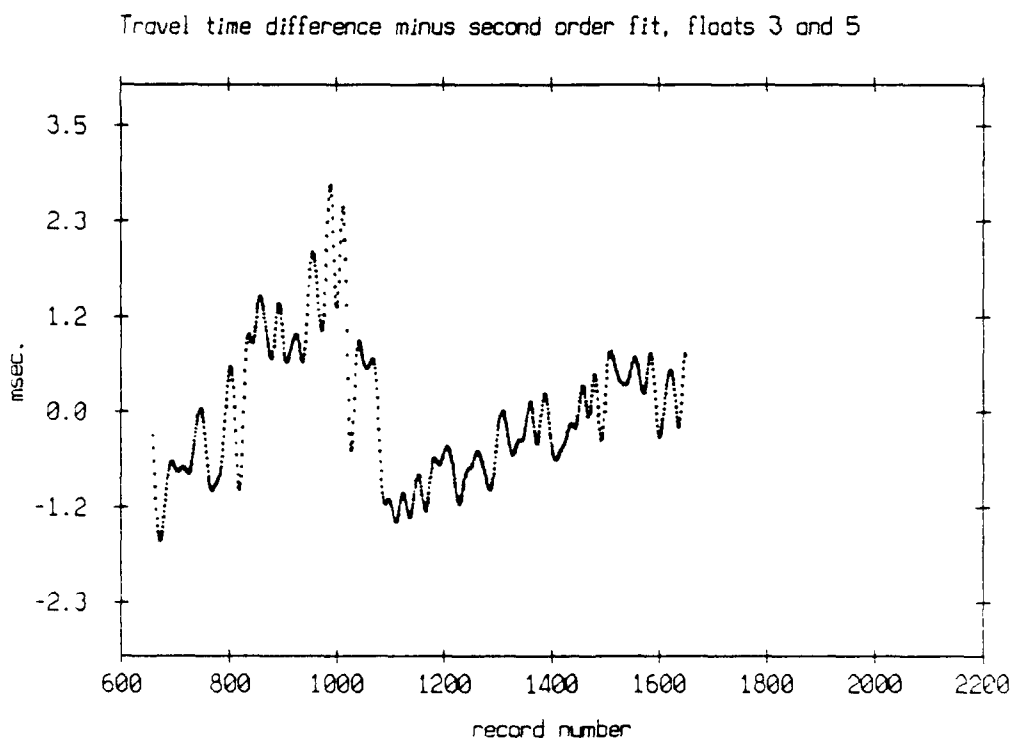
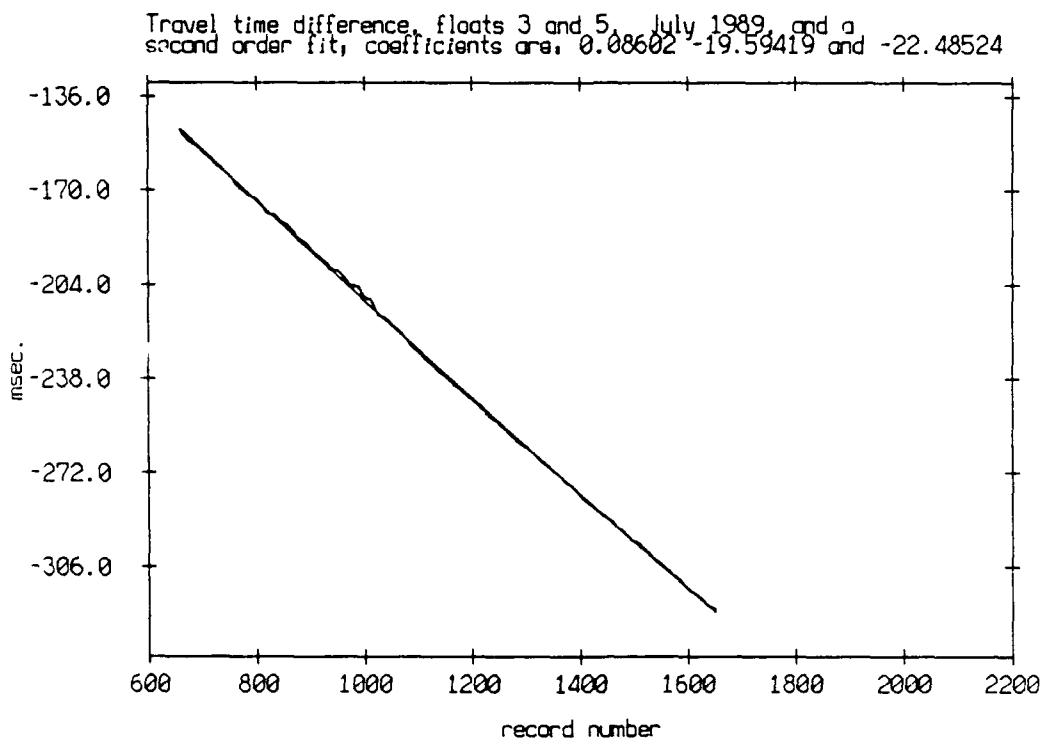


Figure 3.178

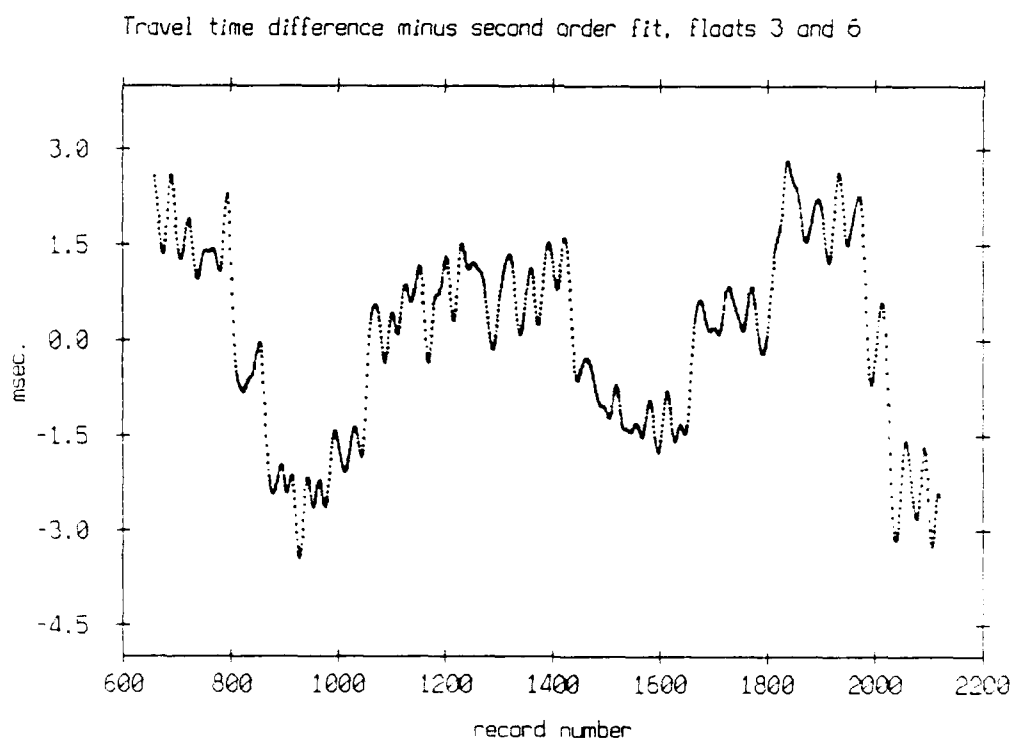
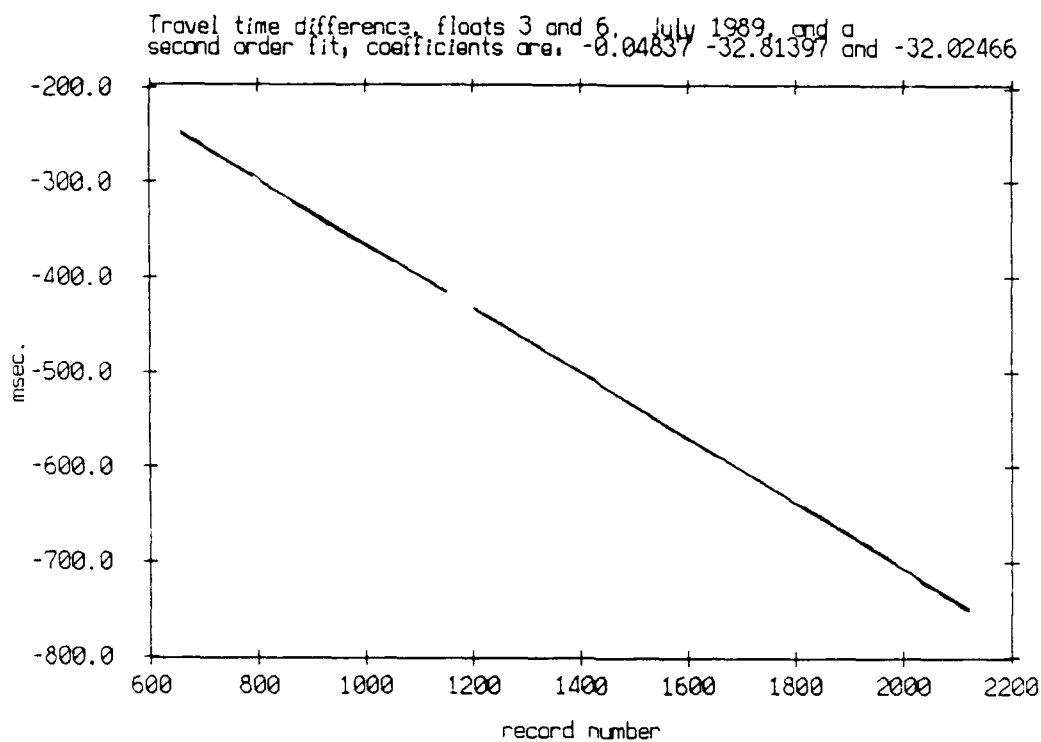


Figure 3.179

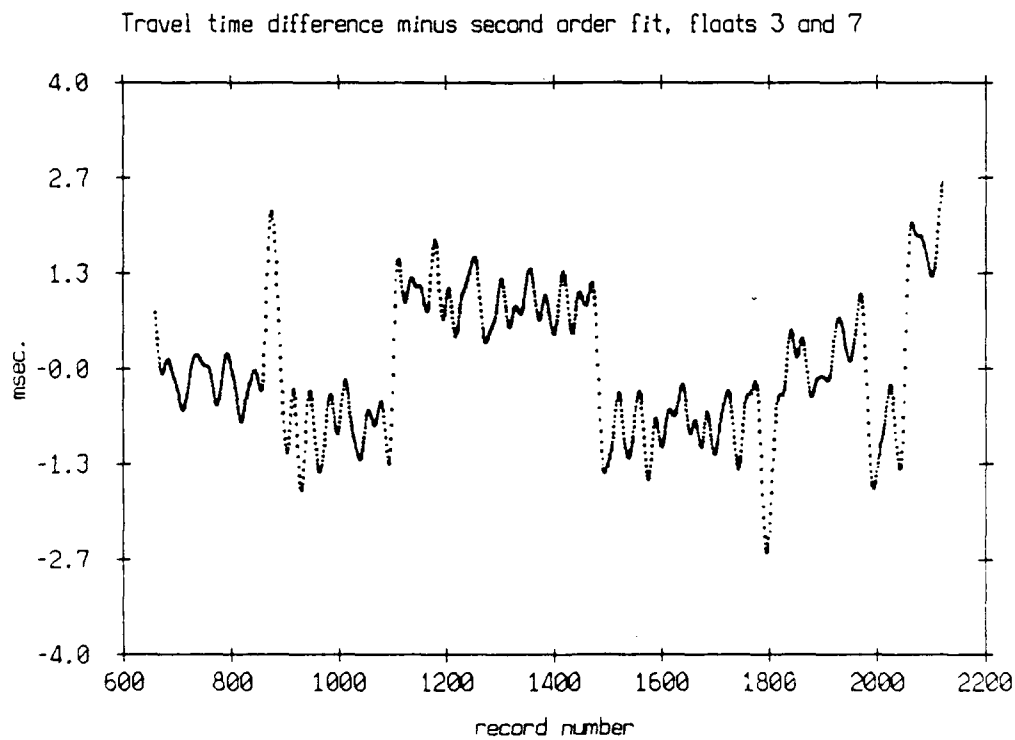
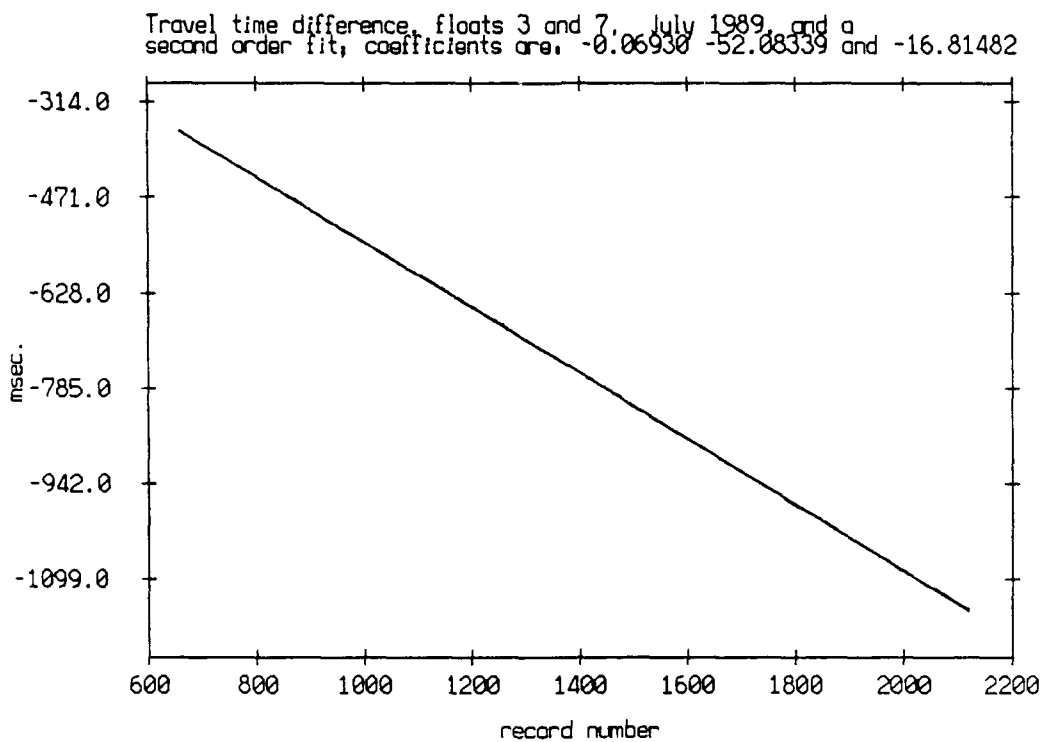
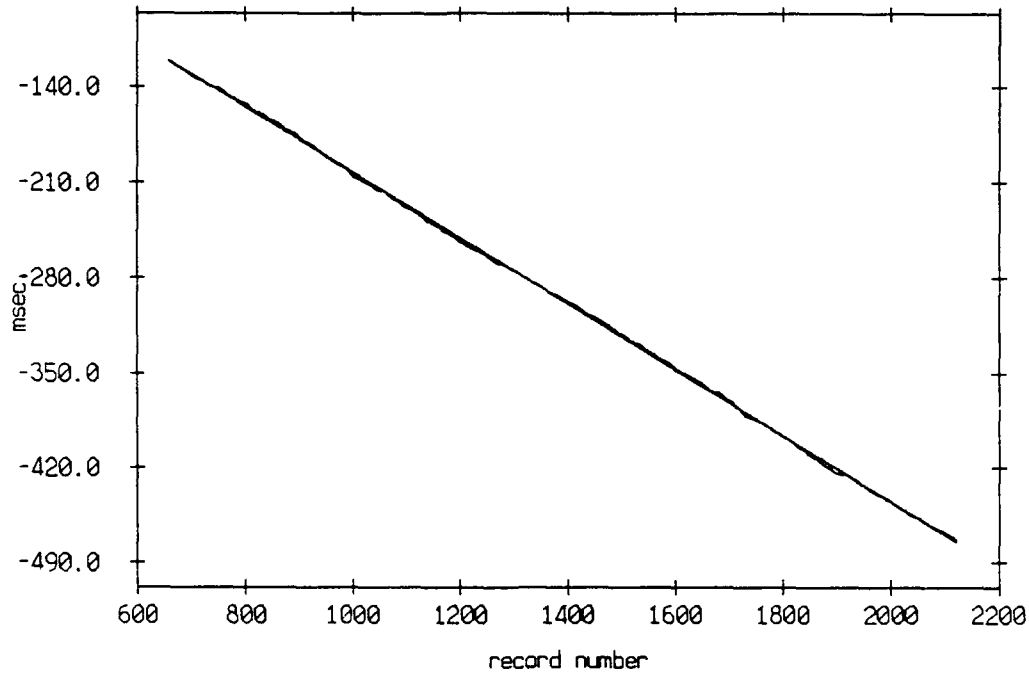


Figure 3.180

Travel time difference, floats 3 and 8, July 1989, and a second order fit, coefficients are, -0.02307 -23.57817 and 35.45761



Travel time difference minus second order fit, floats 3 and 8

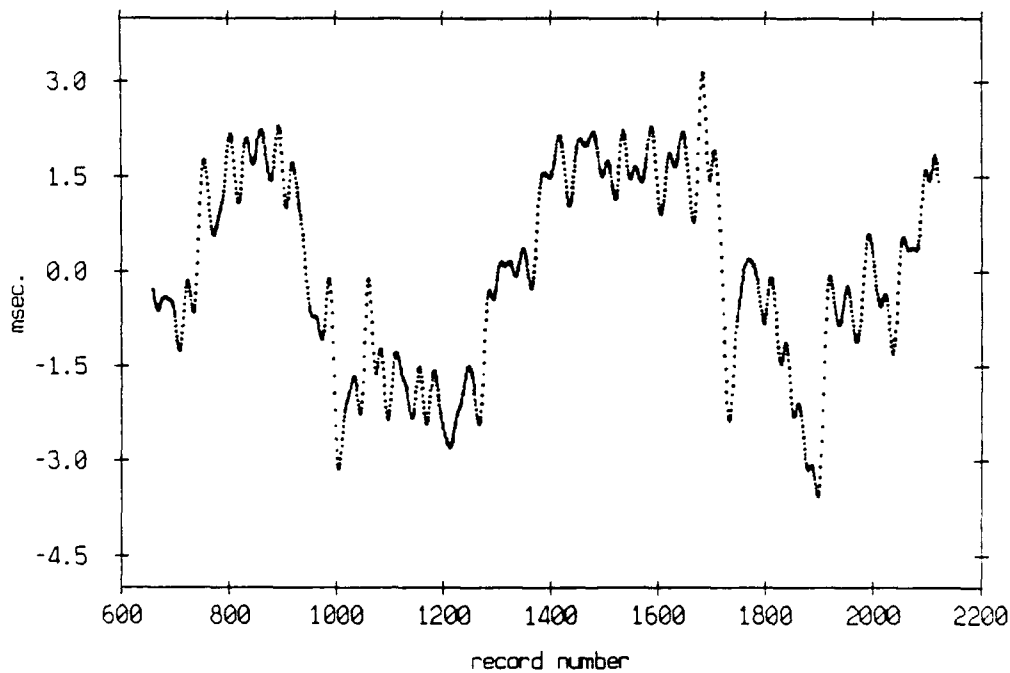
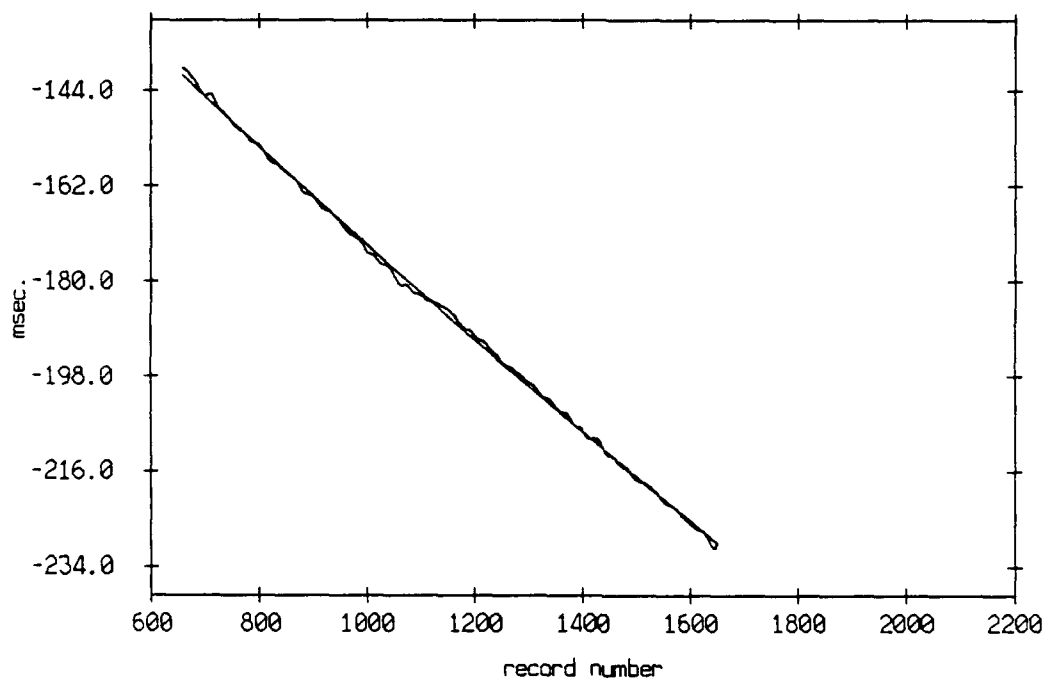


Figure 3.181

Travel time difference, floats 4 and 5, July 1989, and a second order fit, coefficients are, 0.07278 -10.60359 and -74.41269



Travel time difference minus second order fit, floats 4 and 5

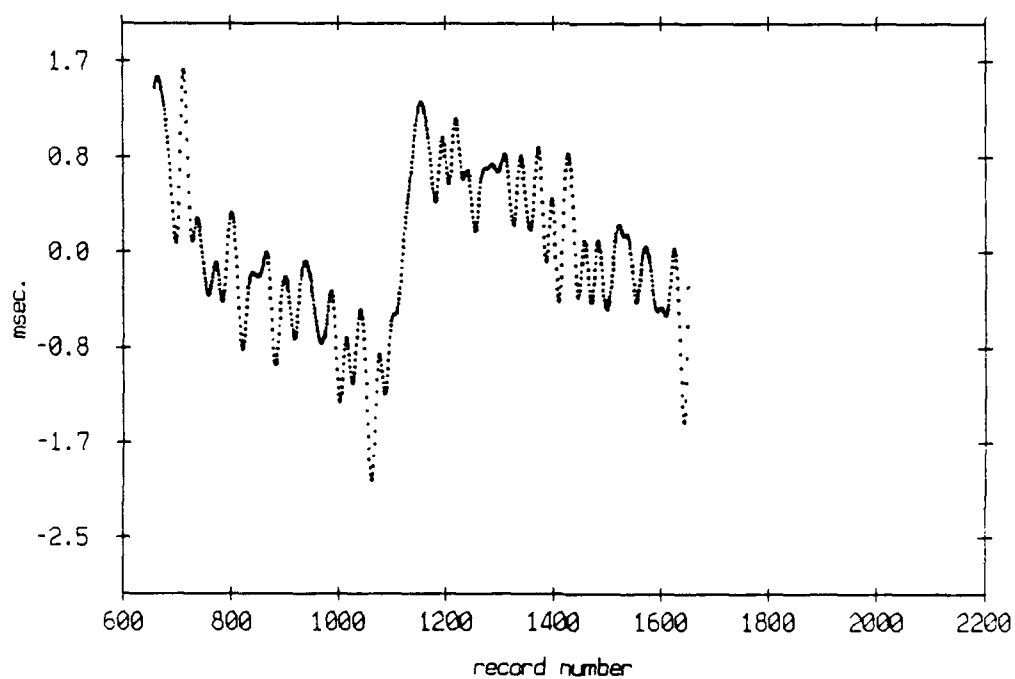
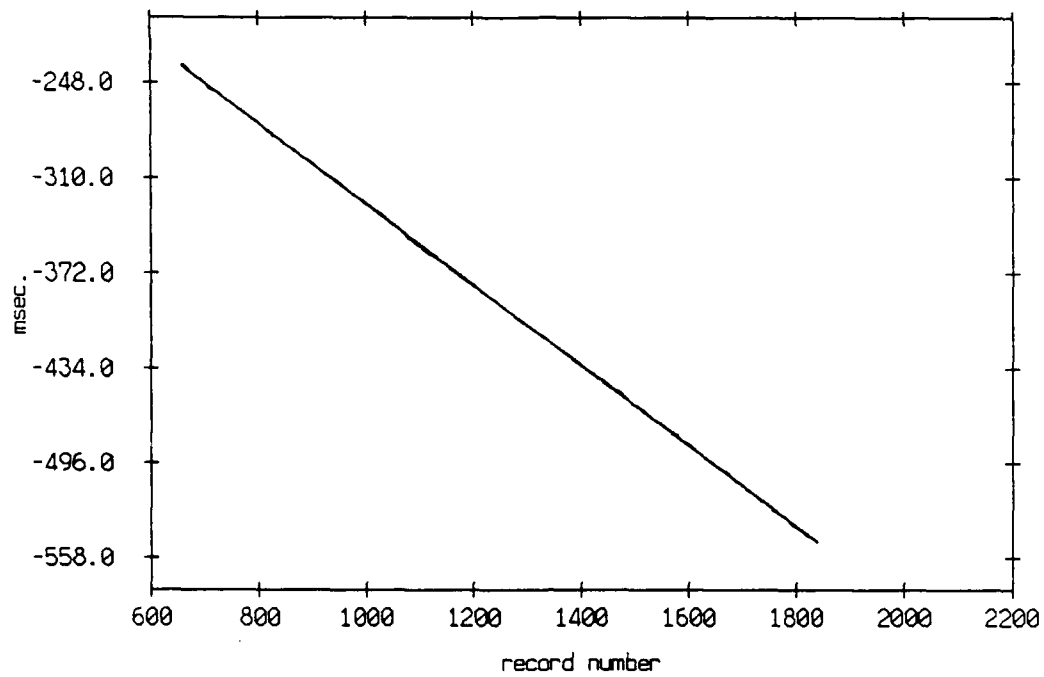


Figure 3.182

Travel time difference, floats 4 and 6, July 1989, and a second order fit, coefficients are, (none) -26.25876 and -64.93631



Travel time difference minus second order fit, floats 4 and 6

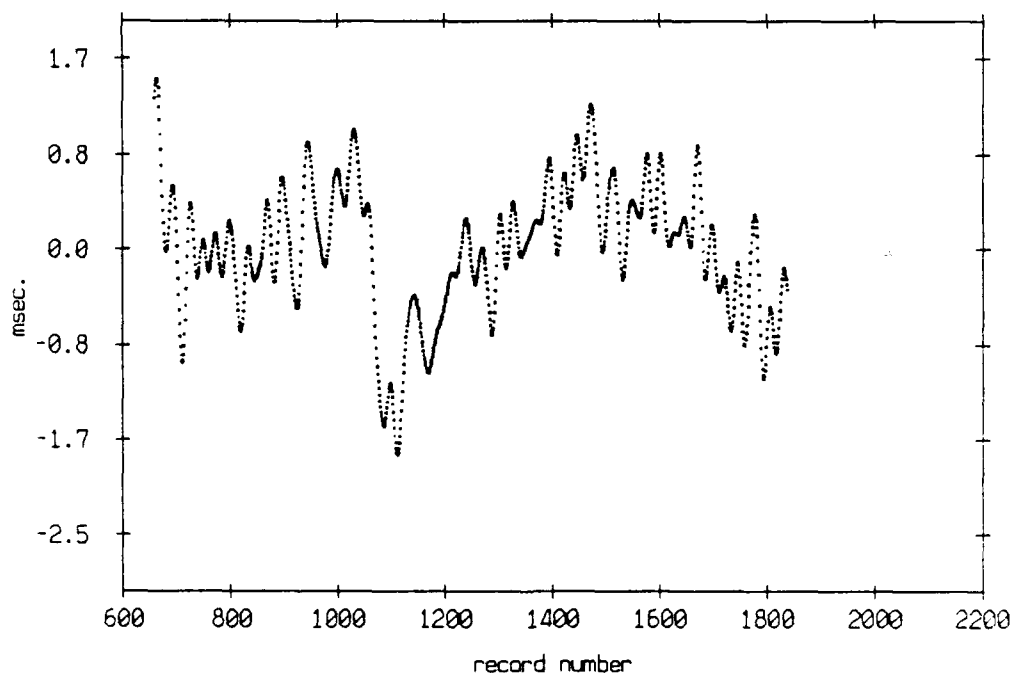
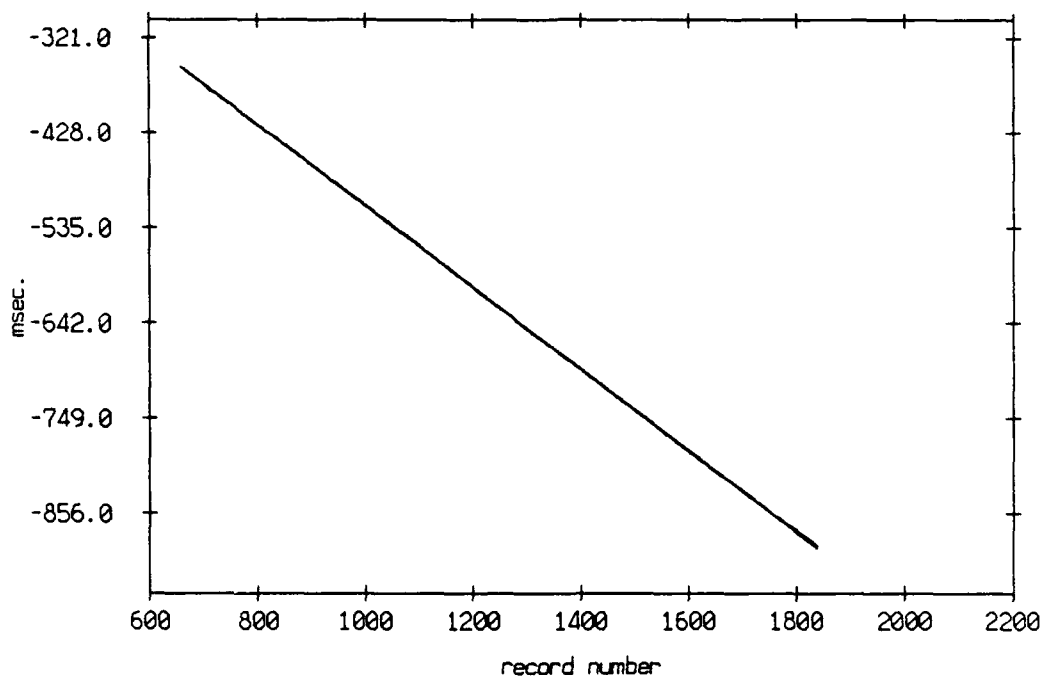


Figure 3.183

Travel time difference, floats 4 and 7, July 1989, and a
second order fit, coefficients are: (none) -45.90385 and -51.37494



Travel time difference minus second order fit, floats 4 and 7

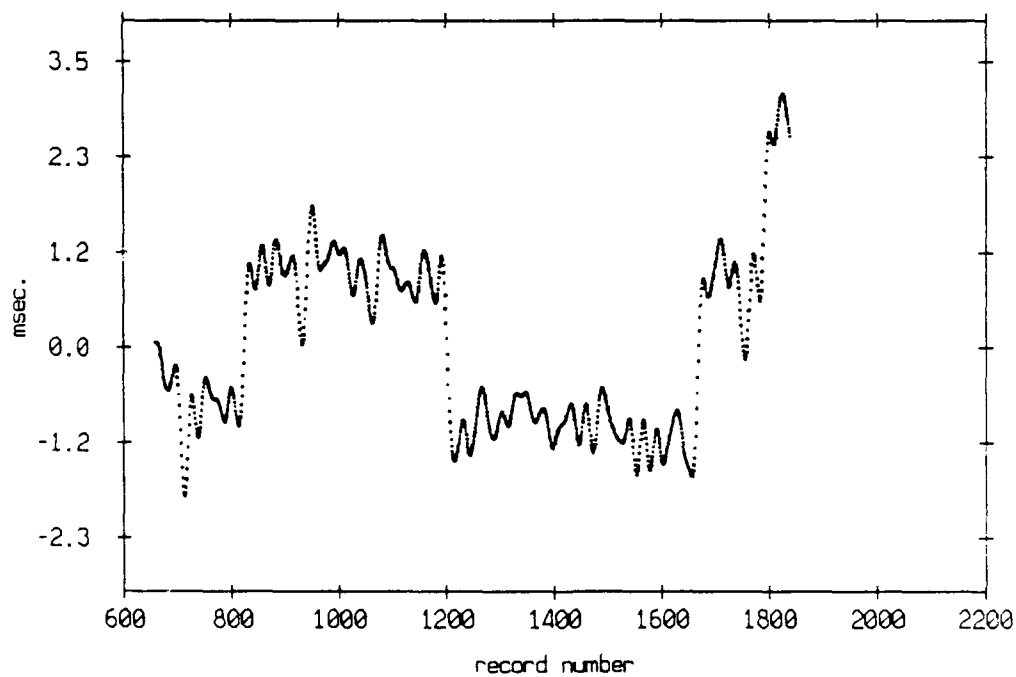
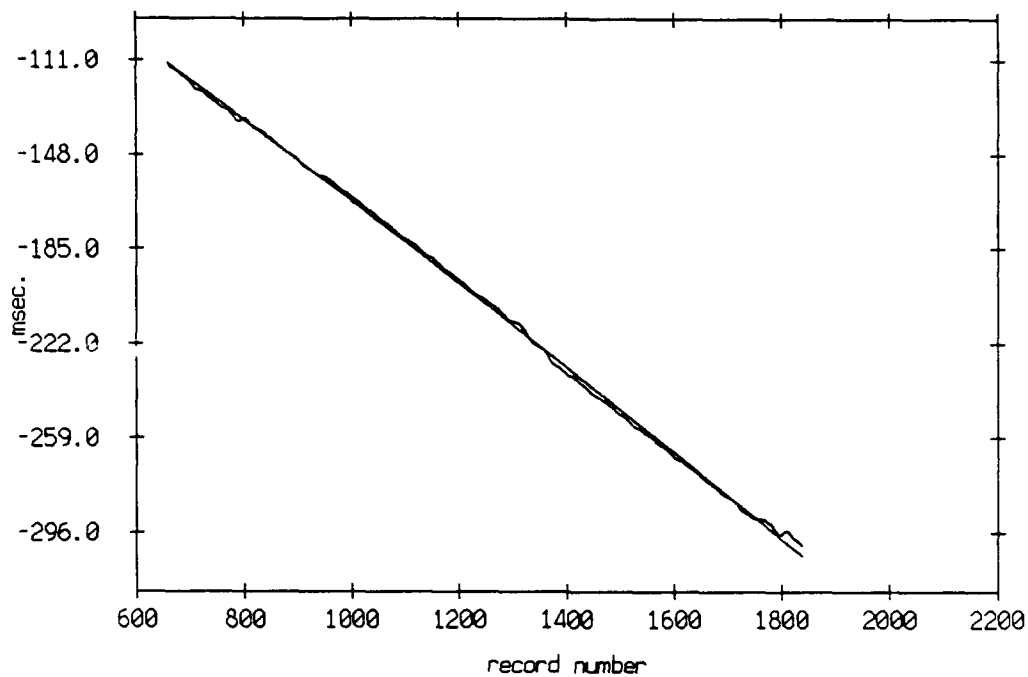


Figure 3.184

Travel time difference, floats 4 and 8, July 1989, and a second order fit, coefficients are: -0.06807 -14.64013 and -13.09142



Travel time difference minus second order fit, floats 4 and 8

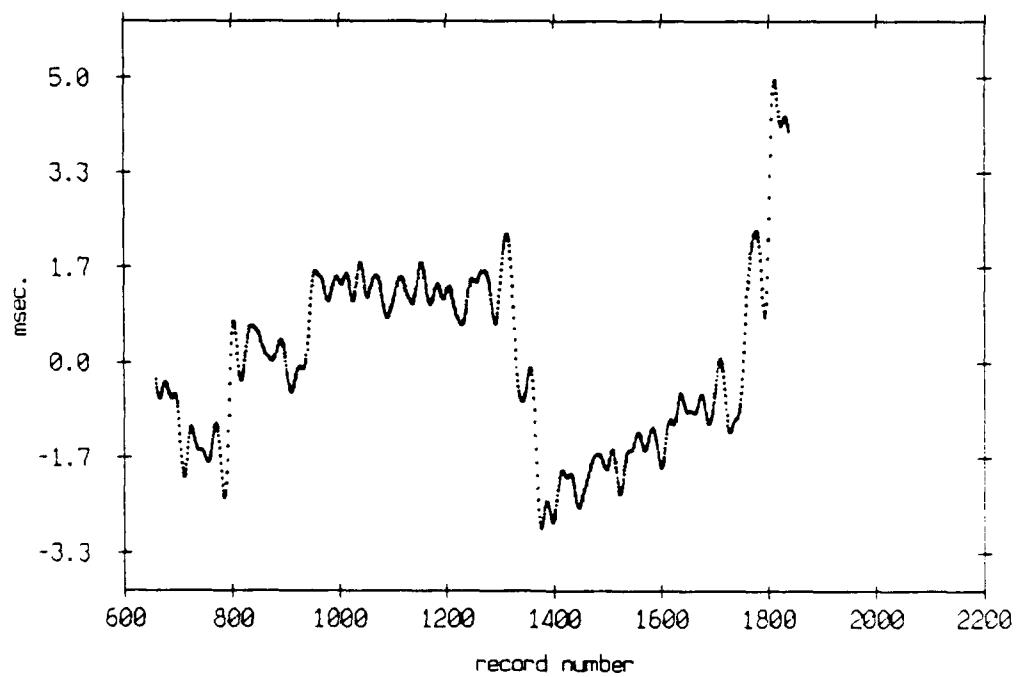
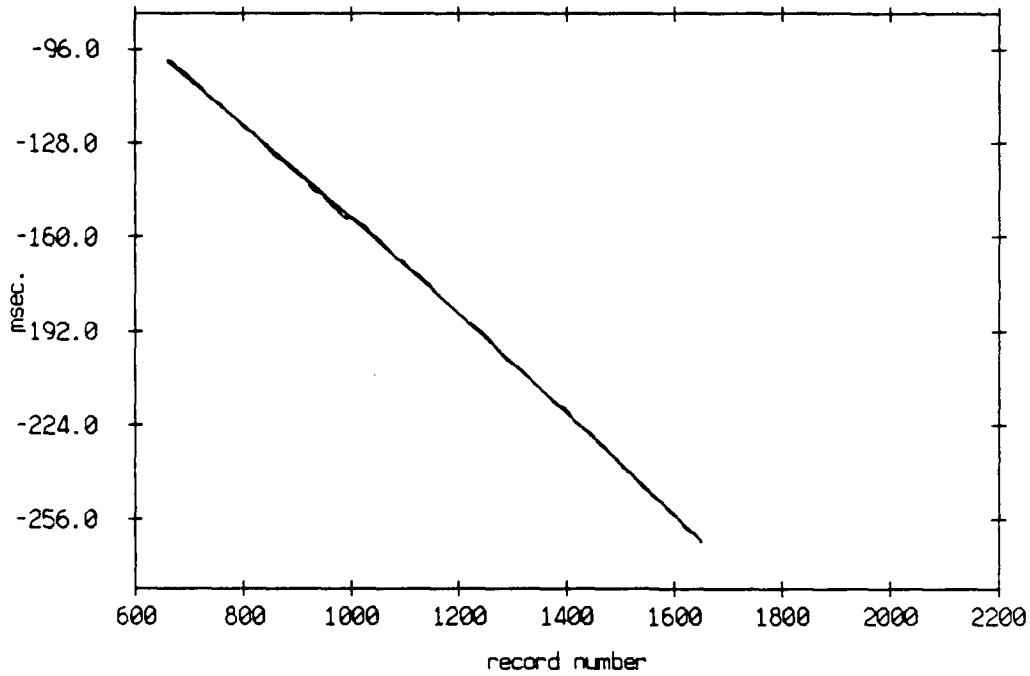


Figure 3.185

Travel time difference, floats 5 and 6, July 1989, and a second order fit, coefficients are, -0.12665 -13.52716 and -5.83221



Travel time difference minus second order fit, floats 5 and 6

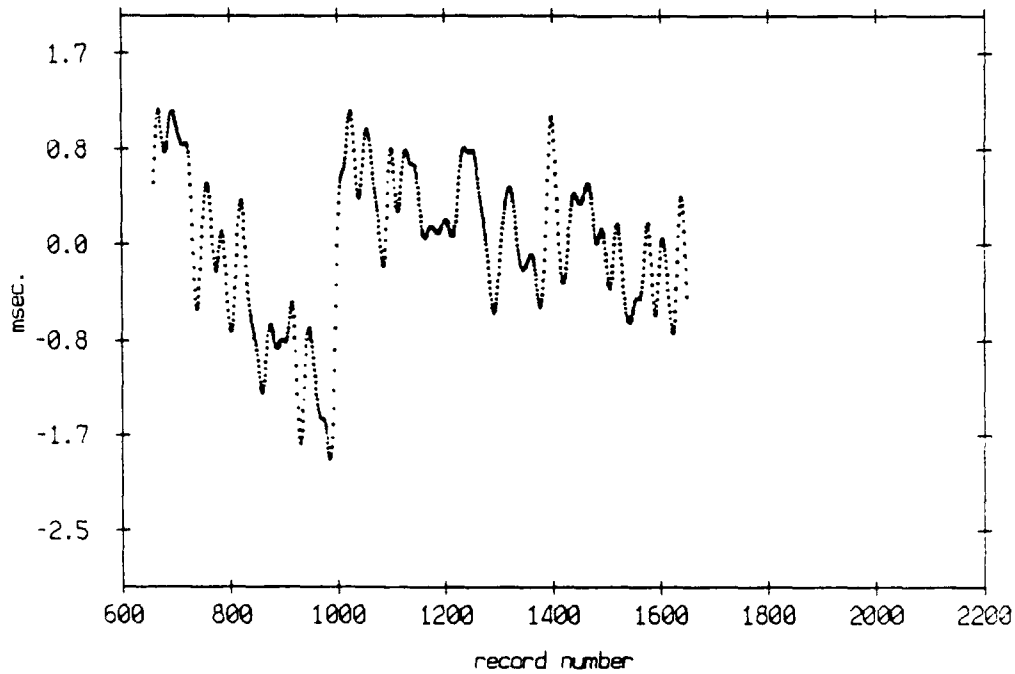
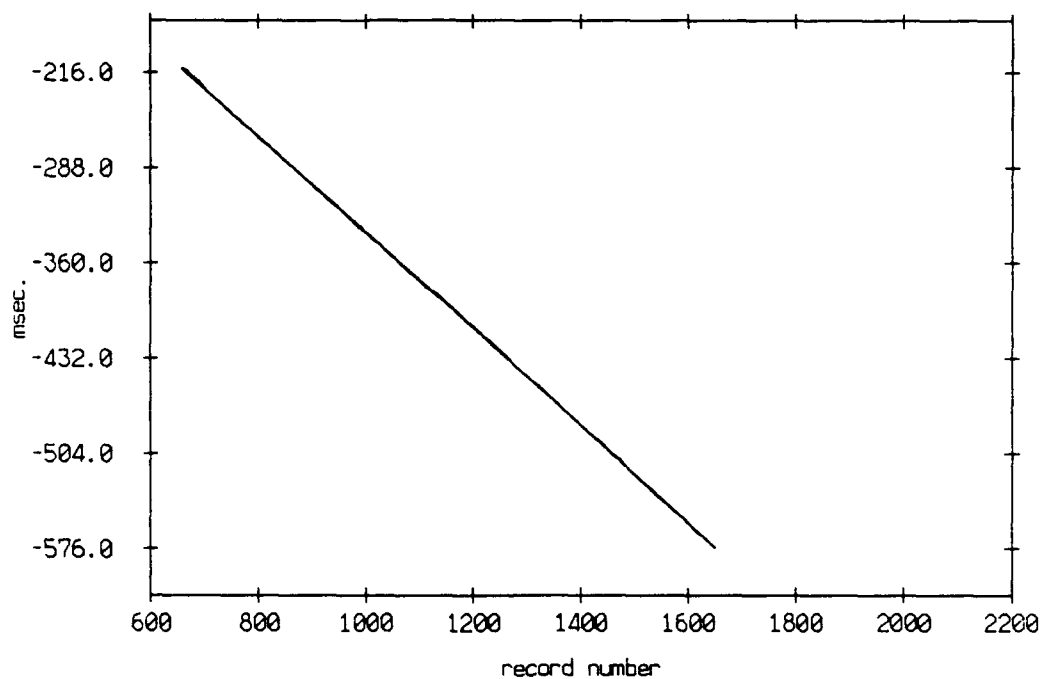


Figure 3.186

Travel time difference, floats 5 and 7, July 1989, and a
second order fit, coefficients are, -0.05768 -35.12783 and 20.22412



Travel time difference minus second order fit, floats 5 and 7

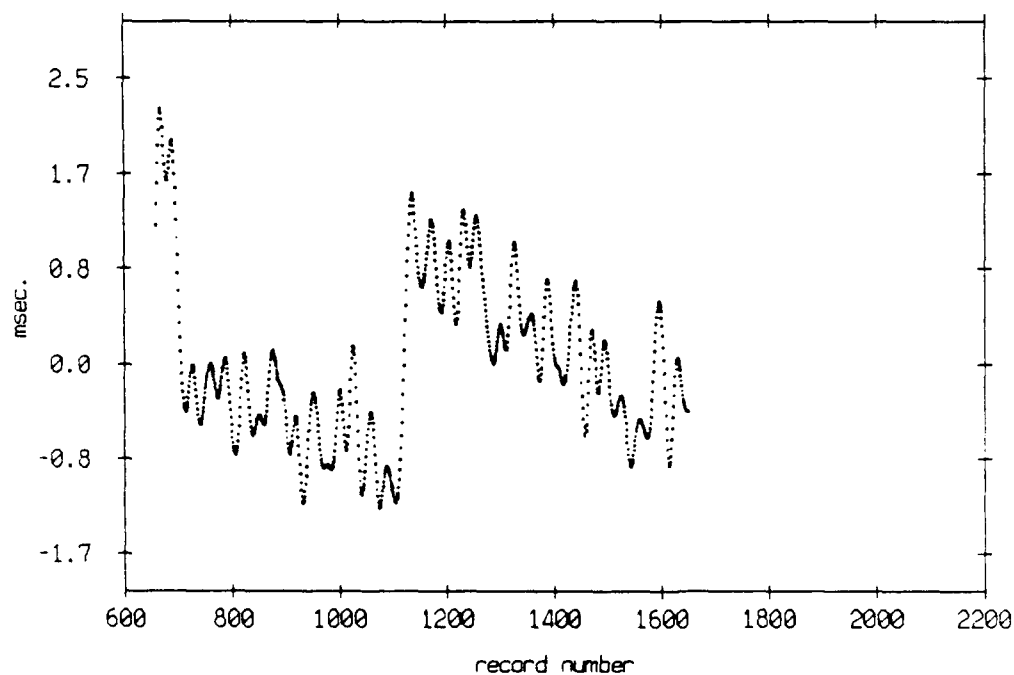
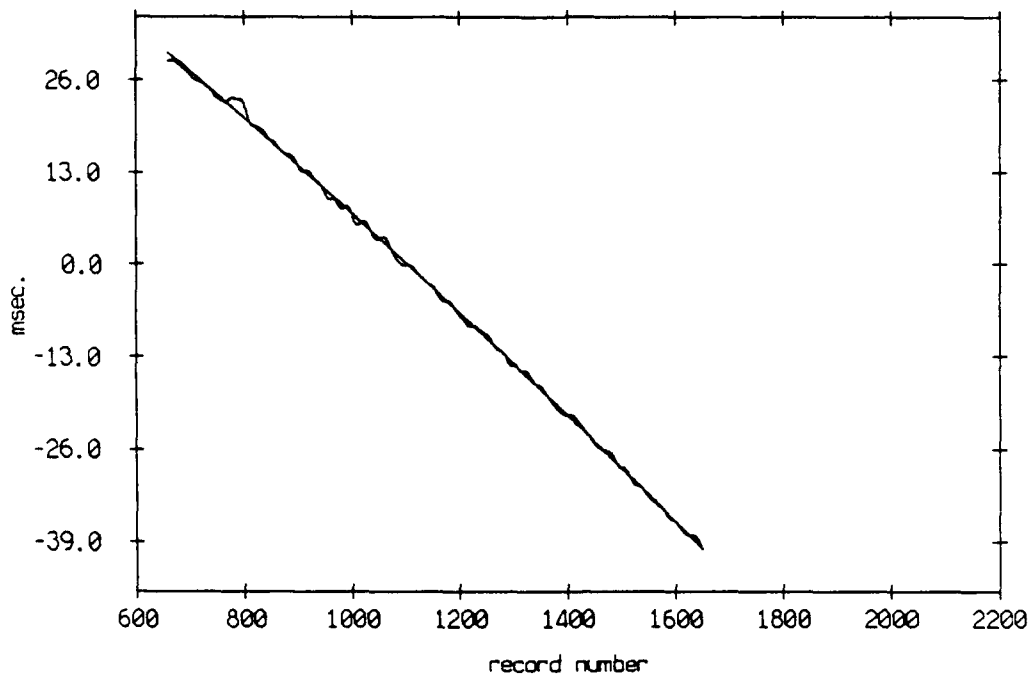


Figure 3.187

Travel time difference, floats 5 and 8, July 1989, and a
second order fit, coefficients are, -0.05973 -5.68480 and 69.97832



Travel time difference minus second order fit, floats 5 and 8

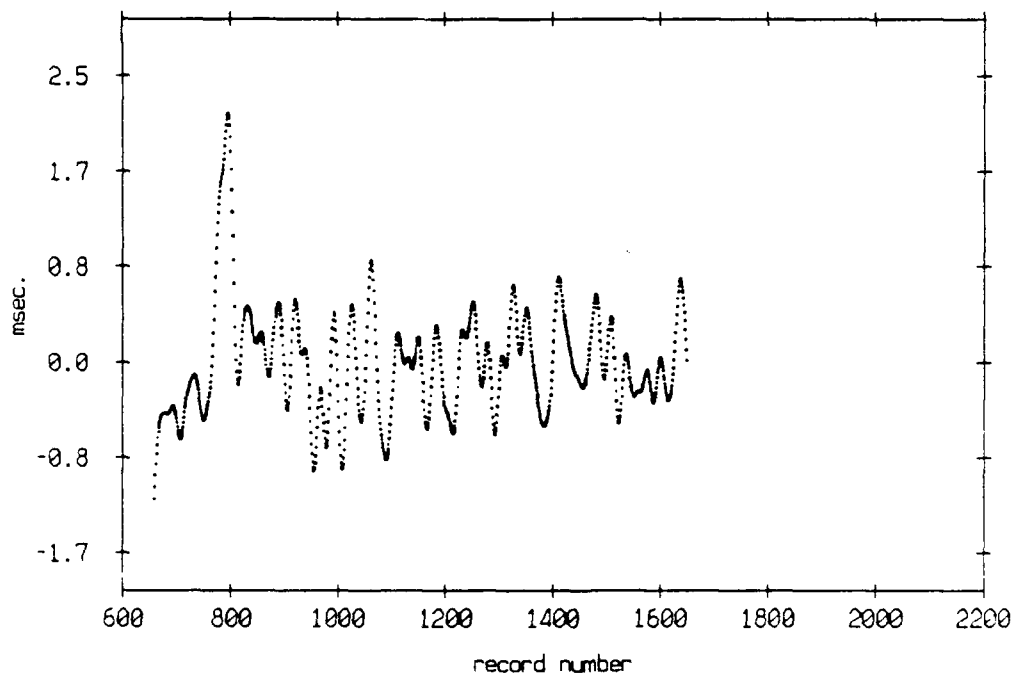
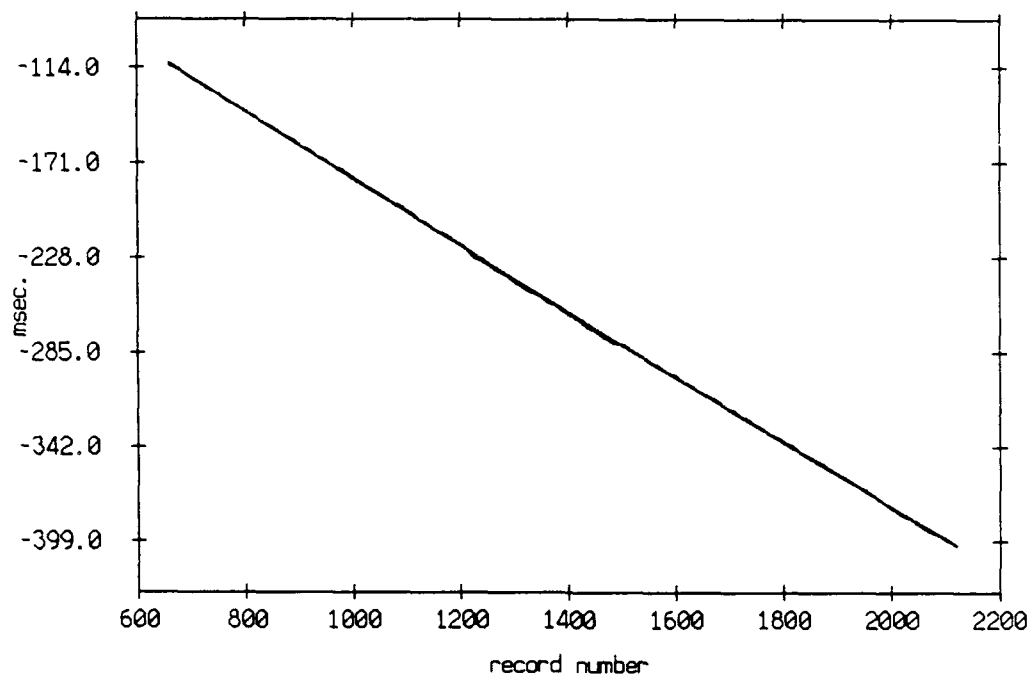


Figure 3.188

Travel time difference, floats 6 and 7, July 1989, and a second order fit, coefficients are: 0.05221 -21.31087 and 26.96481



Travel time difference minus second order fit, floats 6 and 7

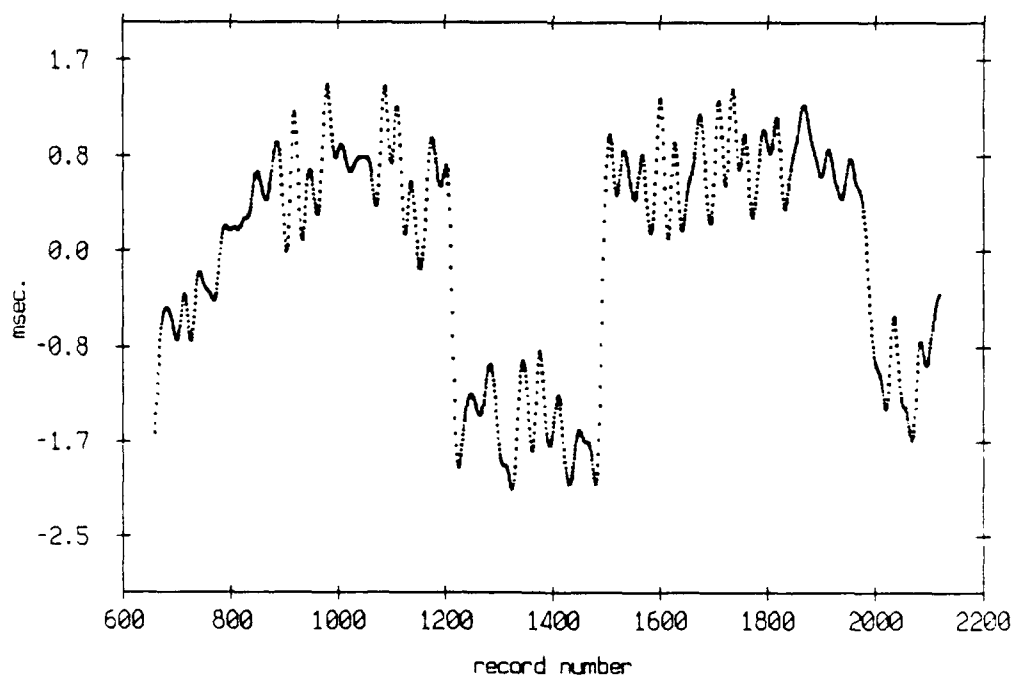
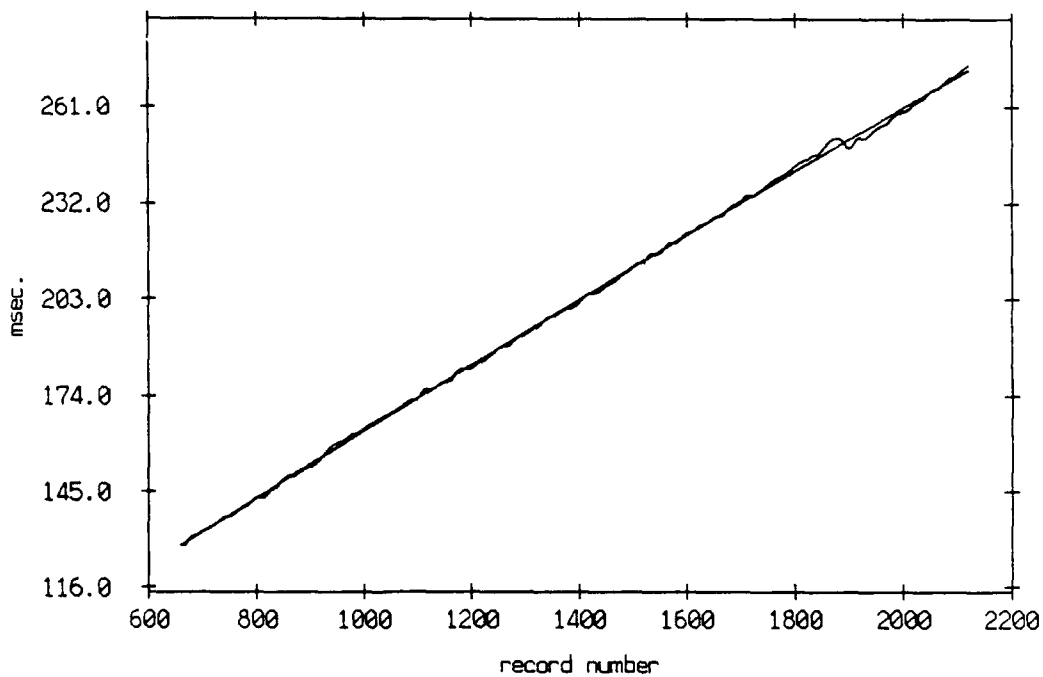


Figure 3.189

Travel time difference, floats 6 and 8, July 1969, and a second order fit, coefficients are: -0.03280 10.73389 and 59.33090



Travel time difference minus second order fit, floats 6 and 8

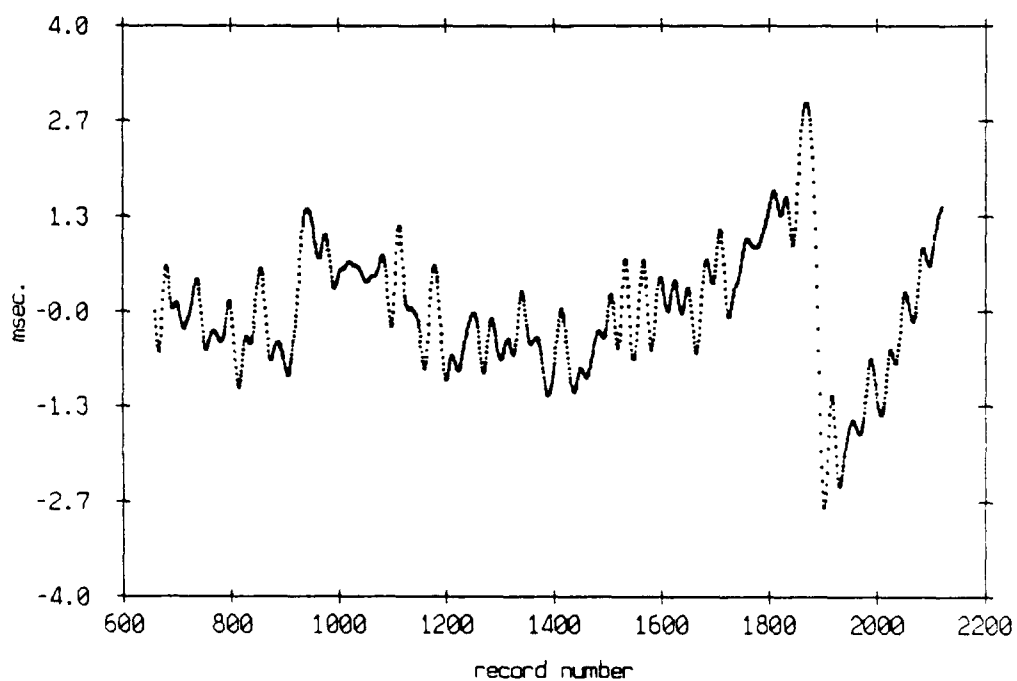
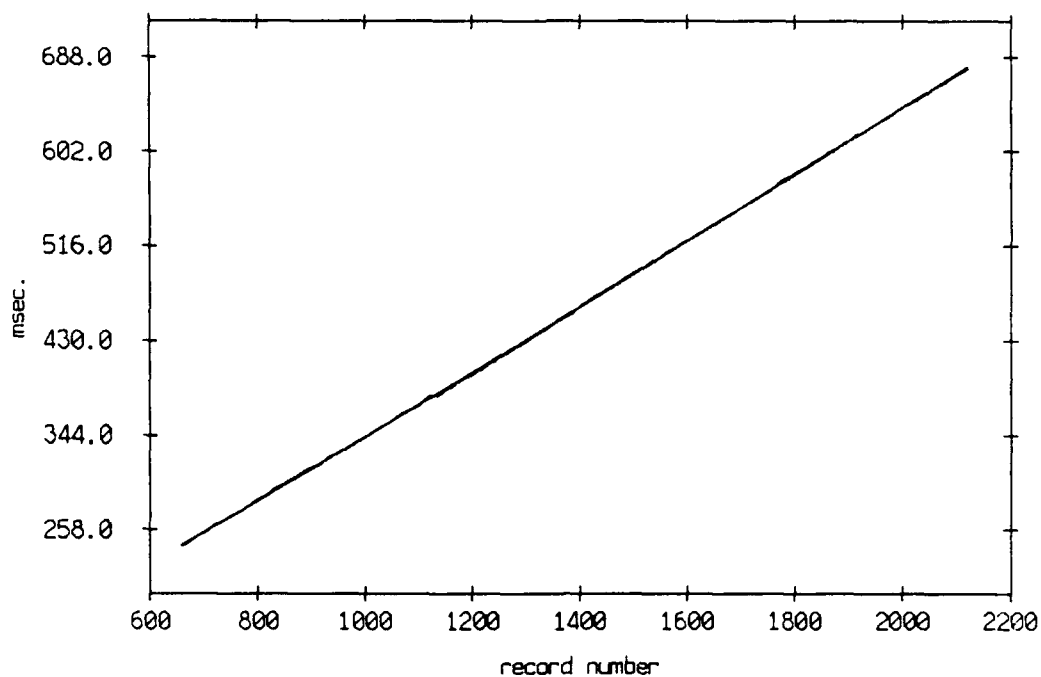


Figure 3.190

Travel time difference, floats 7 and 8, July 1989, and a second order fit, coefficients are: 0.07448 27.69873 and 58.11115



Travel time difference minus second order fit, floats 7 and 8

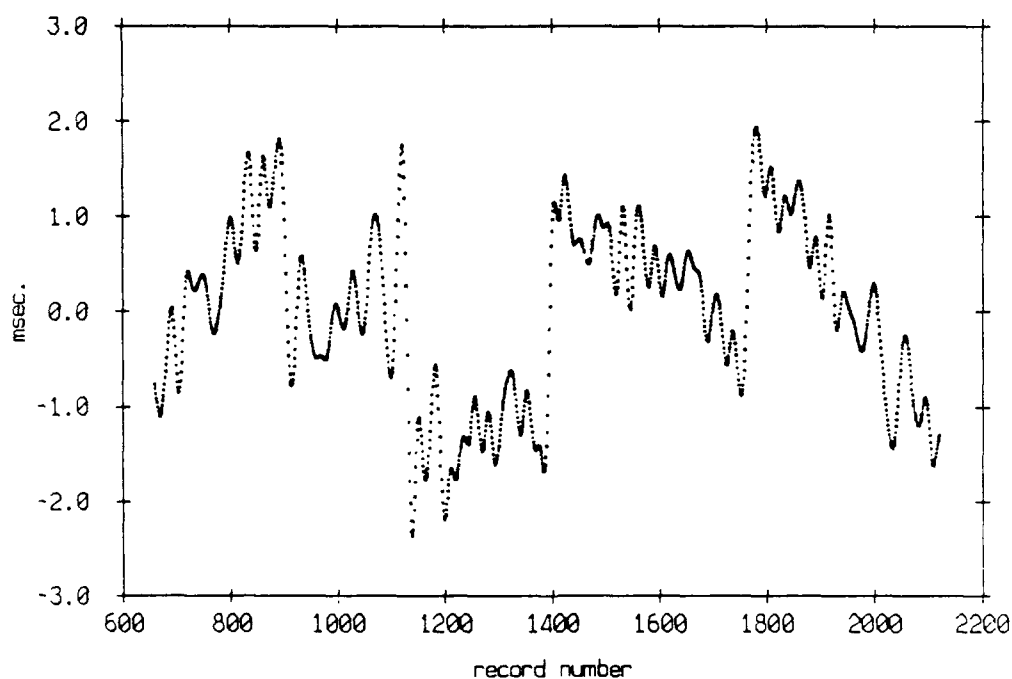
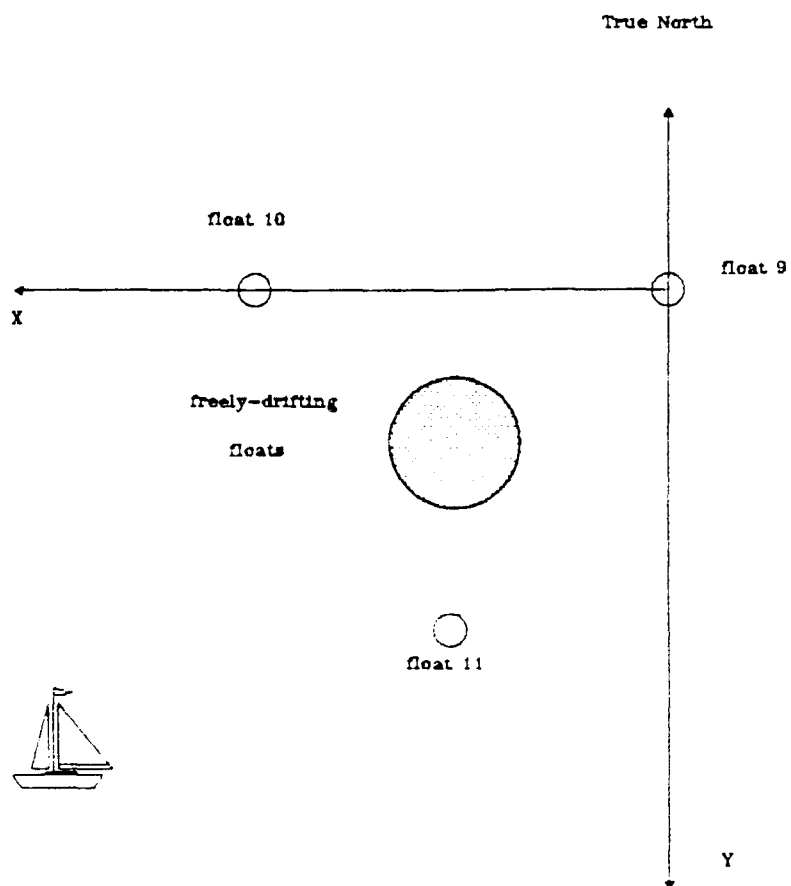


Figure 3.191



Plane view of coordinate system used for float localization

Figure 3.192

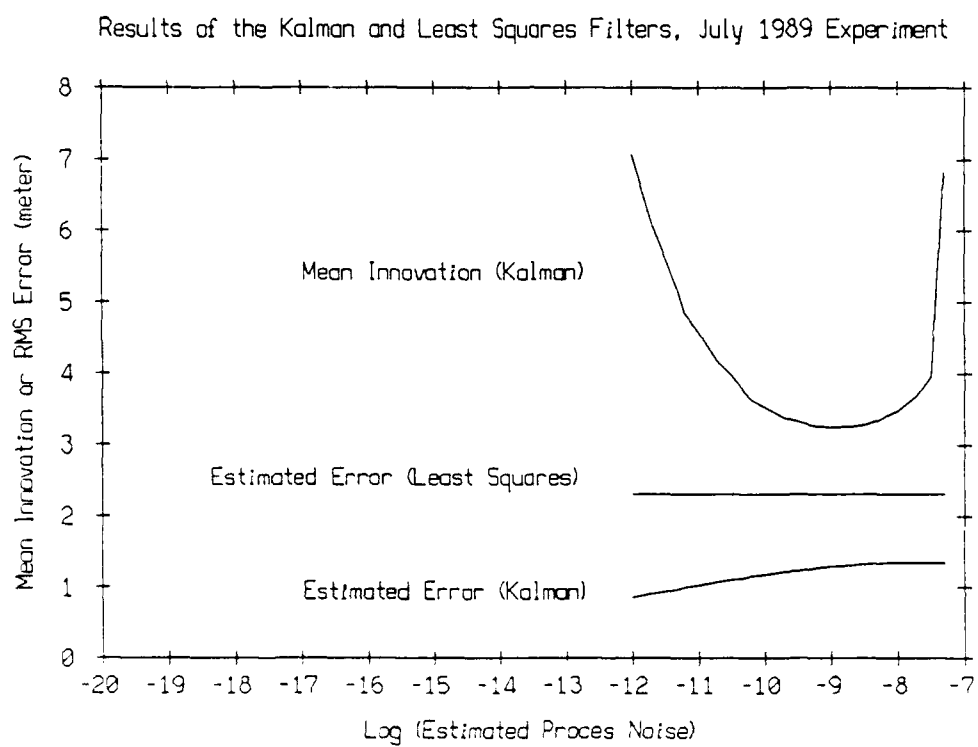


Figure 5.1

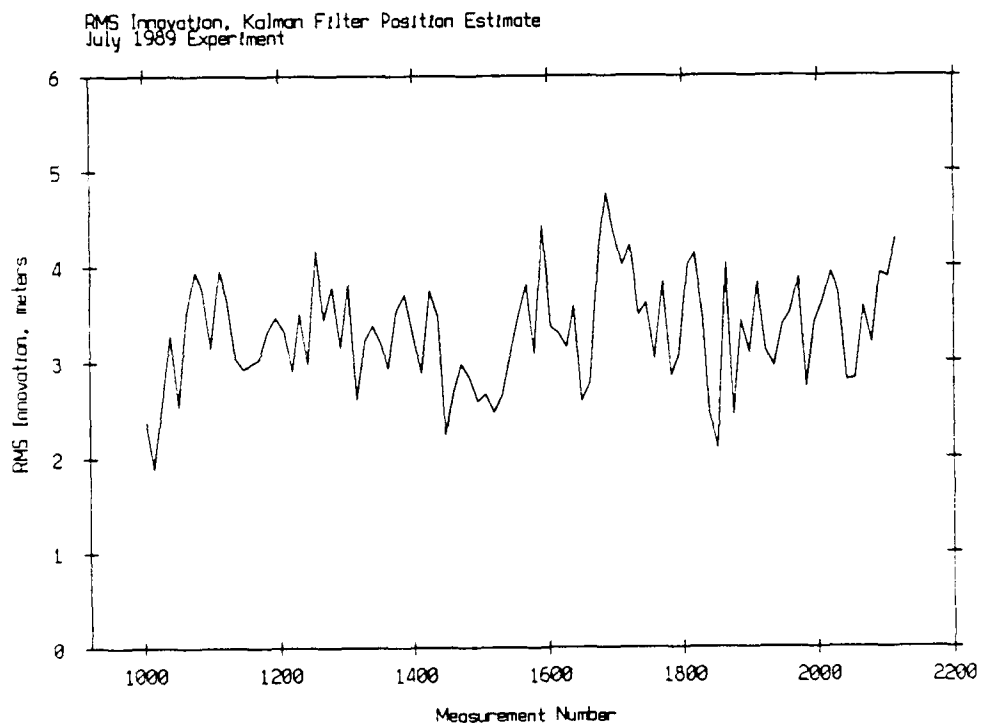
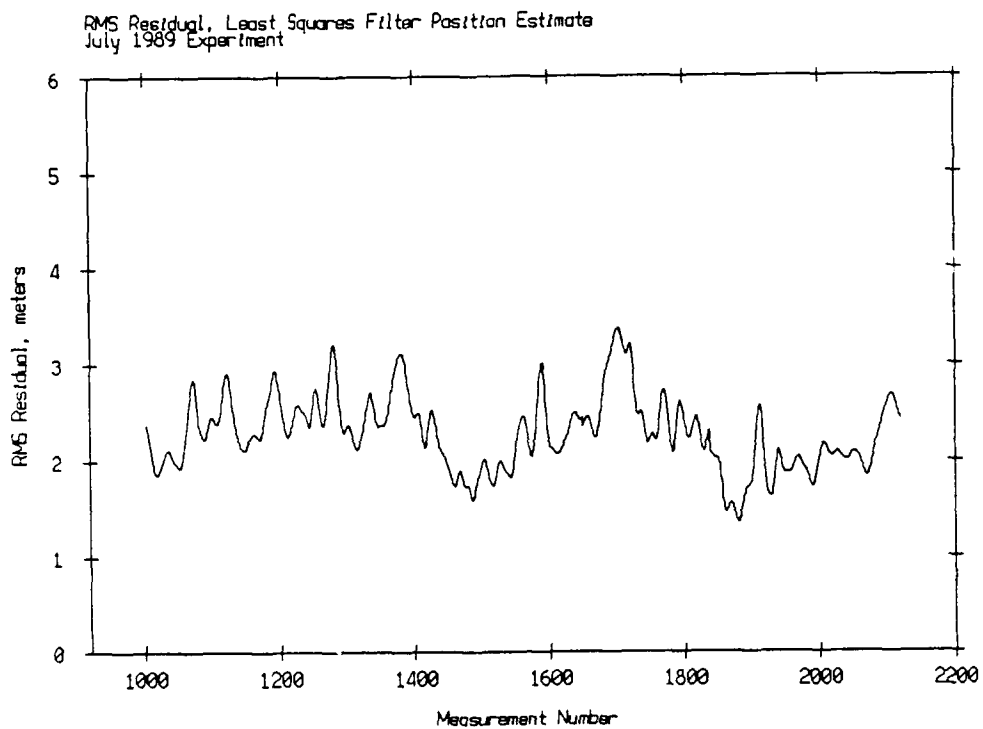


Figure 5.2

Float Locations, Least Squares Filter, July 1989 Experiment
 Records 1003-2120 (00.00 7/9/89 - 13.58 7/9/89)

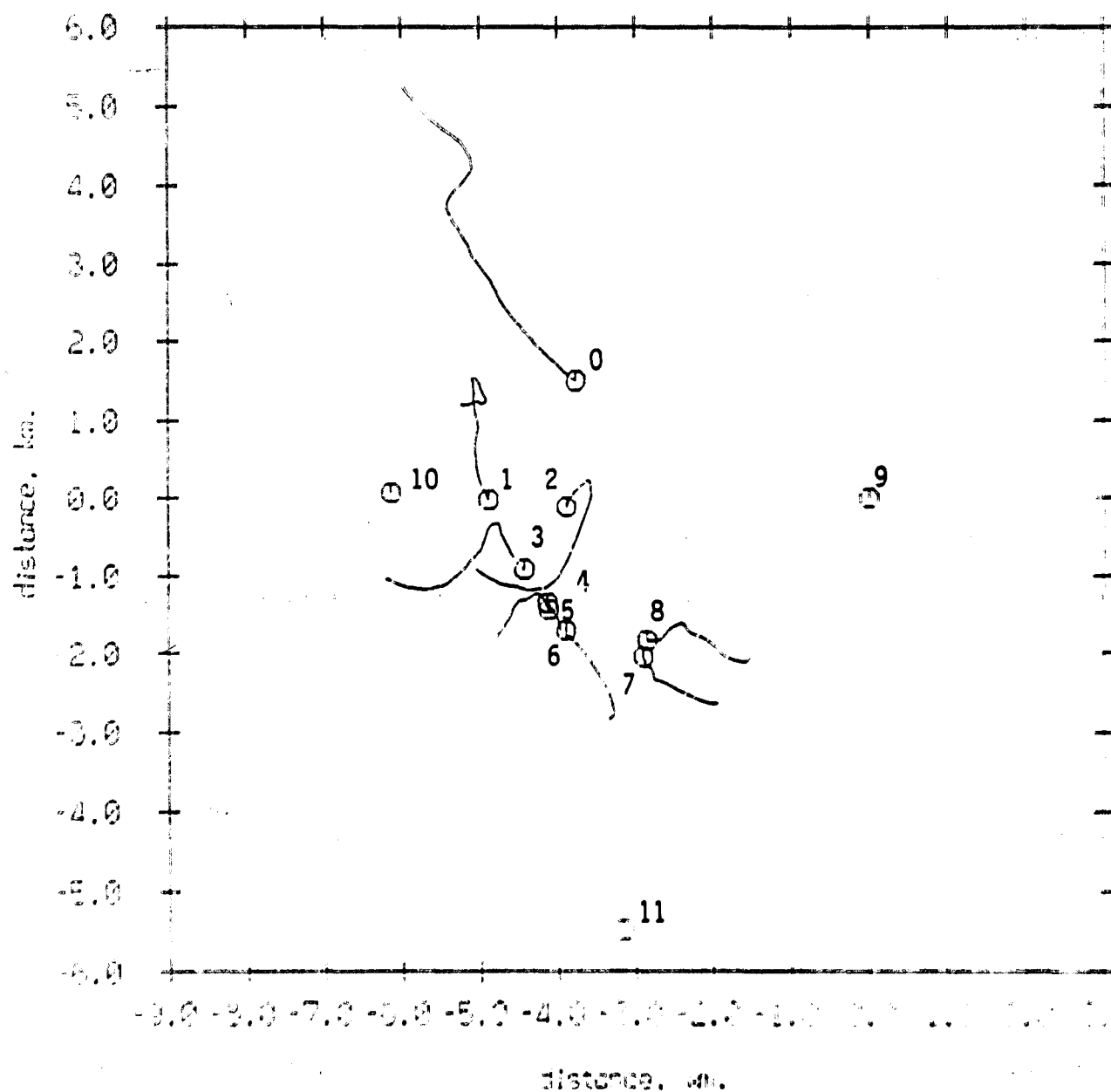


Figure 5.3a

Float Locations, Kalman Filter, July 1989 Experiment
 Records 1003-2120 (00:00 7/9/89 - 13:58 7/9/89)

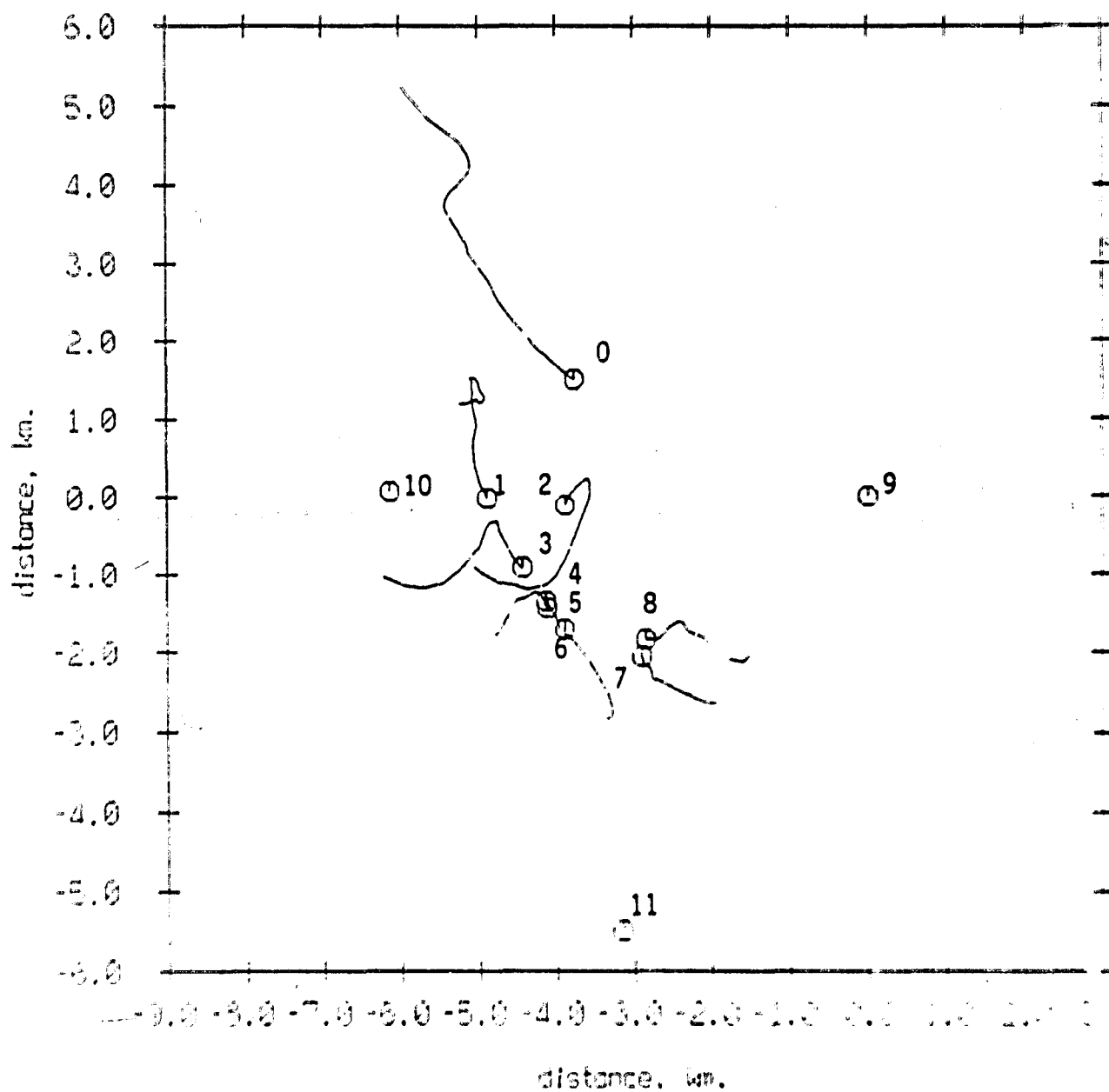


Figure 5.3b

Float Depth Estimates, Least Squares Filter, July 1989 Experiment
 Records 1003-2120 (00:00 7/9/89 - 13:58 7/9/89)

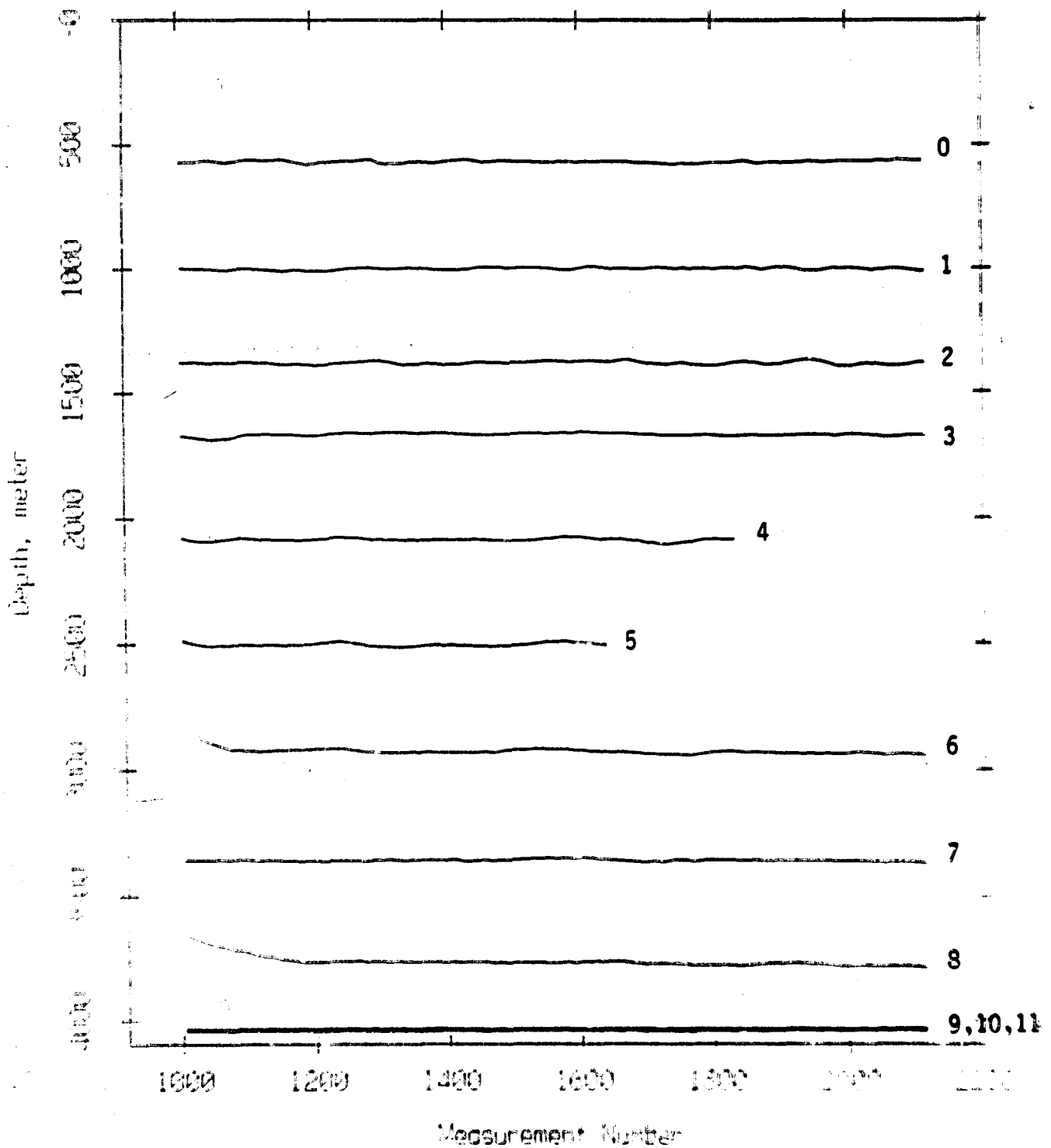


Figure 5.4a

Flood Depth Estimates, Kalman Filter, July 1989 Experiment
 Records 1003-2120 (00:00 7/9/89 - 13:58 7/9/89)

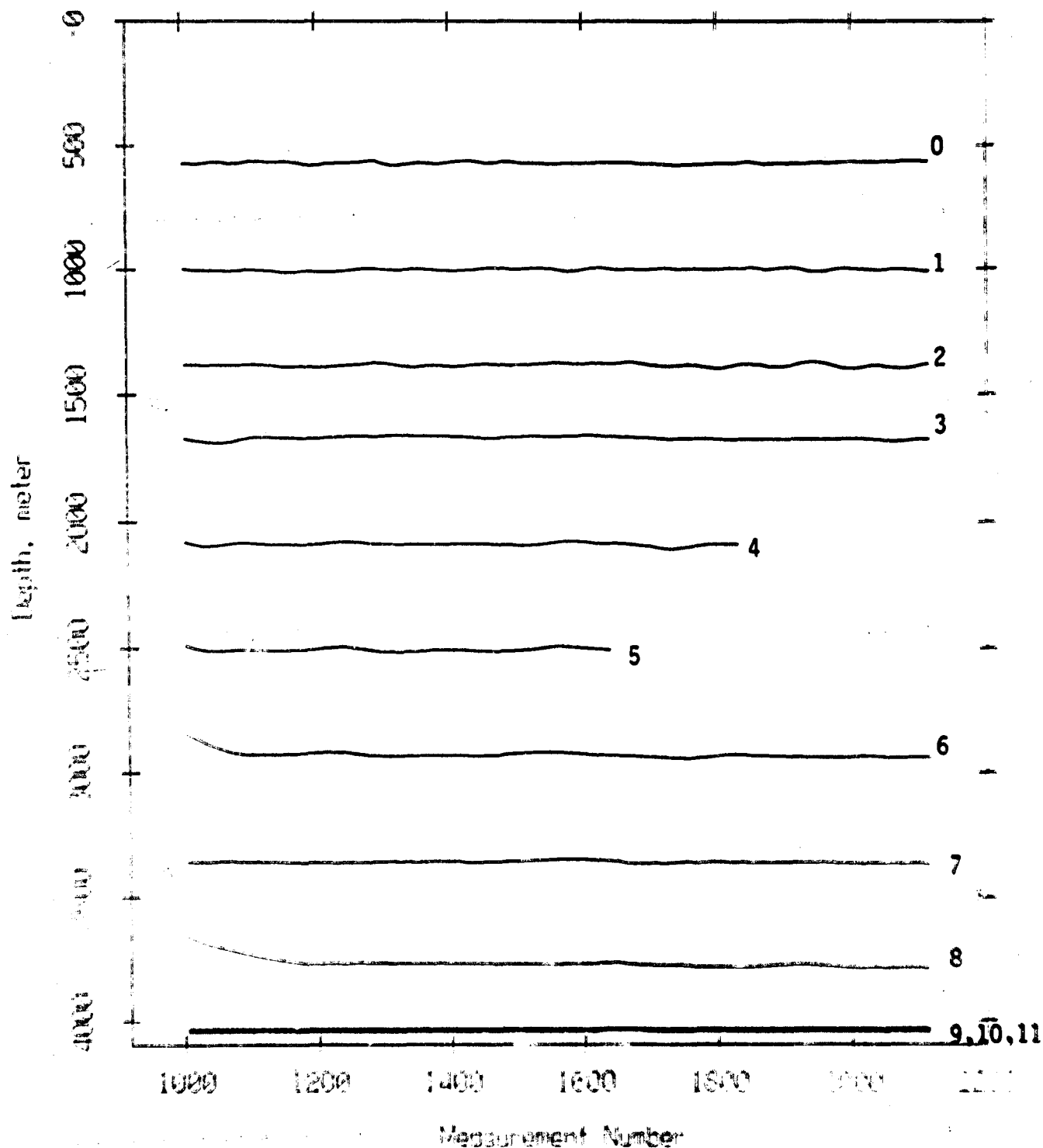


Figure 5.4b

Distance Between Kalman and Least Squares Position Estimates

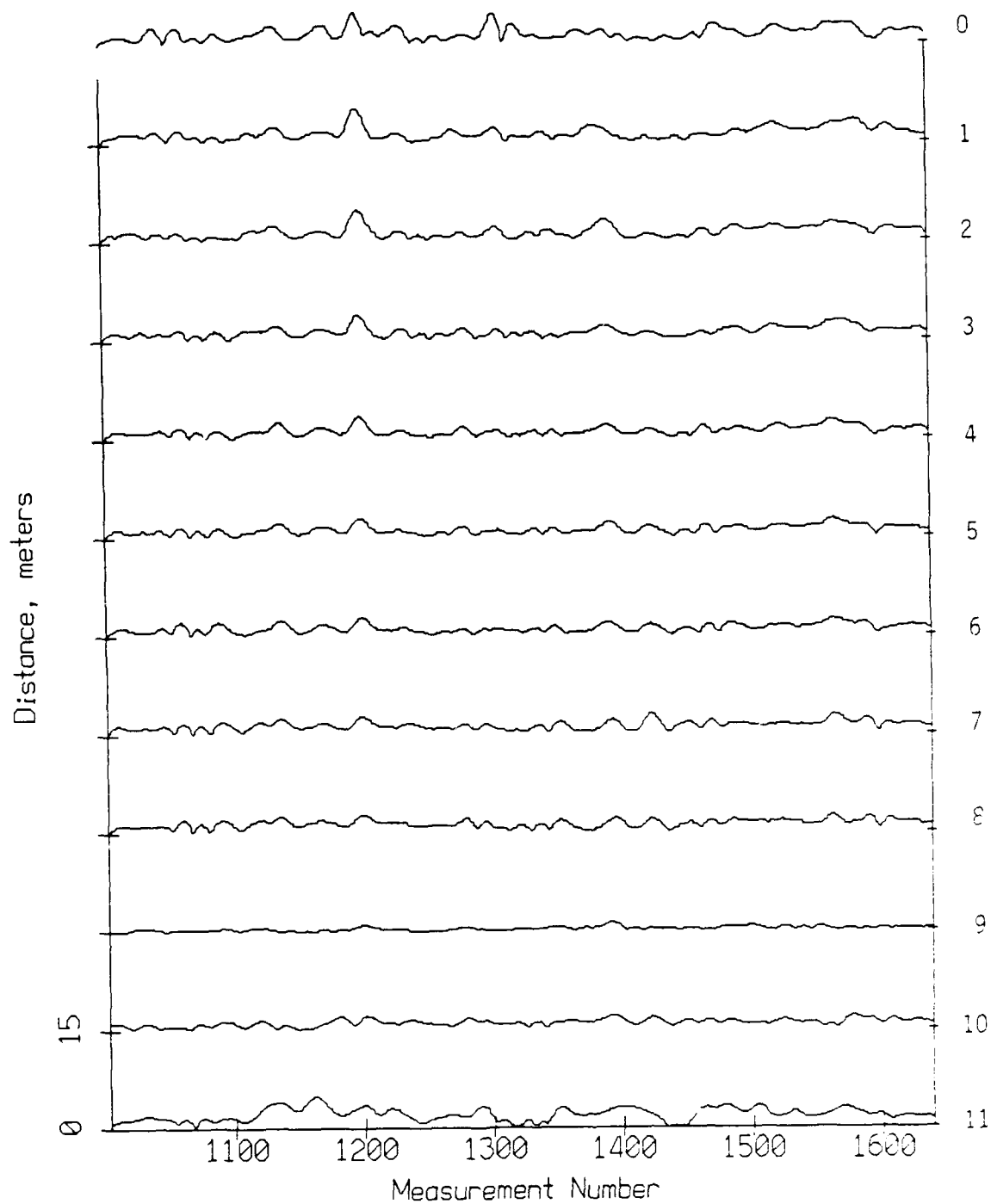


Figure 5.5

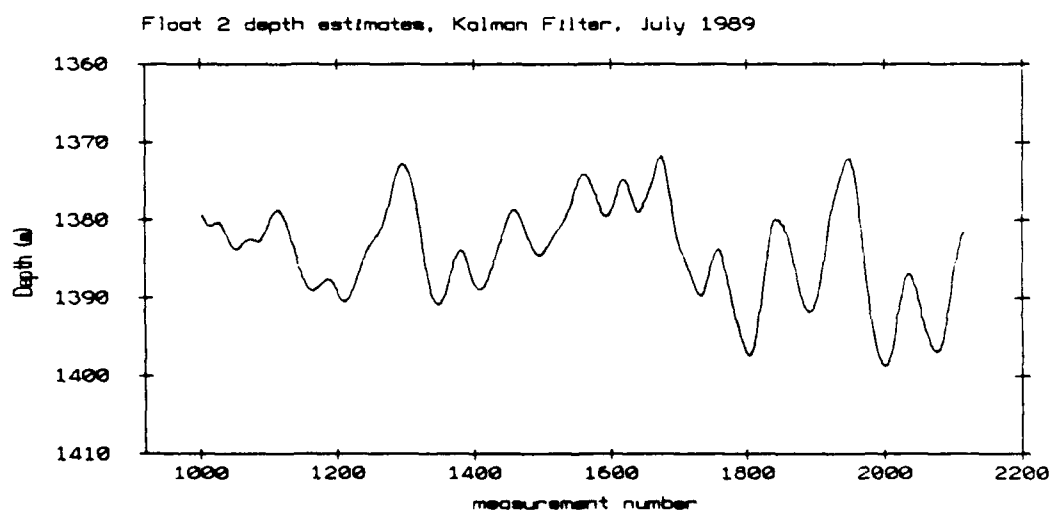
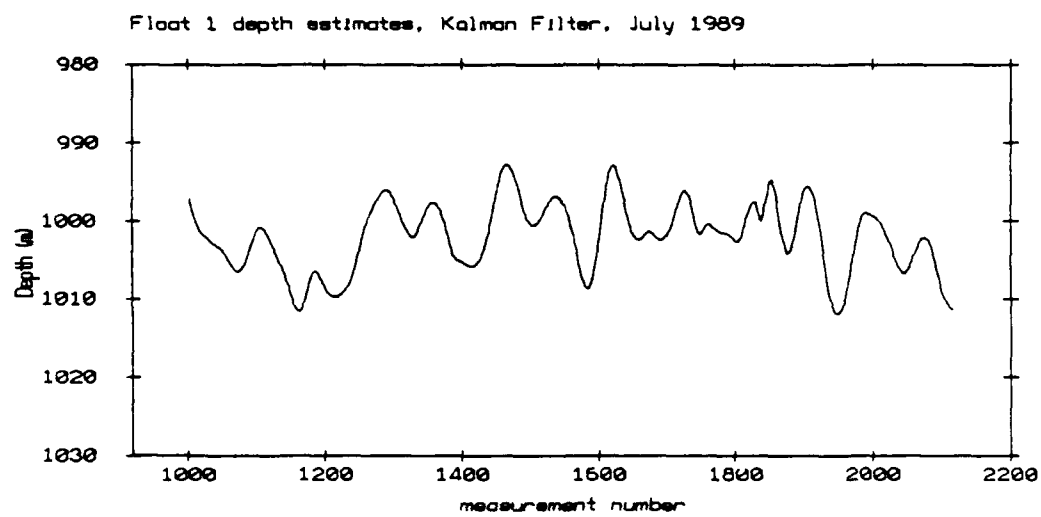
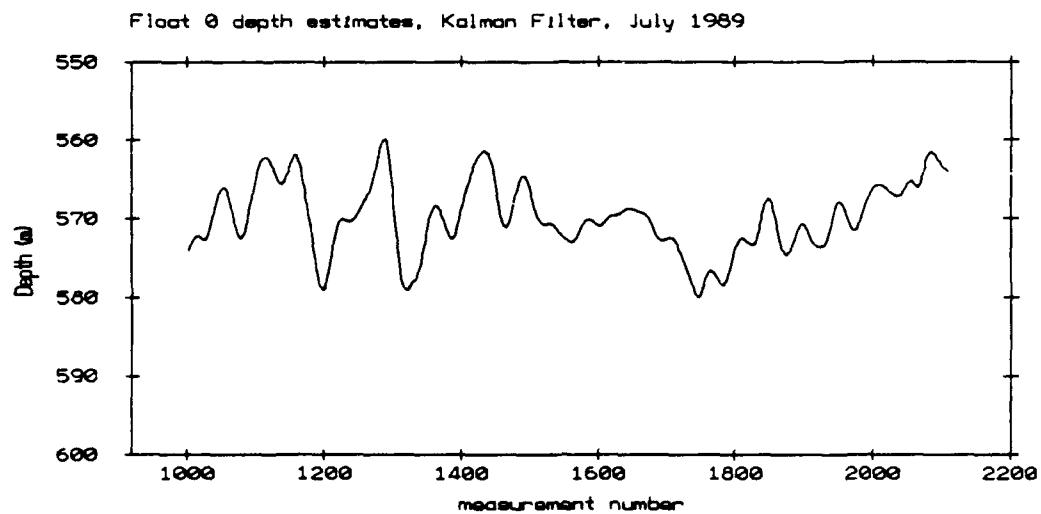


Figure 5.6

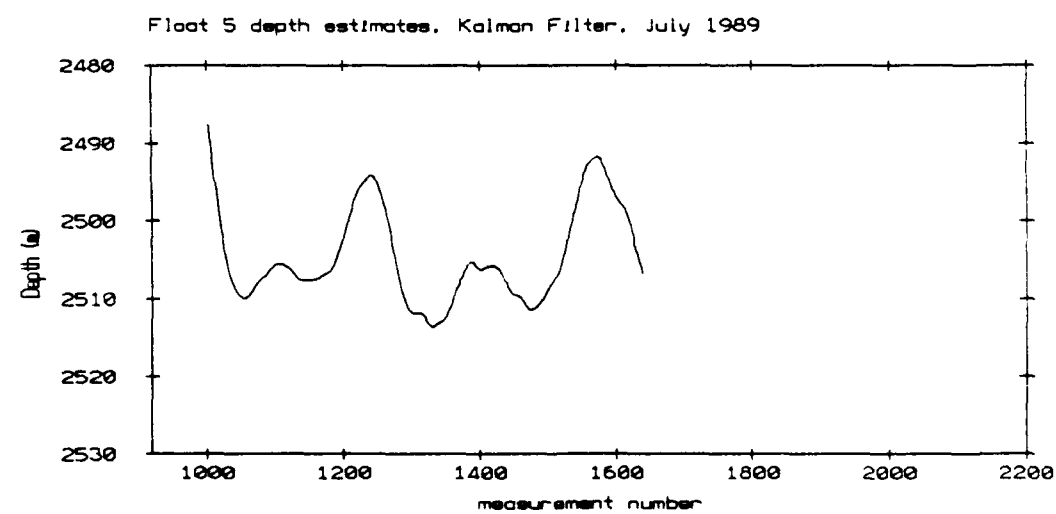
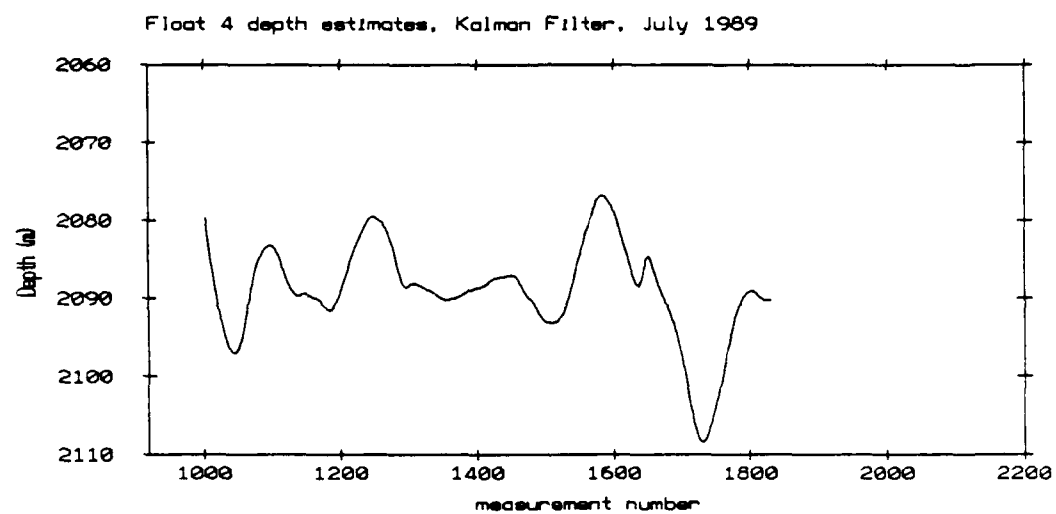
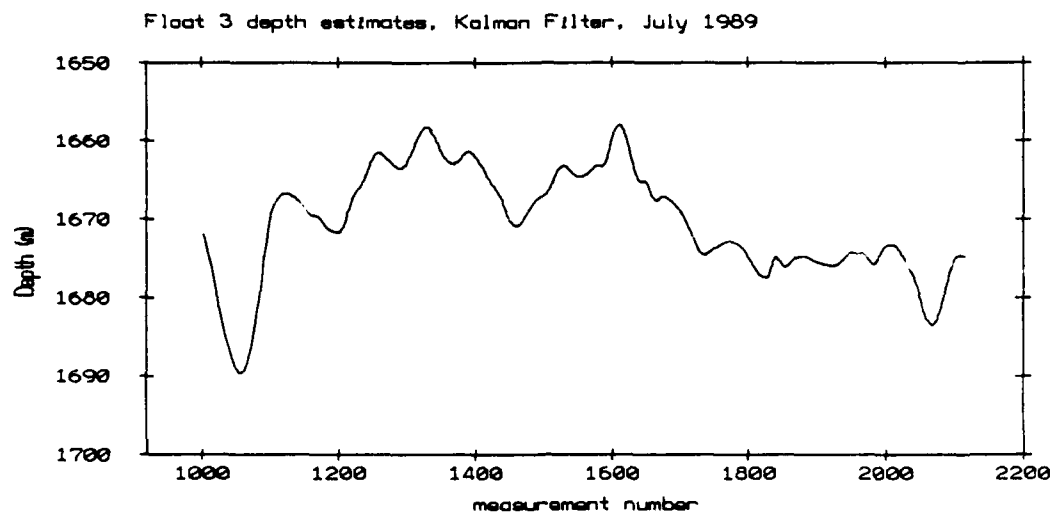
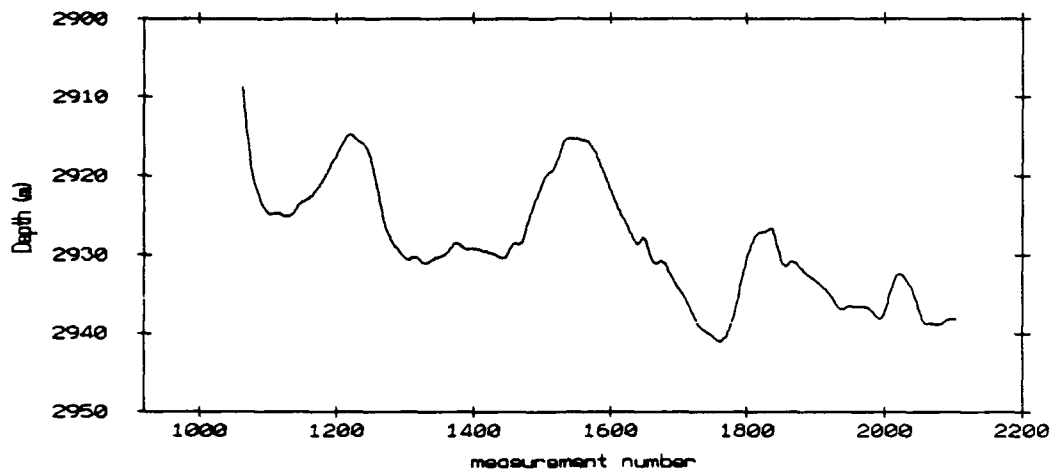
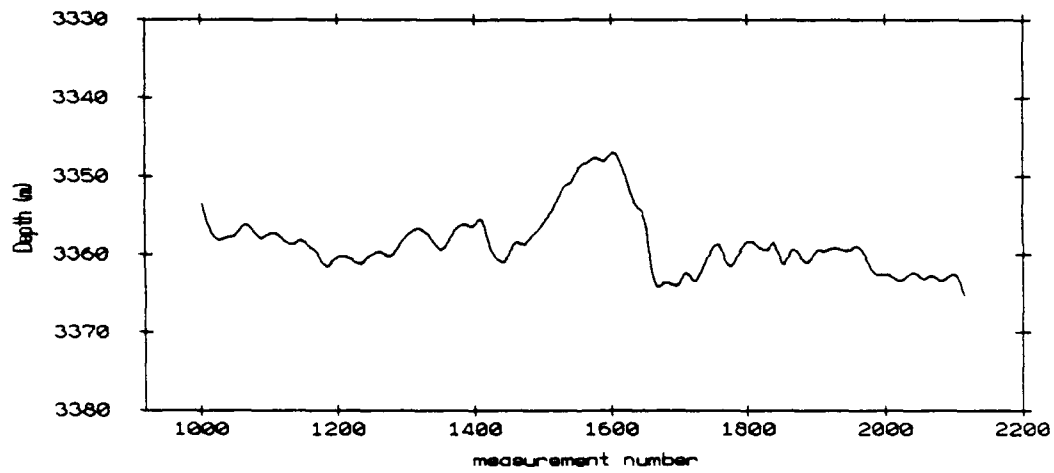


Figure 5.7

Float 6 depth estimates, Kalman Filter, July 1989



Float 7 depth estimates, Kalman Filter, July 1989



Float 8 depth estimates, Kalman Filter, July 1989

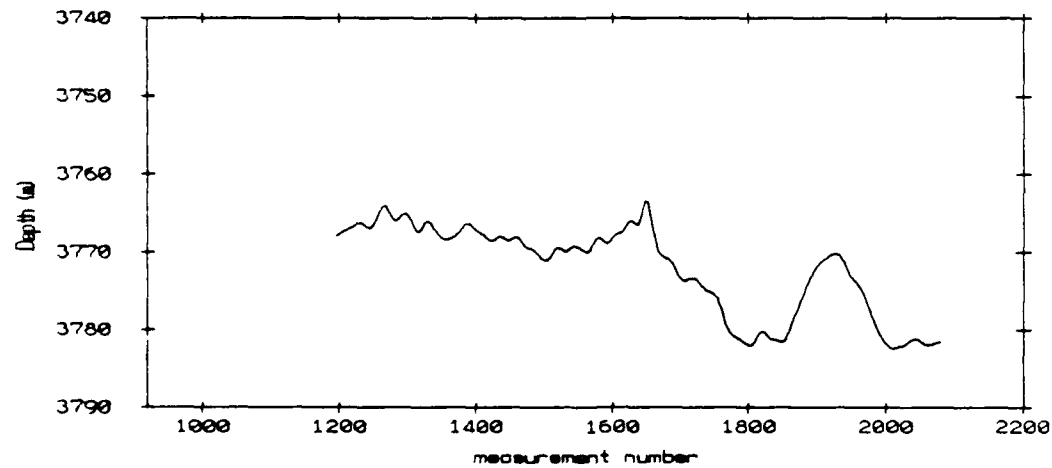


Figure 5.8

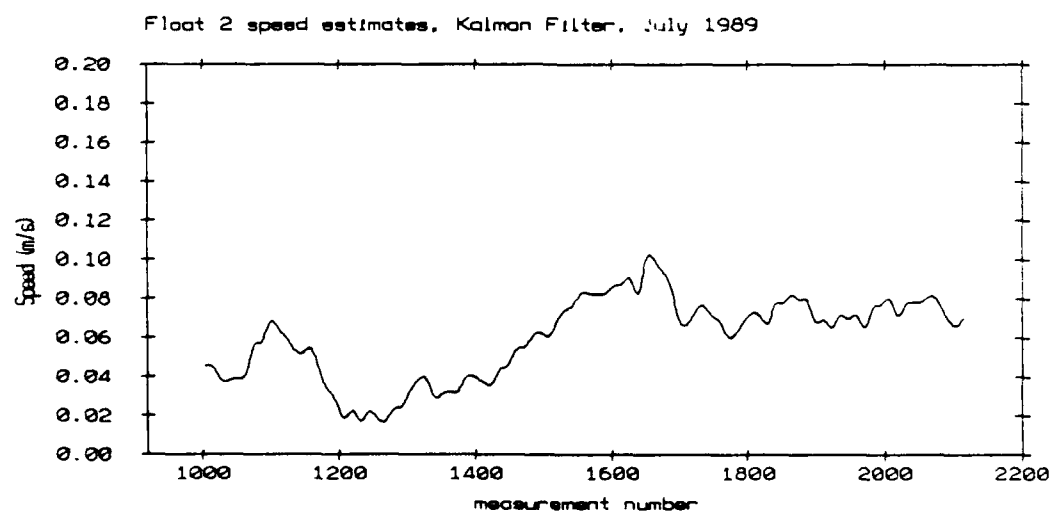
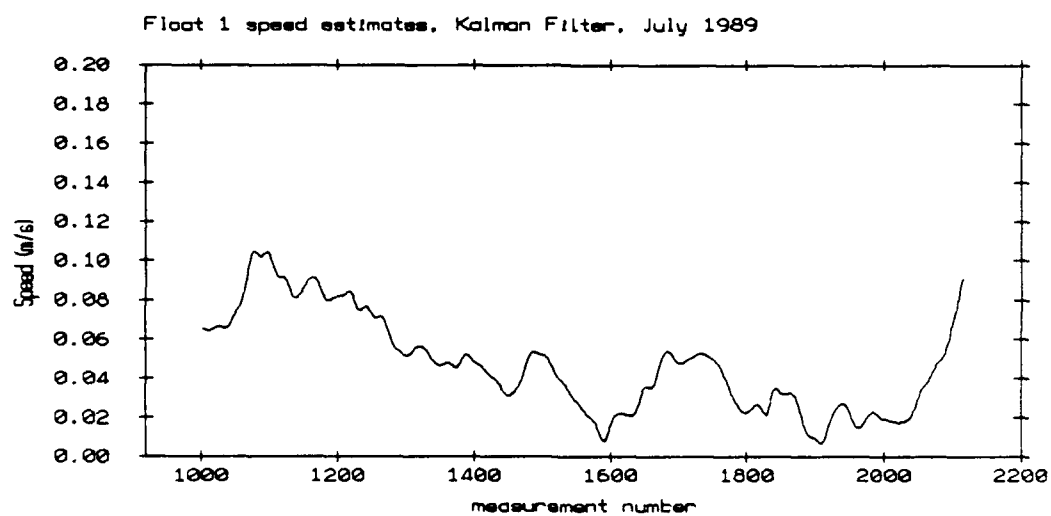
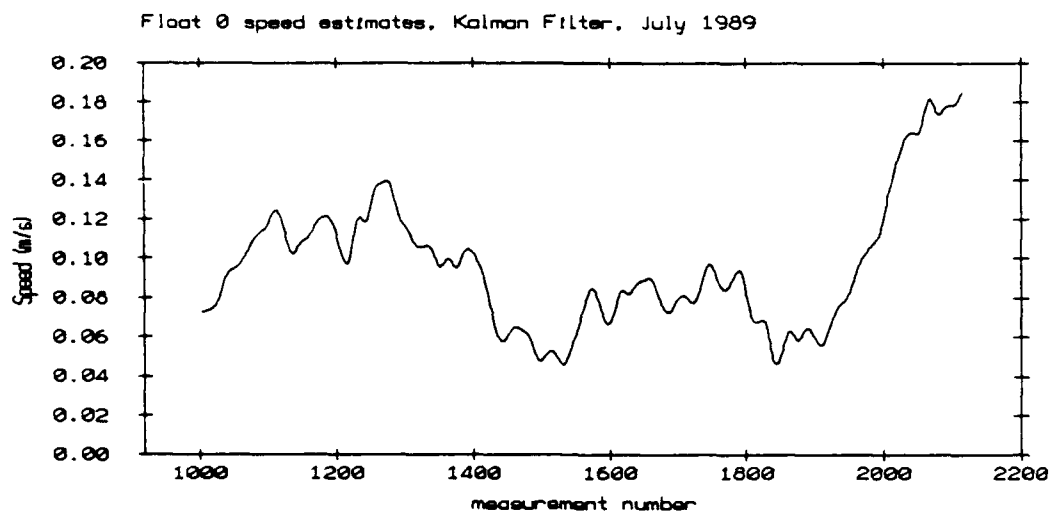
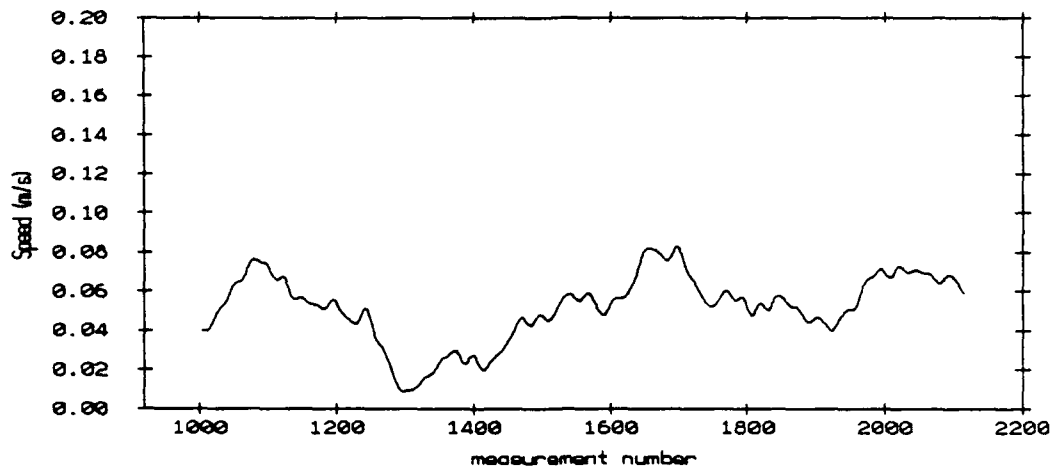
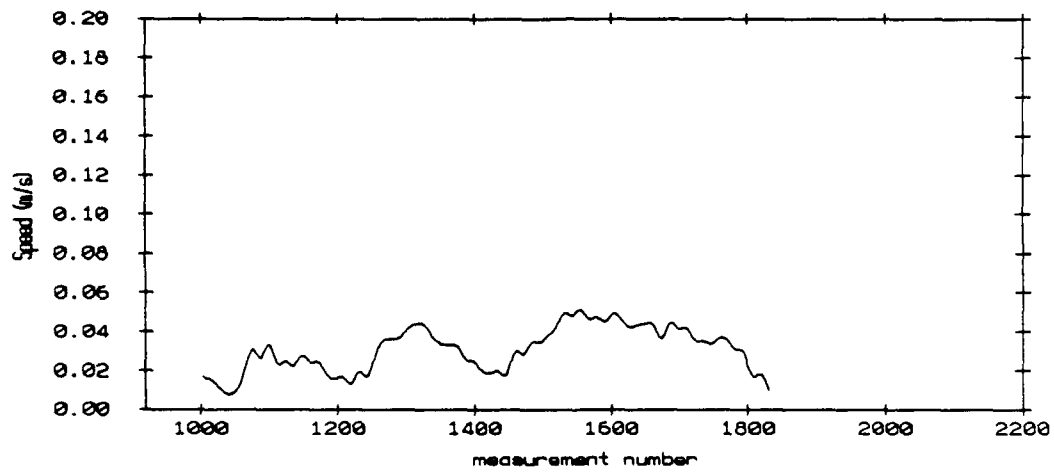


Figure 5.9

Float 3 speed estimates, Kalman Filter, July 1989



Float 4 speed estimates, Kalman Filter, July 1989



Float 5 speed estimates, Kalman Filter, July 1989

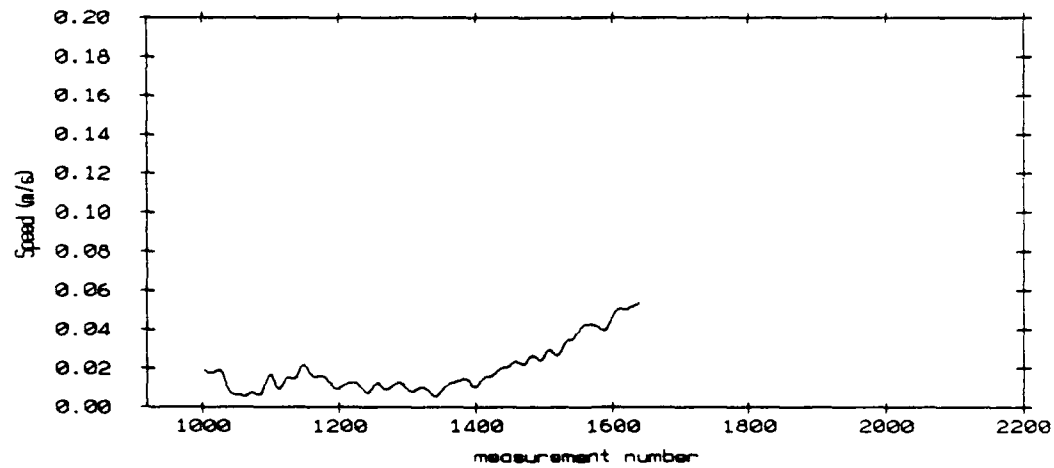


Figure 5.10

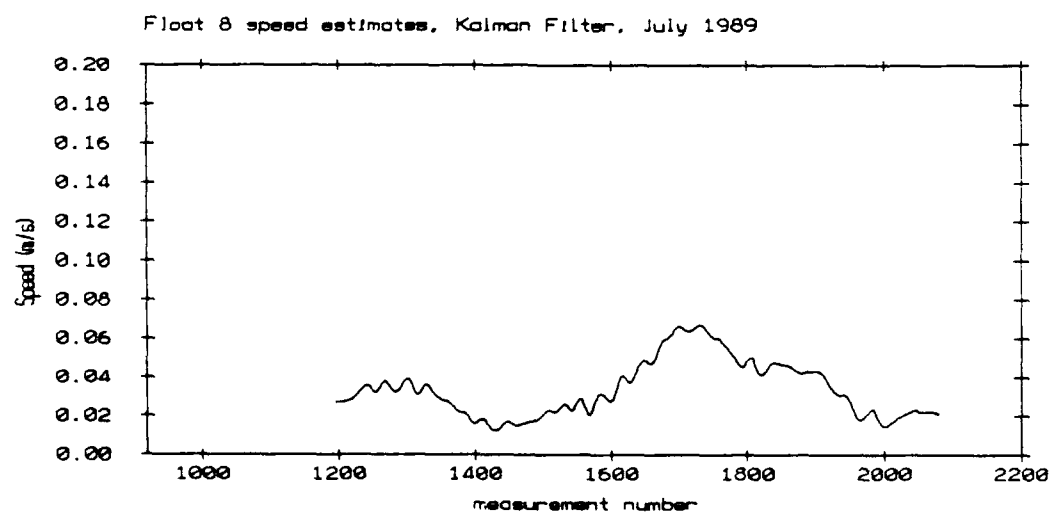
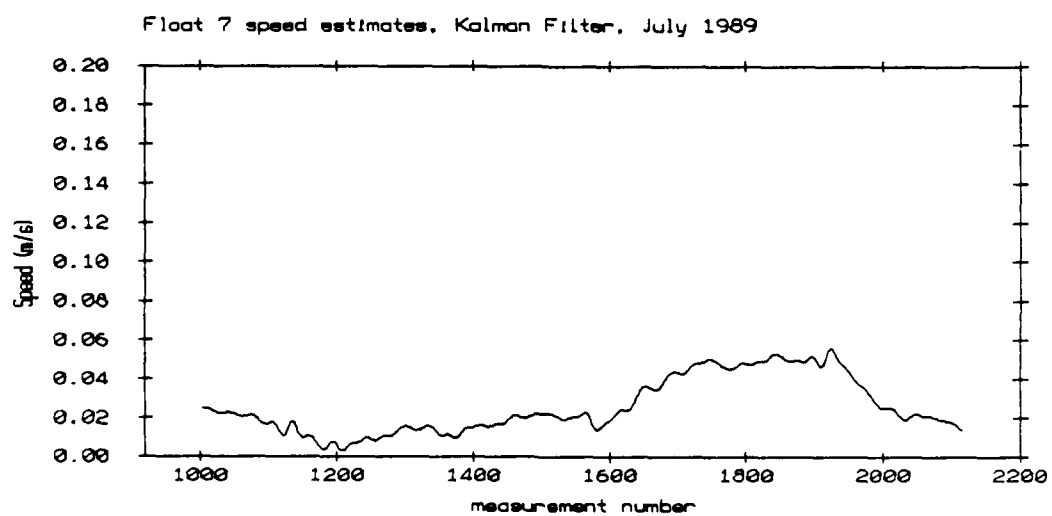
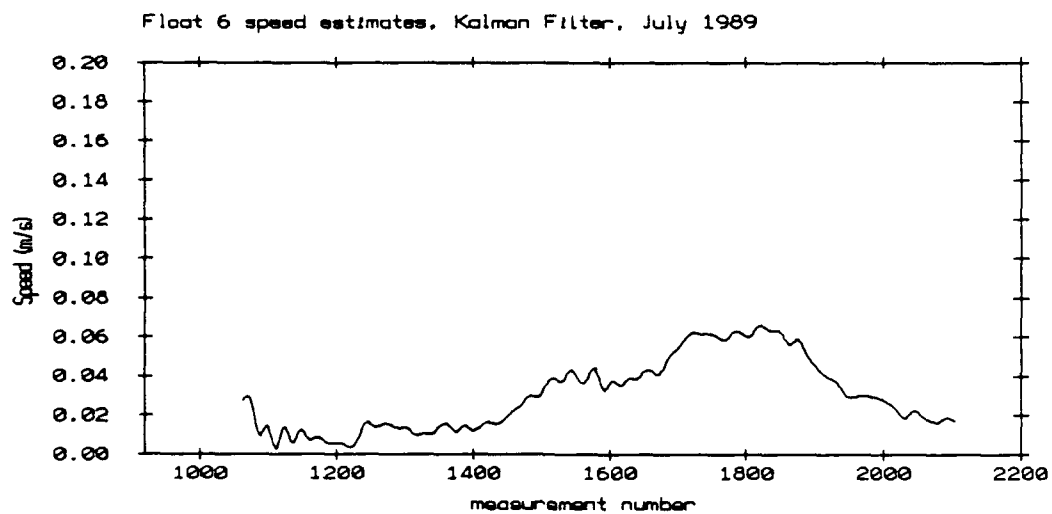


Figure 5.11